2nd International Lund RCM Workshop

21st Century Challenges in Regional-scale Climate Modelling

Lund University, Sweden
4 - 8 May 2009

Workshop Proceedings

Editors: Burkhardt Rockel, Lars Bärring and Marcus Reckermann

Jointly organized by

Swedish Meteorological and Hydrological Institute, Norrköping, Sweden
Lund University, Sweden
International BALTEX Secretariat,
GKSS Research Centre Geesthacht GmbH

Organisers and Sponsors

Lund University

Swedish Meteorological and Hydrological Institute

GKSS Research Centre Geesthacht

U.S. National Science Foundation

World Climate Research Programme

World Meteorological Organization

Swedish Environmental Protection Agency

Swedish Research Council for Environment

Associated Organisations

ENSEMBLES

North American Regional
Climate Change Assessment Programme

BALTEX – The Baltic Sea Experiment

Global Energy and Water Cycle Experiment

Danish Meteorological Institute

Scientific Committee

Raymond Arritt, Iowa State University, USA
Lars Bärring, Swedish Meteorological and Hydrological Institute and Lund University, Sweden
Jens Hesselbjerg Christensen, Danish Meteorological Institute, Denmark
Ole Bøssing Christensen, Danish Meteorological Institute, Denmark
Michel Déqué, Météo-France, France
Congbin Fu, Institute of Atmospheric Physics, Chinese Academy of Sciences, China
Filippo Giorgi, Abdus Salam International Centre for Theoretical Physics, Italy
Richard Jones, Met Office, U.K.
Jack Katzfey, Centre for Australian Weather and Climate Research, Australia
Rupa Kumar Kolli, World Meteorological Organization, Switzerland
René Laprise, Université du Québec à Montréal, Canada
Markus Meier, Swedish Meteorological and Hydrological Institute and Stockholm University, Sweden
Claudio Menendez, Centro de Investigaciones del Mar y la Atmósfera, Argentina
Roger Pielke Sr., University of Colorado, USA
Burkhardt Rockel, GKSS Research Centre, Germany
Markku Rummukainen, Swedish Meteorological and Hydrological Institute, Sweden
Benjamin Smith, Lund University, Sweden
Hans von Storch, GKSS Research Centre and University of Hamburg, Germany

Organising Committee

Lars Bärring, Swedish Meteorological and Hydrological Institute and Lund University, Sweden
Ole Bøssing Christensen, Danish Meteorological Institute, Denmark
Hans-Jörg Isemer, International BALTEX Secretariat, GKSS Research Centre, Germany
Anna Maria Jönsson, Lund University, Sweden
Marcus Reckermann, International BALTEX Secretariat, GKSS Research Centre, Germany
Burkhardt Rockel, GKSS Research Centre, Germany

Preface

This *Second Lund Regional-scale Climate Modelling Workshop* is a follow-up to the first regional-scale climate modelling workshop[1] held in Lund, Sweden in 2004. The overall theme of the first workshop was "High-resolution climate modelling: Assessment, added value and applications." Now, five years later, it is again time to take stock of the scientific progress in the wide range of topics that regional climate modelling spans. These range from theoretical understanding and parameterisation of meso-scale and regional processes in the atmosphere/ocean/land surface/biosphere system, numerical methods and links between regional climate modelling and global climate/earth system models as well as numerical weather prediction models, evaluation of models using various observational datasets, model intercomparison and ensemble-based methods, production and utility of regional climate scenarios, and the application of regional climate modelling output for impact studies.

This *Second Lund Regional-scale Climate Modelling Workshop* summarises developments and progress achieved in the last five years, discusses open issues and focuses on expected future challenges related to regional climate modelling. Thus, the overall theme for this workshop is *21st Century Challenges in Regional-scale Climate Modelling*.

The interest in this workshop was overwhelming. We received over 170 paper contributions from scientists all over the world; a total of about 220 participants from 43 countries registered for the workshop. As time is a tight resource in a 5-day workshop, many high-quality papers which were originally intended as oral presentations had to be realigned as posters. Therefore it is our policy not to distinguish between oral and poster presentations in this proceedings volume. It contains abstracts of all papers presented at the workshop, ordered alphabetically within sessions. Half a day of the workshop is dedicated to group and breakout sessions, some of which are open.

The workshop is organised by the Swedish Meteorological and Hydrological Institute (SMHI), Lund University, the Danish Meteorological Institute (DMI) and GKSS-Forschungszentrum Geesthacht GmbH (GKSS), with support by the International BALTEX Secretariat. The scientific committee was responsible for preparing the workshop content and the scientific programme, while practical and logistic arrangements were managed by the organising committee (see preceding page).

We are grateful for a generous endorsement by the following organisations: the World Meteorological Organization (WMO); the World Climate Research Programme (WCRP); the WCRP Global Energy and Water Cycle Experiment (GEWEX); the U.S. National Science Foundation (NSF); the ENSEMBLES project co-financed by EU FP-6; the North American Regional Climate Change Program (NARCCAP); the Swedish Research Council for Environment, Agricultural Sciences and Spatial Planning (Formas); the Swedish Environmental Protection Agency (Swedish EPA); and the GEWEX-CEOP Regional Hydroclimate Project BALTEX (Baltic Sea Experiment).

This workshop brings together scientists from a wide range of disciplines that share a common interest in regional climate models. We hope that the interdisciplinary programme and the truly international group of participants will stimulate the exchange of views and discussions, and provide a fertile ground for future research directions and new collaborations.

April 2009

Burkhardt Rockel, Lars Bärring, and Marcus Reckermann

Editors

[1] http://www.nateko.lu.se/Elibrary/LeRPG/5/LeRPG5Article.pdf

Contents

Session 1: Dynamical Downscaling

Session 2: New Developments in Numerics and Physical Parameterizations

Session 4: Regional Observational Data and Reanalysis

Session 5: Results from Large Projects

Session 6: The Future of RCMs

Index of Authors

Influence of large-scale nudging on regional climate model simulations

Adelina Alexandru[1,3,4], Ramon de Elia[2,3,4], René Laprise[1,3,4], Leo Separovic[1,3,4], and Sébastien Biner[2]

[1]Université du Québec à Montréal (UQÀM), Montréal (Québec), Canada, adelina@sca.uqam.ca; [2]Consortium Ouranos, Montréal (Québec), Canada; [3]Canadian Network for Regional Climate Modelling and Diagnostics (CRCMD), Montréal (Québec), Canada; [4]Centre pour l'Étude et la Simulation du Climat à l'Échelle Régionale (ESCER), Montréal (Québec), Canada

1. Introduction

The present study examines the impact of various large-scale spectral nudging (SN) configurations on Canadian RCM (CRCM) simulations. The objective is to notice any secondary effects from the application of SN such as a possible reduction of the model's ability to develop small-scale features. A broad series of CRCM experiments is carried out over North America; each experiment, performed for a given SN configuration, consists of four ensembles of 15 runs corresponding to four different domain sizes. In order to evaluate the effects of an "extreme nudging", an additional experiment was carried out nudging the CRCM with the maximum strength of the SN - equivalent to a replacement of the largest waves at all levels.

This study reveals differences in CRCM's behaviour to reproduce regional characteristics when SN has been added to the model driving. SN has diminished in general the model's internal variability (IV), but noticeable effects on statistics of extremes and estimation of simulated precipitation on large domains has been noticed.

2. CRCM Large-Scale Nudging

The present study uses Version 3.6.1 of the CRCM (*Caya and Laprise,* 1999) that has an option for SN, in addition to the standard Davies LBC treatment (*Riette and Caya*, 2002 *Denis et al.* 2002). The current CRCM-SN has three adjustable parameters of SN: the length scale beyond which SN is applied, the maximum strength of the SN ($\propto_{max}$), and the lowest model level (L_0) below which no SN is applied. The SN strength $\propto$ (defined as the fraction of CRCM field that is replaced by the re-analyses at each time step) is taken to vary linearly from 0 (corresponding to $L_{0)}$) to $\propto_{max}$ (at the uppermost model level). The SN can be applied to any model variable; in this study, it is applied to the horizontal wind components only. Figure 1 shows the various profiles of SN used in this paper.

3. Simulation Set-Up

The experiments, performed for different configurations of SN, consist of ensembles of several members (generally 15) generated for four different domain sizes. One experiment is performed without SN ($\propto_{max}$=0); three experiments are made with the same $\propto_{max}$=0.05 but different L_0 (500, 700 and 850 hPa); a fifth experiment is performed with a uniform value of $\propto=\propto_{max}$=1 at all model levels. In this "full SN" case, the large scales of the CRCM are entirely replaced by those of the re-analyses, at all levels from the surface to the model lid (see Fig.1); due to the particularly weak IV, only 10-member ensembles are integrated in the full SN experiment.

All integrations from each ensemble were initialized one day apart, starting the 0000 UTC 5 May 1993 up to the 0000 UTC 20 May 1993; all simulations end on 0000 UTC 1st September 1993, so that all ensemble members for different domain sizes overlap for the full three months of June-July-August 1993, with a spin-up period varying from 11 to 25 days. The integrations share exactly the same LBC for atmospheric fields and the same prescribed SST and sea-ice coverage for the ocean surface (see Table 1).

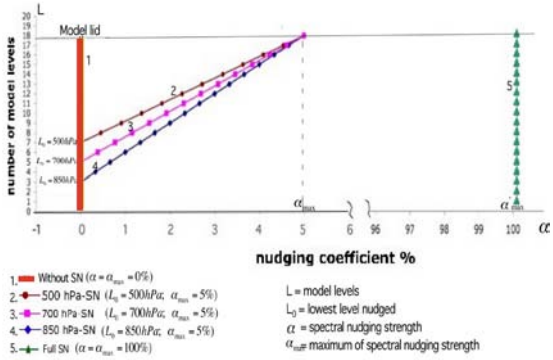

Figure 1. The five CRCM experiments.

Test Experiment	L_0 (hPa)	α_{max} (%)	Number of Ensembles	Domaine Size	Ensemble members
SN from 500 hPa-level to model lid (500 hPa-SN)	500	0.05	4	140×140	15
				120×120	15
				100×100	15
				80×80	15
SN from 700 hPa-level to model lid (700 hPa-SN)	700	0.05	4	140×140	15
				120×120	15
				100×100	15
				80×80	15
SN from 850 hPa-level to model lid (850 hPa-SN)	850	0.05	4	140×140	15
				120×120	15
				100×100	15
				80×80	15
SN from the ground to model lid, at all levels (Full–SN)	1000	1	4	140×140	10
				120×120	10
				100×100	10
				80×80	10

Table 1: Synthesis of the experiments performed.

4. Influence of SN on Internal Variability

The internal variability of the model (IV) is usually estimated by measuring the spread among the ensemble members during the integration period (standard deviation). According to previous studies, the IV of an RCM is sensitive to domain size: larger domains develop large IV while small domains are associated with small IV (see *Alexandru et al.* 2007). The present study shows that a significant SN applied to the model not only reduces the amplitude of IV, particularly true for the large domain sizes, but it also reduces the sensitivity of IV to domain size; the full SN almost suppresses the IV of the model independently on domain size.

5. Influence of SN on the Ensemble Mean

The variability of the seasonal mean (IVS) was estimated as the square root of the variance between individual member seasonal averages. In general, as for IV, the IVS tends to decrease with increasing SN, more significantly for the geopotential height on the largest domain, where IVS values are considerably lower, even with the weak 500 hPa-SN. As expected, the IVS reaches its smallest values in the full SN case with a negligible sensitivity to domain size.

After analyzing the spread between seasonal means of the members in the ensembles (which we termed IVS), we studied the effect of SN on the ensemble mean of different domain sizes. Study shows that the impact of SN on the ensemble mean pattern is quite pronounced for the 140-by-140 domain and much reduced for the smaller 100-by-100 domain when we compare to without-SN case (taken as a reference). This suggests that Davies's control (1976) may be just as effective as SN for small domains. We have also noticed that for stronger SN, there is little variation of the ensemble mean as a function of domain size. Thus, similar results may be obtained by employing large SN regardless of the domain size or, alternatively, by avoiding SN when working with small domains.

6. Influence of SN on Bimodal Solutions

For the largest domains, where the impact of SN is the largest, a difference has been noted between the results without SN (*Alexandru et. al*. 2007) and those with SN concerning bimodal behavior of the ensemble. For the case without SN, the 15 members appear to separate into a group of 5 members producing a low-pressure system over the ocean, close to the Canadian Atlantic Region, and another group of 10 members showing a high-pressure system over the same area and an intense precipitation trough close to the US East Coast (see *Alexandru et al*. 2007). We noticed that when the degree of SN applied to the model is progressively increased, the effect is to foster the development of the solution that is closest to the observed data.

7. Influence of SN on Precipitation Extremes

We note that for the runs without SN on the 140-by-140 domain the largest extremes occur from 10th to 15th of July 1993, associated with the intense precipitation trough given by the group of 10 simulations in the bimodal behaviour of the ensemble, as discussed in the above paragraph. The magnitude of this maximum is progressively attenuated as the degree of SN is progressively increased. Similar behaviour is noted for the 120-by-120 domain: precipitation extremes decrease in number and intensity as the degree of SN is progressively increased.

8. Influence of SN on Power Spectra

When a spectral analysis is performed, the results with 500 hPa-SN show little difference with respect to those without SN, with the exception of the longest wavelengths. As was shown in *Separovic et al.* (2008), long wavelengths at low altitudes tend to be overestimated in CRCM simulations, and SN reduces this overestimation. The configuration with 850 hPa-SN shows a decrease in spectral variance in all wavelengths except in the 200 to 400 km range where it is comparable with the configuration without SN. When full-SN is applied, a very important decrease in spectral variance affects all wavelengths.

9. Conclusion

The general conclusion of this research suggests that SN has, on balance, more positive than negative impacts. On the one hand, SN results in a reduction of IV, reduction of simulation dependence to domain size, and improvement of time means (or at least making them closer to driving data). On the other hand, SN results in a reduction of precipitation maxima and spectral power in the vorticity field, which could be associated to a decrease in the intensity of cyclones. While finding an optimal setup for SN is still elusive, - there are still lingering questions regarding the appropriate nudging intensity and vertical profile, variables to be affected, etc. - a moderate level of SN has been shown to be beneficial.

References

Alexandru, A., de Elia, R., and Laprise, R., 2007 : Internal Variability in RegionalClimate Downscaling at the Seasonal scale. *Mon. Wea. Rev*., **135**, 3221-3238.

Caya, D., and R. Laprise, 1999: A semi-implicit semi-Lagrangian regional climate model: The Canadian RCM. *Mon. Wea. Rev*., **127**, 341-362.

Denis et al. 2002: Spectral Decomposition of Two-Dimensional Atmospheric Fields on Limited-Area Domains Us ing the Discrete Cosine Transform (DCT). *Mon. Wea. Rev*., **130**, 1812-1829.

Riette, S. and D. Caya, 2002: Sensitivity of short simulations to the various parameters in the new CRCM spectral nudging. Res. Act. in Atmos. and Oceanic Modelling, edited by H. Ritchie, WMO/TD - No 1105, Report No. 32: 7.39-7.40.

A comparison of RCM performance for eastern Baltic region and the application of histogram equalization method for RCM outputs

Uldis Bethers, Juris Seņņikovs and Andrejs Timuhins

Faculty of Physics and Mathematics, University of Latvia, 8 Zeļļu street, Riga LV1002, Latvia. bethers@latnet.lv

1. Introduction

The intention of this work was the building of the climate data sets for the territory of Latvia, i.e. the eastern Baltic region. The required data sets were at least temperature and precipitation time series with reasonable spatial resolution which might be considered as characteristic for contemporary climate and climate change scenarios B2 and A2. The further usage of the data series (not covered in this abstract) was foreseen for the assessment of the impact of the climate change on the Latvian inland and coastal water environment.

Authors considered the set of RCM computations publicly available within the framework of PRUDENCE project. The method of comparison of RCM calculation results with the observed data series was proposed. The considered RCMs were ranked according to this comparison. The typical discrepancies between the modeled and observed temperature and precipitation data series were revealed. The method of the histogram equalization was proposed allowing processing of the RCM output, and yielding data series which statistically does not differed from the observed data series for the control time period (contemporary climate). The correction method was applied also for RCM calculations of B2 and A2 cliamate scenarios.

2. Comparison RCM vs. Observations

We considered the collection of the RCM calculations organised in a web-accessible database at Danish Meteorological Institute under EC 5th FP research project "PRUDENCE" EVK2-CT2001-00132 (prudence.dmi.dk). We considered 21 different model for the control period 1961-1991 characterising the contemporary climate. The observations of air temperature and precipitation by Soviet Hydrometeorlogical Agency (www.meteo.ru) in Eastern Baltic area (i.e. in and near the territory of Latvia, see Fig.1) were used. We conisdered 14 observattion stations in Estonia, Russia, Belorus, Lithuania and Latvia. The daily values of all 21 model and 14 observation stations were used.

The penalty function K_i describing the deviation of each i-th RCM from the meteorological observations was constructed. We aimed in evaluation of model accuracy in terms of temperature, precipitation, their monthly and interannual variation, and spatial distribution. Therefore we used four parameters for construction of penalty function: monthly mean temperatures T, monthly net precipitation p, and standard deviation of T, p during the reference 30-year period at all stations. All parameters were normalised to equal their weights. The calculation of penalty function for each RCM allowed for ranking of RCMs according to their agreement with observations in Eastern Baltic region.
Generally, all models reasonably represent the seasonal cycle of temperature, overestimate winter precipitation and underestimate summer precipitation in the study area. The comparison of the observations and RCM, as well as climate change predictions by RCM for Riga is illustrated in Fig. 3. The difference between the model and observations (0.8 degC and 164 mm) is not critical, however one must be careful interpreting the estimated climate change scenarious by RCM, i.e. direct comparison of observations with B2 and A2 calculations may yield to overestimation of expected T and p changes.

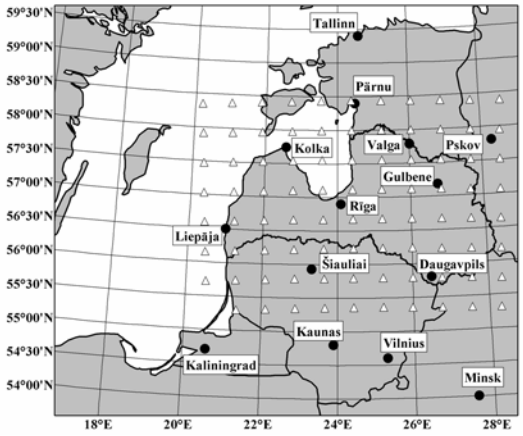

Figure 1. The observation stations and selected nodes of RCM (SMHI HCCTL) calculation grid over the territory of Latvia.

3. Method of Histogram Equalization

We propose a method of RCM data correction, based on the shifting the occurrence distribution of particular daily parameter (temperature or precipitation).

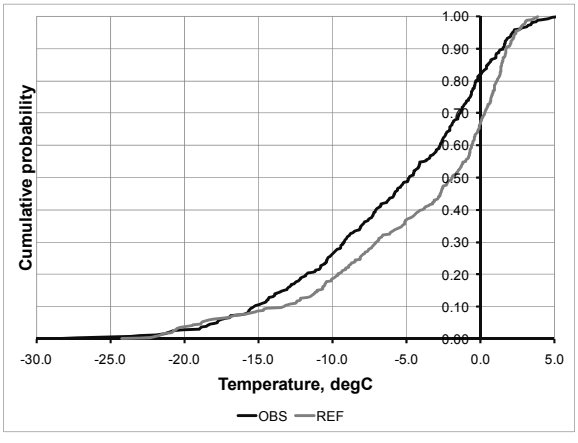

Figure 2. Cumulative probability of temperature (i.e. percentage of occurrence of temperatures below given temperature) for 15-Jan at Riga. Observations and RCM data for reference period.

(1) Two cumulative probability curves – one of the observed data, and one of RCM data – were constructed for each day-of-the-year, for each parameter in each observation station. The data within moving slot of time

(+/- 5 days) were used to increase the number of events to 330 (30 years times 11 days) for each curve. Data was randomly perturbed to ensure smoothness of probability curves.

(2) For each value of model data (say T) we found the probability f(T). We then find the observed temperature T^* for which $f(T^*)=f(T)$, and assume that model temperature correction for T is equal to T^*-T. Thus, the temperature correction is a function of model temperature, and is given by

$$\Delta T(T) = (T - T^*)\Big|_{f(T)=f(T^*)}$$

See the example of the temperature correction for typical winter day in Fig. 2. Correction ensures that the model daily temperatures in the range [-17;+2] degC are decreased to match occurrence of cold events, whilst the higher daily temperatures are increased.

(3) The correction functions of p.(2) were found for each day, for each parameter, and at each observation station. They were spatially interpolated to cover the model domain and applied for the correction of the RCM data. Thus, the dataset "modified RCM data for reference period" was created; it contains the climate signal characteristics from RCM, and in the same time has the statistical properties of the observed data.

(4) The same correction functions of p. (2) were applied for the RCM scenario results, yielding datasets "modified RCM data for climate change scenarios B2 and A2". However, authors at this stage cannot provide arguments defending the validity of this approach.

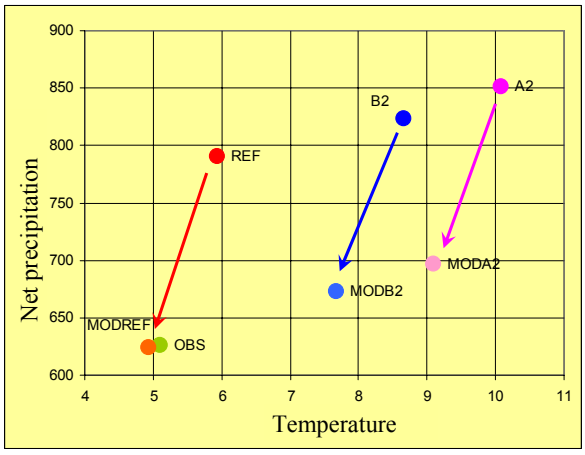

Figure 3. Annual mean temperature and net precipitation for Riga: observations (OBS), RCM calculations for reference period (REF), scenarios B2 (B2) and A2 (A2), and respective modifications of RCM output (MODREF, MODB2, and MODA2)

The T-p plot, indicating the results of the RCM data correction via the histogram equalization is shown in Fig. 3.

Comparison of spatial filters and application to the ENSEMBLES regional climate model simulations

Erasmo Buonomo and Richard Jones

Met Office – Hadley Centre, Exeter, EX1 2HF, UK, erasmo.buonomo@metoffice.gov.uk

1. Background

Regional climate models (RCM) are used to add high-resolution information to climate scenarios obtained from global circulation models and from re-analyses.
It is usually assumed that the RCM are able to keep the large scale features of their driving GCM, in particular the large scale circulation, and that they are also capable to add spatial details at the scales not resolved by the GCMs. These two assumptions are the most basic requirements in the application of the "one-way" nesting approach commonly used in the dynamical downscaling of climate scenarios.
However, a quantitative evaluation of the degree of consistency with the driving conditions and a proper identification and assessment of the mesoscale contribution added by the RCMs are not frequently included in RCM studies. To study these assumptions, the RCM and GCM spatial scales need to be separated; this could be done quantitatively by designing and applying spatial filters defined on the RCM limited area grid.
This work is based on two spatial filters designed for limited areas which have been recently introduced (*Denis et al*, 2002, *Feser and Von Storch*, 2005). These tools are currently being used to assess the consistency with the GCM and the RCM added value of the ENSEMLES set of RCM integrations.

2. Spatial Filters

The standard way of separating spatial scales is the application of Fourier analysis techniques, which are simple and inexpensive for the spectral analysis on regular grids. However, the application of these techniques on the limited areas used in RCMs has to overcome two difficulties; i) the largest scale are not fully represented on the grid and ii) the fields represented on limited areas are aperiodic. These two problems can be solved by removing the components which are aperiodic (***trends***) on the limited area. Since these components are not identifiable in a unique way, different filters have been designed, which mainly differ in the approach used to eliminate these components.
In this study, two filtering techniques have been used, the ***Discrete Cosine Transform*** (DCT), firstly applied by *Denis et al* (2002) to the spectral analysis of field on limited areas, and the ***Discrete Filter*** introduced by *Feser and Von Storch* (2005). In particular, low-pass filters and band-pass filters have been built following the methods described in the paper. From the comparison of these two methods, it is possible to get some estimate of the accuracy of the scale separation and to understand the best conditions to design and apply spatial filters on limited areas. From this comparison, it is possible to conclude that it is easier to design discrete filters, since it is possible to keep the control their spatial extents explicitly; however the DCT filters are cheaper and it is possible to design them to reproduce the discrete filters quite closely.
Finally, the two methods have been compared with a filtering approach commonly used whereby the RCM contribution on a given field is estimated as its difference with respect to the spatial average on an area including (nxn) grid-boxes, assumed to be representative of the GCM resolution. The response functions for the three filters are shown in Figure 1, which illustrate rather clearly the problems associated with this simplified approach.

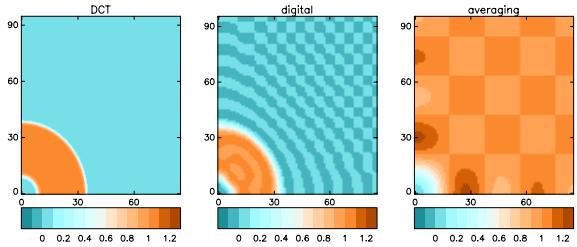

Figure 1 Response functions for the band-pass filters (left and middle panels) designed to separate spatial scales between 100km and 700km on the ENSEMBLES minimal grid. The right panel is the response function for the averaging filter designed to eliminate the same GCM scales from the RCM signal

3. Application to ENSEMBLES integrations

The ENSEMBLES project has produced two sets of RCM integrations. The first set includes 18 different RCM integrations with a horizontal resolution of *25km x 25km* driven by ECMWF ERA-40 boundary conditions. The same RCMs have also been used to downscale a smaller set of GCMs. These RCM integrations have been performed on a common grid.
These two datasets allow to estimate the mesoscale components added by the RCMs and to study their dependence on the driving condition and their robustness with respect to the regional models. These part of the work is currently in progress, a preliminary analysis will be presented at the workshop.

4. Acknowledgement

We acknowledge the ENSEMBLES project, funded by the European Commission's 6th Framework Programme through contract GOCE-CT-2003-505539.

References

Denis, B, J. Côté and R. Laprise, *Mon. Wea. Rev.*, Vol. 130, 1812, 2002

Feser, F and H Von Storch, *Mon. Wea. Rev.* Vol 133, 1774, 2005

Dynamical downscaling: Assessment of model system dependent retained and added variability for two different regional climate models

Christopher L. Castro,[1] Burkhardt Rockel,[2] Roger A. Pielke Sr.,[3] Hans von Storch[2] and Giovanni Leoncini[4]

[1]Department of Atmospheric Sciences, University of Arizona, Tucson, Arizona, USA
[2]Institute for Coastal Research, GKSS Research Centre, Geesthacht, Germany
[3]CIRES/ATOC, University of Colorado, Boulder, Colorado, USA
[4]Meteorology Department, University of Reading, Reading, UK
Corresponding e-mail of lead author: castro@atmo.arizona.edu

1. Motivation and background

Castro et al. (2005) proposed four types of dynamic downscaling with regional atmospheric models. Type 1, which is used for numerical weather prediction, remembers real-world conditions through the initial and lateral boundary conditions. In Type 2, the initial conditions in the interior of the model are "forgotten" but the lateral boundary conditions feed real-world data into the regional model (i.e. through an atmospheric reanalysis). In Type 3, a global model prediction, rather than a reanalysis, is used to create lateral boundary conditions. The global model prediction includes real-world surface data such as prescribed SSTs, sea ice coverage, etc. In Type 4, a global model is run in which there are no prescribed internal forcings. The coupling (interfacial fluxes) among the ocean-land-continental ice-atmosphere are all predicted. Regional climate modeling, in this framework, can be considered Type 2 dynamical downscaling and above. In these types of dynamical downscaling, in which the initial conditions in the interior of the model are "forgotten" but the lateral boundary conditions feed data into the regional model, it is desirable to retain the large-scale features provided by the driving global atmospheric model or reanalysis and add information on the smaller scales. This question is pertinent for regional climate modeling, in which the initial conditions in the interior of the model are "forgotten" but the lateral boundary conditions feed data into the regional model.

Dynamical downscaling was investigated using Type 2 simulations in a suite of experiments with the RAMS model for May 1993 in *Castro et al.* (2005). The main point of this work was to investigate whether or not the regional model retained large-scale features provided by the driving global atmospheric reanalysis and added information on the smaller scales. Both a commonly-used nudging sponge zone at the boundaries and an interior nudging alternative were tested. It was found that interior nudging gives better results for large scales but at the expense of reduced variability at smaller scales. Here we examine: 1) Can the *Castro et al.* (2005) results be confirmed using a different model system? 2) What is the effect of a different interior nudging technique? (i.e., the difference between a 4DDA internal nudging type and spectral nudging) and 3) Is value added on the smaller scales?

2. Model and Methods

We use the regional climate model CLM, a climate version of the German Weather Service (DWD) numerical weather forecast model COSMO to perform simulations. Data used for lateral boundary conditions are from the ERA40 atmospheric reanalysis. Simulations were performed on a small and large model domain with grid spacing ranging from 25 to 200 km. Two different types of nudging were applied: 1) observed state forced upon the model through forcing only in a lateral boundary forcing zone (i.e. classical sponge technique), and 2) a spectral nudging technique. The first type of nudging is commonly used in both regional weather forecasting and regional climate model simulations. In the spectral nudging approach, the lateral "sponge" forcing is kept and an additional steering term is introduced into the interior of the model domain. Consider the expansion of a CLM variable:

$$\Psi(\lambda,\phi,t) = \sum_{j=-J_m,k=-K_m}^{J_m,K_m} \alpha_{j,k}^{m}(t) e^{ij\lambda/L_\lambda} e^{ik\phi/L_\phi}$$

With zonal coordinates λ, zonal wave numbers j and zonal extension of the area L_λ. Meridional coordinates are denoted by ϕ , meriodional wave numbers by K, and the meridional extension by L_ϕ. t represents time. The number of zonal and meridional wavenumbers is J_m and K_m. A similar expansion is done for the analysis. The coefficients of this expansion are labeled $\alpha(a,j,k)$ and the number of Fourier coefficients is $J_a < J_m$ and $K_a < K_m$. The confidence in the realism of the different scales of the reanalysis depends on the wave numbers j and K and is denoted by $\eta_{j,k}$. Interior nudging terms are added in the spectral domain in both directions, in the form:

$$\sum_{j=-J_a,k=-K_a}^{J_a,K_a} \eta_{j,k}\left(\alpha_{j,k}^{a}(t) - a_{j,k}^{m}(t)\right) e^{ij\lambda/L_\lambda} e^{ik\phi/L_\phi}$$

Interior nudging terms are dependent on height, with more weight to the reanalysis given at higher levels in the model. Spectral nudging at each model time step is applied to horizontal wind components u and v above 850 hPa with a height-dependent weighting function. All values for wavelengths larger than the one corresponding to smallest physically resolved wavelength of the reanalysis ($K_{\max}^{*}$) are nudged.

We applied the same two-dimensional spectral analysis applied in *Castro et al.* (2005) to determine the power spectrum $S(k)$ of model variables, where k is the wave number. The fractional change in spectral power ($\Delta S(k)_{frac}$) is computed for each analysis time step.

$$\Delta S(k)_{frac} = \begin{cases} S(k)_{m_1}/S(k)_a - 1, & \text{basic experiments} \\ S(k)_{m_2}/S(k)_{m_1} - 1, & \text{follow-on experiments} \end{cases}$$

where a is the reanalysis, m_1 is the basic experiment without internal nudging and m_2 is the follow-on experiment with internal nudging.

3. Results

The fractional change in spectral power for the column-average total kinetic energy and moisture flux convergence for the last 15 days of May 1993 basic experiment is shown in Fig. 1 for CLM and Fig. 2 for RAMS, as in *Castro et al.* (2005). The results are vary similar. Both models show the same behavior for wave numbers higher than $K^*_{\max}$. The higher the horizontal resolution the higher the added variability. For low wave numbers (less than $K^*_{\max}$), the CLM retains about the same variability as the RAMS version with explicit microphysics and the Kain-Fritch cumulus parameterization scheme turned on. Results from the larger domain are also shown as the dotted curves. Kinetic energy is less retained at large scales on the large domain, whereas there is increased variability on smaller scales k > $K^*_{\max}$. The fractional change in integrated moisture flux convergence (not shown) similarly shows less retention of variability at larger scales for the large domain.

In follow-on experiments, the basic experiments were repeated but with additional interior nudging added. Again, results in kinetic energy confirm the findings by *Castro et al.* (2005). For large scales (i.e. wavenumbers less than $K^*_{\max}$) the values for the RCM are pushed nearer to those of the global reanalysis which means that the value is better retained by applying interior nudging. There are, however, major differences for the small scales between the CLM and RAMS results for moisture flux convergence. RAMS reduces the added variability, whereas in CLM the added variability is preserved, especially on the small domain (not shown). These differences can be attributed to the use of the spectral nudging technique which preserves the added variability on the smaller scale.

Investigation regarding day-to-day differences in the representation of large-scale circulation fields and model simulated precipitation also leads to the same conclusions as for the RAMS simulations. With interior nudging to the model, the amplitude of synoptic features (i.e. ridges and troughs) is preserved and there is a more faithful representation of precipitation as compared to observations.

4. Conclusions

The results for CLM presented here are similar to those found in the RAMS study by *Castro et al.* (2005) for basic experiments using nudging only in a lateral boundary sponge zone. Spectral nudging yields less reduction in added variability of the smaller scales than grid nudging and is therefore the preferred approach in RCM dynamic downscaling. Results suggest the effect to be largest for physical quantities in the lower troposphere. The utility of all regional models in downscaling primarily is not to add increased skill to the large-scale in the upper atmosphere, rather the value added is to resolve the smaller-scale features which have a greater dependence on the surface boundary. However, the realism of these smaller-scale features needs to be quantified, since they will be altered to the extent that they are influenced by inaccurate downscaling of the larger-scale features through the lateral boundary conditions and interior nudging. It should also be assessed if the dynamically downscaled information provides more accuracy than a corresponding statistical downscaling technique.

5. Acknowledgments

Research funded in part by NOAA grant NA17RJ1228 amendment 6, NASA grant NGT5-30344 and the U.S. Department of Defense under cooperative agreement W911NF-06-2-001 and DAAD19-02-2-005, and the University of Colorado at Boulder (CIRES/ATOC). We are grateful to ECMWF for use of ERA-40 data in our CLM simulations.

References

Castro, C.L, R.A. Pielke Sr., and G. Leoncini, Dynamical Downscaling: Assessment of value retained and added using the Regional Atmospheric Modeling System (RAMS), *J. Geophys Res*., **110**, D05108, doi:10.1029/2004JD004721, 2005.

Rockel, B., C.L. Castro, R.A. Pielke, Sr., H. von Storch, and G. Leoncini, Dynamical downscaling: Assessment of model system dependent retained and added variability for two different regional climate models . *J. Geophys. Res.,* **113**, D21107, doi:10.1029/2007JD009461, 2008.

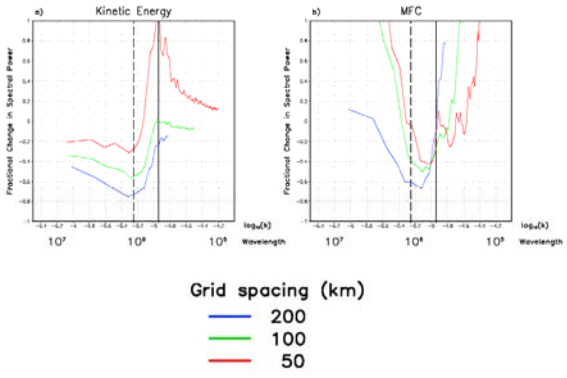

Figure 1. Fractional change in spectral power versus $\log_{10}(k)$ and wavelength, RAMS small domain experiments for (a) column-average total kinetic energy and (b) column integrated moisture flux convergence. The dashed black line and the solid black line indicate the largest physically resolved wavelength and Nyquist frequency, respectively, of the driving reanalysis. k in units of m^{-1}. Wavelength in units of m. Grid spacing of experiments as indicated by colors.

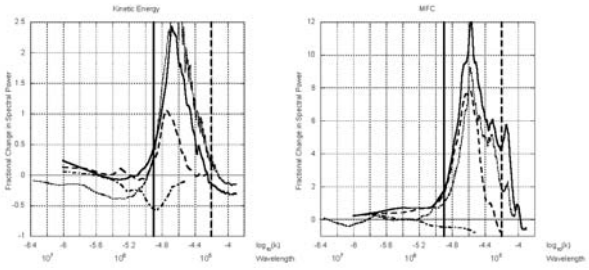

Figure 2. Same as Fig. 1 for CLM experiments. Grid spacing is 100 km, 50 km, and 25 km (dashed-dotted, dashed, solid line, respectively).

Improvement of long-term integrations by increasing RCM domain size

Sin Chan Chou, André Lyra, José Pesquero, Lincoln Alves, Gustavo Sueiro, Diego Chagas, José Marengo and Vladimir Djurdjevic

National Institute for Space Research - INPE, Cachoeira Paulista, SP, Brasil, 12630-000, chou@cptec.inpe.br

1. Introduction

Global models are used to generate climate change according to different future scenarios. However, these models have rather coarse resolution. The nesting of a Regional Climate Model (RCM) over the area of interest allows the reduction of grid size which is more desirable for impact studies. In addition, the climate generated from a regional model is strongly dependent on the lateral boundary conditions (LBC) and, consequently, on the domain size or the position of the LBCs (Xue et al. 2007).

The objective of this work is to show the dependence of the tropical South America climate from a RCM on the choice of the position of the lateral boundary conditions.

2. The models

The driver model is the INGV-SXG coupled GCM (Gualdi et al 2003a,b) which uses ECHAM4 (Roeckner, 1996) as atmospheric component, OPA 8.2 (Madec et al, 1999) as ocean model and LIM as the sea ice model (Fichefet e Morales Maqueda, 1999). The atmospheric resolution is about T106L19.

The RCM is the Eta Model (Black, 1994; Mesinger et al, 1988; Janjic, 1994) configured with 40-km horizontal resolution and 38 vertical layers. The model has been used for weather and seasonal forecasts over South America (Chou et al, 2005) and was adapted to run long-term integrations (Pesquero et al, 2009).

A continuous integration for the present climate period from 1961-1990 was carried out, with the lateral boundary conditions provided at every 6 hours. The sea surface temperature was taken from monthly values produced by the AOGCM. The small domain was setup with 135x293x38 points, with the boundaries positioned about 15 degrees outside the continent in the tropics, and the larger domain with 201x333x38 points, spanned additional 20 degrees in the east-west direction. In the second domain, the Intertropical Convergence Zone can produced by the RCM.

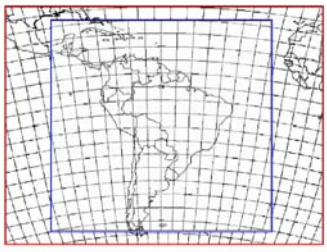

Figure 1. Domains of the Eta Model.

3. Results

During DJF, the austral summer, the major precipitation areas over South America continent occur in the Amazon, northern part of Northeast Brazil, central and southeastern parts of Brazil. These areas are associated with the Intertropical Convergence Zone (ITCZ), the South Atlantic Convergence Zone (SACZ) and frontal passages. The driver model produced the rain band associated to the ITCZ to the south of the observed position; a secondary band was positioned to the north suggesting a double structure (Figure 2). The small domain nested run did not show this double structure, however, the ITCZ rain was very weak, and therefore rains over Amazon region and northern part of Northeast Brazil were underestimated. The larger domain run exhibited the ITCZ rain position more correctly and the rain amounts over Amazonia and northern part of Northeast of Brazil have increased. The precipitation in subtropical areas and southern parts of the continent was not clearly affected by the increase of the domain size. Similar results were found in other seasons of the year

The large positive temperature bias occurred over Amazonia and northern part of Northeast Brazil in the run using small domain area. These errors may have been caused by the reduced amount of precipitation. These positive bias have reduced or changed sign in the larger domain run. Again, negligible temperature effects occurred in subtropical or higher latitudes.

The annual cycle of precipitation over Amazonia region showed substantial improvement in the larger domain setup. The amounts during rainy months were more accurate and the peak occurred in the correct month.

These results are independent of LBC schemes, as it has been shown by Veljovic (2009) that using another scheme (Davies, 1976) large scale structure is retained.

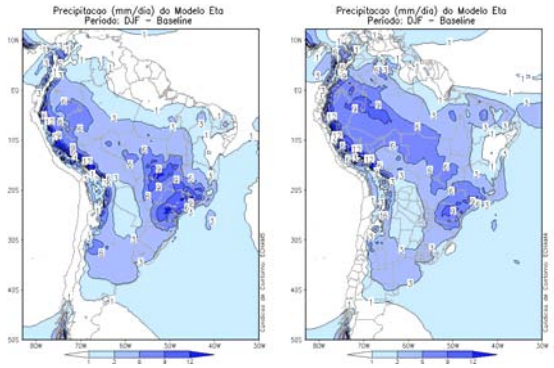

Figure 2. 1961-1990 DJF Eta precipitation (mm/d): small (lhs) and large (rhs) domains.

4. Some Conclusions

The Eta model improved the large scale tropical precipitation and temperatures by positioning the lateral boundaries away from the region of interest. Negligible effects could be noticed outside the tropics.

References

Chou, S.C., Bustamante, J., Gomes, J.L, Evaluation of Eta Model seasonal precipitation forecasts over South America. *Nonlinear Processes in Geophysics*, v.12, pp.537 – 555, 2005.

Pesquero, J.F., Chou, S.C, Nobre, C.A, Marengo, J.A, Climate downscaling over South America for 1961-1970 using the Eta Model, *Theoretical and Applied Climatology,* 2009 DOI: 10.1007/s00704-009-0123-z.

CLM coupled in the RegCM3 model: Preliminary results over South America

Rosmeri P. da Rocha[1], Santiago V. Cuadra, Julio Pablo Reyes Fernandez[2], and Allison L. Steiner [3]

[1] University of São Paulo, São Paulo, Brazil; [2] CPTEC/INPE, [3] University of Michigan,USA; rosmerir@model.iag.usp.br

1. Introduction

The biosphere has a great impact in the South American climate (e.g., Silva Dias et al., 2002). Over the Amazon, the mean evapotranspiration adds from 3.3 to 5.2 mm H_2O day^{-1} to the atmosphere, and the continental fraction of precipitation coming from evapotranspiration (ET/P) varies from 54% to 86% (Marengo, 2006). At same time, many studies have shown the impact of the moisture transport from the Amazon to the La Plata Basin. A unified vision of the monsoons system in Americas was proposed by Vera et al. (2006). They pointed that the soil-vegetation-atmosphere interactions process can control the establishment of monsoons and its interannual variability and intensity. Fu and Li (2004) stressed the importance of latent heat fluxes for the onset of wet season in the Amazon. The land surface scheme used to describe the soil-plant-atmosphere is one of the main components in the climate models, and it has a particular huge relevance in the climatic simulations over South America (hereafter SA). A common problem found in the regional climate simulations over SA using the RegCM3 (Pal et al., 2007) is a deficit of rainfall and sometimes a double peak in the rainy season in the Amazon (Seth et al., 2007). The present paper compares two simulations using different land surface models coupled in the RegCM3. We compare the impact upon the Amazon and La Plata Basin precipitation annual cycle reproduced by the RegCM3 coupled with the BATS (Biosphere-Atmosphere Transfer Scheme; Dickinson et al. 1993) and the CLM (Common Land Model version 3.0; Dai et al., 2003).

2. Methodology

The RegCM3 model is a primitive equation model, compressible in the sigma-pressure vertical coordinate (*Pal et al.* 2007). Several physical parameterizations are available in RegCM3. This work utilizes the boundary layer scheme of Holtslag et al. (1990), the convective prameterization of Emanuel (1991), the Zeng scheme to solve the turbulent fluxes over the ocean and the CLM or BATS as surface model. We used a large domain (Figure 1) with 214 by 148 grid points in the east-west and north-south direction, respectively, and with 60 km of horizontal resolution and 18 vertical levels. The simulation period is from June 1, 2002 to February 1, 2005. For these same grid and period, the RegCM3 was run first using BATS (hereafter RegBATS) and second using CLM (hereafter RegCLM) land surface models. Details about the differences between CLM and BATS surface schemes are given by *Steiner et al.* (2005). The atmospheric initial and boundary conditions are from R2 NCEP reanalysis (*Kanamitsu et al*., 2002) and the sea surface temperature (SST) monthly mean is from the optimum Interpolation SST - OISST V2 of the NOAA (*Reynolds et al.,* 2002).

The simulation results were compared with the analyses known as CMAP (Xie and Arkin, 1996) and WM (Willmott, Matsuura: climate.geog.udel.edu/~climate/).

3. Results

The mean precipitation for DJF (austral summer) of 2003-2004 is shown in Figure 2. The CMAP (Fig. 2a) depicts two main oriented precipitation bands, the Inter-tropical Convergence Zone (ITCZ) and the South Atlantic Convergence Zone (SACZ), and both were simulated by the experiments RegCLM and RegBATS (Fig. 2b-c). Compared with CMAP, the RegBATS overestimates the rainfall intensity in the SA monsoon core and in the continental branch of SACZ (Figure 2c). In these areas, the RegCLM presents a considerable reduction of the RegBATS wet bias. Specifically over the northwestern of Amazon basin, RegCLM shows a better representation of the CMAP rainfall.

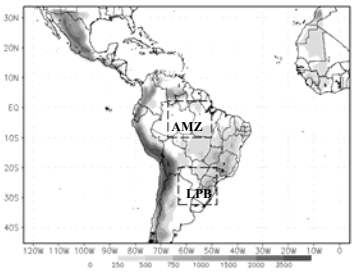

Figure 1. Simulation domain, topography (shaded), and localization of two boxes (AMZ and LPB) referred in the text.

The time series of mean monthly rainfall for Amazon (AMZ) and La Plata Basin (LPB), see Figure 1, areas are presented in the Figure 3. In general the CMAP and WM show good agreement, except for the 2004 dry season over AMZ. Over the AMZ during the peak of the rainy season the RegCLM reduces considerably the RegBATS overestimation of the rainfall and improves agreement with observations. Despite this improvement in the magnitude of precipitation, the RegCLM simulates a rainy season that is about 15-30 days shorter in length than WM or CMAP. While RegBATS overestimates the rainfall in the rainy season over the AMZ, the RegCLM underestimates the rainfall during the dry season. However, in general, the RegCLM more accurately simulates the annual cycle of precipitation compared with observations. The drier dry season simulated by RegCLM could be related with the soil water content, a known deficiency of CLM3.0 (Oleson et al., 2008). This produces an increase of air temperature (Fig. not shown), resulting in a warm bias up to 4^{o}C. As result, the RegCLM simulated temperature annual cycle is controlled by the precipitation, while the observed annual cycle is flat and mainly controlled by solar radiation (colder and warmer in the austral winter and summer, respectively).

As anticipated by figure 2, the differences decrease between RegCLM and RegBATS in the subtropics and extratropics of South America. This is very clear in the time series for LPB area (Figure 3b), where RegCLM presents a dry bias in the austral cold season while RegBATS shows a moist bias during the rainy season. The

air temperature annual cycle (Figure not shown) is well reproduced by RegCLM and RegBATS.

3. Conclusions

Comparisons of the performance of RegCM3 coupled with the BATS and CLM schemes over South America were conducted. The main improvement of the CLM is obtained in the Amazon where the simulated rainfall annual cycle reproduces the observed seasonal maxima in precipitation. However, during the dry season RegCLM produces an excessive decrease of rainfall in this area, resulting in drier soils and warmer air temperature. On the other hand, the BATS scheme produces excessive precipitation, and a smaller temperature bias. Over the subtropics (LPB area), the agreement between RegBATS and RegCLM improves. Improved representation of CLM hydrology (CLM3.5) is included in a recent RegCM3 version, and this version will be used to evaluate its impact on the dry season precipitation and temperature biases.

4. Acknowledgments

This work was funded by CNPq process N° 476361/2006-0. The authors would also like to thank ICTP for provided the RegCM3 code and NCEP by reanalyzes data set.

References

Dai, Y. J., and Coauthors. The common land model. *BAMS*, 84, 1013-1023, 2003.

Dickinson, R. E., A. Henderson-Sellers, and P. J. Kennedy, Biosphere-atmosphere transfer scheme (BATS) version 1E as coupled to the NCAR Community Climate Model. Boulder, Colorado: Technical Note NCAR/TN-387, 72, 1993.

Emanuel, K.A., A scheme for representing cumulus convection in large-scale models. *J. Atmos. Sci*., 48: 2313-2335, 1991.

Holtslag A, D. E. Bruijn E, H.-L. Pan, A high resolution air mass transformation model for short-range weather forecasting. *Mon. Weather Rev., 118,* 1561-1575, 1990.

Kanamitsu, M., W. Ebisuzaki, J. Woollen, J. Potter, and Fiorino, NCEP-DOE AMIP-II Reanalysis (R2). *Bull. Am. Meteorol. Soc., 83*, 1631-1643, 2002.

Marengo, J.A., On the hydrological cycle of the Amazon Basin: A historical Review and current state-of-the-art. *Clivar*, 21, 1-19, 2006.

Oleson, K.W. and coauthors. Improvements to the Community Land Model and their impact on the hydrological cycle, *J. Geophys. Res.*, 113, G01021, doi:10.1029/2007JG000563, 2008.

Pal, J.S. and Coauthors. Regional Climate Modeling for the Developing World: The ICTP RegCM3 and RegCNET. *BAMS*, 88, 1395-1409, 2007.

Reynolds, R. W.; N. A. Rayner; T. M. Smith; D. C. Stokes; W. Wang, 2002: An improved in situ and satellite SST analysis for climate. *J. Climate,* 15, 1609-1625.

Silva Dias, M. A. F., an Coauthors., Clouds and rain processes in a biosphere atmosphere interaction context in the Amazon Region, J. Geophys. Res., 107, 8072, doi:10.1029/2001JD000335, 2002.

Seth, S. A. Rauscher, S. J. Camargo, J.-H. Qian, and J. S. Pal,. RegCM regional climatologies for South America using Reanalysis and ECHAM global model driving fields. *Climate Dyn.,* 28**,** 461–480, 2006.

Steiner, A. L., J. S. Pal, F. Giorgi, R. E. Dickinson, and W.L. Chameides, The coupling of the Common Land Model (CLM0) to a regional climate model (RegCM3). *Theor. Appl. Climatol.*, 82, 225-243, 2005.

Vera C., and Coauthors. The South American Low-Level Jet Experiment. *BAMS*, 87, 63-67, 2006.

Xie, P., and P. A. Arkin. Analyses of global monthly precipitation using gauge observations, satellite estimates, and numerical model predictions. *J. Climate,* 9**,** 840–858, 1996

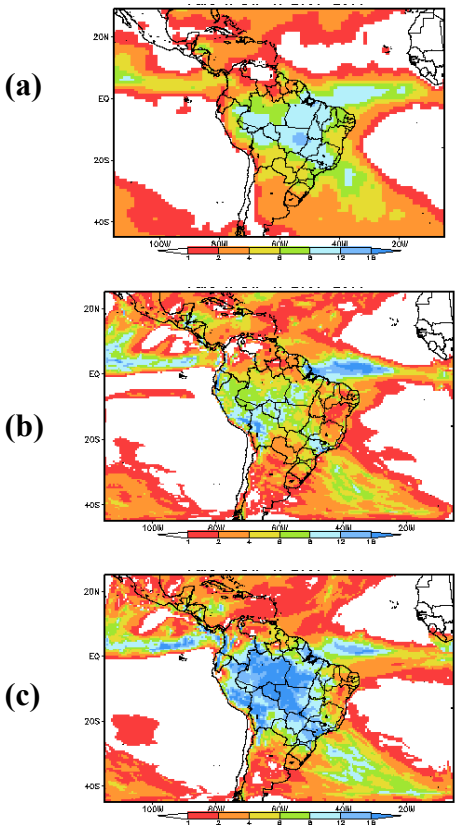

Figure 2. DJF 2003-2004 mean precipitation (mm day^{-1}) from (a) CMAP, (b) RegCLM and (c) RegBATS.

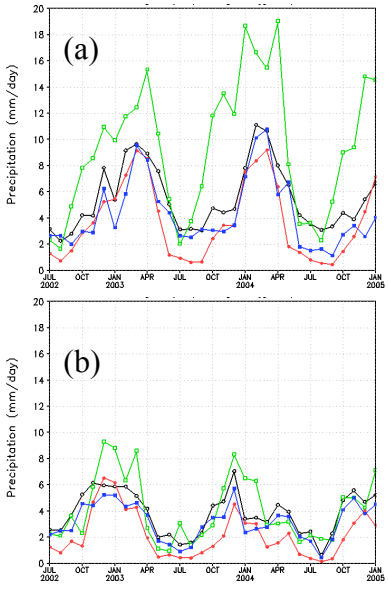

Figure 3. – Time series of the RegCLM (red), RegBATS (green) and from CMAP (black) and WM (blue) monthly mean over the (a) AMZ (b) LPB boxes.

Assessment of dynamical downscaling in river basins in Japan using the Regional Atmospheric Modeling System (RAMS)

Koji Dairaku, Satoshi Iizuka, Wataru Sasaki, Roger A. Pielke Sr., and Adriana Beltrán-Przekurat

3-1 Tennodai, Tsukuba, Ibaraki 305-0006 Japan, e-mail: dairaku@bosai.go.jp

1. Introduction

The responses of the climate system to increases in carbon dioxide concentrations and to changes in land use/land cover and the subsequent impacts of climatic variability on humans and natural ecosystems are of fundamental concern. Because regional responses of surface hydrological and biogeochemical changes are particularly complex, it is necessary to add spatial resolution to accurately assess critical interactions within the regional climate system for climate change impacts assessments. We quantified the confidence and the uncertainties of Type II dynamical downscaling which the lateral and bottom boundary conditions were obtained from Japanese 25-year ReAnalysis (JRA-25) and assessed the value (skill) added by the downscaling to a climate simulation in Japan.

2. Assessment of regional climate models

We investigated the reproducibility of present climate using two regional climate models with 20 km horizontal grid spacing, the atmosphere-biosphere-river coupling regional climate model (NIED-RAMS) and the Meteorological Research Institute Nonhydrostatic Model (MRI-NHM), both of which used JRA-25 as boundary conditions. Two key variables for impact studies, surface air temperature and precipitation, were compared with the Japanese high-resolution surface observation, Automated Meteorological Data Acquisition System (AMeDAS) on 78 river basins. Results simulated by the two models were relatively in good agreement with the observation on the basin scale. The NIED-RAMS bias of 2 m air temperature (2mT) were less than 0.5K and the bias of precipitation (P) were around 10% in most of the river basins on annual averages for three years (2002-2004). The biases over 29 years shown in the long term experiment are similar to those of the three year simulation (Figure 1). The model could add some information as to where the larger scale information was obtained.

3. Sensitivity to domain size and spectral nudging scheme

A regional climate model often has sensitivity to model configurations, such as domain size and nudging scheme. We conducted sensitivity experiments to domain size and nudging scheme using the NIED-RAMS. Smaller domain is 128x144 and larger domain is 216x240 (Figure 2). In each domain, we conducted experiments with/without spectral nudging scheme.

Spatial characteristics of the detected bias of 2mT on river basins in Japan in the large domain were qualitatively similar to that of the small domain. The model bias of 2mT was quantitatively deteriorated in larger domain. On the other hand, model bias of P was not significantly altered in larger domain. The bias of P in June-July-August (JJA) was comparatively strongly influenced by the domain size. It can be attributed to the relatively weak synoptic-scale disturbances in the summer season.

Spectral nudging scheme indicates some impacts on the mean bias of surface variables (2mT and P) particularly in JJA. But overall, the magnitudes of the impacts were not significant. It can be speculated that a large part of the domain area was dominated by the sea where sea surface temperature forcing should play a significant role, "nudging effect", as a boundary condition.

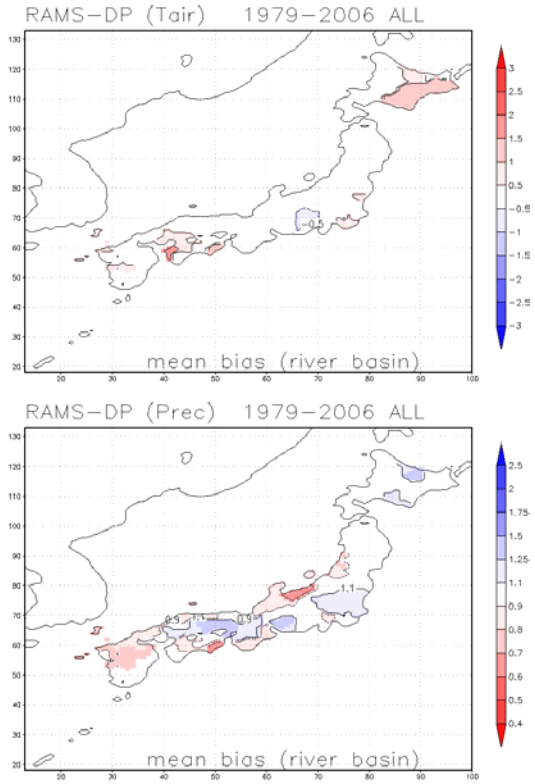

Figure 1. The detected bias of 2m air temperature (°C) (upper) and precipitation (%) (lower) in the NIED-RAMS using station data, Automated Meteorological Data Acquisition System, on 78 river basins in Japan for 29 years.

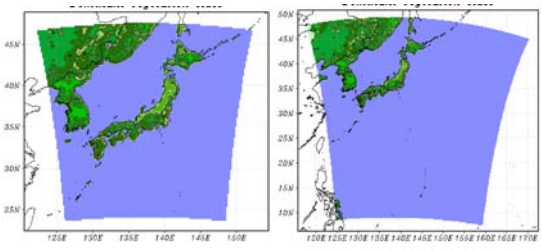

Figure 2. Experimental domains: small domain (left) and large domain (right) in the NIED-RAMS.

Acknowledgements

This research was supported by the Global Environment Research Project Fund (S-5, "Getting a feel for climate change") of the Ministry of the Environment, Japan. Model bias detection program was provided by Prof. Tanaka in Kyoto University.

Sensitivity study of CRCM-simulated climate change projections

Ramón de Elía and Hélène Côté

Ouranos Consortium, Montreal, QC, Canada. E-mail: de_elia.ramon@ouranos.ca

1. Introduction

Regional climate models (RCMs) –as well as climate models in general- have been found to show sensitivity to parameter setting. The origin, consequences and interpretations of this sensitivity are varied, but it is generally accepted that sensitivity studies are very important for a better understanding and a more cautious manipulation of RCM results.

In *de Elia et al. 2008* we presented sensitivity experiments performed on the simulated climate produced by the Canadian Regional Climate Model (CRCM). Results presented here are an extension of that previous work, and concentrate on the sensitivity to parameter variation of the climate change projection simulated by the CRCM.

2. Model description

Different versions of the CRCM have been used for these experiments. For reasons of space and in order to keep a good level of readability, details of each individual model version will not be discussed. Differences between versions are due to model evolution and include changes in surface and convective schemes as well as radiation packages (for a description of the model and a list of references see *Music and Caya. 2007*). All simulations use spectral nudging, and are driven by either of two different versions of the Canadian GCM (CGCM2 and CGCM3). All simulations are run at 45 km resolution, with 29 unequally spaced levels in the vertical, and with a 15 min timestep.

Two domains are used in these experiments (see Fig. 1). The larger one (AMNO; 201x193 grid points) has been used in most experiments, and the smaller one (QC; 112x88 grid points) has been used for testing sensitivity to domain size.

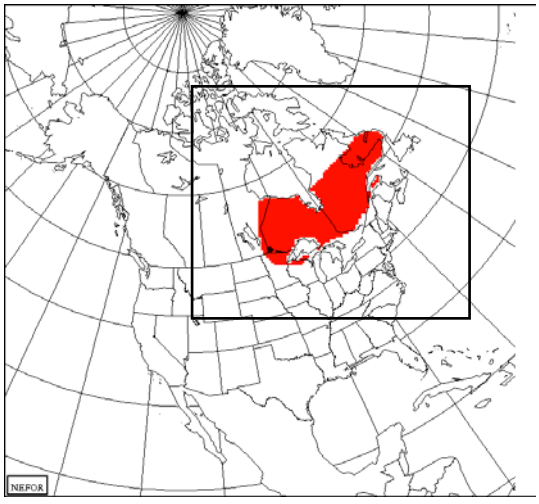

Figure 1. The two domains used in this study. The shaded area indicates the region where average climate change is computed.

3. Experiment design

This section presents the set of experiments used to evaluate the sensitivity of the CRCM-simulated climate change projection. The climate change signal was estimated by computing the difference between simulations performed with future CO_2 concentrations (period 2041:2070) and those with present CO_2 concentrations (period 1961:1990). The GHG scenario used is the A2 (see IPCC report)

Each experiment consists in the estimation of the climate change signal using a pair of control runs (future - present) that is then compared to a climate change signal estimated with a pair of perturbed runs (perturbed future – perturbed present).

The parameters perturbed are the following:

i. Initial conditions: In order to estimate the internal variability of the climate change projection, CRCM initial conditions are modified. Internal variability thus measured defines the threshold that any perturbation must surpass to be considered significant.

ii. Nesting interval: The CRCM driving information (GCM fields) is usually refreshed every 6 hours. Given our access to additional nesting data at a 12-hour interval, we decided to test sensitivity to this change.

iii. Driving GCM: Several studies show that changes in the driving GCM have strong impacts on RCM results. Here the CRCM was driven with two different versions of the CGCM (CGCM2 and CGCM3).

iv. GCM member: GCM climate estimations are sensitive to initial conditions, and this has an impact on the downscaled climate. Here we drive the CRCM with two different CGCM3 members to measure this sensitivity.

v. *CRCM version*: Different CRCM versions have been developed in recent years and these have been used to produce climate change projections.

vi. Domain size: It has been shown in several studies that RCM-simulated climate is sensitive to the choice of domain size. In this study we concentrate on the effect of domain size on the climate change signal.

In order to estimate the robustness of the sensitivity tests described above, more than one experiment per parameter was performed in most cases and these were carried out with different model versions. For reasons of space, at most two experiments for each parameter change are shown.

4. Results

Estimations of the climate change signal and its sensitivity to parameter variation were performed for several variables and statistics, for all seasons and regions in North America. Here we will concentrate on seasonal averages for the region shaded in Fig. 1 (covering mostly northern Ontario and central Quebec), in particular for winter temperature and summer precipitation.

Figure 2a and 2b illustrate the climate change signal for this region for different pairs of simulations (future-present). The different sensitivity tests are indicated in the abscissa.

Each pair of symbols (e.g., triangles) with identical colors represents the values of the climate change signal for the control and perturbed pairs. The distance between identical symbols should be interpreted as the sensitivity of the climate change signal. More than one color is used when more than one set of experiments is present.

In order to simplify the display, the identity of each simulation will not be indicated neither the model version, nor its role as either control or perturbed run.

Figure 2a depicts the projected climate change for winter temperature. The first thing to note is that for all experiments realized temperature increases range between 4 and 6°C. CRCM internal variability seems to be a minor source of uncertainty at regional scale, while the nesting interval also seems to have a small impact. As expected, changes in the driving GCM has a larger impact, but curiously not as large as the change in GCM driving member (we believe that a sampling problem is responsible for this: if more driving data were available for different models, changes in GCMs should have a larger impact than a change in GCM members).

The spread caused by sensitivity to the driving member is the largest of all. It is important to point out that this spread could be considered as the minimum amount of uncertainty associated to a climate change projection. This is because even a perfect RCM driven by a perfect GCM will show dependence on the driving member. Winter temperature shows a weak sensitivity to the CRCM version used and the same can be said of domain size.

Figure 2b depicts the climate change projection for summer precipitation (in percentage). Overall results suggest that an increase of precipitation between 0% and 10% should be expected for this region. As for the case of winter temperature, variation in the driving GCM has the greatest impact through either a change in member or change in model.

Internal variability has a minor role at the regional scale, although it is non negligible at the grid point scale (not shown). The impact of the nesting interval, although considerably larger than that of internal variability, is small compared to other sensitivities.

It can also be seen that a change in the CRCM version has an impact comparable to that of variations in the driving GCM. This result agrees with previous work that finds summer precipitation to be particularly dependent on the regional model used to perform the dynamical downscaling.

Domain size is shown to be a non-negligible source of uncertainty, as was also found in previous studies.

5. Conclusions

In previous experiments (*de Elia et al. 2008*) we have studied the sensitivity of RCM-simulated climate to parameter perturbation. In the present work, we have extended the research to include the sensitivity of the climate change projection to parameter perturbation. These studies account for more than 30 40-year long simulations.

Despite this effort, there still remains a lot of work to do, as many more sensitivity experiments are needed.

Based on experiments to date we can say that issues related to the driving data are the most important, with the exception of summer precipitation where RCM perturbation plays an important role.

This conclusion could be interpreted in two different ways: From one point of view it is a positive result, since it tells us that RCMs are trustworthy tools that do not add too much noise to the driving large scale information. (too much sensitivity to parameter perturbation will be a cause of concern). But it is important to remember that for the case of sensitivity to domain size, this is not the product of chance: effort and resources were invested in the development of spectral nudging in order to alleviate this sensitivity.

From another point of view, it could be argued —and it is a common statement especially in the GCM community--that the dominance of the driving GCM as a source of uncertainty is an indication that RCMs play a minor role in climate downscaling (except for variables dominated by small-scales processes such as summer precipitation).

These two opposing points of view indicate the intricate relation in climate downscaling between questions of uncertainty and those of RCMs potential added value. Both these issues are fundamental in the development of RCMs and deserve unrelenting attention.

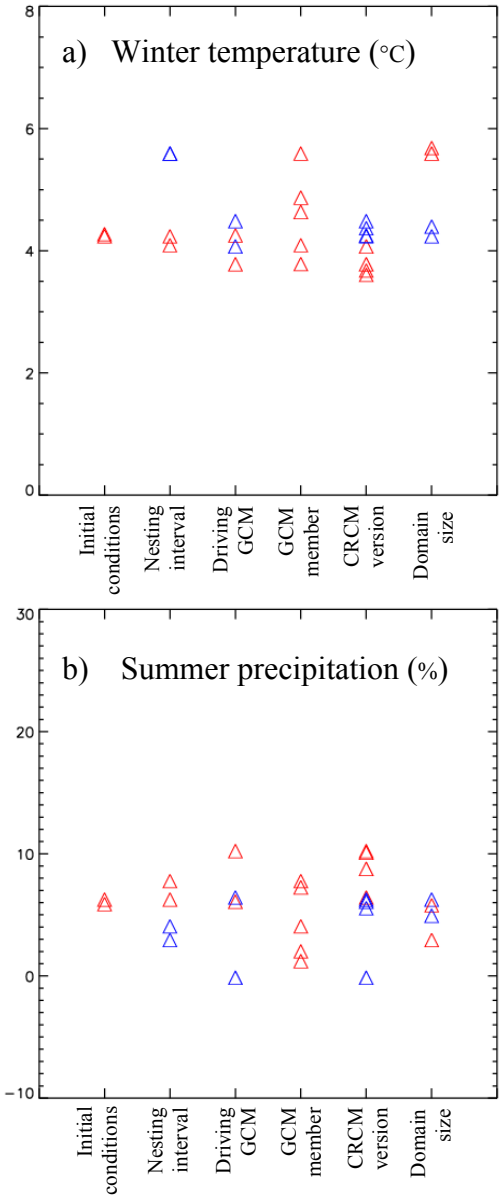

Figure 2. Climate change projections for the seasonal average of the region presented in Fig. 1. Type of sensitivity experiment is defined in the abscissa. Panel **a** depicts winter temperature (in °C), and panel **b** summer precipitation (in %).

References

De Elia, R. and co-authors, Evaluation of uncertainties in the CRCM-simulated North American climate, *Climate Dynamics*, 30, pp. 113-132, 2008.

Music B, and D Caya, Evaluation of the Hydrological Cycle over the Mississippi River Basin as Simulated by the Canadian Regional Climate Model (CRCM). *J. Hydrometeorology*, 8, pp. 969-988, 2007.

Regional precipitation anomalies in eastern Amazon as depicted by observations and REGCM3 simulations

Everaldo B. De Souza, Marcio N. G. Lopes and Alan C. Cunha

Universidade Federal do Pará (UFPA), Faculdade de Meteorologia, Campus Universitário do Guamá, Av. Augusto Correa nº 1, 66075-110 Belém, Pará, Brazil. e-mail: everaldo@ufpa.br. Universidade Federal do Amapá (UNIFAP), Colegiado de Ciências Ambientais, Macapá-AP, Brazil

1. Introduction

In the context of tropical climate dynamics, it is well known that the Brazilian Amazon precipitation variability is related to near-global ocean-atmospheric patterns associated with the El Niño-Southern Oscillation (ENSO) in the Pacific Ocean, as well as the interhemispheric sea surface temperature (SST) Gradient mode in the tropical Atlantic Ocean (Souza et al., 2000). Previous analyses done for two extreme and contrasting climatic scenarios named as unfavorable - El Niño and northward Atlantic SST gradient (favorable - La Niña and the southward Atlantic SST gradient) showed outstanding changes in both the Walker and Hadley cells in association with anomalously weakened (enhanced) ITCZ that, in consequence, yields deficient (abundant) rainfall in most of the Amazon region (Souza et al., 2005).

Here the focus is on eastern Amazon region adjacent to the equatorial Atlantic basin, where most of the precipitation occurs during the rainy season, typically from December to May, i.e., during austral summer (December to February – DJF) and fall (March to May – MAM) seasons. The present work reports the anomalous regional precipitation patterns observed in eastern Amazon and how well the RegCM3 simulations capture such seasonal rainfall distribution during contrasting years associated with the large-scale climate scenarios verified in the Pacific and Atlantic Oceans.

2. Data and Methodology

The observational data consists of a new integrated database containing in situ measurements extracted from 150 raingauge stations scattered in eastern Amazon, during the last 31 years (1978-2008), which it was compiled by the RPCH project at Federal University of Pará, Brazil. Such data represent well the main regional precipitation aspects with reference to others datasets (De Souza et al., 2008).

We used the last version of Regional Climate Model version 3 - RegCM3 developed by International Centre for Theoretical Physics (ITCP), which is third generation of the regional climate model originally developed by NCAR (Giorgi and Bates, 1989; Dickinson et al., 1989) The ITCP RegCM3 is limited-area, hydrostatic, compressible based on primitive equations and employs a terrain following σ-vertical coordinate. Detailed descriptions of the dynamical core, model physics, chemistry, radiation, surface and convective schemes and specifications of initial and boundary conditions can be found by Pal et al. (2007). In the present paper, the RegCM3 domain is set up over eastern Amazon with 80 x 80 points in latitude x longitude (30 Km horizontal resolution). 27 seasonal simulations using Grell and MIT convective schemes are performed for the 1982/83 to 2007/2008 period using lateral boundary conditions updated each 6 hours obtained from NCEP/NCAR reanalysis and SST from NCEP oi.v2 monthly dataset.

Here, the results are investigated as composites anomaly maps obtained from four climatic scenarios in which were observed Pacific ENSO phases (four El Niño events: 1983, 1987, 1992 and 1998; seven La Niña events: 1984, 1985, 1986, 1989, 1996, 1999 and 2000) and Atlantic SSTa gradient phases (two northward gradient events: 1997 and 2002; four southward gradient events: 1985, 1986, 1989 and 1994). Such events are objectively selected by the Trenberth (1997) and De Souza et al. (2005) criterion. Thus, the precipitation anomalies as departures from the 1982-2008 long term mean (for both observations and simulations) are calculated for those composite scenarios. In order to verify the systematic errors of the simulations against observations, it was estimated the local bias and absolute error for each composite.

3. Results

For brevity, we present only composites for Atlantic conditions.

Figure 1 shows seasonal precipitation anomalies observed (RPCH) and simulated by RegCM3 using Grell and MIT schemes as well as the corresponding absolute error maps for the Atlantic northward SSTa gradient phase. This phase is associated with the simultaneous positive/negative SST anomalies over tropical north/south Atlantic basin (Fig. 1a) during DJF and MAM. The impact on the seasonal regional precipitation is presented in Figs. 1b and 1g, so that there are widespread negative rainfall anomalies over the whole eastern Amazon during both seasons. The RegCM3 simulations capture well the spatial pattern of the anomalous negative rainfall distribution (Figs. 1c, 1d, 1h, 1i), however there are systematic errors related to the dry bias predominance using Grell scheme over north/northeast sectors and wet bias over west/south/southeast sectors using MIT scheme (Figs. 1e, 1f, 1j, 1k).

Figure 2 shows the seasonal regional precipitation anomalies observed in eastern Amazon in association with the southward SSTa gradient in the intertropical Atlantic. It is evidenced a positive precipitation anomalies predominance over the whole region (except in the northwest sector during MAM). Such abundant spatial rainfall pattern during rainy season is well simulated by RegCM3 using both Grell and MIT parameterizations. Although the RegCM3 captures well the precipitation sign, there is a dry bias over entire region using Grell (Fig. d) and a dry/wet bias over north/south sector using MIT scheme.

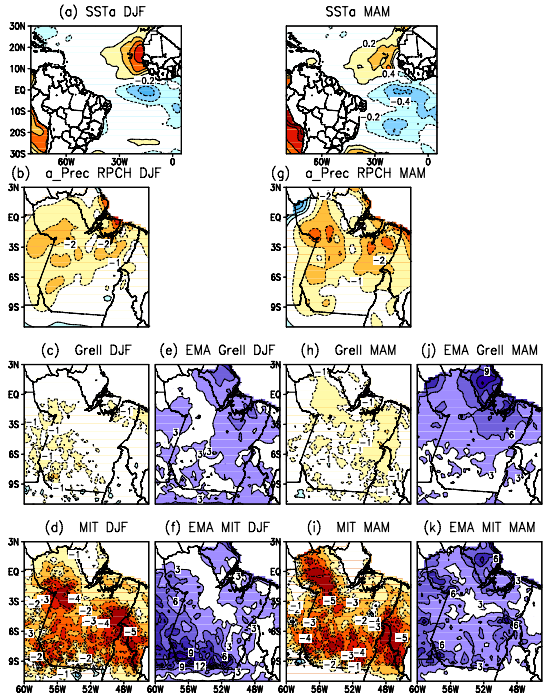

Figure 1. Atlantic northward SSTa gradient composite for (a) SST anomalies during DJF and MAM; precipitation anomalies (mm) observed during (b) DJF and (g) MAM, and simulated precipitation anomalies using Grell (c) DJF and (h) MAM and MIT (d) DJF and (i) MAM; absolute error (EMA) for Grell (e) DJF, (j) MAM and MIT (f) DJF and (k) MAM.

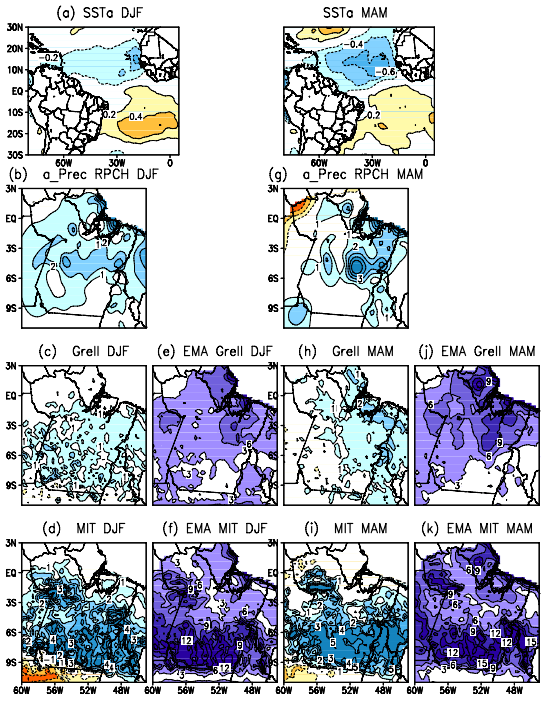

Figure 2. As in Fig. 1, but for the Atlantic southward SSTa gradient composite.

4. Concluding remarks

Previous modeling studies pointed out that the representation of the moist convective processes and the capacity in simulating regional precipitation volume or anomaly and its spatial distribution are a challenge for the scientific community, particularly over Amazon region located entirely over tropical South America. The present paper presents a contribution on tropical climate modeling with emphasis on the seasonal precipitation in eastern Amazon. Based on RegCM3 simulations for a 27 years period (1982 to 2008) considering high resolution domain scale (30 Km) and qualitative and quantitative validations with reference to RPCH observational data extracted from a dense raingauge station network, it was investigated the model performance in capturing anomalous regional precipitation variability during contrasting years associated with large-scale climate scenarios verified in the Pacific and Atlantic Oceans. Overall, the results showed that RegCM3 represent well the spatial patterns of the regional rainfall anomalies, but there are systematic errors related to the dry bias in the north sector and wet bias in the south sector of the eastern Amazon using both Grell and MIT convection schemes.

5. Acknowledgments

The project RPCH “Rede Estadual de Previsão Climática e Hidrometeorológica do Pará” is financed by FINEP/MCT (3641/2006). We also thank CNPq (305390/2007-4 and 570113/2008-3), REDE CELPA for the research support.

References

De Souza, E.B.; Kayano, M.T.; Tota, J. et al. *Acta Amazonica*, 30, 305-318, 2000.

De Souza, E.B, Kayano MT, Ambrizzi T. *Theor.App. Climatol*., 81, 177-191, 2005.

De Souza, E.B., Lopes, M.N.G., Rocha, E.J.P., et al. *Rev. Brasil. Meteorol.*, 2008 (accepted, in press)

Dickinson, R.E., R.M. Errico, F. Giorgi, G. Bates. *Clim. Change*, 15, 383-422, 1989.

Giorgi, F., G.T Bates. *Mon. Wea. Rev*., 117, 2325-2347, 1989.

Pal, J.S., F. Giorgi, X. Bi, et al. *Bull. Amer. Meteor. Soc.*, 88, 1395–1409, 2007.

Trenberth, K.E. Bull. Amer. Meteor. Soc., 78, 12, 2771-2777, 1997.

Assessment of precipitation as simulated by a RCM and its driving data

Alejandro Di Luca[1,3,4], Ramón de Elía[2,3,4] and René Laprise[1,3,4]

[1]Université du Québec à Montréal (UQÀM), Montréal (Québec), Canada, diluca@sca.uqam.ca; [2]Consortium Ouranos, Montréal (Québec), Canada; [3]Canadian Network for Regional Climate Modelling and Diagnostics (CRCMD), Montréal , Canada; [4]Centre pour l'Étude et la Simulation du Climat à l'Échelle Régionale (ESCER), Montréal (Québec), Canada

1. Introduction

The primary and most comprehensive tools to study future climate are the Atmosphere-Ocean General Circulation Models (AOGCMs). Present horizontal grid intervals of the atmospheric component of AOGCMs are insufficient to capture the fine-scale structure of climatic. In this context, an alternative to obtain future regional climate projections is the use of high-resolution Regional Climate Models (RCMs), nested at their lateral boundaries with low-resolution AOGCMs (Giorgi and Bates, 1989; Laprise et al., 2008). Because differences between AOGCMs and RCMs are mainly their resolution, the small scales represent the main potential added value of the high resolution RCM over the AOGCM. We say "potential added value" because the RCM simulation should satisfy several conditions before this potentiality becomes effective. Among them: the one way nesting technique must be reliable in the sense that it should allow a good development of the fine scale with no amplification of driving fields errors; overall regional models errors should be smaller or equal than those from the global model; and, the considered variable must contain information of fine scales.

In this work we focus on the models specific errors, and in order to do so we have studied daily precipitation as simulated by the Canadian RCM (CRCM) and the Canadian GCM (CGCM).

2. Methodology and data

The methodology used to investigate the presence of added value in CRCM simulations is based on the assessment of the RCM performance when compared to its driving model and observed data. We have evaluated some statistics of daily precipitation as simulated by both models in several regions across Canada (see Figure 1) during the period 1971 - 1990.

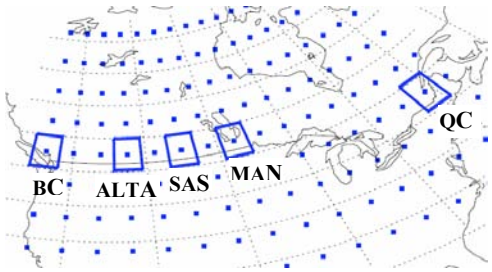

Figure 1. Specification of areas of interest. Blue boxes indicate regions including one CGCM grid point.

A direct comparison between a RCM, a GCM and observed values can be properly done when quantities are equivalent for the three sources of data. In this work, the evaluation is carried out at scales that are greater or equal than that of the coarser resolution data. In our case, the CGCM defines the minimum area (i.e., one CGCM grid box) at which perform the comparison and this forces as to transforms high resolution data into lower resolution. Upscaling RCM and observed results to the GCM level is simply done by computing the spatial-average of all grid-points and stations data within each GCM grid box. Similarly, the fact that the CGCM cumulative precipitation data was archived at 24-hour intervals forces to carry the comparison at this time scale, thus discarding shorter time interval information.

As a result, the considered variable does not explicitly contain spatio-temporal fine scale information produced by the CRCM. The hypothesis of the existence of added value then lies not in the presence of fine scale information but in the assumption that the global model is expected to have little skill near its truncation limit (Laprise, 2003; Feser, 2006).

The global model used in this study is the third generation of the Canadian Centre for Climate Modelling and Analysis Coupled Global Climate Model (CGCM3). The gridded output of precipitation occurs on a 96 by 48 Gaussian grid (output data has a grid spacing of 3.75° in latitude and longitude).

The CRCM simulations were performed at the Ouranos Consortium with horizontal grid spacing of 45 km (true at 60° N) over a North American domain with a total of 201 by 193 grid points. Two CRCM simulations were considered in the present investigation differing only in the lateral boundary conditions used as nesting data. One simulation is driven by the CGCM and will be designated as CRCM (CGCM). The other simulation is nested by the National Centers for Environmental Prediction (NCEP) - National Center for Atmospheric Research (NCAR) reanalyses and will be designated as CRCM (NCEP).

3. Intensity frequency distributions

Intensity frequency distributions are constructed with bin sizes that vary logarithmically in order to account for the reduction on the number of events with increasing intensity. The frequency of each category is calculated using the following thresholds: 1, 2, 4, 8, 16, 32, 64, 128, 256 and 512 mm/day. As an example, Figure 2 shows the intensity frequency distributions as observed and simulated in the BC region for the winter season.

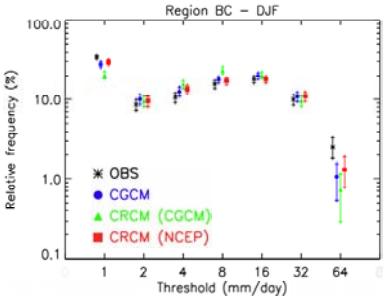

Figure 2. Intensity frequency distributions of precipitation rate in BC for wintertime.

A simple score S (Perkins et al., 2007) that measures the overlap between simulated (f_r^{mod}) and observed (f_r^{obs}) intensity frequency distributions is defined for each region r with the aim of obtaining an objective comparison,

$$S_r^{\mathrm{mod}} = \sum_{k=0}^{9} \min\left(f_r^{\mathrm{mod}}(k), f_r^{obs}(k)\right)$$

where k represents the number of the category. S varies between 0 indicating that no overlap exists among the distributions, and 1, when both distributions are identical.
The S score as calculated from the different data is presented in Figure 3. In winter season, the CGCM and the CRCM display similar skill to simulate the frequency and intensity of observed daily values by showing similar values of the S score, independently of the region considered (with maybe the exception of BC and ALTA regions).
In summer, models have more difficulties to reproduce the observed daily distributions, presenting smaller values of S than in wintertime. The CGCM shows a better agreement with observed data than the CRCM and this improvement is mainly coming from a better simulation of the frequency of observed dry days (not shown).

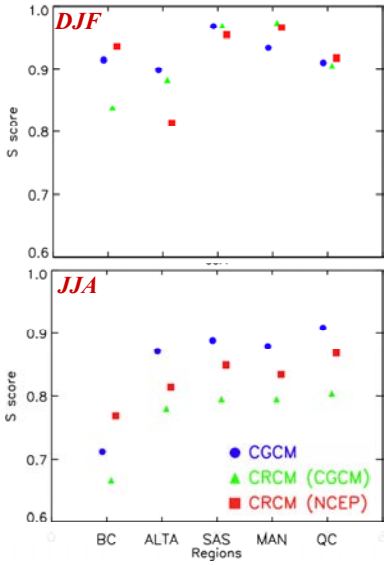

Figure 3. S score calculated between the simulated and observed distribution.

4. Heavier precipitation events

We use the 95th percentile of the distribution to evaluate the performance of models to reproduce the heavier precipitation events (see Figure 4). Seasonal 95-percentiles are estimated from approximately 90 values of precipitation rate (20 years of daily data).

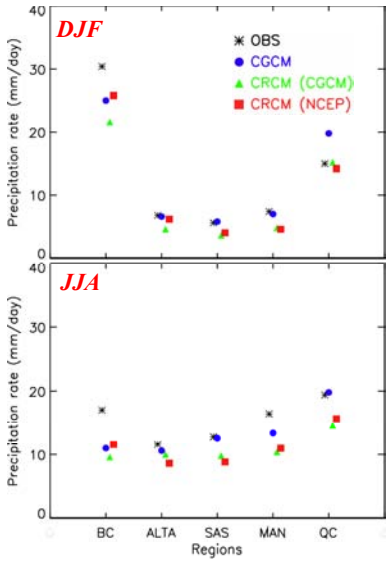

Figure 4. Observed and simulated 95-percentile.

Differences of the 95th percentile values across regions are generally well simulated by both models in both seasons. In summer, the CGCM produces generally a better agreement with observed values than the CRCM. The latter shows a consistent underestimation of the frequency of occurrence of heavy precipitation events as compared with observed frequencies.

5. Summary and discussion

Results of the comparison of daily values of precipitation as simulated by a regional and a global model suggest that there is no evidence of the existence of added value at the scale studied. It is important to emphasise that the approach employed in this study is based on the assessment of spatial and temporal scales of precipitation that are represented by the *two models* although in a much coarser way by CGCM since these scales are near its truncation limit.
Advantages of the RCM simulations due to its higher spatial-temporal resolution have not yet been explicitly explored but it will be part of our next step.
Although the failure of the assumption from which added value should be expected (i.e., that the global model have little skill at their smallest resolved scales) can account for the absence of added value, it can not explain that the CGCM performs better than the CRCM (see for example the simulation of heavier events in Figure 4). Others errors, probably specific to the model seem to play an important role in the simulation of precipitation statistics.
In general, this work highlights the need to further investigate issues related to added value in RCMs. Certainly this work must be extended to studies that explicitly include fine spatial and temporal scale features. For more practical purposes, as when using RCM-simulated scenarios in regional impact studies, a characterization of added value in terms of the variable, climate statistic, surface forcing, weather regime, etc. would be of interest.

References

Feser, F., Enhanced Detectability of Added Value in Limited-Area Model Results Separated into Different Spatial Scales. *Mon. Wea. Rev.* Vol. 134, pp. 2180-2190, 2006.

Giorgi, F., and G.T. Bates: The climatological skill of a regional model over complex terrain. *Mon. Wea. Rev.*, Vol. 117, pp. 2325-2347, 1989.

Laprise, R., Resolved scales and nonlinear interactions in limited-area models. *J. Atmos. Sci.* Vol. 60, pp. 768-779, 2003.

Laprise, R., R. de Elía, D. Caya, S. Biner, Ph. Lucas-Picher, E. P. Diaconescu, M. Leduc, A. Alexandru and L. Separovic, Challenging some tenets of Regional Climate Modelling, *Meteor. Atmos. Phys.* Vol. 100, Special Issue on Regional Climate Studies, pp. 3-22, 2008.

Perkins, S.E., A.J. Pitman, N.J. Holbrook, and J. McAneney, Evaluation of the AR4 Climate Models' Simulated Daily Maximum Temperature, Minimum Temperature, and Precipitation over Australia Using Probability Density Functions. *J. Climate*, Vol. 20, pp. 4356-4376, 2007.

The Asian summer monsoon in ERA40 driven CLM simulations

A. Dobler and B. Ahrens

Institute for Atmosphere and Environment, Goethe-University, Frankfurt am Main, Germany (dobler@iau.uni-frankfurt.de)

1. Introduction

Regional climate simulations using the CLM (the climate version of the COSMO-model, see http://www.clm-community.eu) have been carried out in a South Asian domain. The simulations are driven by ERA40 reanalysis data and have a grid resolution of 0.44°. Similar simulations with CLM are successfully performed for European simulation domains (e.g., Dobler & Ahrens 2008). A shown in Fig. 1 the precipitation climate simulated with CLM in South Asia shows substantial deficiencies. The objective of this paper is to discuss the representation of the monsoonal system in the CLM and its relationship to the realized precipitation fields.

2. Methods

There are several indices available which try to quantify the strength and variability of the South Asian summer Monsoon. These indices are based on rainfall (e.g., *Parthasarathy et al.,* 1992), vertical zonal or meridional wind shear (e.g., *Webster and Yang,* 1992; *Goswami et al.*, 1999), and on combinations of these parameters. In *Wang and Fan* (1999) the choice of the appropriate index is discussed and further indices are introduced.

In this work we apply the indices to the CLM simulations. The results are compared to observations or ERA40 (*Uppala et al.,* 2005) and NCEP (*Kalnay et al.,* 1996) re-analysis data to find possible reasons for the CLM deficiencies.

3. Results

While the magnitudes of the different indices are of similar order in CLM, ERA40 and NCEP, the correlations between the time series of the indices from single data sources vary considerably (not shown). Thus, we take a look at the spatial distribution of the parameter fields involved in the index calculations.

Figs. 1-3 show the spatial distribution of the precipitation model bias of CLM, ERA40 and NCEP data compared to GPCC for JJAS from 1960 to 2000. While the CLM shows an overestimation of precipitation at the Indian west coast, both re-analysis data sets show an underestimation in the same region, but an overestimation just behind the coast. The same holds for the east coast of the Bay of Bengal.

Over the whole Tibetan plateau, both ERA40 and NCEP data show an overestimation of precipitation. Here the CLM shows good agreement with the observational data set.

The differences in the 200-hPa winds are only small (not shown). However, looking at the 850-hPa zonal winds in the CLM model, the ERA40 and the NCEP re-analysis data (Figs. 4-6), we see that the CLM shows higher wind speeds between Somalia and the Indian west coast, and over the Bay of Bengal.

At the foothills of the Himalayas, the CLM shows some significant westward winds, which are not visible in the ERA40 or NCEP data. This is also the region, where the CLM shows the highest underestimation of precipitation. But, we expect that these deficiencies are related to regional phenomena and on only indirectly to the monsoonal system representation.

The meridional 850-hPa winds east of Somalia are also higher in the CLM model than in the re-analysis data (not shown).

4. Conclusions

The generally high wind speeds at 200 hPa show only small differences between the different data sets resulting in vertical wind shear indices, which are of similar magnitude in all three models. Therefore, it is difficult to interpret the monsoonal dynamics in the model simulation based on these indices.

However, looking into the parameter fields involved in the applied monsoon indices allows a preliminary conclusion: the simulation of the 850-hPa winds (especially the zonal component) and in consequence the moisture flux have a strong influence on the simulated precipitation climate in the three models examined.

References

Dobler, A., B. Ahrens, Precipitation by a regional climate model and bias correction in Europe and South-Asia. Meteorol. Zeitschrift, 17(4), 499-509, 2008.

Goswami, B.N., et al., A broad scale circulation index for the interannual variability of the Indian summer monsoon, *Quart. J. Roy. Meteor. Soc.,* 125 (554), pp. 611-633, 1999.

Kalnay, E., et al., The NCEP/NCAR 40-Year Reanalysis Project, *Bull. Amer. Meteor. Soc.*, 77, 437–471, 1996.

Parthasarathy, B., et al., Indian summer monsoon rainfall indices, 1871–1990. *Meteor. Mag.,* 121, pp. 174–186, 1992.

Uppala, S.M., et al., The ERA-40 re-analysis, *Quart. J. Roy. Meteor. Soc.*, 131 (612), pp. 2961-3012, 2005.

Wang, B. and Z. Fan, Choice of South Asian monsoon indices, *Bull. Amer. Meteorol. Soc.*, 80 (4), pp. 629-638, 1999.

Webster P.J. and S. Yang, Monsoon and ENSO: Selectively interactive systems, *Quart. J. Roy. Meteor. Soc.*, 118, pp. 877–926, 1992.

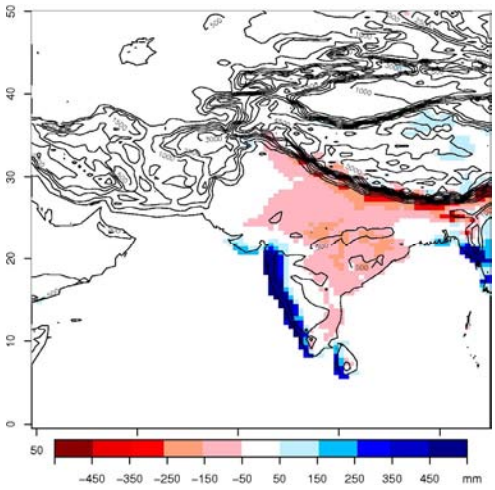

Figure 1: Mean monthly differences between CLM and GPCC precipitation data for the Monsoon months (JJAS) from 1960 to 2000.

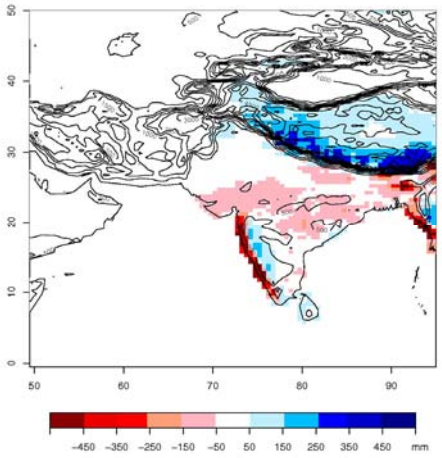

Figure 2: As for Fig. 1, but for ERA40 precipitation data.

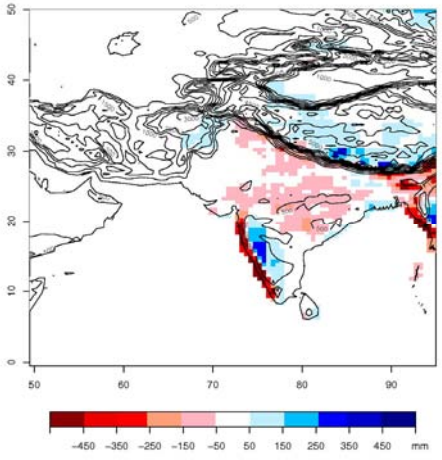

Figure 3: As for Fig. 1, but for NCEP precipitation data.

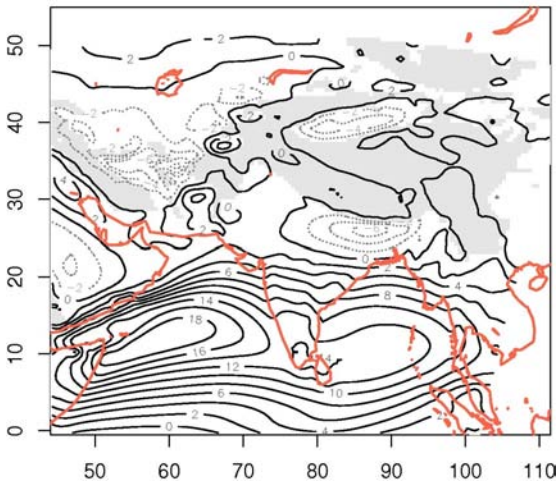

Figure 4: 850 hPa zonal winds averaged over the Monsoon months 1960-2000 in the model region from the CLM simulations. The unit for contour values is m/s. The region where the 850 hPa surface is below ground is shaded.

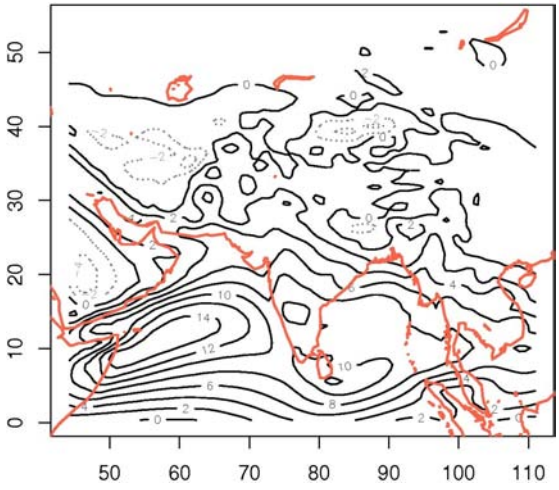

Figure 5: As for Fig. 4, but for ERA40 zonal wind data and without the shading.

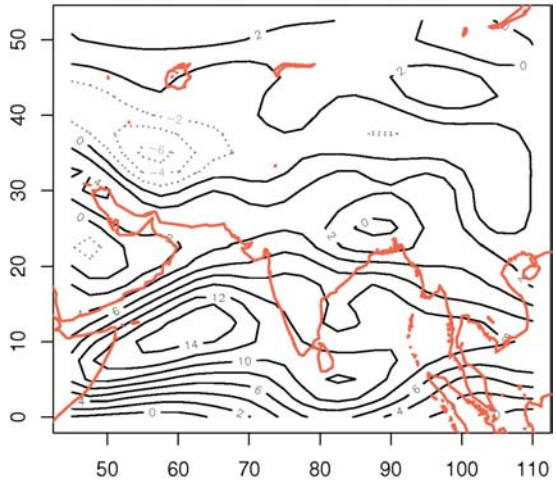

Figure 6: As for Fig. 5 but for NCEP zonal wind data.

Added value of limited area model results

Frauke Feser, Hans von Storch, Jörg Winterfeldt, and Matthias Zahn

Institute for Coastal Research, GKSS Research Center, Geesthacht, Germany, Frauke.Feser@gkss.de

1. Regional Climate Model Results

Regional climate models (RCMs) of the atmosphere are widely used in climate research studies. They serve a variety of purposes, from process studies and weather forecasting to long-term simulations. Such models can process multi-year to multi-decadal large-scale weather information (for the past or for some hypothetical future, e. g. scenarios) and use high-resolution topographic details. The question is: 'Do they return more than the original forcing data's knowledge (specified at the boundaries or as well at the large scales; possibly after some simple downscaling application such as spatial interpolation)?' The additional knowledge is usually termed "added value" – and so far, efforts in determining this added value are rare. Instead general assumptions are made, e. g. that higher grid resolutions should lead to better results. But evidence that the quality of such additional detail is superior to a simple geo-statistical post-processing of the global forcing data is not often provided.

In the present talk, the efforts of our group to determine such added value in multi-decadal simulations with different regional climate models are summarized and evaluated. These simulations were mostly "reconstructions", e. g. simulations of the weather dynamics since 1948 until today of Western Europe or the Northwestern Pacific. Most of these simulations have been done with the constraint of spectral nudging. Thereby the RCM was forced to simulate the assumedly well-resolved large-scale features of the driving fields correctly, while the dynamics at smaller scales were simulated solely by the RCM (*von Storch et al.* (2000)). Conditional upon the model area and the degree of exchange via the lateral boundaries, success in simulating the "right" features at the observed time and location may depend on the constraint of the large-scale dynamics (*Rockel et al.* (2008)).

2. Added Value

We have identified several fields, where added value of RCMs emerges. The better representation of spatially distributed processes allows a more realistic description of meso-scale phenomena – examples are North Atlantic polar lows and East Asian typhoons (e. g. *Zahn and von Storch* (2008); *Feser and von Storch* (2008)).

Features resolved in numerical data are typically of the order four grid boxes or above. For global reanalysis products, this means that phenomena smaller than 800 km are not represented well. In Fig.1 the increased information gained with a RCM is shown for a SLP field including a polar low. Polar lows are meso-scale (200-1000km) sized maritime storms in the Arctic. In the DWD analysis, the polar low is visible with closed isobars off the Norwegian Coast, whereas in the NCEP/NCAR field only a weak pressure trough exists. Using these data to drive a climate mode RCM simulation, it is possible to reproduce the polar low with closed isobars (*Zahn et al.* (2008)).

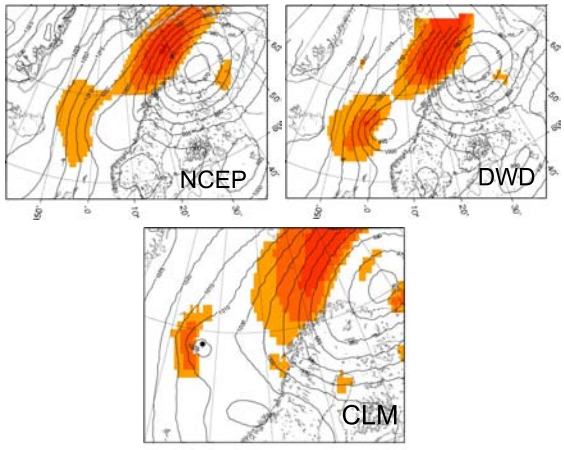

Figure 1. 10m wind speed ≥ 13.9m/s and air pressure (at mean sea level) on 15 October 1993: NCEP/NCAR analysis after interpolation onto the CLM grid, DWD analysis data, CLM simulation. The black dot indicates the positions of the polar low's pressure minimum in the CLM simulation.

The added value of this procedure becomes particularly distinct, when the meso-scale information is extracted from the full MSLP-fields (by applying a band pass filter). In Fig.2 the polar low is comprised in the DWD analysis as well as in the RCM field, but not in the NCEP/NCAR-field.

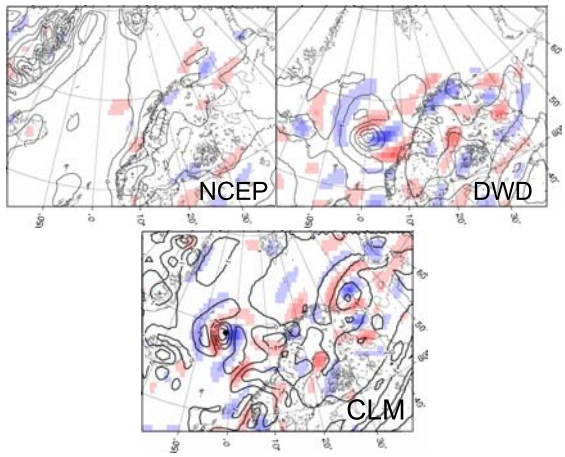

Figure 2. Band-pass filtered MSLP (isolines; hPa) and 10m wind speed anomalies on 15 October 1993: NCEP/NCAR analysis, DWD analysis data, CLM simulation. The black dot indicates the positions of the polar low's pressure minimum in the CLM simulation.

So far these findings were used to automatically detect polar lows in long-term simulations and to investigate their frequency and changing annual numbers.

The higher spatial resolution, compared to the driving large-scale data, will in general not improve the representation of the large-scale dynamics, but presumably mostly the meso-scale dynamics. This can be demonstrated by comparing statistics of meso-scale dynamics simulated in extended RCM simulations with operational regional weather analyses. To do so, suitable digital spatial filters are needed (*Feser and von Storch* (2005)). It turns out that regional models show an added value in describing meso-scale variability compared to the driving global reanalysis, in particular, when the RCM is constrained at the large spatial scales (*Feser* (2006)). Not unexpectedly, the description of the large scales is slightly deteriorated.

The higher resolved description of physiographic details, such as mountain ranges, coastal zones and details of soil properties has the potential of describing the weather and its statistics in such regions closer to reality than the global analyses or simulations. By comparing RCM simulated data with QuikSCAT satellite and with local buoy data, *Winterfeldt and Weisse* (2009) demonstrated that the usage of RCMs indeed leads to an advanced description of wind speed statistics in coastal seas, while conditions in the open ocean were not improved (Fig. 3).

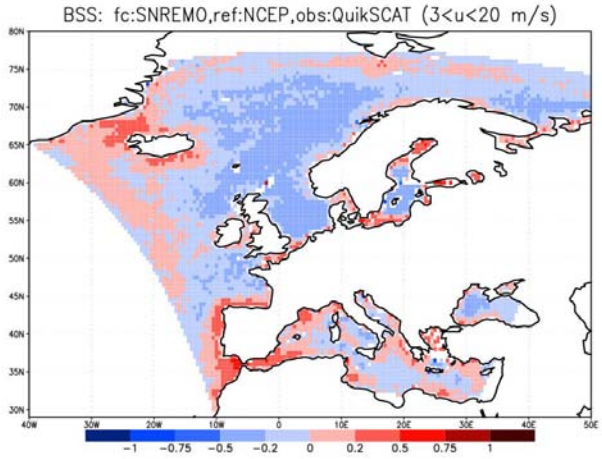

Figure 3. Modified Brier Skill Score calculated from co-locations between QuikSCAT L2B12, NRA_R1 and SN-REMO (SN stands for use of spectral nudging) in the wind speed range from 3 to 20 ms-1 and the years 2000 to 2007, where QuikSCAT L2B12 serves as ``truth``, NRA_R1 as reference ``forecast`` and SN-REMO as ``forecast``. Blue areas indicate value lost, while red areas indicate value added by dynamical downscaling.

The added value of the dynamically downscaled wind was assessed with satellite data, namely QuikSCAT Level 2B 12.5 km (L2B12) wind speed retrievals. After validating the L2B12 data with buoy winds in the eastern North Atlantic (RMSE: 1.7 m/s), L2B12, regional model data (REMO) and global NCEP/NCAR reanalysis (NRA_R1) data were co-located for the years 1999-2007.

Fig. 3 confirms the point stated by *Winterfeldt and Weisse* (2009) for a wide area including the eastern North Atlantic, the Baltic, Mediterranean and Black Sea: dynamical downscaling does not add value to NRA_R1 wind speed in open ocean areas (blue), while it does for complex coastal areas (red).

Finally, an important utility of such multi-decadal model data is that they may be used to quantitatively describe hazards and changing conditions in the regional Earth System – examples are the hydrodynamics of marginal seas, in particular currents, sea level, and thus storm surges or ocean wave conditions and related hazards (CoastDat; *Weisse et al.* (2009)).

References

Feser, F. and H. von Storch, Regional modelling of the western Pacific typhoon season 2004, *Meteorolog. Z.*, 17, 4, pp. 519-528, 2008

Feser, F., Enhanced detectability of added value in limited area model results separated into different spatial scales, *Mon. Wea. Rev.*, 134, 8, pp. 2180-2190, 2006

Feser, F., and H. von Storch, A spatial two-dimensional discrete filter for limited area model evaluation purposes, *Mon. Wea. Rev.*, 133, 6, pp. 1774-1786, 2005

Rockel, B., C. L. Castro, R. A. Pielke Sr., H. von Storch, G. Lencini, Dynamical Downscaling: Assessment of Model System Dependent Retained and Added Variability for two Different Regional Climate Models, *J. Geophys. Res.*, 113, D21107, doi:10.1029/2007JD009461, 2008

von Storch, H., H. Langenberg, and F. Feser, A Spectral Nudging Technique for Dynamical Downscaling Purposes, *Mon. Wea. Rev.*, 128, 10, pp. 3664-3673, 2000

Weisse, R., H. von Storch, U. Callies, A. Chrastansky, F. Feser, I. Grabemann, H. Guenther, A. Pluess, T. Stoye, J. Tellkamp, J. Winterfeldt and K. Woth, Regional meteo-marine reanalyses and climate change projections: Results for Northern Europe and potentials for coastal and offshore applications, *Bull. Amer. Meteor. Soc.*, in press, 2009

Winterfeldt, J. and R. Weisse, Assessment of value added for surface marine wind obtained from two Regional Climate Models (RCMs), submitted to *Mon. Wea. Rev.*, 2009

Zahn, M., H. von Storch, and S. Bakan, Climate mode simulation of North Atlantic polar lows in a limited area model, *Tellus, Ser. A*, 60, pp. 620–631, doi:10.1111/j.1600-0870.2008.00330.x, 2008

Zahn, M., and H. von Storch, A long-term climatology of North Atlantic polar lows, *Geophys. Res. Lett.*, 35, L22702, doi:10.1029/2008GL035769, 2008

Sensitivity of CRCM basin annual runoff to driving data update frequency

Anne Frigon[1] and Michel Slivitzky[1,2]

[1]Ouranos Consortium, Montreal, Canada frigon.anne@ouranos.ca [2]INRS-ETE, Québec, Canada

1. Introduction

Since the inception of Ouranos in 2002, its Climate Simulation Team (CST) has had the responsibility to carry out regional climate change projections over North America. The first simulations were performed with the Canadian Regional Climate Model (CRCM; *Caya and Laprise* 1999), which was originally developed at the Université du Québec à Montréal (UQAM). The CST got strongly involved in the development of its operational version and of later versions of the model. The CRCM was originally built on the physics package of the Canadian GCM2 and so, the first regional projections were driven by its parent GCM.

The more recent CRCM4 (*Music and Caya* 2007) regional climate projections were driven by the latest CGCM3 (*Scinocca et al.* 2008). However, over a total of five members available from CGCM3/T47-A2 runs, the first three were archived at a 12-hour interval, while the last two were 6-hourly (#4 and #5). Up till now, all CRCM simulations have been performed with 6-hourly driving data.

Although it is obviously preferable to drive an RCM with the shortest time interval (6-hourly in our case), some earlier results suggest that a 12-hour interval would produce reasonable results (*Denis et al.* 2003).

For this purpose, we designed a series of experiments to examine the sensitivity of the CRCM to the frequency of driving data (6-hourly VS 12-hourly). We included the two regional domains (Figure 1), typically in use at Ouranos, allowing us also to explore sensitivity according to domain characteristics.

The analysis is performed with 30-year annual series of simulated runoff over 21 basins of interest over Québec (Figure 2); these basins cover from 13 000 to 177 000 km^2. Internal variability is also considered in order to put in perspective our sensitivity results with regard to the model's intrinsic noise.

2. Experimental Configuration

For this sensitivity analysis, pairs of 30-year simulations were performed with the CRCM at a 45-km resolution, where the "reference" run is driven with 6-hourly CGCM3 data, while the "perturbed" run uses re-sampled data at a 12-hourly frequency (00 and 12GMT). Linear interpolation of the driving data is performed to get to the CRCM's 15-minute time steps.

Over the AMNO domain, a total of four pairs of 30-year CRCM_V4.2 simulations were run, driven by members #4 and #5 of CGCM3-A2, over the recent past (1961-1990) and future (2041-2070) periods. Over the smaller QC domain, two pairs of 30-year simulations of CRCM_V4.2 were driven by member #4, over past and future time windows. For all simulations, spectral nudging was applied within the regional domain to large-scale winds in order to keep the large-scale flow close to that of the driving data (*Riette and Caya* 2002).

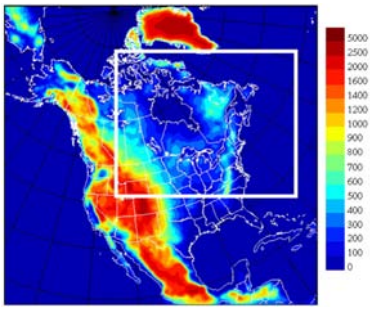

Figure 1. Large AMNO (200x192) and smaller QC (111x88) CRCM domains at 45-km resolution with topography in color shades [meters].

Figure 2. Basins of interest with CRCM's 45-km grid.

3. Results

Figure 3 summarizes sensitivity results over the 21 basins from CRCM's pairs of simulations performed over the large AMNO domain. It presents the difference in the 30-year climate mean and the (centered or unbiased) Root Mean Square Difference (RMSD) obtained from basin simulated annual runoff of each pair of runs. The percent values have been obtained by dividing by the mean of the "reference" run (even though it is arbitrary in the case of internal variability). The black diamonds encompass the sensitivity to driving data frequency (12-hourly VS 6-hourly; from four pairs), while the red stars represent the CRCM's internal variability at basin scale (from three pairs of 30-year "twin" runs, differing only in their initial conditions; *Frigon et al.* 2008). The Figure shows that, for the AMNO domain, the sensitivity to driving data frequency has an effect on basin annual runoff that is comparable but slightly higher than the model's internal variability.

We have also illustrated the influence of the driving GCM's internal variability on the CRCM (i.e., the change produced in the downscaled climate by driving with different GCM members), as shown by the green squares on Figure 3 (from two pairs of 30-year CRCM runs; *Frigon et al.* 2008). This additional information provides

relevant information, considering that RCMs are aimed at providing climate change projections and their associated uncertainty (meaning that they should be driven by different members and various GCMs). It is clear that the sensitivity of basin annual runoff to driving data frequency on AMNO is much smaller than the effect of the GCM member, asserting that sensitivity is within the CRCM's noise level.

Figure 4 presents sensitivity results over the smaller QC domain, in the same form as in Figure 3. Here, the blue stars (from three pairs of 30-year "twin" runs) represent CRCM's internal variability at basin scale. It is clear that sensitivity of basin annual runoff to driving data frequency (black diamonds; from two pairs) is important. It is not only more important than the model's internal variability but it shows a large systematic difference in the 30-year climate mean at basin scale. This implies that changing the driving data frequency on the smaller QC domain alters the simulated climate. However, the effect of driving data frequency on the RMSD of annual runoff is not as important as on the climate means.

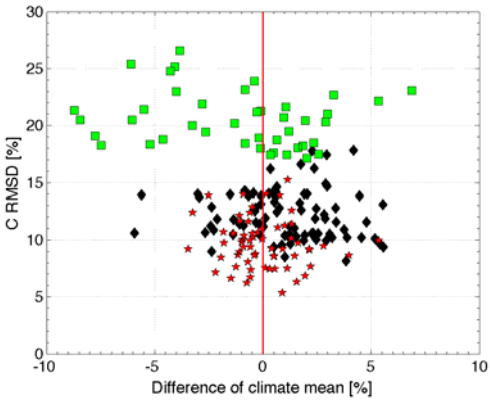

Figure 3. Annual runoff over the 21 basins of interest from CRCM's AMNO domain runs: influence of driving data frequency (black diamonds) compared to the effect of CRCM's internal variability (red stars) and to the effect of driving GCM's internal variability on CRCM run (green squares).

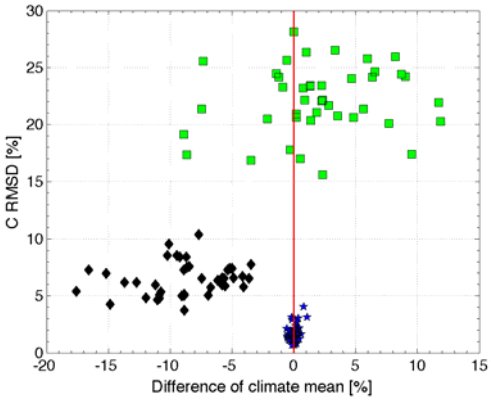

Figure 4. As Figure 3 but from the smaller QC domain runs. CRCM's internal variability at basin scale is represented by the blue stars.

Finally, we have examined the effect of driving data frequency (12-hourly VS 6-hourly) on the *climate change* signal for basin annual runoff (2041-2070 VS 1961-1990) (not shown). With the AMNO domain simulations, climate change becomes more sensitive than would be expected from a simple extrapolation of its effect on the climate. On the other hand, over the QC domain, some compensation effects seem to take place, since the climate change signal becomes less sensitive than would be expected from results depicted in Figures 3 and 4.

4. Discussion

An analysis of the effect of the driving data frequency (12-hourly VS 6-hourly) at the basin scale has provided interesting information. Over the investigated basins, sensitivity to driving data frequency varies according to domain dimension. We know that smaller domains are more constrained by their driving data and we find that the smaller QC domain is very sensitive to a change in driving data frequency, probably because the basins of interest are located much closer to the western inflow lateral boundary.

In answer to our original question, this first analysis indicates that there is potential use for the CRCM4 simulations on the AMNO domain driven by the five CGCM3 members, even though all members are not available at a 6-hourly interval. This does not seem possible with the QC domain because of an important change in the simulated climate. We must mention that all simulations were performed with spectral nudging, which may influence the sensitivity results, particularly over the smaller QC domain.

Although the question treated here was mostly driven by our specific operational needs, the general problem of the impact of a low updating frequency remains open, especially for simulations with increasing resolution.

References

Caya, D. and R. Laprise, A Semi-Implicit Semi-Lagrangian Regional Climate Model: The Canadian RCM. *Monthly Weather Review,* Vol. 127, No. 3, pp. 341-362, 1999

Denis, B., R. Laprise, and D. Caya, Sensitivity of a regional climate model to the resolution of the lateral boundary conditions. *Climate Dynamics*, Vol. 20, pp. 107-126, 2003

Frigon, A., M. Slivitzky, B. Music, and D. Caya, Internal variability of the Canadian RCM's hydrologic variables at the basin scale. EGU Gen. Ass., Vienna (Austria), *Geophysical Research Abstracts*, Vol. 10, EGU2008-A-04093, 2008

Music, B., and D. Caya, Evaluation of the Hydrological Cycle over the Mississippi River Basin as Simulated by the Canadian Regional Climate Model (CRCM). *J. Hydrometeorology,* Vol. 8, No. 5, pp. 969-988, 2007

Riette, S., and D. Caya, Sensitivity of short simulations to the various parameters in the new CRCM spectral nudging. Research activities in Atmospheric and Oceanic Modeling, edited by H. Ritchie, *WMO/TD* - No. 1105, Report No. 32: 7.39-7.40, 2002

Scinocca, J. F., N. A. McFarlane, M. Lazare, J. Li, and D. Plummer, The CCCma third generation AGCM and its extension into the middle atmosphere. *Atmos. Chem. and Phys. Discuss.*, Vol. 8, pp. 7883-7930, 2008

High-resolution dynamical downscaling error components over complex terrain

A. Gobiet[1], M. Suklitsch[1], A. Prein[1], H. Truhetz[1], N.K. Awan[1], H. Goettel[2] and D. Jacob[2]

[1]Wegener Center for Climate and Global Change and Institute for Geophysics, Astrophysics and Meteorology, University of Graz, Austria. [2] Max Planck Institute for Meteorology, Hamburg, Germany
(andreas.gobiet@uni-graz.at)

1. Introduction

Recent regional climate scenarios for are often based on regional climate models (RCMs) operated on 50 km to 25 km spaced grids. The emerging generation of regional climate scenarios is often given on 10 km grids, which is particularly useful in mountainous and climatologically complex areas like the European Alpine region. This resolution enables to resolve climate characteristics of relatively small sub-regions (about 50 x 50 km). However, the typical error characteristics of such high resolution climate simulations and the impact of model setup on model errors are not properly characterized yet.

2. Methods

In this study we quantify the relative importance of major downscaling error components (errors due to spatial setup, model structure, and physical parameterization) of high resolution RCMs (10 km grid spacing) in the European Greater Alpine Region (GAR) on a sub-regional basis (see Fig. 1 for the sub-regions). The study is based on a large ensemble of about 60 one-year simulations performed with four different RCMs (COSMO-CLM, MM5, WRF, REMO) driven by lateral boundary conditions of the ERA-40 reanalysis. We investigate seasonal precipitation and temperature errors (see *Suklitsch et al.* [2008] for such an evaluation for parts of the ensemble) and the relative impact of details in the downscaling strategy on error variability using a similar method as *Déqué et al.* [2007]

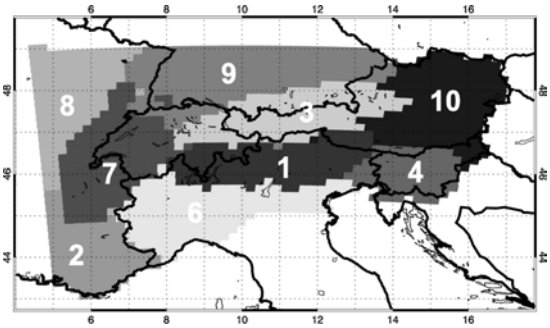

Figure 1. Climatological sub-regions in the Greater Alpine Region (GAR) based on clustering daily precipitation time series (*Suklitsch et al.* [2008]).

3. First Results

First results for a subset of the entire ensemble consisting of 29 COSMO-CLM and MM5 simulations indicate that the selection of the model domain (orange in Fig. 2) plays a major role in the error budget in winter, in higher elevated regions, and near the inflow boundary of the model domain. Error variability due to physical parameterization (green in Fig. 2) is more important in summer and in regions that are orographically shaded from the synoptic flow. Error variability contributed by the type of RCM (blue in Fig. 2) could not yet be reliably quantified due to a too small ensemble size (only 2 RCMs). The full ensemble consisting of 4 RCMs will enable a rough estimation of this error component.

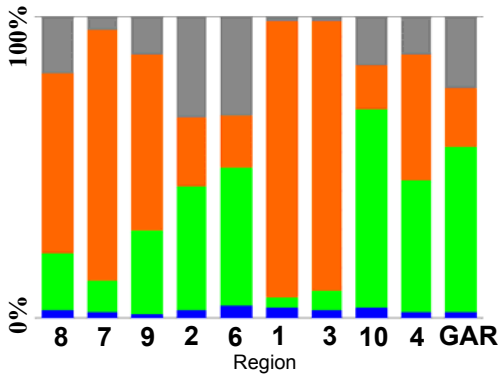

Figure 2. Relative contribution of details in downscaling strategy on the temperature error variability [%] (annual mean): Selection of RCM (blue), physical parameterization (green), domain location and size (orange), further error components (grey).

In addition to the analysis of error components, we'll quantitatively characterize temperature and precipitation errors of high resolution RCMs operated in mountainous areas.

Acknowledgements

The authors thank the University Information Service of the Univ. Graz for the provision of computing infrastructure, the Swiss Federal Institute of Technology Zurich (C. Frei) and Central Institute for Meteorology and Geodynamics and the for the provision of observational data. This study is part of the project NHCM-1 (P19619-N10) funded by the Austrian Science Fund (FWF).

References

Déqué, M., D. P. Rowell, D. Lüthi, F. Giorgi, J. H. Christensen, B. Rockel, D. Jacob, E. Kjellström, M. de Castro, B. van den Hurk, An intercomparison of regional climate simulations for Europe: assessing uncertainties in model projections, Clim. Change, 81, DOI 10.1007/s10584-006-9228-x, 2007.

Suklitsch, M., A. Gobiet, A. Leuprecht and C. Frei, "High Resolution Sensitivity Studies with the Regional Climate Model CCLM in the Alpine Region", *Meteorol. Z.*, 17, 4, pp. 467-476, 2008.

Climate change projections for the XXI century over the Iberian peninsula using dynamic downscaling

J.J. Gómez-Navarro, J.P. Montávez, S. Jerez and P. Jiménez-Guerrero

Departamento de Física, Universidad de Murcia, Edificio CIOyN, Campus de Espinardo, 30100, Spain. (jjgomeznavarro@um.es)

1. Introduction

Climate change is one of the most concerned problems in the actual society, as pointed by the last report of the IPCC (IPCC, 2007). Specifically, the Iberian Peninsula (IP), as part of the Mediterranean Region, has been identified as one of the most responsive regions to climate change (Giorgi, 2006; Diffenbaugh et al., 2007).

Due to its orographic complexity, the IP has many different climates, and a good spatial resolution is needed to understand the details and possible effects of climate change. Nevertheless, the Global Circulation Models (GCM) have a too coarse resolution which makes them unfeasible to study climate change implications over the IP.

For this reason, a regionalization process must be carried out to improve the spatial resolution of climate projections in order to assess the climate change over the IP.

2. Experiments

The simulations have been performed using a climate version of the regional atmospheric model MM5 (Montavez et. al., 2006), over two-way nested domains with resolutions of 90 and 30 km respectively. The inner domain covers the full IP.

Four centennial simulations have been performed using outputs from the GCMs ECHOG and ECHAM5 as driving conditions. The notation for the fours experiments and the time periods covered by each experiment is as follows:

- **ECHOG-A2**: covers the period 1990-2099
- **ECHOG-B2**: covers the period 1990-2099
- **ECHAM5-A2**: covers the period 2001-2099
- **ECHAM5-A1B**: covers the period 2001-2099

3. Methodology

In order to investigate the warming signal along the XXI century an Empirical Orthogonal Functions (EOF) analysis has been used. This approach increases the signal to noise ratio, reduces the huge dimensionality of the problem and makes possible to analyse independently the spatial and temporal features of the 2-m temperature series (von Storch and Zwiers, 2007).

The maximum and minimum 2-m temperature monthly series have been studied for each month separately in each experiment. In all cases, the variance explained by just the first EOF is around 85% percent of the total. This implies than the first EOF contains the warming pattern, as obtained by others authors (e.g. Zorita et al., 2005). For this reason, below only the first EOF is studied, and it is referred as the spatial warming pattern.

4. Results

The spatial structure of the patterns and their temporal evolution have been studied separately.

A very important feature of the warming patterns is that they have an important annual cycle: summer patterns look quite different from the winter ones. For example in the Figure 1 are depicted the spatial patterns for 2-m maximum temperatures for March (up) and July (down), respectively. In summer months, the patterns look more continental, meanwhile in spring and autumn they seem to follow the orography. Nevertheless there are many differences in the behavior of maximum and minimum 2-m temperatures (not shown).

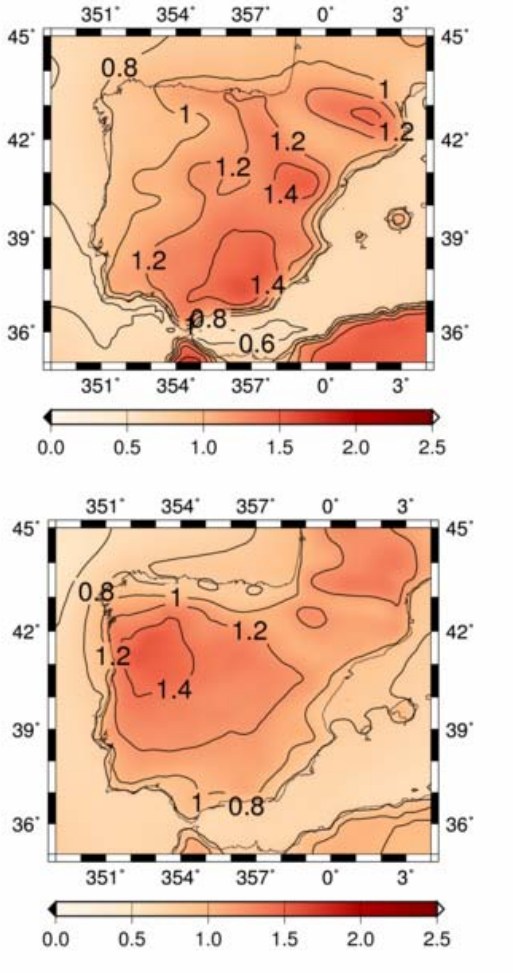

Figure 1: Spatial warming pattern for March (up) and July (down).

There is nevertheless a large agreement between experiments. For a given month, the spatial pattern is very similar, and in fact the spatial correlation is around 90%. This means than the spatial warming patterns found are an inherent characteristic of the domain and the month, not a feature of the GCM neither the SRES scenario used to perform the simulation.

In the temporal evolution, the importance of different scenarios and GCM is found. In the A2 scenario the warming signal is stronger, and it is reflected in a larger trend in the Principal Component associated to the first EOF.

There is also an important difference in the evolution of maximum and minimum 2-m temperatures along the XXI century. The maximum temperatures suffer a higher warming. This could yield in a an increase of the daily temperature range.

Finally, the amount of warming has also an annual cycle. Both the maximum and minimum temperatures have a more marked trend in summer months. This means than the climate could become more continental in the future.

5. Conclusions

A study of the warming patterns over the IP under several scenarios and with different GCM has been performed using a climate version of MM5 mesoescalar model. An EOF analysis has been employed in order to reduce the noise in the warming of 2-m maximum and minimum temperature and reduce the dimensionality of the problem.

It has been found that the first EOF accounts for the main warming pattern, and this depends on the month and on the variable. There is an important annual cycle and an asymmetry in the behavior of maximum and minimum temperatures.

The most important result is that these projections are consistent under different scenarios and using different GCM coupled to the regional climate model. The only difference between scenarios is the intensity of these changes in the IP climate, not the qualitative features.

Finally, the spatial structure of the warming patterns seems to be related to several physical parameters like continentality or height over the sea. Further research should be devoted to fully understand these changes, which could be related to changes in the global circulation.

As future work, others simulations should be performed driven by other GCM. Also, other task involve checking whether these patterns are also present for pre-industrial climate, as obtained by others authors

6. References

Diffenbaugh, N.S., J.S. Pal, F. Giorgi, X.J. Gao. Heat stress intensification in the Mediterranean climate change hotspot. *Geophys.Res. Lett.*, 34(11):53 – 70, 2007.

Giorgi, F. Climate change hot-spots. *Geophys. Res. Lett.*, 33(8):11217 – 11222, 2006.

IPCC. Climate Change 2007 – The Physical Science Basis. *WMO*, 2007.

Montávez, J.P., J. Fernández, J.F. González-Rouco, J. Saenz, E. Zorita, and F. Valero. Proyecciones de cambio climático sobre la Península Ibérica. *Asamblea Hispano Portuguesa de geodesia y geofísica,* 2006.

von Storch, H. and F.W. Zwiers. Statistical Analysis in Climate Research. *Cambridge University Press*, 2007.

Zorita, E., J.F. Gonzalez-Rouco, H. von Storch, J.P. Montavez, and F. Valero. Natural and anthropogenic modes of surface temperature variations in the last thousand years. *Geophys. Res. Lett.*, 32(8):755 – 762, 2005.

Regional climate change scenarios – benefits of modeling in high resolution for central and eastern Europe in Project CECILIA

Tomas Halenka, Michal Belda, Jiri Miksovsky

Dept. of Meteorology and Environment Protection, Charles University, tomas.halenka@mff.cuni.cz

1. Project CECILIA

Resolution of regional climate simulation is an important factor affecting the accuracy of dynamical downscaling of the global changes. Especially the extremes are strongly dependent on the terrain patterns as shape of orography or land use, which can contribute to extreme temperatures or precipitation appearance and distribution. Project EC FP6 CECILIA (Central and Eastern Europe Climate Change Impact and Vulnerability Assessment) is studying the impact of climate change in complex topography of the Central and Eastern Europe in very high resolution of 10 km. The impacts on agriculture, forestry, hydrology and air-quality are studied within the project, and precise information from regional climate simulations is necessary.

2. CECILIA RCMs and simulation strategy

One of the commonly used RCM in the targeted regions is the model RegCM distributed freely from ICTP. The model was originally developed by *Giorgi et al.* (1993a,b) and later augmented as described by *Pal et al.* (2007). Another RCM has been used recently, starting from an operational NWP model used in several national meteorological services in the targeted domain. This is the ALADIN-CLIMATE model and first experiences from its development can be found in *Huth et al.* (2003). The basic objective of modelling activities in CECILIA project is to produce simulations on targeted domains using very high resolution of 10 km for a past period (1961-1990) driven by ERA40 reanalysis used for validation of the models as well as for a reference period (1961-1990) and scenario time slices (2021-2050 and 2071-2100) based on ENSEMBLES 6FP EC IP A1B GCM simulations. Two models have been supposed to be used as source of driving fields over six target areas, ALADIN-Climate family using stretched climate change transient run by ARPEGE/Climat for ENSEMBLES project, RegCM family using RegCM transient ENSEMBLES run for whole Europe in 25km resolution driven by transient run of ECHAM5. While the stretched ARPEGE run provides reasonable resolution in targeted regions for direct application of 10 km resolution RCM, the difference between 10 km resolution of RegCM and the resolution of other common global models is too large, that is why the double-nesting using 25 km RegCM run as an intermediate step was used.

The individual partners running the simulations settled with respect to their purposes and resources available the integration domains (see Fig. 1) when preparing to perform the simulations driven by reanalysis fields, which is necessary for subsequent validation of the models performance. The first effort was given to produce the high resolution runs based on the reanalysis data in targeted areas for the period of 1961-90, allowing spin-up of the models from the beginning of 1960 as starting time, moreover, most partners extended the period till the end of 2000 for more extended validation.

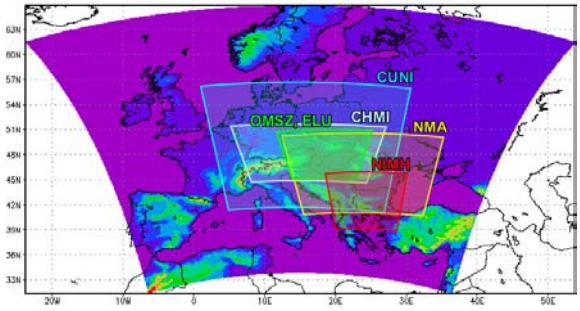

Figure 1. Integration domains for individual partner simulations.

3. Validation of CUNI experiments – output localisation

Comparison of reanalysis run for temperature and precipitation with respect to CRU 10‘ climatology as well as ENSEMBLES gridded data (E-obs, *Haylock et al., 2008*) is available. Reasonable agreement can be seen as well as the similar patterns in interdecadal variations for temperature. The benefit of high resolution is well expressed in the results, especially when going to local scale. There is slight warm bias in January in most region of interest, with pronounced tendency to none or colder bias in the upper locations which might be another demonstration of high resolution benefit as orography of the model terrain is better represented than orography in 10’ CRU resolution. This is similar to July performance where rather cold bias prevails anyway. There is rather overestimation of precipitation due to excessive smaller amounts appearance. Significant wet bias can be seen both for January and July. The problem is not so serious in main domain of interest during July (except the first decade), for January there is again the feature of upper locations expressed, but further analysis has to be performed to get sources of the differences, as well as the tests with modified large scale precipitation parameterization settings. Similarly as for temperature, despite of the biases the potential of high resolution simulation in capturing of orographic features is well pronounced.

The density of information in high resolution and similarity of model terrain and the real topography enables the application of further localization technique adopted by CUNI. It is based on regression analysis of the dependence of the climate characteristics on the orographical height in the vicinity of the point of interest, usually, for validation purposes, the observational site, but for an analysis of scenarios runs e.g. the place for impact study. This way it is possible to get the value of the parameter on real topography and thus to go farer beyond the 10km of model simulation resolution. It should be mentioned that these relations are quite realistically represented in the models especially for temperature parameters where this is more straightforward, but e.g. for ALADIN – Climate it is surprisingly well represented for precipitation as well. There is one advantage of this

technique, as it is based on the analysis of model data only, it can be used the same way for scenarios runs even reproducing possible changes in these dependencies.
The comparison of the results of reanalysis run and control run for reference period is presented in Fig. 2 for selected stations from targeted area after the correction to the real terrain height for temperature. Although annual bias being just nearly exactly zero, in monthly data the warm bias of temperature in GCM driven simulation for colder season is much higher than for reanalysis driven run, while for summer season it is opposite.

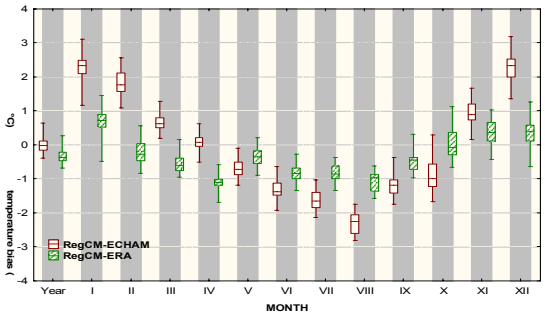

Figure 2. Temperature bias (distribution at 25 Czech weather stations, after correction for altitude mismatch, 1961-1990)

4. Future scenarios

Scenarios runs driven by RegCM@25km forced by GCM ECHAM5 has been performed for 2021-2050 and 2071-2100 with climate change signal analysis with respect to control experiment for period 1961-1990. Fig. 3 presents the preliminary differences based on two decades completed.

Acknowledgements

This work is supported in framework of EC FP6 STREP CECILIA (GOCE 037005). Some contributions to the tasks are supported from local sources as well under Research Plan of MSMT, No. MSM 0021620860, and in framework of the project supported by Czech Science Foundation under No. 205/06/P181. We acknowledge the E-Obs dataset from the EU-FP6 project ENSEMBLES (http://www.ensembles-eu.org) and the data providers in the ECA&D project (http://eca.knmi.nl).

References

Giorgi, F., M.R. Marinucci, and G.T. Bates, Development of a second generation regional climate model (RegCM2). Part I: Boundary layer and radiative transfer processes. *Mon. Wea. Rev.*, 121, 2794-2813, 1993a.

Giorgi, F., M.R. Marinucci, G.T. Bates, and G. DeCanio, Development of a second generation regional climate model (RegCM2). Part II: Convective processes and assimilation of lateral boundary conditions. *Mon. Wea. Rev*., 121, 2814-2832, 1993b.

Haylock, M.R., N. Hofstra, A.M.G. Klein Tank, E.J. Klok, P.D. Jones, M. New, A European daily high-resolution gridded dataset of surface temperature and precipitation. *J. Geophys. Res (Atmospheres)*, 113, D20119, doi:10.1029/2008JD10201, 2008.

Huth, R., R. Mládek, L. Metelka, P. Sedlák, Z. Huthová, S. Kliegrová, J. Kyselý, L. Pokorná, M. Janoušek, T. Halenka, On the integrability of limited-area numerical weather prediction model ALADIN over extended time periods. Studia geoph. geod., 47, 863-873, 2003.

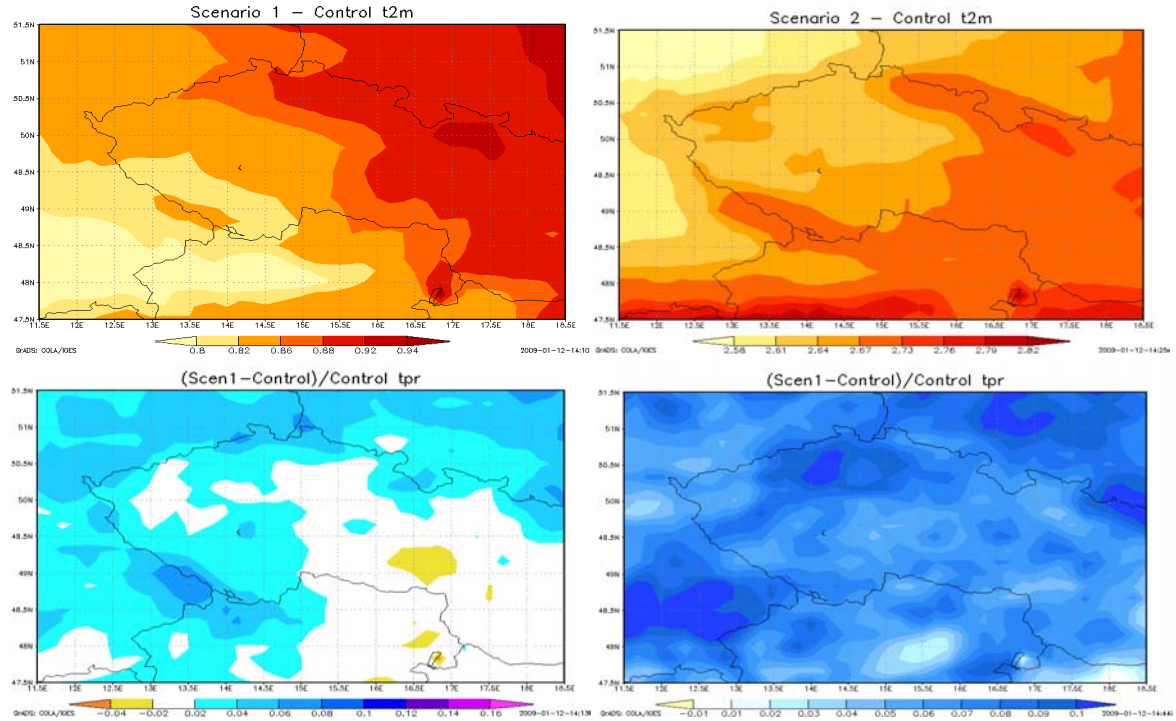

Figure 3. Changes 2021-2040 (left panels) and 2071-2089 (right panels) against CTRL1961-1970 for temperature (upper panels) and precipitation (lower panels).

Climatological feature and heating mechanism of the Foehn phenomena over the north of the central mountain range in Japan by using non-hydrostatic RCM

Noriko Ishizaki and Izuru Takayabu

Meteorological Research Institute, 1-1 Nagamine, Tsukuba 305-0052, Japan. E-mail: nishizak@mri-jma.go.jp

1. Introduction

Foehn phenomena can be observed in many parts of the world, and studies have been made by scientists for many decades. In these days, 3-dimensional numerical simulations have become popular to investigate detailed structure of foehn. The contributions of precipitations for foehn warming often appear to be a controversial point (e.g., *Seibert* 1990, *Zangle* 2003).

In Japan, *Arakawa* (1982) studied condition under which foehn event occurred using observation data-sets. *Inaba* et al. (2002) analyze prolonged foehn along the coast of Japan Sea using observation and AOGCM. They concluded that the PJ pattern and associated synoptic-scale disturbances are important for the persistence of foehn. However, there are few studies of which aim is to reveal local structure of foehn or role of precipitation. The purpose of this study is to capture the climatological feature and heating mechanism of foehn in Japan using RCM.

2. Data and Model

The Automated Meteorological Data Acquisition System (AMeDAS) data, which widely spread in Japan, is utilized to capture climatological aspect of foehn phenomena. To determine the foehn duration, we propose the definition as follows. At first, in each station, the deviation from average value is calculated. The average values are derived using data at the same hour each day from 10 days before to 10 days later. If both the surface temperature and wind speed deviation values exceed 5K and 3m/s respectively, we regard this period as a foehn event. While the conditions are satisfied continuously, it is assumed to be one event.

We used the non-hydrostatic model NHRCM which is based on the operational model of JMA. Details are described in *Sasaki et al*. (2008). We used two sets of RCM configurations. One has 145x155 grids with 20km resolution to examine long-term simulation. Mechanism study is conducted with finer grids model. The horizontal resolution is 10km and domain has 145 by 145 grids and 40 vertical layers as shown in Figure 1. Both configuration sets use Japanese reanalysis (JRA-25) to make initial and boundary condition data.

3. Climatological Aspect

Through the observation analysis, we found that Japan Sea side of the Central Mountainous region often undergoes foehn events. Most of these events occur under strong southerly wind. According to the composite analysis, migratory cyclonic system over Japan Sea is prominent while foehn period observed around north part of Central Mountain region. It has a key role to bring a favorable situation for foehn with strong and persistent winds.

The foehn frequency distribution derived from long-term simulation using 20km-NHRCM, which is covering the whole Japan, is basically similar to those of observation (Fig.2). Furthermore, the typical pressure patterns at the foehn event for each area appear to be similar to each other (Fig.3). Thus, 20km-NHRCM can reproduce basal characteristics features of the foehn.

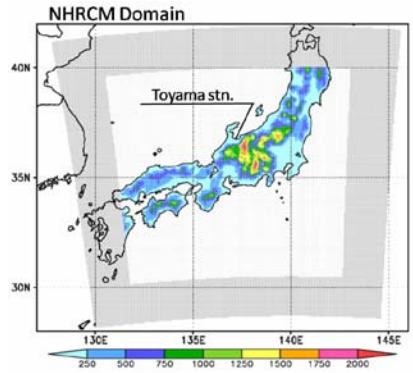

Figure 1. Calculation domain and topography. Gray colored zone indicates buffer zone.

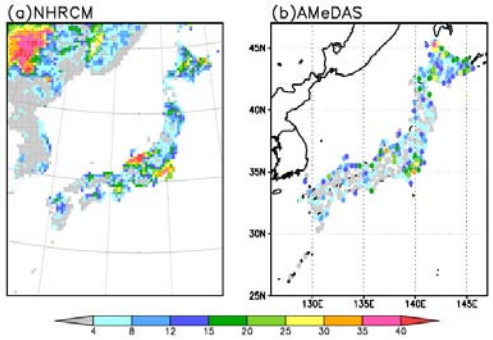

Figure 2. Frequency of occurrence of foehn events from 2002-2004. (a) is for 20km-NHRCM and (b) is derived from observational station.

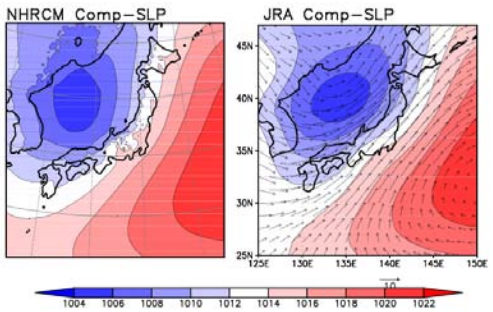

Figure 3. Composited sea level pressure for near Toyama station (see Fig. 1) derived from (a) 20km-NHRCM for 2002-2004 and (b) JRA-25 for 1979-2004.

4. Heating mechanism

In order to clarify the heating mechanism, a numerical simulation is performed. 20km resolution is considered to be insufficient for careful analysis of mechanisms, thus we decided to apply 10km resolution RCM. The calculation period is April 25 to May 6, 1998. This case has the longest foehn duration period in the observational analysis.

Compared to observations, model underestimates the maximum temperature, and enhancement of wind speeds delay. However, model can reproduce the characteristics of the event on the whole.

During the foehn period, the strong southerly wind overcomes the mountains. The potential temperature in the leeward side is much higher than those in the windward side (Fig. 4). The precipitations are observed at the mountains. Equivalent potential temperature, however, is comparable to those in the windward side. Moreover, specific humidity remarkably decreases in the lee side. These facts indicate that the warming over the leeside is associated with diabatic heating.

Backward trajectory analysis using the RCM outputs was also examined for further understanding of heating mechanism. We calculate each term of the static and moist static energy as shown in Figure 5. Gray colored bars mean altitude beneath particles at each time. The parcels travel about 6 hours across the mountain. Concurrently, the static energy increases and alternatively $L\Delta q$ decreases. Comparison of values between the windward and the leeward side shows that reduction of $L\Delta q$ contributes to the increase of $Cp\Delta T$. In other words, the diabatic heating associated with the latent heat release may have a crucial role for warming over the leeward side in this case. We also found the significant difference in the energy variation of the dry-foehn case.

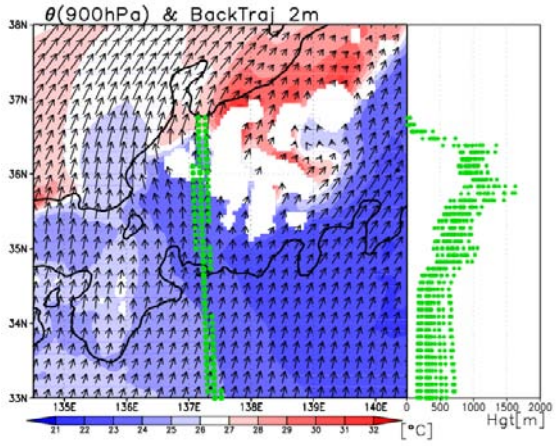

Figure 4. Potential temperature and flow pattern on 900hPa level at 03Z on May 2, 1998. Green colored dots indicate backward trajectory released from Toyama station. The right panel is height-latitude section of the trajectory.

5. Summary

In this study, the climatological feature and heating mechanism of foehn are studied by using a regional climate model. The model can represent the frequency and surrounding condition even with 20km resolution model. The foehn favorable condition can be frequently seen in spring, when many migratory cyclones travel near Japan. As for the north of the Central Mountain region, the cyclonic system or typhoon over Japan Sea is an important role to provide strong and persistent wind.

Furthermore, we attempt to clarify the heating mechanism of foehn occurred on May 2, 1998. In this case, southerly flow loses energy of Lq because of condensation in the windward side of mountains. Instead of this, the static energy increases and results in warming over the leeward side. It is particularly worth noting that there are salient differences of energy variations between wet and dry foehn.

Acknowledgements

This work was supported by the Global Environment Research Fund (S-5-3) of the Ministry of the Environment, Japan. We are deeply grateful to Prof. Kimura in University of Tsukuba for his advices and comments.

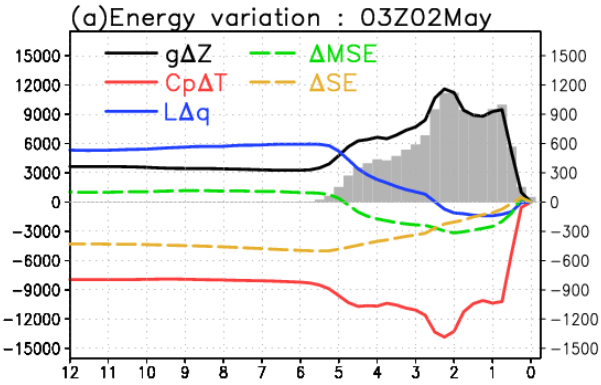

Figure 5. Mean energy variation derived from the back trajectory analysis. Each term is difference from the value at 03Z on May 2. Abscissa means time to reach Toyama station.

References

Arakawa, S., K. Yamada and T. Toya, A study of foehn in the Hokuriku district using AMeDAS data, *Papers in Meteorology and Geophysics*, Vol. 33, No. 3, pp. 149-163, 1982.

Seibert, P., South foehn studies since the ALPEX experiment, *Meteorology and Atmospheric Physics*, Vol. 43, pp. 91-103, 1990

Inaba, H., R. Kawamura, T. Kayahara and H. Ueda, Extraordinary persistence of foehn observed in the Hokuriku district of Japan in the 1999 summer, *Journal of the Meteorological Society of Japan*, Vol. 80, No. 4, pp. 579-594, 2002

Zängl, G., Deep and shallow south foehn in the region of Innsbruck: Typical feature and semi-idealized numerical simulations, *Meteorology and Atmospheric Physics*, Vol. 83, pp. 237-261, 2003

Sasaki H., K. Kurihara, I. Takayabu and T. Uchiyama, Preliminary experiments of reproducing the present climate using the non-hydrostatic regional climate model, *SOLA*, Vol.4, pp. 025-028, 2008

Errors of interannual variability and multi-decadal trend in dynamical regional climate downscaling and their corrections

Masao Kanamitsu, Kei Yoshimura, Yoo-Bin Yhang and Song-You Hong

9500 Gilman Dr. MC0224, La Jolla, CA92093, USA. mkanamitsu@ucsd.edu

1. Introduction

Alexandru et al (2007) discussed that the internal variability in regional downscaling results from two sources: (1) variability forced by the lateral boundary and by the surface characteristics, which is considered to be reproducible and (2) the internal variability simulated by regional model, which is not reproducible. Many people examined the internal variability in detail and concluded that it strongly depends on domain size, resolution, synoptic situation, variables and location.

In this paper, we show that the internal variability can further be separated into two components: (1) physically unpredictable part and (2) time varying model error. In the cases of downscaling of atmospheric analyses, the truth is known for the *analysis fields* whose scales are greater than a predetermined size for which the analysis is considered to be accurate. When estimated from the spatial density of the available observations, this scale is of the order of 500 to 1000km in most of the operationally produced global objective analysis. Thus, in the case of the downscaling of global analysis, it is possible to extract the time varying error component of the internal variability for this scale. Even more, since truth is known, it may be possible to develop a method to reduce or even eliminate the error. If we extend this notion further, in the cases of one-way nested downscaling of global model forecasts or simulations for which truth is not known, it is still reasonable to assume that the scale greater than 500-1000km is accurate in the simulation, or at least more accurate than the prediction with regional models, and thus, we can extract and correct the error part of the internal variability.

We will demonstrate that the "error" part of the internal variability is significant and contaminates the interannual variability of the large scale part and the long term linear trend of the downscaled field. It is also shown that a form of spectral nudging technique is a powerful method to reduce this error.

2. Model and experiments

The ECPC G-RSM is used in this experiment. The model is a spectral model with comprehensive physical parameterizations, and its performance has been well demonstrated in various downscaling works (e.g. Kanamitsu and Kanamaru, 2007). The model grids consist of 129 (west-east) by 86 (north-south) grid pints at approximately 60 km horizontal separation at 60N, and 28 sigma layers in the vertical. The simulations were performed for 25 summers (June 1 to August 31) and winters (December 1 to end of February the following year) from 1979 to 2003. Initial conditions and large-scale forcing are obtained from the 6 hourly NCEP-DOE reanalysis (R-2) data. Observed sea surface temperature (SST) is updated daily from the optimal interpolation SST (OISST) weekly dataset.

Three integrations are performed for summer with no Scale Selective Bias Correction (SSBC, a form of spectral nudging, detailed in Kanamaru and Kanamitsu, 2006), with original SSBC and revised SSBC in which several refinements were applied, the major ones being the use of the rotational part of the wind and removal of area averaged moisture correction. Only two experiments with no-SSBC and Revised-SSBC are performed for winter.

3. Results

Figure 1 displays the year-to-year variability of Root Mean Square (RMS) error of 500 hPa height over the domain for summer (upper panel) and winter (lower panel). The RMS difference of R-2 analysis from long time mean is also plotted as a measure of the interannual variability. It is clearly seen that without any error correction, the error is large and varies significantly from year to year. The error became larger than the interannual variability in 11 summers and 4 winters in 25 years. The error correction is working nicely as expected and the revised version corrects the error within 2-3 meters, with very small interannual variability both in summer and winter.

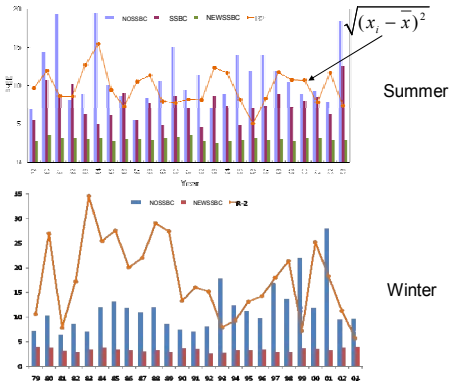

Figure 1. Interannual variability of 500 hPa height root mean square error over the domain for summer (upper panel) and winter (lower panel). NOSSBC stands for without SSBC, SSBC for original SSBC and NEWSSBC for refined SSBC. Unit in meter. Orange line indicates interannual variance of height from R-2 observation.

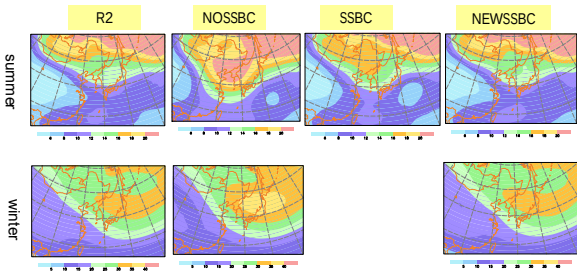

Figure 2. Geographical distribution of interannual variability of seasonal mean 500 hPa height for summer (first row) and Winter (second row). Unit in meter.

The geographical distribution of interannual variability of 500 hPa height in summer, shown in Figure 2 (first row), clearly demonstrates where the error dominates. The variability is nearly the same between R-2 and the new version of SSBC, while the run without SSBC significantly increase the interannual variability in the area near the center of the domain, where the variability is more than 30% larger than R-2. During the winter (Fig. 2, second row), the patterns of interannual variability between R2 and NOSSBA are not far apart, although without SSBC, the variability is enhanced by 10-20% in the middle of the region. The difference in interannual variability becomes more apparent when the variability is decomposed into EOFs (Figure 3). The first mode (top row) in no SSBC (second column) has quite different pattern than the others. Apparently, the regional model error produces its own interannual variability and contaminates the low frequency variability in the global forcing. Mode 2 (2nd row) for no SSBC (second column) is also very different from R2 and others. The original SSBC corrects most of the error in EOFs, but the refined SSBC makes the EOF patterns much closer to those of the R-2.

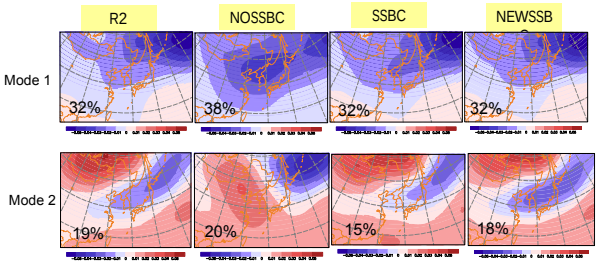

Figure 3. Leading two modes of summer time 500 hPa geopotential height EOF for analysis (R2) and experiments during summer. The percent variance is indicated by percent in each panel.

The linear trend is also affected by the model error, which is shown in Figure 4. The patterns and magnitudes of the linear trends are very different when no correction is applied, while correction works well to correct the problem.

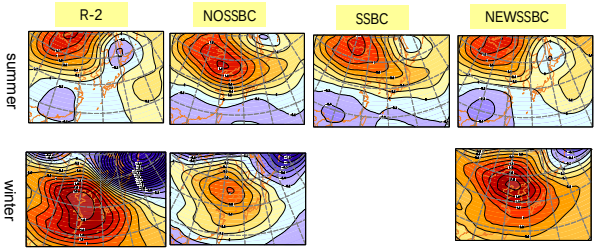

Figure 4. 1972-2005 linear trend of 500 hPa height for summer (upper panels) and winter (lower panels). Unit in meter/10 years.

Figure 5 is the EOF of precipitation during summer for Mode 1, the patterns of model simulations are not so close to the observed pattern, but NEWSSBC and SSBC resemble more with CMAP than that of NOSSBC. Somewhat disorganized EOF patterns in model simulations indicate that the model response is weaker to interannual variability in large scale forcing, but the correction of large scale certainly helps in improving the simulation of precipitation variability.

4. Conclusions

In this paper, it is demonstrated that conventional dynamical downscaling methods without any large scale error corrections suffer from large scale regional model error that contaminates interannual variability and linear trend of downscaled fields. The error also contaminates low frequency variability and trend of derived fields, such as precipitation. The effect of model error on the variability is greater in summer time, as the magnitude of the error is comparable to the interannual variability of seasonal mean.

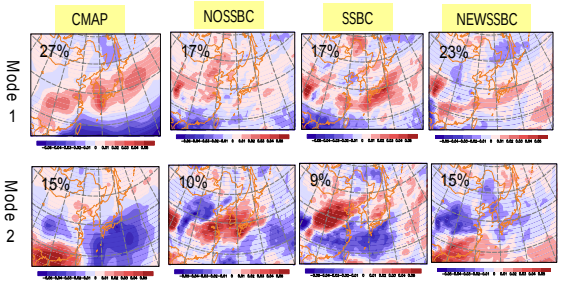

Figure 5. First two leading EOF of seasonal mean precipitation during summer from observation (R-2) and experiments.

These errors can be corrected nicely by introducing Scale Selective Bias Correction method. However, the impact of correcting large scale error in simulating precipitation and near surface temperature was found to be modest. This somewhat reduced impact is due to the inaccuracies in the precipitation process in the model, which is not able to faithfully reproduce observed precipitation given large scale forcing, particularly its interannual variability. However, the modest impact implies that even with somewhat deficient parameterization, the correction to large scale forcing works positively to reduce error and improve dynamical downscaling.

The large scale model error examined in this paper would be a strong function of the choice of the model domain, its location, model resolution and physics of the model. It is very likely that the error increases as the domain size increase. In this regard, it seems important to apply SSBC to all the cases, which have a potential of improving the simulations of mean as well as interannual variability.

Regarding the use of SSBC in the downscaling of GCM simulations, for which truth is not known, our recommendation is to utilize it fully. Although it is not possible to obtain large scale regional model error, it is more logical to faithfully apply the large scale forcing simulated by the global model without altering it by the regional model. It should be emphasized again that the dynamical downscaling is a diagnostic tool to obtain small scale features forced by given large scale forcing, thus the large scale forcing should not be modified during the downscaling procedure.

References

Alexandru, A., R. de Elia, and R. Laprise, 2007: Internal variability in regional climate downscaling at the seasonal scale *Mon. Wea. Rev.* **135**, 3221–3238

Kanamaru H. and M. Kanamitsu, 2006: Scale selective bias correction in a downscaling of global analysis using a regional model, *Mon. Wea. Rev.***135**, 334-350.

Kanamitsu, M. and H. Kanamaru, 2007: 57-year California Reanalysis downscaling at 10km (CaRD10) Part I. System detail and validation with observations. *J. Climate,* **20,** 5527-5552.

Sensitivity of the simulated East Asian summer climatology to convective schemes using the NCEP regional spectral model

Hyun-Suk Kang[1], Song-You Hong[2], and Won-Tae Kwon[1]

[1]Climate Research Laboratory, National Institute of Meteorological Research, Korea Meteorological Administration
[2] Department of Atmospheric Sciences, Yonsei University. [1]Email: hyunsuk@kma.go.kr

1. Introduction

The representation of subgrid-scale precipitation process is known as the cumulus parameterization. Several cumulus parameterization schemes (CPSs) are available for regional and global atmospheric models; however, they do not explicitly resolve the convective clouds. Therefore, the CPS has been considered as one of the most challenging and uncertain aspects in numerical atmospheric modeling. Different CPSs have distinct design history; in some cases, these schemes have completely different conceptual under-printings. In this context, the objective of this study is to examine the sensitivity of the simulated East Asian summer monsoon's (EASM) climatology to the four CPSs within the National Centers for Environmental Prediction (NCEP) Regional Spectral Model (RSM) (Juang and Kanamitsu, 1994; Juang et al., 1997). The RSM is capable of reproducing the EASM in 1987 and 1988 (Hong et al., 1999). In addition, Hong and Choi (2006) investigated the sensitivity of the 1997 and 1998 EASM to three CPSs with the RSM; however, a study on the sensitivity of the long-term climatology of the EASM to physical processes has been rarely conducted.

2. Model and Experiments

The spectral representation of the RSM is a two-dimensional cosine series for perturbations of pressure, divergence, temperature, and mixing ratio, and a sine series for vorticity. Linear computations such as horizontal diffusion and semi-implicit adjustment are only considered as perturbations, which eliminates the error due to the re-evaluation of linear forcing from base fields by the regional model. The physical processes in the RSM follow the package of Hong and Leetmaa (1999).

The model grids consist of 109 (west-east) by 86 (north-south) grid lines at approximately 60 km horizontal separation, and 28 sigma layers in vertical separation. Initial conditions and large-scale forcing are obtained from the 6 hourly NCEP-DOE reanalysis (R-2) data (Kanamitsu et al., 2002). Observed sea surface temperature (SST) is updated daily from the optimal interpolation SST (OISST) weekly dataset. The three-month-long simulations were conducted starting on June the 1st for ten years from 1997 to 2006. Four different CPSs - SAS, RAS, CCM, and KF2 schemes - were used to study the sensitivity of the EASM to cumulus effects. By and large, the four CPSs exhibit unique features. The SAS scheme has been operational in the NCEP global forecast system. Thus, its performance has been evaluated for weather systems all over the world, whereas the RAS outperforms the SAS in reproducing the climate signal in response to the SST anomalies over the tropics. The CCM and KF2 schemes have been successfully applied to climate and mesoscale modeling studies, respectively, using the NCAR CCM and MM5 models. Hence, it would be interesting to clarify the characteristics of the four CPSs in the simulation of summer monsoonal rainfall over East Asia.

3. Results

3.1 Large-scale Circulations

The 10-year averaged JJA precipitation of the GPCP data represents monsoonal rain bands extending northeastward from southern China to the southern part of the Korean peninsula and Japan (Fig. 1a). In association with the monsoonal rain band, the southerly and/or southwesterly low-level jet (LLJ) transports significant moisture from southern China and the South China Sea across Korea to Japan, along the western periphery of a subtropical high over the northwestern Pacific (Fig. 1b). The climatology of the upper atmospheric circulation provides favorable dynamic circulation for the monsoon precipitation in the upper level with an anticyclonic (divergent) circulation above the monsoonal front (Fig. 1c, d).

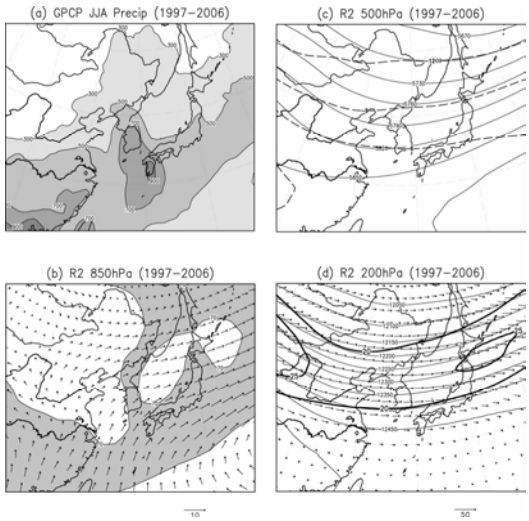

Figure 1. The analyzed 10-year JJA climatology averaged over 1997-2006 for (a) precipitation (mm), (b) 850 hPa winds and relative humidity (> 70%), (c) 500 hPa geopotential height and temperature, and (d) 200 hPa geopotential height and winds.

Overall, the RSM successfully reproduces the large-scale patterns, regardless of the selected CPS. The PC coefficients reveal relatively less skill in the simulation of the lower-level fields. The LLJ transporting warm and moist air from the south to the heavy rainfall region is one of the principle components, which is captured by all experiments, but with a certain systematic biases. A common wet bias appears in northwestern part of the model domain, and a dry bias in its south. Compared to the results from other schemes, dryness is pronounced in the CCM run, particularly, over southern China and the ocean. In the CCM run the humidity bias is the largest, but temperature bias is the smallest. The deviations in the 500 hPa geopotential height (GPH) also show similar error patterns for SAS, RAS, and KF2 runs, which reveal a decrease in height along a continental trough, indicating an exaggerated trough to the west of the Korean peninsula.

The CCM scheme reveals a distinct increase in heights over the domain centered over the East Sea, indicating a weakening of the mid-latitude trough. The bias and RMSE in 500 hPa GPH are relatively small when the KF2 scheme is introduced compared to the other runs.

Figure 2 shows the fractional change in power spectrum for the vertically integrated kinetic energy of zonal wind from the surface to 200 hPa. Both the RAS and CCM runs are not adding any large-scale information compared to that of the SAS run in the long-wave spectral regime. Between the 240 and 450 km range, the RAS and CCM runs produce much more spatial variability than the SAS run, by up to 20~30%, with a slightly more variability in the CCM run near the Nyquist wave number range. The KF2 scheme produces extremely high spatial variability in all length scales compared to the other three runs. This implies that the KF2 scheme effectively adds regional information than any other convection schemes both in the meso- and synoptic-scale (from 240 to 6420 km in this study) regimes.

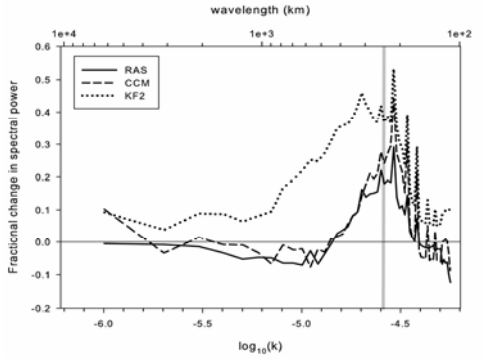

Figure 2. Fractional changes in spectral power versus wave length for the vertically integrated kinetic energy of zonal wind component from the surface to 200 hPa with respect to the spectral power of the SAS run. The thick gray vertical line indicates the wavelength of $4\Delta x$ (240 km).

3.2 Precipitation

Table 1 shows that the simple statistics in the precipitation climatology simulated by the SAS and KF2 schemes are comparable to what was observed. In particular, all three skill scores (bias, RMSE, and spatial correlation) are better in the SAS run than in any other runs. In contrast to the others, in terms of domain average, the CCM run tends to overestimate the amount of precipitation due to the spurious oceanic rainfall at lower latitudes, which is the major characteristic of the CCM scheme and results in the degradation of the simulation skill for precipitation. It is interesting to note that the spatial distribution of monsoonal precipitation simulated by the SAS and KF2 schemes are very similar, although the SAS scheme produces more convective precipitation than the KF2 scheme. The fraction of total precipitation produced by the convective parameterization is more than 20% higher for the SAS scheme and 10% higher for the CCM scheme compared to the KF2 and RAS schemes. The observed monthly rainfall averaged over the entire domain exhibits minimal monthly variation, with a slight precipitation decrease from June to August. None of the schemes reproduced the observed trend; all schemes simulated a relatively enhanced precipitation in August (not shown).

4. Summary

On the whole, there is no single scheme that outperforms the others in all aspects of the simulated climatology. The results show that the SAS and KF2 schemes are capable of reproducing the 10-yr JJA climatology with a certain wet bias over land and dry bias over the oceans. The SAS scheme is capable of resolving the interannual variations of the monsoon precipitation, and the KF2 is able to capture the intraseasonal variation. The RAS scheme reduces significantly precipitation over land compared to other schemes, but interannual variabilities are reasonably reproduced. On the contrary, the CCM scheme significantly overestimates the precipitation over land as well as ocean. Discernable differences among four CPSs are found in the distribution of spatial spectrum, in which the KF2 scheme is the most effective in adding regional details to external large-scale forcing. The feasibility of a physics ensemble using different convection schemes and the impacts of domain size will also discussed in the presentation.

References

Hong, S.-Y., H.-M. H. Juang, and D.-K. Lee, Evaluation of a regional spectral model for the East Asian monsoon case studies for July 1987 and 1988. *J. Meteorol. Soc. Jpn*, 77, 553-572. 1999.

Hong, S.-Y., and J. Choi, Sensitivity of the simulated regional climate circulations over East Asia in 1997 and 1998 summers to three convective parameterization schemes, *J. Korean Meteor. Soc.*, 42(6), 361-378. 2006.

Hong, S.-Y., and A. Leetmaa, An evaluation of the NCEP RSM for regional climate modeling. J. Clim., 12, 592-609. 1999.

Juang, H.-M. H., and M. Kanamitsu, The NMC nested regional spectral model, *Mon. Weather Rev*., 122, 3-26. 1994.

Juang, H.-M. H., S.-Y. Hong, and M. Kanamitsu, The NCEP regional spectral model: An update. *Bull. Am. Meteorol. Soc.*, 78, 2125-2143. 1997

This work was funded by the Grant CATER_2007-4406 of the Korea Meteorological Administration (KMA) and the grant NIMR-2009-B-2 of the National Institute of Meteorological Research/KMA.

Table 1. Statistical skill scores for the simulated precipitation. Bold is the best skill among the experiments and bold italic is the better skills between the physics ensemble and simple average of skill scores from each experiment.

Experiment	Bias (mm/day)	RMSE (mm/day)	Spatial correlation	Fraction of convective rain (%)	Temporal correlation for JJA anomaly	Temporal correlation for daily precipitation
SAS	**-0.02**	**1.65**	**0.70**	78	**0.72**	0.51
RAS	-0.71	1.90	0.59	56	0.66	0.35
CCM	0.70	2.75	0.49	67	0.50	0.35
KF2	-0.26	1.71	0.64	56	0.58	**0.58**
Ensemble	-0.07	***1.67***	***0.66***	66	***0.64***	***0.52***
Average	-0.07	2.00	0.60	64	0.61	0.45

Study of climate change over the Caspian Sea basin using the climate model PRECIS at 2071-2100

Maryam Karimian1,2, Iman Babaeian1,3, Rahele Modirian1,2

1-Climate Change Lab. Climatological Research Institute, Mashad, I.R. of Iran, P.O. Box: 91735-676
2-MSc Student of Physics, Islamic Azad University of Mashhad
3-PhD Student of Climatology, Tabriz University
E-mail: mkarimiyan59@yahoo.com

The Caspian Sea is the largest enclosed body of water on the earth, covering approximately 4×104 Km^2 and sharing its coast whit five countries (Iran, Azerbaijan, Kazakhstan, Russia and Turkmenistan). Because it has no outlet to the ocean the Caspian Sea level (CSL) has undergone rapid shifts in response to climatic forcing, and these have been devastating for the surrounding countries. The Caspian Sea region is of much economic and environmental interest to the world. In addition to being home to many different plant and animal species, it is the major source of oil and natural gas and produce 90% of the world's caviar. In this paper, we present impact of climate change at Caspian Sea region for the period 2071-2100. Interested region has Simulated with A2 & B2 scenario by using Climate model PRECIS at a 50 km grid spacing. In this period, precipitation will be increase over southwestern of Caspian Sea and will decrease in other region. Also, temperature will be increase especially over Caucasus and Elburz mountains.

Key words: Caspian Sea, Climate Change, PRECIS, temperature, precipitation

Performance of pattern scaling in estimating local changes for untried GCM-RCM pairs: Implications for ensemble design

Elizabeth Kendon

Met Office Hadley Centre, Exeter, UK; elizabeth.kendon@metoffice.gov.uk

1. Introduction

Pattern scaling techniques have been widely used to provide climate change projections for time periods and emission scenarios that have not been simulated by GCMs. The assumption underlying these methods is that the geographical pattern of the change is independent of the forcing. Thus the local response of a climate variable is assumed to be linearly related to the global mean temperature change, with the scaling coefficient only dependent on position. This condition is largely satisfied for mean temperature and to a lesser degree precipitation (*Mitchell et al., 1999; Mitchell, 2003*).

In this study, we assess whether pattern scaling methods can be used to estimate changes at the RCM scale for a full range of driving GCMs. The availability of GCM simulations raises the possibility of using anomalies at the GCM scale, rather than global mean temperature change, as the predictor of the local climate response. Thus the change in the RCM for a given variable is expressed as:

$$\Delta\ RCM_{xsye} = A_{xs}\ \Delta\ GCM_{xsye}$$

where the scaling coefficient A depends on position (x) and season (s), but not on year or period (y) or forcing scenario (e). ΔRCM is the change in the RCM and ΔGCM is the corresponding change for the given variable in the nearest GCM grid box. The basis for this 'local scaling' method (Fig. 1) is that regional patterns of precipitation are produced predominantly by the interaction between large-scale systems and the stationary topography (*Widmann et al., 2003*).

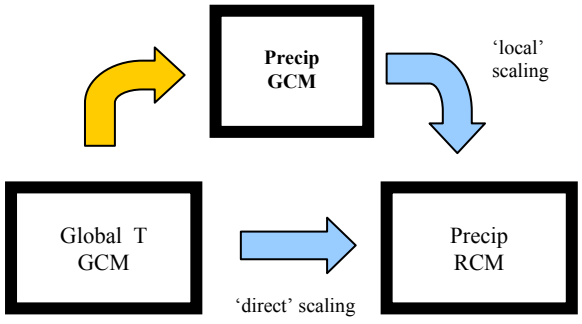

Figure 1. Schematic illustrating the 'local scaling' method as compared to traditional 'direct' pattern scaling techniques.

In this study we examine whether this simple local scaling relationship can be used to predict the local change for untried GCM-RCM pairs i.e. to what extent the scaling coefficient A can be assumed to be independent of the driving GCM. We examine the accuracy of this technique both for time-mean variables and for measures of variability and extremes, focusing on temperature and precipitation across Europe. The implications of this for GCM-RCM ensemble design are discussed.

2. Methodology

We use data from the Rossby Centre regional climate model RCA3 driven by a 3-member initial condition ensemble of ECHAM5 and by 3 members of the Hadley Centre perturbed physics ensemble of HadCM3, specifically the standard model HadCM3-Q0, and the low and high sensitivity experiments HadCM3-Q3 and HadCM3-Q16 respectively. For each of the 6 RCA3 simulations and the corresponding driving models, we calculate various statistics of the daily precipitation and temperature distributions, for each season, for the control 1961-89 and future 2071-99 periods.

The 3-member ensemble of ECHAM5 driven integrations allows us to examine the importance of natural variability. Using the method outlined in *Kendon et al. (2008)* we identify where the change in a given statistic in the RCM is significant compared to natural variability, and in particular, we only assess the performance of pattern scaling where the RCM change is robust.

At each grid box and for each variable, where the change is found to be robust, the scaling coefficient A is calculated using linear regression applied to the 3 member ensemble of ECHAM5 driven runs. The resulting relationship is then used to estimate the RCM change for each of the HadCM3 driving GCMs, and compared with the actual simulated RCM change.

3. Preliminary results

For precipitation in winter, where changes are robust compared to natural variability, local scaling generally performs well in estimating RCM changes for a different driving GCM (with errors from scaling less than 50%). This is true both of changes in mean precipitation, and also changes in variability and extremes. In summer, changes in daily precipitation statistics are not robust compared to natural variability in many regions across Europe. However, where changes are robust in the case of summertime mean precipitation and wet day frequency, local scaling does not perform well.

For temperature, local scaling generally performs well in estimating local changes in mean and extremes, in both winter and summer. However there is some evidence of reduced scaling performance in coastal regions and snow/ice margins in winter and for temperature extremes in a band across central and northern Europe in summer. Changes in temperature variability are found not to be

robust compared to natural variability across much of Europe.

These preliminary results, along with recent further analysis, will be presented and physical explanations suggested for the performance of pattern scaling. The implications for GCM-RCM matrix design, and in particular the extent to which uncertainty in local climate change may be adequately represented using a reduced RCM ensemble, will be discussed.

References

Kendon, E.J., D.P. Rowell, R.G. Jones and E. Buonomo, Robustness of future changes in local precipitation extremes, *J. Climate*, 21, pp. 4280-4297, 2008

Mitchell, J.F.B, T.C. Johns, M. Eagles, W.J. Ingram, and R.A. Davis, Towards the construction of climate change scenarios, *Clim. Change*, 41, pp. 547-581, 1999

Mitchell, T.D., Pattern scaling: An examination of the accuracy of the technique for describing future climates, *Clim. Change*, 60, pp. 217-242, 2003

Widmann, M., C.S. Bretherton and E.P. Salathe, Statistical precipitation downscaling over the northwestern United States using numerically simulated precipitation as a predictor, *J. Climate*, 16, pp. 799-816, 2003

Evaluation of the analyzed large-scale features in a global data assimilation system due to different convective parameterization scheme and their impact on downscaled climatology using a RCM

Jung-Eun Kim and Song-You Hong

Department of Atmospheric Sciences, Yonsei University, Seoul, Korea, japril@yonsei.ac.kr

1. Introduction

Despite the successful application of the RCMs to dynamical downscaling for climate change assessement and seasonal climate predictions, the regional predictability and the evaluation of added values to the GCM outputs are still not clarified. As reviewed by Giorgi et al. (2001), Leung et al. (2003), and Wang et al. (2004), the errors in the downscaled regional climate within a nested RCM result from the 1) uncertainties in the large-scale fields driven by GCM and the related unphysical treatment of the lateral boundary conditions, 2) inaccuracies in the physics and dynamics in the RCM, and 3) inconsistency between the regional and global models in dynamics and physics. The treatment of the lateral boundary conditions, the physics and dynamics in the RCM has significantly been improved by the RCM community. However, the first and fourth issues are still open to the questions.

The skill of an RCM in dynamical downscaling applications is highly dependent upon the skill of the driving GCM. However, substantial differences among several reanalysis datasets, in particular, in the lower-atmospheric circulations and water vapor flux, lead to another complexity in improving the RCM (Annamalai et al. 1999). The consistency between the GCM and RCM is even difficulty issue to explore since the physics package between the two models is usually not consistent. These two issues are rather clear in future development of the RCM, but the uncertainty due to the inconsistency in the internal forcing due to physical parameterizations has to be explored to clarify the RCM's predictability. Our study aims to explore the impact on the regional downscaling embedded within large-scale climate information due to different convective parameterization scheme

2. Experimental Design

The predicted large-scale features are obtained by the perfect large-scale experiments runs (GDAS) that are forced by an analyzed data. The National Centers for Environmental Prediction (NCEP) regional spectral model (RSM) is used in this study for downscaling. A detailed model description is provided by Juang et al. (1997). To discuss the uncertainty due to the inconsistency of different cumulus convective parameterization scheme, two sensitivity experiments are conducted; the simplified Arakawa-Schubert (SAS; Hong and Pan 1998) and community-climate model (CCM; Zhang and McPhalane 1995) schemes. The summer of 2004 was selected in this study, which recorded a near-normal seasonal precipitation in East Asia (Fig.1a).

3. Result

Figures 1b and 1c show the JJA precipitation from the CCM and SAS experiments in GDAS, respectively. It is seen that both runs reproduce the observed precipitation well. Over land, the local maxima in central China, Korea, and southern Japan, are commonly captured, irrespective of the convection scheme in the GDAS. Oceanic precipitation over the sub-tropics is fairly well simulated. Precipitation in Mongolia and Siberia is excessive when the CCM scheme is used in the GDAS run. The pattern correlation of JJA precipitation is 0.52 and 0.70, for CCM and SAS experiments, respectively.

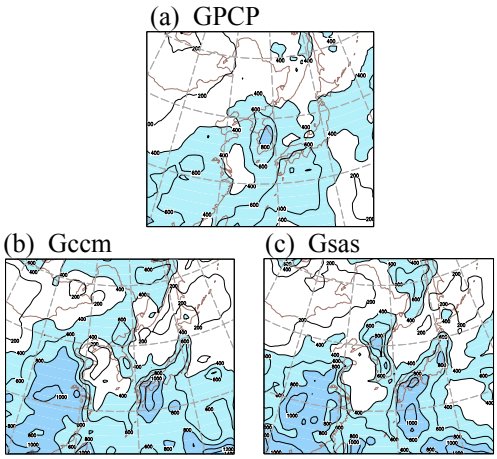

Figure 1. (a) Observed JJA accumulated rainfall from GPCP and the simulated precipitation (mm) from (b) CCM and (c) SAS runs in GDAS.

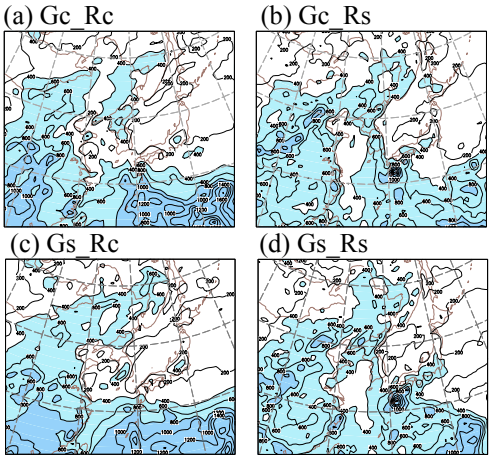

Figure 2. Simulated 3-month (JJA) accumulated precipitation (mm) from RCM experiments forced by GDAS.

Figure 2 shows that the distribution pattern of downscaled precipitation using the RCM depends more on the convection scheme in the RCM, rather than that used in the mother-domain experiments. An excessive precipitation over the southern China and East China Sea regions is commonly observed when the CCM scheme in

used in RCM. To be consistent with excessive precipitation in the low-latitude regions in the case of the RCM runs with CCM, the intensity of trough in China and subtropical oceanic high is strengthened.

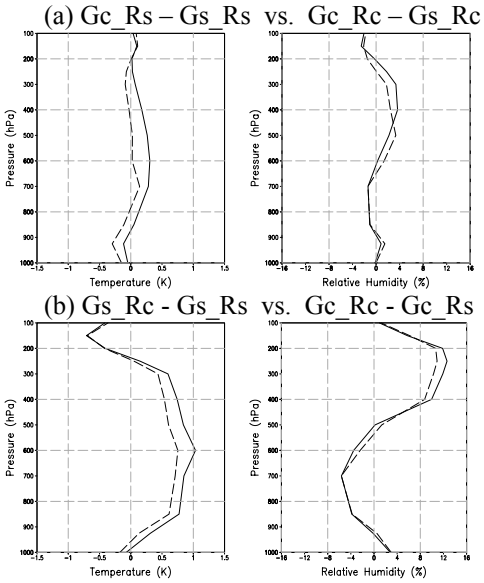

Figure 3. Vertical profiles of the difference in temperature (K) and relative humidity (%). Upper panel designates the difference between Gc_Rs and Gs_Rs (solid line) and Gc_Rc and Gs_Rc (dashed line) and lower panel shows the the difference between Gs_Rc and Gs_Rs (solid line) and Gc_Rc and Gc_Rs (dashed line), respectively.

The influence of the large-scale features from the GDAS is better seen in Fig. 3. In this figure, it is seen that the characteristics of the differences in the vertical profiles of temperature and moisture in the global analyses appear in the downscaled climate. A relative warming in the middle troposphere and cooling in the lower troposphere exist in the case of CCM-GDAS run, as analyzed in the GDAS runs. Moistening in the upper troposphere is also visible. These vertical structures are distinct when the RCM employed the different convection scheme.

4. Summary

This study explores the one of the uncertainties for regional downscaling with the regional climate models (RCMs) of the climate signals from the general circulation models (GCMs); the inconsistency in physical parameterization between GCM and RCM. The results showed that the better large-scale data result in improved regional climate. In the seasonal simulation framework, the dependency of the GCM-generated large-scale conditions on the downscaled climate is as much as the regional model physics in terms of the large-scale forcing. The consistency in physical parameterizations between the GCM and RCM is the one of the factors to alleviate uncertainties in regional downscaling.

References

Annamalai, H., J. M. Slingo, K. R. Sperber, and K. Hodges, The mean evolution and variability of the Asian summer monsoon: Comparison of ECMWF and NCEP-NCAR reanalysis, *Mon. Wea. Rev.,* 127, 1157-1186, 1999

Giorgi, F., and co-authors, Regional climate information-Evaluation and projections. Chapter 10 in Climate Change 2001: The Scientific Basis, *Cambridge University Press, Houghton et al. (Eds.),* 881pp, 2001

Hong, S.-Y., and H.-L. Pan, Convective trigger function for a mass flux cumulus parameterization scheme, *Mon. Wea. Rev.,* 126, 2599-2620, 1998

Juang, H.-M. H., S.-Y. Hong, and M. Kanamitsu, The NCEP regional spectral model: An update, *Bull. Amer. Meteor. Soc.,*78, 2125-2143, 1997

Wang, Y., L. R. Leung, J. L. McGregor, D.-K. Lee, W.-C. Wang, Y. Ding, and F. Kimura, Regional climate modeling: Progress, Challenges, and Prospects, *J. Meteor. Soc. Japan,* 82, 1599-1628, 2003

Zhang G. J., and N. A. McPhalane, Sensitivity of climate simulations to the parameterization of cumulus convection in the Canadian climate centre general circulation model, *Atmos-Ocean,* 33, 407-446, 1995

Sensitivity studies with a statistical downscaling method, the role of the driving large scale model

Frank Kreienkamp, Arne Spekat and Wolfgang Enke

Climate & Environment Consulting Potsdam GmbH, Telegrafenberg A31, 14473 Potsdam,
frank.kreienkamp@cec-potsdam.de

The sensitivity of the statistical downscaling method WETTREG (Enke et al. 2005a, Enke et al. 2005b), will be presented and compared with results of the regional models REMO and CCLM.

WETTREG analyzes the time evolution of circulation pattern frequencies in climate model control runs and scenarios and its consequences for local climate parameters. Several global models (BCCR, CGCM, and ECHAM) and one regional model (CCLM) have been used in their pattern-generating capacity to derive the WETTREG input. Moreover, several generations and runs of the same model are analyzed. In an additional experiment, an extrapolation of the recent trends in pattern frequency into the near future and the resulting short-term temperature and precipitation trends are investigated. The results show model-dependent distinctive features concerning the reconstruction of the current climate, albeit of small magnitude. With respect to short-term climate trends for the target time frame 2011--2030, the model-specific bandwidth is strongest in winter and weakest in summer when temperature is concerned (Figure 1 and 2) and rarely leaves an ± 10% envelope when percentual change of precipitation is concerned (Spekat et al. 2008).

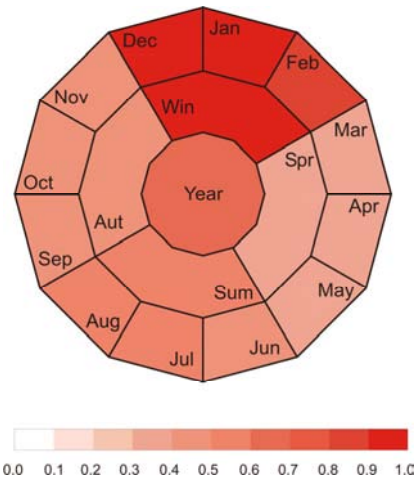

Figure 1: Ring diagram of the temperature signal for the time frame 2010--2030 (scenario A1B) minus 1971--2000 (20C control run) across all models investigated. The outer ring depicts the monthly values, the middle ring gives the seasonal values and the center dodecahedron shows the rise in annual temperature.

Acknowledgements

This work was made possible by funds from the State of Baden-Württemberg, grant 23-8801.10. The authors further acknowledge the assistance of A. Hense, R. Hagenbrock and C. Schölzel of the Bonn University with respect to data acquisition and H.-J. Panitz of the Karlsruhe Research Center with respect to CCLM data processing. The data from the climate stations are courtesy of the German Weather Service.

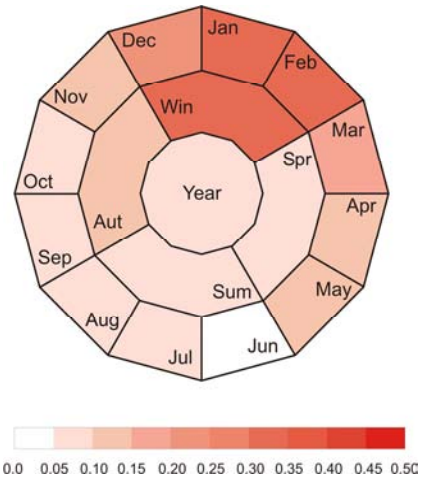

Figure 2: Ring diagram of the temperature variance computed for the time frame 2010--2030 (scenario A1B) minus 1971--2000 (20C control run) across all models investigated. The outer ring depicts the monthly values, the middle ring gives the seasonal values and the center dodecahedron shows the variance of the annual temperature.

References

Enke, W.; Deutschländer, Th.; Schneider, F.: Results of five regional climate studies applying a weather pattern based downscaling method to ECHAM4 climate simulations. *Meteorol Z*, Vol. 14, S. 247-257, DOI: 10.1127/0941-2948/2005/0014-001. 2005

Enke, W.; Schneider, F.; Deutschländer, Th.: A novel scheme to derive optimised circulation pattern classifications for downscaling and forecast purposes. *Theoretical and Applied Climatology*, DOI: 10.1007/s00704-004-0116-x. 2005

Spekat, A.; Enke, W.; Kreienkamp, F. **:** Probabilistische Abschätzung regionaler Klimaänderungen der kommenden Dekaden und ihre Unsicherheiten (PArK): Anwendung von Methoden zur Abschätzung regionaler Klimaänderungen der kommenden Dekaden, Szenarienrechnungen mit WETTREG. Abschlussbericht. Im Auftrage des Landes Baden-Württemberg, vertreten durch das Umweltministerium (UM), dieses vertreten durch die Landesanstalt für Umwelt, Messungen und Naturschutz Baden-Württemberg, Karlsruhe. AZ 23-8801.10. 40pp. 2008

MPI regional climate model REMO simulations over South Asia

Pankaj Kumar, Ralf Podzun and Daniela Jacob

Max Planck Institute for Meteorology, Hamburg, Germany. e-mail: pankaj.kumar@zmaw.de

1. Abstract:

Climatological features associated with South Asian summer monsoon (June-Sept.) is examined on intrannual time scale by Max Planck institute for meteorology (MPI) regional climate model REMO with a focus over India. The objective is to validate the model over the region and identify the strength and weakness of the model. Before making a climate simulation, various sensitivity experiments have been performed to validate the model over the region. Climate simulation have been performed for the period 1979-1993 at 0.5 degree resolution forced by ERA15. Results showed that the regional model is able to simulate the mean monsoon climate reasonably well while comparing with the observed climatologies. The complex topographical precipitation pattern, and the mean annual cycle of precipitation and 2m-temperature is well simulated by the model both over model domain and over the India. Model is showing a cold temperature bias of nearly 1 deg C in DJF season and a positive bias over India of nearly same magnitude in the month of May and June, also during monsoon season model has simulated 10% less mean precipitation over India. The circulation pattern simulated by the model is fairly well though with some limitations.

2. Introduction:

Over 60% of the world population lives over South Asia (SA). The majority of people over this region depend on agriculture for their livelihood, that primarily depend on monsoon rainfall. Rainfall occurrence over this region is very limited and occurs mainly during summer accounting 70-90% over major part of the region and has a strong influence on the whole economy of the region. In view of the importance of SA monsoon on the economy of the region, it will be interesting to examine the phenomenon using a regional climate model (RCM).

Climate modelling over SA region is a challenging task due highly complex interaction between land, ocean and atmosphere and most of the GCMs fails to simulate the spatial pattern of precipitation both over land and ocean, *Gadil and Sajaini* (1998). Developing a high resolution models on a global scale is not only computationally prohibitively expensive for climate change simulations, but also suffers from errors due to inadequate representation of climate processes.

Regional model studies over SA, *Jacob and Pozdum* (1997), *Rupa Kumar et al.* (2006), *Ratnam et al* (2008) have reported an improvement in the simulation of spatial and temporal distribution, particularly land precipitation but also a general over estimation of the rainfall over ocean.

In the present study, Max-Planck Institute for Meteorology, REgional MOdel (REMO) has been used to the study the SA summer monsoon with a focus over India to validate the model over the region for climate change studies.

3. Data and Model:

Data: The observational data of precipitation and surface air temperature (2m) used to validate the model results have been taken from Climate Research Unit (CRU) of the University of East Anglia, which covers the entire globe at a horizontal resolution of 0.5^0 x 0.5^0 (hereafter referred as CRU) for the period 1979-1993, *New et al.* (2000).

The initial and lateral boundary conditions for regional model simulation is derived from ERA15 at a horizontal resolution of T106 (1.125^0 x$1.1.25^0$) at a interval of 6hr. The ERA15 data are interpolated to model grid and levels to compare the model results.

Model: REMO is a three dimensional hydrostatic atmospheric circulation model which solve the discretization primitive equations of the atmospheric motion. REMO, *Jacob* (2001) is a combination of two models, dynamical core and discretization in space and time has been taken from European Model and Physics has been taken from ECHAM4 (GCM of MPI).

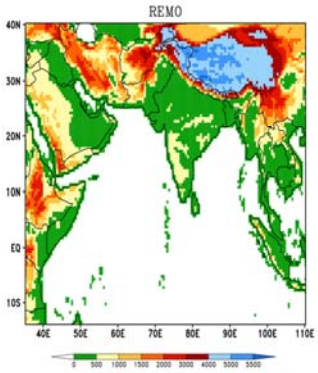

Figure-1: Orography and model domain over south Asia

Three sensitivity experiment have been performed for the period 1987-1988 to validate the model over the region. REMO was run on climate mode with a horizontal resolution of 0.5^0 (~55 Km) using physical parametrization scheme from ECHAM4/T106 for the period 1979-1993 forced by ERA15 reanalysis. Model domain and topography are shown in in Figure-1, it has 151x109 horizontal grids and 27 vertical levels.

4. Sensitivity experiments

In REMO, soil hydrology can be represented by two ways: First by a bucket type soil module *Dumenil and Todini* (1992) where each gridbox is represented by a single soil water reservoir i.e. the depth of the bucket and therefore the water available for evaporation, is defined by the rooting depth of the plants. This scheme is called without five soil layer (W5SL). Second, by a five soil layer (5SL) scheme, in which soil hydrology is defined in five discrete layers up to 10 meters or bedrock.

The model simulation with 5SL for the period 1987-1988, shows a positive 2m temperature bias over the Indian subcontinent when compared to observed CRU, whereas second simulation for the same period W5SL have shown a similar result but the magnitude was less compared to 5SL. In REMO soil has been described as medium moist, whereas over SA, soil is basically dry throughout the year except for the monsoon months, therefore, we have changed the heat capacity and diffusivity of the soil from medium moist type to dry type *Gordon B.* (2002) and made a third simulation (Ref) for the same period. Results are presented in the figure-2. Upper panel is the difference from Ref to W5SL, which show a significant realistic drop in 2m temperature over Indian subcontinent by 2-4 ^{0} C, whereas middle panel show the difference form Ref to

5SL, the results suggest that 5SL is much warmer then the W5SL

Air sea interaction plays a important role in influencing the monsoon circulation. The ocean roughness determines the the turbulence level near the air sea interface and wind stress. Charnok's relation, *Charnok* (1995) as a function of wind stress determines the ocean roughness length. Its value depend on the surface condition and varies from 0.01 to 0.048 for an average wind speed greater the 5m/s and is a dimensionless quantity. In REMO standard version the Charnok constant value is 0.0123. To check the impact of Charnok constant over Indian ocean (IO) we have made two model simulation one by increasing the value 0.032 and other by decreasing the value to 0.0012. By decreasing the the Charnok value over IO have showing significant improvement over ocean and land precipitation. Figure-2 lower panel shows the difference plot of precipitation intensities between Ref and 5Sl simulation, significant realistic difference both over IO, Bay of Bengal and over Indian plains, almost similar results were noticed with W5SL. Model is showing a much better simulation with dry soil and reduced Charnok's constant value. Therefore, climate simulations are performed by incorporating all these changes in the model with W5SL version for the period 1979-93 forced by ERA15 lateral boundary conditions. Results are highlighted in the next section.

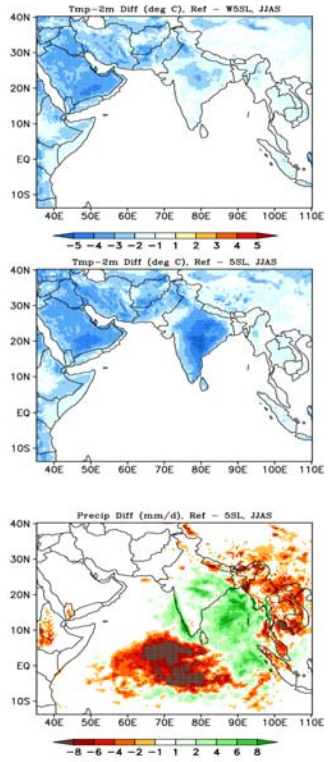

Figure-2: Difference plot of REMO 2m temp, upper panel is Ref. run -W5SL and middle panel is Ref – 5SL. Lower panel is the precipitation intensities difference form Ref - 5SL.

5. Results

The main highlights of the climate simulation are as follows

- The annual cycle of precipitation and 2m temperature is well simulated by the model both over model domain (Fig-3) and over India (Fig. not shown). Over model domain (India) schematic cold bias is noticed during the winter up to 1^0 C (2^0 C) and mean JJAS monsoon precipitation is 10% less simulated by the model over India, when compared to CRU.
- The Somali jet at 850 hPa and tropical easterly Jet (TEJ) at 200hPa is well simulated by the model, though the intensity of TEJ is 2-4 m/s less when compared to observed (ERA15).
- The spatial pattern of model simulated mean JJAS precipitation shows that the chief features like rainfall maxima over land, orographic precipitation over western ghats and foothills of Himalaya is well simulated by the model, but over Indo-Gangetic belt (monsoon trough region) model is simulating less precipitation, witnessed by anomalous high 2m temperature extended up to NE Pakistan, over the same region cloud cover was also 10-20% less when compared to observed.
- REMO is showing good skill in capturing the SA summer monsoon and can be used for climate change studies.

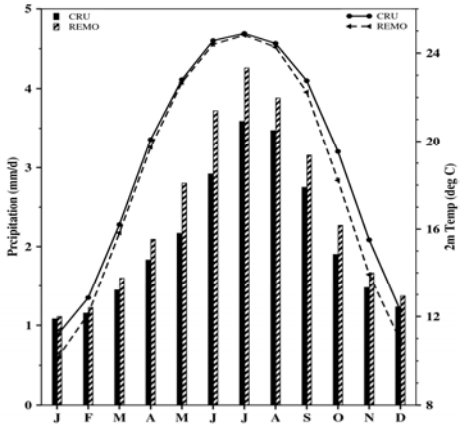

Figure-3: Annual cycle of REMO and CRU precipitation and 2m temp over model domain.

6. Acknowledgement

First author has been supported by Max Planck Institute for Meteorology Visiting scientist fellowship.

7. References

Gordon B, Eclogical climatology: concepts and applications, Cambridge University Press, pp 678, 2002

Charnock H, Wind stress on a water surface, Quart. J. Roy. Meteor. Soc. Vol. 81, pp 639, 1955

Gadgil S, Sajani S, Monsoon precipitation in the AMIP runs, Clim. Dyn., Vol. 14, pp 659-689, 1998

Dumenil L, Todini E, A rainfall-runoff scheme for use in the Hamburg climate model. In: Kane JP (ed) Advances in theoretical hydrology – a tribute to James Dooge. Elsevier Science, Amsterdam, pp 129–157, 1992

Jacob D and Podzum R, Sensitivity studies with the Regional Climate Model REMO, Meteor. Atmos. Phys., Vol No 63, pp 119–129, 1997

Jacob D, A note to the simulation of the Annual and Interannual Variability of the Water Budget over the Baltic Sea Drainage Basin, Meteorology and Atmospheric Physics, Vol. 77, No. 1-4, pp 61-74, 2001

New M, Hulme M, Jones P, Representing twentieth-centuary space-time climate variability. PartII: Development of 1901-1996 Monthly grids of terrestial surface climate, J. Climate, Vol. 13, pp 2217-2238, 2000

Ratnam JV, Giorgi F, Aakshara K, Stefano C, Simulation of Indian monsoon using RegCM3-ROMS regional coupled model, Clim. Dyn., in press, 2008

Rupa Kumar K, A. K. Sahai, K. Krishna Kumar, S. K. Patwardhan, P. K. Mishra, J. V. Revadekar, K. Kamala, G. B. Pant, High-resolution climate change scenarios for India for the 21st century, Current Science, pp 334-345, 2006

Settled and remaining issues in regional climate modelling with limited-area nested models

René Laprise[1,4,5], Ramón de Elía[2,4,5], Daniel Caya[2,4,5], Sébastien Biner[2], Philippe Lucas-Picher[3], Emilia Diaconescu[1,4,5], Martin Leduc[1,4,5], Adelina Alexandru[1,4,5], Leo Separovic[1,4,5] and Alejandro di Luca[1,4,5]

[1]Université du Québec à Montréal (UQÀM), Montréal (Québec), Canada, laprise.rene@uqam.ca; [2]Consortium Ouranos, Montréal (Québec), Canada; [3]Danish Meteorological Institute (DMI), Copenhagen, Denmark; [4]Canadian Network for Regional Climate Modelling and Diagnostics (CRCMD), Montréal (Québec), Canada; [5]Centre pour l'Étude et la Simulation du Climat à l'Échelle Régionale (ESCER), Montréal (Québec), Canada

1. Introduction

A pragmatic approach to reduce the computing cost of high-resolution global climate models is to apply the high resolution over only a subset of the globe, a technique known as nested Regional Climate Modelling. Lower resolution data, either simulated by Coupled Global Climate Models (CGCM) or from reanalyses of observations, are interpolated in time and in space on the high-resolution grid of a limited-area Regional Climate Model (RCM) and serve to define the lateral (and often the ocean surface) boundary conditions (LBC). Like all models, RCMs are subject to a variety of sources of errors and uncertainty, as well as to scepticism about their potential usefulness. But in addition, there are specific issues that arise with RCMs relating to their geographically limited computational domain, the nesting technique, the resolution jump between the RCM and the driving data, the update frequency of the LBC, and the imperfections in LBC data.

This presentation will summarise the work presented in Laprise (2008), Laprise et al. (2008) and references therein.

2. Dynamical Downscaling Hypothesis

The *ansatz* behind the "dynamical downscaling" technique is that an RCM, driven by large-scale fields at its LBC, generates fine scales that are dynamically consistent with, and somehow preconditioned by the LBC. Initialised and driven by data without small-scale information, nested models develop small-scale variance even in the absence of strong surface forcing. Hence RCM are expected to act as a kind of magnifying glass that reveals details that cannot be resolved on a coarse mesh. The small scales represent the main potential added value of high-resolution RCM. A more controversial issue concerns the potential improvement of the large scales in the case of driving by low-resolution CGCM data.

The spin-up of fine scales proceeds fairly rapidly. Within a few days in the simulation, atmospheric variance spectra and forecast error spectra become independent of the time since the simulation's initiation and of the presence or absence of small scales in the initial and LBC. The hypothesised development mechanisms include fine-scale surface forcing, hydrodynamic instabilities, mesoscale processes, and nonlinear interactions cascading information from the large to the small scales.

3. Deterministic Forecast *Vs* Climate Skill

In idealised forecast experiments for mid-latitude domains with 100 by 100 grid points on a 45-km mesh, scales larger than about 800 km appear to retain extended deterministic predictability, while scales smaller than about 400 km loose predictability in a fashion similar to global models. For the small scales, the shorter the length scale, the shorter the predictable time. Hence even when fine scales are present initially and in the LBC, they do not retain deterministic temporal coherence (at the right place at the right time) beyond a day or so. This implies that part of the downscaling is not deterministic, i.e. not entirely determined or preconditioned by LBC. A non-deterministic, "free" component exists (free in the sense of its stochastic-like character) which is also reflected in the presence of some level of internal variability (IV) in nested models.

Hence small scales are generated by nested models, but not with deterministic skill. Climate statistics of small scales appear to be skilful though, lending some confidence in the potential usefulness of RCMs in climate simulations and climate-change projections. IV puts however severe limitations on the usefulness of single-season, single-simulation experiments. While IV may not be a major problem for climate applications as far as low-order statistics are concerned (when the domain size is not too big; see next section), as long as the user of an RCM is aware of its presence in the interpretation of results.

4. Regional Domain Size

In idealised experiments, it is seen that fine scales develop in RCM within a few days, and they have the right amplitude and the right statistics. It has been shown however that the full spin-up of small scales within the regional domain requires rather large domains, particularly in the upper troposphere in mid-latitudes where the flow is strong. Due to the continuous transport of low-resolution information from the lateral boundary, some distance is required for the spin-up process to proceed. The spin-up distance on the inflow side of domain is larger for stronger ventilation flow through the domain. For mid-latitude domains, this distance is thus larger in winter and at upper levels due to stronger winds. The physically meaningful portion of the limited-area domain must exclude the spin-up distance, in addition to any sponge or buffer zone used as part of the lateral boundary nesting.

The downscaling skill has been documented through a set of idealised "perfect prog" tests. Over small domains (e.g. 70 linear grid points), the small-scale transient eddies are amplitude deficient, especially at upper levels. With larger domain (e.g. of the order of 200 linear grid points), small-scale transient eddies are simulated with the correct amplitude, but with very little time correlation with the reference. Lack of time synchronicity is of secondary importance for climate applications, but must be taken into consideration for process studies. Failure to reproduce the correct monthly or daily anomalies may however have important consequences for the downscaling skill in seasonal prediction and even for some climate applications.

By their nature, nested RCM require externally provided data to drive them. Over mid-latitude domain, the application of LBC is usually sufficient to control the large-scale circulation through the RCM domain. There

are however occasional episodes in RCM simulations when the circulation within the regional domain (the inner solution) decouples substantially from that of the driving data (the outer solution). This phenomenon is referred to as "Intermittent Divergence in Phase Space". IDPS is particularly frequent with large computational domain and under conditions of weak ventilation flow through the domain. These episodes result in unphysical flow artefacts near the outflow boundary. The application of the alternative nesting technique called large-scale (or spectral) nudging (SN) that forces the large-scale flow throughout the entire regional domain, is effective in suppressing this occurrence.

5. Impact of Imperfections in Lateral Boundary Conditions

The impact of errors in the driving data is an issue when low-resolution CGCM-simulated or global model forecasts data are used to drive an RCM. According to a strict interpretation of dynamical downscaling, RCM are expected to simply reproduce the large-scale errors supplied as LBC. Some forecast experiments carried over very large domains have shown some promise at correcting part of the large-scale forecast errors over the regional domain, due to reduced numerical truncation and improved treatment of some mesoscale forcings. On the other hand, it has been argued that planetary-scale circulation may be poorly handled over limited-area domain, and there are indications of some attenuation in the amplitude of the largest scales in RCM simulations. Idealised experiments with a perfect-prog approach over intermediate domain sizes (e.g. 100 linear grid points) indicate that the large scales that are supplied at the LBC are essentially replicated within the regional domain, without reduction nor amplification of their errors. As ought to be expected, the fine scales that are generated suffer degradation in proportion to the large-scale errors (this is referred to as "garbage-in, garbage-out").

6. Internal Variability

In ensembles of RCM runs driven by identical LBC but initialised from slightly different initial states, differences develop in time between instantaneous values simulated by the various members. Hence the fine-scale structures that develop in RCM are not uniquely defined, but they are subject to some internal variability (IV), defined as inter-member spread. Different variables exhibit different degree of IV; compared to natural variability, relative IV of precipitation rate for example is much larger than that of mid-tropospheric geopotential. IV is rather episodic, staying around small background values for extended periods of time, with episodes of rapid growth and decay. IV varies with domain size, location, season, and weather regime. The intensity of IV is negligible on small domains (e.g. less than 70 linear grid points), and it increases with domain size, reflecting the reduced control exerted by LBC with larger domains. With large domains (e.g. 200 linear grid points), IV occasionally and locally approaches natural variability. For climate applications, the RMS IV of time-averaged variables is inversely proportional, on average, to the square root of the averaging period. For process studies or testing model sensitivity to changing parameters, it is important to acknowledge the presence of IV in the interpretation of the results.

7. Influence of Large-Scale Nudging

Nudging of the large scales (SN) throughout the entire RCM domain is becoming increasingly more common in dynamical downscaling, with some positive and some undesirable effects. On the positive side, studies confirm that lateral-boundary numerical artefacts, domain-size sensitivity and IV all decrease with increased SN strength. But our results also indicate a noticeable reduction of precipitation extremes as well as low-level vorticity amplitude in almost all length scales, as negative side effects of SN, particularly when applied with strength. Overall results indicate that the use of "mild" SN may constitute a reasonable compromise between the risk of IDPS when using large domains without SN, and an excessive control of the large scales, with concomitant effects on the smaller scales, with strong SN.

8. Jump in Resolution

Successful simulations have been achieved with very large jumps in resolution between the RCM mesh and the driving data, with changes by factors as large as 25 (e.g. from 250-km mesh driving data to 10-km RCM mesh) without using a cascade with intermediate-resolution meshes. There is some empirical evidence that what matters is not so much the resolution jump, but that the RCM domain should span several (e.g. 10 or more linear) grid points of the driving data in both horizontal directions.

With respect to the update frequency of LBC, it appears that six-hourly data are sufficient for 45-km mesh RCM; it can be expected that the acceptable time interval scales with the RCM mesh size.

9. Conclusions

Several issues of regional climate modelling call for further investigation. The following is a partial list of remaining RCM issues, as we perceive them. There is a need to improve our knowledge of the sensitivity of RCM to a number of arbitrary parameters related to the nesting approach, such as domain size (both in terms of physical dimension and number of grid points), location of domain (climate regime, ventilation flow), resolution jump, nesting time interval, and nesting technique. Little is known on the influence of the nesting technique on processes such as nonlinear scale interactions and the cascade of variance, the presence of artificial domain circulations, the ability to capture interannual variability, the ability of nested RCM to maintain the integrity of large scales used to drive and possibly to correct their errors. What are the dynamical mechanisms responsible for the time variations of IV? What is the spectral signature of IV during episodes of high and low IV? And beyond these specific issues, there remains the fundamental question of RCM added value. This question is intertwined with topics that defy a simple classification and that depend on spatio-temporal scales, the metrics used, the local topography, as well as the users needs, to name just a few. These are still open questions that are topics of active investigation.

References

Laprise, R., R. de Elía, D. Caya, S. Biner, Ph. Lucas-Picher, E. P. Diaconescu, M. Leduc, A. Alexandru and L. Separovic, Challenging some tenets of Regional Climate Modelling, *Meteor. Atmos. Phys.* Vol. 100, Special Issue on Regional Climate Studies, pp. 3-22, 2008.

Laprise, R., Regional climate modelling, *J. Comp. Phys.* Vol. 227, Special issue on Predicting weather, climate and extreme events, pp. 3641–3666, 2008.

Regional climate model skill to develop small-scale transient eddies

Martin Leduc, René Laprise, Mathieu Moretti-Poisson and Jean-Philippe Morin

Canadian Regional Climate Modelling and Diagnostics (CRCMD) Network - ESCER Centre - Université du Québec à Montréal, Montréal, Canada, leduc@sca.uqam.ca.

1. Introduction

Over the last few years, the perfect-model approach has been used in several experiments to measure the sensitivity of the Canadian Regional Climate Model (CRCM) to various parameters characterizing its nesting technique. Leduc and Laprise (2008, hereafter LL08) recently conducted a domain-size experiment that highlighted a well-known characteristic of RCM: the control of the lateral boundary conditions (LBC) on the large-scale component of the solution becomes weaker when using wide domains (unless spectral nudging at large scales is applied). Another effect measured after changes in domain size is related to the small-scale transient activity, not excited by the LBC but generated within the RCM domain by local forcing and through non-linear interactions. Evidence has been found that the generation of such variability can be highly penalized over a region of interest if located near to the inflow boundary. This region where small-scale transient eddies are deficient in intensity has been interpreted as the characteristic distance of spin-up that the large-scale inflow must travel to generate small-scale features with sufficient intensity. Similarly, de Elía (2006) measured the characteristic spin-up time for the small scales when developed from initial conditions containing only large-scale features.

The LL08 experiment has been performed by running the CRCM for the winter season over midlatitudes. In order to generalize, we have extended this work to include the summer season, where the flow is rather turbulent and subject to strong convective processes. These new results give a homogenous spatial spin-up overall the domain of interest since summer circulation shows frequent changes in the domain ventilation regime.

An additional experiment has been made by reproducing the winter experiment but including spectral nudging at large scales (SN). This technique strongly diminishes variations of the large-scale flow between two simulations using different domain sizes. It hence facilitates to unambiguously attribute differences in small-scale transient patterns to the distance traveled by the large-scale inflow from the lateral boundaries. In the following, the perfect-model approach is used to evaluate the skill of an RCM to develop small-scale features, for both winter and summer and under conditions of strong SN.

2. Experimental framework

The perfect-model approach consists of integrating an RCM over a large domain, called the Big-Brother simulation (BB). Secondly, BB is low-pass filtered to result in a coarsely detailed dataset, similar to what usually constitutes the LBC for driving an RCM. This filtered time series is used to drive the same RCM over a smaller domain, called the Little-Brother (LB), which is finally compared to the unfiltered reference (BB) solution.

The BB simulations produced for winter and summer seasons are labeled BW and BS respectively. These short "climates" consist of appending four February (winter) and four July (summer) months by driving the CRCM with NCEP reanalyses for the years 1990 to 1993. The BB domain of integration covers 196x196 grid points with a center located over Québec, Canada. LB simulations for winter are named L1W, L3W and L4W for domains of 144x144, 96x96 and 72x72 grid points respectively. Also, the smallest domain (72x72) has been integrated for the summer season (L4S). Finally, L1W have been repeated with the use of a strong SN (L1WN). In Tab. 1 are summarized the labels and characteristics defining the CRCM simulations analyzed here. A common domain of 38x38 grid points is used for comparing the simulations.

In the following, we focus on the small-scales features of the flow, which have been extracted by Fourrier filtering and correspond to the length scales smaller than 1080 km, including a smooth transition that reaches 2160 km. Reader is invited to refer to Leduc and Laprise (2008) for a detailed description of the experimental procedure.

Name	Season	Domain size	SN strength
BW, BS	W, S	196^2	no
L1W	W	144^2	no
L3W	W	96^2	no
L4W, L4S	W, S	72^2	no
L1WN	W	144^2	yes

Table 1 Characteristics of the simulations where winter and summer are respectively represented by W and S and domain sizes are given in grid points.

3. Small-scales features sensitivity to season

The RCM skill to develop small-scale features are compared for winter and summer experiments. The transient eddies of the small-scales features are plotted on Fig. 1 for the 700-hPa relative humidity field. Virtual reference simulations (BW and BS) are displayed for both seasons (Fig. 1 a and b) with associated Little-Brother (Fig. c and d) integrated over a very small domain (L4W and L4S on Tab. 1). The first noticeable feature of LBs compared to BBs is that they display important underestimations of transient activity. Averaged over the displayed domain, L4W regenerates 46% of the BW transient variance while for L4S a value of 59% is obtained. When attention is devoted to the shape of patterns compared to the BBs, spatial correlation (R*) for L4W is poor (R* = 50%) compared to L4S which gives a value of 90%. The winter small-scale transient pattern is highly distorted due to a strong westerly inflow and proximity of the western boundary from the domain of interest. For the summer case, L4S retains the general features of the BS pattern, as the northern maximum and the south-north gradient of relative humidity. Better skill of the summer simulation to preserve BB pattern in both intensity and spatial correlation in comparison to same domain size in winter is partly due to the fact that summer inflow is weaker and often changes in direction over short periods (few hours). It results in a spatial spin-up that is homogenously distributed over the domain of interest, unlike the winter case where spatial spin-up is concentrated on a specific region. Also, a better ability to reproduce small-scale transient variability in summer may be related to stronger convective processes occurring in

this season, as well as the higher residency time (Picher et al. 2008) that could provide a longer time for small-scale features spin-up.

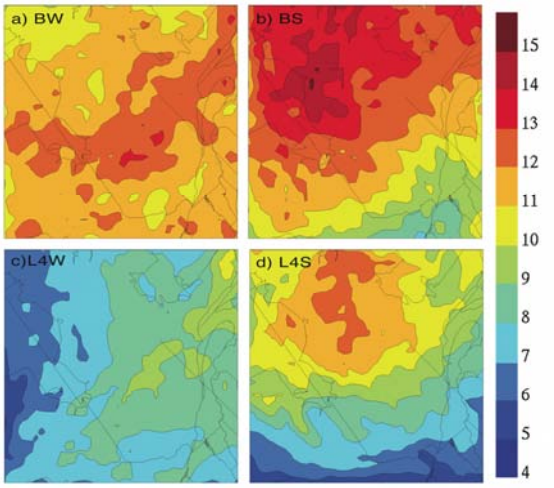

Figure 1. Small-scale transient eddies of the 700-hPa relative humidity for a) BW, b) BS, c) L4W and d) L4S. The scale is given in %. The spatial correlation coefficient (R*) with BW and BS for L4W and L4S are of 50 and 90% respectively.

4. Effect of spectral nudging at large scales

This section focuses on how applying SN can affects development of small-scale features simultaneously with variations of the domain size. On Fig. 2 are shown the small-scale transient eddies of the 700-hPa relative vorticity for the virtual reference simulation (BW; Fig. 2 a), the large-domain Little-Brother using SN (L1WN; Fig. 2 b) and without SN (L1W; Fig. 2 c) and a smaller domain Little-Brother with no SN (L3W; Fig. 2 d). See Tab. 1 for an overview of simulations.

Let's first concentrate on the similarities between patterns by using the spatial correlation coefficient of the Little-Brothers with the virtual reference climate (BW). L1W displays the most different pattern with R* = 50% compared to 79 and 72% for L1WN and L3W respectively. Since small-scales features are somewhat preconditioned by the large-scale information penetrating the domain through its lateral boundaries, the fact that L1W shows such a different small-scale pattern is principally attributable to the use of a large domain without applying SN. Such conditions engender a weak control of the LBC on the RCM large-scale solution, and have a consequence on the small-scale features. For the cases of L1WN and L3W, skills for pattern matching with BW are higher than L1W for two different reasons. L1WN uses a strong SN allowing a sufficient control of the nesting data on the large-scale solution, in despite of its large domain. Also, the large domain allows for a sufficient distance needed to spin-up the small-scale transient eddies. For L3W, SN does not seem required to obtain a significant matching in small-scale feature patterns since proximity of the lateral boundaries from the validation area provides the control needed for keeping the large-scale flow similar to the driving data.

Another interesting point is about potential side effects that may be related to the use of a strong SN (Alexandru et al. 2009). From the results presented on Fig. 2, effect of SN on intensity of small-scale transient eddies is not significant when averaged overall the domain. However, it is clearly visible that the southern maximum is not captured by the large-domain simulation without SN (Fig. 2 c). This seems to be attributable to the fact that the different large-scale circulation occurring in L1W does not allow such feature to develop.

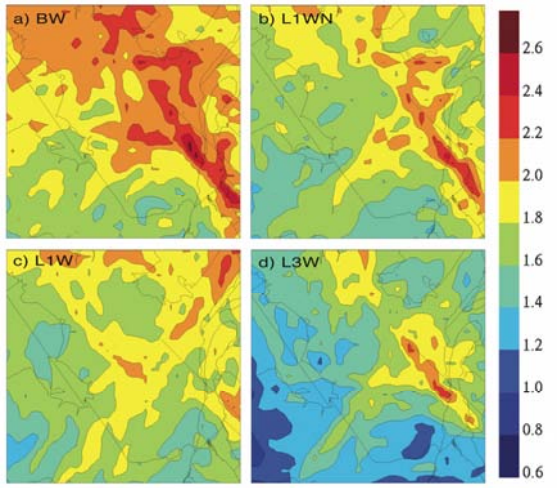

Figure 2. Small-scale transient eddies of the 700-hPa relative vorticity for a) BW, b) L1WN, c) L1W and d) L3W. The scale is given in 1.0e-05 s^{-1}. The spatial correlation coefficient (R*) with BW for L1WN, L1W and L3W gives respective values of 79, 50 and 72 %.

5. Conclusions

The domain-size perfect-model experiment for a winter short climate (LL08) has been compared with new results obtained for the summer season. Simulations presented here display a seasonal dependence of the domain-size effect on the small-scale transient eddies. For winter, a small domain of integration engender lacks in the transient variability of the small-scale features, particularly on the inflow side of the domain. In summer, simulations also display such underestimations but those are homogenously distributed overall the domain of interest. Differences in the ventilation regimes that depend on season seem to partly explain such different spatial spin-up. By performing supplementary winter experiments using a strong SN permitted a direct comparison of the small-scales features for different domain sizes since the large-scale flow remains approximately the same. By this way, it has been possible to isolate the effect of the distance traveled by the inflow to explain the differences residing in the intensity of small-scales transient eddies.

References

Alexandru, A., R. de Elia, R. Laprise, L. Separovic and S. Biner, 2009: Sensitivity Study of Regional Climate Model Simulations to Large-Scale Nudging Parameters. Mon. Wea. Rev. (accepted)

de Elía R, Laprise R, Denis B, 2006: Forecasting skill limits of nested, limited-area models: a perfect-model approach. Mon. Wea. Rev., 130:2006–2023

Leduc, M. and R. Laprise, 2008: Regional Climate Model sensitivity to domain size. Clim. Dyn., (Published online, DOI 10.1007/s00382-008-0400-z).

Lucas-Picher, P., D. Caya, S. Biner and R. Laprise, 2008: Investigation of regional climate models' internal variability with a ten-member ensemble of 10-year simulations over a large domain. Mon. Wea. Rev., 136:4980-4996.

Evaluation of dynamical downscaling of the East Asian regional climate using the HadGEM3-RA: Summer monsoon of 1997 and 1998

Johan Lee[1], Suhee Park[1], Wilfran Moufouma-Okia[2], David Hassell[2], Richard Jones[2], Hyun-Suk Kang[1], Young-Hwa Byun[1], and Won-Tae Kwon[1]

[1]National Institute of Meteorological Research/Korea Meteorological Administration, Seoul, Republic of Korea, Johan.lee@kma.go.kr, [2]Met Office Hadley Centre, Exeter, UK

1. Introduction

The HadGEM3-RA is a regional atmospheric model based on the global atmospheric model of the Met Office Hadley Centre (MOHC). Korea Meteorological Administration (KMA) has a plan to adopt this model for dynamical downscaling from seasonal to decadal scales over the East Asian region according to the collaboration agreement between MOHC and KMA.

As the first stage of this effort, the performance of the HadGEM3-RA for the East Asian summer monsoon is investigated. The East Asian summer monsoon is the most prominent feature in the East Asian region climate and a distinct component of the Asian summer monsoon system. Therefore, it is important to examine the model's capability to simulate the East Asian summer monsoon before utilizing the model for downscaling for longer time scales over the East Asian region.

In this paper, we will show a preliminary evaluation of its performance for the East Asian summer monsoon.

2. Experiment design

The model domain is the East Asian monsoon region including Korean Peninsula, East China, Mongolia, and Japan. Number of grid points are 190 (in west-east) by 158 (in north-south) and horizontal resolution is selected to be 0.22 degree, about 25 km. The buffer zone for lateral boundary conditions is 8 grids for each direction. Configuration of HadGEM3-RA for the East Asian region is almost the same as that of the HadGEM3-A, except that the dynamic settings are taken from the operational limited area model. Dynamics core and physical packages are described in Davies et al. (2005) and Martin et al. (2006), respectively.

Atmospheric initial conditions were obtained from the European Centre for Medium-Range Weather Forecasts (ECMWF) 40-year reanalysis (ERA40) data. Lateral boundary conditions to drive HadGEM3-RA were derived from the 6-hourly data. Sea surface temperature and sea ice were prescribed by Atmospheric Model Inter-comparison Project (AMIP) II data.

We selected two summer seasons to examine the model's capability to simulate the East Asian summer monsoon and its interannual variation. The model integration periods are 3 months from 0000 UTC 1 June 1997 and 1998, respectively. Typical characteristics of the East Asian summer are heavy rainfall from June to July and heat waves from late July to August. The two selected summers represented extreme climatic events which were opposite extremes in terms of precipitation. In summer of 1997, there were drought and heat waves in North China. In the other hand, there were abnormal heavy rains in summer of 1998 which had caused severe flooding in the Yangtze River valley and northeast China and record-breaking daily precipitations over the Korean Peninsula. Therefore, the model's capability to capture interannual variability of the summer monsoon can be evaluated by comparing the simulations of 1998 and 1997.

3. Results and discussions

Figure 1 shows observed and simulated precipitations for summer of 1998. As mentioned above, East Asia experienced severe heavy rainfall in summer of 1998. In Fig. 1a, there are intense rainbands over central China around the Yangtze River basin, the Korean Peninsula, and Japan. On the contrary the major rainband is weaker and shifted southward (not shown) in 1997. Therefore, in the difference between 1998 and 1997, positive anomalies occur in central China, Korea, and the northwest Pacific Ocean, and a negative anomaly in south China and Taiwan (Fig.1b). HadGEM3-RA reproduces well the observed features of both summers in terms of the distribution of seasonal precipitation. The pattern correlation coefficients are 0.53 and 0.61 for 1998 and 1997, respectively, and the model reproduces well the anomaly from 1998 to 1997 (Table 1). In Fig. 2b, the rainfall deficit over south China and its surplus across central China and the Korean Peninsula are distinct as in the observations. However, the HadGEM3-RA tends to overestimate the intensity of precipitations. Simulated precipitations of 1998 and 1997 are greater than observations and wet biases are 66.5% and 47.9%, respectively (Table 1).

Simulations of surface air temperature are better than those of precipitation. The pattern correlations are 0.96 for both summers (Table 1) with the distribution and magnitude of surface air temperature very close to observations (not shown). In addition, the features of 1998 and 1997 anomalies are well captured, e.g. the cold anomaly in north China and warm anomalies in south China and the north-eastern region of Asia. The simulated surface air temperature is generally warmer than observations with area averaged biases of 0.5 °C and 0.9 °C respectively (Table 1).

Table 1. Comparison of statistical values for precipitation and surface air temperature of observation and simulations. In case of biases of precipitation, the ratio (%) of bias to observation is presented in parentheses.

	Precipitation		Temperature	
	1998	1997	1998	1997
Observed mean	5.27	4.35	21.0	21.4
Simulated mean	8.78	6.44	21.5	22.3
Bias	3.51 (66.5)	2.09 (47.9)	0.5	0.9
RMSE	4.32	2.66	1.0	1.3
Pattern Correlation	0.53	0.63	0.96	0.96

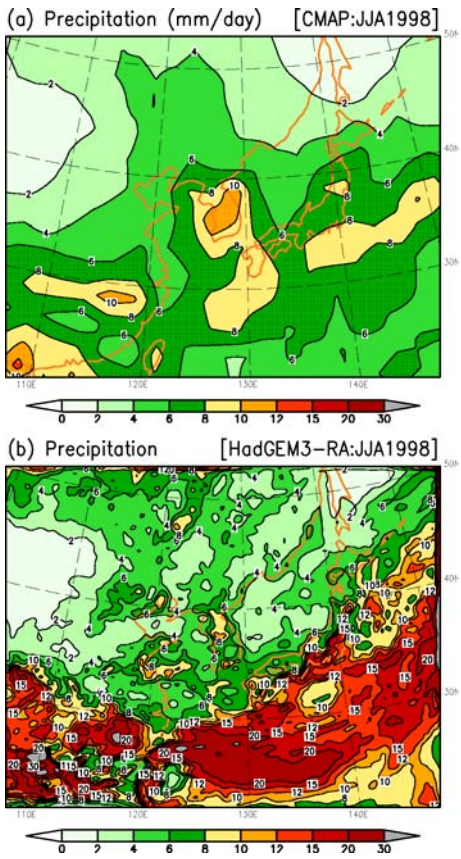

Figure 1. Precipitation rate (mm day^{-1}) for summer (JJA) 1998 from (a) the CMAP data as observation and (b) the simulation by the HadGEM3-RA

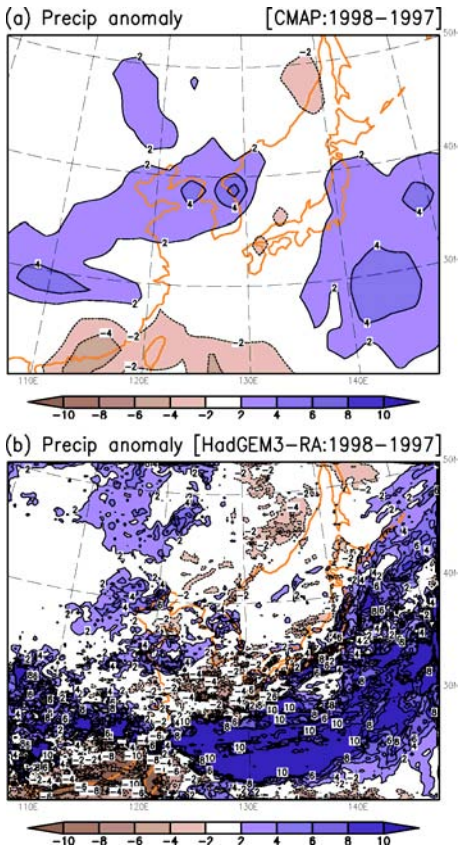

Figure 2. Differences of summer precipitation rate (mm day^{-1}) from 1998 to 1997, obtained from (a) the observation and (b) the simulation.

There are coherent bias patterns in the simulated East Asian summer monsoon of 1998 and 1997 (not shown). The HadGEM3-RA overestimates precipitation over most of the region and underestimates over the centre of model domain. There are warm biases over north China, Manchuria, and northern continent and small cold biases over south China and Japan. In 500 hPa geopotential height, there is a negative bias over the centre of model domain and positive biases near the north and west lateral boundaries. Biases of sea level pressure are negative over the centre and positive near the lateral boundaries of the domain. In the lower troposphere there are south-westerly biases near the southern boundary and dry biases over most of the domain. In vertical profiles of the biases of air temperature and specific humidity, there are distinct warm and dry biases within lower troposphere, with maximum warming and drying at 850 hPa. In contrast, there are warm and wet upper tropospheric biases with a maximum at 300 hPa.

These coherent bias patterns seem to indicate the following mechanism; strong south-westerlies in the south of the domain supply warm and moist air and that enhances convective activity over south China and northwest Pacific Ocean. Active convection transports moisture from lower to upper levels. At the same time, cyclonic flow related to the active convections leads to reduced moisture supply into north of the region of convection. Therefore, precipitation is underestimated over the centre of model domain, such as the Korean Peninsula region.

4. Concluding remarks and future works

It is found that the HadGEM3-RA reproduces well extreme seasonal timescale climatic events of the East Asian monsoon, such as flooding in China and Japan during summer of 1998, and is able to capture the interannual variation between the East Asian monsoon seasons of 1997 and 1998. However, the HadGEM3-RA exhibits systematic errors, such as wet bias in precipitation, warm bias in surface air temperature, and strong south-westerly bias near southern and eastern lateral boundaries.

To improve model performance, we will conduct sensitivity experiments to physics and simulation domain size. After sensitivity experiments on seasonal scale, we will conduct a multi-annual climatological simulation.

References

Davies, T., M. J. P. Cullen, A. J. Malcolm, M. H. Mawson, A. Staniforth, A. A. White, and N. Wood, A new dynamical core for the Met Office's global and regional modelling of the atmosphere. Quart. *J. Roy. Meteor. Soc.*, **131**, 1759–1782. 2005.

Martin, G. M., M. A. Ringer, V. D. Pope, A. Jones, C. Dearden, and T. J. Hinton, The physical properties of the atmosphere in the new Hadley Centre Global Environmental Model (HadGEM1). Part I: Model description and global climatology. *J. Climate*, **19**, 1274–1301. 2006.

Interpolating temperature fields using static and dynamic lapse rates

Chris Lennard

Climate Systems Analysis Group, University of Cape Town, Cape Town, South Africa. email: lennard@csag.uct.ac.za

1. Introduction

Gridded climate data are important in many climate applications such as the validation of simulated results and understanding land-atmosphere interactions. Point source data often forms the basis of the gridded product and involves the interpolation of these data to a specified grid size. The nature of point source, observational temperature data is usually spatially heterogeneous and often lacks temporal consistency thus many interpolation techniques have been developed to aid the spatial generalization of point source data into a gridded product (e.g. Cressman 1959, Willmott *et al.* 1985, Biau *et al.* 1999). Here, we present a novel approach, which uses empirical and dynamical methods, in the preparation of station data for interpolation as well a a more traditional approach. The latter used a static lapse rate field to get station data to a common level for interpolation whereas the new approach a dynamic lapse rate field. Each method is presented as well as the results from both and the merits of each discussed. We examined 36 years of station data over the Cape Fynbos region and used the Cressman interpolation scheme.

2. Data and Methods

The two preparation methods used lapse rates to reduce/raise station temperature data to a common level at which the interpolation was performed. The traditional approach reduced the station data at a constant lapse rate of 0.6 degrees per 100 m to sea level where the interpolation was performed. However, this method is unlikely to capture local scale phenomena such as temperature inversions, berg winds and localized orographic effects. In an attempt to capture these phenomena, the new method used empirical and dynamic methods to establish lase rate fields. First, self organizing maps (SOMs) were used to produce 12 characteristic synoptic circulations over South Africa for the 36 year time period (Fig. 1).

Then, for each of these states, a regional climate model was run at a resolution of 3 km to generate 12 high resolution archetypal lapse rate fields. Figure 2 shows the lapse rate field for Cape Town International Airport for each of the synoptic states over 29 sigma levels.

Every day in the station record mapped to one of the 12 characteristic circulations so every station was raised by the SOM-specified lapse rate to a common level at the top of the atmosphere. The interpolation was then performed at this level. The interpolated temperature fields were then returned to the surface along respective lapse rates. We present the technique and the interpolated results and assess the value of using a dynamic lapse rate field versus a static one.

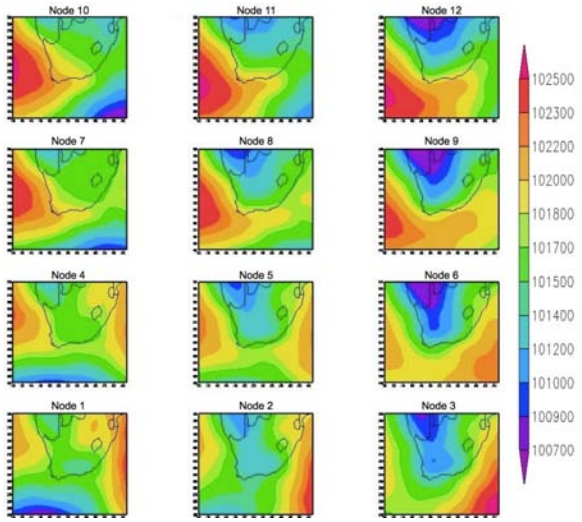

Fig.1. Sea level pressure maps of the 12 characteristic synoptic states.

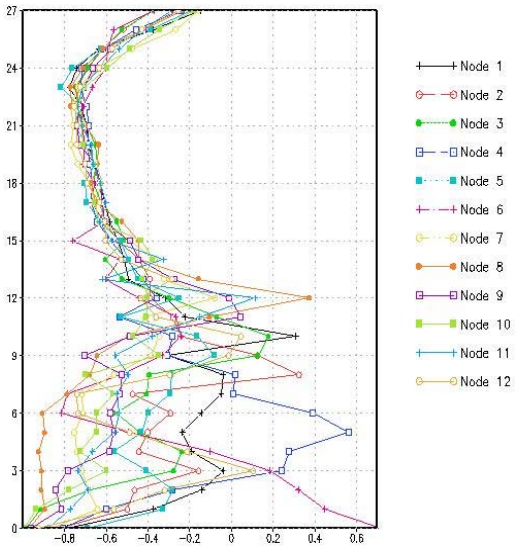

Fig. 2. Lapse rate fields for the SOM circulations above Cape Town International Airport. Sigma levels are not evenly spaced with height, more levels are at lower altitudes to capture boundary dynamics here. Sigma level 15 is at approximately 3000 m, level 21 at approximately 6000 m and level 30 at about 15000 meters.

References

Biau. G., E. Zorita, H. von Storch, and H. Wackernagel, Estimation of precipitation by kriging in the EOF space of the sea level pressure field. J. Climate, 12, 1070-1085, 1999.

Cressman. G. P., An operational objective analysis system. Mon. Wea. Rev., 87. 367-374, 1959.

Willmott. C. J., C. M. Rowe, and W. D. Philpot, Small-scale climate maps: A sensitivity analysis of some common assumptions associated with grid-point interpolation and contouring. Amer. Cartogr., 12, 5-16, 1985.

Regional modelling of climate and extremes in southeast China

Laurent Li(1), Weilin Chen(2) and Zhihong Jiang(2)

(1) Laboratoire de Météorologie Dynamique, CNRS/IPSL, Université Paris VI, France, li@lmd.jussieu.fr
(2) Nanjing University of Information Science and Technology, Jiangsu Key Laboratory of Meteorological Disaster, China

A variable-grid atmospheric general circulation model, LMDZ, with a local zoom over southeast China is used as a traditional regional model to investigate climate changes in terms of both mean and extremes. This regional version of LMDZ can also be interactively coupled to the global version of LMDZ in a two-way nesting manner.
Two time slices of 30 years are chosen to represent respectively the end of the 20th century and the middle of the 21st century. The boundary conditions were taken from the outputs of three global coupled climate models. An evaluation of the simulated temperature and precipitation for the current climate shows that in general LMDZ reproduces well the spatial distribution of mean climate and extremes in southeast China, but the model has systematic cold bias in temperature and tends to overestimate the extreme precipitation.
Scenario results show that in all seasons there is a significant increase for mean, maximum and minimum temperature in the entire region, associated with a decrease in the number of frost days and with an increase in the heat wave duration. The magnitudes and main spatial patterns of the changes in temperature extremes show a quite good consistency among the three global scenarios. A warming environment also gives rise to changes in extreme precipitation events. Precipitation extremes increase over most of southeast China, in a quite consistent manner among the three global scenarios

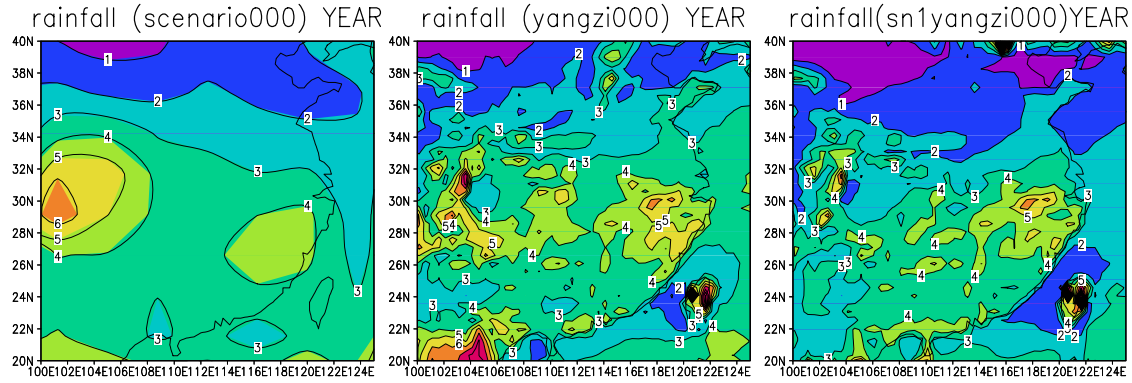

Fig. 1: Annual-mean precipitation rate (mm/day) in the global model (left), in the regional model driven by the global model (middle), and in the regional model operated interactively with the global model (right).

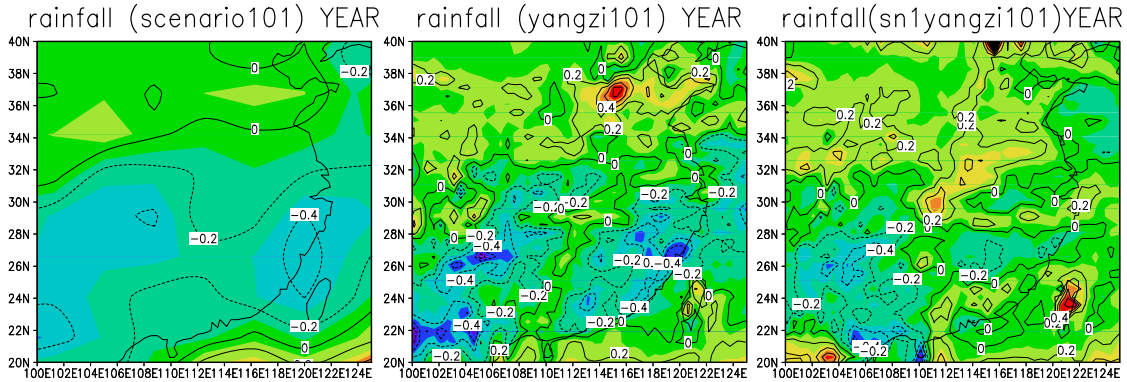

Fig.2: As in Fig.1, but for changes of precipitation (2050-2000).

Investigation of regional climate models' internal variability with a ten-member ensemble of ten-year simulations over a large domain

Philippe Lucas-Picher[1,2,4,5], Daniel Caya[3,4,5], Ramón de Elía[3,4,5], Sébastien Biner[3] and René Laprise[2,4,5]

[1]Danish Meteorological Institute (DMI), Copenhagen, Denmark, plp@dmi.dk; [2]Université du Québec à Montréal (UQÀM), Montréal (Québec), Canada; [3]Consortium Ouranos, Montréal (Québec), Canada; [4]Canadian Network for Regional Climate Modelling and Diagnostics (CRCMD), Montréal (Québec), Canada; [5]Centre pour l'Étude et la Simulation du Climat à l'Échelle Régionale (ESCER), Montréal (Québec), Canada.

1. Introduction

Regional climate models (RCM) are chaotic in their nature since they are built on the physical laws describing the behavior of a chaotic system. Therefore, different solutions can emerge from an ensemble of RCM simulations launched with slightly perturbed initial conditions. However, these simulations will keep a certain level of correlation throughout the simulation because they share the same lateral boundary forcing.

There appears to be a link between the internal variability (IV), computed with the inter-member spread, and the control exerted by the lateral boundary control (LBC). This control seems to be associated to the so-called flushing regime that is dependent of the size of the domain, its geographical location and the strength of the atmospheric circulation (von Storch, 2005). The flushing regime is governed by the atmospheric circulation, which depends on the synoptic conditions. It is thought to be an indicator of the efficiency of the steering exerted by the LBC on the RCM.

Thus, this work introduces a new tool, an aging tracer, to quantify the lateral boundary forcing of a RCM. Its also extends previous RCM IV studies using a large ensemble of multi-years simulations performed with the Canadian Regional Climate Model over a large domain covering North America. This presentation will summarize the work presented in Lucas-Picher et al. (2008a and 2008b).

2. Methodology

An ensemble of 10 simulations of 10 years (1980-1989) was produced with the Canadian Regional Climate Model (CRCM) over a domain covering most of North America. The domain contains 193 x 145 grid cells of 45 km resolution and 29 vertical levels. To construct the ensemble, the simulations were launched with different initial conditions obtained by lagging the start of the simulations or by adding small random perturbations. The source of the perturbations has no influence on the IV 15 days after the beginning of the simulation. The simulations were driven at the lateral boundary with the NCEP/NCAR reanalysis data and the sea surface temperature (SST) comes from AMIP monthly-means.

A new tool is implemented in the simulations. This tool is an aging tracer that computes the time the air parcels spend inside the limited-area domain of a RCM. The aging tracers are initialized to zero when the air parcels enter the domain and grow older during their migrations through the domain with each time step in the integration of the model. The residency time is treated and archived as the other simulated meteorological variables, therefore allowing computation of its climate diagnostics.

3. Results

The IV is computed with the inter-member variance. To describe the spatial distribution of the IV, the climatology of the IV is computed with the time-average of the inter-member variance. The maximum of IV computed with the inter-member variance of a large ensemble of regional simulations is equal to the temporal variance (TV) when the members of the ensemble are completely uncorrelated and unbiased. The temporal variance also corresponds to the global climate models' (GCM) IV where simulations become uncorrelated after a few weeks of simulation. Thus, to remove the portion of the IV due to the temporal variance in the analysis, the IV computed as the inter-member variance (hereinafter described by the absolute internal variability (AIV)) can be normalized by the temporal variance to obtain the relative internal variability (RIV). The latter varies between 0 and 1. A RIV of 0 means that there is no internal variability, that simulations are perfectly correlated and that the lateral boundary forcing is strong. At the opposite, a RIV of 1 means that the internal variability is at its maximum, that simulations are uncorrelated and that the lateral boundary forcing is too weak to have any control on the simulation, making the RCM to behave as a GCM.

Figure 1 presents the 1980-1989 summer and winter spatial distributions of the AIV, TV and RIV for mean-sea-level pressure (MSLP). The spatial distribution of the AIV for MSLP is similar for each season with larger values in the northeast of the domain. The temporal variance of MSLP is larger in winter than in summer, with a south-to-north gradient. This behavior can be explained by the strong cyclonic activity in winter in North America. The RIV is closer to 1 in summer than in winter, and larger values are located in the northeast of the domain. The RIV is related to the general atmospheric circulation. The RIV is stronger near the outflow boundary in the northeast of the domain where the lateral boundary forcing is weak. At the opposite, it is weaker in the west part of the domain, close to the boundary inflow, where the lateral boundary forcing is strong. The larger values of the RIV in summer than in winter are explained by the weaker lateral boundary forcing in summer, which is related to the slower atmospheric circulation.

Figure 2 presents the 1980-1989 summer and winter climatology of the ensemble-mean residency time, geopotential heights and wind vectors at 850 hPa, thus allowing a clear identification of the mean inflow and outflow boundaries. The small values of the residency time and the incoming wind vectors on the western side of the domain identify the mean inflow boundary, while the large values of the residency time and the outgoing wind vectors in the northeast of the domain identify the mean outflow boundary. Generally, the residency time increases from west to east due to the aging of the tracer during its migration towards the east following the westerly general atmospheric circulation. We can also see that the residency time is shorter in winter than in summer due to the faster atmospheric circulation in winter. Furthermore, the residency time decrease with increasing height according to the faster atmospheric circulation in higher levels (not shown).

The 1980-1989 spatial distributions of the residency time at 850 hPa in Fig. 2 exhibit clear similarities with the RIV in Fig. 1. To illustrate and quantify the relationship between these two variables, a scatter diagram linking the RIV and the residency time is generated. Figure 3 shows the scatter diagram of the 1980-1989 time-average residency time at 850 hPa and RIV for mean-sea-level pressure in summer and in winter. The data clouds generated for the summer and winter seasons are well mixed together. Linear fits for both seasons present similar correlation coefficients (0.92 in summer and 0.95 in winter) and slopes (0.05 in summer and 0.04 in winter).

4. Conclusion

A general message arising from the presented scatter diagrams is that the RIV increases linearly at a similar rate in summer and winter with the residency time. This analysis supports the hypothesis that the internal variability is associated to the control of the LBC linked to the atmospheric circulation that is described by the residency time. As shown by the strong relation between the RIV and the residency time, the latter is a good indicator to quantify the forcing exerted by the LBC on the RCM simulation. The residency time can thus be used as a tool to compare objectively the forcing from the LBC on the RCM. It could also be useful to estimate the level of IV for different RCM configurations by avoiding the high-computational cost of a large ensemble of simulations.

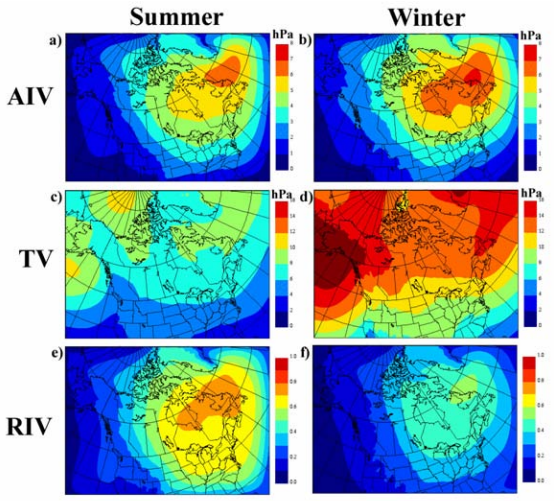

Figure 1. 1980-1989 climatology of a) the absolute internal variability (AIV), c) temporal variability (TV) and e) relative internal variability (RIV) for mean-sea-level pressure in summer. Same figures but for winter in b), d) and f).

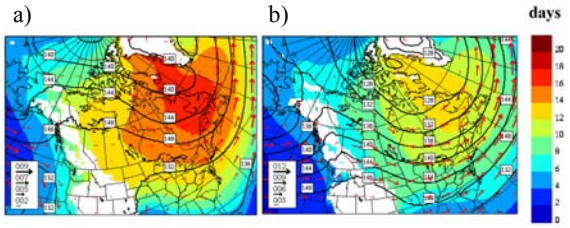

Figure 2. 1980-1989 ensemble-mean residency time (colours; days), geopotential heights (black contours; decameters) and mean wind vectors (red arrows; m/s) in a) summer and b) winter at 850 hPa.

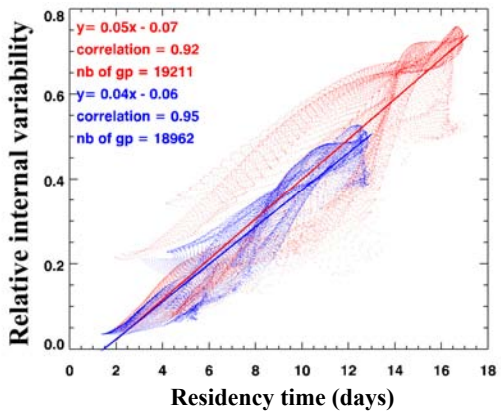

Figure 3. Scatter diagram of the 1980-1989 time-average ensemble-mean residency time at 850 hPa and the 1980-1989 time-average relative internal variability for mean-sea-level pressure. Blue is for winter while red corresponds to summer.

References

Lucas-Picher, P., D. Caya, R. de Elia and R. Laprise, Investigation of regional climate models' internal variability with a ten-member ensemble of 10-year simulations over a large domain, *Clim. Dyn.* Vol. 31, pp. 927-940, 2008a.

Lucas-Picher, P., D. Caya, S. Biner and R. Laprise, Quantification of the lateral boundary forcing of a regional climate model using an aging tracer, *Mon. Wea. Rev.* Vol. 136, pp. 4980–4996, 2008b.

von Storch, H., Models of global and regional climate, Encyclopedia of Hydrological Sciences, Part 3. Meteorology and Climatology, Chapter 32, pp. 478-490, 2005.

Selected examples of the added value of regional climate models

H.E. Markus Meier[1/5], Lars Bärring[1], Ole Bössing Christensen[2], Erik Kjellström[1], Philip Lorenz[3], Burkhardt Rockel[4], and Eduardo Zorita[4]

[1]Swedish Meteorological and Hydrological Institute, Norrköping, Sweden, markus.meier@smhi.se, [2]Danish Climate Center, Danish Meteorological Institute, Copenhagen, Denmark, [3]Max Planck Institute for Meteorology, Hamburg, Germany, [4]GKSS-Research Centre Geesthacht GmbH, Geesthacht, Germany, [5]Stockholm University, Stockholm, Sweden

1. Background

Regional Climate Models (RCMs) can be used for (1) dynamical downscaling of Global Climate Models (GCMs), (2) regional reanalyses utilizing data assimilation schemes, (3) sampling network design, (4) supplying hypotheses, among others guiding detection and attribution studies, and for (5) testing dynamical hypotheses and new parameterizations. However, the question is how to infer the added value by studying these topics with RCMs instead of using a global model framework or statistical analysis of observational evidence derived from a network. To discuss the issue of added value a BALTEX working group was formed (www.baltex-research.eu/organisation/ bwg_rcm.html). The working group on the "Utility of Regional Climate Models" will be active during a three-year period (2007-2010), conducting working group meetings, organizing workshops open for all interested scientist on the topic, and setting up international collaborations and projects financed by the EU, BONUS or national funding agencies. An example of such a project proposed within BALTEX is ECOSUPPORT (An advanced modelling tool for scenarios of the Baltic Sea Ecosystem to support decision making) addressing the question how to regionalize GCM simulations to assess the impact of changing climate on the Baltic Sea ecosystem (*Meier, 2008*). Various scientific questions related to the tasks of the working group may be addressed using results of a RCM forced with lateral boundaries either from the ERA40 reanalysis or from transient global simulations. The working group will prepare a brief report summarizing the results of the discussions and of common projects until the next BALTEX conference in 2010. Preliminary results will be presented at the workshop in Lund.

2. Small-scale variability

RCMs can generate small-scale variability in a realistic way. This is shown for instance in the Big Brother experiment (e.g. *Denis et al., 2002; 2003*). In particular fine-scale structures related to orography and land-sea contrasts are improved. Strongly localised forcing leads to more improvements. This is a clear indication that RCMs provides added value compared to the forcing AOGCMs. However, the utility of the RCM is not primarily to add increased skill to the large scale. An example is presented by *Zahn et al. (2008)*. They investigated polar lows in the coarse-resolution NCEP reanalysis compared to high-resolution RCM results from CLM (Figs. 1 and 2). The RCM improves the wind speed and sea level pressure anomalies connected with a polar low.

3. More detailed processes

RCMs can include more detailed processes operating on the local and regional scales of interest. This also implies added value compared to the forcing data. As an example simulated extreme precipitation over Denmark in control and scenario simulations are shown (Fig.3). Using point wise daily precipitation data covering land and sea points around Denmark for a current period (1961-1990), extremes of daily precipitation have been analyzed as a function of regional model resolution. Fig. 3 illustrates that the high-resolution simulation results in much higher and more realistic extremes in precipitation (compare the pink observational curve with the thick black 12km and the solid orange 50km curves). This effect is not just a trivial effect of aggregation, as is illustrated in the thin solid black curve, where daily values for the 12km grid point were aggregated to 50km grid points before the analysis of extremes; this curve is more realistic than the original 50km simulation.

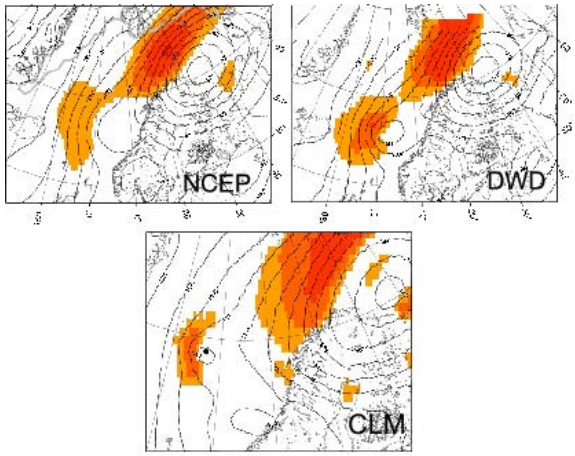

Fig. 1: 10m wind speed ≥ 13.9 m/s and air pressure (at mean sea level) on 15 October 1993: NCEP/NCAR analysis after interpolation onto the CLM grid, DWD analysis data, CLM simulation. The black dot indicates the positions of the polar low's pressure minimum in the respective untreated field of the CLM simulation.

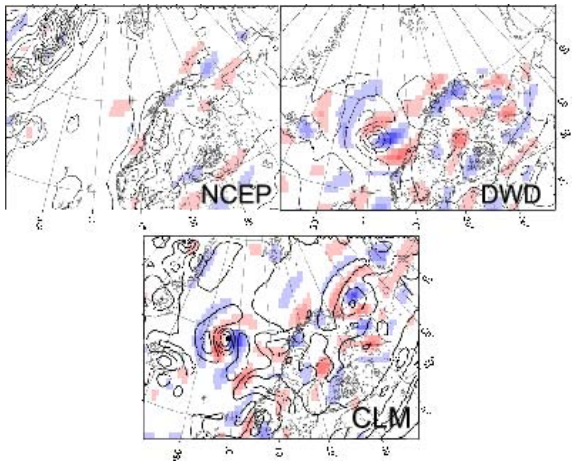

Fig. 2: Band-pass filtered mslp (isolines; hPa) and 10m wind speed anomalies on 15 October 1993: NCEP/NCAR analysis after interpolation onto the CLM grid, DWD analysis data, CLM simulation. The black dot indicates the positions of the polar low's pressure minimum in the respective untreated field of the CLM simulation.

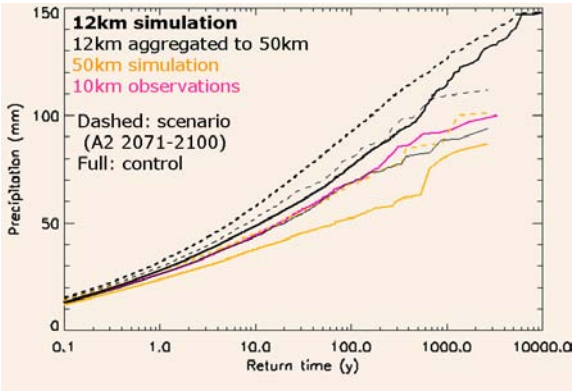

Fig.3: Precipitation over Denmark as a function of the return period in HIRHAM4 in various horizontal resolutions for the period 1961-1990.

With the HIRHAM4 model at the Danish Meteorological Institute, simulations were performed in 50km, 25km and 12km resolution in the setup used in the PRUDENCE project (*Christensen et al., 2007*). Data are compared to a gridded 10km observational data set of the DMI. Individual points from the 30-year simulations are pooled, giving nominal return times up to 10000 years.

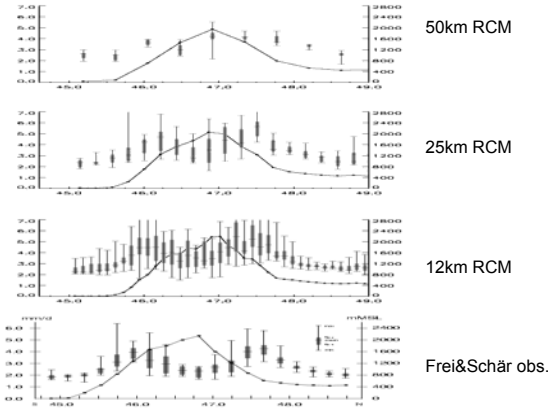

Fig. 4: Longitudinal averaged precipitation as a function of latitude over the Alps in various horizontal resolutions.

In Fig. 4 we show the precipitation as a function of latitude and averaged over longitudes between 11°E and 13.5°E (the Alps). These simulations are compared with a station-based plot from *Frei and Schär* (1998). For simulation results the error bars correspond to the spread among lattice points; for the observation-based plot the spread is among observation stations. It is clear from the plots that the precipitation in the lowest-resolution simulation does not capture the dip on the top of the mountains, whereas the 25km and particularly the 12km resolution simulations have realistic precipitation on the slopes of the mountain range.

4. Added value compared to other methods

RCMs improve small scales compared to the forcing data and sometimes even compared to statistical downscaling methods. For instance, *Schmidli et al. (2006)* found that RCM downscaling improved the precipitation patter over the Alpine region, not just compared to the forcing data, but also to statistical downscaling methods. This is an important finding as it tells us that there is added value to RCMs not just compared to the coarser AOGCMs but also compared to other methods.

5. Consistent scenario simulations

For climate change impact studies on land or in the ocean the output of dynamically consistent high-resolution RCM simulations are often needed because various variables like air temperature, precipitation, sea level pressure, wind, cloudiness, etc. are used together as forcing fields for mechanistic dynamical impact models. To this end, RCMs provide an essential added value because the output fields are physically consistent in time and space, as well as across the fields. For applications in the marine environment actually coupled atmosphere-ice-ocean models are needed. Otherwise SSTs over the Baltic Sea might not be realistically represented because SSTs from GCM simulations are often not appropriate lower boundary data for atmospheric RCMs. Thus, two regional coupled model systems have been developed: RCAO (*Döscher et al. 2002*) and BALTIMOS (*Lehmann et al. 2004*). Although the results of GCMs on the regional scale may differ substantially, RCMs can help to identify common features in climate change scenarios. Albeit a completely different climate change signal of the large scale patterns in future change in wind speed (*Räisänen et al.*, 2004) the detailed RCAO model shows the common feature of increasing wind speed in the Bothnian Bay due to changes in the atmospheric stability when sea ice disappears. The higher resolution and better description of relevant processes in RCAO allows to identify robust climate change signals on the regional scale.

References

Christensen, J. H., T. R. Carter, M. Rummukainen and G. Amanatidis. *Clim. Ch*. **81** 1-6, 2007

Denis, B., R. Laprise, D. Caya and J. Côté, Downscaling ability of one-way –nested regional climate models: The Big-Brother experiment. *Clim. Dyn.*, 18, 627-646, 2002:

Denis, B., R. Laprise and D. Caya, Sensitivity of a regional climate model to the spatial resolution and temporal updating frequency of the lateral boundary conditions, *Clim. Dyn.*, 20, 107-126, 2003

Döscher, R., U. Willen, C. Jones, A. Rutgersson, H.E.M. Meier, U. Hansson, and L.P. Graham, The development of the regional coupled ocean-atmosphere model RCAO. *Boreal Env. Res.*, 7, 183-192. 2002

Frei, C., and C. Schär. A precipitation climatology of the Alps from high-resolution rain-gauge observations. *Int. J. Climatol.*, 18, 873-900, 1998

Lehmann, A., D. Jacob and P. Lorenz, Modelling the exceptional Baltic Sea inflow events in 2002–2003, Geophysical Research Letters, Vol. 31, L21308, 2004

Meier, H.E.M., ECOSUPPORT - An advanced modeling tool for scenarios of the Baltic Sea ECOsystem to SUPPORT decision making, *BALTEX Newsletter*, GKSS, Geesthacht, Germany, 12, 7-10, 2008

Meier, H.E.M., B. Broman, H. Kallio, and E. Kjellström, 2006: Projections of future surface winds, sea levels, and wind waves in the late 21st century and their application for impact studies of flood prone areas in the Baltic Sea region. In*: Schmidt-Thome, P. (ed.), Sea level changes affecting the spatial development of the Baltic Sea region, Geological Survey of Finland, Special Paper,* 41, Espoo, 23-43.

Räisänen, J., U. Hansson, A. Ullerstig, R. Döscher, L.P. Graham, C. Jones, H.E.M. Meier, P. Samuelsson, and U. Willen, 2004: European climate in the late twenty-first century: regional simulations with two driving global models and two forcing scenarios. *Clim. Dyn.*, 22, 13-31.

Schmidli, J., C. Frei and P.L. Vidale, Downscaling from GC precipitation: A benchmark for dynamical and statistical downscaling methods, *Int. J. Climatol.*, 26, 679-689, 2006

Zahn, M., H. von Storch, and S. Bakan, Climate mode simulation of North Atlantic polar lows in a limited area model, *Tellus*, Ser. A, 60, 620–631, 2008

The climate change in Europe simulated by the regional climate model COSMO-CLM

Kai S. Radtke and Klaus Keuler

Brandenburg University of Technology, Environmental Meteorology, 03044 Cottbus, Germany, radtke@tu-cottbus.de

1. Introduction

A small ensemble of regional climate simulations (Hollweg et al., 2008) was performed with the climate version (Böhm et al., 2006) of the numerical weather prediction model COSMO ('COnsortium for SMall scale Modelling', formerly known as LM) (Steppeler et al., 2003). The COSMO-CLM has been forced by output of the ECHAM5/MPIOM global climate model, which contributed to the fourth climate assessment report of the 'International Panel on Climate Change' (IPCC, 2007). The simulations were performed by the Model and Data group (M&D) of the Max Planck Institute for Meteorology. The configuration of the model was developed by the CLM Community (http://www.clm-community.eu/). In this context, three realisations of the climate of the 20th century (1961-2000) were simulated. Each of the IPCC scenarios A1B and B2 (Nakićenović, 2000) for the climate of the 21st century (2001-2100) was simulated twice. The model grid has a resolution of 0.165° and covers Europe nearly complete.

Here, the climate change signal and its variability with regard to the different scenarios, the different realisations and different time periods as well as regional and seasonal differences are considered. Simulation results for the 2 m air temperature and the precipitation sum are presented.

2. Temperature

The annual mean temperature for the climate of the 20th century (1961-1990) amounts 280.77 K to 281.07 K for Central Europe. Thus, the different realisations vary up to 0.3 K.

The 70-year climate change signals (2031-2060 vs. 1961-1990) amount from 1.39 to 1.95 K for the A1B scenario (figure 1) and from 0.84 to 1.30 K for B1. The variability is caused by considering the different realisations. Six paired comparisons between the two realisations of the future climate and the three realisations of the climate of the 20th century were taken into account for both scenarios. These variability amounts to 0.56 K for the A1B scenario and to 0.46 K for B1, approximately 25-50% of the absolute value of the simulated climate change. The warming is 0.55 to 0.65 K larger in the A1B scenario than in B1 for Central Europe.

The annual cycle of temperature change for the A1B scenario (figure 1) shows the strongest warming in summer and winter and a moderate warming in spring. The B1 scenario feature a similar shape of the seasonal distribution of climate change, but the warming is always lower.

The 100-year climate change signal (2061-2090 vs. 1961-1990) is more intense than the 70-year signal, but it shows for both scenarios a similar structure. The warming for Central Europe amounts from 2.81 to 3.19 K in the A1B scenario and from 1.79 to 2.13 K in the B1 scenario. The shape of the annual cycle of the climate change is similar to the 70-year signal, but the values are larger. For the B1 scenario, this increase in time is somewhat lower.

The simulated warming is in southern, southwest and northern Europe relative strong, but in Central Europe more moderate. The increase in annual mean temperature for northern Europe (A1B, 70-year: 1.8 to 2.2 K for Scandinavia) and southern Europe (1.8 to 1.9 K for the Iberian Peninsula) has a similar magnitude. But the seasonal trends of global warming are completely different. The warming in southern Europe is strongest in summer. In contrast, it is strongest in winter time in northern Europe. This fact is characteristic for both scenarios.

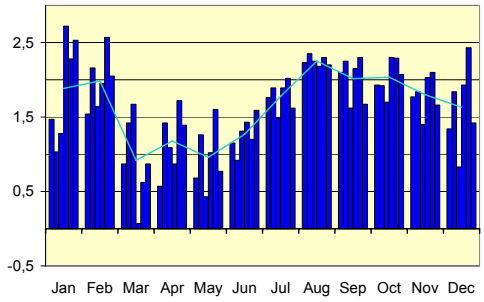

Figure 1. The 70-year climate change (2031-2060 vs. 1961-1990) for the near surface temperatures for Central Europe for the scenario A1B in K. Six paired comparisons (A1B (realisation 1) minus climate of the 20-th century (realisation 1 to 3) and the same for A1B (realisation 2)) are given for any month. The line shows the average of all paired comparisons.

3. Precipitation

The 30-year averages of annual precipitation sums vary for the climate of the 20th Century from 1021 to 1036 mm for Central Europe. The 70-year climate change signal amounts from 4 to 21 mm for A1B, from -17 to 34 mm for B1. So, the change of the precipitation in Central Europe is low (the largest value is lesser than 5% of the total precipitation amount). The variability of the simulated climate change for the different paired comparisons is relatively large. Increases as well as decreases are simulated. Thus, the simulations show no reliable change of the annual precipitation sum for Central Europe. But they feature a shift of precipitation from summer to winter. This shift is more clearly developed in the 100-year climate change signal (figure 2). Furthermore, it's stronger in the A1B scenario. The 100-year time period also does not show a reliable climate change for the annual precipitation sum for both scenarios for Central Europe. The changes amount from -16 to 12 mm for the A1B scenario and from -2.5 to 18 mm for the B1 scenario.

Central Europe is in the transition zone between two domains in Europe. An increase of annual precipitation is simulated in the area of northern Europe (A1B, 70-year: 41 to 97 mm for Scandinavia). It's strongest in the winter. But, the model produces a decrease in annual precipitation for south and southwest Europe (-145 to +2 mm for the Iberian Peninsula). This decrease is mainly caused by the summer months. Both scenarios show that spatial pattern.

These structures are more intense in the 100-year climate change signal.

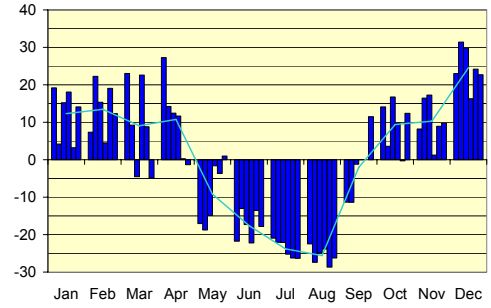

Figure 2. The 100-year climate change (2061-2090 vs. 1961-1990) for the precipitation sum for Central Europe for the scenario A1B in %. Six paired comparisons (A1B (realisation 1) minus climate of the 20-th century (realisation 1 to 3) and the same for A1B (realisation 2)) are given for any month. The line shows the average of all paired comparisons.

References

Böhm, U., M. Kücken, W. Ahrens, A. Block, D. Hauffe, K. Keuler, B. Rockel, A. Will, CLM – The climate version of LM: Brief description and long-term application. Proceedings from the COSMO General Meeting 2005, *COSMO Newsletter*, No. 6, pp. 225 – 235, 2006

Hollweg, H.-D., U. Böhm, I. Fast, B. Hennemuth, K. Keuler, E. Keup-Thiel, M. Lautenschlager, S. Legutke, K. Radtke, B. Rockel, M. Schubert, A. Will, M. Woldt, C. Wunram, Ensemble Simulations over Europe with the Regional Climate Model CLM forced with IPCC AR4 Global Scenarios, *Max Planck Institute for Meteorology, M&D Series, Technical Report*, No. 3, pp. 152, 2008

IPCC, Solomon, S., D. Qin, M. Manning, Z. Chen, M. Marquis, K. B. Averyt, M. Tignor, H. L. Miller (Eds.), IPCC Fourth Assessment Report, Intergovernmental Panel on Climate Change, The Physical Science Basis, *IPCC, Cambridge University Press*, pp. 996, 2007

Nakiećenović, N., R. Swart (Eds.), Special report on emissions scenarios, Intergovernmental Panel on Climate Change, *IPCC, Cambridge University Press*, pp. 599, 2000

Steppeler, J., G. Doms, U. Schättler, H. W. Bitzer, A. Gassmann, U. Damrath, G. Gregoric, Meso-gamma scale forecasts using the non-hydrostatic model LM, *Meteorol. Atmos. Phys.,* No. 82, pp. 75-96, 2003

Simulation of South Asian summer monsoon dynamics using REMO

Fahad Saeed, Stefan Hagemann and Daniela Jacob

Max Planck Institute for Meteorology, Hamburg, Germany. fahad.saeed@zmaw.de

1. Abstract

This study investigates the capability of regional climate model REMO in simulating the South Asian summer monsoon. The experiment consists of 40 year integration from 1961 to 2000, with 0.5 degree resolution. The ability of REMO to simulate the dynamics of the summer monsoon is tested by comparing a number of fields with observations. Surface and upper level circulation patterns yield results close to ERA40 reanalysis. Simulated temperatures show a warm bias over the Indian plains in comparison to observations; however temperatures over the Tibetan Plateau and along the coast are ably simulated. The model captures the pattern of precipitation over Western Ghats and over the plains but overestimates the precipitation in Northern India and Bangladesh. The East-West oriented precipitation pattern, at the border of India and Nepal is more consistent in REMO than observational data representing the sparse density of stations used for the construction of observational fields in that region. Other dynamical features like seasonal reversal of tropospheric temperature gradient and strengthening of easterly vertical shear compare well with observations. Further, summer monsoon onset dates match reasonably well with the values found in literature. The results indicate that the REMO model can be a useful tool for examining the monsoon behavior under climate change. This work is carried out under WATCH project.

Analysis of precipitation changes in Central Europe within the next decades based on simulations with a high resolution RCM ensemble

Gerd Schädler, Hendrik Feldmann, Hans-Jürgen Panitz

Institute for Meteorology and Climate Research, University/Forschungszentrum Karlsruhe, Germany,
Gerd.Schaedler@imk.fzk.de

1. Introduction

The 4th IPCC report summarises the effects on precipitation for Europe based on global climate models (GCM) simulations as follows: In northern Europe the climate will become moister – especially during winter – and the Mediterranean region will be much drier in the future – especially for the summer months - than it is today. Central Europe lies in the transition region between these two regimes. This is reflected in the fact that the current GCMs do not give a consistent picture of the precipitation characteristics for this region in the 21st century. Possible reasons for that may be that mountain ridges like the Alps are not adequately accounted for in the coarse resolution of GCMs and that climate change induced changes in weather patterns are highly variable in this region.

In this study we focus on that part of Central Europe situated between 47.5°N to 52°N and 5°E to 13°E (cf. Fig. 1).

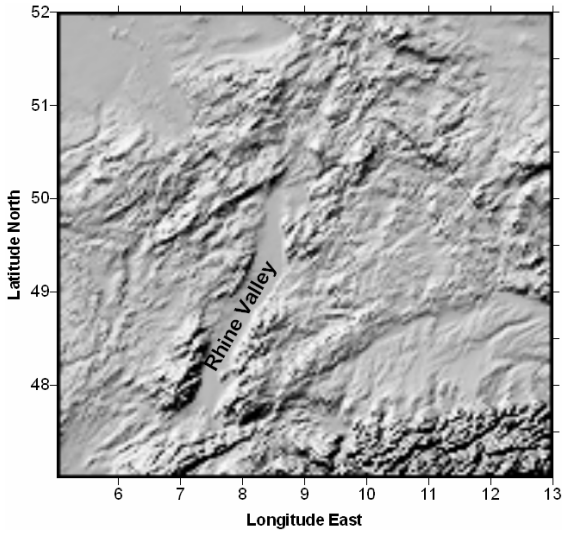

Figure 1: Orography detail of the study area.

This includes regions with complex topography north of the Alps from eastern France to Bavaria, for instance the Upper Rhine Valley and the Black Forest, regions where trends in temperature and precipitation over the last decades have been observed to be significant and higher than average. Furthermore, it includes densely populated narrow valleys prone to flash floods, making detailed knowledge of future precipitation scenarios - including uncertainty estimates – essential for the development of adaptation measures. Therefore, high-resolution simulations with regional climate models (RCMs) are necessary to derive reliable estimates of the upcoming changes in the precipitation pattern.

We analyse climate simulations over several decades performed with RCMs on grid sizes below 20 km for Central Europe and focus on possible precipitation changes until the middle of this century. We will discuss climatological precipitation as well as heavy precipitation events with a 10-year return period.

2. Ensemble Description

Our ensemble is based on a number of long-term simulations performed with the RCMs COSMO-CLM (with 18 km and 7 km resolution) and REMO (with a horizontal resolution of 10 km). Up to now, all RCM simulations are driven by ECHAM5 IPCC runs. The RCM simulations have been comprehensively evaluated against gridded observation data (*Feldmann et al.*, 2008) and include different realisations of present day and future climate as well as different IPCC scenarios for future emissions.

Table 1: List of ensemble simulations. Numbers after the underscore indicate the realisation.

Model/Data set	Grid size	Period	Simulations
REMO UBA simulations	10 km	1971-2000	C20_1
		2011-2040	A1B_1, B1_1, A2_1
COSMO CLM Consortial Runs	18 km	1971-2000	C20_1, C20_2, C20_3
		2011-2040	A1B_1, A1B_2, B1_1, B1_2
CCLM	7 km	1971-2000	C20_1, C20_3
		2011-2040	A1B_1, A1B_3

The 30 year projection covers the period 2011 – 2040. During this phase the greenhouse gas emissions of the different scenarios do not differ much, but the variations still have an effect on the internal variability. The climate change effects during the projection period are compared to a reference period from 1971 – 2000. Overall the ensemble consists of 6 members for the present-day climate simulations and 9 members for the projections.

3. Methodology

An important aspect is the assessment of the uncertainty of regional projections. For that purpose, we evaluate the ensemble of simulations to establish estimates and assess the regional changes in the precipitation regime. In addition, the use of a set of realizations provides the opportunity to broaden the data basis for an extreme values analysis for a given period.

A good representation of the present day climate in the models is necessary but not sufficient to derive reliable estimates of future climate. As an additional criterion we use the agreement between the ensemble members: if a majority of simulations shows a similar behaviour in a given region, despite their different setups or states of internal variability, we can have more confidence in the climate change estimates.

For the climatological precipitation, the statistical significance of the changes has been calculated using the non-parametric Wilcoxon test. The extreme values have been calculated using the peak-over-threshold approach and fitting a Kappa distribution on the highest 10% of the distribution (Früh et al. 2008). Here the significance of the climate change signal has been derived by calculating confidence intervals via bootstrapping.

4. Results

We will discuss the following findings:

RCM simulations provide added value: whereas by construction the GCMs see no spatial variability below their grid size and exhibit low ensemble agreement, the RCM ensemble results show considerable spatial variability of the precipitation distribution. Although the results for the different models and setups show discrepancies especially in some regions with complex topography, there are distinct regions of high ensemble agreement concerning increase/decrease of precipitation (Fig. 2).

The different realisations of future climate do not differ significantly between the emissions scenarios used (possibly in contrast to temperature). However, there are larger variations between the different realisations of each emission scenario. This indicates that for precipitation the internal variability is dominant over the differences between the IPCC SRES scenarios until the middle of the 21st century. Also, the three realisations for the present-day climate (CLM-CR C20) do not differ significantly.

Future and present-day mean precipitation differs significantly for yearly totals and the winter season, but less for the summer season.

There is a marked tendency towards increased variability (standard deviation/mean) in the future precipitation for all seasons, with higher 95th percentile during all seasons and lower 5th percentile of summer precipitations, i.e. a tendency towards a more extreme climate.

Changes in the spatial patterns of heavy precipitation events are not necessarily coincident with the patterns for climatological precipitation.

There seems to be a northwest to southeast gradient in the precipitation changes indicating a combination of the transition from the Mediterranean to northern European regime with the transition from Atlantic to continental conditions.

5. Outlook

In a next step, we will augment the ensemble by RCM simulations driven by other GCMs.

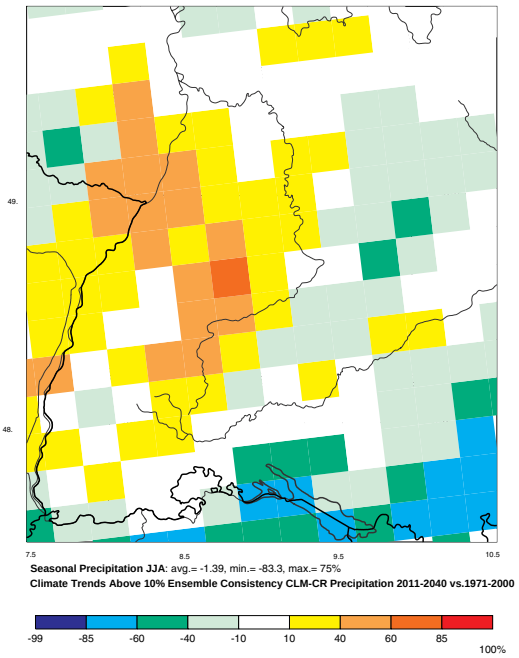

Figure 2: Percentage agreement between the ensemble members for the climate change signal 2011 – 2040 vs. 1971 – 2000 for JJA mean precipitation changes above 10% (absolute).

References

Feldmann, H., B. Früh, G. Schädler, H.-J. Panitz, K. Keuler, D. Jacob, P. Lorenz, Evaluation of the precipitation for South-western Germany from high resolution simulations with regional climate models, *Meteorol. Zeitschrift*, Vol. 17, No. 4, pp. 455-465, 2008

Früh, B., H. Feldmann, H.-J. Panitz, G. Schädler, D. Jacob. P. Lorenz, K. Keuler, Determination of precipitation return values in complex terrain and their evaluation, submitted to: *J. of Climate*, 2008

Sensitivity studies of model setup in the alpine region using MM5 and RegCM

Irene Schicker, Imran Nadeem, Herbert Formayer

Institute of Meteorology, University of Natural Resources and Applied Life Sciences, Peter-Jordan-Straße 82, A-1190 Vienna, Austria, irene.schicker@boku.ac.at

1. Introduction

Regional climate modeling in the alpine area is a challenging task. Currently, our institute is participating in two projects, CECILIA (http://cecilia-eu.org) and Reclip:century (Basic Data Set of Regional Climate Scenarios), to study regional climate change in the Alpine region using two different meteorological models, MM5 (*Grell et al., 1994*) and RegCM (*Pal et al., 2007*). The present study is a part of these projects and focuses on selection of domain, nesting versus direct runs, comparison of different physical parameterization schemes and lateral boundary conditions. The horizontal resolution of 10 km is used to capture the effects of the complex topographical and land use features of the region.

The case study is carried for the year 1999. This year is particularly interesting because of flooding in Danube Catchment in May followed by the storm in December.

2. Domain and Model setup – MM5

As the innermost domain should cover both the Alpine ridge and the eastern parts of Austria and comparability with the Greater Alpine Region (GAR) (*Auer et al*., 2007) should also be given, no changes on the horizontal domain size have been made. For the outermost domain, four different grid box setups have been tested. Results of two of them, domain ML and domain L, are shown here (see Fig. 1). Due to computational limitations 30 vertical half σ levels have been used.

Zängl options for alpine modeling (z-diffusion, orographic shadowing) implemented in MM5V3.7 have been used in all the test runs. One test run used additional improvements in the NOAH LSM scheme implemented by G. Zängl and his group (*Mauser and Strasser, 2007*). Table 1 gives an overview of the different setups and physical parameterizations used.

Table 1. Setups of the different sensitivity runs. Cumulus schemes used are BM for the outermost domain and Grell for the innermost domain.

	ML1	ML2	L1	L2
PBL	ETA/MRF	ETA	ETA/MRF	ETA
radiation	RRTM	RRTM	RRTM	RRTM
Land use	NOAH	5 layer soil	NOAH	5 layer soil
cumulus scheme	BM/Grell	BM/Grell	BM/Grell	BM/Grell
explicit moisture	Reisner 2	Reisner 2	Reisner 2	Reisner 2

3. Domain and Model setup – RegCM

The innermost domain used by RegCM3 simulations closely resembles that of MM5. The boundary conditions used for various simulations were ECMWF Interim Re-Analysis (ERA-Interim, 0.75° and 1.5° grid spacings, 6-h intervals), the ECMWF 40 Years Re-Analysis (ERA40, 1° and 2.5° grid spacings, 6-h interval) and finally the 2.5°, 6-h NCEP/DOE AMIP-II Reanalysis (Reanalysis-2). Sea Surface Temperature for the simulated periods was obtained from a UK Met Office Global Ocean Surface Temperature (GISST), a set of SST data in monthly 1° area grids. Table 2 summarizes different domain settings and Nesting strategies for RegCM3 simulations.

Table 2. Setup of RegCM sensitivity runs.

Reanalysis	Resolution	Nesting		Physics
		2 / 3 nests	1 / 2 nest	
ERA 40	30 km → 10 km	1 way	direct	Grell Conv.,PBL (Holtslag), BATS1e Radiation: NCAR CCM3 SUBEX
ERA Interim	30 km→ 10 km	1 way	direct	
NCEP/DOE AMIP-II	90 km → 30 km→ 10 km	1 way	30 km→ 10 km	

Domain setup of the RegCM runs is shown in Figure 1.

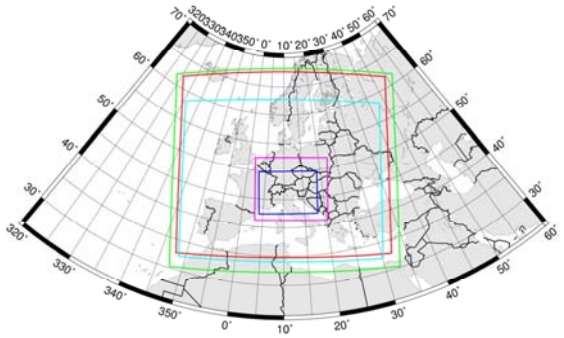

Figure 1. MM5 and RegCM domains. In magenta MM5 domain 2, which has been used in all three domain settings. In blue RegCM domain 2 and 3 respectively. In green MM5 domain1 L, in red MM5 domain ML. RegCM domain 1 is shown in cyan.

4. Results

Very first results of the May 1999 case study simulated with MM5 show that the general patterns of the precipitation are very well captured if using grid nudging options to avoid drifting of the model. As grid nudging is not advisable when performing climate simulations, also some runs without grid nudging have been performed. First results of the May 1999 flooding event of two different L1 runs, without grid nudging, are shown in Figures 3 and 4. In Figure 2 the 72 h precipitation sum, obtained from the gridded observation data set of *Frei and Schär (1998)* is shown for comparison.

The RegCM3 simulation driven with ERA40 and ERA-Interim shows that direct downscaling to 10km produces better results than Nested Run 30km→10km. When recently released ERA-Interim Reanalysis was used as lateral and boundary conditions, the simulated

precipitation field was more closer to observations than simulated by the model driven with other boundary conditions (see Figure 5). Comparison between hydrostatic model RegCM3 and non-hydrostatic model MM5 will also be carried out.

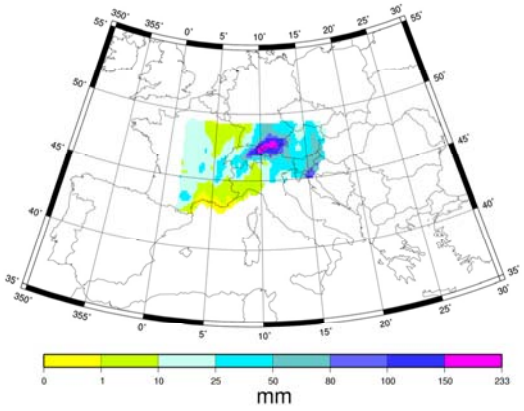

Figure 2. 72 h sum of the heavy flood event of 20 May 1999 to 22 May 1999, based on data of *Frei and Schär (1998)*.

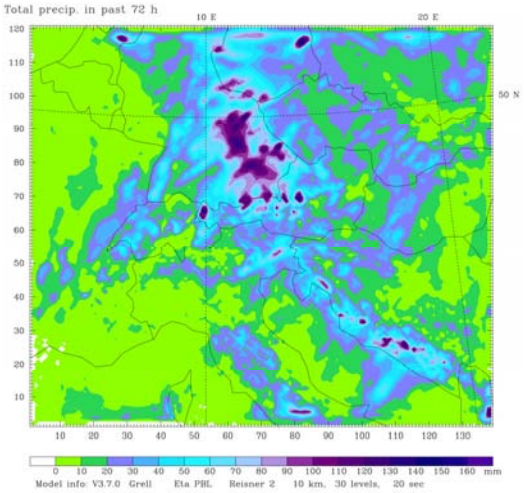

Figure 3. Total precipitation in the past 72 h of the May event of run L1 with the additional changes made by Zängl (*Mauser and Strasser, 2007*) in the NOAH LSM.

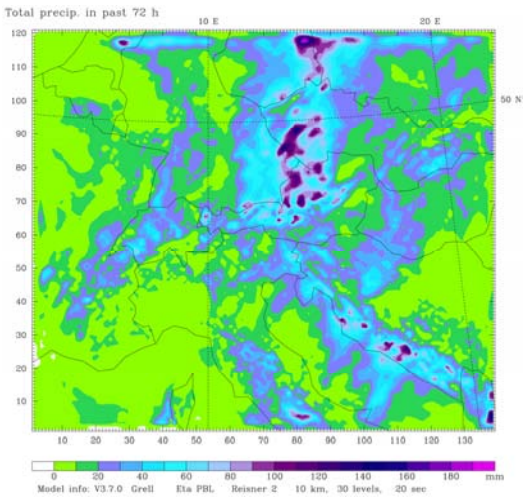

Figure 4. Same as Figure 3 but without the additional changes in the NOAH LSM model.

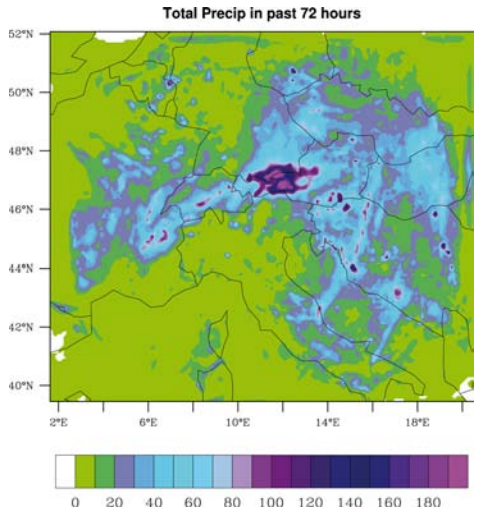

Figure 5. Same as Figure 3 but of one of the RegCM simulations.

References

Auer, I., R. Böhm, A. Jurković, W. Lipa, A. Orlik, R. Potzmann, W. Schöner, M. Ungersböck, C. Matulla, K. Briffa, P. Jones, D. Efthymiadis, M. Brunetti, T. Nanni, M. Maugeri, L. Mercalli, O. Mestre, J.-M. Moisselin, M. Begert, G. Müller-Westermeier, V. Kveton, O. Bochnicek, P. Stastny, M. Lapin, S. Szalai, T. Szentimrey, T. Cegnar, M. Dolinar, M. Gajic-Capka, K. Zaninovic, Z. Majstorovic, and E. Nieplova, HISTALP - historical instrumental climatological surface time series of the Greater Alpine Region, *International Journal of Climatology*, 27, 1, 17-4166. (doi:10.1002/joc.1377), 2007

Frei, C. and C. Schär. A precipitation climatology of the Alps from high-resolution rain-gauge observations, *Int. J. Climatol.*, 18, 873 – 900, 1998

Grell G., Dudhia J. and Stauffer D, A Description of the Fifth-Generation Penn State/NCAR Mesoscale Model (MM5), *NCAR/TN-398+STR*, (http://www.mmm.ucar.edu/mm5/documents/mm5-desc-doc.html), 1994

Mauser, W. and U. Strasser (Eds.), GLOWA-Danube: Integrative Techniken, Szenarien und Strategien zur Zukunft des Wassers im Einzugsgebiet der Oberen Donau, Department für Geographie, *Lehrstuhl für Geographie und Geographische Fernerkundung Ludwig-Maximilians-Universität München*, (http://www.glowa-danube.de/PDF/reports/abschlussbericht_phase2.pdf, accessed 06.02.2009), 2007

Pal, J.S., F. Giorgi, X. Bi, N. Elguindi, F. Solmon, X. Gao, S.A. Rauscher, R. Francisco, A. Zakey, J. Winter, M. Ashfaq, F.S. Syed, J.L. Bell, N.S. Diffenbaugh, J. Karmacharya, A. Konaré, D. Martinez, R.P. da Rocha, L.C. Sloan, and A.L. Steiner, Regional Climate Modeling for the Developing World: The ICTP RegCM3 and RegCNET. *Bull. Amer. Meteor. Soc.*, **88**, 1395–1409. 2007

Parameter perturbation study with the GEM-LAM: the issue of domain size

Leo Separovic[1,3,4], Ramon de Elia[2,3,4] and René Laprise[1,3,4]

[1]Université du Québec à Montréal (UQÀM), Montréal (Québec), Canada, separovi@sca.uqam.ca; [2]Consortium Ouranos, Montréal (Québec), Canada; [3]Canadian Network for Regional Climate Modelling and Diagnostics (CRCMD), Montréal (Québec), Canada; [4]Centre pour l'Étude et la Simulation du Climat à l'Échelle Régionale (ESCER), Montréal (Québec), Canada.

1. Introduction

Fine-scale processes that are not resolved explicitly in models are parameterized with bulk formulae that depend on large-scale variables. A number of poorly constrained parameters employed in these parameterizations rely on a mixture of theoretical understanding and empirical fitting. The skill level of a model is achieved through the process of tuning in which parameters are adjusted on the trial-and-error basis. However, due to the large number of parameters present in the model, it is impossible to run the model for every combination of their plausible value and examine all possible skill scores. Hence, tuning does not guarantee neither an optimal skill level nor that this skill is not achieved as a compensation of model errors.

This study aims at quantifying uncertainty in dynamical downscaling originating in poorly constrained Regional Climate Model (RCM) parameters. For this purpose we are currently designing a Perturbed-Parameters Ensemble (PPE) of RCM simulations. Currently underway is the exploratory phase that should allow for an optimized trade-off between the available computational/human resources and ensemble size necessary to formally quantify parameter uncertainty.

Important decisions in the PPE design are related to the domain size and position as well as integration period. The domain (integration period) should be as small (short) as possible due to the enormous computational cost of the PPE, but sufficiently large to allow extrapolation of results to the typical operational RCM simulations. Here we discuss the sensitivity of 3-month averages of model's variables to parameter perturbations obtained using two domains of different size, focusing on the issue of detection of model response to perturbations against internal variability noise. Currently underway is the study of the nonlinearity of the model output in the parameter space in order to verify whether summing up the responses to perturbations of individual parameters can approximate the response to simultaneous multiple-parameter perturbations.

2. Methodology

The model is the limited-area version of the Global Environmental Multi-scale (GEM) model, described in *Yeh et al.* (2002). It is a non-hydrostatic grid-point model based on the semi-Lagrangian, semi-implicit time discretization scheme. It includes a terrain-following vertical coordinate based on hydrostatic pressure with 58 levels in the vertical and the horizontal discretization on an Arakawa C grid.

The ensemble integrations are performed over a single year at two domains shown in Fig 1. The large (small) domain consists of 120x120 (72x50) grid points in the zonal and latitudinal direction, respectively, both at the resolution of ~55 km. The domains shown in Fig 1 include a 10-point relaxation zone at the perimeter of their boundaries. The initial and Lateral Boundary Conditions (LBC) are provided by ERA40 reanalyses and ocean surface is from AMIP2.

Figure 1. Two domains (large – 120x120 and small, denoted by the rectangle – 72x50 grid points).

For each domain, the PPE consist of the standard (unperturbed) version of the model and single-parameter perturbations. Regardless of its origin and magnitude, perturbations also excite internal variability noise. In order to distinguish the model sensitivity to perturbations from this noise, each member of the PPE consists of 5 identical integrations initialized from November 01 trough 05, 1992, each at 00UTC, 24 hours apart. All simulations end on December 01, 1993 at 00UTC, thus providing a 12-month integration period (November 1992 being excluded from consideration). For each model run, time averages are computed for the four distinct seasons. The only exception is the standard model version for which 10 lagged integrations with perturbed initial conditions are performed in order to provide a more robust estimate of noise statistics.

The noise standard deviation is estimated by the RMSD of 10 lagged seasonal averages obtained by the standard model version. The model response to a parameter perturbation is quantified by the difference between the two means: that computed from 5 integrations given a parameter perturbation and that from 10 runs of the standard version. This is further referred to as the signal. The statistical significance of the signal is quantified by the rejection level of the null hypothesis (H_0) that the two means are drawn from the same distribution, under the two-tailed t-distribution test. Finally, results obtained using the two domains (Fig. 1) are compared over the area of the smaller domain, excluding its lateral boundary relaxation zone.

The somewhat unusual shape of the small domain (Fig. 1) is chosen to shorten the residence time within the domain of air parcels carried by the climatological zonal flow, while keeping a large latitudinal span for comparison with the results obtained using the large domain. It is shown in *Lucas-Picher et al.* (2008) that the internal variability noise decreases with decreasing average residence time of air parcels within the domain.

3. Results

Fig. 2 shows the analysis of sensitivity of summer (JJA) time-averaged precipitation to a moderate perturbation of the threshold vertical velocity in the trigger function of the Kain-Fritch deep convection scheme. This parameter is perturbed from its standard value of 3.4 cm/s to 4.8 cm/s. In Fig. 2 the noise standard deviation (a), the signal (b) and the level of rejection of H_0 (c), all computed for summer precipitation are shown. Results obtained with the large domain are on the left and those with the small domain on the right.

It can be seen that internal variability noise standard deviation in the large domain (Fig. 2a, left) exhibit very large values that locally reach 2 mm/day. In the same time, in response to the parameter perturbation (Fig. 2b, left), there is a decrease of precipitation over the continent and the southeast portion of the domain, comparable to the noise level. The signal is scarcely distinguishable from internal variability since the level of rejection of H_0 is predominantly below 90% (Fig. 2c, left).

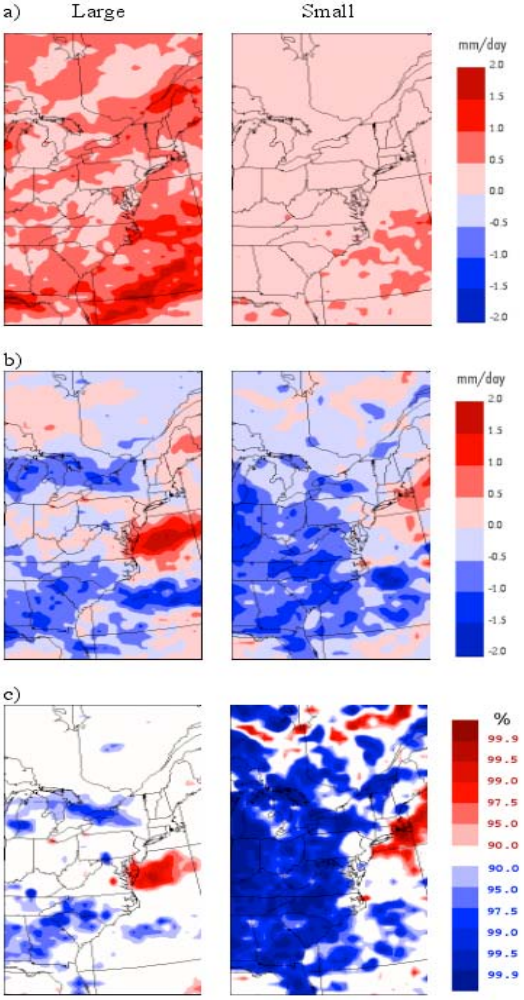

Figure 2. Summer seasonal-average precipitation (left – large domain, right – small domain): (a) internal variability noise standard deviation (mm/day); (b) change in response to positive perturbation of the threshold vertical velocity in the Kain-Fritch deep convection (mm/day), and (c) the statistical significance of the change (%).

Clearly, more simulations with perturbed initial conditions are necessary to provide statistical significance in the large domain. Some more confidence can be attributed to the signal pattern over the continent, since a perturbation of the same parameter and magnitude but of the opposite sign produces a similar pattern of model response but with the opposite sign (not shown). This indicates a strong linear component of the sensitivity to the given parameter. It is also worth noting that the internal variability exhibits a pronounced annual cycle, with maximum in summer and minimum in winter. Hence, the rejection level of H_0 is larger in the remaining seasons. However, the magnitude and the pattern of the signal also considerably vary through seasons.

Reduction of domain size decreases the noise magnitude roughly by factor of 3 (Fig. 2a, right). In the same time, comparison of Figs. 2b left and right shows no evidence that the sensitivity of summer precipitation is reduced. One exception is the area of the positive sensitivity off the coast of Virginia. Over land the absolute change in precipitation is locally even larger in the smaller domain. This is reflected in a substantial increase in statistical significance of the signal: the level of rejection of H_0 becomes larger than 99% over a considerable part of the area of comparison (Fig. 2c, right).

4. Discussion and concluding remarks

It is clear that reduction in domain size decreases the computational cost of the PPE, both directly through reduction of the number of computational points and indirectly – reducing the number of identical simulations with perturbed initial conditions needed to provide the statistical significance of the signal. Given that the computational resources are usually limited by external funding and thus non-negotiable, the lowering of noise is an important advantage of the small domain because it allows allocation of resources to the PPE size (*e.g.*, more parameters and perturbations can be included in the study). Furthermore, noise can render very difficult the quantification of non-linear components of the model response to simultaneous multiple-parameter perturbations.

There are, however, two important disadvantages of the small domain to be noted. Firstly, the results obtained in the small domain are representative for a small region and are of little value for typical RCM domains to which this study is addressed. Secondly, it can be argued that in a too small domain, control of the large-scale interior flow by the LBC may be excessive and suppress the signal. Suppression of the model sensitivity to parameter perturbations would decrease spread among the members of the PPE and yield an underestimation of the uncertainty range with respect to that in typical RCM simulations. Our results provide no evidence that this happens with seasonal precipitation but the concern still remains when less small-scale dominated variables are considered.

References

Lucas-Picher, P., D. Caya, S. Biner, and R. Laprise, Quantification of the Lateral Boundary Forcing of a Regional Climate Model Using an Aging Tracer. *Mon. Wea. Rev.*, 136, 4980–4996, 2008.

Yeh, K.-S., J. Côté, S. Gravel, A. Méthot, A. Patoine, M. Roch, and A. Staniforth, The CMC–MRB Global Environmental Multiscale (GEM) model. Part III: Nonhydrostatic formulation. *Mon. Wea. Rev.*, 130, 339–356, 2002.

Modeling climate over Russian regions: RCM validation and projections

Igor Shkolnik, S. Efimov, T. Pavlova, E. Nadyozhina

Voeikov Main Geophysical Observatory, 7, Karbyshev str., 194021, St.-Petersburg, Russia, igor@main.mgo.rssi.ru

Increased levels of atmospheric greenhouse gases will have bigger effects on climate in northern Eurasia than in most of other regions of the Earth. In this study the estimates of climate and its change potential are obtained using Voeikov Main geophysical observatory regional climate model (RCM) applied to the two major domains in the northern Eurasia (western Russia and Siberia) within the framework of the Northern Eurasia Earth Science Partnership Initiative (NEESPI).

The RCM demonstrated satisfactory performance skill in reproducing 20th century climate and its variability over the northern Eurasia. The presented analysis, in particular, addresses aspects of model validation strategies over the regions with sparce observations (e.g. Siberia and the Russian Far East) at 50 and 25 km resolution. The discretization of RCM output at daily time intervals makes it feasible to investigate statistics of high frequency climate variability and associated rare events. These events at limited modeling resolution are manifested in large-scale slowly evolving climate (weather) anomalies that can be utilized to feed different impact models for more practical assessment. Considered are some changes in the extreme indices of temperature and precipitation in 21st century over Russia. Additionally, changes in cryosphere characteristics over parts of northern Eurasia are shown.

Owing to the largest climate variability the northern Eurasia exhibits significant uncertainties in climate projections. In order to decrease the uncertainties (including those due to natural variability, model sensitivity to prescribed forcings and due to forcings themselves), large samples of RCM simulations are apparently required. Estimates of extreme events and their frequencies of occurrence also require massive RCM ensemble simulations over the region.

Is the position of the model domain over the target area related to the results of a regional climate model?

Kevin Sieck, Philip Lorenz and Daniela Jacob

Max Planck Institute for Meteorology, Hamburg, Germany, kevin.sieck@zmaw.de

1. Introduction

Most studies to investigate uncertainties in regional climate modelling concentrated on the influence of domain sizes (e.g. Laprise et al., 2008), treatment of the lateral boundary conditions (e.g. Lorenz & Jacob, 2005) and uncertainties due to different lateral forcings (PRUDENCE, ENSEMBLES). However, the decision on the position of the model domain over a certain target area was not in the focus of the community. By now it is mainly done by experience and subjective decisions. This study shows that results of a regional climate model can depend on the position of the model domain.

2. Experimental setup

All simulations were performed with the regional climate model REMO (Jacob et al., 2007) at a horizontal resolution of 0.5° (~55 km) over Europe with a domain-size of 81x91 gridboxes. The forcing at the lateral boundaries came from the ERA-15 reanalysis dataset and ECHAM5/MPIOM (Roeckner et al., 2003) simulations of the 20th century. The integration periods for the first forcing were 10 years (1979-1988) and for the latter 20 years (1950-1969). Several members with slight shifts up to 2 gridboxes around a centred control domain were integrated for both forcings.

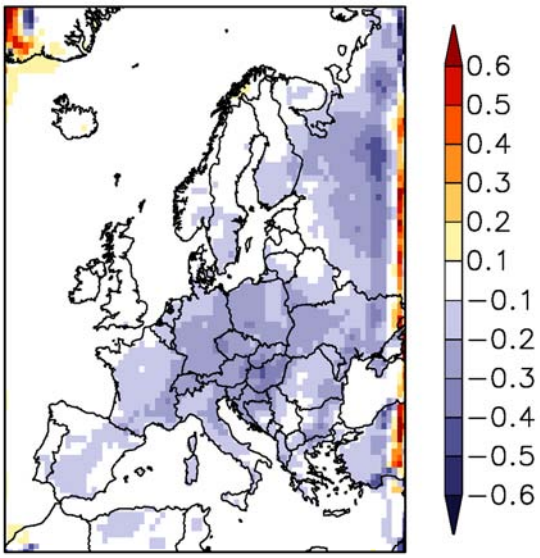

Figure 1. Temperature difference in [K] between two ERA-15 driven runs. Shown is the difference between a run where the model domain was shifted two grid-boxes to the west and the control domain for the period 1979-1988.

3. Results

Results from the ERA-15 driven runs show that shifts of the model domain by one gridbox lead to a systamatic cooling or warming of the near surface temperatures compared to the control domain depending on the direction of the shift. Eastward shifts result in a warming whereas westward shifts show a cooling in central Europe up to 0.2 K between 1979 and 1988. This effect is even stronger if the model domain is shifted by two gridboxes (see Figure 1). Connected to this cooling is an anomalous low pressure system located over the Czech Republic.
To determine if this is a feature of the regional model ECHAM5/MPIOM forcing was used to run REMO. Results show that no systematic variations appear when shifting the model by two gridboxes.

4. Conclusions

The anomalous temperature and pressure patterns found in the ERA-15 driven runs seem to be dependent on the forcing that is used, because they are not showing up in ECHAM5/MPIOM forced integrations. Nevertheless, for ERA-15 forcing this feature seems to be quite robust.

5. Further studies

Further analysis on weather type frequencies for the different runs can show if ERA-15 forcing tends to give the regional model more freedom in developing mesoscale features, so that a small shift in the model domain can lead to significant differences in the climate due to internal variability.

References

Jacob, D., Barring, L., Christensen, O. B., Christensen, J. H., de Castro, M., Deque, M., Giorgi, F., Hagemann, S., Lenderink, G., Rockel, B., Sanchez, E., Schar, C., Seneviratne, S. I., Somot, S., van Ulden, A., van den Hurk, B. & UL, An inter-comparison of regional climate models for Europe: model performance in present-day climate, *Climatic Change*, 81, 31-52, 2007

Laprise, R., R. de Elia, D. Caya1, S. Biner, P. Lucas-Picher, E. Diaconescu, M. Leduc, A. Alexandru, L. Separovic, Challenging some tenets of regional climate modelling, *Meteorol Atmos Phys*, 100, 3-22, 2008

Lorenz, P. & D. Jacob, Influence of regional scale information on the global circulation: A two-way nesting climate simulation, *Geophysical Research Letters*, 32, L18706, 2005

Roeckner, E., Bäuml, G., Bonaventura, L., Brokopf, R., Esch, M., Giorgetta, M., Hagemann, S., Kirchner, I., Kornblueh, L., Manzini, E., Rhodin, A., Schlese, U., Schulzweida, U. & Tompkins, A., The atmospheric general circulation model ECHAM5: Model description, Max Planck Institute for Meteorology, Hamburg, Report Nr. 349, 127pp., 2003

Estimating the Mediterranean Sea water budget: Impact of the design of the RCM

Samuel Somot[1], Nellie Elguindi[2], Emilia Sanchez-Gomez[1], Marine Herrmann[1] and Michel Déqué[1]

(1) Météo-France/CNRM-GAME, 42 av. G. Coriolis, 31057 Toulouse Cedex, France, samuel.somot@meteo.fr
(2) CNRS / Laboratoire d'Aérologie, Toulouse, France

1. Motivations

The Mediterranean Sea can be considered as a thermodynamic machine that exchanges water and heat with the Atlantic Ocean trough the Strait of Gibraltar and with the atmosphere through its surface. Considering the Mediterranean Sea Water Budget (MSWB) multi-year mean, the Mediterranean basin loses water by its surface with an excess of the evaporation over the freshwater input (precipitation, river runoff, Black Sea input). Moreover the MSWB largely drives the Mediterranean Sea water mass formation and therefore a large part of its thermohaline circulation. This could even have an impact on the characteristics of the Atlantic thermohaline circulation through the Mediterranean Outflow Waters that flow into the Atlantic at a depth of about 1000 m. From a climate point of view, the MSWB acts as a water source from the Mediterranean countries and then plays an important role on the water resources of the region.

2. Scientific issues

The regional physical characteristics of the Mediterranean basin (complex orography, strong land-sea contrast, land-atmosphere coupling, air-sea coupling, relative importance of the river inflow, Gibraltar Strait constraint and complex ocean bathymetry) strongly influence the various components of the MSWB. Moreover extreme precipitation events over land and strong evaporation over the sea due to local winds can play a non-negligible role on the mean MSWB.

Therefore, modelling the mean behaviour, the interannual variability and the trends of the MSWB is a challenging task of the Regional Climate Model community in the context of the climate change. It is actually one of the highlighted issues of the future HyMex project planned for the 2010-2020 period. We propose here is to investigate some key scientific issues of the regional modeling of the Mediterranean Sea Water Budget using a wide range of regional climate simulations performed by Météo-France or in the framework of European projects (ENSEMBLES, CIRCE). The addressed scientific questions are the impact of:

A. the horizontal resolution
B. the modelling technique (stretched-grid model, versus limited area model)
C. the nudging technique (spectral versus grid-point)
D. the regional air-sea-river coupling
E. the choice of the RCM
F. the RCM internal variability

In our study, we assume that the volume of the Mediterranean is constant over a long period of time and we define the Mediterranean Sea Water Budget as:

$E - P - R - B \approx G$

Where E is the evaporation, P the precipitation, R is the river discharge into the Mediterranean Sea (see figure 1), B the input from the Black Sea and G the Gibraltar Strait net volume transport.

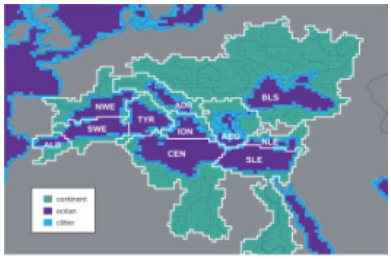

Figure 1. River catchment basin of the Mediterranean Sea (extracted from Ludwig et al. 2009) also used for the TRIP routing scheme model

3. RCM experiments

Various RCM experiments are used to answer the scientific issues define in section 2. The global ARPEGE-Climate model is used at different horizontal resolution (up to 50 km) to answer question A. The global stretched-grid version of ARPEGE-Climate nudged towards ERA40 (see figure 2a) is compared with the limited area model ALADIN-Climate driven by ERA40 (see figure 2b) to answer question B. The same resolution and the same physics are used in both models. Question C is addressed using spectral nudging technique either in the stretched-grid ARPEGE or in ALADIN-Climate.

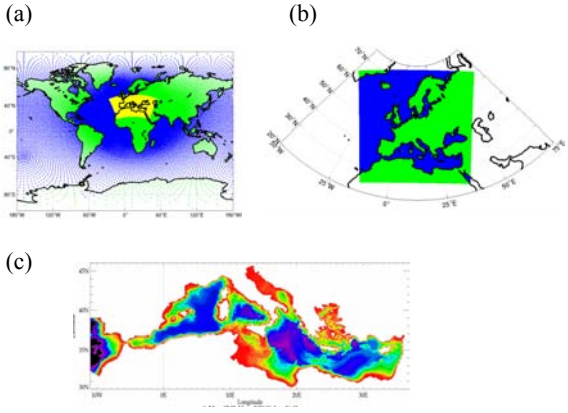

Figure 2. Domain definition of (a) the stretched ARPEGE-Climate, (b) the ALADIN-Climate grid used in ENSEMBLES and (c) the NEMO-MED8 model used for the ocean component.

The AORCM coupling the RCM ARPEGE-Climate or ALADIN-Climat; a Mediterranean version of NEMO (NEMOMED8, see figure 2c) and the routine scheme TRIP (see figure 1) is used to conclude about question D (European project CIRCE) whereas an ensemble of 13 RCMs driven by ERA40 (at a 25 km resolution) and run in the framework of ENSEMBLES can serve to assess

question E. Finally a 10-member ensemble of ALADIN-Climate forced in a Perfect Big Brother approach allows to assess the impact of the internal variability of RCMs. The numerical set-up of this suite of RCM experiments is described in detailed in the following papers: Elguindi et al. (in preparation, question A); Herrmann and Somot (2008, question C), Radu et al. (2008, question C); Somot et al. (2008, question D), SanchezGomez et al. (2008, question E) and SanchezGomez et al. (in preparation, question F).

4. Observations estimates

In the literature, using surface observational datasets, the MSWB estimates range from 520 to 950 mm/yr whereas the Gibraltar Strait estimates of the water budget range from 630 to 1135 mm/yr. Other authors estimated the MSWB using low resolution reanalysis and obtained a lower range going from 391 to 524 mm/yr.

In our study, different surface datasets have been used to estimate the MSWB. This surface datasets are derived from in-situ and/or satellite measurements (see Table 1). This observation estimates are used to evaluate and to sort out between the different modeling techniques.

Variable	Dataset	Period
Evaporation	OAFlux	1958-2006
	HOAPS	1988-2006
Precipitation	GPCP	1979-2003
	HOAPS	1988-2006
River discharge	*Ludwig et al*. (2009)	1960-2000
Black sea discharge	*Stanev et al*. (2000)	1923-1997
Short wave	ISCCP	1983-2008
	NOC	1983-2006
Long wave	ISCCP	1983-2008
	NOC	1983-2006
Latent Heat	OAFlux	1958-2006
	NOC	1983-2006
Sensible Heat	OAFlux	1958-2006
	NOC	1983-2006

Table 1: Observation dataset allowing to evaluate the Mediterranean Sea Water Budget and its components.

5. Results

Following the 6 main scientific issues defined in section 2 and the RCM experiments defined in section 3, we analyze how the design of the RCMs impacts the mean behaviour, the interannual variability and the trends of the MSWB.

The increase in spatial resolution from IPCC-like model to state-of-the-art RCM improves the representation of the MSWB in increasing the total water loss by the Mediterranean Sea surface in agreement with the Gibraltar Strait observed estimates. The choice of the RCM (same resolution, same LBC, different set-up and physics) leads to a large spread in terms of MSWB estimates. The high-frequency air-sea coupling seems also to impact the MSWB even if other coupled simulations are required to legitimate this result. Impact of the RCM internal variability, of the nudging technique and of the modeling technique is also investigated.

6. Perspectives

A large part of the results relies on the ARPEGE-ALADIN-Climate models and can therefore be model-dependent. A broader analysis of the Mediterranean Sea Water Budget using other AORCM or Regional Earth System model should be carried out. Moreover the uncertainty of the observed estimates of the MSWB can be considered as a limitation of such a study and should be reduced in the future through a intense in-situ and remote observing effort. Both tasks are planned in an international coordinated framework during the 2010-2020 HyMex project (www.cnrm.meteo.fr/hymex/).

References

Elguindi N., Somot S., Déqué, M., Ludwig, Climate chnage evolution of the hydrological balance of the Mediterranean, Black and Caspians Seas: impact of climate model resolution, *Clim. Dyn*, in preparation.

Ludwig, W., Dumont, E., Meybeck, M., and Heussner, S., River discharges of water and nutrients to the Mediterranean Sea: Major drivers for ecosystem changes during past and future decades, *Progress In Oceanography*, accepted, 2009

Radu R., Déqué M. and Somot S., Spectral nudging in a spectral regional climate model*, Tellus,* 60A(5):885-897. doi: 10.1111/j.1600-0870.2008.00343.x, 2008

SanchezGomez E., S. Somot, M. Déqué, Ability of an ensemble of regional climate models to reproduce the weather regimes during the period 1961-2000. *Clim. Dyn.,* doi:10.1007/s00382-008-0502-7, 2008

SanchezGomez E, S. Somot, N. Elguindi, S. Josey, Simulation of the Water and Heat budgets in the Mediterranean Sea by an ensemble of high resolution Regional Climate Models experiments, *Clim. Dyn*., in preparation

Somot S. , Sevault F., Déqué M., Crépon M., 21st century climate change scenario for the Mediterranean using a coupled Atmosphere-Ocean Regional Climate Model. *Global and Planetary Change,* 63(2-3), pp. 112-126, doi:10.1016/j.gloplacha.2007.10.003, 2008

Herrmann, M. J., and S. Somot, Relevance of ERA40 dynamical downscaling for modeling deep convection in the Mediterranean Sea, *Geophys. Res. Lett.,* 35, L04607, doi:10.1029/2007GL032442, 2008

Stanev E.V. Le Traon P.Y. and Peneve E.L., Sea level variations and their dependency on meteorological and hydrological forcing : analysis of altimeter and surface data for the Black Sea, *J. Geophys. Res*., 105, 17203-17216, 2000

Comparison of climate change over Europe based on global and regional models

Lidija Srnec, Mirta Patarčić and Čedo Branković

Croatian Meteorological and Hydrological Service, Grič 3, Zagreb, HR-10000, CROATIA, srnec@cirus.dhz.hr

1. Introduction

In this study seasonal projections of several future surface parameters based on the difference between future minus present climate are presented. Applying data of global EH5OM model at the RegCM lateral boundaries, it is possible to infer a potential benefit of dynamical downscaling in comparison with global model results.

2. Data and method

The dynamical downscaling is applied to the two 30-year periods: 1961-1990 for "present" climate and 2041-2070 for future climate under A2 IPCC emission scenario, taken from the global circulation model EH5OM. The regional climate model used here is the third version of RegCM, originally developed by Giorgi et al. (1993a,b). The downscaling is done for a small ensemble of three integrations for each climate. The comparison of climate change between global and regional model is studied from seasonal climate averages for all seasons; winter (DJF), spring (MAM), summer (JJA) and autumn (SON).

In our study, the horizontal resolution used was 35 km in the area of 128x90 grid points centred at 46N and 7.5E. The model was run with 23 vertical levels up to 10 hPa.

3. Discussion

Preliminary results are shown in Fig.1 for winter and Fig.2 for spring. Here we present the differences for the shorter 20-year time slices: 2041-2060 minus 1961-1980.

An increase of the near-surface temperature is clearly seen in both seasons for both models. Although both models shows similar gradient with the highest temperatures towards northeast part of domain, the temperature increase is more pronounced in the results obtained by RegCM.

In winter, over the Mediterranean there is a decrease in precipitation and increase over the northern part of domain. Although both models give qualitatively similar pattern of change, spatial distribution in RegCM follows a better represented orography. In spring, lack of precipitation prevails over a broader part of the domain. A small precipitation increase in the northeastern part of Europe is more pronounced in RegCM than in EH5OM.

Changes in convective precipitation are small in both seasons indicating a small decrease over Atlantic and the Mediterranean.

An increase in surface pressure over a large part of the domain indicates an increase in frequency of anticyclonic weather types or a decrease in the frequency of cyclonic situations (i.e. more stable winters).

4. Further plans

Our further intention is to complete analysis for the 30-year periods and for all seasons. Because of different resolutions, a better comparison would be obtained by interpolating models' results to the same grid. In addition, discussion in terms of future variability and its significance would certainly improve results.

References

Giorgi, F., M.R. Marinucci and G.T. Bates, Development of second-generation regional climate model (RegCM2): Part I: Boundary-layer and radiative transfer processes, *Mon. Wea. Rev.,* 121, 2794-2813, 1993a

Giorgi, F., M.R. Marinucci, G.T. Bates and G. De Canio, Development of the second-generation regional climate model (RegCM2), Part II: Convective processes and assimilation of lateral boundary conditions, *Mon. Wea. Rev.,* 121, 2814-2832, 1993b

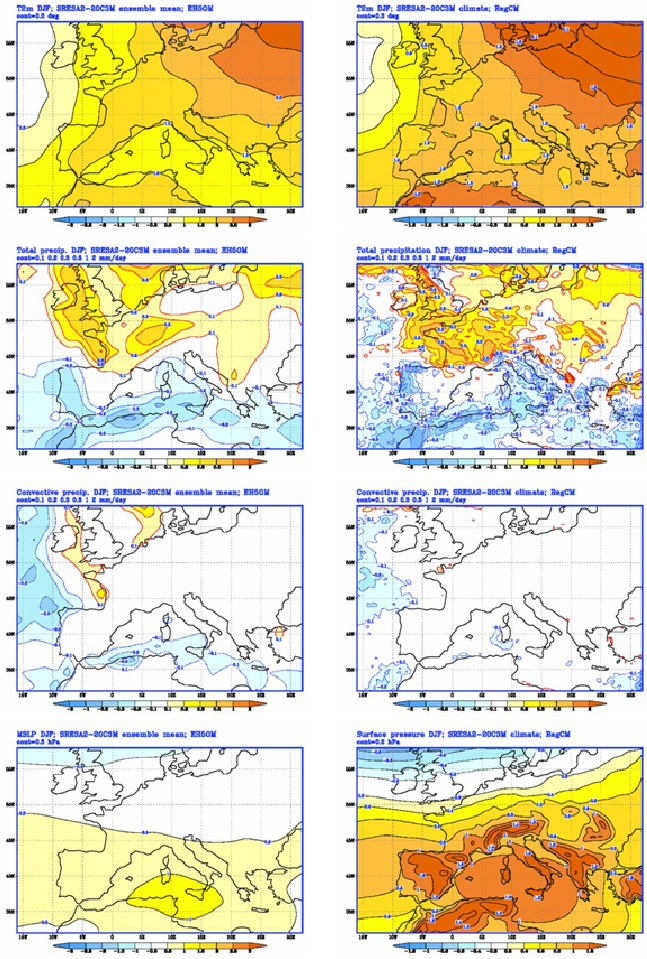

Figure 1. Ensemble mean difference between future and present climate for temperature at 2m (deg), total precipitation (mm/day), convective precipitation (mm/day) and surface pressure (hPa) for DJF obtained by EH5OM (left column) and RegCM (right column).

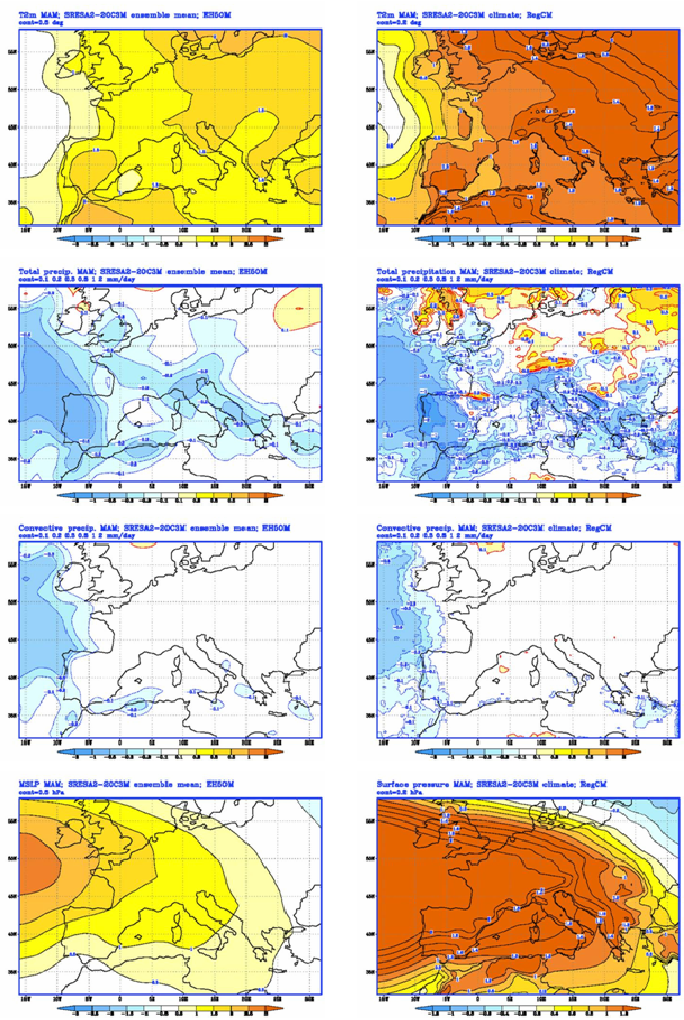

Figure 2. Same as in Fig.1 but for MAM.

Investigation of added value at very high resolution with the Regional Climate Model CCLM

Martin Suklitsch and Andreas Gobiet

Wegener Center for Climate and Global Change and Institute for Geophysics, Astrophysics and Meteorology, Institute of Physics, University of Graz, Leechgasse 25, 8010 Graz, Austria (martin.suklitsch@uni-graz.at)

1. Introduction

Based on a large ensemble of sensitivity simulations at a horizontal resolution of 10 km with the Regional Climate Model CCLM (*Will et al.*, submitted), merits and shortcomings of this particular RCM have been demonstrated (*Suklitsch et al.,* 2008). In this study we additionally deploy finer grids of 3 and 1 km horizontal resolution for single month simulations in a winter and a summer case in two test areas within the Alpine Region and analyze the added value due to finer spatial resolution.

2. Method

In order to reach the very high horizontal resolution of 1km a triple nesting approach is applied. Starting from ERA-40 (*Uppala et al.*, 2001) lateral boundary data at roughly 120km horizontal grid spacing we first simulate the entire Greater Alpine region at 10 km (red rectangle in fig. 1), then the Eastern Alps (east of Innsbruck; green in fig. 1) at 3 km and finally the two test regions at 1 km (blue): One hilly region with relatively smooth orography, located in the southeastern part of Styria, and a mountainous one, with steep orography located in the "Hohe Tauern" region of the Alps.

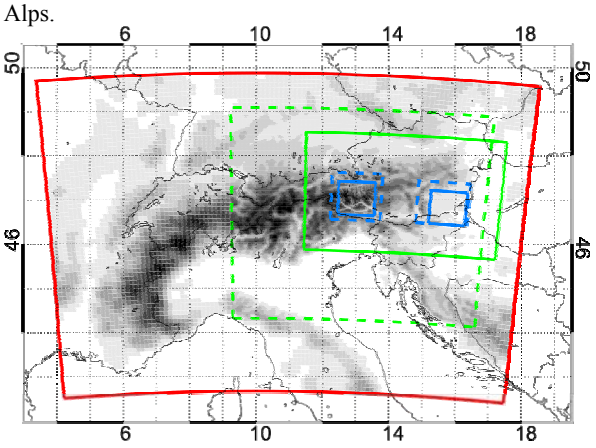

Figure 1. Domains used for this study. Red: 10 km, green: 3 km and blue: 1 km horizontal resolution. Dashed lines indicate extended domains, solid lines the default ones.

3. First results

Figure 2 shows the 2m air temperature at each of the three resolutions for the Hohe Tauern region. Here it is clearly visible that the increased resolution yields more realistic results. The value of the increased resolution will be quantified using observational data of the Austrian Weather Service (ZAMG), of the avalanche warning services of Tyrol, Salzburg and Carinthia, and from the new high resolution observation network WegenerNet (*Kirchengast et al.*, 2008).

A preliminary evaluation of the resolution chain (based on selected examples) shows the following main features:

(1) There is a cold bias (area average in hilly region) at any resolution. The cold bias ranges from −0.9K (July) to −2.4K (January) at 10 km resolution, from −2.0K (July) to −2.6K (January) at 3 km resolution, and amount to −1.8K (July and January) at 1 km resolution. Qualitatively similar results for one location in the Hohe Tauern region are shown in figure 3, where the mean diurnal cycle of the three resolution steps is compared to observation data.

(2) Precipitation (not shown) is overestimated at 10 and 3 km resolution, but underestimated at 1 km resolution. The latter however strongly depends on the physical parameterization: in case of the setup where graupel is included in the microphysics scheme precipitation is

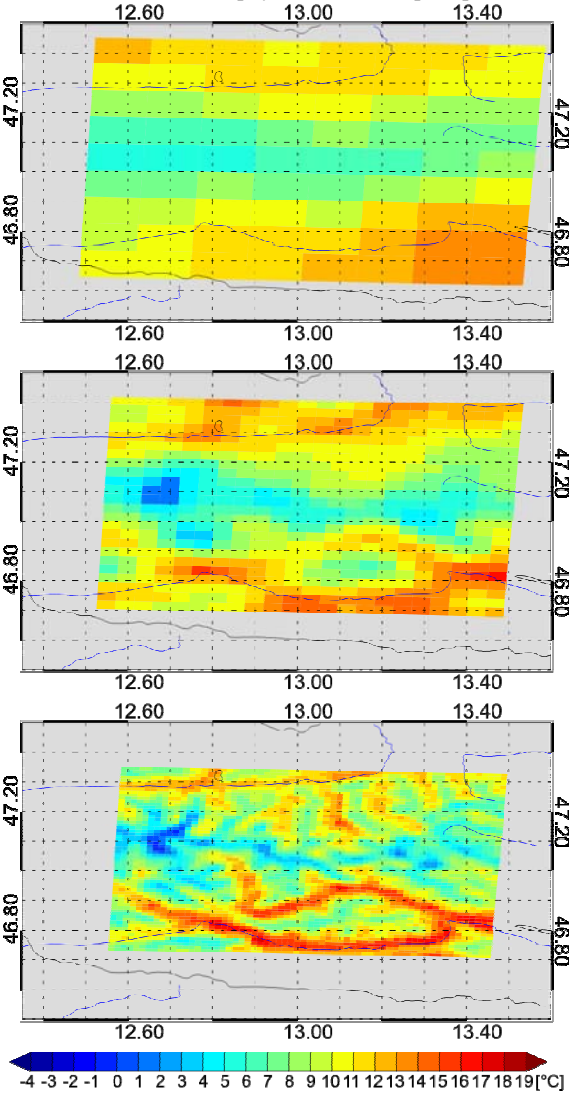

Figure 2. 2m air temperature for the "Hohe Tauern" region in July 2007 as forecast by CCLM at 10, 3 and 1 km horizontal resolution (top to bottom).

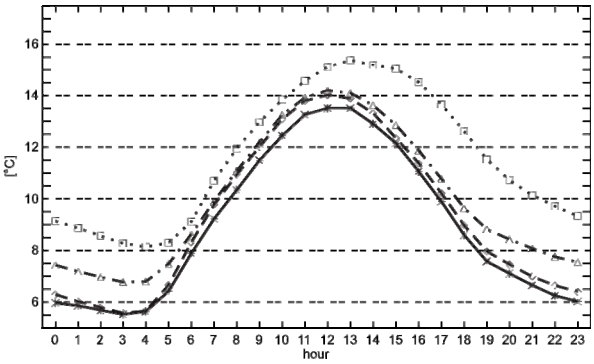

Figure 3. Monthly mean of the diurnal cycle of the 2m temperature in July 2007 as simulated with CCLM for the gridpoint next to Obervellach (808m ASL) in the Hohe Tauern region. Solid: 10 km resolution; dashed: 3 km; dash-dotted: 1 km; dotted: observation. The height difference between the four members is taken into account using a constant lapse rate of 6.5K per km.

overestimated also in the 1 km domain.
The diurnal cycle of precipitation shows that at the 10 km resolution there are two maxima of precipitation, one in the morning around 8 UTC, one in the late evening around 22 UTC. The two other resolutions have the first maximum two to three hours later while the second maximum occurs one hour earlier. The intensity is captured well at all resolutions.

4. Conclusions so far

The preliminary results show that increased model resolution does not necessarily mitigate model biases (after altitude correction) but yield more realistic spatial patterns and partially improve the diurnal cycle. Further, more systematic evaluation results will be presented..

Acknowledgements

The authors would like to thank the University Information Service of the University of Graz for the provision of the computing infrastructure, the Central Institute for Meteorology and Geodynamics and the avalanche warning services of Tyrol, Salzburg and Carinthia for providing observation data. This study is part of the project NHCM-1 (P19619-N10) funded by the Austrian Science Fund (FWF).

References

Kirchengast, G., T. Kabas, S. Binder, A. Leuprecht, C. Bichler, "Pionierexperiment WegenerNet Klimastations-netz: Ein neuartiges Messnetz in der Region Feldbach (Steiermark/Österreich) zur Beobachtung von Wetter und Klima mit sehr hoher Auflösung", *Wegener Center Verlag Graz*, Wiss. Ber. Nr. 23-2008, 2008

Suklitsch, M., A. Gobiet, A. Leuprecht and C. Frei, "High Resolution Sensitivity Studies with the Regional Climate Model CCLM in the Alpine Region", *Meteorol. Z.*, 17, 4, pp. 467-476, 2008.

Uppala, S. M., P. W. Kållberg, A. J. Simmons, U. Andrae, V. da Costa Bechtold, M. Fiorino, J. K. Gibson, J. Haseler et al, "The ERA-40 re-analysis", *Quart. J. Roy. Meteor. Soc.*, 131, 2961-3012, 2005

Will, A., M. Baldauf, B. Rockel, A. Seifert, "Physics and Dynamics of the COSMO-CLM", *Meteorol. Z.*, submitted

A general approach for smoothing on a variable grid

Dorina Surcel and René Laprise

Canadian Network for Regional Climate Modelling and Diagnostics, Centre ESCER, Université du Québec à Montréal, 550 Sherbrooke St. West, 19th Floor, Montréal (Québec) Canada; colan@sca.uqam.ca

1. Introduction

Regional climate modelling using a variable-resolution global approach are an alternative to the widely used nested limited-area models. A variable-resolution GCM do not require lateral boundary conditions and it provides self-consistent interactions between global and regional scales of motion (*Laprise* 2006, *Fox-Rabinovitz et al*. 2006). The concentration of the resolution over a subset of the Earth's surface increases computational efficiency, but this does not come free of some problems owing to the variation of resolution. The non-uniformity and anisotropy of the computational grid can result in contamination of the solution, as is the case near the poles with latitude-longitude grids.

Variable resolution can be achieved in different ways, but the stretched-grid (SG) approach will be in our attention for the purpose of this paper. The technique of grid stretching is one of the most extensively used methods for including the variable resolution in climate models. The resolution of the latitude-longitude grid is smoothly and gradually decreased outside a uniform fine-resolution area that constitutes the region of interest.

The implementation of the SG approach for climate simulations requires addressing some problems arising from grid irregularities such as computational dispersion or the pole problem (*Fox-Rabinovitz et al*. 2008). Even when appropriate stretching constraints are applied for the mesh design, the anisotropy of the grid outside the uniform high-resolution area can result in aliasing of short scales into large scales. One way to avoid this problem is to remove the scales that are improperly represented in the stretching areas to obtain a clean smoothly varying representation on the entire mesh.

A general convolution filter has been developed and successfully tested in one- and two-dimensional Cartesian geometry. The filter has the property of using a limited spatial stencil for the convolution to reduce computational cost. The filter has also been adapted for polar geometry and tested for different test-functions, first to control the pole problem specific of the latitude-longitude models and second to effectively remove the anisotropy and noise outside the high-resolution area of a polar stretched grid. This filter can be applied for scalars and vectors with appropriate definition constraints.

2. Theoretical approach

Variable-resolution stretched grids are designed to have a uniform fine resolution over the area of interest; outside this area the grid intervals are increasing in both horizontal directions, usually as a geometric progression with a constant local stretching factor. To control the undesirable computational problems due to the anisotropy of the grid, a numerical filtering operator is built to remove the unnecessary small-scale signal outside the high-resolution area.

The convolution operator was chosen to design the filtering formula. For a signal ψ, the filtered value $\overline{\psi}$ will be:

$$\overline{\psi}(x) = (\psi * w)(x) = \int_{-\infty}^{\infty} \psi(s) \cdot w(x-s)\, ds$$

We have demonstrate (*Surcel* 2005) that the weighting function « *w* » needed for the convolution is the inverse Fourier transform of the response function. It is necessary to establish the properties of the filter; we here impose that the filter will remove all the scales that are not correct represented outside the high-resolution region. The response is defined as follows:

$$R(k) = \begin{cases} 1 & 0 \le k \le a = \pi/\Delta X \\ \cos^2 \dfrac{\pi}{2}\left(\dfrac{k-a}{b-a}\right) & a < k < b \\ 0 & b \le k \le \pi/\Delta x \end{cases},$$

where ΔX is the maximum grid-point distance and Δx is the minimum grid-point distance in the high-resolution area.

We find then:

$$w(x) = \frac{\pi}{2} \cdot \frac{\sin ax + \sin bx}{x} \cdot \frac{1}{\pi^2 - x^2 (b-a)^2}.$$

This function is dependent on the wavenumbers *a* et *b*. The parameter *a* is well determined, $a = \pi/\Delta X$; the parameter *b* is chosen such as to minimise the Gibbs phenomenon.

3. Adapting the filter for 2D geometry

The formal approach developed in 1D was generalized for the two-dimensional domain. The two-dimensional convolution uses a weighting function that is the product of two one-dimensional functions, similar with those used in the first case. The filtered function is:

$$\overline{\psi}(x,y) = \int_{-\infty}^{\infty}\int_{-\infty}^{\infty} \psi(s,t) w(x-s, y-t)\, ds\, dt$$

$$= \int_{-\infty}^{\infty}\int_{-\infty}^{\infty} \psi(s,t) w_x(x-s) w_y(y-t)\, ds\, dt$$

$$= (\psi * w_x) * w_y$$

For a polar grid, the filter formulation is obtained by the application of the convolution in radial and azimuthally directions, so:

$$\overline{\psi}(r,\lambda) = \overline{\left(\overline{(\psi)}^{r}\right)}^{\lambda}(r,\lambda) = (\psi * w(d_r)) * w(d_\lambda)$$

where : $\begin{cases} r = (x^2 + y^2)^{1/2} \\ \lambda = tan^{-1}\left(\dfrac{y}{x}\right) \end{cases}$, $0 \le r < \infty$, $0 \le \lambda \le 2\pi$

represent the polar coordinates.

When the convolution is computed on a discrete set of points on a variable grid, the surface area associated with each grid point used in the convolution must be considered.

If the polar grid is represented by (r_i, λ_j) and in every point the signal to be filtered is

$\psi_{i,j} = \psi(r_i, \lambda_j)$ with $i = 1, \ldots, n; \quad j = 1, \ldots, m$; $r_i \in [0, ar]; \quad \lambda_j \in [0, 2\pi[$., then the convolution formula is written as follows:

$$\overline{\psi}^{r,\lambda}(r_i, \lambda_j) = \frac{\sum_{\substack{k \\ d^r_{i-k} \le d_{max}}} \overline{\psi}^{\lambda}(r_k, \lambda_j) \cdot w(d^r_{i-k}) \cdot s(d^r_{i-k})}{\sum_{\substack{k \\ d^r_{i-k} \le d_{max}}} w(d^r_{i-k}) \cdot s(d^r_{i-k})}$$

$$= \frac{\sum_{\substack{k \\ d^r_{i-k} \le d_{max}}} \sum_{\substack{l \\ d^{\lambda}_{j-l} \le d_{max}}} \psi(r_k, \lambda_l) \cdot w(d^{\lambda}_{j-l}) \cdot w(d^r_{i-k}) \cdot s(d^r_{i-k}) \cdot s(d^{\lambda}_{j-l})}{\sum_{\substack{k \\ d^r_{i-k} \le d_{max}}} \sum_{\substack{l \\ d^{\lambda}_{j-l} \le d_{max}}} w(d^{\lambda}_{j-l}) \cdot w(d^r_{i-k}) \cdot s(d^r_{i-k}) \cdot s(d^{\lambda}_{j-l})}$$

where d^r_{i-k} and d^{λ}_{j-l} are the radial and azimuthally distances between two points (r_i, λ_j) and (r_k, λ_l), and $s(d^r_{i-k})$ and $s(d^{\lambda}_{j-l})$ are the surface areas around the (r_k, λ_l) point.

The convolution is calculated up to a user prescribed distance d_{max} between the application point and all other points necessary for the convolution.

When the convolution is applied for the components of a vector (e.g. the horizontal winds), we must consider the representation of the vector components relative to the same referential centred on the application point.

The polar grid was used in this project as an intermediate step to the application of the filter on a spherical latitude-longitude stretched grid. In both cases, at the origin of a polar coordinate system or at the north and south poles of the sphere, the lines of constant polar angle or constant longitude converge in a single point. This convergence has consequence a severe time-stepping limit (the so-called «pole problem»). One way to stabilize the solution of a numerical differential equation near the pole is to damp the waves that are unstable for a chosen timestep at a rate that exceeds the exponential growth (*Williamson and Laprise* 2000).

4. Results

We present in this section two sets of tests performed with this smoothing operator. In both cases we used a large-scale cosine signal represented into a polar domain. An artificial noise was added to represent the small-scale noise to be removed.

We first verified the efficiency of the convolution operator to act as polar filter using a uniform polar grid. In figure 1 is presented the total signal (a) and the filtered signal (b). We find that the amplitude of the large-scale scale signal is unchanged and that the short-scale noise is removed.

In the second case we used a stretched polar grid and the filter was applied outside the uniform high-resolution area to remove the anisotropy. When the filter was built, we had decreased the resolution with 8% in the radial direction and with 3.8% in azimuthally direction for every grid point in the stretching zones. The total stretching factor is almost 6 in both directions. The large-scale signal was represented on the entire domain and the noise was added in the stretching zones. The initial signal is represented in figure 2a and the filtered signal is represented in figure 2b. One thing to remark is that the filtering operator conserves the quantities and keeps unchanged the amplitude of the long waves.

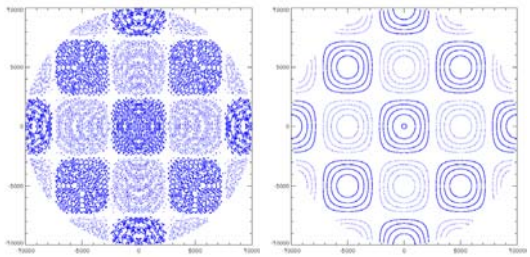

Figure 1: The initial signal composed from a large-scale signal and a small-scale noise in (a) and the filtered signal in b).

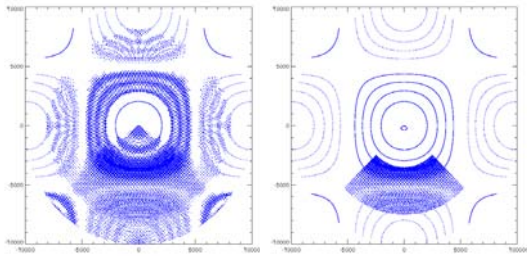

Figure 2: The initial signal composed of a long wave and the noise added in the stretching zones in a) and the filtered signal in b).

References

Fox-Rabinovitz, M., J. Côté, B. Dugas, M. Déqué and J.L. McGregor, Variable resolution general circulation models: Stretched-grid model intercomparison project (SGMIP), *J. Geophys. Res*., 111, D16104, doi:10.1029/2005JD006520, 2006.

M. Fox-Rabinovitz, J. Côté, B. Dugas, M. Déqué, J.L. McGregor and A. Belochitski, Stretched-grid Model Intercomparison Project: decadal regional climate simulations with enhanced variable and uniform-resolution GCMs, *Meteorology and Atmospheric Physics,* Volume 100, Numbers 1-4, pp. 159-178, 2008.

R. Laprise, Regional climate modelling, *J. Comput. Phys*., doi:10.1016/j.jcp.2006.10.024, 2006.

Surcel, D., Filtres universels pour les modèles numériques à résolution variable, Mémoire de maîtrise en Sciences de l'atmosphère, Université du Québec à Montréal, 104 pp., 2005.

Williamson, D., and R. Laprise: Numerical approximations for global atmospheric General Circulation Model, P. Mote and A. O'Neil (eds.) *Numerical modeling of global atmosphere in the climate system*, Kluwer Academic Publishers, 127-219, 2000.

What details can the regional climate models add to the global projections in the Carpathian Basin?

Gabriella Szépszó, Gabriella Csima and András Horányi

Hungarian Meteorological Service, Budapest, Hungary (szepszo.g@met.hu)

1. Motivation

Recently the continuously improving global climate models are providing solid basis and realistic projections for the synoptic scale characteristics of the climate, however they are at the moment largely insufficient for detailed regional scale estimations. The use of regional climate models ensures a dynamics-based opportunity to interpret and enhance the global results for regional scale. A couple of years ago two regional climate models were adapted at the Hungarian Meteorological Service (HMS): the ALADIN-Climate model developed by Météo France on the basis of the internationally developed ALADIN modelling system and the REMO model developed by the Max Planck Institute for Meteorology in Hamburg. It is anticipated in Hungary that these models are able to give realistic regional climate estimations not only for the next few decades but also for the end of 21st century, particularly for the area of the Carpathian Basin. This area of interest is especially important considering the fact that one of the largest uncertainties in climate projections can be found over the Carpathian Basin as it had already been identified by former large international projects.

2. Model experiments

Firstly, the models were integrated for a past period (1961–1990) with the use of ERA-40 re-analyses as lateral boundary conditions in order to explore the main characteristics of the models' behaviour in case of "quasi-perfect" forcing. The model domains include continental Europe with approximately 25 km horizontal resolution. The models were also integrated with lateral boundary conditions provided by global atmosphere-ocean general circulation models: by ARPEGE/OPA in the case of ALADIN-Climate and ECHAM5/MPI-OM in the case of REMO. With the latter regional climate model a hundred-year transient run was accomplished for the period of 1951–2050, while the ALADIN-Climate simulations covered three thirty-year time slices in 1961–1990, 2021–2050, 2071–2100 over a smaller domain in its focus with Hungary on 10 km horizontal resolution. The regional models were forced with the A1B SRES emission scenario, which is considered as a "realistic" estimate for the evolution of the greenhouse gas concentrations until the end of the 21st century.

3. Results

Naturally, the validation of regional climate models for the past climate is an indispensable ingredient in understanding the behaviour of RCMs. This is originating from the considerations that on the one hand successful climate projections can be only expected if the models are already capable to reasonably simulate the past climate and on the other hand the biases of the model for the past might indicate and anticipate biases for the future. The model experiments for the past were validated against the CRU-dataset focusing on two main variables: the mean temperature and precipitation. Regarding the future projections the change of the same parameters was investigated for the 2021–2050 period with respect to the reference 1961–1990 one. The analysis was concentrating not only on the regional results but also taking into account the driving global models' results, in order to carefully scrutinize the possible added value of the regional climate models with respect to the global ones and to draw reliable and robust conclusions in terms of quantitative uncertainties in the projections.

Figure 1 shows the change of the annual and winter precipitation over Hungary for 2021–2050 with respect to the model means in 1961–1990 on the basis of the ALADIN-Climate and REMO results. It can be concluded, that the annual change is a non-significant decrease projected quite similarly by both RCMs, however in the case of seasonal changes large differences can be experienced, which is pointing towards large uncertainties.

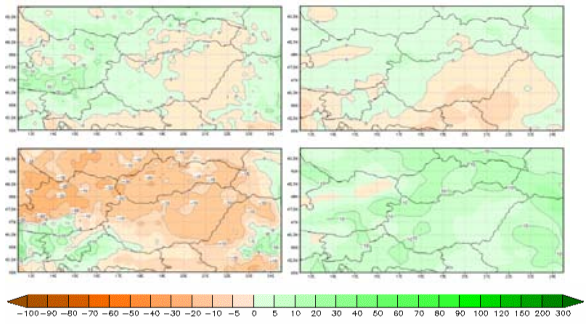

Figure 1. The annual (top) and the winter (bottom: DJF) precipitation change over Hungary for 2021–2050 with respect to the model means in 1961–1990 based on two RCMs (left: ALADIN-Climate; right: REMO).

This workshop contribution will give an overview about the results of regional climate models applied at the HMS with special emphasis on their inter-comparison and evaluation with respect to the global models.

References

Csima, G. and Horányi, A.: Validation of the ALADIN-Climate regional climate model at the Hungarian Meteorological Service, *Időjárás*, 112., 3-4, pp. 155-177, 2008

Szépszó, G. and Horányi, A.: Transient simulation of the REMO regional climate model and its evaluation over Hungary, *Időjárás*, 112., 3-4, pp. 203-231, 2008

Investigation of precipitation of the contiguous China using the Weather Research and Forecasting (WRF) model

Jian Tang and Tang Jianping

School of Atmospheric Science, Nanjing University, HanKou Road 22, Nanjing, P.R. China; tangjian@smail.nju.edu.cn

1. Introduction

The booming of the area of regional climate models makes RCMs being more and more used in climate research to meet the increasing demands for high resolution simulations by its downscaling skills. Regional climate research began in the late 1980s when the global climate models' (GCMs) coarse resolutions of 300-500km cannot produce enough climate information to satisfy the needs for investigating climate change (Leung et al., 2003). It is commonly accepted the regional climate model driven by a large-scale circulation (generated by either reanalysis data or GCMs) can be integrated from an initial condition and generate realistic high-resolution (spatial and temporal as well) simulations. Since late 1980s, much remarkable progress has been made in the field of the regional climate modeling. (e.g., Dickinson et al. 1989; Giorgi 1990; Jones et al. 1995; Fu and Giorgi 1996; Christensen et al. 1997; Machenhauer et al. 1998). Giorgi and Mearns (1991) has recommended that long-term continuous RCM integrations can generate more pronouncing information than ensembles of short simulations, including minimal effect from atmospheric spin-up, improved equilibrium between the regional climate and surface hydrology cycle, accurate representation of the model internal climatology and better detection of systematic model physics deficiencies.

China is a typical monsoon area with distinct geographical configurations: west terrain high and low in the east, with ocean surrounds its south and east. In this paper, in order to understand the performance of the Weather Research and Forecasting (WRF) model in China, we run a twenty-year simulation to get better understanding of the large climate variability in China. The purpose of this study is to investigate the capability of an RCM to reproduce the observed annual cycle of the contiguous China and to get better understanding of model climatology biases. The twenty-year mean climatology is long enough to be robust significant.

2. Model simulation and validation

The WRF model, driven by the NCEP/DOE reanalysis data, is used to simulate the regional climate change from 1982 to 2001 in China. The model was integrated form 1 December to December 31 1981 with a resolution of 30km (Figure 1) .The simulation results are compared to observations as well as the NCEP/DOE reanalysis data to study the WRF's downscaling skill and uncertainty over China. The WRF simulations show its remarkable downscaling skills for precipitation and precipitation annual cycle, producing more realistic regional details.

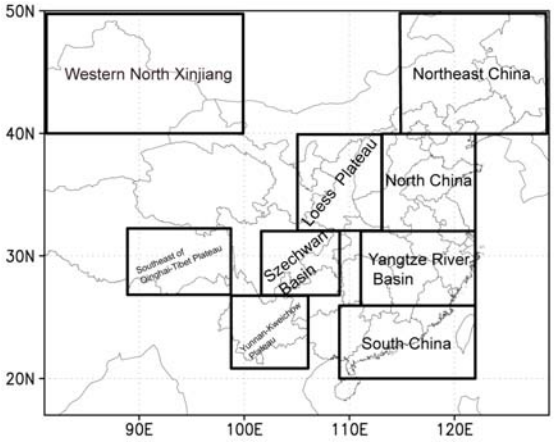

Figure 1. Outlined are nine key regions with distinct climate characteristics and/or model biases.

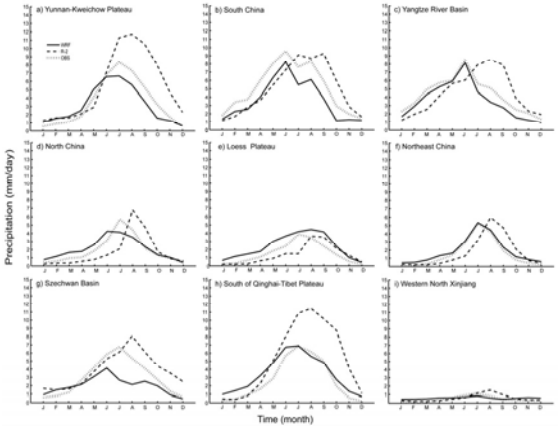

Figure 2. Monthly 1982-2001 mean precipitation (mm day-1) variations averaged over the nine key regions in China for observation (OBS; thin dashed), the WRF baseline integration (WRF; thick solid), and the R-2 model output (R-2; thick dashed).

Figure2 compares the observed, the R-2 and WRF simulated monthly precipitation variations averaged over nine key regions (see specification in Fig. 1). These regions have distinct climate characteristics and/or model biases. The WRF simulates most accurately in the region of Yangtze River Basin, South China and Northeast China. In South China, the WRF simulation has corrected the R-2 precipitation seasonal cycle with less precipitation than observation in all seasons. Similar biases exist in Northeast China and Yangtze River Basin. The R-2 poorly simulates the seasonal cycle and the month with maximum precipitation has been postponed one month, and the rainfall amount is largely overestimated. For the Yunnan-Kweichow Plateau, North China and South of Qinghai-Tibet Plateau, the WRF simulations are generally realistic

in winter and spring, while substantial underestimations are identified in summer and fall. The R-2 simulations in these regions has the similar flaw like regions described above, overestimating the precipitation in august. For Szechwan Basin, the WRF simulation is basically underestimating precipitation all season (except spring), while R-2 generates substantially larger (smaller) rainfall in fall and winter (spring and summer). For south of Qinghai-Tibet Plateau, the WRF simulates larger rainfall than observation except for august, while the R-2 simulates larger rainfall all year than the observation. In Western North Xinjiang area, the WRF simulates larger (smaller) rainfall than the observation in spring, fall and winter (summer), while the R-2 biases mainly exist in excessive summer precipitation.

3. Conclusion

The precipitation simulation is more skillful in DJF/SON than in MAM/JJA in most area of China, and produces more convincing results in East China than the west. Hence the WRF downscaling provides an incredible way to improve reanalysis data in China, which has its distinct geographical configurations: west terrain high and low in the east, with ocean surrounds its south and east. The results that fall and winter simulation is better than spring and summer are possible due to the weakness of modeling convections in spring and summer. Overall, based on a number of objective measures of climate simulation skill, the WRF reproduces observed spatial and seasonal precipitation patterns better than the R-2 simulations.

References

Dickinson, R. E., R. M. Erroco, F. Giorgi, and G. T. Bates, 1989: A regional climate model for the western United States. *Climate Change*, 15, 383–422.

Christensen, O. B., J. H. Christensen, B. Machenauer, and M. Bozet, 1998: Very high-resolution regional climate simulations over Scandinavia—Present climate. *J. Climate*, 11, 3204–3229.

Fu, C. and F. Giorgi, 1996: development of coupled climate, ecology, chemistry regional modeling activities for East Asia and study of environmental effects of anthropogenic activities over the region. Proposal to START-TEA (Temperature East Asia region). 21pp. Available from authors.

Giorgi, F., 1990: On the simulation of regional climate using a limited area model nested in a general circulation model. *J. Climate*, 3, 941–963.

Giorgi, F. and Mearns, L. O.: 1991, 'Approaches to the Simulation of Regional Climate Change: A Review', *Rev. Geophys*. 29, 191–216.

Giorgi, F., C. S. Brodeur, and G. T. Bates, 1993a: Regional climate change scenarios over the United States produced with a nested regional climate model. *J. Climate*, 7, 375–399.

Jones, R. G., J. M. Murphy, and M. Noguer, 1995: Simulation of climate change over Europe using a nested regional climate model, I, Assessment of control climate, including sensitivity to location of lateral boundary conditions. *Quart. J. Roy. Meteor*. Soc., 121, 1413–1449.

Leung, L.R., Mearns, L.O., Giorgi, F., and R. Wilby, 2003: Workshop on regional climate research: Needs and opportunities, *Bull. Amer. Met. Soc*. (in press).

Liang, X.-Z., L. Li, K. E. Kunkel, M. Ting, and J. X. L. Wang (2004), Regional climate model simulation of U.S. precipitation during 1982–2002. Part 1: Annual cycle, *J. Climate,* 17, 3510–3528.

Machenhauer, B. Windelband, M., Botzet, M., Christensen J.H., Déqué, M., Jones, R.G, Ruti, P., and Visconti, G. (1998) Validation and analysis of regional present-day climate and climate change simulations over Europe *MPI for Meteorology report* 275, 87pp.

Impacts of the spectral nudging technique on simulation of the East Asian summer monsoon in 1991

Jianping Tang and Shi Song

School of Atmospheric Sciences, Nanjing University, Nanjing, China, 210093 jptang@nju.edu.cn

1. Introduction

Traditionally, the regional climate models (RCMs) are nested in the global models to provide detailed regional information. The method of Davies (1976) has been widely applied to the formulation of lateral boundary conditions (LBCs). However, the relaxation does not handle larger scales correctly, and distorts the long waves reflecting and interfering within the domain. One of the most substantial issues in regional climate modeling is that the RCM integrations are limited by the errors induced by the LBCs (Risbey and Stone 1996; Christensen et al. 1998; Menendez et al. 2001; Misra et al. 2003), especially the synoptic-scale systematic errors during the long-term RCM integrations.

To improve the downscaling performance of the RCMs, the method of adding nudging terms in the spectral domain has been developed to incorporate large-scale regulations inside the RCM domain (Waldron el al 1996; von Storch et al 2000). The basic idea of spectral nudging is that the regional model should not modify the large-scale field in the regional domain, which is from the coarse-resolution base field and considered accurate in regional downscaling. The spectral nudging method has been widely assessed in the downscaling experiments in Western Europe (Feser 2006), contiguous U.S. (Miguez-Macho et al. 2004) and North America (Kanamaru and Kanamitsu 2007) and has been proved a demonstrative ability in improving RCM's performance.

The purpose of this paper is to evaluate the ability of the spectral nudging method in the regional climate simulation over China.

2. Model Description and numerical experiments

The regional climate model used in this study is NCAR-MM5v3, a three-dimensional, limited-area, primitive-equation model. The simulation domain centered at 35°N and 105°E with 107×93 horizontal grid points and 50-km grid spacing covering most of East Asia. Initial and boundary conditions are provided by the 2.5°×2.5°NCEP/NCAR reanalysis (NNRP) data, and sea surface temperature (SST) are from the NOAA weekly OI SST data.

The experiments are initialized on 16 May 1991 and integrated until 1 Sep 1991. The control (CTL) integration is the regular MM5 runs without any spectral nudging applications, the spectral nudging method is applied to the wind fields at and above 850 hPa in the spectral nudging (SN) run.

3. Results

3.1 Large-scale circulation

Figure 1 shows the differences of JJA-averaged geopotential height (GPH) field at 500hPa between model simulations and the NNRP data in 1991. Clearly there is a dominant negative bias in the CTL run in most part of the domain, with a maximum locates at the southwest, and a less severe positive bias in northeast of the domain. The SN run is able to reduce the dominant negative bias to much smaller values although slightly increase the positive bias in the north of the domain. In addition, differences of the JJA-averaged 500hPa temperature field between the model simulations and the NNRP reanalysis are analyzed. Similar to those of the mass field, the SN run largely reduces the northern positive bias and the southern negative bias (Figure not shown).

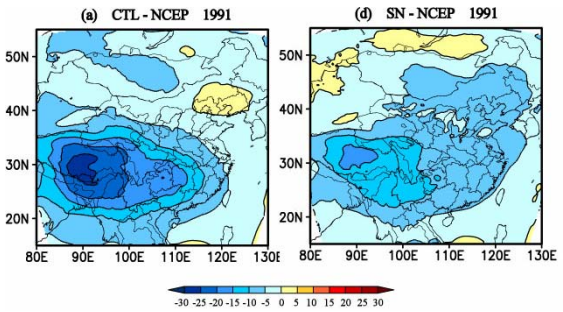

Figure 1. Difference of JJA-averaged geopotential height at 500hPa between model simulations and NNRP.

3.2 Regional simulations of daily precipitation events

Figure 2 presents the model simulated and the observational time series of regional-averaged daily precipitation rates in Northeast China, North China, the Yangtze River basin, and South China. Obviously, the SN run successfully reproduce the observed individual precipitation events with day to day variations, while the CTL runs show relatively larger discrepancies. Note that the three heavy rain periods of 1991 over the Yangtze River basin are captured markedly better by SN runs than CTL runs. And the SN run diminishes most false precipitations generated by the CTL run, i.e. in the North China in late August. The correlation coefficient between the observation and the SN run is 0.69, which is remarkably better than that of the CTL run (0.42).

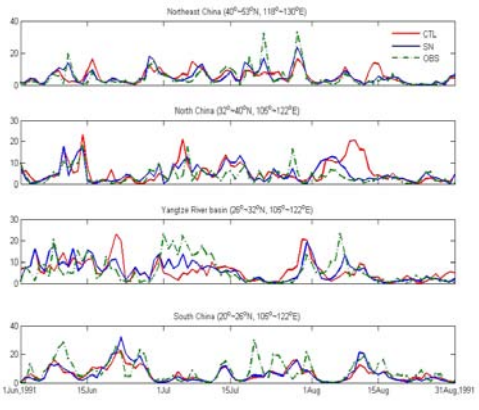

Figure 2. The model simulated and the observational time series of regional-averaged daily precipitation rates.

4. Conclusions

The spectral nudging technique prevents the regional model from generating internal states inconsistent with the driving fields as well as grants the model with freedom to develop regional and small-scale patterns. The simulations using the spectral nudging method show demonstrative skill in dynamical downscaling by (1) significantly reducing the model's systematic error in simulating forcing variables; (2) largely improving the simulation of individual precipitation events, i.e. the intra-seasonal variability of regional precipitation.

References

Risbey JS, Stone PH (1996) A case study of the adequacy of GCM simulations for input to regional climate change assessments. J. Climate, 9, 1441–1467.

Christensen OB, Christensen JH, Machenhauer B, Botzet M (1998) Very high-resolution regional climate simulations over Scandinavia—Present climate. J. Climate, 11, 3204–3229.

Menendez CG, Saulo AC, Li ZX (2001) Similation of South America wintertime climate with a nesting system. Climate Dyn., 17, 219–231.

Misra V, Dirmeyer PA, Kirtman BP (2003) Dynamic downscaling of regional climate over South America. J. Climate, 16, 103–117.

Waldron KM, Paegle J, Horel JD (1996) Sensitivity of a spectrally filtered and nudged limited-area model to outer model options. Mon. Wea. Rev., 124, 529–547.

von Storch H, Langenberg, Feser F (2000) A spectral nudging technique for dynamical downscaling purposes. Mon. Wea. Rev.,128, 3664–3673.

Feser F (2006) Enhanced Detectability of Added Value in Limited-Area Model Results Separated into Different Spatial Scales. Mon. Wea. Rev., 134, 2180–2190.

Miguez-Macho G, Stenchikov GL, Robock A (2004) Spectral nudging to eliminate the effects of domain position and geometry in regional climate model simulations. J. Geophys. Res., 109, D13104, doi:10.1029/2003JD004495.

Kanamaru H, Kanamitsu M (2007) Scale-selective bias correction in a downscaling of global analysis using a regional model. Mon. Wea. Rev., 135, 334–350.

Extremes and predictability in the European preindustrial climate of a regional climate model

L. Tomassini, Ch. Moseley, A. Haumann, R. Podzun, and D. Jacob

Max Planck Institute for Meteorology, Hamburg, Germany (lorenzo.tomassini@zmaw.de)

1. Abstract

We investigate extreme events in a 300-years control simulation with the regional climate model REMO for Europe assuming constant preindustrial greenhouse gas concentrations. The extreme events in the preindustrial control run of the regional climate model are compared to recent observed extraordinary seasons like the summer 2003 or autumn 2006 in Central Europe. We examine the main causes of these incidents and ask whether the recently observed extreme events show a new quality and unprecedented characteristics that are not present in the control simulation of the regional climate model. Statistical assumptions underlying common estimates of return periods of such climatic outliers are discussed.
Furthermore we explore the potential predictability of the European preindustrial climate. Here we focus on three major large-scale modes of variability, MOC, ENSO and NAO, their effects on surface air temperature and precipitation in Europe, and the role of soil moisture as a memory-inducing factor. These aspects are of importance for studies trying to produce seasonal or decadal predictions of the climate in Europe.

2. Extreme events

We selected eight seasons in a 300-years control simulation each for temperature and precipitation that were extreme in one or several of the PRUDENCE regions in Europe.
Figure 1 shows mean temperature for a selection of the 8 PRUDENCE regions and different seasons. The red lines depict corresponding observations of the years 1961 to 2006, the blue circles indicate the extreme events.
Events that are similar to e.g. the unusually hot summer 2003 in Central Europe are present in the 300-years control run of the regional climate model. Spatial and temporal characteristics of the atmospheric circulation and other climatic properties that detail these extraordinary incidents are described and discussed.

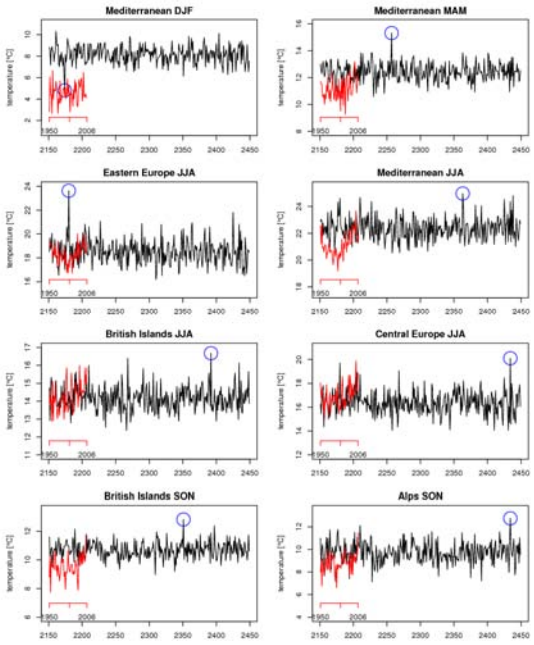

Figure 1. Seasonal mean temperatures for a selection of the 8 PRUDENCE regions and different seasons. Red lines indicate observations of the years 1961 to 2006, blue circles mark the extreme events. The x-axes correspond to (dummy) years of the preindustrial control run.

3. Potential predictability of the European climate

In order to investigate the potential influence of variations in MOC on European climate, we selected two 20-years periods in the preindustrial control simulation, one with high MOC (years 2210 to 2229), and one with low MOC (years 2327 to 2346) values. Figure 2 shows mean SST anomalies over the two respective periods. Cross-correlations of MOC with yearly or seasonal means of temperature or precipitation for the different PRUDENCE regions are typically small and not significant.
Therefore, instead, we explore the differences in extreme events and estimate the distribution of the 100 warmest days for each of the high MOC years and the low MOC period. To assess the robustness of the results the same distributions are computed for ten randomly chosen 20-years periods. The results are summarized in Figure 3. One can see that generally the differences between the low MOC and the high MOC period lie within the uncertainty indicated by the results from the ten randomly chosen reference periods.

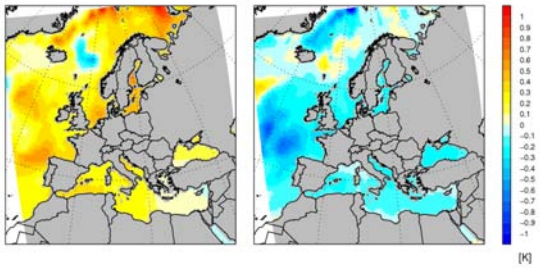

Figure 2. Mean SST anomalies for the high MOC period (left panel) and the low MOC period (right panel).

A similar analysis is carried out for the 100 coldest days, and the 100 days with largest precipitation totals (results not shown).

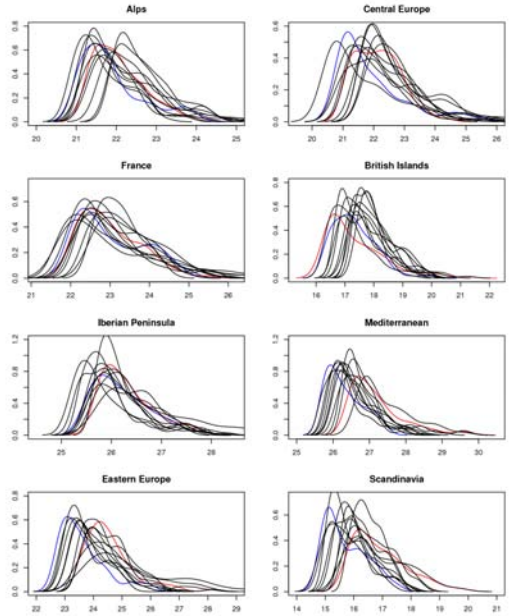

Figure 3. Distributions of 100 warmest days for different PRUDENCE regions. Red lines correspond to the high MOC period, blue lines to the low MOC years. The black curves show the results for ten randomly chosen 20-years periods. The unit of the x-axes is degrees Celsius.

In order to investigate the potential predictability induced by variations in the NAO and ENSO, we introduce a measure for extremal dependence and explore correlations between anomalous NAO or ENSO years with temperature or precipitation extremes in the different PRUDENCE regions. Furthermore, storm track statistics are calculated for the periods exhibiting high/low MOC and ENSO indices, and the role of soil moisture as a memory-inducing factor for seasonal forecasts is explored.

References

Brönnimann S., E. Xoplaki, C. Casty, A. Pauling, J. Luterbacher, ENSO influence on Europe during the last centuries, *Climate Dynamics,* 28, pp. 181-197, 2007

Pohlmann H., F. Sienz, M. Latif, Influence of the multidecadal Atlantic Meridional Overturning circulation variability on European climate, *Journal of Climate*,19, pp. 6062-6067, 2006

Schär Ch., P.L. Vidale, D. Lüthi, Ch. Frei, Ch. Häberli, M. A. Liniger, Ch. Appenzeller, The role of increasing temperature variability in European summer heatwaves, *Nature*, 427, pp. 332-336, 2004

Van Oldenborgh G.J., How unusual was autumn 2006 in Europe, *Climate of the Past,* 3, pp. 659-668, 2007

Large-scale skill in regional climate modeling and the lateral boundary condition scheme

Katarina Veljović[1], Borivoj Rajković[1] and Fedor Mesinger[2]

[1]Institute of Meteorology, Faculty of Physics, University of Belgrade, Serbia, katarina@ff.bg.ac.yu
[2]NCEP Environmental Modeling Center, Camp Springs, Maryland, and Earth System Science Interdisciplinary Center, Univ. Maryland, College Park, Maryland

Several points are made concerning the somewhat controversial issue of regional climate modeling: should a regional climate model (RCM) be expected to maintain the large scale skill of the driver global model that is supplying its lateral boundary condition (LBC)? Given that this is normally desired, is it able to do so without help via the fairly popular large scale nudging? Specifically, without such nudging, will the RCM kinetic energy necessarily decrease with time compared to that of the driver model as strongly suggested by a recent study using the Regional Atmospheric Modeling System (RAMS) model? Finally, can the lateral boundary condition scheme make a difference: is the almost universally used but somewhat costly relaxation scheme necessary for a desirable RCM performance?

Experiments are made to explore these questions running the Eta model in two versions differing in the lateral boundary scheme used. One of these schemes is the traditional relaxation scheme, and the other the Eta model scheme in which information is used at the outermost boundary only, and not all variables are prescribed at the outflow boundary. Forecast lateral boundary conditions are used, and results are verified against the analyses. Thus, skill of the two RCM forecasts can be and is compared not only against each other but also against that of the driver global forecast. A presumably novel verification method is used in the manner of customary precipitation verification in that forecast spatial wind speed distribution is verified against analyses by calculating bias adjusted equitable threat scores and bias scores for wind speeds greater than chosen wind speed thresholds. In this way, focusing on a high wind speed value in the upper troposphere, verification of large scale features we suggest can be done in a manner that may be more physically meaningful that verifications via spectral decomposition that are a standard RCM verification tool.

The results we have at this point are to a degree limited in view of the integrations having being done only for 10-day forecasts. Even so, one should note that they are among very few done using forecast as opposed to reanalysis global driving data. They suggest that (1) running the Eta as an RCM, no significant loss of large-scale kinetic energy with time seems to be taking place; (2) no disadvantage from using the Eta LBC scheme compared to the relaxation scheme is seen, while enjoying the advantage of being significantly less demanding than the relaxation given that the Eta scheme needs driver model fields of the outermost domain boundary only; and (3) the Eta RCM skill in forecasting large scales seems to be just about the same as that of the driver model, or, in the terminology of Castro et al.(2005), the Eta RCM does not lose "value of the large scale" which exists in the larger global analyses used for the initial condition and for verification.

References

Castro, C. L., R. A. Pielke Sr., and G. Leoncini (2005), Dynamical downscaling:Assessment of value retained and added using the Regional Atmospheric Modeling System (RAMS), *J. Geophys. Res.,* 110, D05108, doi:10.1029/2004JD004721

Does dynamical downscaling with regional atmospheric models add value to surface marine wind speed from re-analyses?

Jörg Winterfeldt and Ralf Weisse

Institute of Coastal Research, GKSS Research Centre, Geesthacht, Germany, ralf.weisse@gkss.de

1. Assessment of added value using buoy wind

The hindcast surface marine wind speed fields from the regional atmospheric model REMO in two configurations and the regional atmospheric model CLM are investigated with regard to their added value in comparison to the driving wind field from the NCEP/NCAR reanalysis (NRA_R1). To do so in a first step wind speed measurements from buoys, light ships and platforms in the eastern North Atlantic are considered as “truth”. Added value from the regional models is obtained when correspondence with both the measured statistical distribution and instantaneous wind speeds is higher than that of the reanalysis. Wind speed fields from NRA_R1, REMO and CLM are bilinearly interpolated to measurement locations and statistically compared.

Winterfeldt and Weisse (2009) demonstrated that for instantaneous wind speeds the regional models do not have an added value both in "open ocean" areas and the German Bight. However, in the English Channel, where local topography and associated local wind regimes become important, the regional model shows an added value for instantaneous wind speeds.
Concerning the wind speed distribution there's a clear indication for an added value of the regional models in coastal regions, especially for higher wind speed percentiles, while in "open ocean" areas the NRA_R1 is better reflecting observed distributions.

2. Assessment of added value using QuikSCAT wind speed retrievals

The added value of the dynamically downscaled wind was assessed with satellite data, namely QuikSCAT Level 2B 12.5 km (L2B12) wind speed retrievals following the thorough validation of the quality of L2B12 data with buoy winds in the eastern North Atlantic (RMSE: 1.5 m/s) by *Winterfeldt et al.* (2009). For that purpose L2B12, REMO and global NCEP/NCAR reanalysis (NRA_R1) data were co-located for the years 1999-2007. Co-location criteria between REMO and L2B12 data are within 0.1° and 0.06° in longitudinal and latitudinal distance from REMO model grid points and within 20 minutes, leading to a high quality L2B12 gridded wind speed data set with REMO grid dimensions. NRA_R1 data was interpolated in time and space onto the REMO grid.

A slightly modified Brier Skill Score (BSS) was used to test to what extent the regionally modelled wind gives a better reproduction of QuikSCAT wind speed than the NRA_R1. The modified version of the BSS varies between -1 and +1 and simplifies the comparability of positive (value added) and negative (value lost) scores.

Fig. 1 confirms the point stated by *Winterfeldt and Weisse* (2009) for a wide area including the eastern North Atlantic, the Baltic, Mediterranean and Black Seas: dynamical downscaling does not add value to NRA_R1 wind speed in open ocean areas (blue), while it does for complex coastal areas (red).

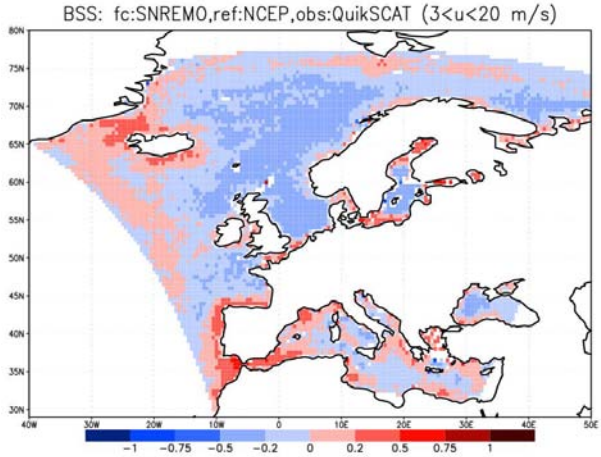

Figure 1. Modified Brier Skill Score calculated from co-locations between QuikSCAT L2B12, NRA_R1 and SN-REMO (SN stands for use of spectral nudging) in the wind speed range from 3 to 20 ms-1 and the years 2000 to 2007, where QuikSCAT L2B12 serves as ``truth``, NRA_R1 as reference ``forecast`` and SN-REMO as ``forecast``. Blue areas indicate value lost, while red areas indicate value added by dynamical downscaling.

3. Seasonal variability of added value

Strong interseasonal differences exist, in winter enhanced cyclonic and meso-cyclonic activity increases the potential of dynamical downscaling. In winter time the added value is more pronounced around Iceland and Greenland, south of Iceland and within the Gulf of Lyon/Mistral region (see Fig. 2 and 3).

Summarizing QuikSCAT is a valuable tool to identify marine regions where dynamical downscaling of wind speed makes sense.

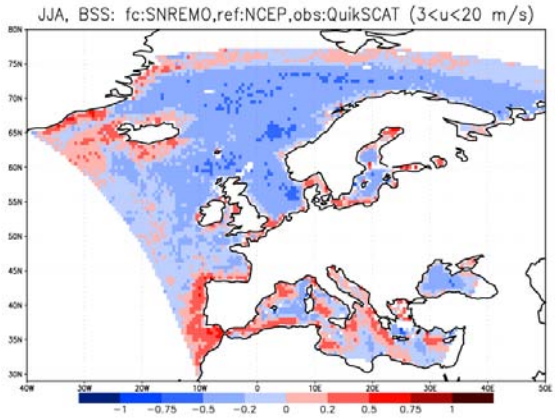

Figure 2: As Figure 1 but for Summer (JJA).

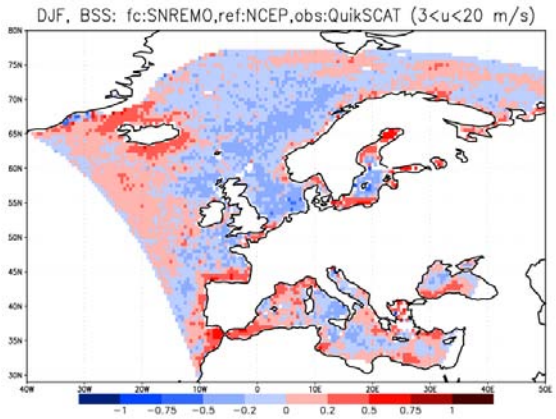

Figure 3: As Figure 1 but for Winter (DJF).

References:

Winterfeldt, J. and R. Weisse, Assessment of value added for surface marine wind obtained from two Regional Climate Models (RCMs), submitted to *Mon. Wea. Rev.*, 2009

Winterfeldt, J., Andersson, A., Klepp, C., Bakan, S. and R. Weisse, Assessment of value added for surface marine wind obtained from two Regional Climate Models (RCMs), submitted to *IEEE Trans. Geosciences and Rem. Sens.,* 2009

Present climate simulations (1982-2003) of precipitation and surface temperature using the RegCM3, RSM, and WRF

Yoo-Bin Yhang, Kyo-Sun Lim, E-Hyung Park and Song-You Hong, ybyhang@yonsei.ac.kr

1. Introduction

Interannual variations of precipitation and surface air temperature are integral parts of the climate system, where remote controls by planetary circulation and global surface anomalies act together with local influences by regional mesoscale surface characteristics. These two broad factors (remote and local) can be distinguished by using a regional climate model (RCM), in which planetary signals are integrated through lateral boundary conditions while mesoscale impacts are internally resolved (e.g., Giorgi et al., 1993; Liang et al., 2001). Given the inadequacies of general circulation models (GCMs) to simulate regional climate variability, the RCM downscaling has become a powerful alterative and is widely applied in studies of seasonal-interannual climate prediction and future climate change projection.

It is imperative that any RCM must be rigorously validated in reproducing historical observations, including both mean climate and temporal variability, before credible application for climate change projection. In the published literature, numerous studies have demonstrated the RCM skill enhancement for downscaling regional characteristics, especially of precipitation and surface air temperature, focusing on mean climate (long-term averaged) biases such as in the annual cycles (Pan et al., 2001; Roads et al., 2003).

In this study, three different RCMs, the Weather Research and Forecasting model (WRF), National Centers for the Environmental Prediction (NCEP) Regional Spectral Model (Juang et al., 1997), and Regional Climate Model version 3 (RegCM3, Pal et al., 2007), are chosen to examine downscaling skill. The downscaling sckills of RCMs are compared with the driving reanalysis, against observation of interannual variations of precipitation and surface temperature during 1982-2003 over East Asia. This is facilitated by using empirical orthogonal function (EOF) and correlation analyses.

2. Model and experimental design

Three regional climate models used in this study are the RSM, WRF, and RegCM3. The RSM is a primitive equation model using the sigma-vertical coordinate. The model includes parameterizations of surface, boundary layer (BL), and moist processes that account for the physical exchanges between the land surface, the boundary layer, and the free atmosphere. The RegCM3 is a primitive equation, compressible, sigma-vertical coordinate, and limited area model of which the dynamical core is based on the hydrostatic version of the fifth-generation Penn State University-National Center for Atmospheric Research (PSU-NCAR) Mesoscale Model (MM5; Grell et al. 1994). The Advanced Research WRF (ARW; Skamarock *et al*. 2005) is a community model suitable for both research and forecasting.

Three-month-long simulations for the summer season (June-July-August; JJA) were performed for 22 years from 1982 to 2003. The model grids consist of 109 (west-east) by 86 (north-south) grid lines at 60 km horizontal separation with the polar stereographic map projection. The model configurations used for each model are summarized in Table 1. The simulations are performed with reanalyses-derived boundary forcing.

	RegCM3	RSM	WRF
vertical levels	σ-23 layers	σ-28 layers	σ-28 layers
dynamics numerics	hydrostatic finite difference	hydrostatic spectral computation	nonhydrostatic finite difference
CPS	Grell (Grell, 1993)	SAS 2005 (Byun and Hong, 2007)	Kain-Fritsch (Kain and Fritsch, 1993)
PBL	Holtslag (Holtslag ,1990)	YSUPBL (Hong et al., 2006)	YSUPBL (Hong et al., 2006)
LSM	BATS (Dickinson et al., 1986)	OSU (Mahrt and Pan, 1984)	Noah (Chen and Dudhia, 2001)
RAD	CCM3 (Kiehl, 1998)	GSFC (Chou and Suarez, 1999)	simple cloud-interactive (Dudhia, 1989), RRTM (Mlawer et al., 1997)

3. Dominant interannual variation patterns

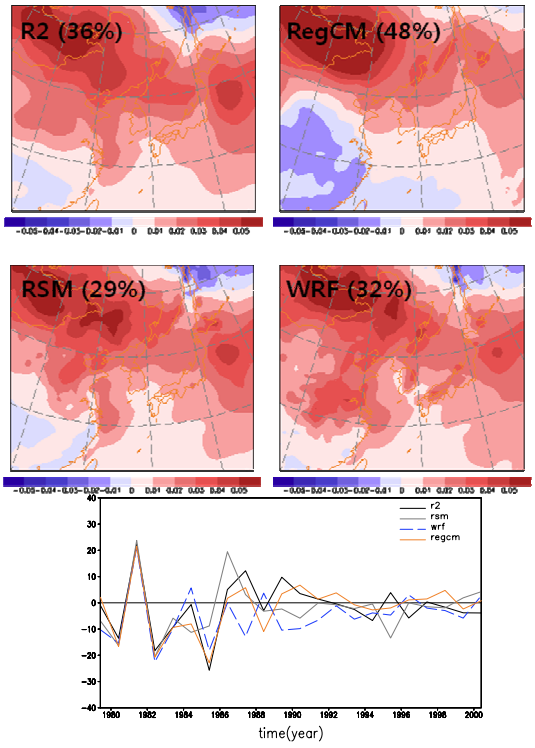

Figure 1. The first EOF mode and corresponding principal component of surface temperature.

Figure 1 shows the first EOF mode of summer temperature and the corresponding principal component (PC) reanalysis data and simulated by the RegCM3, RSM, and WRF, where summer is defined as the average of JJA. The first dominant mode of the reanalysis explains 36% of the total variance in the model domain, which is characterized by positive values over the whole domain.

The models capture this pattern with the variance of 48% by the RegCM, 29% by the RSM, and 32% by the WRF. The spatial patterns are quite consistent with the corresponding modes from the R2. The spatial correlation coefficients with the first modes from reanalysis data are 0.8, 0.94, and 0.91 by the RegCM, RSM , and WRF, respectively. The corresponding temporal correlation coefficients are 0.89, 0.65, and 0.60 by theh RegCM, RSM, and WRF.

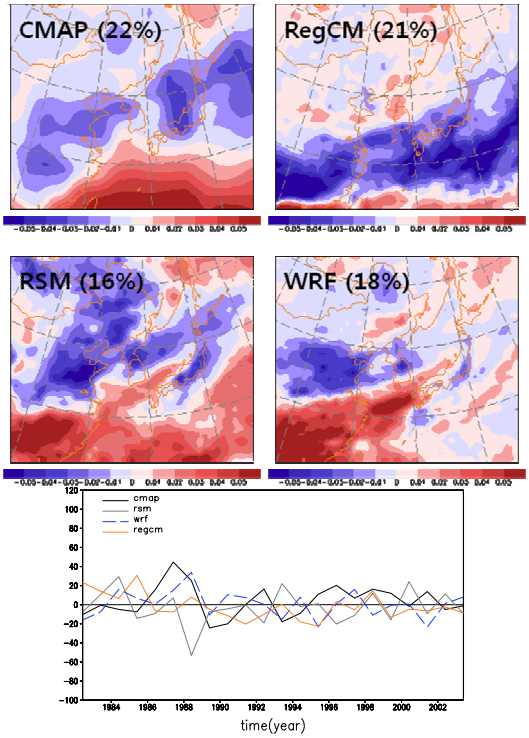

Figure 2. Same as in Fig. 1 except for precipitation.

Figure 2 compares the EOF patterns and PC time series of the observed and simulated precipitation. The first eigenvector of the observed summer precipitation explains 22% of total variance that is smaller than that for temperature. The interannual variation of precipitation is more complex and also more difficult to model than temperature. The first modes of simulated precipitation by three RCMs explain 21%, 16%, and 18%. The CMAP precipitation is characterized by positive-negative pattern in the north-south direction. The RegCM and RSM capture these patterns, however, the negative area is biased southward in the RegCM and band-shape is not reproduced in the RSM compared to the CMAP. The spatial correlations with the observed mode are 0.43, 0.29, 0.05 for the RegCM, RSM, and WRF, respectively. The correlation of the PC time series between the observed and simulated precipitation for the first mode is about -0.1, 0.33, and 0.23 by the RegCM, RSM, and WRF, respectively. In contrast to the PC time series obtained from the surface temperature, correlation coefficients between the CMAP and simulated precipitation is low.

References

Byun, Y.-H., and S.-Y. Hong, Improvements in the subgrid-scale representation of moist convection in a cumulus parameterization scheme: Single-column test and impact on seasonal prediction. *Mon. Wea. Rev*, 135,2135-2154, 2007.

Chen, F., and J. Dudhia, Coupling an advanced land surface–hydrology model with the Penn State–NCAR MM5 modeling system. Part I: Model implementation and sensitivity. *Mon. Wea. Rev*, 129, 569–585, 2001.

Dickinson, R., Henderson-Sellers, A. and Kennedy, P., Biosphere-atmosphere transfer scheme (bats) version 1e as coupled to the ncar community climate model, *Technical report, National Center for Atmospheric Research,* 1993.

Dudhia, J., Numerical study of convection observed during the winter monsoon experiment using a mesoscale two-dimensional model. *J. Atmos. Sci*., 46, 3077-3107, 1989.

Giorgi, F., M. R. Marinucci, and G. T. Bates, Development of a second-generation regional climate model (RegCM2). Part II : Convective processes and assimilation of lateral boundary conditions. *Mon. Wea. Rev.*, 121, 2814-2832, 1993.

Grell, G., Prognostic evaluation of assumptions used by cumulus parameterization, *Mon. Wea. Rev,* 121, 764-787, 1993.

Holtslag, A.A.M., De Bruijn, E.I.F., Pan, H.-L., A High Resolution Air Mass Transformation Model for Short-Range Weather Forecasting. *Mon. Wea. Rev.* 118, 1561–1575, 1990.

Hong, S.-Y., Y. Noh, and J. Dudhia, A new vertical diffusion package with an explicit treatment of entrainment processes. *Mon. Wea. Rev*., 134, 2318–2341, 2006.

Juang, H.-M. H., S.-Y. Hong, and M. Kanamitsu, The NCEP regional spectral model: An update, *Bull. Amer. Meteor. Soc.,* 78, 2125-2143, 1997.

Kain, J., and M. Fritsch, Convective parameterization for mesoscale models : The Kain- Fritsch scheme. *The representation of cumulus convection in numerical models, Meteor. Monogr*., No. 24, Amer. Meteor. Soc., 165-170, 1993.

Kiehl, J., Hack, J., Bonan, G., Boville, B., Breigleb, B., Williamson, D. and Rasch, P., Description of the ncar community climate model (ccm3), *Technical report, National Center for Atmospheric Research*,1998.

Liang, X.-Z., K. E. Kunkel, and A. N. Samel, Development of a regional climate model for U. S. Midwest applications. Part I : Sensitivity to buffer zone treatment, *J. Climate*, 14, 4363-4378, 2001.

Mahrt, L. and H.-L. Pan, A two layer model of soil hydrology. *Bound.-Layer Meteor*., 29, 1-20, 1984.

Mlawer, E. J., S. J. Taubman, P. D. Brown, M. J. Iacono, and S. A. Clough, Radiative transfer for inhomogeneous atmosphere: RRTM, a validated correlated-k model forthe long wave. *J. Geophys. Res.,* 102(D14), 16 663-16 682, 1997.

Pal, J. S., F. Giorgi, X. Bi, N. Elguindi, F. Solomon, X. Gao, R. Francisco, A. Zakey, J. Winter, M. Ashfaq, F. Syed, J. L. Martinez, R. P. da Rocha, L. C. Sloan, and A. Steiner, RegCM3 and RegCNET: Regional climate modeling for the developing world. *Bull. Amer. Meteor. Soc.,* 88, 1395-1409, 2007.

Pan, Z., J. H. Christensen, R. W. Arritt, W. J. Gutowski Jr., E. S. Takle, and F. Otieno, Evaluation of uncertainties in regional climate change simulations. *J. Geophys. Res*., 106, 17753-17751, 2001.

Roads, J., S.-C. Chen and M. Kanamitsu, U. S. regional climate simulations and seasonal forecasts. *J. Geophys. Res.*, 108, 8606, doi:10.1029/2002JD002232, 2003.

Skamarock, W. C., J. B. Klemp, J. Dudhia, D. O. Gill, D. M. Barker, W. Wang and J. G. Powers, A Description of the Advanced Research WRF Version 2. NCAR technical note, NCAR/TN-468+STR, 88 pp. [Available at http://www.mmm.ucar.edu/wrf/users/docs/arw_v2.pdf], 2007.

Incremental interpolation of coarse global forcings for regional model integrations

Kei Yoshimura and Masao Kanamitsu

9500 Gilman Dr. MC0224, La Jolla, CA92093, USA. k1yoshimura@ucsd.edu

1. Introduction

Until now, the numbers of forcing levels and time frequencies have been somewhat arbitrarily chosen for regional model integrations and very high resolutions in the vertical and in time, of the order of 25 hPa in the vertical and 6 hours in time, are believed to be required. Unfortunately, this high resolution forcing output restricts the number of cases of downscaling that can be performed. For example, NARCCAP limits the number of global warming simulation models to only four. The slow progress in the downscaling of ensemble seasonal forecast is also due to the practical difficulties in storing high resolution output from large ensemble members.

In this study, we will examine the impact of the vertical resolution of the forcing field and introduce a new interpolation scheme that arrows the use of coarse vertical resolution without losing accuracy with only a small overhead. Similar idea can be applied to the interpolation in time. Using this method, global forcing with only 5 levels in the vertical and time frequency of daily is sufficient to force regional model, thus reducing the required volume of forcing files by a factor of 30 or more.

This work also presents the importance of specification of the forcing data. Since vertical levels of forcing fields are generally different from those of regional models and the vertical interpolation may have significant deteriorating effects on dynamical downscaling. This problem has not been studied intensively because these errors were considered to have only a minor influence on the regional simulation. This may be true for a short-range regional forecast problem for which the initial condition is of greater importance, while the lateral boundary condition has less influence. However, the lateral boundary conditions may have a significant influence on the downscaling at climate time-scale, since they continuously influence the interior of the regional domain. The external forcings will be even more important for their use within the regional domain when the spectral nudging is applied.

For further detail, please see *Yoshimura and Kanamitsu* (2009).

2. Incremental Interpolation

A method we introduce here is a common procedure used widely in objective analysis, called incremental interpolation (*e.g.*, *Bloom et al.*, 1996). This method uses short range forecast with a global coarse resolution model as a guess, and vertically interpolates the difference between the external forcing field and the guess at the standard pressure levels to model levels. Since only the increment is interpolated, the fine structure in the guess field is preserved after the interpolation.

If we use incremental interpolation used in objective analysis to the vertical interpolation of the forcing, the forcing field F_{INC} will be written as:

$$F_{INC} \equiv F_g + \Im_{p\to s}(\Im_{s\to p}(F_a)) - \Im_{p\to s}(\Im^*_{s\to p}(F_g)) \quad (1)$$

where F_g and F_a are initial guess field and analysis fields in full sigma-level coordinate, and $\Im_{p\to s}$ and $\Im_{s\to p}$ are interpolation operators from pressure-to-sigma and sigma-to-pressure coordinates, respectively. Summation of the second and third terms on the right hand side of Eq.(1) gives you the "interpolated increment." Note that the interpolation operators used in $\Im_{s\to p}(F_a)$ and in $\Im^*_{s\to p}(F_g)$ are generally not exactly the same, since vertical interpolation (frequently called post-processing) used in the models between analysis and guess models are different. As schematically shown in Figure 1, the incremental interpolation maintains the small scale vertical structure in the guess field, thus errors are much smaller than the simple interpolation.

Two streams of regional integrations are taken place with different processes applied for forcing fields in pressure-level; simple vertical interpolation scheme (P2S) and the new incremental interpolation scheme (INC), and they are compared with a reference integration (CTL), in which forcing fields in fully identical sigma levels are used. We used ECPC RSM, which a type of the spectral nudging (selective scale bias correction; *Kanamaru and Kanamitsu*, 2006) is applied. The domain of all the experiments covers part of North and Central America including the U.S. and Mexico, (135-65W and 10-50N), with 50 km horizontal and 28-level vertical resolutions. The original forcing data are taken from R2. The integration period is January 1-11, 1985, which is somewhat arbitrarily chosen. Each set of experiments consists of 4 ensemble members that start at 00Z on the 1st, 2nd, 3rd, and 4th, respectively, and all end at 00Z January 11. For each of the streams, the following five combinations of pressure levels to generate the forcings; *i.e.*, 17, 9, 7, 3, and 2 levels.

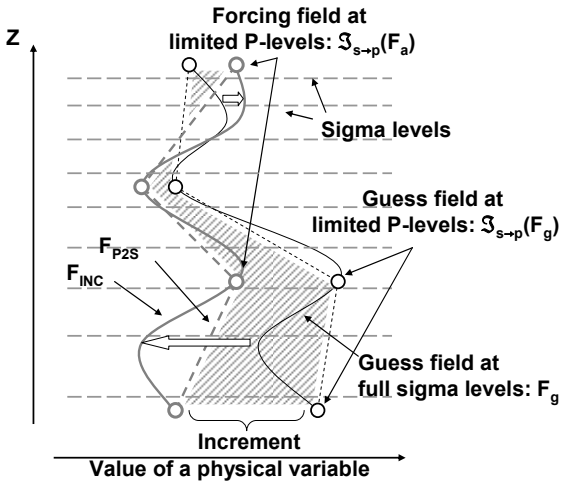

Figure 1. Schematic representation of the vertical incremental interpolation.

3. Results

Figure 1 present a comparison of the root mean square difference (RMS) of surface air temperature, surface wind, and precipitation between CTL and the experiments with different forcing level specifications (17, 9, 6, 3, and 2 levels.) The left-most gray bars, the mean RMS among the ensemble members, indicate the variance

of the simulations due to the difference of the initial conditions. The dark bars in Figure 2 show the results from the simple vertical interpolation (P2S), whereas the white bars indicate the incremental interpolation (INC). The incremental interpolation significantly improves regional simulation for nearly all ranges of pressure levels with the exception of precipitation in 17L, 9L, and 3L. The performance of the 7L results became very similar to that of 17L without the incremental interpolation (P2S-17L), and even 3L produced a reasonably good regional simulation compared to P2S-17L. Therefore, from a practical point of view, approximately 5 pressure levels will be sufficient to obtain reasonably accurate regional simulations. We should note that the improvement is more apparent for 2-meter temperature and 10-meter winds. Reasonable improvement is also seen in precipitation.

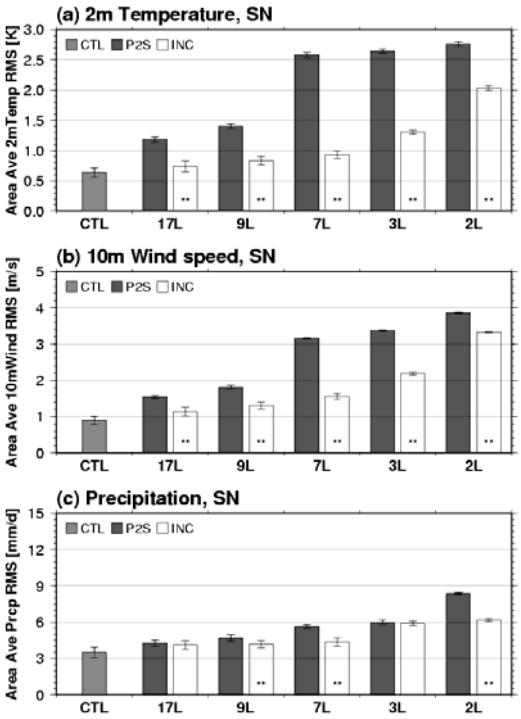

Figure 2. Ensemble means of area averaged RMS between CTL and experiments with different numbers of vertical levels used as forcings are shown for 2-meter air temperature (a), 10-meter wind speed (b) and precipitation (c).

4. Application to Regional Future Projection

Though highly expected, few of IPCC/WCRP's CMIP3 simulation results can be directly used as lateral boundary condition for dynamical downscaling study because these data are archived with small number of vertical levels and scarce temporal interval (at most daily). We therefore investigated the impact of small number of vertical levels and longer intervals of forcing data, particularly focused on a purpose of the regional future projection. Japanese T106 MIROC simulation results are used, and all 23-level data are used as lateral boundary for the control regional integration (CTL). Similarly to the previous section, we applied the simple vertical interpolation from coarse vertical data (COA) and the incremental interpolation (INC) from the lowest 9 levels (up to 200 hPa). In this experiment, we used the ECPC RSM, but for a domain covering western U.S.A. and Mexico and vicinity oceans in 10 km horizontal resolution. Integration was done for one year (year of 2047 in A1B scenario, according to MIROC experiment) with identical initial conditions.

Figure 3 shows monthly precipitation distributions and their difference from CTL. Due to less vertical information given by the forcing data, more precipitation is simulated over the Central Valleys in COA, whereas the wet condition is fixed in INC, even though exactly same amount of information has been used. As shown in Figure 4, this is mainly due to more surface convergence simulated in COA.

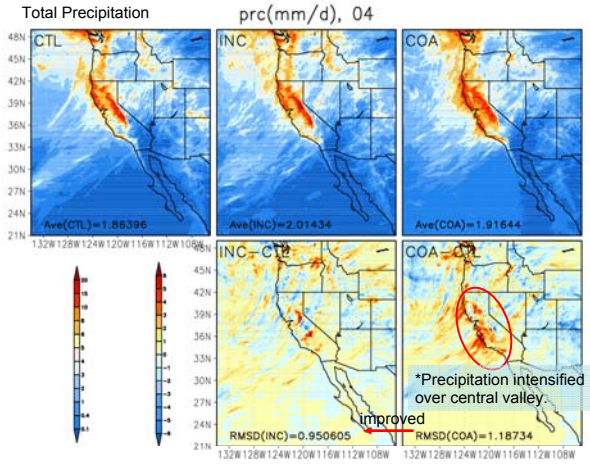

Figure 3. Monthly precipitation from 10-km regional dynamical downscaling of MIROC's global future projection results. Upper panels show monthly distribution and lower panels show difference from the control (CTL).

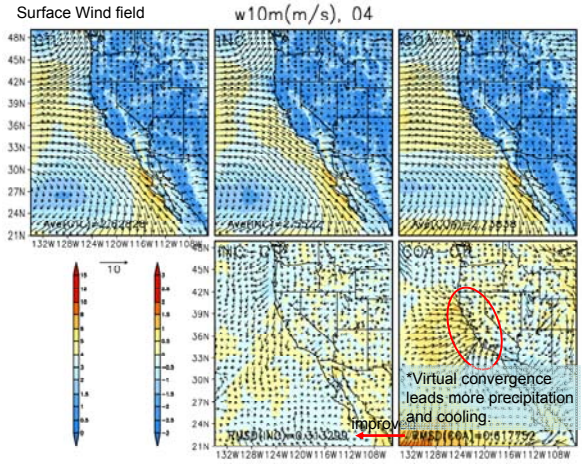

Figure 4. Same as Figure 3, but for surface wind fields.

References

Yoshimura, K. and M. Kanamitsu, Specification of external forcing for regional model integrations, *Mon. Wea. Rev.*, 2009. (in print)

Kanamaru, H. and M. Kanamitsu, Scale-selective bias correction in a downscaling of global analysis using a regional model, *Mon. Wea. Rev.*, **135**, 334–350, 2006.

Development of a long term climatology of North Atlantic polar lows using a RCM

Matthias Zahn and Hans von Storch

Institute for Coastal Research, GKSS Research Center, Geesthacht, Germany, matthias.zahn@gkss.de

1. Introduction - polar lows

Polar lows are intense mesoscale ground level storms, which occur in the subpolar maritime regions of both hemispheres during the winter seasons. They usually develop in instable atmospheric conditions and are often triggered by convective processes (cf. *Rasmussen and Turner* (2003)). Only since the advent of satellite imagery it became possible to discover a large proportion of these features reliably. However the period covered by such data usually does not allow for any statements on the long-term behavior of polar lows.

For investigations of atmospheric features on timescales of several decades, often so called global reanalysis data are used. These reanalyses contain the past state of the whole atmosphere on a relatively coarse grid, approximately 200 x 200 km. As polar lows are phenomena sized beyond the resolved scales of the reanalyses, we used a RCM for our approach to develop a long-term climatology of polar lows in the North Atlantic.

2. Method - reproducing polar lows with a RCM

This widely used method to gain higher resolved atmospheric fields is called "dynamical downscaling" and post processes reanalysis-data by means of RCMs. However, for a number of applications, it is not clear if the expected additional value of the higher resolved fields justifies this computationally intensive procedure. E.g. *Winterfeldt and Weisse* (2009) show, that an additional value for wind speed statistics in maritime areas in RCMs is only gained in coastal areas, which are influenced by topography.

In our talk we show that driving a RCM with global reanalysis-data is a reasonable way for our aim, namely to reproduce polar lows. In RCM simulations polar lows do emerge, whereas in the driving fields, they are not clearly contained. This extends what *Feser et al.* (2009) report on the "added value of limited area model results" on this workshop.

It is further shown, that polar lows can more reliably be reproduced, when a spectral nudging method, which integrates large scale information from the reanalyses into the RCM-simulation, is applied. This holds for an ensemble of case studies as well as for an ensemble of two year long simulations (*Zahn, M. et al.* (2008), *Zahn, M. and H. von Storch* (2008a))

Considering these results we carried out a multidicadal (approx. 60 years) simulation of the atmosphere above the North Atlantic and counted the seasonal numbers of polar lows.

3. Results – the climatology of polar lows

Figure 1 shows the number of counted polar lows per winter season over the investigated period of 60 years. There is large interannual variability in this number, expressed by a standard deviation of about +/- 13 cases, but no long-term changes can be seen (cf. *Zahn, M. and H. von Storch* (2008b)).

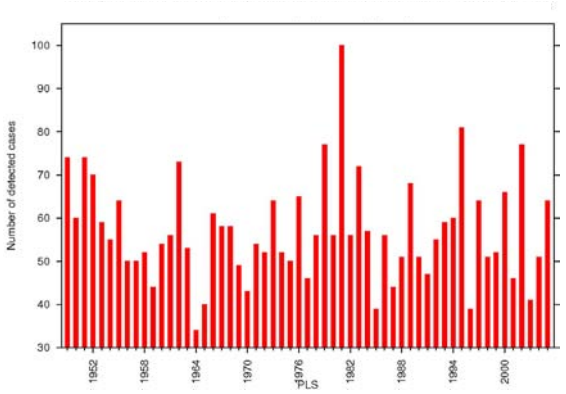

Number of detected polar lows per polar low season (PLS). One PLS is defined as the period starting 1 July and ending 30 June the following year.

Further characteristics of the climatology such as regional distribution and the resemblance to limited observational evidence are also presented. Finally, first results for future projections, which assess the behavior of the number of polar lows in presumed changing climate conditions, are discussed.

References

Frauke Feser, Hans von Storch, Jörg Winterfeldt, and Matthias Zahn, Added value of limited area model results, this workshop, 2009

Rasmussen, E. J. Turner, Polar Lows: Mesoscale Weather Systems in the Polar Regions. – Cambridge University Press, Cambridge. 2003

Winterfeldt, J. and R. Weisse, Assessment of value added for surface marine wind obtained from two Regional Climate Models (RCMs), submitted to *Mon. Wea. Rev.*, 2009

Zahn, M., H. von Storch, and S. Bakan, Climate mode simulation of North Atlantic Polar Lows in a limited area model, *Tellus, Ser. A*, 60, pp. 620–631, doi:10.1111/j.1600-0870.2008.00330.x, 2008

Zahn, M. and H. von Storch, Tracking Polar Lows in CLM, Meteorologische Zeitschrift,17(4), 445 - 453, doi:10.1127/0941-2948/2008/0317, 2008a

Zahn, M., and H. von Storch, A long-term climatology of North Atlantic Polar Lows, *Geophys. Res. Lett.*, 35, L22702, doi:10.1029/2008GL035769, 2008b

Examining the relative roles convective parameterization precipitation and cloud material feedback

Christopher J. Anderson

3010 Agronomy Hall, Iowa State University, Ames, 50011-1010, cjames@iastate.edu

1. Introduction

Mesoscale convective systems (MCSs) produce unique regional climate signals in the central United States that include nocturnal precipitation maximum, eastward nocturnal propagation of precipitation, and mixing line (Anderson and Arritt 2007, Markowski and Stensrud 1998) but are notoriously difficult to simulate with grid spacing >1km (Bryan et al. 2003, Correia et al. 2008). The challenge arises in simulating an upscale transition of dynamical forcing. MCSs begin as independent convective storms that self-organize into larger dynamical scale circulation by means of low-level outflow, gravity waves, and mid-level virtual warming (Bryan et al. 2003, Cotton et al. 1989, Pandya et al. 2000). The scale and configuration of latent heat release and evaporative cooling are very important in the evolution of these processes and are represented within a regional climate model (RCM) by the convective and moist physics parameterizations. In this paper, the role of precipitation and cloud material generated by convective parameterization is examined in simulations of a two-month period in which MCSs are prevalent (Anderson and Arritt 1998).

2. Experimental Design

A suite of RCM experiments were used to systematically study sensitivity of climate characteristics of MCSs to the partitioning of water vapor flux within the convective parameterization into precipitation and cloud material. The simulation period was 1993 June 1 – July 31. More than 35 large MCSs occurred during this period, which equates to about one occurrence per two days (Anderson and Arritt 1998).

The simulations were performed with the Weather Research and Forecast (WRF; Skamarock et al. 2001) model, using the Kain-Fritsch (KF) convective parameterization (Kain 2004). Initial and boundary conditions were provided by the NCEP-DOE Renalysis-II (R2; Kanamitsu 2002).

The fundamental experiment was designed to compare two versions of the KF scheme. A control simulation was made in which the RCM used the default KF scheme and was compared to a test simulation in which the KF scheme was altered to produce cloud material at the expense of precipitation. Comparison of results from the default and modified KF scheme provides insight into the importance of producing widespread mid-level cloudiness and latent heating, and low-level evaporative cooling relative to local heating and cooling profiles from the convective parameterization. A number of experiments were performed by varying the moisture physics parameterization, trigger function in the KF scheme, and model grid point spacing.

3. Results

The diabatic theta change, KF scheme theta change, and KF scheme water species change, where change refers to the one time-step update to the RCM theta and water species, were accumulated over all time steps and over a 10^{O}x10^{O} region centered on the observed maximum of two-month precipitation. The accumulated values are converted to daily average values and shown in profile in Figure 1.

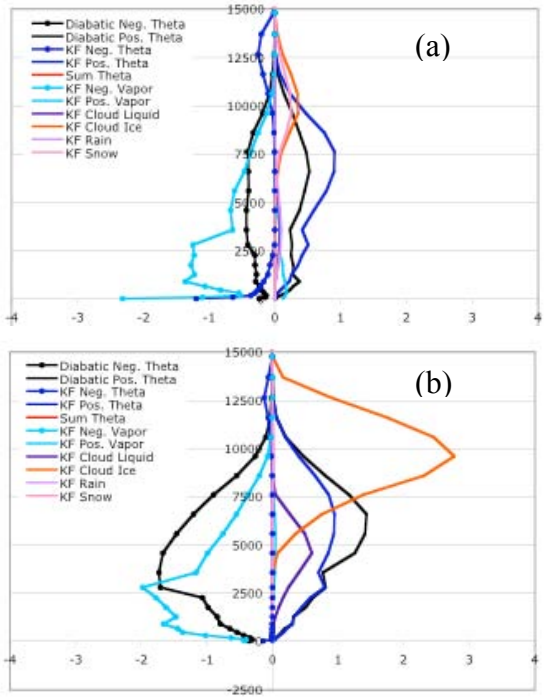

Figure 1. Sixty-one day average of daily diabatic theta change, KF theta change, and KF water species change for (a) default KF scheme and (b) altered KF scheme. 'figure'.

Large differences are evident in the average daily change of diabatic theta, KF theta, and KF water species. In the context of MCSs, the notable differences are a large increase in positive diabatic change 3000-7500 m AGL and larger magnitude of negative diabatic change below 7500 m AGL. The positive KF theta change is nearly identical in both simulations; whereas, the negative KF theta change is slightly larger in magnitude below 3000 m and much, much smaller in magnitude near the surface.

The increase in mid-level positive diabatic theta change occurs in the transition zone from large values of KF cloud water and KF cloud ice change. This result shows that the microphysics parameterization is engaged by altering the KF scheme to produce cloud material at the expense of precipitation. In particular, the diabatic heating appears to occur within a vertical level in which cloud water would freeze to form cloud ice. Likewise, the increase in magnitude of negative diabatic theta change at mid- and low-level altitude is evidence of the activities of the microphyiscs parameterization. In this case, melting of frozen water and evaporation of liquid water create cooling.

The absence of the very shallow, near surface negative KF theta change when using the altered KF scheme is due to the severe reduction in precipitation produced by the KF scheme. The downdraft model uses a fraction of the precipitation to generate an evaporatively cooled downdraft that detrains in the lowest model layer. In the altered version of the KF scheme, precipitation is nearly absent and the water vapor is partitioned into cloud material so that the downdraft model produces very little cooling.

4. Summary

An altered version of the KF scheme in which water vapor flux is converted into cloud material rather than precipitation is examined. The results from simulations of a two-month period in which large propagating MCSs were frequent showed dramatic differences in diabatic heating profiles.

At the workshop, additional results will be discussed that show just as dramatic differences in precipitation characteristics. In particular, the phase of the diurnal cycle of precipitation is significantly delayed and more accurate in when using the altered KF scheme, and with this modified scheme the eastward, nocturnal propagation of precipitation is more pronounced. The sensitivity to microphysics parameterization and grid point spacing will be discussed as well.

References

Anderson, C. J., and R. W. Arritt, An alternative mass flux profile in the Kain-Fritsch convective parameterization and its effect on seasonal precipitation. *J. Hydrometeor.*, Vol. 8, No. 5, pp. 1128-1140, 2007.

Anderson, C. J., and R. W. Arritt, Mesoscale convective complexes and persistent elongated convective systems over the United States during 1992 and 1993, *Mon. Wea. Rev.*, Vol. 126., pp. 578—599, 1998.

Bryan, G. H., J. C. Wyngaard, J. M. Fritsch, Resolution requirements for simulation of deep moist convection, *Mon. Wea. Rev.*, Vol. 131, No. 10, pp. 2394—2416, 2003.

Correia, J. Jr., R. W. Arritt, and C. J. Anderson, Idealized mesoscale convective system structure and propagation using convective parameterization, *Mon. Wea. Rev.*, Vol. 135, No. 7, pp. 2422—2442, 2008.

Cotton, W. R., M.-S. Lin, R. L. McAnelly, and C. J. Tremback, A composite model of mesoscale convective complexes, *Mon. Wea. Rev.*, Vol. 104, 765—783, 1989.

Kain, J. S., The Kain-Fritsch convective parameterization: An update, *J. Appl. Meteor.*, Vol. 43, pp. 170—181, 2004.

Kanamistsu, M., W. Ebisuzaki, J. Woollen, S.-K. Yang, J. J. Hnilo, M. Fiorino, and G. L. Potter, NCEP-DOE AMIP-II reanalysis (R-2), *Bull. Amer. Meteor. Soc.*, Vol. 83, pp. 1631—1643, 2002.

Markowski, P. M., and D. J. Stensrud, Mean monthly diurnal cycles observed with PRE-STORM surface data, *J. Climate*, Vol. 11, No. 11, pp. 2995—3009, 1998.

Pandya, R. E., D. R. Durran, M. L. Weisman, The influence of convective thermal forcing on the three-dimensional mesoscale circulation around squall lines, *J. Atmos. Sci.*, Vol. 57, No. 1, 29—45, 2000.

Skamarock, W. C., J. B. Klemp, and J. Dudhia, Prototypes for the WRF (Weather Research and Forecasting) model, Preprints, Ninth Conf. on Mesoscale Processes, Fort Lauderdale, FL, Amer. Meteor. Soc., J11—J15, 2001.

Dynamical coupling of the HIRHAM regional climate model and the MIKE SHE hydrological model

Martin Drews[1], Søren H. Rasmussen[1], Jens Hesselbjerg Christensen[1], Michael B. Butts[2], Jesper Overgaard[2], Sara Maria Lerer[2] and Jens Christian Refsgaard[3]

[1]Danish Meteorological Institute, Lyngbyvej 100, DK-2100 Copenhagen E, Denmark, mad@dmi.dk
[2]DHI Water and Environment, Agern Alle 11, DK-2970, Hørsholm, Denmark
[3]Geological Survey of Denmark and Greenland, Øster Voldgade 10, DK-1350 Copenhagen K, Denmark

Introduction

Traditionally, the hydrological impacts of climate change have been based on driving hydrological models with the output of global or regional climate models, e.g. Graham et al. (2007). This means that the feedbacks to the atmosphere are neglected, which has an unknown impact on the predictions of climate change, particularly at the local scale. Furthermore, climate models often operate at spatial and temporal scales that are much larger than the scales required for analyzing the effects on the hydrological system. This means that the representation of the hydrology in these climate models is often very simplified and therefore not suitable for detailed hydrological analyses.

To develop improved methods for assessing the effects of climate change on water resources, a fully coupled hydrological and climate modelling system is being developed using two state-of-the-art model codes: the climate model code HIRHAM, Christensen et al. (1996), and the hydrological model code MIKE SHE, Graham and Butts (2006) The coupling will exploit new OpenMI technology that has recently emerged from the water sector for coupling model components. OpenMI provides a standardized interface to define, describe and transfer data on a time basis between software components that run simultaneously thus supporting systems where feedback between the modelled processes is necessary, Gregersen et al. (2007). Therefore, OpenMI is ideally suited to linking hydrological and climate models and allows linking with different spatial and temporal representations and across different platforms. This new technology will also be effective in linking the meteorological and hydrological modelling communities.

MIKE SHE

MIKE SHE is an advanced, flexible framework for hydrologic modeling, Butts et al., (2004); Graham & Butts (2006). MIKE SHE covers the major processes in the hydrological cycle and includes process models for evapotranspiration, overland flow, unsaturated flow, groundwater flow, and channel flow and their interactions. Each of these processes can be represented at different levels of spatial distribution and complexity according to the goals of the modelling study, the availability of field data and the modeller's choices, Butts et al. (2004).

A new energy-based evapotranspiration model has been implemented in MIKE SHE, Overgaard et al. (2007), and will be used to model the feedback processes between the land surface and atmosphere. This new evapotranspiration model was successfully evaluated against observations of energy fluxes collected during the First International Satellite Land Surface Climatology Project (ISLSCP) Field Experiment (FIFE). FIFE was conducted in a 15x15 km area near Manhattan, Kansas, in and around the Konza Prairie.

HIRHAM

HIRHAM is a regional atmospheric climate model, cf. Christensen et al. (1996), based on a subset of the HIRLAM, cf. Undén et al. (2002) and ECHAM models, cf. Roeckner et al. (2003), combining the dynamics of the former model with the physical parameterization schemes of the latter. A new and updated version, HIRHAM5, has recently been developed in collaboration between the Danish Meteorological Institute and the Potsdam Research Unit of the Alfred Wegener Institute Foundation for Polar and Marine Research and was released in 2006, cf. Christensen et al. (2006).

Coupling scheme

The coupling will be made such that HIRHAM's standard, simple land surface parameterization scheme (hydrological model) will be utilized in regions not covered by the MIKE SHE model. This will make it possible to apply the coupled code without having to set up MIKE SHE on the entire regional scale covered by HIRHAM, and it will therefore save both personal time and computational power. The following parameters are passed from the climate model to the hydrological model: air temperature, precipitation, wind speed, relative humidity, global radiation, and air pressure, whereas sensible and latent heat flux and surface temperature is passed to the climate model.

Since the HIRHAM code is designed to run efficiently on a massively parallel UNIX/LINUX system, while MIKE SHE runs primarily on a WINDOWS PC, a critical task is to develop a suitable method for cross-platform communication, i.e. in order to facility the exchange of parameters at run-time. Here, we exploit the OpenMI standard interface technology. In brief, an OpenMI compliant version of MIKE SHE has been built to run on a WINDOWS PC along with a similarly compliant "proxy" version of the HIRHAM model. The proxy component is linked to a HIRHAM wrapper on the UNIX/LINUX side, which implements the smallest subset of the OpenMI standard methods and provides a direct interface to the modified model code. In this way any of the model components, i.e. HIRHAM or MIKE SHE, may be seamlessly exchanged or new ones added, e.g. to build a regional Earth system model.

Concluding remarks

This poster presentation provides further details on the coupled model system and the OpenMI interface. Also, we present preliminary results from coupled feasibility studies carried out on the basis of data from the FIFE project as well as reanalysis data from the CRU and ERA-40 archives.

Acknowledgements

This work is part of the "HYACINTS" project, www.hyacints.dk, and has been funded by the Danish Council for Strategic Research under the Programme Commision on "Sustainable Energy and Environment".

References

Butts MB, Payne JT, Kristensen M and Madsen H. An evaluation of the impact of model structure on hydrological modelling uncertainty for streamflow prediction. Journal of Hydrology, 298, pp 242-266, 2004.

Christensen JH, Christensen OB, Lopez P, van Meijgaard E, Botzet M. The HIRHAM4 Regional Atmospheric Climate Model; DMI Scientific Report 96-4. Danish Meteorological Institute, 1996.

Christensen OB, Drews M, Christensen JH, Dethloff K, Ketelsen K, Hebestadt I, Rinke A. The HIRHAM Regional Climate Model Version 5β; DMI Technical Report 06-17. Danish Meteorological Institute, 2006.

Graham DN and Butts MB, Flexible, integrated watershed modelling with MIKE SHE. In Watershed Models, Eds. V.P. Singh & D.K. Frevert, pp 245-272, CRC Press. ISBN: 0849336090, 2005.

Graham LP, Hagemann S, Jaun S, Beniston M. On interpreting hydrological change from regional climate models, 81 Suppl. 1, 97-122. doi: 10.1007/s10584-006-9217-0, 2007.

Gregersen JB, Gijsbers PJA, Westen SJP. OpenMI: Open modelling interface. Journal of Hydroinformatics, 09.3, 175-191. doi: 10.2166/hydro, 2007.

Overgaard J, Butts MB, Rosbjerg D. Improved scenario prediction by using coupled hydrological and atmospheric models. In: Quantification and Reduction of Predictive Uncertainty for Sustainable Water Resources Management (Eds: Boegh E, Kunstmann H, Wagner T, Hall A, Bastidas L, Franks S, Gupta H, Rosbjerg D Schaake J), IAHS Publ. 313, pp 242-248, 2007.

Overgaard J, Butts MB, Rosbjerg D, Gregersen J. Coupling hydrological and meteorological models using OpenMI to investigate land-use and climate change. Proceedings of the 7th International Conference on Hydroinformatics Editted by P. Gourbesville, J. Cunge, V. Guinot, S-Y Liong., HIC 2006, Nice, France, September 2006, Vol III, 2040-2047, 2006.

Roeckner E, Bäuml G, Bonaventura L, Brokopf R, Esch M, Giorgetta M, Hagemann S, Kirchner I, Kornblueh L, Manzini E, Rhodin A, Schlese U, Schulzweida U, and Tompkins A. The atmospheric general circulation model ECHAM5. Part 1. Model description. Report no. 349, Max-Planck-Institut für Meteorologie (MPI-M), 2003.

A parameterization of aircraft induced cloudiness in the CLM regional climate model

Andrew Ferrone, Philippe Marbaix, Ben Matthews, Ralph Lescroart and Jean-Pascal van Ypersele

Institut d'astronomie et de géophysique G. Lemaître (ASTR), Université catholique de Louvain (UCL)
2, chemin du cyclotron 1348 Louvain-la-Neuve, Belgium

1. Introduction

Under well defined conditions (see Schumann, 2000) the hot and moist engine exhaust gases of airplanes at cruise level trigger the formation of condensation trails (contrails) in the wake or the aircraft. If the surrounding air is ice-supersaturated these contrails become persistent and transform into cirrus clouds and can persist for several hours (IPCC,1999).

It has been shown (IPCC, 1999, IPCC, 2007) that this so-called aircraft induced cloudiness (AIC) has a warming impact on climate, although the magnitude of the impact is not well determined. This study aims at modeling the contrail formation and their evolution into cirrus clouds with the regional climate model CLM over Europe. A regional model has been chosen as its cloud microphysics are generally more detailed than in global climate models. The higher resolution of the model (20km x 20km) permits a more detailed representation of small-scale structures like contrails. The global contrail coverage is spatially very inhomogeneous. Therefore Europe has been chosen as a model domain as it presents very high coverage due to the high traffic density over this region.

2. Model and contrail parameterisation

The regional climate model CLM (Climate version of the Lokal Model) (Will et al., 2008) has been chosen for this study. This regional climate model is derived from the operational non-hydrostatic weather-forecast model COSMO used among others by the German Weather Service (DWD).

The cloud microphysical scheme is a one moment, two category ice-scheme based on (Lin et al., 1983). To this scheme a parameterization was added (figure 1) that creates supplementary ice clouds when the meteorological conditions permit the creation of contrails (Schmidt-Appleman criterion, see Schumann, 2000) and the air is ice-supersaturated. The subgridscale growth of contrails in the model is based on results by Lewellen and Lewellen (2001) and depends on the ambient supersaturation level. The supplementary ice created is then fully integrated into the microphysics of the climate model, which allows the simulation of the growth of linear contrails into cirrus clouds.

3. Some preliminary results

For these preliminary runs a homogeneous flight distribution has been assumed (i.e. a plane is continuously flying in every grid-cell). In all grid boxes the flown distance has been set to the average over Europe derived from the AERO2k database (Eyers et al., 2005)

Figure 2 shows the difference of ice mass between the run with the homogeneous contrail forcing and a reference run, without contrails averaged over January 2005 and all model levels. This tells us the location of regions which are more prone than others to form persistent contrails

This experiment shows that especially over the northern Iberian peninsula, but also over the English Channel and the North-Sea, conditions are present to form many persistent contrails, whereas the region west of the Alps shows a rather low potential. These findings are in accordance with satellite based observations of linear contrails (Meyer et al., 2002).

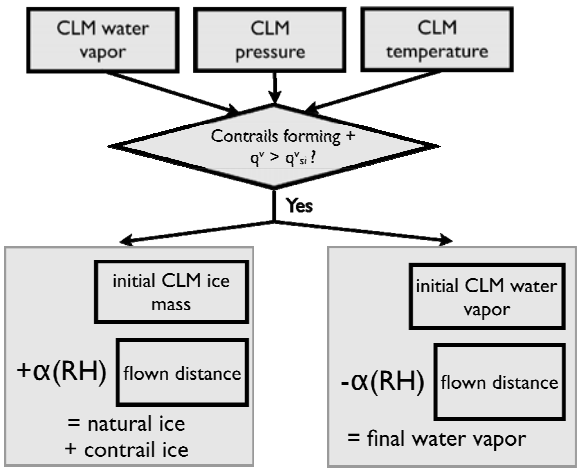

Figure 1. Schematic representation of the contrail parameterization in the model, with q^v the specific humidity calculated by CLM, q^v_{si} the specific ice saturation humidity, α a parameter to account for the sub-grid scale growth of contrails and RH the relative humidity

Figure 3 shows a vertical slice through the model domain at the black line indicated in figure 2. Even though in this theoretical experiment planes are flying at every altitude (including the stratosphere) it can be seen that contrails form only between 8 and 12 km, which are the heights where most ice-supersaturation is observed (Gettelman et al., 2006).

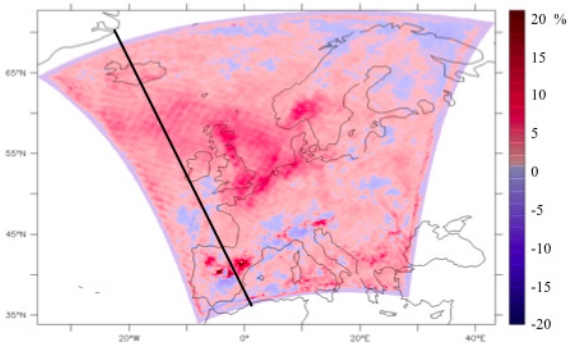

Figure 2. Relative difference (in %) of the mass of ice given by model, averaged over all model levels between the reference run and a run including the contrail parameterisation, for January 2005. The darker the red aera the more ice has been formed by aircrafts in this idealised case (see text)

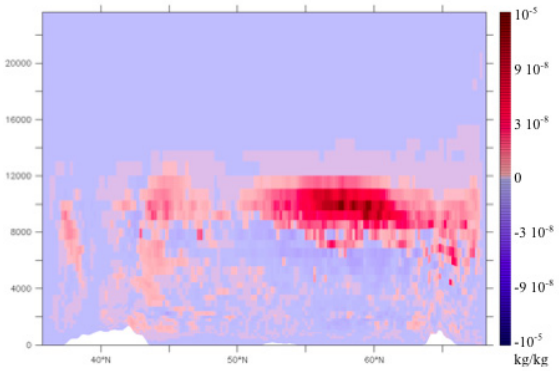

Figure 3. Slice through the model domain at the line indicated in black on figure 2 of the relative difference (in %) of the mass of ice given by model, between the reference run and a run including the contrail parameterisation, for January 2005.

The impact of this additional ice mass on the high cloud cover (> 8km) as calculated by CLM (Xu and Randall, 1996) is shown in figure 4. The increase of up to 8% of cloud cover is in accordance with recent simulations of AIC in a global model (Burhardt et al., 2008).
We can again see a high increase over e.g. the North Sea. However in regions which are less prone to from persistent contrails, such as Southern France, the change in cloud cover is slightly negative. This is due to a slight temperatures increase just below the contrail cover, which is advected in regions with low contrail coverage and leads to a decrease in cloud cover that becomes visible in these areas.

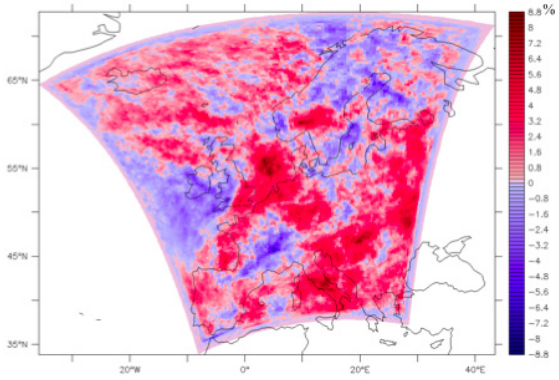

Figure 4. Difference of the high cloud cover (> 8km, in % of coverage), between the reference run and a run including the contrail parameterisation, for January 2005.

4. Outlook and future work

The next step will be to perform runs based on data derived from real flights (e.g. from AERO2k, see Eyers et al., 2005). As this database is on a 1°x1° grid, a downscaling has been performed to the model grid of 0.2° x 0.2°. Once a model run with these data has been done it will be interesting to compare the additional cloudiness with the "homogenous traffic" case in order to what extent the observed patterns by satellite are based on the inhomogeneities in the air traffic, or on different climatic conditions.
As the parameterisation is dependent on the correct calculations of supersaturation it is important to validate it in the CLM model, by comparing model output to satellite data. Also the simulated AIC needs to be validated on longer time scales and other seasons, which can be done by a comparison with satellite observations from (Meyer et al., 2002), covering 2000-2005.
Once the approach has been validated the model will be used to evaluate the impacts of AIC on different climatic indicators, such as the diurnal temperature range and the total cloud cover.

References

ABCi: W. Hecq, S. Meyer, J. Van Mierlo, J. Matheys, C. Macharis, T. Festraets, J.P. van Ypersele, A. Ferrone, P. Marbaix, B. Matthews, Aviation and the Belgian Climate Policy: Integration Options and Impacts: Final report, phase I, Belgian Public Planning Service Science Policy Rue de la Science 8 - Wetenschapsstraat B-1000 Brussels 87p., 2008

Burkhardt, U., B. Kärcher, M. Ponater, K. Gierens, and A. Gettelman , Contrail cirrus supporting areas in model and observations, Geophys. Res. Lett., 35, L16808, doi:10.1029/2008GL034056, 2008

Eyers C., P. Norman, J. Middel, M. Plohr, S. Michot, and K. Atkinson, AERO2k Global Aviation Emissions Inventories for 2002 and 2025, 2004

Gettelman A., W. D. Collins, E. J. Fetzer, A. Eldering, F. Irion, W. P. B. Duffy, and G. Bala. Climatology of upper tropospheric relative humidity from the atmospheric infrared sounder and implications for climate. J.Climate, 19, 23, pp. 6104–6121, 2006

IPCC: J. E. Penner, D. H. Lister, D. J. Griggs, D. J. Dokken, and M. McFarland, editors, Aviation and the Global Atmosphere, Cambridge University Press, Cambridge, United Kingdom and New York, NY, USA, 1999

IPCC: S. Solomon, D. Qin, M. Manning, Z. Chen, M. Marquis, K. Averyt, M. Tignor, and H. Miller, editors, Climate Change 2007: The Physical Science Basis. Contribution of Working Group I to the Fourth Assessment Report of the Intergovernmental Panel on Climate Change, Cambridge University Press, Cambridge, United Kingdom and New York, NY, USA, 2007

Lewellen D. C. and W. S. Lewellen, The effects of aircraft wake dynamics on contrail development, Journal of the Atmospheric Sciences, 58(4), pp. 390–406, 2001

Lin, Y.-L., R. D. Rarley, and H. D. Orville, Bulk parameterization of the snow field in a cloud model. J. Appl. Meteor, 22, pp. 1065-1092, 1983

Meyer R., H. Mannstein, R. Meerkötter, P. and Wendling, Contrail and cirrus observations over Europe from 6 years of NOAAAVHRR data, EUMETSAT Meteorological Satellite Conference, edited by EUMETSAT, vol. EUM P 36, pp. 728–735, 2002

Schumann U., Influence of propulsion efficiency on contrail formation. Aerosp. Sci. Technol, 4(6), pp. 391–401, 2000

Will A., M. Baldauf, B.Rockel, A. Seifert, Physics and Dynamics of the COSMO-CLM, Meteorol. Z., submitted, 2008

Xu, K.-M., and D. A. Randall, 1996: A semiempirical cloudiness parameterization for use in climate models. J. Atmos. Sci., 53, pp. 3084-3102, 1996

Stratospheric variability and its impact on surface climate

Andreas Marc Fischer(1,2), Isla Simpson(3), Stefan Brönnimann(2), Eugene Rozanov(2,4), Martin Schraner(2)

(1) Federal Office of Meteorology and Climatology, MeteoSwiss, Kraehbuehlstr. 58, 8044 Zurich, Switzerland
(2) Institute for Atmospheric and Climate Science, ETH Zurich, 8092 Zurich, Switzerland. (andreas.fischer@env.ethz.ch)
(3) Department of Physics, Imperial College, London, UK
(2) PMOD/WRC, Dorfstrasse 33, 7260 Davos, Switzerland.

1. Introduction

The stratospheric layer plays a key role in communicating climate variability over vast regions of the Earth's atmosphere. Some of its variability is attributable to natural drivers such as variations in El Niño Southern Oscillation (ENSO), solar irradiance, or volcanic eruptions and is manifest on different timescales from days to seasons and even longer timescales. Through downward wave propagation, variability in the stratosphere can impact on tropospheric climate variability modes and hence surface climate on different spatial scales. One of the most prominent stratospheric influence are sudden stratospheric warmings (SSWs) leaving an imprint on weather at the ground even a few weeks later (*Baldwin and Dunkerton*, 2001).

Figure 1 shows the observed surface air temperature (SAT) and sea level pressure (SLP) response with respect to five major tropical volcanic eruptions and to ENSO since 1880. The volcanic signal in the first boreal winter months after the eruption is characterized by a cooling over the oceans and a warming over the northern extra-tropical land masses. Several dynamical feedback mechanisms including the propagation of planetary waves have been proposed to explain the pathway of climate anomalies originating from the stratosphere (see e.g., *Stenchikov et al.*, 2004).

Over recent years much attention has been drawn to the climatic effect of El Niño on the northern extra-tropical stratosphere and its manifestation on surface. While the surface climate response over the North Pacific and North American region is well known, the signal over the North Atlantic European sector (negative North Atlantic Oscillation accompanied by cold (mild) temperatures over Northern (Southern) Europe) is subject to a large variability among individual El Niño events which complicates its interpretation. *Ineson and Scaife* (2009) provided evidence for a global teleconnection pathway from the Pacific region to Europe via the stratosphere. They showed that, in presence of SSWs, the stratosphere plays an active role in the manifestation of the European regional climate pattern.

A better knowledge of the impact of stratospheric variability on regional surface climate is therefore highly relevant with respect to detection and attribution studies as well as improvements of seasonal prediction schemes.

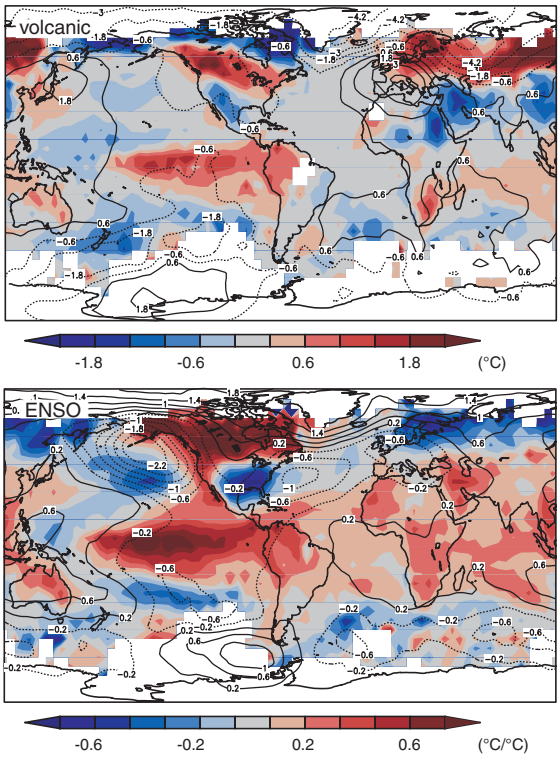

Figure 1. Effect of tropical volcanic eruptions (top) and ENSO (bottom) on boreal winter (Jan-Mar) SAT and SLP since 1880. Temperature and SLP data were detrended. The top panel shows a composite of the first winters after five tropical eruptions (Krakatoa, Santa Maria, Mt. Agung, El Chichón, Pinatubo). The bottom panel shows regression coefficients using a NINO3.4 index (Sep-Feb average) after removing two winters after each major volcanic eruption

2. Model Simulations

To study stratosphere-troposphere exchange processes global chemistry-climate models (CCMs) have proven to be indispensable tools as they incorporate all relevant dynamical, radiative, and chemical processes in the atmosphere (*Eyring et al.*, 2006).

Here we present results of two different kinds of simulations with the CCM SOCOL (*Schraner et al.*, 2008): (a) ensemble simulations (9 members) in transient mode across the 20th century (*Fischer et al.*, 2008a); (b) time-slice simulations (20 ensemble members) of an anomalously strong El Niño (1940-42) and a weak La Niña (1975-76) (*Fischer et al.*, 2008b). SOCOL is a combination of the middle atmosphere version of ECHAM4 (MPI, Hamburg) and the chemistry-transport model MEZON (PMOD/WRC, Davos). The simulations

were forced by sea surface temperature, sea ice distribution, volcanic aerosols, solar variability, greenhouse gases, ozone depleting substances, land surface changes, and the quasi-biennial oscillation. The model output was extensively validated against a number of observational and (prior to 1957) reconstructed datasets.

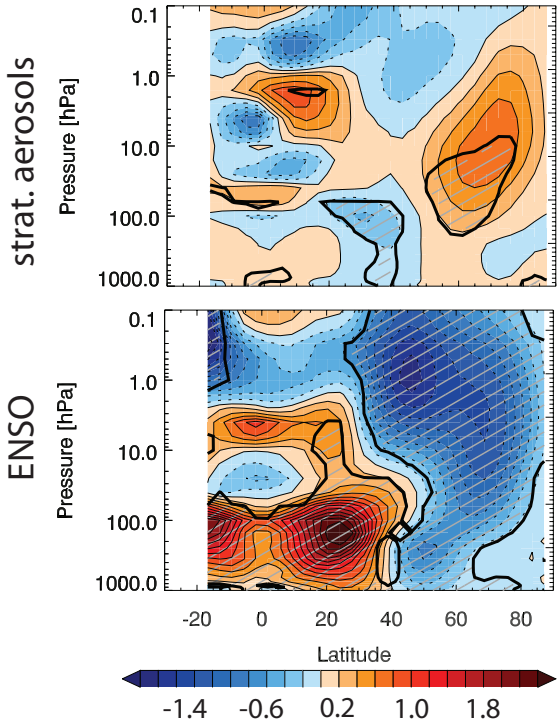

Figure 2. Regression coefficients (in m/s) of zonally averaged zonal wind in the winter northern hemisphere (JFM) upon stratospheric aerosols (upper panel) and ENSO (lower panel). Units of coefficients are with respect to one standard deviation of the explanatory variable. (Shaded areas mark statistical significance.)

3. Drivers of Variability

Figure 2 shows the winter northern hemispheric ensemble mean response in zonally averaged zonal wind upon variations of stratospheric aerosols and ENSO. Enhanced levels of stratospheric aerosols as observed after major volcanic eruptions lead to a significant strengthening of the polar vortex as a result of a stronger equator-to-pole temperature gradient and a reduction of the vertical planetary wave flux. On the contrary, zonal wind at polar latitudes during warm ENSO phases is characterized by reduced wind speeds with a signal penetrating well into the troposphere at mid-latitudes. In time-slice simulations the tropospheric ENSO signal was further analyzed and stratified according to the strength of the northern polar vortex in the stratosphere (above or below the ensemble mean). Preliminary results show that in the model this tropospheric signal is irrespective of the stratospheric response and surface pressure anomalies of El Niño minus La Niña do not show significant differences over large parts of the northern hemisphere between the two cases (see figure 3). Similar to figure 1 both composites reveal changes in surface pressure resembling a negative Arctic Oscillation mode.

In the presentation we will further compare the ENSO response looking particularly at the spatial manifestation and contrasting it to observations. Additionally, we will present the impact of variability drivers on circulation indices in the troposphere and the stratosphere for both models and observations/reconstructions.

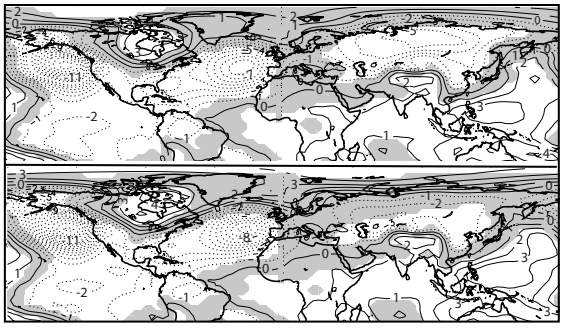

Figure 3. Surface pressure anomalies (in hPa) stratified according to the zonal wind response of the polar vortex averaged over 61N to 79N and 6 to 15 hPa. The upper (lower) panel shows averages of El Niño ensemble members with a wind response greater (smaller) than the mean. The ensemble mean of La Niña simulations is subtracted from both panels. (White areas mark statistical significance.)

References

Baldwin, M. P., and Dunkerton, T. J., Stratospheric harbingers of anomalous weather regimes, *Science*, 294, pp. 581-584, 2001.

Eyring, V., et al.: Assessment of temperature, trace species, and ozone in chemistry-climate model simulations of the recent past, *J. Geophys. Res.*, 111, D22308, doi:10.1029/2006JD007327, 2006.

Fischer, A. M., et al., Interannual-to-decadal variability of the stratosphere during the 20th century: ensemble simulations with a chemistry-climate model, *Atmos. Chem. Phys.*, 8, pp. 7755-7777, 2008a.

Fischer, A. M., Shindell, D. T., Winter, B., Bourqui, M. S., Faluvegi, G., Brönnimann, S., Schraner, M., and Rozanov, E., Stratospheric Winter Climate Response to ENSO in three Chemistry-Climate Models, *Geophys. Res. Lett.*, 35, L13819, doi:10.1029/2008GL034289, 2008b.

Ineson, S., and Scaife, A. A., The role of the stratosphere in the European climate response to El Niño, *Nature Geoscience*, 2, pp. 32-36, 2009.

Schraner, M., et al., Technical Note: Chemistry-climate model SOCOL: version 2.0 with improved transport and chemistry/microphysics schemes, *Atmos. Chem. Phys.*, 8, pp. 5957-5974, 2008.

Stenchikov, G., Hamilton, K., Robock, A., Ramaswamy, V., and Schwarzkopf, D., Arctic oscillation response to the 1991 Pinatubo eruption in the SKYHI general circulation model with a realistic quasi-biennial oscillation, *J. Geophys. Res.*, 109, D03112, doi:10.1029/2003JD003699, 2004.

Effects of numerical methods on high resolution modelling

Holger Göttel

Max Planck Institute for Meteorology, Bundesstr. 53, 20146 Hamburg, Germany, holger.goettel@zmaw.de

1. Introduction

One of the remaining challenges in climate predictions as well as in weather forecasts is the correct modelling of heavy precipitation. The reason is the high temporal and spatial variability of cloud formation and precipitation. Models with a resolution of several kilometres (50 to 10 km in regional climate models) are not able to resolve small scale features like convective clouds explicitly. To account for these features they use convective parameterisations which are normally only based on few observations. It is unclear that these parameterisations are still valid under climate change conditions and for all current convection types due to the limits of observations.

One solution is to increase the horizontal resolution to few kilometres where the model is able to resolve convective clouds explicitly. The increased computer power in the last decade allows an increase of resolution from 50 to 10 kilometres. A further increase of resolution, which might be possible in the near future, has consequences for some simplifications in state of the art climate models. These approximations (e.g. the hydrostatic balance and the neglect of advection of precipitation) are not realistic at these scales.

With the regional climate model REMO – a hydrostatic model which was extended with an evolutionary approach (Janjic et al., 2001) to a non-hydrostatic model – the limits of the Tiedtke scheme for convective systems in cold-air-outbreaks and the ability of the non-hydrostatic model to simulate such extreme events are investigated.

2. REMO

The regional climate model REMO (Jacob, 2001; Jacob et al., 2001; Jacob and Podzun, 1997) is a three-dimensional, hydrostatic atmospheric circulation model which solves the discretised primitive equations of atmospheric motion. Like most other RCMs, REMO has been developed starting from an existing numerical weather prediction (NWP) model: the Europa-Modell (EM) of the German Weather Service DWD (Majewski, 1991). Additionally, the physical parameterisation package of the general circulation model ECHAM4 (Roeckner et al., 1996) has been implemented, optionally replacing the original EM physics. In numerous studies, the latter combination (i.e., the EM dynamical core plus the ECHAM4 physical parameterisation scheme) proved its ability to realistically reproduce regional climatic features and is therefore used as the standard setup in recent applications, including the present study.

This hydrostatic model was extended in this study to a non-hydrostatic model using the evolutionary approach proposed by Janjic et al. (2001). Additionally, a diagnostic advection scheme for precipitation is implemented which can be used online and offline (Göttel, 2009).

3. Results

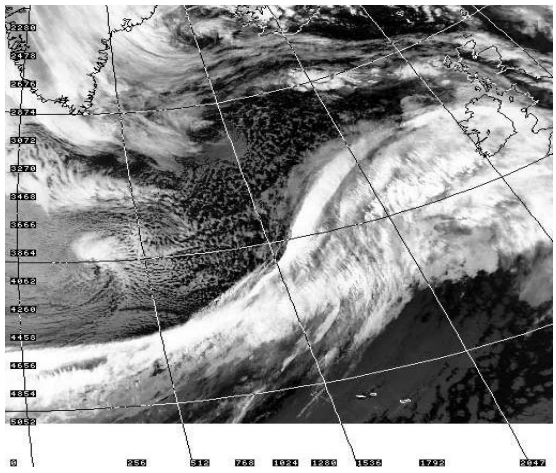

Figure 1. AVHRR channel 5 retrieval from 17 February 1997

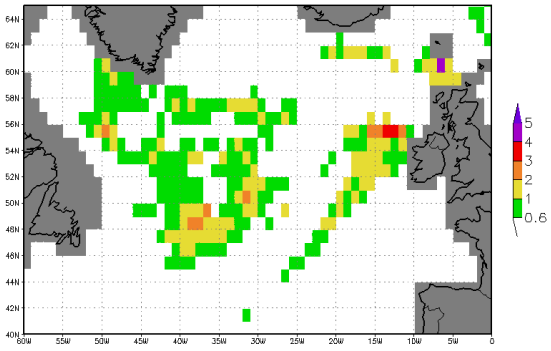

Figure 2. HOAPS estimated precipitation fluxes [mm/h] valid for 9:00 UTC 17 February 1997

The AVHHR (Figure 1.) show clouds in the postfrontal area due to a cold air outbreak over the open ocean. The cold air outbreak induces convection with intense precipitation. The precipitation estimates of HOAPS (Figure 2.) reaches in the postfrontal area precipitation similar values like in the cold front of the low “Caroline”. This precipitation which is validated by ship observations doesn’t appear in the ECMWF model as well as in the regional model REMO (Figure 3.). The missing precipitation in the models is caused by deficits in the cloud convection scheme. A re-calculation of this event with the non-hydrostatic version of REMO shows, that this model is able to reproduce postfrontal precipitation (Figure 4.).

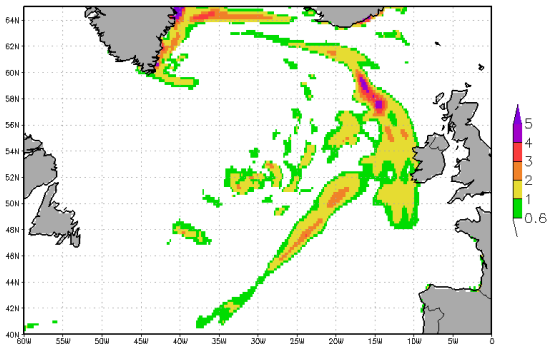

Figure 3. REMO: precipitation [mm/h] valid for 9:00 UTC 17. February 1997

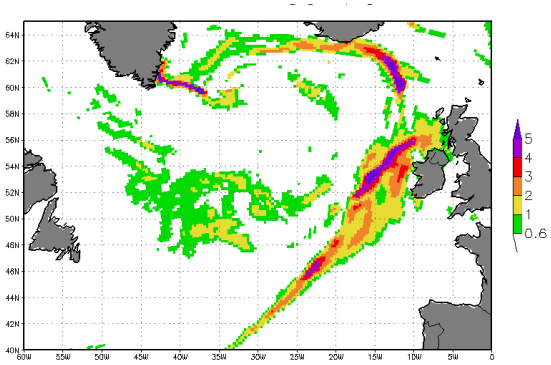

Figure 4. REMO (non-hydrostatic): precipitation [mm/h] valid for 9:00 UTC 17. February 1997

Acknowledgements

This work has been supported by the German Science Foundation (2004-2009) within the Program: Collaborative Research Centre 512 - Cyclones and the North Atlantic Climate.

References

Göttel, H. (2009): Einfluss der nichthydrostatischen Modellierung und der Niederschlagsverdriftung auf die Ergebnisse regionaler Klimamodellierung, Dissertation, University of Hamburg

Jacob, D. und R. Podzun (1997): Sensitivity studies with the regional climate model REMO, Meteorological Atmospheric Physics, 63, 119-129.

Jacob, D. (2001): A note to the simulation of the annual and inter-annual variability of the water budget over the Baltic Sea drainage basin, Meteorological Atmospheric Physics, 77, 61-73.

Jacob, D., B. van den Hurk, U. Andræ, G. Elgered, C. Fortelius, L.P. Graham, S.D. Jackson, U. Karstens, C. Koepken, R. Lindau, R. Podzun, B. Roeckel, F. Rubel, B.H. Sass, R.N.B. Smith, X. Yang (2001) : A comprehensive model intercomparison study investigating the water budget during the BALTEX PIDCAP period, Meteorological Atmospheric Physics, 77, 19-43.

Janjic, Z. I., Geritty JR., J. P., and Nickovic, S. (2001) An Alternative Approach to Nonhydrostatic Modeling. Monthly Weather Review, 129, 1164-1178.

Majewski, D. (1991): The Europa-Modell of the Deutscher Wetterdienst. ECMWF Seminar on Numerical Methods in Atmospheric Models, 2, 147-191.

Roeckner, E., K. Arpe, L. Bengtsson, M. Christoph, M. Claussen, L. Duemenil, M. Esch, M. Giorgetta, U. Schlese, U. Schulzweida (1996): The atmospheric general circulation model ECHAM4: Model description and simulation of present-day climate, Report Nr. 218, Max-Planck-Institut für Meteorologie, Hamburg

Development of a climate model with dynamic grid stretching

William Gutowski[1], Babatunde Abiodun[2], Joseph Prusa[3] and Piotr Smolarkiewicz[4]

[1]Iowa State University, Ames, Iowa, USA (gutowski@iastate.edu), [2]University of Cape Town, Cape Town, South Africa, [3]Teraflux Corp., Boca Raton, Florida, USA, [4]NCAR, Boulder, Colorado, USA.

1. Introduction

Regional features of climate can potentially affect much larger scales. Exploring such upscaling requires a model that can resolve regional behavior for a targeted location while covering the globe. One approach is through grid stretching applied to a global climate model. We describe here a fully operational atmospheric GCM that can employ static or dynamic grid stretching.

Our focus is on continuous grid deformation methods that offer local enhancements of resolution where it is most desired. To date, we have developed a generalized-coordinate model that enables continuous dynamic grid adaptation in the non-oscillatory, forward-in-time dynamics model EULAG developed by Smolarkiewicz and colleagues [see *Prusa et al.* (2008) for a review], while concurrently producing a global, adaptive-grid atmospheric climate model.

We present here a brief description of the model, results of simulations using standard tests, and an application that yields understanding dynamic processes affecting tropical convection and circulation.

2. CAM-EULAG

EULAG is an established parallel computational model for simulating thermo-fluid flows over a wide range of scales and physical scenarios (*Prusa et al.* 2007). It is noteworthy for its non–oscillatory forward-in-time (NFT) integration algorithms (*Smolarkiewicz* 2006), robust elliptic solver (*Smolarkiewicz* et al. 2004), and generalized coordinate formulation enabling grid adaptivity (*Prusa and Smolarkiewicz* 2003; *Smolarkiewicz and Prusa* 2005). The underlying analytic formulation of EULAG used in this study assumes the non-hydrostatic, deep moist-anelastic equations of motion of *Lipps and Hemler* (1982). We have tested the code as a potential dynamics core in a global model, using tests described by *Jablonowski and Williamson* (2006).

The stretched-grid model couples EULAG to the physics package of the NCAR Community Atmospheric Model, Version 3 (CAM3) (*Abiodun et al.* 2008a). We have tested the model as a dynamics core in CAM-EULAG. We also have exploited the coupled model's grid-stretching to explore dynamical influences on tropical convection (*Abiodun et al.* 2008b).

3. Baroclinic wave test

Jablonowski and Williamson (2006) have formulated a short-term (several day) test of dynamics cores that involves simulating a growing and decaying baroclinic wave and its scale interactions. We have conducted this test after formulating the boundary conditions appropriately for our model's coordinate system.

The test consists of a steady flow that is perturbed. From the perturbation emerges a growing baroclinic wave. In our testing without a perturbation, the flow remains steady for 20 days (the duration of the simulation). The L^2 norm for (u-u_e), where u_e is a specified initial zonal wind and u is the instantaneous local zonal wind, is at 10^{-3} at 20 days, and is below 10^{-5} for the first 12.5 days. In comparison, the best result in *Jablonowski and Williamson* (2006) shows an L^2 norm of $\sim 10^{-2}$ (Eulerian result in their Fig. 4). When perturbed, a wave emerges that grows ~ exponentially from 3 to 9 days. The resulting surface pressure fields during this period of exponential growth compare well to those in *Jablonowski and Williamson* (Fig.1).

4. Aqua-planet simulation

We have performed aqua-planet simulations to test the performance of CAM-EULAG with full physics turned on and to exercise its grid stretching. Several-month simulation with uniform grid shows spectral energetics that decay with increasing wave number without showing excessive energy near the truncation limit, even though the dynamics core uses no explicit diffusion. The model's NFT numerics are capable of controlling the spectral flow of energy near the truncation limit (Fig. 2).

In further simulation we have used grid stretching to resolve selectively smaller and smaller scales in the tropics in aqua-planet simulation (*Abioudun et al.* 2008b). The degree to which equatorial Rossby waves are resolved affects the character of tropical convection. At low resolution, the model's Hadley cell produces a single maximum in its latitudinal distribution of tropical precipitation. As equatorial Rossby waves become better resolved using higher tropical resolution, they change the pattern of tropical moisture convergence and produce a double maximum (Fig. 3). In contrast, increasing extratropical resolution increases the magnitude of tropical precipitation, through stronger dynamic forcing of the Hadley cell, but the precipitation retains a single maximum (not shown).

5. Conclusion

We have produced a dynamics core using advanced numerics that can increase resolution either statically or dynamically through grid stretching at select locations. The code performs well in tests often used for dynamics cores. Further applications planned include tracking select features with higher resolution, such as the evolution of tropical storms and mesoscale convective systems. We will give a demonstration of the model's dynamic stretching at the workshop.

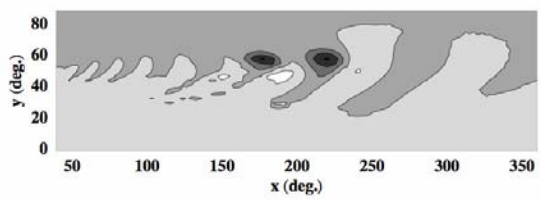

Figure 1. Surface pressure field at 9 days in the baroclinic wave test simulation (2.82° x 2.82°). Contour interval is 10 mb.

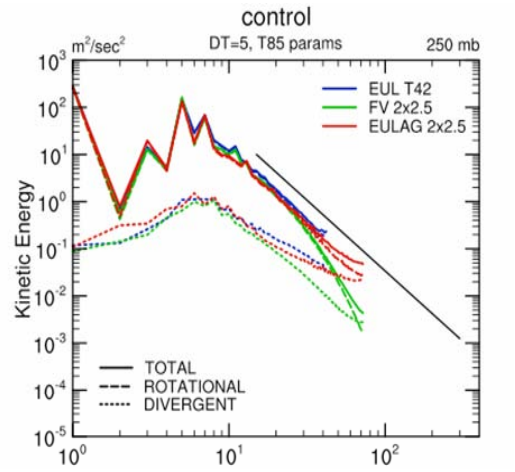

Figure 2. Energy spectra of CAM-EULAG in aqua-planet simulation compared with spectra from CAM simulations using either Eulerian spectral or finite volume dynamics cores.

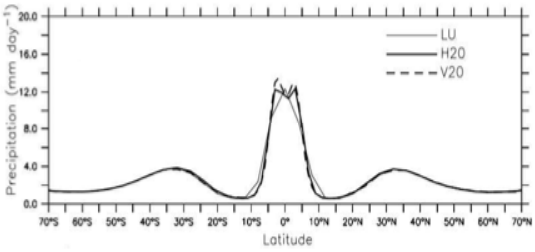

Figure 3. Time and zonal average precipitation vs. latitude for a uniform low-resolution case [LU - 4˚(lat)], a case with high resolution for (20S-20N) [H20 – 2˚(lat)] and a case with very high resolution for (20S-20N) [V20 – 1˚(lat)]. Resolution outside the tropics is 4˚(lat) in all cases.

References

Abiodun, B.J., J.M. Prusa and W.J. Gutowski, Implementation of a Non-hydrostatic, Adaptive-Grid Dynamics Core in CAM3. Part I: Comparison of Dynamics Cores in Aqua-Planet Simulations. *Clim. Dynamics,* **31,** 795-810 [DOI: 10.1007/s00382-008-0381-y], 2008a.

Abiodun, B.J., W.J. Gutowski and J.M. Prusa, Implementation of a Non-hydrostatic, Adaptive-Grid Dynamics Core in CAM3. Part II: Dynamical Influences on ITCZ Behavior and Tropical Precipitation. *Clim. Dynamics,* **31,** 811-822 [DOI: 10.1007/s00382-008-0382-x], 2008b.

Jablonowski ,C., and D.L. Williamson, A baroclinic instability test case for atmospheric model dynamical cores, *Quart. J. Roy. Meteor. Soc.,* **132,** 2943-2975, 2006.

Lipps, F.B., and R.S. Hemler, A scale analysis of deep moist convection and some related numerical calculations. *J Atmos Sci,* **39,** 2192–2210, 1982.

Prusa, J.M., P.K. Smolarkiewicz, An all–scale anelastic model for geophysical flows: dynamic grid deformation. *J Comput Phys,* **190,** 601–622, 2003.

Prusa, J.M., P.K. Smolarkiewicz, A.A. Wyszogrodzki, EULAG, a computational model for multiscale flows. *Comp. & Fluids* [doi:10.1016/j.compfluid.2007.12.001], 2008.

Smolarkiewicz P.K., Multidimensional positive definite advection transport algorithm: an overview, *Int. J. Numer. Meth. Fluids,* **50,** 1123-1144, 2006.

Smolarkiewicz P.K., Temperton, C., Thomas, S.J. and Wyszogrodzki,A.A., Spectral Preconditioners for nonhydrostatic atmospheric models: extreme applications. *Proceedings of the ECMWF Seminar Series on Recent developments in numerical methods for atmospheric and ocean modelling*, 6-10 September 2004, Reading, UK, 203-220, 2004.

Smolarkiewicz, P.K., and J.M. Prusa, Toward mesh adaptivity for geophysical turbulence: continuous mapping approach. *Int J Num Meth Fluids,* **47,** 789-801, 2005.

Study of the capability of the RegCM3 in simulation of precipitation and temperature over the Khorasan Razavi province, case study: Winters of 1991-2000

Maryam Karimian1,2, Iman Babaeian1,3, Rahele Modirian1,2

1-Climate Change Lab. Climatological Research Institute, Mashad, I.R. of Iran, P.O. Box: 91735-676
2-MSc Student of Physics, Islamic Azad University of Mashhad
3-PhD Student of Climatology, Tabriz University

Ability and skill of the nesting version of the RegCM3 Regional Climate Model in simulation of monthly and seasonal amount of precipitation and temperature by using four different cumulus parameterization of Grell-AS, Grell-FC, Emanuel and Kuo have been studied over khorasan area including three provinces of North Khorasan, Khorasan Razavi and South Khorasan. In this regards, 40 control runs by using NNRP1 reanalysis data have been done for winter seasons of 1991-2000 over the area under study. Errors of the modeled data computed by comparing with CMAP precipitation data, NCEP temperature data and observed data of 15 synoptic weathers stations that located inside the study area. Bias and mean absolute errors were calculated monthly and seasonally. Results show that among four parameterizations methods used in this research, monthly and seasonal bias of the Grell-FC and Grell-AS with amount of +2.1 and -1mm is lower than other parameterizations scheme. Smallest bias of monthly and seasonal temperature have been found in Emanuel parameterization by amount of -0.8˚C and +0.7˚C, respectively. Results of this research can be used in development of regional climate models for issuing seasonal forecast over Northeast of Iran.

Keywords: RegCM3, regional climate modeling, cloud parameterizations, calibration, khorasan, winter.

Simulating aerosol effects on the dynamics and microphysics of precipitation systems with spectral bin and bulk parameterization schemes

L. Ruby Leung[1], Alexander P. Khain[2], and Barry Lynn[2]

[1]Pacific Northwest National Laboratory, Richland, WA, USA; Email: Ruby.Leung@pnl.gov
[2]The Hebrew University of Jerusalem, Israel

1. Introduction

An increase in atmospheric aerosol particles serving as cloud condensation nuclei (CCN) can increase the concentration and reduce the size of cloud droplets. Although the relationship between aerosol concentrations and cloud drop size is relatively well established through observations and modeling, the effects of aerosols on precipitation are less well understood because aerosols can influence both the microphysical and dynamical structure of clouds. Despite the importance of evaluating how air pollution may potentially influence the global and regional hydrologic cycle, to date, simulating the effects of aerosols on precipitation remains a challenge, as simulation results and observations often diverge in their quantification of aerosol effects on precipitation. This study compares two microphysical schemes and their quantification of aerosol effects on precipitation in different cloud systems including the squall line and orographic clouds.

2. Results

A new spectral bin microphysical scheme (SBM) was implemented into the Weather Research and Forecasting (WRF) (Skamarock et al. 2005) model (referred to as Fast-SBM), which uses a smaller number of size distribution functions than the previous (standard) version of SBM (referred to as Exact-SBM). The Exact-SBM scheme has been described by Khain et al (2004) and Lynn et al (2007). The scheme is based on solving the kinetic equation system for size distributions of seven types of hydrometeors: water drops, three types of crystals (columnar-, plate- and branch-type), aggregates (snow), graupel and hail. Each hydrometeor type is described by a size distribution function defined on the grid of mass (size) containing 33 mass bins.

The WRF model was applied to a 2D domain to simulate the structure of a squall line. It was shown that both the Fast SBM and Exact SBM reproduced the typical structure of an idealized squall line quite realistically. The schemes simulated similar dynamical and microphysical structures, and there was excellent agreement in the simulated precipitation amounts between the schemes under a very wide range of aerosol conditions in which initial condensation nuclei concentration varied from 100 cm^{-3} to 3000 cm^{-3}. Moreover, the Fast-SBM uses about 40% of the computing power of the exact-SBM, allowing it to be used for "real-time" simulations over limited domains.

The results of SBM simulations have been compared with a modified version of the Thompson bulk parameterization scheme within the same dynamical framework (2D WRF). The bulk scheme has been extended to simulate the process of drop nucleation, so that drop concentration is no longer prescribed a priori, but rather calculated depending on the prescribed aerosol concentration. This scheme is referred to as DROP scheme. A large set of sensitivity studies have been performed, in which the sensitivity of results (microphysical parameters and precipitation) to aerosol concentration, droplet nucleation above cloud base, etc. has been compared with the results from the SBM.

Comparison of the results from the DROP scheme and SBM scheme shows that the SBM scheme produces more realistic dynamical and microphysical structure of the squall line. The addition of the DROP scheme did relatively little to change the underlying results of the bulk scheme, and unlike the SBM simulations, that show different precipitation sensitivities to aerosol concentrations in relatively clean and polluted environments, the drop scheme simulates large monotonic decrease in precipitation with increasing aerosol concentrations.

Both the SBM and DROP schemes are being applied to simulate orographic clouds to further elucidate the effects of aerosols on orographic precipitation. Both 2D and 3D simulations are being performed and compared with observations collected during the SUPRECIP field experiment (Rosenfeld et al. 2008) in northern California.

References

Khain A., A. Pokrovsky and M. Pinsky, A. Seifert, and V. Phillips, 2004: Effects of atmospheric aerosols on deep convective clouds as seen from simulations using a spectral microphysics mixed-phase cumulus cloud model Part 1: Model description. *J. Atmos. Sci., 61, 2963-2982.*

Lynn B., A. Khain, D. Rosenfeld, William L. Woodley, 2007: Effects of aerosols on precipitation from orographic clouds. *J. Geophys. Res.,* 112, D10225, doi:10.1029/2006JD007537.

Rosenfeld, D., W.L. Woodley, D. Axisa, E. Freud, J.G. Hudson, A. Givati, 2008: Aircraft measurements of the impacts of pollution aerosols on clouds and precipitation over the Sierra Nevada. J. Geophys. Res., 113, D15203, doi:10.1029/2007JD009544

Skamarock, W.C., Klemp J.B., Dudhia, J., Gill D.O., Barker D.M., Wang W., and Powers J.G., 2005: A description of the Advanced Research WRF Version 2. NCAR Tech Notes-468+STR.

Evaluation of the land surface scheme HTESSEL with satellite derived surface energy fluxes at the seasonal time scale.

Erik van Meijgaard[1], Louise Wipfler[2], Bart van den Hurk[1], Klaas Metselaar[2], Jos van Dam[2], Reinder Feddes[2], Bert van Ulft[1], Sander Zwart[3], and Wim Bastiaanssen[3]

[1]Royal Netherlands Meteorological Institute, PO Box 201, NL-3730 AE De Bilt, The Netherlands; vanmeijg@knmi.nl
[2]Soil Physics, Ecohydrology and Groundwater Management Group, Wageningen University, The Netherlands
[3]WaterWatch, Wageningen, The Netherlands

1. Introduction

A problem often reported in numerical regional climate studies is a systematic summer drying that results in too dry and too warm simulations of summertime climate in southeastern Europe (*Hagemann et al.* 2004). This summer drying is associated with a strong reduction of the hydrological cycle, dry soils, strong evaporation stress and reduced precipitation. Precipitation and evaporation are coupled processes, but these models often overemphasize the positive feedback. Presumably, land surface processes play an important role in this feedback, and their representation may be subject to improvement.

Lenderink et al. (2003) pragmatically reduced a summer continental dry bias in the KNMI regional climate model RACMO2 by enhancing the soil reservoir depth in the land surface scheme (LSS). Yet, it is unclear how realistic this solution is, and whether it is still valid when extrapolating to changing climate conditions.

Here we evaluate the LSS HTESSEL and modifications therein with satellite inferred evaporation estimates during a single growing season. Focus is on the Transdanubian region in Hungary, a region that was found particularly sensitive to summer drying in previous integrations with RACMO2. The modifications that are examined relate to soil water issues, i.e. water storage capacity, water stress in vegetation covered soils, and water supply from groundwater. In the evaluation, we focus on the model ability to reproduce the range of evaporative responses seen in the observations. Details can be found in *Wipfler et al*. (in prep).

2. HTESSEL reference version

In the LSS TESSEL (Tiled ECMWF Scheme for Surface Exchange over Land; *van den Hurk et al.,* 2000) and its successor Hydrology-TESSEL, introduced in ECMWF IFS cy33r1 (*Balsamo et al*. 2009), the tiled land surface in each atmospheric model grid cell is partitioned between bare soil, low and high vegetation, intercepted water, shaded and exposed snow deck. For each tile a separate surface energy balance is calculated. Total fluxes are calculated as area weighted averages over the tiles. The soil heat flux G serves as upper boundary condition to a 4-layer vertical column with fixed depth (2.89m) using a standard diffusion scheme. Sensible (H) and latent heat (LE) fluxes from each tile are calculated applying a commonly used resistance analogy. Of relevance to this study is the sensitivity of evaporation to soil moisture content which strongly affects the seasonal evolution of evaporation in water-constrained conditions. This is controlled by the so called water stress function

$$f_2^{-1} = (\theta - \theta_{pwp})/(\theta_{cap} - \theta_{pwp})$$

with θ denoting the actual root density weighted column average soil water content, while θ_{pwp} and θ_{cap} are soil moisture content at permanent wilting point and field capacity (in units m^3/m^3).

The hydrology of a snow free land grid cell is depicted in Figure 1. Precipitation accumulates in the interception reservoir until it is saturated. Excess precipitation is partitioned between surface runoff and infiltration into the soil column. Soil water flow is described by the diffusivity form of the Richard' equation using the same 4-layer mesh as for soil temperature. The hydraulic conductivity and diffusivity are described with the analytical functions proposed by van Genuchten. Free drainage is assumed at the bottom of the soil column. Excess water leaves the domain as surface or subsurface runoff. Capillary rise of groundwater is not considered, nor is horizontal exchange of soil water.

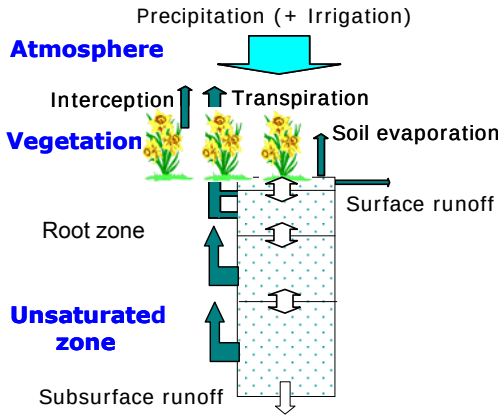

Figure 1. Schematic representation of the water component of the (H)TESSEL land-surface scheme.

3. Modifications to HTESSEL

A parameter analysis with a detailed soil-water-atmosphere model showed that the evaporative responses of HTESSEL to a controlled forcing are particular sensitive to i) the characteristics of the water stress function, ii) soil column depth, and iii) the treatment of the lower boundary condition. In addition it was indicated that a finer mesh of the soil column yields improved convergence. Based on these findings we have investigated the following modifications:

i) formulation of the water stress function f_2 in terms of the more commonly used soil water pressure head:

$$\tilde{f}_2^{-1} = (\psi - \psi_{pwp})/(\psi_{cap} - \psi_{pwp})$$

with ψ_{pwp} and ψ_{cap} set to -15 and -0.1 bar.

ii) introduction of additional spatially variable soil depths classes with shallower depths to account for rocky material in the soil. In the region of interest about 30% of the area is found to have a soil depth of 1 meter or less.

iii) inclusion of extra water storage to represent the presence of a shallow ground water table. This acts as an additional supply of moisture. In the region of interest about 40% of the area is potentially affected by a shallow water table.

In addition, the number of soil layers was doubled to 8.

4. Evaporation estimates from SEBAL

Maps of evaporation have been derived by application of the energy-partitioning algorithm SEBAL (Surface Energy Balance Algorithms for Land, *Bastiaanssen et al.* 1998) on the basis of MODIS images. Information at pixel scale (1km) is aggregated to 0.25° to match the typical RCM resolution. The temporal resolution is about one week, primarily determined by the occurrence of cloud free scenes. Figure 2 shows the SEBAL inferred evaporative fraction averaged over the growing season of 2005. The accuracy of the evaporation estimates is 3-5% on a seasonal basis.

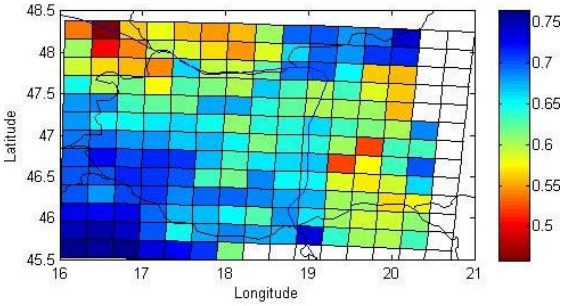

Figure 2. SEBAL inferred evaporative fraction across Hungary for the growing season of 2005

5. Experimental setup

HTESSEL standalone versions are set up across the domain of interest and forced with 3-hourly fluxes of precipitation, incoming radiation and near surface meteorological fields from a RACMO2@25km hindcast run driven by ECMWF operational analyses. Weekly total amounts of precipitation and incoming short wave radiation are scaled with the observed amounts used to constrain the SEBAL algorithm, for consistency. Incoming radiation has been calibrated with in-situ measurements, while precipitation amounts have been inferred from TRMM estimates.

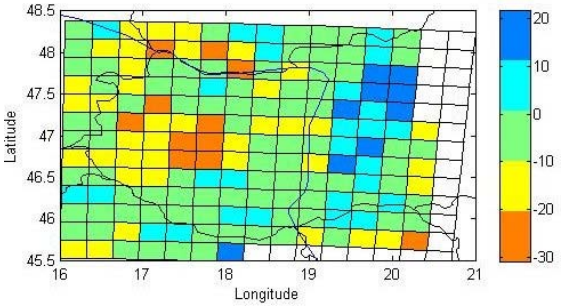

Figure 3. Relative difference in seasonal evaporative fraction between HTESSEL and SEBAL.

6. Results and Conclusions

The difference in seasonal evaporative fraction between HTESSEL and SEBAL is shown in Fig.3. The areas with underprediction are found to match reasonably well with areas where P-E accumulated over the season is negative. It is yet unknown whether this points to a model inadequacy or to a problem with irrigation as a missing source term. Figure 4 shows a scatter plot of ranked evaporative fraction obtained from integrations with HTESSEL (reference and modified versions) against ranked SEBAL evaporative fraction. The reference version follows the SEBAL range of variability reasonably well, but with a tendency of underestimating the low amounts. Modifying the water stress clearly results in increased seasonal evaporative fractions, especially in the higher end of the distribution. Shallower soil depths produce lower values of evaporative fraction, in particular in the central part of the distribution. Inclusion of capillary rise from a shallow ground water table shows little impact. The combination of all three modifications yields a marginally improved result in the lower part of the distribution (fraction smaller than 0.60), but in the higher end the combined result is strongly dominated by the modification in water stress.

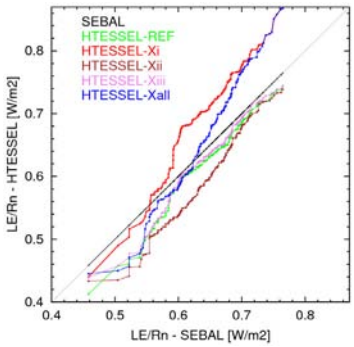

Figure 4. Ranked evaporative fraction from HTESSEL compared to SEBAL

7. Outlook

HTESSEL has been implemented in RACMO2. Integrations of the present-day European climate are ongoing The evaluation assessment will focus on the seasonal cycle and interannual variability of land surface feedbacks

Acknowledgements: This work was carried out within the programme Climate changes Spatial Planning.

References

Bastiaanssen, W.G.M., M. Menenti, R.A. Feddes and A.A.M. Holtslag: The Surface Energy Balance for Land (SEBAL): Part 1 formulation, *J. Hydrology*, 212-213, 198-212, 1998

Balsamo, G., P. Viterbo, A. Beljaars, B. van den Hurk, M. Hirschi, A.K. Betts and K. Scipal, A revised hydrology for the ECMWF model: Verification from field site to terrestial water storage and impact in the ECMWF-IFS, Tech. Memo. 563, 28 pages, 2008.

Hagemann, S., B. Machenhauer, R. Jones, O.B. Christensen, M. Déqué, D. Jacob and P.L Vidale, Evaluation of water and energy budgets in regional climate models applied over Europe. *Climate Dynamics*, 23, pp. 547-567, 2004

Lenderink, G, B. van den Hurk, E. van Meijgaard, A. van Ulden, and H. Cuijpers: Simulation of present-day climate in RACMO2: First results and model developments, KNMI Tech. Report 252, pp. 24, 2003.

Van den Hurk, B.J.J.M., P. Viterbo, A.C.M. Beljaars and A.K. Betts: Offline validation of the ERA-40 surface scheme; ECMWF Tech. Memo. 295, 2000.

Wipfler, E.L, K. Metselaar, J. C. van Dam, R A. Feddes, E. van Meijgaard, L.H.. van Ulft, B. van den Hurk, S. J. Zwart and W.G.M. Bastiaanssen, Seasonal evaluation of the ECMWF land surface scheme against remote sensing derived energy fluxes of the Transdanubian region in Hungary, *in preparation*

Simulation of the precipitation and temperature over the Khorasan province using RegCM3, case study: Autumns 1991-2000

Rahele Modirian 1,2, Iman Babaeian1,3, Maryam Karimian 1,2

1-Climate change lab, Climatological Research Institute, Mashad, I.R. of Iran, P.O. Box: 91735-676
2-MSc Student of Physics, Islamic Azad University of Mashhad
3-PhD Student of Climatology, Tabriz University

A ten years Climate of khorasan during 19991-2000 has been modeled regarding to the role of autumn precipitation in providing water resource and role of precipitation and temperature for water requirement over khorasan and for calibration of the RegCM3 as a Research and Seasonal Predictions tool. In this research RegCM3 with 15 km horizontal resolution and four different conversion parameterizations of Grell-FC, Grell-AS, Kuo and Emanuel has been used. Modeled precipitations have been compared by both observed and CMAP data and modeled temperatures have been compared by observed and NCEP reanalysis data. Minimum monthly and seasonal bias are found in Kue parameterization scheme by -0.9 and -7.1 mm, respectively and minimum mean absolute errors are found in Grell-FC scheme by 19.3 and 21.3 mm. Comparing the modeled temperature shows that the minimum monthly and seasonal biases are found in Grell-FC scheme by -1.1 mm. Results of this paper can be used in operational seasonal predictions and research porposes as well.

Key Words: Climate Modeling, RegCM3, Precipitation, temperature, autumn, khorasan

Diffusion impact on atmospheric moisture transport

Ch. Moseley[1], J. Haerter[1], H. Göttel[1], G. Zängl[2], S. Hagemann[1] and D. Jacob[1]

[1] Max Planck Institute for Meteorology, Hamburg, Germany (christopher.moseley@zmaw.de)
[2] German Weather Service, Offenbach, Germany

1. Numerical diffusion on height levels

To ensure numerical stability, many global and regional climate models employ numerical diffusion to dampen short wavelength modes. Terrain following sigma diffusion is known to cause unphysical effects near the surface in orographically structured regions. They can be reduced by applying z-diffusion on geopotential height levels (*Zängl* (2005), Figure 1). We investigate the effect of the diffusion scheme on atmospheric moisture transport and precipitation formation at different resolutions in the European region. For our study, we perform a sequence of simulations of the regional climate model REMO over Europe, and compare the standard sigma diffusion simulation with z-diffusion results. For these simulations, REMO was forced at the lateral boundaries with ERA40 reanalysis data for a five year period. For our higher resolution simulations we employ a double nesting technique.

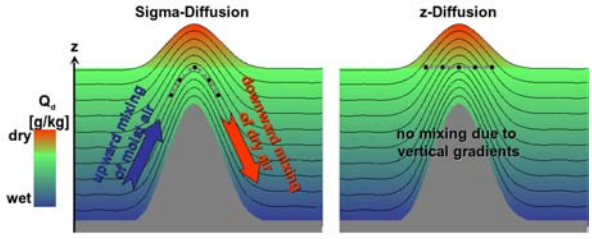

Figure 1: Diffusion on z-levels reduces unphysical mixing on vertical orographic gradients.

2. Study regions

With respect to a better understanding of diffusion in current and future grid-space global models, current day regional models may serve as the appropriate tool for studies of the impact of diffusion schemes: Results can easily be constrained to a small test region and checked against reliable observations, which often are unavailable on a global scale. Special attention is drawn to the Alps - a region of strong topographic gradients and good observational coverage. Our study is further motivated by the appearance of the "summer drying problem" in South Eastern Europe. This too warm and too dry simulation of climate is common to many regional climate models and also to some global climate models, and remains a permanent unsolved problem in the community (*Hagemann et al.* (2004), Figure 2). We perform a systematic comparison of the two diffusion-schemes with respect to the hydrological cycle. In particular, we investigate how local meteorological quantities - such as the atmospheric moisture in the region east of the Alps - depend on the spatial model resolution. Higher model resolution leads to a more accurate representation of the topography.

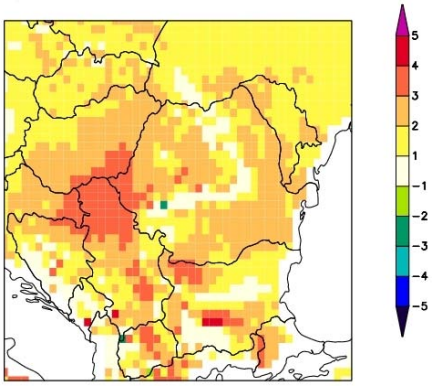

Figure 2: The "summer drying problem": Temperature bias (°C) of ERA40 driven REMO simulation with gridded dataset provided from EU-ENSEMBLES project (*Haylock et al.* (2007)): Mean over summer season for years 1960-1979.

References

Zängl, G., An Improved Method for Computing Horizontal Diffusion in a Sigma-Coordinate Model and Its Application to Simulations over Mountainous Topography, *Monthly Weather Review,* 130, pp. 1423-1432, 2002

Hagemann, S., B. Machenhauer, R. Jones, O.B. Christensen, M. Deque, D. Jacob, P.L. Vidale, Evaluation of water and energy budgets in regional climate models applied over Europe, *Clim. Dyn.*, 113, , 2004

Haylock, M.R., N. Hofstra, A.M.G. Klein Tank, E.J. Klok, P.D. Jones, M. New, A European daily high-resolution gridded dataset of surface temperature and precipitation, *J. Geophys. Res.*, 113, D20119, doi:10.1029/2008JD010201, 2008

Climate simulations over North America with the Canadian Regional Climate Model (CRCM): From operational Version 4 to developmental Version 5.

Dominique Paquin[1], René Laprise[2,4,5], Katja Winger[2,4], Ramon de Elía[1,4,5], Ayrton Zadra[3,4,5] and Bernard Dugas[3,4,5]

[1]Consortium Ouranos, Montréal (Québec), Canada, paquin.dominique@ouranos.ca; [2]Université du Québec à Montréal (UQÀM), Montréal (Québec), Canada; [3]Meteorological Service of Canada, Montréal (Québec), Canada; [4]Canadian Network for Regional Climate Modelling and Diagnostics (CRCMD), Montréal (Québec), Canada; [5]Centre pour l'Étude et la Simulation du Climat à l'Échelle Régionale (ESCER), Montréal (Québec), Canada

1. Farewell to old model, what about the new one

Developed in the early nineties at UQÀM, the Canadian Regional Climate Model (CRCM) has been based on the coupling of the semi-Lagangian and semi-implicit dynamical core of MC2 (Mesoscale Compressible Community Model, *Laprise et al*. 1997) with an ensemble of parameterizations describing physical processes. The original physical processes formulation followed the second-generation Canadian GCM, AGCM2 and was later updated to the AGCM3 (*Scinocca et al.* 2008) package by the Ouranos Climate Simulations Team. Other modifications, such as a new convection scheme and large-scale nudging, were also included. All versions, from number 1 to the last up-to-date 4.3 have been (and still are) used during the last 15 years to perform regional climate change projections over Canada and North America (e.g. *Plummer et al*. 2006), including the Canadian participation in the TAR and AR4 IPCC Reports, and for such projects as ENSEMBLES and NARCCAP.

The next generation of RCMs will need to operate at high resolution at a reasonable speed, which the current dynamical core cannot do. Therefore, the Canadian Network for Regional Climate Modelling and Diagnostics (CRCMD) has chosen the Global Environmental Multiscale (GEM) to be the dynamical core of the next-generation model, CRCM5. GEM has been developed for Numerical Weather Prediction (NWP) in Canada and has the most welcomed advantage of being able to operate at high resolution in a highly parallelized computational environment. GEM will eventually be coupled to AGCM4 physics, but for now it uses the NWP physics.

In what follows we will present some preliminary results comparing, for both CRCM4 and CRCM5, climate simulations over North America for recent past, 1960-2000, driven by ERA40 and AMIP2.

2. Operational model CRCM4.2.3

The operational CRCM_v4.2.3 is a one-way nested limited-area climate model based on a semi-implicit semi-Lagrangian algorithm. The model equations are solved on an Arakawa-C grid on polar stereographic projection and Gal-Chen scaled-height vertical coordinates. The nesting follows Davies over the sponge zone (9-grid points) and large-scale nudging (*Biner et al*. 2000) is applied over the entire domain for horizontal wind. The physical parameterization is mostly based on the AGCM3, including CLASS_V2.7 surface scheme, but the moist convection follows Bechtold-Kain-Fritsch.

Documented features of this version over North America include good mean precipitation but underestimation of strong events, noisy signal over Rockies topography and lack of precipitation over the Mississippi basin in winter. Too cold minimum screen temperature in winter, especially in the northern part of the domain has been noticed, although lack of reliable long-term observations in this region does not guarantee a fair evaluation. Cloud-free radiation is fairly good, but all-sky radiation suffers from a large negative bias in cloud cover and an underestimation of downward longwave radiation throughout the year. See figures 2 and 3 (top panels) for a comparison against CRU observations for winter precipitation and minimum screen temperature.

3. Developmental model CRCM5.0.1

The dynamical kernel of CRCM5 is the LAM version, rotated uniform latitude-longitude grid, of the GEM model, which can also be run global uniform and stretched. GEM can be run parallel in MPI and OpenMP. The nonhydrostatic formulation uses hydrostatic pressure as the basis for its vertical coordinate and a semi-implicit semi-Lagrangian time discretization scheme. The free domain is surrounded by a blending zone for nesting plus a halo region.

The physical parameterizations are described in detail in *Zadra et al*. (2008). In particular, Kain-Fritsch convection, ISBA land-surface scheme and correlated-k radiation are used.

At the time of writing this abstract only a few simulations have been done in climate mode, so main features are still to be documented. However, it has been shown that contribution of trace gases included in the radiation package gives a certain advantage to CRCM5 with respect to CRCM4.

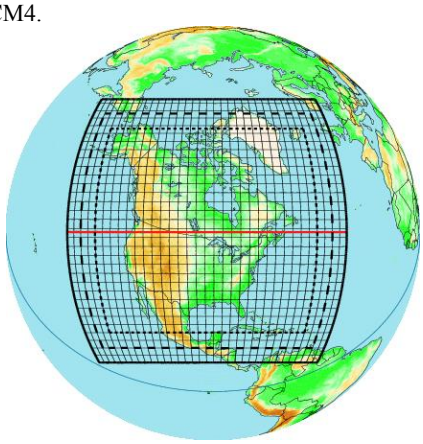

Figure 1. CRCM5 North American 0.5 deg grid. 170x158, including 10-point halo region and 10-point blending zone. Every 5th grid points are shown.

4. 1961-2000 simulations against observations.

Simulations over North America by CRCM4 at 45 km true at 60 deg North and CRCM5 at 0.5 deg over North

America, both driven ERA40 and AMIP2 are compared with observations. CRU2 data are used for precipitation and minimum and maximum (not shown) screen temperature.

Preliminary results show that CRCM5 produces an acceptable climate over North America, with, *as usual*, some improvements and some deteriorations compared to CRCM4, depending on the variable, the region and the season. For instance, precipitation is less noisy over the Rockies, compared with CRCM4 (see Fig. 2). The typical problematic under-representation by most regional models (as preliminary results from NARCCAP suggest) of Mississippi delta winter precipitation does not seem to appear in CRCM5. Summer maximum screen temperature has a slightly reduced warm bias compared to CRCM4, albeit over a different region, while minimum screen temperature warm biases have increased (see Fig. 3). For winter, a warm minimum screen temperature bias (4-5º) located specifically over boreal forest in Canada is particularly notable and may be related to snow formulation in ISBA or to geophysical characteristics (to be confirmed).

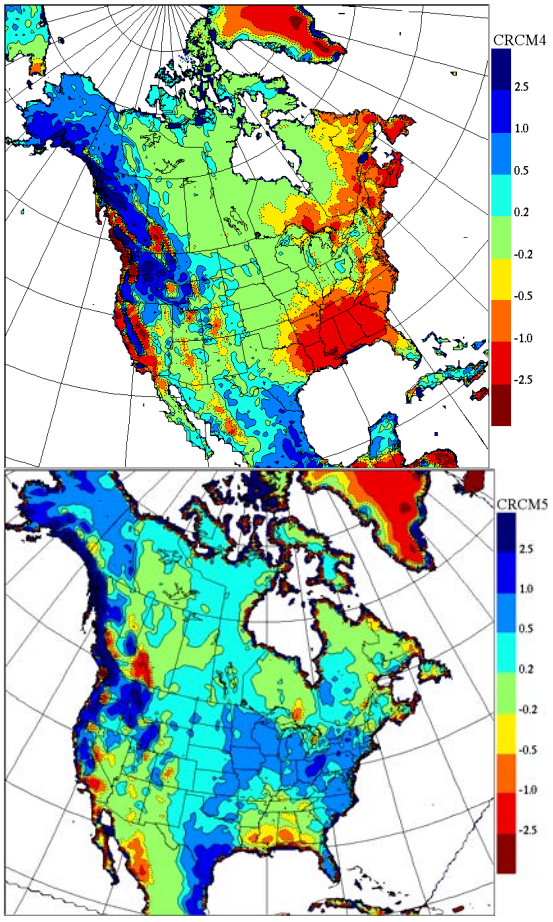

Figure 2. CRCM4 and CRCM5 1961-2000 DJF precipitation difference with CRU2 (mm/d).

5. Conclusion

A new version of the CRCM (CRCM5) is under development. For now, only the NWP physics coupling with the dynamics is done, while the CGCM4 climate physics coupling is still under way. For now, 40-year recent past (1961-2000) climate simulations for both operational (CRCM4) and developmental (CRCM5) versions are compared with observations. First results with CRCM5 are promising, particularly for precipitation and radiation, however not without some remaining challenges. Boreal forest in winter seems particularly problematic.

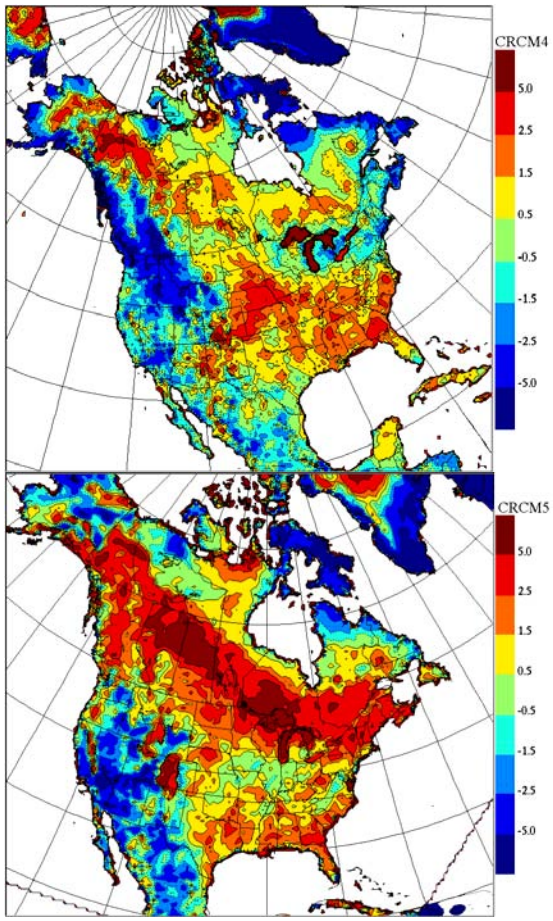

Figure 3. CRCM4 and CRCM5 1961-2000 DJF minimum screen temperature difference with CRU2 (°C).

References

Biner, S., D. Caya, R. Laprise and L. Spacek, Nesting of RCMs by Imposing Large scales. *Research Activities in Atmospheric and Oceanic Modelling*, Ed. H. Ritchie. Report N 30, WMO/TD No 987, pp. 7.3-7.4, 2000.

Laprise, R., D. Caya, G. Bergeron and M. Giguère, The formulation of André Robert MC2 (Mesoscale Compressible Community) model. *Atmos.-Ocean*, Vol. 35, No. 1, pp. 195-220, 1997.

Plummer D. A., D. Caya, A. Frigon, H. Côté, M. Giguère, D. Paquin, S. Biner, R. Harvey, R. de Elia, Climate Change over North America as Simulated by the Canadian RCM. *Journal of Climate*. Vol 19, No 13, pp. 3112-3132, 2006.

Scinocca, J. F., N. A. McFarlane, M. Lazare, J. Li, and D. Plummer, The CCCma third generation AGCM and its extension into the middle atmosphere. *Atmos. Chem. Phys. Discuss.*, Vol. 8, pp. 7883-7930, 2008.

Zadra A., D. Caya, J. Côté, B. Dugas, C. Jones, R. Laprise, K. Winger and L.-P. Caron, The next Canadian Regional Climate Model. *Physics in Canada,* Vol. 64, No. 2, pp. 75-83, 2008.

Soil organic layer: Implications for Arctic present-day climate and future climate changes

Annette Rinke[1)], Peter Kuhry[2)] and Klaus Dethloff[1)]

1) Alfred Wegener Institute for Polar and Marine Research, Potsdam, Germany; Annette.Rinke@awi.de;
2) University of Stockholm, Department of Physical Geography and Quaternary Geology, Stockholm, Sweden

1. Introduction

A top layer of organic material is a dominant feature of northern forest and tundra soils, and plays a prominent role in ground temperature and moisture regimes because of its distinct thermal and hydraulic properties.
Previous modelling studies have focussed on the impact of organic soil on the ground temperature and moisture, and surface energy fluxes (*Lawrence and Slater*, 2008). However, it is important to indicate that changes in ground heat flux necessarily affect turbulent heat fluxes which have consequences for the regional Arctic climate. In this study, we investigate these potentially critical feedbacks on Arctic climate, and its impact on Arctic climate change estimates.

2. Simulations

The regional climate model HIRHAM is applied on a pan-Arctic domain. It has been improved by coupling it to the sophisticated land-surface model LSM from NCAR (*Bonan*, 1996; *Saha et al.*, 2006). Further, moss, lichen and peat have been included as additional texture types. Their thermal and hydraulic parameters have been specified according to *Beringer et al*. (2001). The top organic layer has been prescribed according to land surface type. For the main types it is as follows: non-wood tundra, 0–10 cm peat; forest tundra, 0–10 cm moss and 10–30 cm peat; forests, 0–10 cm moss/lichen. In deeper layers, the original mineral ground texture has been kept.
The following HIRHAM simulations have been performed:
(i) For present-day climate, the model has been run over 21 years (1979–1999), driven by ERA40 analyses. The first 11 years are devoted to spin-up the deep ground conditions in order to obtain a balanced ground-atmosphere system. The remaining 10 years (1990–1999) have been analyzed.
(ii) For future climate change, the model has been run over 1980-1999 and 2080-2099, driven by ECHAM5/MPI-OM 20C control and A1B emission scenario data. The difference between both periods quantifies the simulated change by the end of the 21st century.
To investigate the implications of a top organic layer the differences between the runs without any organic layer and the runs including such a layer have been analyzed for both present-day and future climate.

3. Results

The inclusion of a top organic layer modifies not only the ground thermal and hydrological regimes, but also dynamically feeds back into the atmosphere (*Rinke et al.*, 2008).
The low thermal conductivity and high heat capacity of the top organic layer cause an effective insulation of the underlying ground, contributing there to slightly warmer ground temperatures in winter and much cooler conditions in summer. The strongest response is simulated for summer. It reduces the ground temperatures by 0.5°C to 8°C. It is shown that the ground temperature changes vary strongly from region to region due to the specific climatological and hydrological conditions. The addition of the top organic layer has also effects on the energy exchange from and to the surface. The most important calculated response is the increased latent heat flux in summer due to a strong increase in ground evaporation which causes a significant 2m air temperature decrease. Furthermore, the dynamical response due to the turbulent heat flux changes affects the large-scale atmospheric circulation. The regional mean sea level pressure (SLP) changes over land are directly thermally driven: An increase of SLP over those land regions characterized by an air temperature cooling is calculated. Furthermore, a remote SLP response over the Arctic Ocean appears. In winter, the SLP is reduced over the Barents- and Kara Seas which is an improvement compared to observations.
Based on the GCM-driven simulations, the uncertainty of the future climate change signal in 2m air temperature and atmospheric circulation concerning the set-up of the land surface model LSM is presently being quantified.

Acknowledgment. This research was supported by the 6th EU Framework Programme (CARBO-North project) and the Bert Bolin Climate Research Centre of Stockholm University.

References

Beringer, J., A.H. Lynch, F.S. Chapin III, M. Mack, G.B. Bonan, The representation of Arctic soils in the Land Surface Model (LSM): The importance of mosses, *J. Clim.*, 14, 3324-3335, 2001

Bonan, G.B., A land surface model for ecological, hydrological and atmospheric studies: Technical description and user guide, *Tech. Rep. NCAR/TN-417+STR*, Boulder, USA, 1996

Lawrence, D.M., A.G. Slater, Incorporating organic soil into a global climate model, *Clim. Dyn.*, 30, 145 – 160, 2008

Rinke, A., P. Kuhry, K. Dethloff, Importance of soil organic layer for Arctic climate: A sensitivity study with an RCM, *Geophys. Res. Lett*., 35, L13709, 2008

Saha, S.K., A. Rinke, K. Dethloff, P. Kuhry, Influence of a complex land surface scheme on Arctic climate simulations, *J. Geophys. Res.*, 111, D22104, 2006

Impact of surface waves in a Regional Climate Model

Anna Rutgersson[1], Björn Carlsson[1], Alvaro Semedo[1] and Øyvind Sætra[2]

1) Department of Earth Sciences, Uppsala University, Sweden, Anna.rutgersson@met.uu.se
2) Norwegian Meteorological Institute, Oslo, Norway

1. Introduction

When modelling the atmosphere it is of crucial importance to correctly describe the boundary conditions. The atmospheric-ocean boundary is an important source of turbulence and there is a significant exchange of momentum, heat and moisture. The marine atmospheric boundary layer (MABL) has a considerable impact on global climate atmospheric models since 70 % of the global surface is covered with water. The turbulence in the atmosphere as well as the surface fluxes is different over the ocean since the roughness of the surface (the waves) changes as a response to the atmospheric forcing. Surface waves can be divided into growing sea (young sea) and decaying sea (swell) with very different impact on the atmosphere.

2. Model

The atmosphere model RCA3 (Rossby Centre atmospheric regional climate model) is developed at SMHI (Swedish Meteorological and Hydrological institute) and its domain covers Europe. It is a hydrostatic model, with terrain-following coordinates and the calculations are semi-Lagrangian, semi-implicit and with 30-min time step. The horizontal resolution is c. 44 km and resolved in the vertical by 24 levels between 90 m above the surface and 10 hPa. The model is forced at the lateral boundaries by ERA40 data and from below by sea surface temperature (and ice) and phase speed of the dominant waves from the same data set. For more details, see e.g. *Jones et al. (2004)*.

The atmosphere is coupled to the WAM wave model. The WAM model is a state-of-the-art third generation wave model *(Komen et al, 1994)*. RCA and WAM are coupled with a two-way coupling each time-step (see Figure 1).

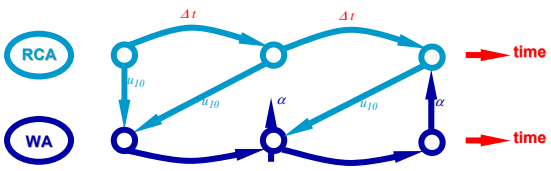

Figure 1. Sketch of the RCA-WAM coupled system.

In addition wave-data from the ERA40 re-analysis are used as wave-input to the RCA model for one part of the investigation.

3. Theory

The situation with decaying sea (swell) has in several experimental investigations been shown to give significantly lower friction at the surface as well as altered wind profiles and atmospheric turbulence (*Smedman et al, 1999; Rutgersson et al, 2001*). The lower friction at the surface can be expressed by a reduced drag coefficient (Figure 2).

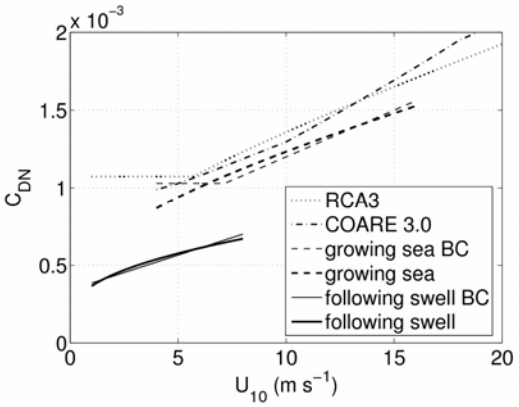

Figure 2. Drag coefficient for growing sea (dashed and dashed-dotted lines show different expressions) and swell (solid lines). Figure from *Carlsson et al (2009)*.

The altered wind profiles with a low level wind maximum can also be reproduced by an analytical model Figure 3 (*Semedo et al, 2009*).

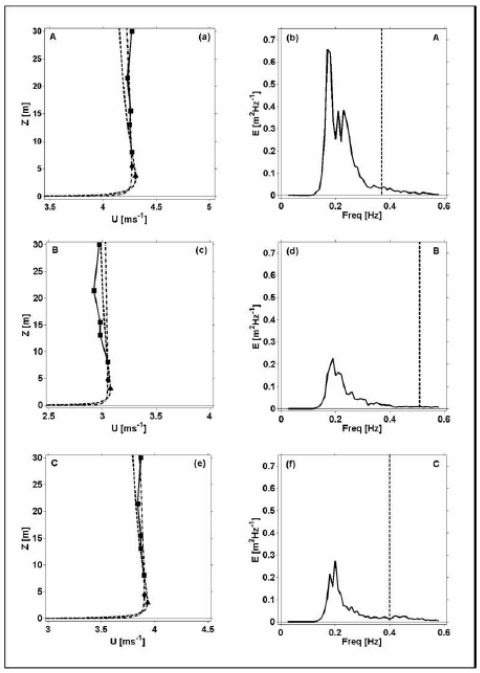

Figure 3. Measured and modeled wind profile for three different cases (left). Measured wave spectra for the corresponding situations (right).

4. Results

The method how to do the coupling can be done using different methods and this has some impact on the response of the atmosphere. In general are the higher wind speeds slightly reduced when the feed-back of the waves are also included. When correctly including the impact of swell waves the momentum transport is significantly reduced, this includes reduced turbulence in the atmosphere and has a significant impact on heat fluxes as well as other secondary parameters. Figure 4 shows the change precipitation patterns modelled by the RCA model as mean difference for one year when including swell compared to when not including swell.

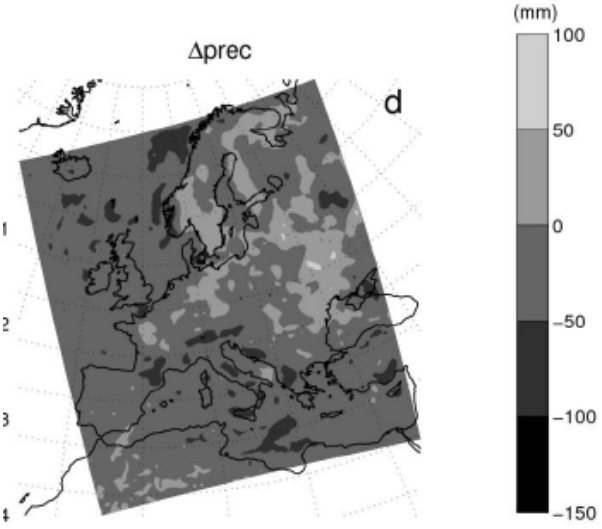

Figure 4. Annual mean precipitation difference when including swell and not including swell in the RCA model. Figure from *Carlsson et al (2009)*.

5. Conclusions

It is of importance to correctly represent the impact of the surface roughness. Having correct description alters the surface roughness, but may also change the pressure patterns over the sea.

References

Carlsson B., A. Rutgersson and A. Smedman, 2009a : Impact of swell on a regional atmospheric climate model. *Under revision in Tellus.*

Carlsson B., A. Rutgersson and A. Smedman, 2009b : Investigated the effect of including wave effects in the process oriented model PROBE-Baltic. *Accepted for publ. in Bor. Env Res.*

Jones, C. G., Willén, U., Ullerstig, A. and Hansson, U. The Rossby Centre Regional Atmospheric Climate Model Part I: Model Climatology and Performance for the Present Climate over Europe. *Ambio 33:4-5*, 199-210.

Komen, G. J., L. Cavaleri, M. Donelan, K. Hasselmann and P.A.E.M. Janssen, Dynamics and Modelling of Ocean Waves. In: , Cambridge University Press, Cambridge (1994), p. 512.

Rutgersson, A., Smedman, A.-S., Högström, U. 2001: Use of conventional stability parameters during swell. *J. Geophys. Res.,* **106** , 27,117-27,134.

Semedo, A., Sætra, Ø., Rutgersson, A., Kahma, K., Pettersson, H. 2009: Wave induced wind in the marine boundary layer. J. Atmos. Sci. in press.

Smedman, A., Högström, U., Bergström, H., Rutgersson, A., Kahma, K., and H. Pettersson 1999. A case-study of air-sea interaction during swell conditions. *J. Geophys. Res*., **104**, 25,833-25,851.

Sensitivity of a regional climate model to physics parameterizations: Simulation of summer precipitation over East Asia using MM5

Shi Song[1] and Jian-ping Tang[1,2]

1. School of Atmospheric Sciences, Nanjing University, Nanjing, China, 210093
2. Key Laboratory of Mesoscale Severe Weather of Ministry of Education, Nanjing University, China, 210093

1. Introduction

A number of studies address that the uncertainty due to model parameterizations is one of the major sources of errors in dynamical downscaling. The concept of ensemble climate prediction has been raised to alleviate prediction errors arising from model physical parameterizations (Krishnamurti et al., 1991). The sensitivity of a regional climate model (RCM) in modeling summer precipitation over East Asia to cumulative parameterization schemes (CUPAs) is significant because the skill of CUPAs has great effect on the performance of the RCM on the simulation of the summer precipitation. It has recently been demonstrated that spectral nudging can effectively incorporate large-scale regulations inside the RCM domain and thus improve model performance (von Storch et al. 2000; Feser et al., 2006; Castro et al., 2005). Therefore, this study is to investigate (1)how does the downscaling method of spectral nudging perform over the region of East Asia, especially in the simulations of summer precipitation over East Asia and (2)how sensitive is the RCM solution to the choice of physical parameterization scheme before and after incorporating spectral nudging method.

2. Model, Experiments and Data

The case examined here is the rainy season (JJA) in East Asia in the years 1998. Two groups of numerical experiments are conducted: the control runs (CTLs) which refer to traditional MM5 simulations without any form of nudging, and the spectral nudging runs (SNs), which are the runs with spectral nudging method adopted in MM5. Each group includes three experiments with different CUPA schemes: the KF2 scheme, the GR scheme, and the BM scheme. It is designed to study the sensitivity of the model to CUPAs. The RCM simulations are evaluated against the NCEP/NCAR Reanalysis data and NCEP/CPC precipitation analysis data.

In each group of experiments with different CUPAs, we calculate the PC between each two members of the three and then obtain the group average, which indicates the similarity among three simulation fields with different CUPAs. We speculate that the spectral nudging can diminish model's sensitivity to physical parameterization schemes, and therefore we expect in all cases the average values of PCs of SNs are generally larger than those of CTLs.

3. Results

Compared to the experiments without interior nudging, experiments using interior nudging can reproduce more realistic large-scale circulations in the upper levels of the atmosphere as well as near the surface. So we further investigate the model performance of simulating precipitations.

Monthly precipitation fields

Figure 1 shows the observed and simulated monthly mean precipitation fields of August of 1998. There are two features: (1) the simulation ability are largely improved by using interior nudging because the results of SN runs are in more consistence with the observation; (2) the large discrepancy among CTL runs under different CUPAs are largely reduced in the SN runs, which is confirmed by the skill socres in Table 1. Similar results can be seen in the simulations of other months.

Individual precipitation fields

igure 2 shows the time series of regional-averaged daily precipitation rates in JJA of 1998 in North China and the Yangtze River basin. Overall, most results of SNs markedly outperform those of CTLs: RMSEs of CTLs are generally reduced by averaging 20~30% in SNs; temporal correlation coefficients of CTLs are significantly increased in SNs (skill scores not shown). Furthermore, the discrepancy between individual runs of SN group is far less than that of the CTL group.

4. Conclusions

The sensitivity of a regional climate model (RCM) in modeling summer precipitation over East Asia to cumulative parameterization schemes are tested using a regional climate model PSU–NCAR MM5. The effect of interior (spectral) nudging is also assessed. In conclusion, this study demonstrates that compared to the experiments without interior nudging, the results indicate three major improvements by using interior nudging: (1) the RCM can reproduce more realistic large-scale circulations in the upper levels of the atmosphere as well as near the surface; (2) the precipitation fields in both monthly mean and intra-seasonal (daily) variability are improved; and (3) the sensitivities of the RCM simulations to the choice of cumulative parameterization schemes are reduced.

Therefore we argue that the discrepancies of model simulations using different cumulative parameterization schemes could be reduced by spectral nudging method, the multi-CUPA ensemble simulation can demonstrate an improved skill to some extent, especially in the simulation of summer precipitation over East Asia.

References

Krishnamurti TN, and Coauthors. 1999: Improved weather and seasonal climate forecasts from multi-model superensemble. Science 285:1548–1550

Castro CL, Pielke RA Sr., Leoncini G. 2005: Dynamical downscaling: Assessment of value retained and added using the Regional Atmospheric Modeling System (RAMS), J. Geophys. Res., 110, D05,108

von Storch, H, Feser F. 2000: A spectral nudging technique for dynamical downscaling purposes. Mon. Wea. Rev.,128, 3664–3673.

Feser F. 2006: Enhanced Detectability of Added Value in Limited-Area Model Results Separated into Different Spatial Scales. Mon. Wea. Rev., 134, 2180–2190.

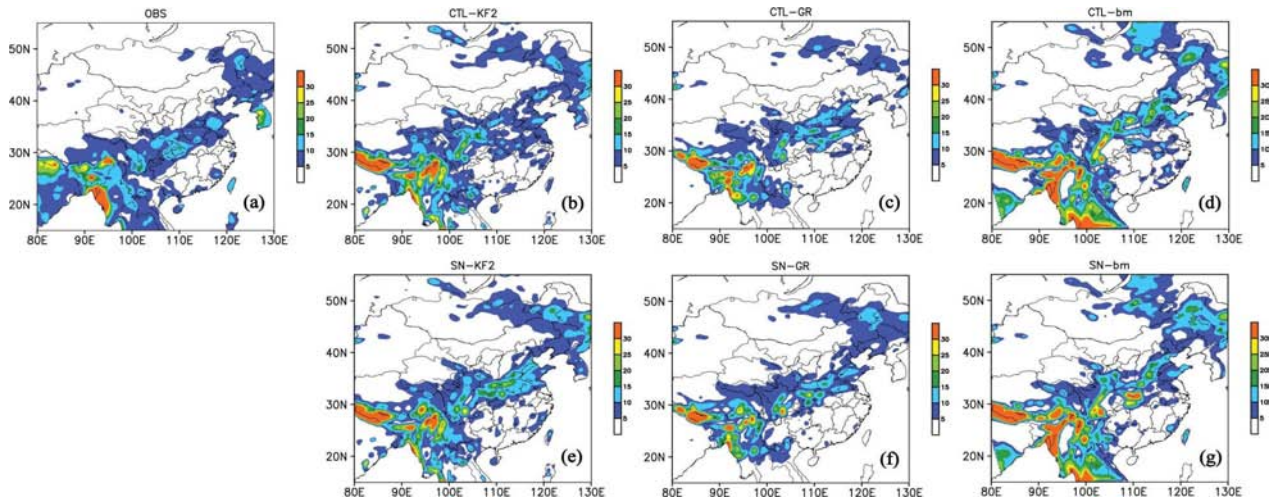

Figure 1. Observed (a) and simulated (b,c,d) for CTL and (e,f,g) for SN runs) monthly mean precipitation of August 1998

Table 1. Pattern correlation coefficients between monthly precipitation fields produced by the experiments with different CUPAs and the overall average.

experiment	Period	KF2 - GR	GR - BM	KF2 - BM	average
CTLs-98	June	0.76	0.52	0.64	0.64
	July	0.71	0.61	0.63	0.65
	August	0.66	0.60	0.60	0.62
SNs-98	June	***0.81***	***0.65***	***0.73***	***0.73***
	July	***0.77***	0.52	0.60	0.63
	August	***0.84***	***0.72***	***0.69***	***0.65***

*Bold italic indicates the SNs outperform that of the CTLs.

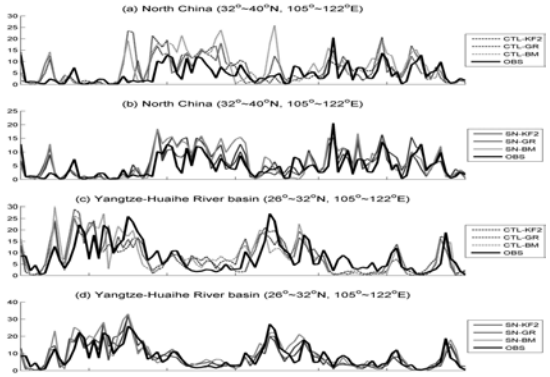

Figure 2. Observed and simulated (panel(a, c) for CTL runs and (b, d) for SN runs) time series of regional averaged precipitation in 1998 JJA of North China(top two) and Yangtze-Huaihe River basin(bottom two) in Figure 1

Overview of recent developments of COSMO-CLM numerics and physical parameterizations for high resolution simulations

Andreas Will (1) and Ulrich Schättler (2)

(1) Chair of Environmental Meteorology, Brandenburg University of Technology (BTU), P.O. Box 10 13 44, D-03013 Cottbus, Germany, e-mail: will@tu-cottbus.de
(2) Research and Development (FE13), Deutscher Wetterdienst, Offenbach, Germany

1. Motivation

Several RCMs are based on NWP models. They use the NWP dynamical core and extend the model physics relevant on long time scales. This is also the case with COSMO-CLM.

One basic idea of the COSMO-CLM development is that a model improvement should reduce the inaccuracy of operational numerical weather prediction and of regional climate simulations with perfect boundary conditions.

From version 4 on the COSMO-CLM is a unified model for NWP and RCM designed for high resolution applications of up to 100m horizontal resolution. In NWP mode the model is developed and tested at the 2 to 7 km space and the synop tic time scale. The corresponding RCM mode is used and evaluated at space scales between 2 and 50 km and climatological time scales. Both "views"

- the time development of single weather situations (case studies) investigated in NWP mode and

- the statistics of climate investigated in RCM mode
are regarded as complementary pictures and contribute to the further improvement of the model system.

The main issue of the presentation is to give an overview of the COSMO-CLM model system, to present the recent developments of numerics and of physical parameterizations and to discuss their relevance for regional climate simulations.

2. Developments of Model Physics and Numerics for High Resolution Simulations

The basic non-hydrostatatic model version LM_3 / CLM_3 of the COSMO-CLM uses the leapfrog-dynamical method as proposed by Klemp-Wilhelmson, moist physics for rain and snow, 1d radiation scheme of Ritter-Geleyn and a multi-layer deep soil model (see Steppeler et al. (2003) for details). This model dynamics has the advantage of efficiency and exhibits an acceptable local accuracy in NWP (LM) and regional climate mode (CLM) (see Hollweg et al (2008)).

The model physics of the LM_3 was designed for resolutions between 10 and 50km and had to be further developed for applications at much higher resolutions. The strong relation between the physical parameterizations of unresolved processes and the simulation of grid scale phenomena led to the development of a new dyanamical core in order to achieve higher local accuracy.

A new dynamical core based on a non-dissipative 3rd order Runge-Kutta time integration method has been introduced together with 3rd and 5th order upwind advection schemes in order to reduce the phase error. Furthermore, different schemes for passive tracer fields (water constituents) have been introduced and the so called "shallow atmosphere approximation" was removed. Now all advection compo nents and all coriolis terms are implemented.

At meso-scale resolving simulations also more and more physical processes are explicitely resolved and/or become important. In COSMO-CLM the horizontal transport, evaporation of falling water constituents and a further type of precipitation (graupel) have been introduced, the cloud microphysics and the convection scheme have been modified and a shallow convection parameterization has been introduced.

The improved numerics (RK dynamics) and higher spatial resolutions modified the unresolved dynamics, which has to be parameterized. In COSMO-CLM an explicit parame terization of the effect of the unresolved orography on the dynamics has been introduced (Lott and Miller (1997)) and a prognostic turbulent kinetic energy equation is solved.

At higher resolutions and for climate applications the heterogenity of the land surface becomes more important. A lake model has been introduced to calculate the surface temperature of the grid scale lakes and the albedo of snow covered evergreen forests has been introduced. The last improves the model behavior especially in late winter.

The developments have not been evaluated independently on climatological time scales and/or for different regions on the globe. Therefore, results will be presented illustrating the influence of each of the developments for idealized test cases (numerics), extreme weather conditions and/or on seasonal to inter-annual time scales.

References

Hollweg, H.-D., U. Boehm, I. Fast, B. Hennemuth, K. Keuler, E. Keup-Thiel, M. Lautenschlager, S. Legutke, K.Radtke, B. Rockel, M. Schubert, A. Will, M. Woldt, C. Wunram, Ensemble simulations over Europe with the regional climate model CLM forced with IPCC AR4 global scenarios. *M&D Technical Report*, No. 3, 145 pp. Max-Planck-Institute for Meteorology, 2008, *www.mad.zmaw.de/projects-at-md/sg-adaptation/*

J.Steppeler, G.Doms, H.-W.Bitzer, A.Gassmann, U.Damrath and G.Gregoric, Meso-gamma scale forecasts using the nonhydrostatic model LM, Meteorology and Atmospheric Physics (2003), 82, 75-96

Evaluation of the Rossby Centre Regional Climate model (RCA) using satellite cloud and radiation products.

Ulrika Willén

Rossby Centre, SMHI, 601 76 Norrköping, Sweden. Email: Ulrika.Willen@smhi.se

1. Introduction

We have compared monthly mean cloud and radiation fields from the EUMETSAT Climate Monitoring SAF (CM-SAF, http://www.cmsaf.eu) data base with the clouds and radiation simulated by the Rossby Centre regional climate model (RCA) and by the European Centre Medium range Weather Forecast model (ECMWF) over Europe and North Africa for the time period January 2005 to December 2008.

2. Data

The CM-SAF data is derived from both geostationary satellites and polar orbiting satellites with different instruments on board. This gives rise to differences in the derived variables such as cloud fraction depending on e.g. the viewing geometry (Johnston and Karlsson 2007). The cloud fractions in their turn are used in derivation of the surface radiation fluxes. We have used both types of satellite data in this study.

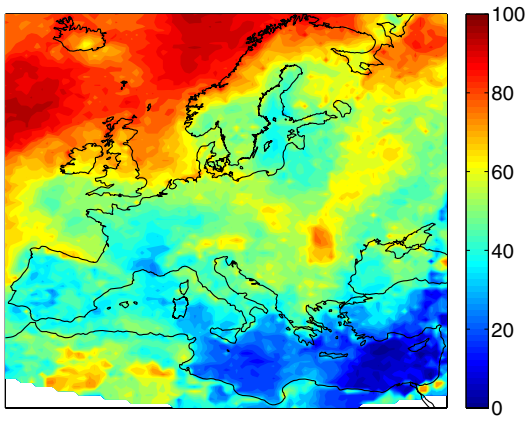

Figure 1. CM-SAF cloud fraction (%) for June 2006.

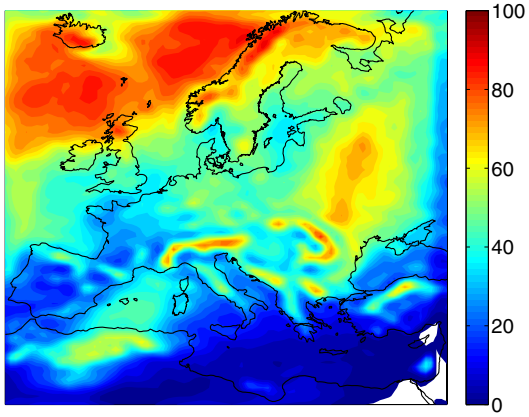

Figure 2. RCA cloud fraction (%) for June 2006.

The Rossby Centre Atmospheric regional climate model is a hydrostatic gridpoint model with semi-Lagrangian dynamics originally based up on the numerical weather prediction model HIRLAM (Undén et. al. 2002). Most physical parameterisations have been replaced and the model has been developed to perform optimally in the 10-50km horizontal resolution range with 24 or 40 vertical levels (Jones et. al. 2004 and Kjellström et. al. 2005). We will present results for two versions of the model RCA3 and RCA3.5 for different horizontal and vertical resolutions.

3. Results -Europe

RCA and ECMWF overestimate the cloud fraction by 20% over snow covered regions in the north east of Europe and overestimate the surface downwelling longwave radiation (SDL) by 20-40W/m^2 and surface outgoing longwave radiation by 10-30W/m^2. The RCA-simulated clouds have too much cloud water in northern Europe in summer and in autumn and they therefore reflect too much shortwave radiation at the TOA (TRS) and this also leads to an underestimation of the incoming shortwave radiation (SIS) at the surface. The latest version of RCA has greatly improved cloud water and radiative fluxes.

Over most of Europe and over sea ECMWF (all year) and RCA (in winter-spring) underestimate the cloud fraction which could explain a corresponding underestimate of TRS, overestimate of SIS and underestimate of SDL. The satellites overestimate cloud cover over sea due to problems in the treatment of sub-pixel cloudiness and therefore the models underestimates are larger over sea. Mainly RCA but also ECMWF overestimate cloud fraction on top of mountains and underestimate it along mountain ranges and have corresponding differences in the TOA and surface radiation fluxes compared to the CM-SAF data.

4. Results - North Africa

Over North Africa RCA underestimates TRS by -11W/m^2 and overestimates the TOA emitted thermal radiation (TET) by 8W/m^2. ECMWF underestimates TRS by -28W/m^2 and overestimates TET by 14W/m^2. These errors are similar to what has been found for many other global models and are attributed to clear sky errors either due to too high surface temperatures, errors in emissivity, albedo or lack of aerosols. Adding clear and cloudy skies radiation fluxes to the CM-SAF data base would help us to understand the reasons for ECMWF and RCA errors. The polar orbiting satellite retrieval for 2005-2006 erroneously overestimated cloud fraction over North Africa, which also affects the CM-SAF derived surface radiation fluxes.

References

Jones CG, Willén U, Ullerstig A, Hansson U., The Rossby Centre Regional Atmospheric Climate Model Part I: Model Climatology and Performance for the Present Climate over Europe. AMBIO: A Journal of the Human Environment, Vol. 33, No. 4 pp. 199–210, 2004

Kjellström, E., Bärring, L., Gollvik, S., Hansson, U., Jones, C., Samuelsson, P., Rummukainen, M., Ullerstig, A., Willén U. and Wyser, K., A 140-year simulation of European climate with the new version of the Rossby Centre regional atmospheric climate model (RCA3). RMK report 108, SMHI, SE-60176 Norrköping, Sweden, 54 pp. 2005

Undén P. and co-authors, HIRLAM-5 Scientific Documentation, (hirlam.knmi.nl), 2002

Simulating aerosols in the regional climate model CCLM

Elias Zubler[1], Ulrike Lohmann[1], Daniel Lüthi[1], Andreas Mühlbauer[2] and Christoph Schär[1]

(1) Institute for Atmospheric and Climate Science, ETH, Zurich (elias.zubler@env.ethz.ch), (2) Department of Atmospheric Sciences, University of Washington, Seattle

1. Introduction

Since aerosols serve as cloud condensation and ice nuclei they influence the microphysical properties of clouds and precipitation [indirect aerosols effects: *Lohmann and Feichter* (2005)]. Increasing the aerosol number in a cloud leads to more but smaller cloud droplets and, hence, a deceleration of hydrometeor growth and a reduction in warm-phase precipitation [cloud lifetime effect: *Albrecht* (1989)], a higher cloud albedo [cloud albedo effect: *Twomey et al.* (1984)] and may also cause significant changes in ice formation [*Cantrell and Heymsfield* (2005)]. However, larger concentrations of heterogeneous ice nuclei could also enhance the Wegener-Bergeron-Findeisen process and, thus, potentially increase snowfall or conversion to graupel [cloud glaciation effect: *Zubler et al.* (in prep.), *Lohmann et al*. (2002)]. On the regional scale, aerosols may therefore alter precipitation patterns, possibly affecting the hydrological cycle [*Ramanathan et al*. (2001)]. Aerosols also interact directly with the radiation as they scatter and absorb sunlight [direct aerosol effect: *Wild et al.* (2005), and semi-direct effect: *Ackerman et al.* (2000)]. Hence, the representation of complex cloud and aerosol microphysics is crucial to narrow down current uncertainties in regional climate modelling.
Here, a regional climate model (RCM) is coupled to a sophisticated aerosol module and a 2-moment cloud microphysics scheme. This setup is used to study the effects of aerosols on the regional climate of Europe with focus on the hydrological cycle in the Alpine region.

2. RCM

In the present study, the regional climate model CCLM4.0 [*Will et al.* (subm.)] is coupled to a sophisticated aerosol microphysics module [*Vignati et al*. (2004)] and a 2-moment bulk cloud scheme [*Seifert and Beheng* (2006)]. Figure 1 shows the schematic of the RCM setup.

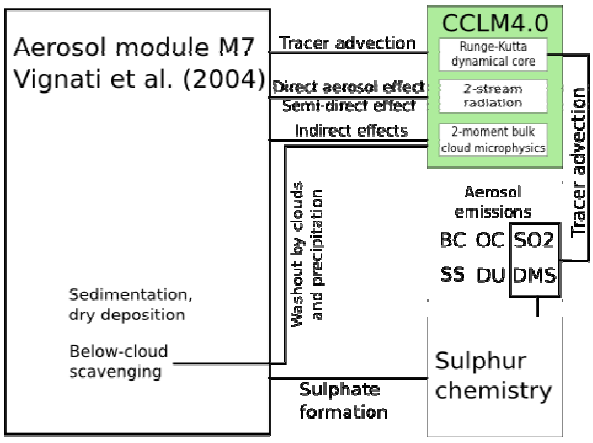

Figure 1. CCLM4.0 setup with coupled aerosol module and 2-moment cloud microphysics scheme.

The aerosol module accounts for the life cycle (emission, chemical evolution through condensation of soluble material onto the particles and water uptake, coagulation, in- and below-cloud scavenging, sedimentation and dry deposition) of major aerosol species such as sulfates, seasalt, soil dust, black and organic carbon. A 2-moment approach with lognormal size distributions is applied for the aerosol particles. The 2-moment cloud microphysics scheme allows for the prognostic representation of both mass and number concentrations for five different types of cloud and precipitation particles (cloud, rain, ice, snow and graupel). The following cloud microphysical processes are considered: autoconversion of cloud droplets to rain drops and accretion by rain drops, aerosol activation and heterogeneous nucleation of cloud droplets and ice-crystals [via immersion and contact freezing], homogeneous freezing, cloud-graupel and snow-cloud riming, aggregation of ice-crystals and snowflakes, self-collection of rain, ice and snow, sublimation of ice-crystals, evaporation and break-up of rain drops. Vapor diffusion onto cloud droplets and ice-crystals, Hallett-Mossop ice multiplication as well as graupel shedding are also taken into account.
Simulations with the new CCLM setup are conducted from 1960-2000 driven by ERA-40 reanalysis, applying aerosol boundary data from the global atmospheric circulation model ECHAM5-HAM [*Stier et al.* (2005)]. The horizontal resolution is 50 km.

3. Preliminary results

An overview of the physical parameterizations and first results with the newly coupled version of CCLM4.0 are shown. The new model version produces physically consistent results. For example, the model simulates the scavenging rates depending on aerosol and precipitation particle size. Scavenging below clouds is found to be most efficient for the largest as well as the very smallest aerosol particles. For the largest aerosols, impaction is the dominant removal process. The smallest particles are scavenged due to Brownian diffusion. Consequently, intermediate size particles accumulate, which has a significant effect on the radiative as well as the microphysical properties of the aerosol population.
In our simulations, emitted insoluble soot and dust particles grow by coagulation, sulfate condensation and water uptake. Particle growth is shown to increase the activated fraction, providing more cloud condensation nuclei. This increases the number of cloud droplets and reduces their size. It is also discussed that the change toward smaller droplet radii has the expected effect on cloud albedo and cloud lifetime. In a simplified 2D setup, the model is shown to reproduce a decline in surface net short-wave radiation. An increase in cloud lifetime is found in terms of reduced autoconversion and accretion rates. This slows down warm-phase precipitation formation. In cloud-resolving simulations with our model, rainfall patterns in orographic terrain are changed as a consequence of this effect, such that more moisture is transported to the drier lee side and a loss of precipitation is observed on the windward side of the corresponding mountain ridge.

4. Summary

This study illustrates the primary steps that were taken to provide a framework for regional climate predictions with the CCLM model, including a sophisticated representation of aerosol and cloud microphysics. Model development is finished and the newly coupled schemes are validated. Here, the complexity of aerosol-cloud-precipitation interactions and the underlying processes are highlighted and an overview of the corresponding parameterizations is given. Furthermore, we show first results of climate simulations with the new RCM configuration.

References

Ackerman, A. S., O. B. Toon, D. E. Stevens, A. J. Heymsfield, V. Ramanathan, E. J. Welton, Reduction of tropical cloudiness by soot, *Science*, 288, 1042–1047, 2000

Albrecht, B., Aerosols, cloud microphysics, and fractional cloudiness, *Science*, 245, 1227–1230, 1989

Lohmann, U., J. Feichter, Global indirect aerosol effects: A review, *Atmos. Chem. Phys.*, 4, 7561–7614, 2005

Lohmann, U., A glaciaton indirect effect caused by soot aerosols, *Geophys. Res. Lett. Sci.*, 29 (4), 10.1029/2001GL014357, 2002

Cantrell, W., and A. Heymsfield, Production of ice in tropospheric clouds, *Bull. Amer. Meteor. Soc.*, 86 (6), 795-807, 2005

Ramanathan, V., P. J. Crutzen, J. T. Kiehl, and D. Rosenfeld, Aerosol, climate and the hydrologicalal cycle, *Science*, 294, 2119–2124, 2001

Seifert, A. and K. D. Beheng, A two-moment cloud microphysics parameterization for mixed-phase clouds. Part I: Model description, *Meteorol. Atmos. Phys.*, 92, 45–66, 2006

Vignati, E., J. Wilson, and P. Stier, M7, An efficient size-resolved aerosol microphysics module for large-scale aerosol transport models, *J. Geophys. Res.*, 109, D22 202, 2004

Stier, P., J. Feichter, S. Kinne, S. Kloster, E. Vignati, J.Wilson, L. Ganzeveld, I. Tegen, M.Werner, Y. Balkanski, M. Schulz, O. Boucher, A. Minikin, and A. Petzold, The aerosol-climate model ECHAM5-HAM, *Atmos. Chem. Phys.*, 5, 1125–1156, 2005

Twomey, S., M. Piepgrass, and T. Wolfe, An assessment of the impact of pollution on global cloud albedo, *Tellus, Ser. B*, 36, 356–366, 1984

Will, A., M. Baldauf, B. Rockel, A. Seifert, Physics and dynamics of the CLM, submitted: *Meteorol. Z.*

Zubler, E., U. Lohmann, D. Lüthi, A. Muhlbauer, C. Schär, Evidence of a glaciation indirect aerosol effect in 2D sensitivity studies of mixed-phase orographic precipitation, *in preparation*

Moisture availability and the relationship between daily precipitation intensity and surface temperature

Peter Berg, Jan Haerter, Peter Thejll, Claudio Piani, Stefan Hagemann, Jens Hesselbjerg Christensen

Institute for Meteorology and Climate Research, University/Forschungszentrum Karlsruhe, Germany, Peter.Berg@imk.fzk.de

1. Introduction

What is the connection between precipitation intensity and the surface temperature? A claim commonly made when studying global warming is that precipitation intensity increases as the troposphere warms (e.g. Semenov and Bengtsson, 2002; Trenberth et al., 2003). This claim has its origin in the relationship between the air's moisture-holding capacity and the temperature, as stated by the Clausius-Clapeyron (C-C) equation. For the precipitation intensity to follow this increase in capacity at the same rate, the supply of moisture must then increase sufficiently to enable saturation leading to condensation and cloud formation. To what extent is the atmospheric moisture content actually limited by the C-C relationship? Are there other factors that inhibit a potential increase in the precipitation intensity as the globe warms?

In this study, further described in Berg et al. (submitted to JGR), we explore the relationship between surface temperature and precipitation intensity for a gridded observational data set of daily values covering all of Europe, similar to what has earlier been carried out for a single precipitation station in the Netherlands (Lenderink and van Meijgaard, 2008). We explicitly resolve the intra-seasonal behaviour and investigate in which seasons the precipitation intensity dependence on temperature can be understood using the C-C relation, and why this concept breaks down in other seasons. The results are compared to, and further explored using three RCMs.

2. Data and models

We use the gridded 0.44 degree resolution observational data set of daily precipitation and temperature over European land areas, constructed for the ENSEMBLES project (Haylock et al., 2008). We focus on the period 1961—1990, where there is good spatial and temporal coverage of precipitation and temperature stations in the domain. The below analysis was also performed on station data directly, with similar results, so the gridded data are found to be reliable.

To complement the observations we use ERA40-reanalysis driven simulations by the HIRHAM4, REMO and HadRM3 RCMs from the ENSEMBLES project. The models use a 0.44 degree horizontal resolution, and we use only model data over land, to be consistent with the observations.

3. Methodology

We consider daily precipitation intensity, larger than 0.1 mm/day, and the two-meter daily mean temperature. However, the variable for studying an increase in the moisture holding capacity, and precipitation intensity changes, would be the cloud level temperature. A study of the relationship between the two-meter temperature and the cloud level temperature, using the RCMs, showed the two-meter temperature to be proportional to the cloud level temperature, with no systematic deviations. Thus we can use this directly to compare with the precipitation intensity.

We divide the data into months, and study the intra-seasonal relationship between temperature and precipitation intensity. This performed by dividing the temperature range into two Kelvin bins, and calculating the 70^{th}, 90^{th}, 99^{th} and 99.9^{th} percentiles for each bin. The two higher percentiles are calculated by a Generalized Pareto Distribution (GPD) fit to the upper 20% of the data. All the calculated percentiles show similar, i.e. parallel, results so in the rest of this text we restrict to only discuss the 99^{th} percentile.

4. Results

The observations show a general monotonous positive relationship with increasing temperature in winter, while in summer there is a negative relationship (Fig. 1). However, the negative trend in summer shows signs of being interrupted and level out for the temperature range of about ten to twenty degrees.

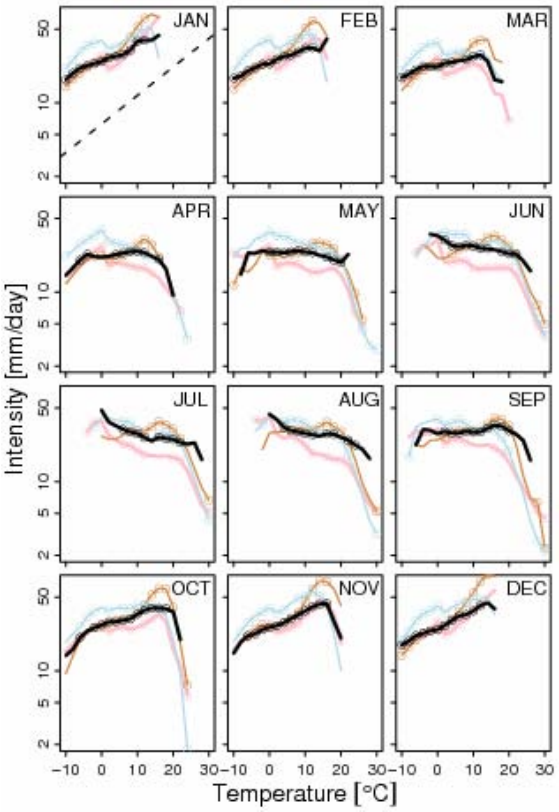

Figure 1: The 99^{th} percentile of precipitation intensity larger than 0.1 mm/day as a function of daily average temperature for observations (black), HIRHAM4 (pink), REMO (light brown), and HadRM3 (light blue). The dashed line in the January panel shows a C-C like increase with temperature. Note the logarithmic vertical axis.

The RCM simulations show a very similar behaviour as the observations (Fig. 1). The models separate between large-scale and convective precipitation events, depending on the circumstances leading to the precipitation event. We utilize this separation between the precipitation types to investigate their individual behaviour.

We find the large-scale precipitation (Fig. 2, blue curves) to have a positive trend in winter, and a negative trend in summer, much like that found in the observations. In winter, the large-scale precipitation is mainly due to the migration of large scale moist air masses from the Atlantic and Arctic oceans. As the continental air is cold and easily saturated, there will be an increase in the cloud and precipitation formation with rising temperatures. In summer, the warmer air is not as readily saturated, in fact it gets more difficult to saturate the higher the temperature. Therefore, the large-scale precipitation, which has a typical time scale of one day, decreases with increasing temperature as there is simply not enough water vapor available for cloud formation. The atmospheric moisture variables are further studied in Berg et al. (submitted to JGR)

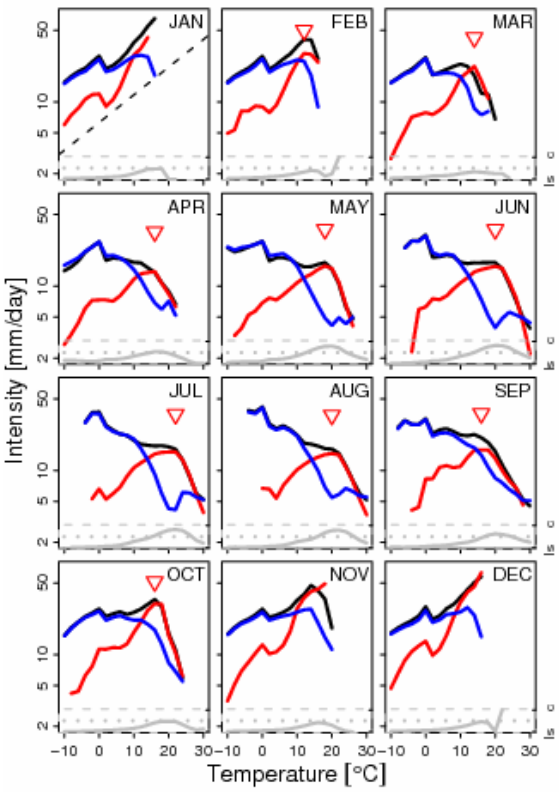

Figure 2: The 99th percentile of precipitation intensity larger than 0.1 mm/day as a function of daily average temperature for the HIRHAM4 model. The curves indicate the total (black), convective (red), and large-scale (blue) precipitation. The dashed line in the January panel shows a C-C like increase with temperature. Note the logarithmic vertical axis. The relative contribution to the total precipitation of the two sub types of precipitation is shown in the gray inserted curve at the bottom of each plot. The dotted line in the middle indicates equal contributions, while above (below) the convective (large-scale) type dominates.

The convective precipitation (Fig. 2, red curves) has a much shorter time scale, and a more intense convection, so it is not bound in the same way to the availability of moisture. That is to say, even if there is not enough moisture available for large-scale cloud formation on the daily scale, a smaller scale convective event with a shorter time scale can still collect enough moisture to produce an intense precipitation event. Furthermore, we find the convective precipitation to increase at a rate similar to the C-C rate, but that it has peak intensity at between ten to twenty degrees, depending on the month, thereafter it shows a steep negative trend. The peak coincides closely with the range for the interruption of the negative summertime trend in the observational data. When studying the sum of the convective and large-scale precipitation we see that the large-scale is generally dominating, except for in the warm season at the higher end of the temperature range.

5. Discussion

The results presented here, and further in Berg et al. (submitted to JGR), shows that the precipitation intensity is restricted by the C-C relationship in winter, while for summer, the general trend is toward weaker events with higher temperature. The convective precipitation shows a different dependence on temperature compared to the large-scale precipitation, but it too shows a negative trend at the higher end of the temperature range. This leads us to argue that also the convective precipitation is limited by the availability of moisture and the level to reach for saturating the atmosphere at the higher temperatures. To further explore this argument we need to look further into sub-daily data to properly resolve the convective events. Furthermore, it would be interesting to study these phenomena in other regions of the world to assess the generality of the results.

6. Acknowledgments

We acknowledge the funding of the European Union FP6 project WATCH (contract nr. 036946). We further acknowledge the model data sets contributed by the HIRHAM, REMO and HadRM groups, and the observational data set from the ECA&D project (http://eca.knmi.nl), through the ENSEMBLES project.

References

Berg, P., J. Haerter, P. Thejll, C. Piani, S. Hagemann, J. H. Christensen, Moisture availability and the relationship between daily precipitation intensity and surface temperature, submitted to JGR.

Haylock, M.R., N. Hofstra, A.M.G. Klein Tank, E.J. Klok, P.D. Jones, M. New, A European daily high-resolution gridded dataset of surface temperature and precipitation. *J. Geophys. Res*, 113, D20119, doi:10.1029/2008JD10201, 2008

Lenderink, G., E. van Meijgaard, Increase in hourly precipitation extremes beyond expectations from temperature changes, *Nature Geosciences*, 1, 511-514, 2008

Semenov, V.A., L. Bengtsson, Secular trends in daily precipitation charateristics: greenhouse gas simulation with a coupled AOGCM, *Clim. Dyn*, 19, 123-140, 2002

Trenberth, K.E., A. Dai, R.M. Rasmussen, D.B. Parsons, The changing character of precipitation, *Bull. Am. Meteor. Soc*., 84, 1205-1217, 2003

Temperature and precipitation scenarios for the Caribbean from the PRECIS regional climate model

J. Campbell, M. A. Taylor, T. S. Stephenson, F. S. Whyte and R. Watson

jayaka.campbell@uwimona.edu.jm

Scenarios of rainfall and temperature changes into the 2080s under the A2 and B2 SRES scenarios are examined using the Hadley Centre PRECIS (Providing Regional Climates for Impacts Studies) regional climate model (RCM). The model simulates 'present-day' (1979-93) rainfall and temperature climatologies reasonably well, capturing the characteristic bi-modality of Caribbean rainfall and the boreal summer maximum and winter minimum temperatures. Observed annual spatial patterns are reproduced, albeit rainfall amounts are underestimated (~ 4cm) over Cuba, Jamaica, Hispaniola and Puerto Rico. Temperatures over the region are overestimated by 1°- 3°C. For seasonal maps, the November-January (NDJ) pattern was not as well simulated as the other seasons. The study highlights 3 key features evident from the climate change scenarios obtained. (i) There is an intensification of the climatological gradient pattern for NDJ, i.e. the northern Caribbean (i.e. north of 22^{o}N) is projected to get wetter and southern (i.e. south of 22^{o}N) drier. This potentially points to an intensification of the northern hemisphere winter circulation patterns; (ii) There is a robust June-October drying signal which bolsters the projections of summer drying obtained from global climate models simulations; and (iii) While there is evidence of increased temperatures across all seasons, the rainfall response varies with seasons (i.e. the northern Caribbean is wetter for November-April but largely drier for May-October). This points to a need to investigate circulation parameters to determine what changes produce this response under increased temperatures.

Use of the Weather Research and Forecasting Model (WRF) towards improving warm season climate forecasts in North America

Christopher L. Castro[1] and Francina Dominguez[2]

[1]Department of Atmospheric Sciences and [2]Department of Hydrology, University of Arizona, Tucson, Arizona, USA
Corresponding e-mail of lead author: castro@atmo.arizona.edu

1. Motivation and background

Official U.S. seasonal climate forecasts by the National Oceanic and Atmospheric Administration (NOAA) are issued by the Climate Prediction Center (CPC), a branch of the National Center for Environmental Prediction (NCEP). CPC uses the Climate Forecast System (CFS) global coupled ocean-atmosphere model as numerical modeling component of these forecasts (*Saha et al*. 2006). In a retrospective ensemble hindcasts for 1980-2004 over the contiguous U.S., CFS demonstrates: an increase in skill when a greater number of ensemble members are used; an ability to forecast tropical Pacific SSTs and large-scale teleconnection patterns (at least as evaluated for the winter) for seasonal leads; and greater skill in forecasting winter than summer climate. Winter climate is largely dependent on synoptic-scale mid-latitude storms. The decrease in CFS skill during the warm season is due to the fact that the physical mechanisms of rainfall at this time are more related to mesoscale processes, specifically the diurnal cycle of convection, low-level moisture transport, propagation and organization of convection (e.g. development of mesoscale convective systems), and surface moisture recycling. In general, these are poorly represented in global atmospheric models.

A regional climate model (RCM) may potentially add value in representation of warm season climate in North America. RCMs with a grid spacing of tens of kilometers have been shown to be useful because they can improve the representation of the mesoscale processes (e.g. *Castro et al.* 2007). Large-scale circulation patterns may also still be reasonably represented in the driving global atmospheric model. A major large-scale feature of importance at this time is an upper-level high pressure ridge in the interior of the continent related to development of the North American Monsoon. The "monsoon ridge" causes in the continental-scale pattern of precipitation as the summer proceeds, such that precipitation increases in Southwest U.S. and northwest Mexico and decreases in the central U.S Our prior work conclusively demonstrates that time-evolving teleconnections in the warm season (i.e. quasi-stationary Rossby wave responses) related to interannual and interdecadal variability in Pacific sea surface temperature (SST) significantly affects the positioning of this ridge and, consequently, the warm season precipitation in each of these respective regions (*Castro et al.* 2007). If an accurate representation of the synoptic scale features is present in data from a driving global model, seasonal climate prediction simulations of North America with a RCM for the warm season may be a viable possibility. This is one of the major scientific goals of the recent North American Monsoon Experiment (NAME).

2. The Weather Research and Forecasting (WRF) model

The Weather Research and Forecasting (WRF) Model has been developed as a collaborative effort among numerous research institutions, most notably the Mesoscale and Microscale Meteorology (MMM) Division at the National Center for Atmospheric Research (NCAR) and NOAA NCEP. Similar to other regional atmospheric models, WRF is designed primarily for mesoscale and cloud-scale atmospheric phenomena. The version of WRF we use is the Advanced Research WRF (ARW), developed at NCAR. The ARW solver is fully three dimensional; nonhydrostatic; includes telescoping, interactive nested grid capabilities; and has schemes for initial and boundary conditions (*Skamarock et al. 2005*). The model physical parameterizations that will are used for the proposed work are consistent with those of the existing WRF numerical weather prediction system at the University of Arizona.

An issue that is being increasingly recognized with respect to use of RCMs is the loss of synoptic scale variability from the driving GCM when the limited area model is forced only at its lateral boundaries (e.g. *Castro et al.* 2005). The loss of synoptic scale variability can then affect how the RCM represents the mesoscale processes. An alternative approach to lateral boundary nudging in a buffer zone may be spectral nudging, in which selective nudging at only the largest scales takes place throughout the whole domain of the model for prognostic fields like geopotential height, winds, and temperature. The nudging is confined to the upper-levels of the atmosphere. In this way, the variability of the synoptic scale circulation features may be maintained during the model integration, while allowing the RCM to still add value at the smaller scales. A RCM simulation with spectral nudging is typically more realistic with respect to observations, if global reanalysis data are used as the driving data (e.g. *Miguez Macho et al.* 2005). For this work, we use the spectral nudging technique described in *Miguez Macho et al.* (2005) recently implemented in the WRF model.

3. Dynamical downscaling procedure for retrospective CFS model ensembles

We are using archived CFS hindcast ensembles from NCEP for the years 1980-2005 as the driving condition for WRF RCM simulations. Each CFS ensemble consists of approximately 10 members, generated by different initializations by NCEP Reanalysis 2. The specific CFS forecasts that will be used for dynamical downscaling start at the beginning of May of the given year and last approximately the duration of the warm season (through at least August). Data from the NCEP Reanalysis 2 will be is also being downscaled for the same period as a control to assess the performance of the RCM assuming "perfect" boundary forcing. The domain for these simulations will cover the contiguous U.S. and Mexico with a grid spacing of 32 km. Spectral nudging according to *Miguez-Macho et al.* (2005) will be employed for scales greater than four times the grid spacing of the driving CFS, in accordance with *Castro et al.* (2005). The initial soil moisture is specified by the North American Regional Reanalysis, as the land surface model is consistent with that in WRF.

4. Preliminary results for downscaling one CFS ensemble member with WRF

Thus far we have executed two tests dynamically downscaling one CFS ensemble member for the 1993 warm season. For the first test, only standard lateral boundary nudging is applied to the outer five grid points of the model domain, equivalent to what is traditionally done in WRF numerical weather forecast applications and oftentimes in regional climate modeling applications. For the second test, both standard lateral boundary nudging and internal nudging (at all wavelengths) is applied according to the standard WRF FDDA options.

Precipitation results for June 1993 are shown for the original CFS ensemble member (Figure 1), and the WRF test downscaling experiments described above (Figure 2). The precipitation for the original CFS ensemble member demonstrates that the CFS model is able to capture warm season teleconnections that lead to increased rainfall in the central U.S., consistent with the precipitation observations at this time. The WRF experiment with only lateral boundary nudging, however, produces a diminished amount of precipitation in the central U.S. as compared to the original CFS ensemble member. Thus, this experiment appears to actually take away value from CFS model. An analysis showed that the large-scale circulation patterns in this WRF experiment are significantly different than in the driving CFS model ensemble member data, in a manner consistent with *Castro et al.* (2005). By an improved representation of the large-scale circulation, the WRF experiment with lateral boundary nudging and internal nudging dramatically improves the forecast June precipitation. The positioning of the precipitation maximum in the central U.S. shifts slightly southward and the amount of precipitation there is increased compared to the original CFS ensemble member, more closely matching the observed precipitation. Later months in the summer (not shown) also show a much improved representation of the North American Monsoon in the Southwest U.S.

5. Conclusions and ongoing work

The preliminary results of dynamically downscaling a CFS ensemble member with WRF for the warm season in North America are quite promising. Provided that the regional model is able to retain the variability in the large scale circulation fields, WRF used as a RCM can potentially add value to representation of the warm season climate. This is primarily realized by an improved representation of warm season convective precipitation. These results appears to validate the hypothesis posed by *Castro et al*. (2007) that RCMs can add value to the representation of warm season climate provide the driving global model produces reasonably accurate teleconnection patterns and that these are retained in the RCM. We anticipate the results here will improve further with the incorporation of spectral nudging in the CFS-WRF simulations.

6. Acknowledgements

This work is supported by National Science Foundation under grant number ATM-0813656. We thank Dr. Gonzalo Miguez-Macho of the University of Santiago de Compostela for providing the spectral nudging code for WRF.

Selected References

Castro, C.L., R.A. Pielke, Sr., and G. Leoncini, Dynamical Downscaling: Assessment of value restored and added using the Regional Atmospheric Modeling System (RAMS), *J. Geophys. Res*., **110**, D05108, doi:10.1029/2004JD004721, 2005.

Castro, C.L., R.A. Pielke, Sr., J.O. Adegoke, S.D Schubert, and P.J. Pegion. Investigation of the Summer Climate of the Contiguous U.S. and Mexico Using the Regional Atmospheric Modeling System (RAMS). Part II: Model Climate Variability. *J. Climate*, **20**, 3888-3901, 2007.

Miguez-Macho, G., G.L. Stenchikov, and A. Robock. Regional Climate Simulations over North America: Interactions of Local Processes with Improved Large-Scale Flow. *J. Climate*, **18**, 1227-1246, 2005.

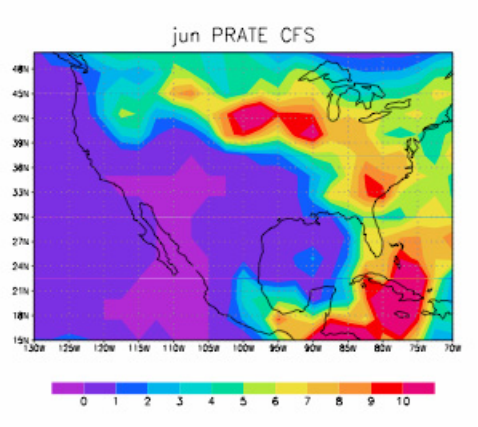

Figure 1. June 1993 CFS precipitation (mm day^{-1}) from sample ensemble member.

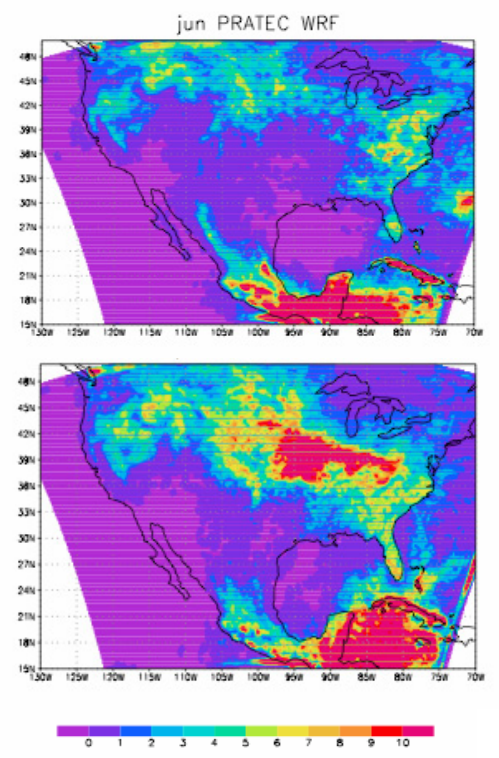

Figure 2. June 1993 CFS-WRF downscaled precipitation (mm day^{-1}) using lateral boundary nudging only (top) and interior nudging (bottom).

Modeling of the Atlantic tropical cyclone activity with the RegCM3

Daniela Cruz-Pastrana[1], Ernesto Caetano[1] and Rosmeri Porfírio da Rocha[2]

[1]National Autonomous University of Mexico, Mexico; [2]São Paulo University , São Paulo, Brazil;
daniela@atmosfera.unam.mx

1. Introduction

The North Atlantic basin (including North Atlantic Ocean, Caribbean Sea and Gulf of Mexico) has a substantial interdecadal and interannual variability which modulates tropical cyclone activity over the region (Goldenberg et al., 2001). Additionally this activity according some authors (eg Emanuel, 2005, Mann and Emanuel, 2006, Trenberth and Shea, 2006) has been enhanced due to global warming.
The dynamic simulations of tropical cyclones over Atlantic basin permit to the study the controlling factors of the variability and long-term trend. However, the typical resolution global climate models are often unsuitable for this kind of simulations. Knutson et al. (2007) used the Geophysical Fluid Dynamics Laboratory (GFDL) Regional Atmospheric Model (Pauluis and Garner, 2006) to simulate successfully various aspects of tropical storms, obtaining a high correlation between observed and simulated variability and trends.
The Northern Hemisphere interannual variability cyclone activity is assessed through simulations with the RegCM3 (Pal et al., 2007) and applying an algorithm for the detection and tracking of cyclones based on the relative vorticity and warm cores.

2. Methodology

RegCM3

The RegCM3 is a primitive equations model, compressible, in sigma vertical coordinates (Pal et al., 2007). The turbulent surface fluxes over the ocean are parameterized using the Zeng scheme (Zeng et al., 1998) and the convective scheme proposed by Grell (1993) with the Fritsch Chappell cloud- model (Pal et al., 2007).
The simulation period was January 1982 to December 1991 for the domain from 110 °W to 10 °W and 6 °S to 36 °N. The initial and boundary conditions are provided by the NCEP-NCAR Reanalysis 1 (Kalnay et al., 1996) and the sea surface temperature (SST) is the average weekly from OISST (Optimum Interpolation SST) dataset with 1°x 1° resolution (Reynolds et al., 2002). The model horizontal resolution is 25 km with 18 sigma levels in the vertical, with the top of model at 75hPa.

Hurricane tracking

The algorithm used for identification and tracking of cyclones was developed by Sugahara (2000) and adapted by Reboita (2008) for extratropical cyclones. The numerical scheme uses a similar method proposed by Sinclair (1994) through the identification of the minimum (maximum) cyclonic relative vorticity. We performed an adaptation to tropical cyclones taking the account the consideration of Knutson et al. (2007) to identify warm cores from vortices that correspond to hurricanes. Before applying the tracking method, the zonal and meridional wind at 850hPa and mean sea level pressure were interpolated to a regular grid of 1° x 1°.

3. Results

The modeled tropical cyclone activity is higher in the central part of the basin and the lower over the Gulf of Mexico compared (Fig. 1a) with the best-track of National Hurricane Center dataset (Fig.1b). (HURDAT; http://www.aoml.noaa.gov/hrd/hurdat/) Additionally the simulated cyclone trajectories are more erratic and lasting less than those observed.
The simulated daily average cumulated rainfall (Fig.2b) for August to October is underestimated for the region of the InterTropical Convergence Zone (ITCZ) and in the northern Gulf of Mexico while it is overestimated at the basin central part compared with the CMAP (CPC Merged Analysis of Precipitation) (Xie and Arkin, 1997) (Fig 2a).

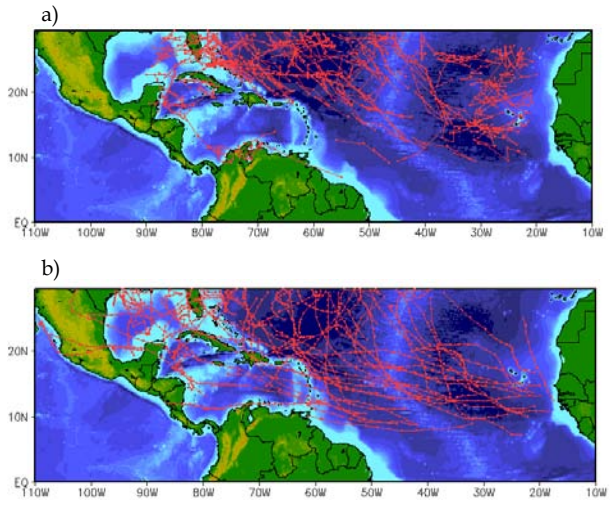

Figure 1. Tropical cyclones trajectories for the 1982-1991 period: (a) RegCM3 with the Sugahara modified algorithm; (b) best-track from National Hurricane Center dataset.

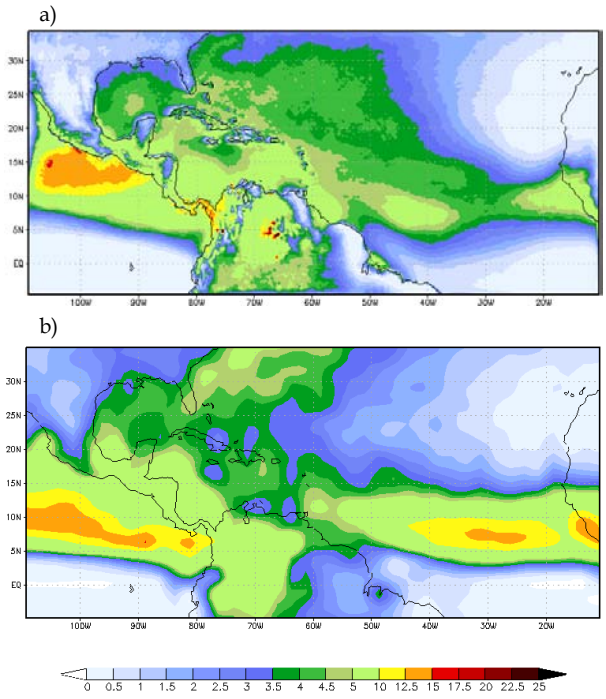

Figure 2. The 1982-91 daily average accumulated precipitation (mm/day) for August to October: (a) Observed (CMAP); (b) Simulated (RegCM3).

4. Conclusions

The objective was to evaluate the ability of the RegCM3 using Sugahara modified algorithm to simulate tropical cyclones a algorithm to locate and tracking their trajectories. Comparing the simulations with observations and it is found that the model has little ability to simulate long lasting tropical cyclones and this is enhanced over the Gulf of Mexico region

5. Acknowledgments

This work was funded by CNPq process Nº 476361/2006-0 and scholarship CONACyT CVU46942. The authors would also like to thank ICTP for provided the RegCM3 code and NCEP by reanalyzes data set.

References

Emanuel, K., Increasing destructiveness of tropical cyclones over the past 30 years. *Nature*, 436, 686-688, 2005.

Goldenberg S.B., C.W. Landsea, A.M. Mestas-Nuñez and W.M. Gray, The Recent Increase in Atlantic Hurricane Activity: Causes and Implications. *Science*, 293, 474-479, 2001.

Grell G.A., Prognostic Evaluation of Assumptions used by Cumulus Parametrizations. *Mon. Wea. Rev.*, 121, 764-787, 1993.

Kalnay, E. and Coauthors, The NCEP/NCAR 40-Year Reanalysis Project. *BAMS*, 77, 437-471

Knutson, T.R., J.J. Sirutis, S.T. Garner, I.M. Held and R.E. Tuleya, Simulation of the recent multi-decadal increase of Atlantic hurricane activity using an 18-km grid regional model, *BAMS*, 1549-1565, 2007.

Mann, M. and K. Emanuel, Atlantic hurricane trends linked to climate change. *EOS*, 87, 233-241, 2006.

Pal, J.S. and Coauthors, Regional Modeling for the Developing World: The ICTP RegCM3 and RegCNET. *BAMS*, 88, 1395-1409,2007.

Pauluis, O. and S.T. Garner, Sensitivity of radiative-convective equilibrium simulations to horizontal resolution. *J. Atmos. Sci.*, 63, 1910-1923, 2006.

Reboita, M.S., Ciclones Extratropicais sobre o Atlântico Sul: Simulação Climática e Experimentos de Sensibilidade. PhD Thesis, Universidade de São Paulo, 294pp, 2008.

Reynolds, R.W., N.A. Rayner, T.M. Smith, D.C. Stockes and W. Wang, An improved in situ and satellite SST analysis for climate. *J. Climate*, 15, 1609-1625, 2002.

Sinclair, M.R., An Objetive Cyclone Climatology for the Southern Hemisphere. *Mon.Wea.Rev.*, 122, 2239-2256, 1994.

Sugahara, S., Variação Annual da Freqüencia de Ciclones no Atlântico Sul. In: *Congresso Brasileiro de Meteorologia*, Rio de Janeiro, RJ, 16 a 20 do outubro de 2000.

Trenberth, K. E. y D. J. Shea, Atlantic hurricanes and natural variability in 2005. *Geophys. Res. Lett.*, 33, L12704, doi:10.1029/2006GL026894, 2006.

Xie and Arkin, Global Precipitation: A 17-year monthly analysis based on gauge observations, satellite estimates, and numerical model outputs. *BAMS*, 78, 2539-2558, 1997.

Zeng, X., M. Zhao and R.E. Dickinson, Intercomparison of Bulk Aerodynamic Algorithms for the Computation of Sea Surface Fluxes Using TOGA COARE and TOA Data. *J. Climate*, 11, 2628-2644, 1998.

Regional modelling of recent changes in the climate of Svalbard and the Nordic Arctic (1979-2001): Comparing RCM output to meteorological station data

Jonathan Day[(1)], Jonathan Bamber[(1)], Paul Valdes[(1)] and Jack Kohler[(2)]

[(1)] School of Geographical Sciences, University of Bristol, U.K., (jonathan.day@bristol.ac.uk).
[(2)] Norwegian Polar Institute, Tromsø, Norway.

1. Motivation and region of interest

Svalbard is one of the largest glaciated regions in the Arctic with over 2,100 glaciers and ice caps. In a topographically complex region like Svalbard corse resolution general circulation model (GCM) data fail to accurately capture local climate. We simulate climatic changes in the region over the period 1979-2001 using the regional climate model (RCM) HadRM3, the high resolution limited area version of the U.K. met office's general circulation model (GCM) HadCM3 (Gordon et al 200).

2. Model and Forcing

Wind, temperature, water vapour and surface pressure from the European Centre for Medium-Range Weather Forecasts' ERA-40 reanalysis are used to force a 50km resolution RCM at the lateral boundary. Using reanalysis to force the RCM and comparing the output to meteorological station data provides a method to isolate any systematic bias in the RCM.

Figure 1. Map of Svalbard, located in the Norwegian Arctic.

3. Downscaling and validation

There are a large number of emerging "downscaling" methods to relate regional (50 km resolution) climate model output to a local (point). We use ERA-40 and meteorological station data over this period to calculate downscaling factors for precipitation, temperature and solar radiation similarly to Rivington et al (2008). This will improve estimates of climate change impacts when the RCM is forced with a GCM under different emission scenarios.

References

Gordon C, Cooper C, Senior C A, Banks H, Gregory J M, Johns T C, Mitchell J F B, Wood R A. The simulation of SST, sea ice extents and ocean heat transports in a version of the Hadley Centre coupled model without flux adjustments, *Climate Dynamics*, 16, 2-3, pp. 167-168, 2000

Rivington M, Miller D, Matthews K B, Russell G, Bellocchi G, Buchan K, Downscaling regional climate model estimates of daily precipitation, temperature and solar radiation data, *Climate Researchl*, 35, 3, pp. 181-202, 2008

Effects of variations in climate parameters on evapotranspiration in the arid and semi-arid regions

Saeid Eslamian , Mohammad Javad Khordadi, Arezou Baba Ahmadi, Jahangir and Abedi Koupai

Associate Professor, Isfahan University of Technology, Department of Water Engineering, College of Agriculture, Isfahan University of Technology, Isfahan, Iran
Email:prof.eslamian@gmail.com

Postgraduate Student, Isfahan University of Technology, Department of Water Engineering, College of Agriculture, Isfahan University of Technology, Isfahan, Iran

Graduate student, Chalmers University, Department of Civil Engineering, Geo and Water Engineering Master Program, Gothenburg, Sweden Email: arezoob@student.chalmers.se (Corresponding author)

Associate Professor, Isfahan University of Technology, Department of Water Engineering, College of Agriculture, Isfahan University of Technology, Isfahan, Iran

The main objective of this study is to investigate the effects of climatic parameters variability on evapotranspiration in five climatologically different regions of Iran. The regions include Tehran, Esfahan, Shiraz, Tabriz and Mashhad. Fifty four-year monthly records of temperature, relative humidity, sunshine duration, wind speed, and precipitation depth from 1951 to 2005 comprise the database. Trend and persistence analyses of the data are performed using the Mann–Kendall test, the Cumulative Deviation test, Linear Regression, and the Autocorrelation Coefficient. A sensitivity analysis of meteorological variables in these five regions is carried out using Penman-Monteith formula. In all of studied regions, temperature and relative humidity are the most sensitive parameters in Penman-Monteith formula respectively. The results of this study indicate that the effective climatic variables in evapotranspiration are changing, though in each region the variables have significant long-term trends and persistence.

Regional climate change projections using a physics ensemble over the Iberian Peninsula

P. Jimenez-Guerrero (1), S. Jerez (1), J.P. Montavez (1), J.J. Gomez-Navarro (1), J.A. García-Valero (2) and J.F. Gonzalez-Rouco (2)

(1) Universidad de Murcia, Spain (sonia.jerez@gmail.com), (2) AEMET, Murcia, Spain, (3) Universidad Complutense de Madrid, Spain

1. Introduction

Some of the most widely used Regional Climate Models (RCMs) contain large numbers of parameterizations which are known, individually, to have a significant impact on simulated climate (Zhiwei et al., 2002). Up to date, considerable uncertainties exist in the the extent to which different choices of parameter-settings or schemes may influence present climate simulations and different projections for the future climate. The most thorough way to investigate this uncertainty is to run ensemble experiments in which relevant parameter combination is investigated. The use of ensemble techniques in regional climate modeling has been shown in several studies (such as the PRUDENCE -Christensen et al., 2007-, ENSEMBLES projects) as feasible for obtaining projections of climate change (Vidale et al., 2007) and to study the capacity of RCMs to reproduce the observed climatology (Lenderink et al., 2007).

This work explores the sensitivity of different physical parameterizations (microphysics, cumulus and PBL schemes) within a regional climate version of the MM5 model (Grell et al., 1994) when applied in a complex an heterogeneous area such as the Iberian Peninsula (IP).

2. Experiments

A multi-physics ensemble of eight climate change projections (2070-2099 vs. 1970-1999) have been performed with MM5 driven by ECHAM5 global climate model outputs, forced by the SRES A2 scenario for the future period. This ensemble is the result of the combination of two of the available options for cumulus (Grell and Kain-Fritsch), microphysics (Simple Ice and Mixed Phase) and PBL (Eta and MRF) parametrizations (Tab. 1). Common physics options are RRTM scheme for radiation and Noah Land-Surface Model. Documentation is available in the website http://www.mmm.ucar.edu/mm5.

Spatial configurations of the domains employed in the simulations consists of two two-way nested domains, arising a resolution of 30 km over the IP. Vertically, 24 sigma levels with the top at 100 mb are considered.

Table 1: Experiments identifiers. The last two are still under development.

Experiment	Microphysics	Cumulus	PBL
1	Simple Ice	Grell	Eta
2	Simple Ice	Grell	MRF
3	Simple Ice	kain-Fritsch	Eta
4	Simple Ice	kain-Fritsch	MRF
5	Mixed Phase	Grell	MRF
6	Mixed Phase	kain-Fritsch	Eta
7	Mixed Phase	Grell	Eta
8	Mixed Phase	kain-Fritsch	MRF

3. Results

The analysis focuses on multiyear seasonly mean values of two variables: 2-meter temperature and precipitation.

3.1. Temperature

The ensemble spread is caused by changes in the PBL scheme (being negligible the changes in other parameterizations). Overall, the MRF scheme for the PBL provokes the highest temperature increase (and also the highest absolute values), meanwhile the Eta scheme leads to the minimum variation and values. The average rise in the temperature is about 2 degrees for wintertime and more than 5 degrees during the summertime in the Iberian Peninsula (Fig. 1); however, it should be highlighted that the spread of these results is up to 50% of the estimated warming in some areas (Fig. 2).

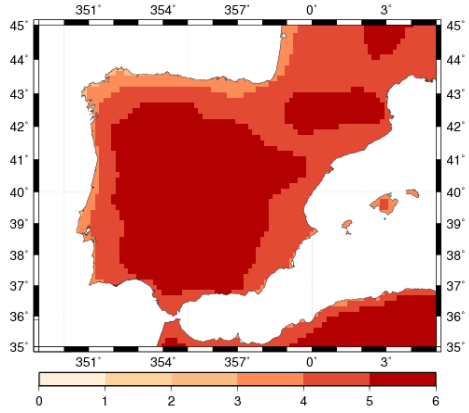

Figure 1: Mean JJA temperature increase projected, weighting all the ensemble members equally.

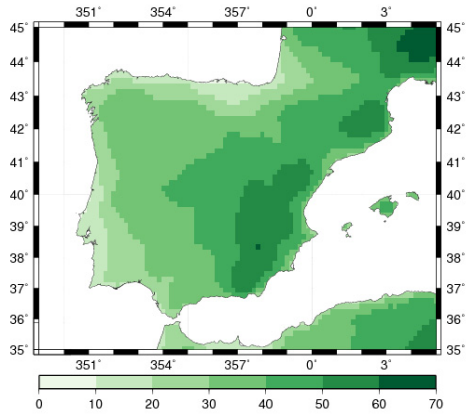

Figure 2: Ensemble spread in the projected JJA temperature increase in % with respect to the mean projected increase (shown in Fig. 1).

3.2. Precipitation

The ensemble spread is caused both by the selection of the PBL scheme and the cumulus parameterization, specially during the Autumn period. In contrast to other seasons and areas, an important increase in precipitation takes place in the eastern IP for that season (about 40% with respect to the reference period, Fig. 3), where convective precipitation dominates. The spread in the simulated data with the different schemes may achieve 100% in the aforementioned area (also in others), but all individual experiments project such increase (such agreement in the trend does not occur everywhere). For precipitation, no experiment is found to cause a dominant increase or decrease in the IP.

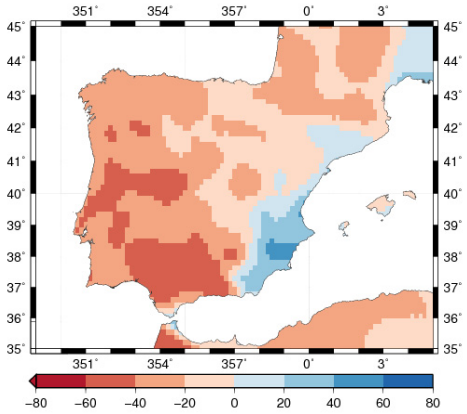

Figure 3: Mean SON precipitation change projected (in % with respect to the reference period), weighting all the ensemble members equally.

Figure 4 analises in detail the mentioned area located in the southwestern IP, where all experiments project an increase of the precipitation amount in Autumn. The leading parametrization regarding to the projected change is the PBL. The second factor of importance is the cumulus scheme employed, and there are no significant differences between experiments that only diffrer in the microphysics parametrization.

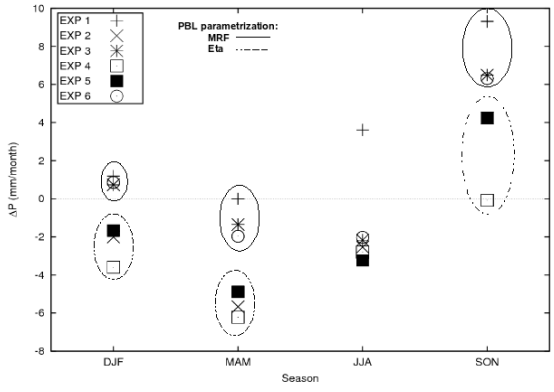

Figure 4: Precipitation change projected by each individual ensemble member averaged for the south-east area where all the emsemble members project an increase of the precipitation amount in Autumn. Note that experiments with different PBL parametrization are surrounded by different line types, and that in each subgroup the simulation with Grell cumulus parametrization provides the highest value.

4. Conclusions

The first conclusion is that RCMs are far away of being free of uncertainties, even in the hypothetical case that initial and boundary conditions were perfect (do not forget that the main uncertainty in order to simulate future projections cames from the inherent uncertainty of the future emision scenario (Giorgi et al., 2000; Déqué et al., 2007). Spreads of 50% and over 100% in the projected changes of temperature and precipitation, respectively, are found changing only the PBL parametrization in the described simulations. Therefore, given a fixed data base to the dynamical downscaling, this work shows that spreads from a multi-physics ensemble could be on the order of that from a multi-model ensemble (Déqué et al., 2007).

Nevertheless, some common signals are found and it allows to extract conclusions qualitatively. For example, no experiment projects a decrease in temperature for any season, and all project a higher increase for summer season. The unexpected signal of an increase of precipitaction in Autumn in the southwestern IP also appears in all the experiments, and all confirm that in this area the cumulus parametrization becomes greatly influential.

Also, precipitation projections present a larger disagreement between experiments that those for the temperature; leading schemes are the PBL for both temperature and precipitation, and also cumulus scheme in the case of precipitation. This kind of result could guide the modelers about where it is more necessary to stress for enlarging the confidence of such projections.

References

Christensen, J.H. and Christensen O.B., A summary of the PRUDENCE model projections of changes in European climate by the end of this century, *Climatic Change,* 81, 7-30, 2007

Grell, G.A., J. Dudhia and D.R. Stauffer, A description of the fifth-generation Penn State/NCAR Mesoscale Model (MM5), *Technical Report*, NCAR/TN-398+STR, 1994

Déqué, M., D.P. Rowell, D. Lüthi, F. Giorgi, J.H. Christensen, B. Rockel, D. Jacob, E. Kjellström, M. de Castro and B. van den Hurk, An intercomparison of regional climate simulations for Europe: assessing uncertainties in model projections, *Climatic Change,* 81, 53–70, 2007

Lenderink, G., A. van Ulden, B. van den Hurk and E. van Meijgaard, Summertime inter-annual temperature variability in an ensemble of regional model simulations: analysis of the surface energy budget, *Climatic Change,* 81, 233–247, 2007

Vidale, P.L., D. Lüthi, R. Wegmann and C. Schär, European summer climate variability in a heterogeneous multi-model ensemble, *Climatic Change,* 81, 209–232, 2007

Zhiwai, Y. and R.W. Arritt, Tests of a Perturbed Physics Ensemble Approach for Regional Climate Modeling, *American Meteorological Society,* 15, 2881-2896, 2002

Effect of internal variability on regional climate change projections

Klaus Keuler, Kai Radtke, and Andreas Will

Chair of Environmental Meteorology, Brandenburg University of Technology (BTU), P.O. Box 10 13 44, D-03013 Cottbus, Germany, e-mail: keuler@tu-cottbus.de

1. Motivation

Results of climate change projections are generally associated with uncertainties due to three major reasons:

- the insecurity of the future development of greenhouse gas (GHG) concentrations,
- the inaccuracy and diversity of the climate models used,
- the internal (natural) variability of the modeled climate system.

The main issue of this paper is to investigate the influence of the internal variability of a dynamically coupled global-regional climate model system on the results of a climate projection for the 21st century. The internal variability, which represents the natural variability of the climate system, is determined by comparing several simulations (realizations) of the same climate forcing (GHG rise) with the same unchanged model system.

2. Simulations

The model system being used in this study consists of the global climate model ECHAM5-MPIOM of the Max-Planck Institute in Hamburg and the regional climate model CLM 3.1, which is based on the operational weather forecast model COSMO-LM of the German Meteorological Service. The regional model operates at a horizontal resolution of 0.165° (about 18 km) in a rotated coordinate system with 32 vertical layers and is dynamically nested into six-hourly results of the global spectral model with the horizontal resolution T63 (about 180 km). The regional model domain includes whole Europe and the entire Mediterranean area with parts of northern Africa.

The global simulations start in 1860 and are continuously performed until 2100. Three simulations have been carried out with the same model configuration and the same GHG-forcing according to the emissions scenario SRES-A1B. The three simulations only differ in their initial state at January 1st 1860. Their results are incorporated into the IPCCC AR4 analysis of global climate scenarios.

The regional simulations downscaling the global model results cover the period from 1960 to 2100 and use the same GHG concentrations as the global simulations. The 20th-century period until the year 2001 has been simulated three times but has only been continued by 2100 for two of the three global realizations. Further details of the simulations and an extended quality analysis are given by *Hollweg et al.* (2008).

3. Results

The different realizations of the same climate forcing produce different temporal developments of the atmospheric conditions in the regional simulation. As a consequence, the daily, monthly and annual mean values of any meteorological variable are completely uncorrelated between the different realizations. However, on longer time-scales (several years to decades) their climatological means converge against each other. Figure 1 shows the annual means of temperature and precipitation of all three regional simulations averaged over the region of Germany. The curves partly show contrary developments of the annual values during time periods of several years and longer. Temperature values of single years can deviate up to 3 K, precipitation sums by more than 300 mm. The climatological means calculated over the entire 100 years of the scenario period, however, only differ by less than 0.1 K and 3 mm, respectively. This demonstrates that both realizations of the A1B-scenario represent the same climate conditions but also that the internal variability of the climate system leads to considerable different decadal variations along possible ways into the modified climate state.

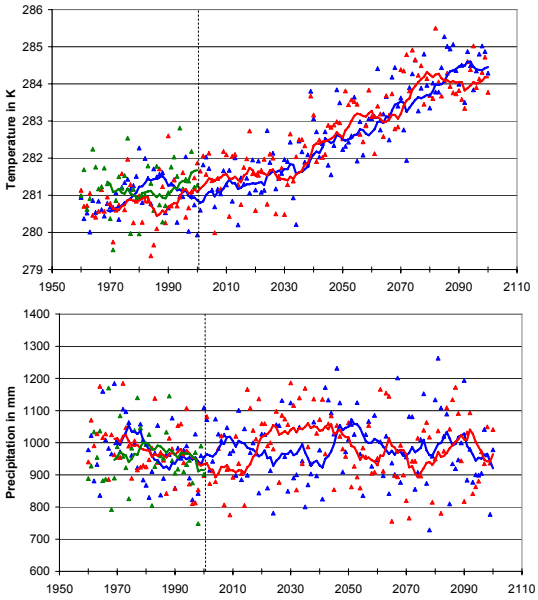

Figure 1. Temporal development of annual values (triangles) of 2-meter temperature (top) and precipitation sum (bottom) for Germany from different realizations of the A1B-scenario. The curves represent 10-year running means. The green one marks the 3rd realization of 20th century conditions which has not been continued beyond year 2000.

As climate change signals are usually determined by calculating the difference of multi-year climatological means of two separated periods, this variability causes different results for different realizations. These differences between the climate change signals of different realizations of the same climate forcing are a direct consequence of the internal variability of the climate system and provide an estimation of the "natural" or statistical uncertainty of climate change projections.

In order to quantify this uncertainty, climatological means of both scenario realizations are compared with the corresponding means of the three 20th century realizations (present-day climate reference). The selected periods are 2051-2080 and 1961-1990. The spread of the six differences between these periods – two representing the future scenario, three the present day conditions – expresses the natural uncertainty of the climate change projection. Its

knowledge is essential to assess confidence of the simulated tendencies.

Figure 2 summarizes the simulated climate changes for temperature and precipitation calculated from all six comparisons of the two periods. The areas between the upper and lower curves represent the uncertainty ranges of the simulated climate changes for the monthly means and the annual average. The values in this figure refer to the area average of Germany.

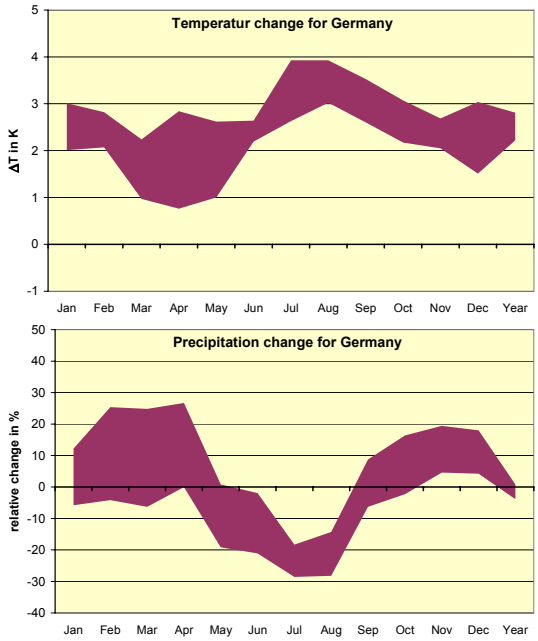

Figure 2. Climate change of 2-meter temperature (top, absolute change in K) and precipitation (bottom, relative change in %) for Germany from different realizations of the A1B-scenario. Values represent differences between the periods 2051-2080 and 1961-1990.

The increase of annual mean temperature varies between 2.2 and 2.8 K. The strongest warming occurs in August with values of 3 to 4 K. A reduced warming with less than 1 K seems possible in spring, but here the range of uncertainty with up to 2 K is larger than in other seasons. Despite the partly large spread of temperature changes a significant rise of temperature throughout the year seems very likely

The simulated changes of precipitation show a different behavior during the year. The annual sum does not change within the range of uncertainty. Summer precipitation, however, considerably decreases with maximum values in June and August between -14 and -28 %. Because the reduction is much stronger than the range of uncertainty, the drying in summer has to be regarded as confidential. The reduction in summer is compensated by an increase of precipitation during the other seasons particularly from October to May. The increase in winter and spring, however, is connected with a large range of uncertainty (up to 30 %) which reduces the level of confidence.

The precipitation changes of the corresponding global climate simulations calculated for the same region show a similar seasonal cycle (figure 3). However, the reduction in summer with up to -50 % is significantly stronger and expands over a longer period than in the regional simulation. Furthermore, the decrease is not fully compensated by the increase during the rest of the year. This leads to an overall reduction of annual precipitation by 10 %, which lies well outside of the calculated natural variability. This documents that the higher resolved regional simulations can significantly modify the projections of the global model.

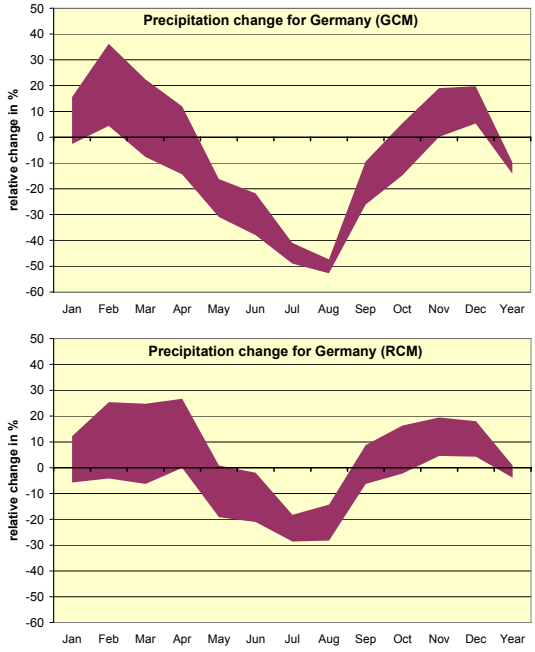

Figure 3. Precipitation changes for Germany form global (top) and regional (bottom) model simulations for the A1B-scenario.

4. Conclusions

The analysis of a small single model ensemble of climate simulations for Europe with the regional climate model CLM provides a first estimate of the effect of internal variability on the simulated climate changes for temperature and precipitation. The knowledge of this unavoidable natural uncertainty is a necessary precondition to assess the reliability (confidence) of climate change signals. The results further show, that the changes of climatological means as simulated by the regional model can significantly differ from those of the driving global simulation. "Significantly" means in this context that the deviations between global and regional projections are larger than explained by their internal variability.

References

Hollweg, H.-D., U. Boehm, I. Fast, B. Hennemuth, K. Keuler, E. Keup-Thiel, M. Lautenschlager, S. Legutke, K.Radtke, B. Rockel, M. Schubert, A. Will, M. Woldt, C. Wunram, Ensemble simulations over Europe with the regional climate model CLM forced with IPCC AR4 global scenarios. *M&D Technical Report*, No. 3, 145 pp. Max-Planck-Institute for Meteorology, 2008, *www.mad.zmaw.de/projects-at-md/sg-adaptation/*

An ensemble of regional climate change simulations

Erik Kjellström, Grigory Nikulin, Lars Bärring, Ulf Hansson, Gustav Strandberg and Anders Ullerstig

SMHI, SE 60176 Norrköping, Sweden, erik.kjellstrom@smhi.se

1. Introduction

Uncertainties in future climate change are related to uncertainties in external forcing, model formulation and natural variability. A common way to deal with uncertainties in external forcing is to use different emission scenarios thereby sampling a multitude of possible outcomes *Nakićenović et al*. (2000). By using multiple climate models or an ensemble of simulations with one model perturbed in its formulation of the physics, parts of the uncertainties related to how changes in forcing influence the climate can be assessed (*e.g. Meehl et al.*, 2007, *Murphy et al.*, 2007). To get a grip on the natural variability one may use several simulations with one climate model under the same emission scenario differing only in initial conditions. A way to handle all three main uncertainties is to perform several simulations constituting an ensemble. Previous attempts to do this on the regional scale in the European projects PRUDENCE (*e.g. Déqué et al.*, 2007) and ENSEMBLES (*Sanchez-Gomez et al*, 2008) have limitations in that only a few GCMs have been used to provide lateral boundary conditions (PRUDENCE) or that only one emission scenario has been considered (ENSEMBLES). At the Rossby Centre, a regional ensemble has been created that makes use of a number of GCMs, several emission scenarios, and in some case several simulations differing only in initial conditions in the GCM. The ensemble can be used to illustrate uncertainties on the regional scale and to produce probabilistic climate change information in a region.

2. Model and simulations

We use the regional climate model RCA3 (*Kjellström et al*., 2005) to dynamically downscale several experiments with global coupled atmosphere-ocean general circulation models (AOGCMs). Table 1 summarizes the experiments in terms of AOGCM (references for these are given in *Meehl et al.* (2007), emission scenario and horizontal resolution. In particular we study a subset of the simulations all under the A1B emission scenario and with five different forcing AOGCMs. This subset is denoted ENS5 in the following.

Table 1. Simulations in the Rossby Centre regional climate change ensemble. Number of simulations is given in parenthesis if more than 1. 3* denotes that 3 different members from the perturbed physics ensemble with HadCM3 are used. Simulations in italics constitute the "sub-ensemble" ENS5.

AOGCM	Emission scenario	Horizontal resolution (km)
BCM	*A1B*	25, 50
CCSM3	A2, *A1B*, B2	50
CNRM	*A1B*	50
ECHAM4	A2, B2	50
ECHAM5	*A1B* (3 at 50km), B1, A2	12.5, 25, 50
HadCM3	*A1B*	25, 50(3*)
IPSL	A1B	50

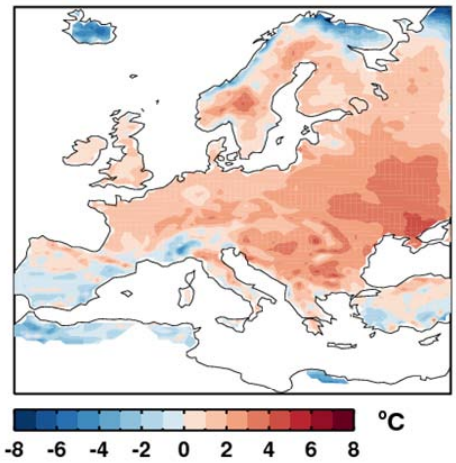

Figure 1. Difference in seasonal mean T_{2m} between ENS5 and the ENSEMBLES gridded dataset (*Haylock et al.*, 2008) for winter (DJF) conditions in the 1961-1990 period.

3. The recent past climate

We evaluate the ability of RCA3 to reproduce the recent past climate when forced on the lateral boundaries by the different AOGCMs. As the AOGCMs, and thereby RCA3, in general show a somewhat too zonal climate during winter the simulated temperature climate is too warm (Fig. 1) and too wet (not shown) over much of the continent.

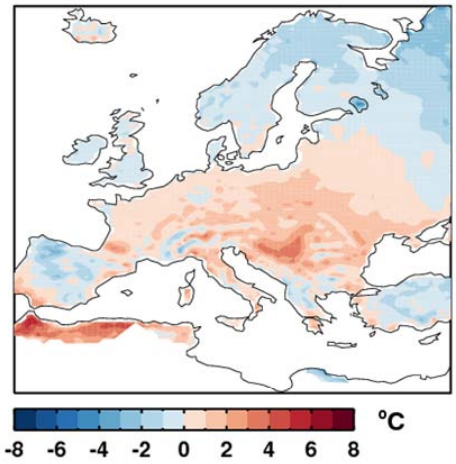

Figure 2. Difference in seasonal mean T_{2m} between ENS5 and the ENSEMBLES gridded dataset (*Haylock et al.*, 2008) for summer (JJA) conditions in the 1961-1990 time period.

In summer there is also a (weaker) warm bias in central Europe but now also a cold bias in the northeastern part of the domain (Fig. 2). The cold bias in the northeast is seen also in experiments in which RCA3 is forced by reanalysis data (*Kjellström et al*. 2005). In summer there are no

pronounced biases in the simulated MSLP fields (not shown) indicating that the biases in temperature and precipitation are more related to the regional climate model than to the large-scale circulation.

4. Climate change scenarios

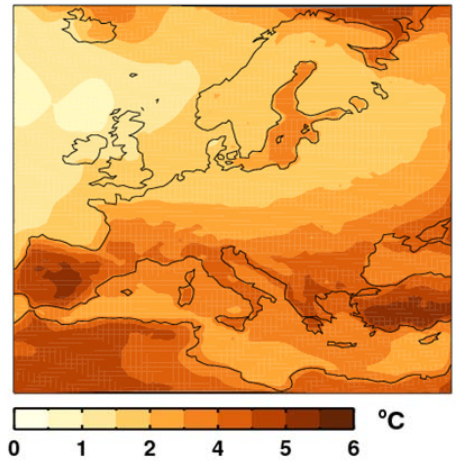

Figure 3. Change in seasonal mean T_{2m} between ENS5 2071-2100 compared to 1961-1990 for summer (JJA) conditions.

The ensemble mean (ENS5) shows a gradual evolution of the climate change signal with time both for temperature (Fig. 3) and precipitation (not shown). However, if single scenarios are considered, large differences can occur for single years, decades and even 30-year periods (not shown). Such differences can to some part be explained by natural variability as several scenarios with the same AOGCM differ substantially. Also daily variability changes with time. We note that these changes are largest where the signal is largest, as illustrated for summer in Figs. 3&4.

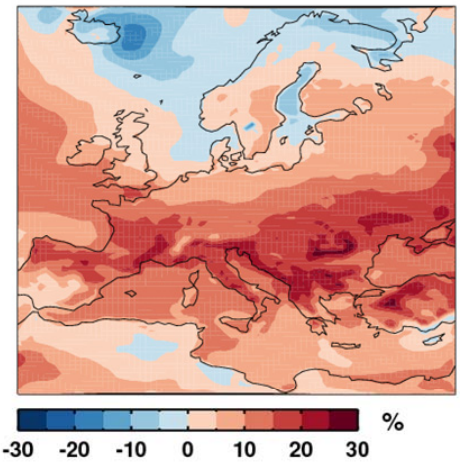

Figure 4. Relative change in daily standard deviation of T_{2m} for the ENS5 simulations for the time period 2071-2100 compared to 1961-1990 for summer (JJA) conditions.

5. Summary

The Rossby Centre regional climate change ensemble can be used to illustrate parts of the undertainties related to emission scenario, forcing AOGCM and natural variability. The results show that the main uncertainties by the end of the century are related to choice of forcing AOGCM and emission scenario. For the nearest few decades the role of natural variability is large.

6. Acknowledgements

This work is part of the Mistra-SWECIA programme, funded by Mistra (the Foundation for Strategic Environmental Research), and of the ENSEMBLES project funded by the EC through contract GOCE-CT-2003-505539. The GCM groups are acknowledged for providing models and boundary data. The model simulations with RCA3 were performed on the climate computing resource Tornado funded with a grant from the Knut and Alice Wallenberg foundation. We acknowledge the E-Obs dataset from the EU-FP6 project ENSEMBLES (http://www.ensembles-eu.org) and the data providers in the ECA&D project (http://eca.knmi.nl).

References

Déqué, M., et al., 2007. An intercomparison of regional climate simulations for Europe: assessing uncertainties in model projections. *Climatic Change*. 81, 53-70.

Haylock, M.R., et al. 2008: A European daily high-resolution gridded dataset of surface temperature and precipitation. J. Geophys. Res (Atmospheres), 113, D20119, doi:10.1029/2008JD10201

Kjellström, E., et al., 2005. A 140-year simulation of European climate with the new version of the Rossby Centre regional atmospheric climate model (RCA3). Reports Meteorology and Climatology, 108, SMHI, SE-60176 Norrköping, Sweden, 54 pp.

Meehl, G.A., et al., 2007: Global Climate Projections. In: Climate Change 2007: The Physical Science Basis. Contribution of Working Group I to the Fourth Assessment Report of the Intergovernmental Panel on Climate Change [Solomon, S.,D. et al., eds.)]. Cambridge University Press, Cambridge, United Kingdom and New York, NY, USA.

Murphy, J. M., et al., 2007. A methodology for probabilistic predictions of regional climate change from perturbed physics ensembles. *Phil. Trans. R. Soc. A*, 365, 1993-2028.

Nakićenović, N., et al., 2000. Emission scenarios. A Special Report of Working Group III of the Intergovernmental Panel on Climate Change. Cambridge University Press, 599 pp.

Sanchez-Gomez E. , et al., 2008: Ability of an ensemble of regional climate models to reproduce weather regimes over Europe-Atlantic during the period 1961-2000 , Clim. Dyn., 10.1007/s00382-008-0502-7.

Detailed assessment of climate variability of the Baltic Sea for the period 1950/70-2008

Andreas Lehmann, Klaus Getzlaff, Jan Harlass and Karl Bumke

Leibniz Institute of Marine Sciences at University of Kiel , alehmann@ifm-geomar.de

1. Introduction

The warming trend for the entire globe (1861-2002) is 0.05°C/decade. A specific warming period started around 1980 and continued at least until 2006. The temperature increase of that period is about 1°C (0.4 °C/decade). This trend is equally well evident for many areas on the globe, especially on the northern hemisphere in observations and climate simulations (IPCC 2007: WG1 AR4). Consequently, this warming appeared also for the Baltic Sea catchment. From 1960 to 1980 the air temperature for the catchment was close or slightly below the long-term mean with respect to the period 1871-2004, only between 1965-1975 the temperature was slightly above the mean. Then with the beginning of the 1980s the annual mean temperature increased by about 1°C until 2004.

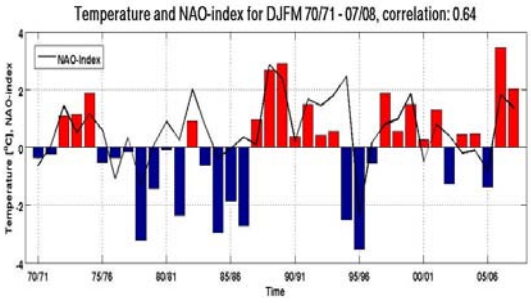

Figure 1 Winter air temperature anomaly (DJFM) at Kiel Lighthouse derived from SMHI-meteorological data base for the period 1970-2008 and winter NAO-index.

A similar warming trend could be observed for the SST of the Baltic Sea (Siegel et al. 2006; MacKenzie and Schiedek 2007). Since 1985, summer SSTs have increased at nearly triple the global warming trend, and for the period 1985-2002 summer SSTs have risen by 1.4°C, 2-5 times faster than in any other season. Even the annual mean water temperatures averaged spatially and vertically for the deep basins of the Baltic Sea show similar trends (Hinrichsen et al. 2007). Figure 1 shows the winter air temperature anomaly at Kiel Lighthouse for the period 1970-2008 based on the SMHI-meteorological data base. The number of anomalous warm winters has strongly increased for the period 1988-2008. The winter 2006/07 was about 3.5°C warmer than the seasonal mean over the period 1970-2008. The winters 2006/07 and 2007/08 were not only mild in the south-western Baltic area. The maximum sea ice extent in these years was extraordinarily small: for 2006/07 it was 139,000 km², and for 2007/08 a new low ice record was document, the ice cover being only about 49,000 km² which is the smallest since 1720 (Vainio and Isemer, 2008).

2. Methods and concepts

As climate, to a large extent, controls patterns of water circulation and biophysical aspects relevant for biological production, such as the vertical distribution of temperature and salinity, alterations in climate may severely impact the trophic structure and functioning of marine food webs. Since the mid-1980s an acceleration of climate warming has occurred which agrees remarkably well with a regime shift in the pelagic food webs (Hinrichsen, et al. 2007). To answer which are the processes linking changes in the marine environment and climate variability it is essential to investigate all components of the climate system. This will be performed by a detailed analysis of about 2 decades-periods before and after the regime shift.

Most of the studies of climate change in the Baltic Sea area have been restricted to the analysis of temperature records. The detailed analysis of changes in variability of atmospheric heat, radiation and momentum fluxes and their impact on the Baltic Sea has not been studied in detail. Her we will provide a detailed assessment of the variability of atmospheric variables and the corresponding response of the Baltic Sea including temperature, salinity and circulation for different time slices seasonally resolved within the period 1970-2008. NCEP/NCAR re-analysis data are available for the northern hemisphere for the period 1948-2008. However, NCEP/NCAR re-analysis data are only poorly resolved (2.5x2.5°, 6 hours) for the Baltic Sea area. Thus, the approach is to use additionally atmospheric data from the SMHI meteorological data base (1x1°, 3 hours, 1970-2008) together with COADS-data (at present 1949-2004), ICES Oceanographic data, IFM-GEOMAR atmospheric and oceanographic measurements (1987-2008) and BSH SSTs (1990-2008).

The main idea is to investigate in detail the climate variability of the Baltic Sea area as a whole and for the different sub-basins to assess the regional difference in response to the large scale atmospheric forcing.

3. Results

We used statistical analysis including basic and higher order statistics to discriminate the climatological conditions between different time slices and identify significant changes in atmospheric and oceanic variables.

As one example of our comprehensive analysis, Figure 2 shows the wavelet analysis of air temperature at the position of Kiel Lighthouse and NAO DJFM-winter indices (Figure 1). Interesting is the common structure of the wavelet analysis for temperature and NAO which reflects the high correlation between them. For the periods 1970-1987 and 1988-2008 there is also a change in the spectral characteristics of both temperature and NAO winter index. After 1985, higher variability occur at periods of about 2.5 and 5 years. Before 1985 highest

variability was concentrated at a period of about eight years which slightly shifted to longer periods.

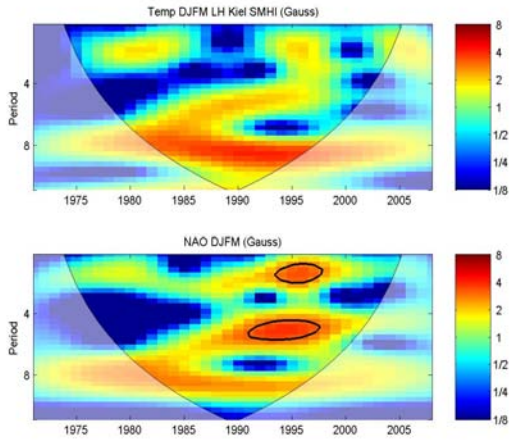

Figure 2. Wavelet analysis of air temperature at Kiel lighthouse and NAO DJFM winter indices. The thick black contour designates the 5% significance level against red noise and the cone of influence where edge effects might distort the picture is shown in lighter shade.

Additionally to the changes in temperature there is also a change in prevailing winds for the periods under consideration. Figure 3 shows the decrease in frequency of wind from westerly directions for autumn (SON) and an increase for winter (DJF). This shift in wind directions is associated also with a decrease of strong wind events during autumn and a corresponding increase in winter.

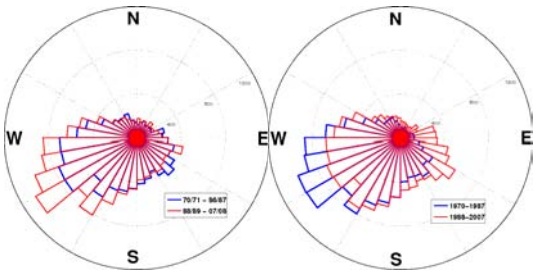

Figure 1. Frequency of wind events for autumn SON (left) and winter DJF (right) for the periods 1970-1987 (blue) and 1988-2008 (red).

From NCEP/NCAR reanalysis MSLP data, we calculated the first EOF for DJF for both periods (Fig. 4). Comparing the first with the second period reveals an intensification of the NAO/AO pattern and a slight shift to the east of the centers of action.

Hilmer and Jung (2000) observed a similar shift of the NAO pattern to the east when comparing the periods 1958-1977 and 1978-1997. Cassou et al. (2004) explained the shift by the asymmetry of the NAO pattern. For positve phases the NAO is located more easterly than for negative phases.

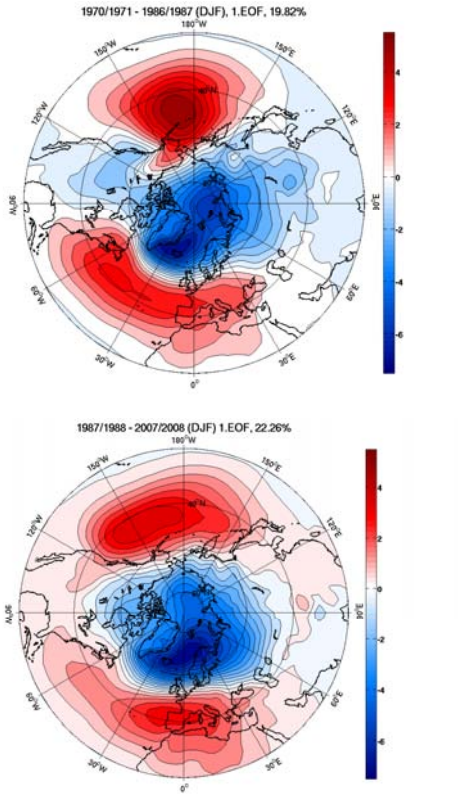

Figure 2. First EOF of MSLP data for DJF calculated from NCEP/NCAR reanalysis data for the period 1970-1987 and 1988-2008.

References

Cassou, C., Terray, L. Hurrell, J.W., Deser, C. North Atlantic winter climate regimes: Spatial asymmetry, stationarity with time, and oceanic forcing. *Journal of Climate* 17, 1055-1068.

Hinrichsen H.-H., Lehmann A., Petereit C., Schmidt, J. Correlation analysis of Baltic Sea winter water mass formation and its impact on secondary and tertiary production. *Oceanologia*, 49, 381-395, 2007

IPCC 2007, WG 1 AR4, www.ipcc.ch

Hilmer, M., Jung, T. Evidence for a recent change in the link between the North Atlantic Oscillation and Arctic sea ice export. Geophysical Research Letters, 27, 989-992, 2000.

Lehmann, A., Hinrichsen, H.H., Krauss, W. Effects of remote and local atmospheric forcing on circulation and upwelling in the Baltic Sea. *Tellus* 54: 299-316,2002

MacKenzie B.R., Schiedek, D. Daily ocean monitoring since the 1860s shows record of warming northern European seas. *Global Change Biology*, Vol. 13, 7, 1335-1347, 2007

Siegel H., Gerth M., Tschersich G. Sea surface temperature development of the Baltic Sea in the period 1990-2004. *Oceanologia*, 48, 119-131, 2006

Vainio, J., Isemer, H.-J. Mildest Ice winter ever in the Baltic Sea. BALTEX Newsletter No. 11.

Diurnal variation of precipitation over central eastern China simulated by a regional climate model (CREM)

Jian Li[1], Rucong Yu[1], Tianjun Zhou[2], Wei Huang[2] and Hongbo Shi[21]

1. State Key Laboratory of Severe Weather (LaSW), Chinese Academy of Meteorological Sciences (CAMS), China Meteorological administration, Beijing, China, lijian@cams.cma.gov.cn

2. State Key Laboratory of Numerical Modeling for Atmospheric Sciences and Geophysical Fluid Dynamics, Institute of Atmospheric Physics, Chinese Academy of Sciences, Beijing, China

This paper describes and evaluates the performance of a regional climate model developed at the State Key Laboratory of Numerical Modeling for Atmospherics Sciences and Geophysical Fluid Dynamics / Institute of Atmospheric Physics (LASG/IAP). The model has been developed based on the numerical forecast model, Advanced Regional Eta-coordinate Model (AREM), of LASG/IAP. An advanced radiation package and a common land surface scheme have been included into the AREM. The new model is regarded as the Climate version of AREM and named as CREM. To evaluate its performance in reproducing the summer climate over eastern China, the CREM was integrated from 1 May to 1 September of 1995-2004. The lateral boundary forcing data is derived from the NCEP-DOE (National Centers for Environmental Prediction-Department of Energy) reanalysis data at 6-h intervals. Evaluations on the model performance indicate that the CREM can reasonably reproduce the diurnal variation of summer precipitation over central eastern China. The late night peak of rainfall over South China and Northeast China is reproduced by CREM. Rainfall over the region between the Yangtze and Yellow Rivers is characterized by a semi-diurnal cycle, which peaks both in the early morning and in the late afternoon. The CREM can partly simulate this two-peak pattern. However, the regional model fails to reproduce the midnight maximum of rainfall in the eastern part of the Tibetan Plateau and the upper-middle Yangtze River valley.

Investigation of 'Hurricane Katrina' type characteristics for future, warmer climates

Barry H. Lynn[1], Richard J. Healy[2] and Leonard Druyan[2]

[1]Weather It Is, LTD, Efrat, Israel 90435 (barry.lynn@weather-it-is.com)
[2]Center for Climate Systems Research, Columbia University, New York, NY, USA.

1. Abstract

The goal of this study was to ascertain the potential impact of climate change on a "Hurricane Katrina' type storm. Hurricane Katrina was a devastating hurricane that made a direct hit on New Orleans, Louisiana. Extremely high winds and tides led to severe damage along the Louisiana coastline, as well as severe flooding in New Orleans. It has been suggested that warmer sea surface temperatures combined with higher atmospheric moisture humidity will lead to even worse storms during the rest of this century.

2. Approach

Evidence suggests that regional climate model simulations nested within GCM generated climate data are often compromised by unrealistic characteristics of the driving GCM (Rojas and Seth, 2003; Misra and Kanamitsu, 2004). Lynn et al. (2008) found that MM5 regional models running over the US and driven by NCEP reanalysis generated a more realistic frequency of heavy versus light precipitation events than when driven by the Goddard Institute for Space Studies Atmospheric-Ocean GCM (GISS AOGCM). They postulated that this was because reanalysis provided more realistic daily variability in the synoptic fields than the AOGCM. This presents a great challenge for regional climate studies that use GCM projections for downscaling climate change due to anthropogenic forcing.

The problem is especially acute in the current study, which aims to simulate the short-term variability of a Hurricane Katrina type storm, since important meteorological forcing cannot be supplied by the coarse- grid AOGCM.

To address this deficiency, this research introduces a new method, "mean-signal nesting," which strives to overcome some of the limitations of GCM inadequacies by creating more suitable initial and lateral boundary conditions (LBC) for driving a regional mesoscale model, in this case the Weather Research and Forecasting model (WRF; Skamarock et al., 2005). Misra and Kanamitsu (2004) improved initial and lateral boundary conditions (LBC) from a GCM by replacing GCM climatology with reanalysis climatology, while preserving the GCM's short-term variability. Their approach was suitable for correcting against model drift, thereby improving regional model seasonal forecasts. However, such an approach cannot be used for a 5-day simulation of hurricane development, where the sub-daily variability of the boundary conditions is crucial. Moreover, there is need here to account for climate change due to anthropogenic forcing. Hence, in the current study, AOGCM projections of future climate are combined with realistic 4x per day variability taken from August 2005 NOAA/NCEP Global Forecast System analysis data (GFS) on a 1° x 1° grid. More specifically, in mean-signal nesting, a mean climate-change signal (CCS) representing decadal climate evolution is derived from AOGCM projections and combined with the GFS to create initial conditions and LBC for driving WRF simulations. This approach is offered here as an alternative to exclusive AOGCM forcing. Just as mesoscale models can be driven with unadjusted GFS to downscale the current climate, the new approach uses the (adjusted) analysis data combined with the climate change signal as LBC for WRF simulations that project future climate scenarios.

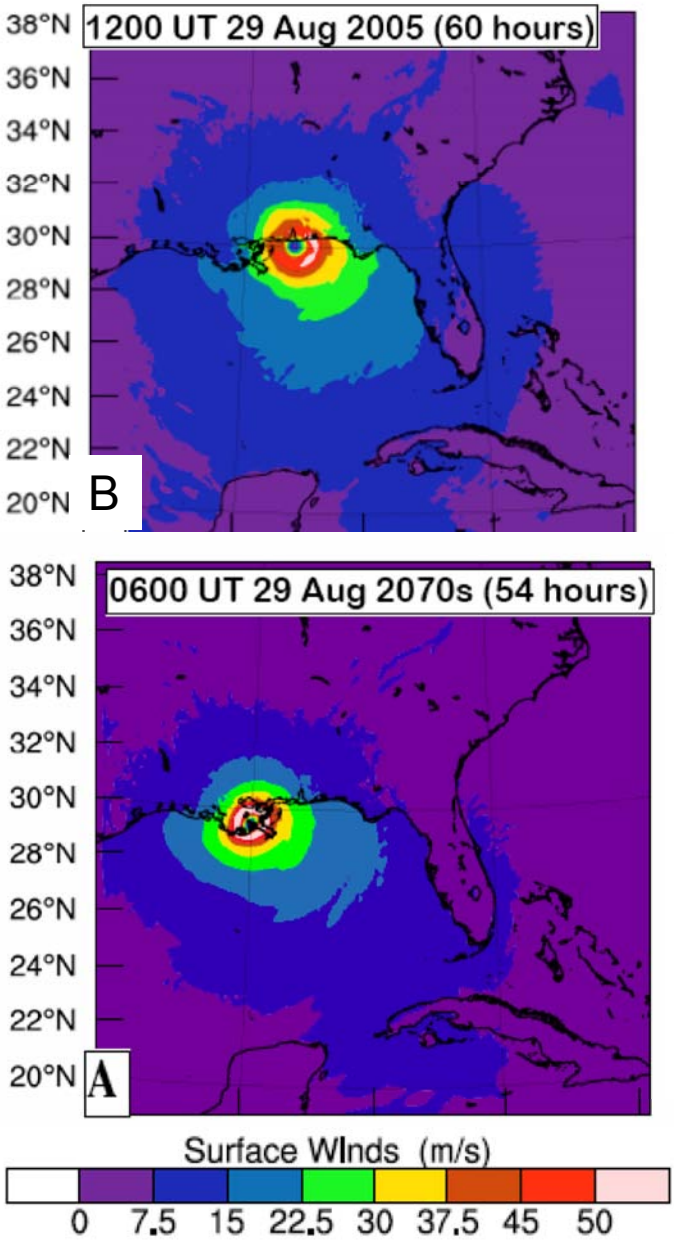

Figure 1. WRF simulated surface wind speed for A) 2070s and B) 2005 (control)

3. Experimental Design

The simulations of Katrina characteristics were made with the Weather Research and Forecasting (WRFv2.1) model run over a limited area. The WRF domain included the Gulf of Mexico, southeast US and the adjacent North

Atlantic Ocean (19-39°N, 75-95°W). WRF horizontal grid spacing was 9 km and the model was integrated at 31 vertical levels. All simulations covered the period August 27-31. WRF simulations were forced by data derived from the A2 climate change scenario defined by the IPCC (2007), as simulated by the GISS AOGCM (Russell et al. 1995; Rangwala et al. 2006). The AOGCM uses a 4° x 5° horizontal grid at nine vertical atmospheric levels and 13 vertical ocean levels.

4. Results

Simulations of Hurricane Katrina using the WRF model on a 9 km grid over the Gulf of Mexico and the Southeast US were analyzed during the period August 27-30, 2005. The control captured many of the observed characteristics of Katrina (not shown), although the predicted center was about 150 km to the actual land falling position. WRF storm tracks were determined from the locations of minimum sea-level pressure every three hours. (not shown). The tracks of the storms in the first half of the century were mostly east of the simulated (control) 2005 storm. Tracks in the second half the century were mostly west of the control.

Vertical profiles of the Gulf of Mexico averaged u-wind component from the GCM for simulations representing the earlier decades showed a large positive vertical shear relative to the CTL, reaching maxima between approximately 12-16 km altitude. Profiles from the latter decades showed a negative anomaly shear up to about 8-10 km altitude. Each consistent with the differences in tracks discussed above. The vertical shear of the zonal wind is proportional to north-south temperature gradients. The negative shear in the simulations representing the second half of this century indicates a weakening or a reversal of the usual south to north temperature gradient. This can occur when the continent north of the Gulf of Mexico becomes excessively warm compared to the water temperature. In contrast, the GCM sea surface temperatures were predicted to fall in the first two decades, explaining in part the positive anomalies in the u-wind component during this time. However, predicted Gulf of Mexico sea surface temperatures exceeded those of the present decade from the 2030s onward, increasing by about 3 ^{o}C by the 2090s.

Fig. 1 compares the horizontal distribution of surface wind speed of the 2070s to the control. After 54 hours (06 UT on August 29). the 2070s storm center crossed the Louisiana coastline at 90°W, displaced further west from the control. The 2070s storm is more compact than the control. For example, the diameter within which its wind speeds exceed 30 m/s is about 20% smaller than for the control (2.9° versus 3.6°). Hence, the average wind speeds within, for example, 180 km of the core were less than in the control. Nevertheless, the future storm maintained its core of very high winds better than the control as it approached the coast. The 2070s storm shows narrow rings of wind speeds in excess of 50 m/s. but unlike the control its bands of wind speed exceeding 50 m/s completely surround the storm center. Similar results were obtained for the simulated storm in the 2080s.

5. Sensitivity Tests

Figure 2 shows WRF simulated hurricane minimum surface pressures versus Gulf of Mexico sea-surface temperatures. There is a good relationship between the two, except in the 2090s (when an anomalous track of the storm sent it to close to the Florida Pan Handle). Hence, one might wonder why there are not larger *and* more severe hurricanes in the second half of the 20th century.

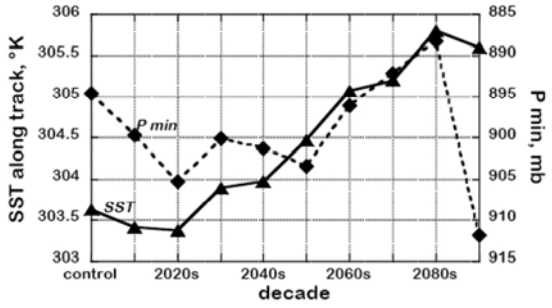

Figure 2. WRF simulated minimum hurricane pressures versus Gulf of Mexico averaged sea-surface temperatures in each decade.

Sensitivity tests showed that predicted, decadal increases in atmospheric temperature anomalies (with peak values of 12 ^{o}C found at about 10 km) prevented further storm intensification.

6. Conclusions

Results suggest that during the latter part of the 21st century, the radius of strong winds in a Katrina- like storm will decrease, but the pressure minimum will be more extreme and maximum wind speeds will be higher and more prolonged after landfall. Thus, the extremely low minimum pressures for 2070s and 2080s storms were apparently caused by the very high SST the storms encountered over the Gulf of Mexico, while their relatively small diameters may reflect the high vertical thermal stability of the late decades. Our results, using real boundary conditions modified by a climate change signal, suggest that the danger to coastal locations from the high winds of severe hurricanes could increase in the latter half of this century.

References

Lynn, B, Healy R, Druyan L, 2008: Quantifying the sensitivity of simulated climate change to model configuration. Climatic Change. 92, p. 275.

Misra V, Kanamitsu M, 2004: Anomaly Nesting: A methodology to downscale seasonal climate simulations from AGCMs. J Climate 17: 3249-3262.

Rangwala I, Miller J R, Russell G L, Xu M, 2006: Analysis of global climate model experiments to elucidate past and future changes in surface insolation and warming in China. Geophys Res Lett 33: L20709, doi:10.1029/2006GL027778.

Rojas M, Seth A, 2003: Simulation and Sensitivity in a Nested Modeling System for South America. Part II: GCM Boundary Forcing. J Climate 16: 2454-2471.

Russell G L, Miller J R, Rind D, 1995: A coupled atmosphere-ocean model for transient climate change studies. Atmosphere-Ocean 33: 683–730.

Skamarock W C, Klemp J B, Dudhia J, Gill D O, Barker D M, Wang W, Powers J. G., 2005: A description of the advanced research WRF version 2. NCAR Technical Note NCAR/TN-468+STR, National Center for Atmospheric Research (NCAR), Boulder Colorado (Revised January 2007).

Evaluation of seasonal forecasts over the northeast of Brazil using the RegCM3

Rubinei Dorneles Machado[1] and Rosmeri Porfírio da Rocha[1]

[1] University of São Paulo, São Paulo, Brazil; rmvip@usp.br

1. Introduction

Several works discussed the limitations of AGCMs (Atmospheric General Circulation Models) for climate forecasting due to the low horizontal resolution typically used in these models (*Giorgi and Mearns,* 1999). The interest in regional climate models (RCMs) is associated with the more appropriated physical parameterizations and higher spatial resolution that they can utilizes providing better representation of the sub-grid processes and thus reducing the errors found in AGCMs (*Sen et al.* 2004).

Over northeastern Brazil *Misra* (2006) shows that the COLA AGCM did not present any ability to predict February-March-April rainfall anomalies during the years considered as normal, i.e. without influence of the large-scale phenomena like El-Niño/La-Niña. A common systematic error in some AGCMs is the overestimation of the austral summer precipitation over the northeast Brazil (*Cavalcanti et al.*, 2002). Climate studies using RCMs are becoming more frequent and important as they can reduce the systematic errors of AGCMs in some regions (*Seth et al.*, 2007). The RCMs have been used not only for hindcasts of past climate, but also for seasonal climate predictions (*Chou et al.*, 2001) with the aim of also capture the regional aspects of the climate. Considering the interest in the application of the RegCM3 (Regional Climate Model version 3; Pal et al., 2007) for seasonal forecasting, *Cuadra and da Rocha* (2007) studied the sensitivity of the simulations on the southeastern South America to the specification of SST (sea surface temperature). They show that the persisted SST affects little the simulation of austral summer anomalies of precipitation and air temperature over the continental parts of south-southeast Brazil. For this work, the goal is to investigate the performance of seasonal forecasting over northeast Brazil using the RegCM3 nested in the CPTEC/COLA (Center for Weather Forecasting and Climate Studies/Center for Ocean-Land-Atmosphere Studies) AGCM.

2. Methodology and Data Set

The RegCM3 is a primitive equation model, compressible, and in the sigma-pressure vertical coordinate. A recent description is given in *Pal et al.* (2007). In this study the RegCM3 was integrated in the domain of Figure 1 using 60 km of horizontal resolution, 18 vertical levels, and Grell convective scheme with the Fritsch-Chappell closure. The RegCM3 forecasts used the initial and boundary conditions of the CPTEC/COLA AGCM, which is described by *Cavalcanti et al*. (2002), and over the Oceans the persisted SST was specified. The 27 forecasts analyzed were initiated at 00 UTC of day 16 of each month. The first 14-15 days of integrations were considered as spin-up and the quarter of validation correspond to the average of the following three months. This average is referred as seasonal forecasts.

For validation of precipitation we used the rainfall data from CPC (Climate Prediction Center) analysis that has horizontal resolution of 1 ° x 1 ° latitude by longitude (*Silva et al.*, 2007). The air temperature was compared with the NCEP re-analysis (*Kalnay et al*. 1996) that is in a Gaussian grid with about 1.875º of horizontal resolution.

To perform an objective analysis on the subdomain Northeast (NDE) (Figure 1) were calculated quarter averages of seasonal climate forecasts, the linear correlation coefficient and the index of efficiency of *Nash and Sutcliffe (1970)* of time series. This index indicates the skill of RegCM3 forecasts regarding the average of the observations.

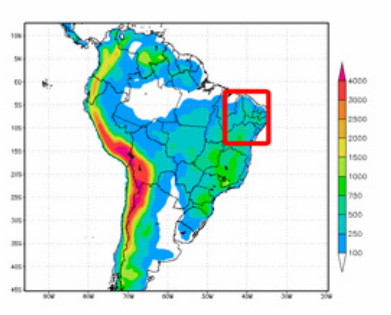

Figure 1. Forecast domain and topography (shaded with scale at right) and the NDE subdomain (red box) used to evaluate the RegCM3 forecasts.

3. Results

The Figure 2a shows over the NDE the area average seasonal rainfall provided by CPC analysis, CPTEC/COLA and RegCM3. It is important to note the lack of ASO/2006 values due to the post-processing problems. Figure 2a shows the overestimation of seasonal rainfall by the CPTEC/COLA model in all quarters, except in FMA/2006. Apparently there is a displacement of the rainy season from FMA of the CPC to MAM in CPTEC/COLA forecasting. According to *Oyama* (2006) and our seasonal maps (Figure not shown) errors in the positioning of ITCZ (Intertropical Convergence Zone) and SACZ (South Atlantic Convergence Zone) found in low horizontal resolutions AGCMs, including CPTEC/COLA, can justify the wet bias in the northeast Brazil. In contrast, Figure 2a indicates that RegCM3 produces a superior forecasting of seasonal precipitation during all the 27 quarters. This improvement could be due to higher horizontal resolution of the RegCM3 that also improves the ITCZ localization.

The area average air temperature over NDE (Figure 2b) presents small annual amplitude with maximum and minimum values during the dry and wet seasons, respectively. Both RegCM3 and CPTEC/COLA models underestimates the air temperature during all seasons (Figure 2b). However, Figure 2b shows that inter-seasonal air temperature variability is well reproduced by RegCM3, while CPTEC/COLA is out of phase regarding the analysis as well as it occurs for rainfall (Figure 2a). This is due to the control of the rainfall over the air temperature. In the NDE area, located near the equator, the solar radiation is almost constant throughout year. During the rainy season there is an increase of cloudiness that reduces the net solar radiation and the air temperature. The opposite behavior is obtained during the dry periods.

The linear correlation coefficients show that RegCM3 had superior performance than CPTEC/COLA to reproduce the inter-seasonal variability of precipitation (0.84 against 0.64) and air temperature (0.90 against 0.30) in the NDE area. This is associated to the correction by RegCM3 of the out of phase seasonal values of the CPTEC/COLA forecasts (Figure 2).

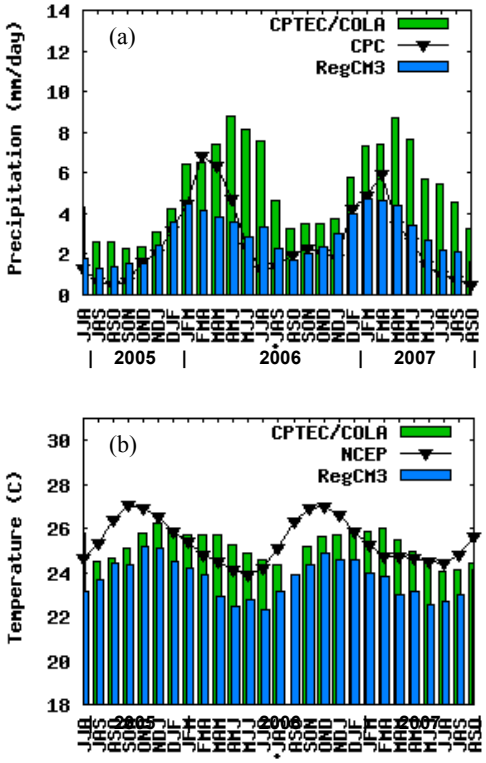

Figure 2. Seasonal averages over NDE of precipitation (a) and air temperature (b).

The efficiency coefficient (E) for RegCM3 is positive (0.62; Table 1), what indicates that the model is better predictor of the seasonal rainfall than the average (calculated for all the 27 seasons) of the analysis of the CPC. The systematic negative bias of air temperature in RegCM3 forecasts produces a negative E coefficient (Table 2). However, if this bias is removed of the time series, the efficient coefficient (E_b) increases to 0.8 indicating the superior forecast of RegCM3 over the mean of observations. The CPTEC/COLA presents negative E values for both precipitation and air temperature (Table 1) and this is justified by the bias and out phase seasonal values (Figure 2) found in these forecasts. Comparatively, the efficiency coefficient indicates that RegCM3 is better predictor of seasonal rainfall and air temperature over the NDE than CPTEC/COLA model.

4. Conclusions

This study evaluated the seasonal climate forecasts on the Northeast of Brazil using the RegCM3 nested in the CPTEC/COLA AGCM. The 27 seasonal forecasts were compared with analysis of the CPC (precipitation) and NCEP re-analysis (air temperature). The most important result is that RegCM3 correct simulates systematic out of phase mean values of rainfall and air temperature that is found in the CPTEC/COLA AGCM forecasts. This implied that RegCM3 was better predictor of mean seasonal rainfall than the mean of analysis with efficiency coefficient near 1 and temporal correlation of 0.84. This high correlation indicates that RegCM3 reproduces the inter-season variability of seasonal rainfall similar to the analysis. For air temperature, RegCM3 seasonal mean also shows high correction with the analysis (0.89) and after the correction of it systematic cold bias the efficiency coefficient approximates of 1. This coefficient sensitize that RegCM3 (CPTEC/COLA) is better (worse) preditor of the mean seasonal values of air temperature and rainfall than the mean of observations in the period analysed.

5. Acknowledgments

The present study was supported by CNPq and FAPESP (Grant #2001/13925-5). We thank the NCEP, CPC/NOAA and ICTP for providing the data set and model.

Table 1 – Averages of the 27 quarter for the analysis (CPC or NCEP) and RegCM3 and CPTEC/COLA forecasts, coefficient of efficiency (E) and linear correlation (r) for precipitation and air temperature. The value in parenthesis is the E after bias correction.

Precipitation	Mean (mm/day)	r	E
CPC	2.6	-	-
RegCM3	2.9	0.84	0.62
CPTEC/COLA	5.2	0.64	-1.86
Air Temperature	**Mean (^oC)**		
NCEP	25.4	-	-
RegCM3	23.7	0.89	-2.27 (0.80)
CPTEC/COLA	25.2	0.30	-0.05

References

CAVALCANTI, I. F. A; MARENGO, J. A., SATYAMURTY, P., *et al.* Global climatological features in a simulation using CPTEC/COLA AGCM. *J. of Climate,* Boston v.15, p. 2965-2988, 2002.

CHOU, S. C.; Nunes, A. M. B.; Cavalcanti, I. F. A. Extended range forecasts over South America using the regional eta model. *J. Geophys. Res.*, v. 105, n. D 8, p. 10147-10160, 2001.

CUADRA, S. V.; da ROCHA, R. P. Sensitivity of regional climatic simulation over Southeastern South America to SST specification during austral summer. International. *J. of Climatology*. v. 27, p. 793-804, 2007.

GIORGI, F.; MEARNS, O. Introduction to special section: regional climate modeling revisited. *J. Geophys. Res.*, v. 104, p. 6335-6352, 1999.

KALNAY, E., *et al* 1996: NCEP/NCAR 40-year Reanalysis project. *Bull. Amer. Meteor. Soc.*, 77, 437-471.

MISRA, V. et al.: Dynamic Downscaling of Seasonal Simulation over South American. *J. Climate*, Boston, v. 16, p. 103-117, 2003.

SEN, O. L., WANG, Y.; Wang, B. Impact of Indochina deforestation on the East-Asian summer monsoon. *J. Climate*, Boston. v. 17, p. 1366–1380, 2004a.

MISRA, V. Understanding the predictability of seasonal precipitation over northeast Brazil. *Tellus*, v . 58A, p. 307-319, 2006.

NASH J. E., SUTCLIFFE J. V., 1970: River flow forecasting through conceptual models part I — A discussion of principles. *J. Hydrology*, Volume 10, Issue 3, Pages 282-290.

OYAMA, M. D. Erros sistemáticos no clima da região tropical da América do Sul simulado pelo modelo regional MM5 em baixa resolução horizontal. *RBMET*, v. 21, n. 1, p. 118-133, 2006.

PAL, J.S. and Coauthors. Regional Climate Modeling for the Developing World: The ICTP RegCM3 and RegCNET. *BAMS*, v. 88, p. 1395-1409, 2007.

SETH, A.; RAUSCHER, S.A.; CAMARGO, S. J.; *et al.* RegCM3 regional climatologies for South America using reanalysis and ECHAM global model driving fields. *Clim. Dyn.*, v. 28. p. 461–480, 2007.

SILVA, S. B. V., KOUSKY, E. V., SHI, W.; *et al.* An Improved Gridde Historical Daily Precipitation Analysis for Brazil. *J. Hydrometeorology*. v. 8, p. 848-861, 2007.

An evaluation of surface radiation budget over North America in a suite of regional climate models

M. Markovic[1], C. G. Jones[1], P. Vaillancourt[2], K. Winger[1], D. Paquin[3]

[1]Department of Earth and Atmospheric Sciences, UQAM, 550 Sherbrooke West, 19th floor, West Tower, Montreal H3A 1B9, Canada, [2]Numerical Forecast Research Branch, Environnment Canada, [3]Consortium Ouranos, Montreal, Canada
e-mail: markovic@sca.uqam.ca

In this study we evaluate the components of the surface radiation budget (SRB) (downwelling longwave, DLR and incoming shortwave radiation, ISR) in three regional climate models (RCMs): CRCM (The Canadian Regional Climate Model), GEM-LAM (Regional version of Global Environmental Multiscale Model) and RCA3 (Regional model of Rossby Centre, Sweden) against surface observations. All three RCMs use different radiation and cloud schemes, characterizing systematic errors in the SRB as a function of climatic conditions will aid in model improvement.

The RCMs will be directly compared with available surface-based measurements (SURFRAD Network) over different conditions. We will determine the quality of the simulated radiation budget in the respective models and target the areas and climatic conditions where the models give the worst results. By evaluating the surface radiation budget in a variety of climate conditions, for cloudy and clear conditions separately and as function of season and time of day, we aim to isolate conditions and situations where the respective cloud and radiation schemes operate poorly and identify aspects of the parameterization schemes that are causing these simulation errors.

While surface based radiation observations offer accuracy at high temporal resolution, they do not allow full evaluation of the simulated SRB and cloud cover across the entire North America. In order to compare the RCMs over wider geographical domain we first evaluate ISR, DLR and cloud cover for various possible observational surrogate datasets: ERA40 (ECMWF Reanalysis), NARR (North American Regional Reanalysis, NCEP) and ISCCP (International Satellite Cloud Climatology Project).

Climate change assessment over Iran during future decades by using the MAGICC-SCENGEN Model

Majid Habibi Nokhandan 1 , Fatemeh Abassi 2, Azade Goli Mokhtari,3 and Iman Babaeian 4

1.Assistant Prof (ASMIRC) and Director of CRI, habiby_2001@yahoo.com
2.Msc of Meteorology -Climatological Research Institute(CRI)
3.Phd Student of Geomorphology
4.Phd Student of climatology, Tabriz University and deputy of Kh.Razavi Met office Mashad, I.R. of Iran.,

In this paper, we modeled the climate of Iran for future periods. Each period is a 30-years period centered on a year. The range of periods is from 2000 (i.e., 1986-2015) to 2100 (i.e., 2086-2115). This was made using 2 General Circulation Models (ECHAM4 and HadCM2) and 18 IPCC scenarios. MAGICC-SCENGEN was used as a tool for downscaling GCM low resolution output data. Result of HadCM2 model shows a 2.5% decrease in precipitation until 2100 but ECHAM4 shows a 19.8% increase for this period. Another difference between results of these 2 models is that HadCM2 predicts an increase in precipitation in next decades for Mazandaran, Golestan, Khorasan Shomali, Khorasan Razavi, Semnan, Tehran and some parts of Gilan and Ghazvin provinces, while ECHAM4 predicts a decrease for that regions. HadCM2 predicts precipitation decrease for southeast of country (Hormozgan, Kerman, Bushehr, south of Fars and some parts of sistan va Baloochestan, but in ECHAM4 that regions will have precipitation increase in similar period. About temperature, both HadCM2 and ECHAM4 agree in temperature increase in next decades for all provinces. These 2 models predict, on the average, 3 to 3.6□c increases in temperature until decade 2100. Maximum increase in decadal temperature in ECHAM4 is about 1°C more than HadCM2 and both of them are in conformity with each other in spatial distribution of decadal temperature.

Key Words: Climate Change, General Circulation Model, Magicc-Scengen, ECHAM4, HadCM2

Dynamical downscaling of ECMWF experimental seasonal forecasts: Probabilistic verification

Mirta Patarčić and Čedo Branković

Croatian Meteorological and Hydrological Service, Gric 3, 10000 Zagreb, Croatia, patarcic@cirus.dhz.hr

1. Introduction

Predictability of the atmosphere on seasonal time scales mostly depends on lower boundary forcings such as sea surface temperature, surface albedo, soil moisture and snow cover. They are defined on global scales and have influence on distant regions. Therefore, seasonal forecasts are made with global coupled atmosphere, ocean and land surface models. One way of increasing spatial and temporal scales of a global model's results is dynamical downscaling by a regional climate model. In this study we used the 50-km Regional Climate Model (RegCM, Pal et al. 2007) to dynamically downscale ECMWF experimental seasonal integrations from the EU ENSEMBLES project.

Due to uncertainties in initial conditions and uncertainties in representation of physical processes, predictions on seasonal time scales are inherently probabilistic. Reliable seasonal forecasts can be made by using ensembles of integrations that enable probabilistic approach to a particular event. In order to assess the quality of probability forecasts it is necessary to perform forecast verification. Verification of probabilistic forecasts of summer 2m temperature has been done for both models.

2. Experiments

Dynamical downscaling has been done for nine-member ensembles for summer (July-September, JAS) season for the 11-year period (1991-2001). RegCM domain covered central and southern Europe and the Mediterranean.

The data from Climatic Research Unit (CRU) from University of East Anglia (New et al. 2002) were used for verification.

3. Methods of analysis

Probabilistic verification of seasonal ensemble integrations for global and regional model is made with emphasis on Brier score, reliability and resolution.

Brier score is the mean squared error of the probability forecasts (Palmer et al. 2000 and Wilks, 2006):

$$BS = \frac{1}{N}\sum_{i=1}^{N}(p_i - v_i)^2, \quad 0 \le p_i \le 1, \; v_i \in \{0,1\}$$

where p_i is probability, v_i is observation and N is the number of forecast-event pairs over all ensemble members and grid points in 11 years. Probabilities are calculated as a fraction of ensemble members predicting particular event forming 10 probability bins.

Reliability diagrams are constructed by plotting hit rate (HR) for each probability bin against corresponding forecast probability. HR for each probability bin is defined as:

$$HR_n = \frac{O_n}{O_n + NO_n}$$

where n is the number of nth bin, O_n is number of observed occurrences and NO_n number of observed non-occurrences in each probability bin.

Relative operating characteristic (ROC) diagrams are constructed by plotting hit rate against false alarm rate (FAR) for accumulated probability bins (i.e. for each probability threshold P_n).

For each probability threshold P_n HR and FAR are defined as:

$$HR_n = \left(\sum_{i=n}^{N} O_i\right) \Big/ \left(\sum_{i=1}^{N} O_i\right)$$

$$FAR_n = \left(\sum_{i=n}^{N} NO_i\right) \Big/ \left(\sum_{i=1}^{N} NO_i\right)$$

where N is total number of probability bins.

For verification purposes global and regional model outputs were interpolated to CRU grid (0.5deg). Since the CRU data are defined over land, verification was performed for land points only. 2m temperature anomalies were calculated as differences of seasonal means and model/verification climatology.

4. Results

Skill measures have been calculated for 2m temperature anomalies for the summer season for the whole regional model domain and southern part of the domain (south of 48°N). Brier score, reliability diagram and relative operating characteristic were determined for three events: JAS 2m temperature anomaly above normal (0.0 K), above 0.1 K and 0.5 K.

According to all skill measures for temperature anomalies above normal, both models have better results for the southern part of the domain than for the entire domain indicating an increased potential seasonal predictability for south Europe.

Brier score, which is negatively oriented, for global model in the southern part is 0.20, and for the whole domain 0.25.

Forecasts are more reliable in the southern part of the domain, which is indicated by the proximity of the curve to the diagonal line in reliability diagram in Fig. 1.

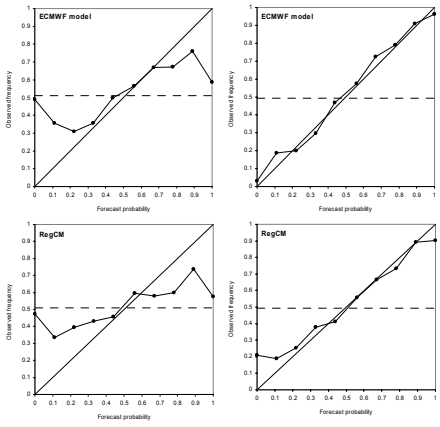

Figure 1. Reliability diagram for global (upper panels) and regional model (lower panels), for entire (left) and southern part of the domain (right) for JAS 2m temperature above normal.

For relative operating characteristic, measure of skill is given by the area under ROC curve (A). Perfect forecasts will have A=1, and no-skill forecasts will have A=0.5. For global model and the entire domain A=0.65, and in the southern part A=0.76 (upper panels in Fig.2).

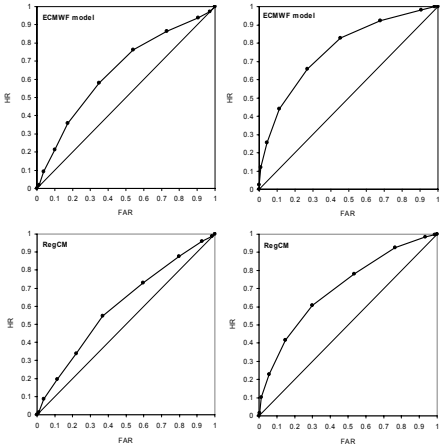

Figure 2. Relative operating characteristic for global (upper panels) and regional model (lower panels), for entire (left) and southern part of the domain (right).

We obtained similar results for both models for the other two thresholds. Table 1. gives a summary of Brier scores and areas under the ROC curves for both models/domains and all thresholds. In all cases (both domains and all thresholds) the global model is more skilful than the regional model.

Table 1. Brier score (BS) and area under the ROC curve (A) for both models/domains and all thresholds.

threshold	0.0 K		0.1 K		0.5 K	
	BS	A	BS	A	BS	A
entire domain						
ECMWF	0.25	0.646	0.25	0.652	0.22	0.659
RegCM	0.26	0.603	0.26	0.607	0.23	0.610
southern Europe						
ECMWF	0.20	0.760	0.20	0.760	0.18	0.732
RegCM	0.22	0.702	0.22	0.701	0.19	0.685

References

New M, D. Lister, M. Hulme and. I. Makin, A high-resolution data set of surface climate over global land areas. Clim. Res., Vol. 21, pp. 1-25, 2002

Pal, J.S., F. Giorgi, X. Bi, N. Elguindi, F. Solmon, X. Gao, S.A. Rauscher, R. Francisco, A. Zakey, J. Winter, M. Ashfaq, F.S. Syed, J.L. Bell, N.S. Diffenbaugh, J.Karmacharya, A. Konare, D. Martinez, R.P. da Rocha, L.C. Sloan and A.L. Steiner, Regional climate modelling for the developing world, Bull. Amer. Meteor. Soc., Vol. 88, No. 9, pp. 1395-1409, 2007

Palmer T.N., C Brankovic and D.S. Richardson, A probability and decision-model analysis of PROVOST seasonal multi-model ensemble integrations, Q. J. R. Meteorol. Soc., Vol. 126, No. 567, pp. 2013-2033, 2000

Wilks D.S., Statistical methods in the atmospheric sciences (2nd ed.). Academic Press, p. 648, 2006

Cutoff-Low Systems: Comparison NCEP versus RegCM3

Michelle Simões Reboita[1], Raquel Nieto[2], Luis Gimeno[2], Rosmeri Porfírio da Rocha[1] and Tércio Ambrizzi[1]

[1] University of São Paulo, São Paulo, Brazil; [2] University of Vigo, Ourense, Spain; reboita@model.iag.usp.br

1. Introduction

Cutoff low pressure systems (COLs) are usually closed circulations in the middle and upper troposphere developed from a deep trough in the westerlies (*Palmén and Newton*, 1969). These systems are different of other upper level lows because become completely detached from the main westerly current. COLs intensity is higher in the upper troposphere, decreasing downward. The troposphere below COLs is unstable and convective severe events can occur, depending on surface conditions.

COLs have been extensively studied in the Northern Hemisphere (*Nieto et al.*, 2008 and their references), but much less attention has been paid to those occurring in the Southern Hemisphere (SH). *Fuenzalida et al.* (2005) determined a climatology of COLs over the SH from 1969 to 1999. It was observed that the COLs tend to occur over three main continental areas: Africa, Australia and South America (SA). Marked seasonal cycles with winter maxima were found in SA and Africa but not over Australia. On the other hand, *Campetella and Possia* (2007) found higher COLs frequency in fall over SA from 1979 to 1988. *Garreaud and Fuenzalida* (2007) simulated a case of COL over the subtropical southeast Pacific during March 2005 (near SA western coast). The model used by these authors simulated well the COL and it allowed a detailed three-dimensional structure description, as well as an evaluation of the vorticity and temperature budgets. Another experiment without Andes topography was done and the COL exhibited similar position, strength, and extension as in the control simulation. This indicates that the Andes has little influence on COL's formation and intensification. Climatological simulations using regional climate models are rare. In this work we try to simulate COLs over SA and South Atlantic Ocean from 1990 to 1999 using a Regional Climate Model, RegCM3.

2. Methodology

2.1 RegCM3 and Simulations

The RegCM3 is a primitive equation model, compressible, and in the sigma-pressure vertical coordinate (*Pal et al.* 2007). For RegCM3 applications, different physical parameterizations scheme options are available. In this study, the surface turbulent fluxes over the ocean were parameterized using the Zeng scheme (*Zeng et al*., 1998) and the moist processes were parameterized following the Grell convective scheme (*Grell,* 1993) with the Fritsch-Chappell closure (*Pal et al.* 2007).

The simulation was carried out from September 1989 to the January 2000 in a domain between 84°W-15°E and 60°S-5°S. The atmospheric initial and boundary conditions are from R2 NCEP reanalysis (*Kanamitsu et al*. 2002). Over the ocean, the sea surface temperature (SST) monthly mean has a horizontal resolution of 1.0° x 1.0° (*Reynolds et al.* 2002). The topography and land data are specified by using the 10' horizontal resolution global archives from, respectively, United States Geological Survey (USGS) and Global Land Cover Characterization (GLCC), described by *Loveland et al*. (2000). The simulation used 60 km of horizontal resolution and 18 sigma-pressure vertical levels (model top at 80 hPa).

2.2 COLs Identification

The COLs were identified using the objective method by *Nieto et al.* (2005) based on imposing the three main physical characteristics of the conceptual model of COLs (*Winkler et al*., 2001): the 200 hPa geopotential minimum, cutoff circulation, and the specific structure of both equivalent thickness and thermal front parameter fields. This first identification was done using R2 NCEP reanalysis with 2.5º x 2.5º resolution; the second one was made using RegCM3 data. Due the different data resolution, the RegCM3 data were interpolated to the same grid as R2 NCEP reanalysis to eliminate small scale noise and guarantee that we were seeking the same type of systems in both databases.

3. Results

Figure 1a shows all grid points that fulfilled the exigencies of the COLs algorithm using R2 NCEP. Higher frequency of COLs is found over the continent between 25°-40°S and 70°-50°W. This spatial distribution is similar to *Fuenzalida et al.* (2005) and *Campetella and Possia* (2007) climatologies. Figure 1b shows RegCM3 simulation. This result points to that RegCM3 underestimates the COL number over the continental area between 25°-40°S and overestimates over the central part of South Atlantic Ocean (30°-20°W), and between 10°-20° S.

The cause of differences between R2 NCEP and RegCM3 COLs climatologies was investigated computing the geopotential height and air temperature differences at 200 hPa during 1990.

The difference field (Figure 2a) shows that the RegCM3 simulates higher (lower) geopotential height than R2 NCEP in the region where underestimates (overestimates) COLs. Since the COLs are identified using geopotential minimum, this can explain the absence of COLs in the RegCM3 simulations near Paraguay-Uruguay region and the excessive frequency of COLs at lower latitudes from 15°S. Other fact is that the RegCM3 is colder poleward 40°S and warmer equatorward 40°S (Figure 2b) that implicates a more intense upper level jet (*Reboita*, 2008). This is unfavorable to COLs' detection because these systems need weaker winds to detach from the main westerly current.

4. Conclusions

The purpose of this work was evaluating the performance of the RegCM3 model to simulate the spatial distribution of COLs over SA and South Atlantic Ocean during 1990-1999. The simulation was compared with R2-NCEP reanalysis. The results show that RegCM3 is not the best regional model to identify COL systems. The higher geopotencial height and warmer air at 200 hPa level reproduced by the model could explain the absence of COLs surrounding Paraguay-Uruguay region in the RegCM3 simulation. The opposite pattern could be

responsible for the excessive simulation of COLs between 10°-15°S.

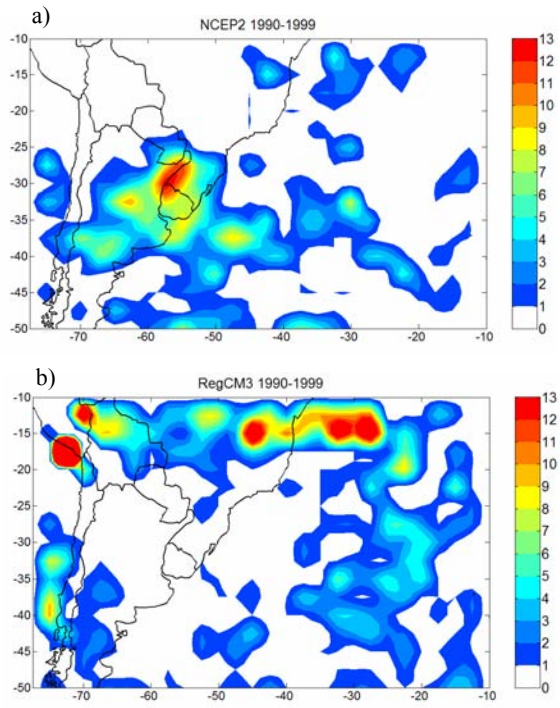

Figure 1. Number of COL points from 1990 to 1999: (a) R2 NCEP and (b) RegCM3.

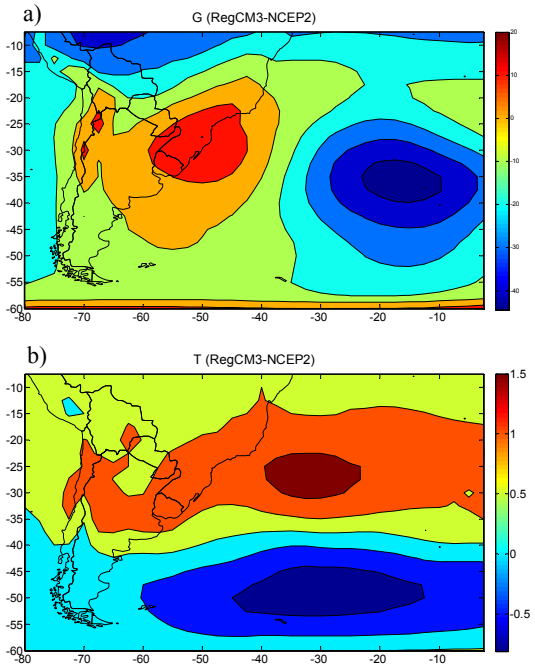

Figure 2. RegCM3/R2-NCEP average difference of a) geopotential and b) air temperature at 200 hPa for 1990.

5. Acknowledgments

This work was funded by FAPESP process N°. 04/02446, CAPES process N°. BEX 0626/08-2, and CNPq process N° 476361/2006-0. The authors would also like to thank ICTP for provided the RegCM3 code and NCEP by reanalyzes data set.

References

Campetella, C. M.; N. E. Possia: Upper-level cut-off lows in southern South America. *Meteorol. Atmos. Phys.*, 96, 181-191, 2007.

Fuenzalida, H. A.; R. Sánchez; R. Garreaud: A Climatology of Cutoff Lows in the Southern Hemisphere., *J. Geophys. Res*., 110 (D18101), 1-10, 2005.

Garreaud, R. D.; H. Fuenzalida: The Influence of the Andes on Cutoff Lows: A Modelling Study. *Mon. Wea Rev*., 135, 1596-1613, 2007.

Grell, G. A.: Prognostic Evaluation of Assumptions used by Cumulus Parameterizations, *Mon. Wea. Rev*., 121, 764-787, 1993.

Kanamitsu, M., and co-authors: NCEP-DOE AMIP-II Reanalysis (R-2). *Bull. Am. Met. Soc*., 83, 1631-1643, 2002.

Loveland, T. R.; B. C Reed; J. F. Brown; D. O. Ohlen; J. Zhu; L. Yang; J. W. Merchant: Development of a global land cover characteristics database and IGBP DISCOVER from 1-km AVHRR Data. *International Journal of Remote Sensing,* 21, 1303-1330, 2000.

Nieto, R., and co-authors: Climatological Features of Cutoff Low Systems in the Northern Hemisphere. *J. Climate*, 18, 3085-3103, 2005.

Nieto, R.; M. Sprenger; H. Werli; R. M. Trigo; L. Gimeno: Identification and Climatology of Cut-off Lows neart the Tropopause. Annals of the New York Academy of Sciences, 256-289, 2008.

Pal, J.S., and co-authors: The ITCP RegCM3 and RegCNET: Regional Climate Modeling for the Developing World. *Bull. Amer. Meteor. Soc.*, 88 (9), 1395-1409, 2007.

Palmén, E.; C. W. Newton: *Atmospheric Circulation Systems: Their Structure and Physical Interpretation*. New York: Academic Press, 603 p., 1969.

Reboita, M. S.: *Ciclones Extratropicais no Atlântico Sul: Simulação Climática e Experimentos de Sensibilidade*. PhD. Thesis in Meteorology (in portuguese), IAG/USP, 294 p., 2008.

Reynolds, R. W.; N. A. Rayner; T. M. Smith; D. C. Stokes; W. Wang: An improved in situ and satellite SST analysis for climate. *J. Climate,* 15, 1609-1625, 2002.

Winkler, R.; V. Zwats-Meise: Manual of Synoptic satellite meteorology. Conceptual models, Vers. 6.0. (Available at Central Institute for Meteorology ans Geodynamics, Hohe Warte 38, 1190 Vienna, Austria).

Zeng, X.; M. Zhao; R. E. Dickinson: Intercomparison of Bulk Aerodynamic Algorithms for the Computation of Sea Surface Fluxes Using TOGA COARE and TAO Data. *J. Climate*, 11, 2628-2644, 1998.

Relative role of domain size, grid size, and initial conditions in the simulation of high impact weather events

Himesh S[1], Goswami P[1], and Goud BS[2]

1. CSIR Centre for Mathematical Modeling and Computer Simulation, NAL Belur Campus, Wind Tunnel Road, Bangalore-560037, India. Email:himesh@cmmacs.ernet.in

2. UVCE, Department of Civil Engineering, Bangalore University, Bangalore-560056, India

1. Summary

The limited domain, and the associated artificial lateral boundaries, introduces several uncertainties and errors into simulation of Limited Area Models (LAM). The size of the model domain with its implicit geographical coverage also implicitly determines the large-scale dynamics and terrain effects. Thus, domain size and resolution together will determine the spectrum of resolved scale and the nature of scale interaction in the model dynamics. A comparative, comprehensive and quantitative estimation of the relative role of domain size, horizontal grid size (horizontal grid spacing) and initial condition in the simulation of mesoscale events is however, lacking. We investigate this issue using a mesoscale model (MM5V3) with respect to heavy rainfall event with a series of ensemble (5 initial conditions) simulations. We first use a high-resolution (10-km) bench mark simulation to show the model's performance in simulating extreme rainfall events. The sensitivity simulations (varying domain size and grid distance) are carried out at coarser resolutions in view of the large number of simulations involved, and as our emphasis is on relative roles and not on precise forecast. Our results show that along with initial conditions and grid distance the size of the domain also significantly affects simulated quantities like total rain, maximum rain and other dynamical fields. While the quantitative aspects of this conclusion are likely to change based on type and location of the event, the results show that domain size play as much an important role as that of horizontal resolution and initial condition in the simulation of high impact weather events like heavy rainfall.

2. Introduction

Genesis and evolution of mesoscale events are strongly determined by local inhomogenities of boundary forcings in addition to non-hydrostatic dynamics that is characterized by small spatial scales. Limited area or mesoscale models (LAM) thus continue to be the most popular and effective tools for simulating and forecasting mesoscale events. Numerous studies have demonstrated the ability of high resolution mesoscale models to successfully simulate high impact weather events like extreme rainfall and their associated synoptic features. A necessary price for such high horizontal resolution, however, is a small numerical domain of integration due to computational constraints. In reality, both resolution and the size of the mesoscale domains play critical role in the quality of the simulation. The size of the domain implicitly determines the large-scale dynamics and terrain effects, while the horizontal resolution determines the smallest resolvable scale. Thus the size of the domain and the resolution together determine the spectrum of resolved scales and the associated scale interaction in the model dynamics. Warner et al (1997**)** described the Lateral Boundary Conditions (LBC) as potential limitation and an inevitable problem of regional weather prediction. Giorgi et al (1999) discussed the importance of the choice of model domain in mesoscale simulation and concluded that it was not feasible to evolve general criteria for the choice of model domain but to depend largely on trial and error approach. One of the necessary requirements in mesoscale simulations to minimize the adverse impact of lateral boundary condition on the model solution is to keep the lateral boundaries away from the region of interest (Pielke, 2002). The question of relative sensitivity of domain size, horizontal grid distance and initial conditions on the quality of mesoscale simulation, however, has not yet been studied in depth in the context of high impact weather events. The objective of the present study is to investigate this issue in the context of high impact weather event occurred in Indian Monsoon region.

3. Brief Synoptic Description of the Event

The extreme rainfall event that flooded the metropolis of Mumbai on the west coast of India (72.52E and 18.52N) was an intense and highly localized meso-scale (meso-β) convective system, with a spatial scale of only about 30 Km. It was also a short-lived system, with recorded rainfall of around 94 cm in 24 hours between 26 -27th July 2005, with most of the rainfall occurred in the afternoon of July 26th, 2005. Satellite pictures had shown the event as a centre of intense precipitation along with a few other precipitation centers in the west-east direction. Satellite images also showed deep cloud system (one form east and the other from Arabian Sea) over the region. The overall synoptic situation was that of intense convective activity with strong continuous convergence of offshore winds (westerlies).The other features were; the presence of low pressure system (22N, 85.5E) and its associated cyclonic circulation up to 300mb, offshore trough was also seen at 10N-20N.

4. Design of Experiments

In our study we have considered Extreme Rainfall Event occurred over Mumbai (west coast of India, July 26-27, 2005). Fifth generation NCAR /Penn State mesoscale model (MM5V3) was used in this study. This is a non-hydrostatic model [Dudhia, 2004] with multiple choices for parameterization of various processes like cumulus convection, Planetary Boundary Layer (PBL) and nesting capability. All simulations in this study were carried out with a single domain and with same physics options (cumulus parameterization-Anthes-Kuo, Boundary Condition-Relaxation., Microphysics-Simple Ice, Radiation Scheme- Dudhia, Vertical levels-23). We have considered three grid distances (90, 60 30 and 10-km) in our study to examine the relative role of domain size and horizontal grid distance in the simulation of extreme rainfall event. While it could be argued that proper simulation of mesoscale events require much higher grid distance, the focus here is on quantitative assessment of relative roles of domain size versus grid distance through large number of sensitivity studies. Seven domains (D1 to D7, Fig.1.) of varying longitudinal and latitudinal extent were chosen for this study, out of which five domains (D2 to D6) were common to all the three grid distances (90, 60

and 30km). Domains D1 (90 and 60-km) and D7 (90-km) were considered for only coarser grid distance due to computational constraints. Domains D4 and D5 which have same longitudinal extents but different latitudinal extents were re-run to verify and validate results at finer grid distance. As mentioned above, the larger scales simulated in model dynamics will depend not only on the size of the domain but also on the geographical coverage. The seven domains were thus chosen to provide an ensemble of large-scale dynamics and terrain effects as affected by different domains. For each of the domains mentioned above, the model was integrated for 5 days starting from five different initial conditions 6-hours apart beginning from 00UTC, 24th July 2005. Although the event was highly localized in both space and time, we have considered a spatial window of $2^{o}x2^{o}$ centered on the general event location and a time window of 24-hour (06UTC, 26th July to 06UTC, 27th July 2005) for diagnosis and analysis.

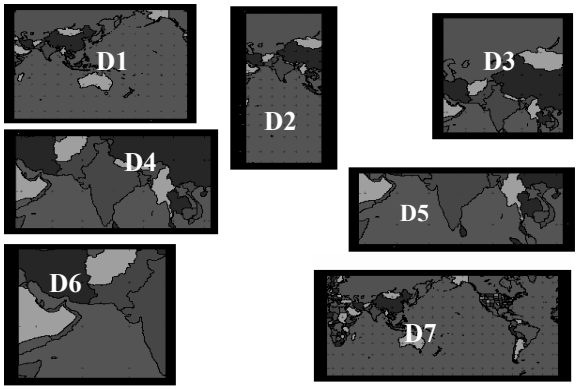

Figure 1. Experimental domains.

5. Benchmark Simulation

Due to large number of simulations involved , high resolution simulations (10-km) were carried out for only two domains (D4 and D5) which are comparable in size but vary in geographical coverage. These simulations and their comparison with observations are then used as benchmark for the acceptability of simulations with coarser resolutions. We then, compared the spatial distribution of 24-hour accumulated simulated rainfall for these domains at four horizontal resolutions (10, 30, 60 and 90-km) and found that a localized intense rainfall event around Mumbai was seen for all the resolutions and for both the domains. In particular, both high (10-km) and coarse (30-km) resolution simulations could capture the distribution reasonably well especially in terms intensity when compared with satellite data.

6. Results and Discussion

Comparison of spatial distributions of 24-hour (event window) accumulated, simulated ensemble rainfall based on five initial conditions for five domains of 30-km resolution with satellite data has shown considerable inter-domain variations in the simulated distribution of rainfall. Simulations with resolutions of 90 and 60 km also have shown significant variations in the distribution and intensity of the simulated rainfall with the size and geographical coverage of the domain. This inter-domain variability in the distribution of rainfall is profound at higher grid spacing. It was also found that the domain D5 (which included equatorial belt) simulated the observed distribution better than all the other domains, and for all the three resolutions. The effects of changes due to longitudinal or latitudinal extents or both on the 24-hour accumulated area averaged rainfall (R_{av}) and the maximum rainfall (R_{max}) were analyzed. The results are from ensemble average simulations with the five leads (initial conditions) described above. It was shown that changes in the domain size results in significant changes in R_{av} and $R_{max,}$ it was true for domains of different resolutions as well. This variability of R_{av} and R_{max} due to change in domain size and coverage in terms of Standard Deviation (SD) as percentage of mean across different domains was in the range of 30 to 40 % and 34 to 40 % respectively. It was seen that effects of change in the domain size in general are larger for lower resolutions. This implies the need for an optimum model configuration with appropriate domain size or ensemble of domains and resolution to resolve both ends of the spectrum of scales. We next examined the relative role of resolution on R_{av} and $R_{max.}$ Dispersion of forecasts due to changes in initial conditions provides both a measure of reliability of the forecasts and a measure of variation in mesoscale forecasts due to changes in the large scale conditions (initial fields). In particular, we expect the response to different initial conditions to be a strong function of the domain size and geographical coverage as the large scale fields evolve differently over different domains. Summary of the relative variability or sensitivity of R_{av} and R_{max} in terms of SD (as % mean) with respect to different domains, resolutions and IC's are summarized in Table.1. As another measure of relative sensitivity of the simulations to domain size we have considered standard deviation (as % of mean) in terms of 24-hour accumulated total rain over event location (R_T) for different domains (with varying number of domains depending on the resolution). Time evolution of this standard deviation indicated that variation due to change of domain is typically 40 % and can be as much as 70 to 80%; in comparison a change of resolution doesn't change this dispersion that significantly except at isolated hours and not more than by a factor of 2.

Table 1. Summary of variability of R_{av} and R_{max} in terms of SD as % of mean for different domains, resolution and Initial Conditions.

Rain	Model Domain	Resolution	Initial Condition
R_{av}	30-40	10-30	11-50
R_{max}	34-40	21-43	6-40

References

Dudhia, J., PSU/NCAR Mesoscale Modeling System Tutorial Class Notes and User's Guide; MM5 Modeling System Version 3, 2004

Giorgi, F., and L.O. Mearns, Introduction to special section: Regional climate modeling revisited. *J.Geophys. Res*., Vol.**104**, No. 6, pp. 6335-6352, 1999

Pielke, R.A., Mesoscale Meteorological Modeling. Academic Press, pp. 673, 2002

Warner, T.T., Peterson, R.A. and Treadon R.E., Tutorial on lateral boundary condition as a basic and potentially serious limitation to regional numerical weather prediction. *Bull. of the Amer.Meteor.Soc*., No.78, pp. 2599-2617, 1997

Weighting multi-models in seasonal forecasting – and what can be learnt for the combination of RCMs

Andreas P. Weigel, Mark A. Liniger and C. Appenzeller

Federal Office of Meteorology and Climatology, MeteoSwiss, Switzerland
Email: andreas.weigel@meteoswiss.ch

1. Introduction

Multi-model combination (MMC) is a pragmatic approach to estimate the range of uncertainties induced by model error. MMC is now routinely applied on essentially all time scales, ranging from the scale of weather forecasts to the scale of climate-change scenarios, and its success has been demonstrated in many studies (e.g. *Palmer et al.* 2004). Simple multi-models can be easily constructed by pooling together the available single model predictions with equal weight. However, given that models may differ in their quality and prediction skill, it has been suggested to further optimize the effect of MMC by weighting the participating models according to their prior performance (e.g. *Giorgi and Mearns 2002*). How can such weights be objectively estimated? How robust are such estimates, and what are the consequences if "wrong" weights are applied, i.e. if the weights are not fully consistent with the true model skill? It is the aim of this study to discuss these questions at the example of seasonal forecasts as well as synthetic toy model forecasts, i.e. prediction contexts where a sufficient number of training and verification data is available. Potential implications of the results for the construction of weighted RCM multi-models will be discussed.

2. Model weighting in seasonal forecasting

The weighting method presented in this study has been described in detail in *Weigel et al.* (2008). Essentially, optimum weights are obtained by minimizing a universal skill metric called ignorance (*Roulston and Smith 2002*), a score which is derived from information theory. The ignorance quantifies the information deficit (measured in bits) of a user who is in possession of a probabilistic prediction, but does not yet know the true outcome. This metric has its fundamental justification in the fact that it is the aim of any prediction strategy to maximize the available information about a future event, respectively to minimize the information deficit. The method has been applied and tested in cross-validation mode on a set of 40 years of hindcast data from two models of DEMETER database (*Palmer et al.* 2004). The models have been combined (a) with equal weights and (b) with optimum weights. The weights have been determined grid-pointwise. The corresponding skill maps (skill metric: debiased ranked probabilitiy skill score, RPSSd, *Weigel et al.* 2007) are shown in Fig. 1 and reveal that, on average, model weighting can improve the prediction skill significantly.

3. Weight robustness

The success of weighted MMC depends on the robustness of the weights obtained. For the example shown above the average uncertainty of the weight estimates is, despite 40 years of available reforecasts, on the order of 10%. The uncertainties grow if the number of independent training data decreases. Model weighting in the context of climate change scenarios is particular problematic, since the verification context is strongly limited to a few, rather dependent samples. To evaluate the potential effects of these uncertainties more systematically, a stochastic and Gaussian forecast generator has been applied to generate large numbers of multi-model forecasts (consisting of two models) and corresponding verifying observations. The combination has been carried out (i) with equal weights (this is the benchmark), (ii) with optimum weights, and (iii) with perturbed weights.

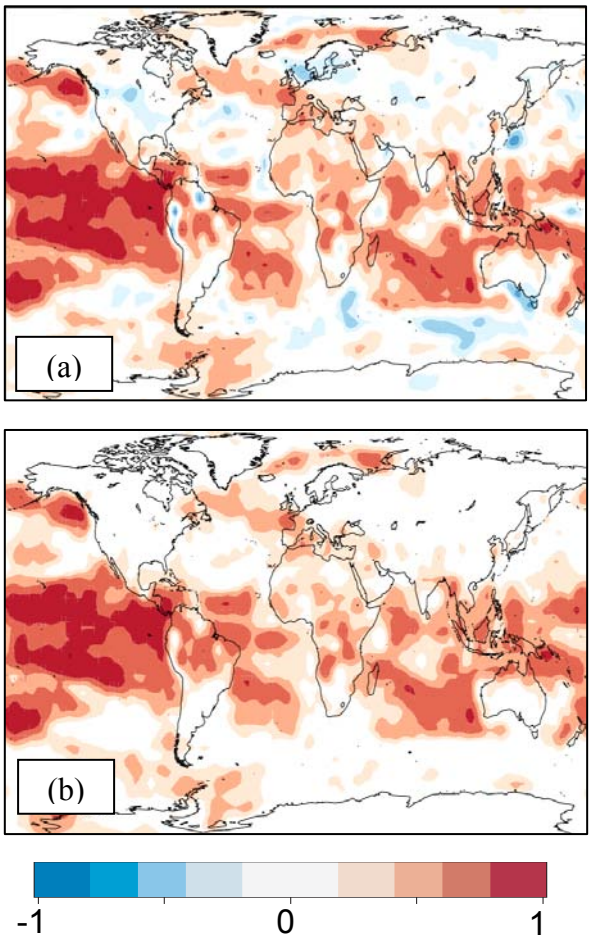

Figure 1. Skill maps (RPSSd) of combined seasonal forecasts (June, July, August; initialization 1 May) of 2m temperature for the period 1960-2001. Two models (ECMWF's System 2 and the UK Met Office's GloSea 2) from the DEMETER database have been combined (a) with equal weights, and (b) with optimum weights (determined grid-pointwise).

The toy model experiments confirm that the forecast information content can be substantially improved by weighted multi-models. However, they also show that even more information can be lost if the uncertainty in the weights becomes too large, i.e. if the weights which are applied are not consistent with the true model skill. This

can be seen in Fig. 2, where the information gain or information loss with respect to unweighted multi-models is shown for (i) optimally weighted multi-models and (ii) randomly weighted multi-models.

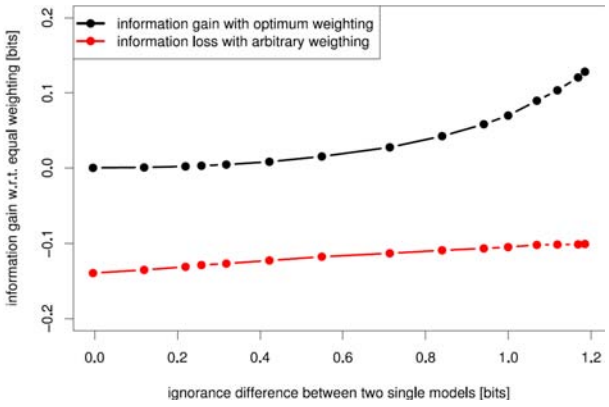

Figure 2. Information gain/loss of weighted multi-models (black: optimum weights; red: random weights) with respect to unweighted multi-models, plotted as a function of skill-difference between the two participating single models. Each value represents the average of 100,000 toy model combination experiments.

4. Implications for the combination of RCMs

The key conclusion to be drawn from this study is that the application of a weighting method can significantly enhance the prediction quality of a multi-model. However, it is essential that robust weights are applied, since otherwise more information may be lost than can potentially be gained. While the issue of weight estimation is already challenging in the context of seasonal forecasts, particularly if only a short number of independent training data is available and more than two models are to be combined, it is even more complicated in the context of climate change scenarios with RCMs, because:

- The assumption must be made that weights obtained on the basis of a present or past control climate equally hold under different climate conditions in the future.
- The predictand is typically a climate change signal and is as such evaluated over long time periods (on the order of decades). Consequently, the number of independent training data to obtain an optimum weighting is much smaller than in the case of seasonal forecasts.
- The quality of coupled GCM-RCM climate change scenarios is not only determined by the RCM quality alone, but also by the quality of the driving GCMs. Weights determined on the basis of observation-driven RCM control runs may therefore not be representative for the overall skill of a coupled GCM-RCM scenario.

When climate change scenarios are to be estimated on the basis of weighted RCM-multi-models, these aspects should be considered and their potential impacts on scenario reliability estimated.

Acknowledgments

This study was supported by the Swiss National Science Foundation through the National Centre for Competence in Climate Research (NCCR Climate).

References

Giorgi F. and L. O. Mearns, Calculation of average, uncertainty range, and reliability of regional climate changes from AOGCM simulations via the "Reliability Ensemble Averaging" (REA) Method, *J. Clim.*, 15., 1141-1158, 2002

Palmer and Coauthors, Development of a European multimodel ensemble system for seasonal-to-interannual prediction (DEMETER), *Bull. Amer. Met. Soc*, 85, 853-872, 2004

Roulston M.S. and L.A. Smith, Evaluating probabilistic forecasts using information theory, *Mon. Wea. Rev.,* 130, 1653-1660, 2002

Weigel A.P., M.A. Liniger and C. Appenzeller, Generalization of the discrete Brier and ranked probability skill scores for weighted multi-models, *Mon. Wea. Rev.,* 135, 118-124, 2007

Weigel A.P., M.A. Liniger and C. Appenzeller, Can multi-model combination really enhance the prediction skill of ensemble forecasts? *Quart. J. Roy. Met. Soc.*, 134, 241-260, 2008

Weigel A.P., M.A. Liniger and C. Appenzeller, Seasonal ensemble forecasts: Are recalibrated single models better than multi-models? *Mon. Wea. Rev.*, in press, 2009

High-resolution simulation of a windstorm event to assess sampling characteristics of windstorm measures based on observations

Lars Bärring[1], Włodzimierz Pawlak[2], Krzysztof Fortuniak[2] and Ulf Andrae[1]

[1]Swedish Meteorological and Hydrological Institute, Norrköping, Sweden, lars.barring@smhi.se;
[2]University of Łódź, Department of Meteorology and Climatology, Łodź, Poland

1. Background

Extra-tropical cyclone frequency and intensity are currently under intense scrutiny because of the destruction recent windstorms have brought to Europe, and because they are a major meridional heat transport mechanism that may respond to differential latitudinal warming trends. There are two fundamental questions that arise in this context; how has the wind climate varied back in time; and what future variations and possible changes do the climate change scenarios suggest? The former question is analysed using observational data, mainly indirect measures based on sea-level pressure that is less influenced by inhomogeneity problems compared to direct wind observations (Carretero et al., 1998). The latter question is addressed using climate models scenarios (e.g Ulbrich et al., 2008, Weisse et al., 2009).

The two different data types have sampling characteristics: observational point data from (usually rather sparse) station networks and observation frequency of typically 2-4 times per day, and gridded climate model data, typically having 20-50 km spatial resolution (regional models) or 100-250 km (global models) and temporal frequency of 0.5-6 h. To gain insight in how these two sources of information on historic and future wind climate can be related to each other the effect of these differences need to be assessed.

Here we use the high-resolution NWP model *AROME* (http://www.cnrm.meteo.fr/gmap/accueil.html) to analyse the sampling properties of several common measures of observed wind conditions. The measures include high percentiles of geostrophic wind (Schmidt and von Storch, 1993; Alexandersson et al. 1998, 2000; Trenberth et al. 2007; Matulla et al. 2007), and Eulerian storminess indices (Alexandersson et al. 1998; Carretero et al., 1998; Bärring and von Storch, 2004; Bärring and Fortuniak, 2009).

2. Data and Methods

The *AROME* ("Applications of Research to Operations at MEsoscale") non-hydrostatic NWP model is currently under development by an international consortium lead by CNRM and MétéoFrance and involving collaboration with SMHI (Andrae, 2006) and others. For this experiment *AROME* is used to downscale the Gudrun windstorm event that caused severe damage in southern Sweden. The domain covers southern Sweden (Fig. 1) and surroundings with a resolution of 2.5 km. The simulated period runs from 2005-01-08 00UTC to 2005-01-09 00UTC. Initial conditions and lateral boundary conditions are taken from the operational *Hirlam* 11 km analysis. The time-step is 30 s and data is stored for every 10 minutes.

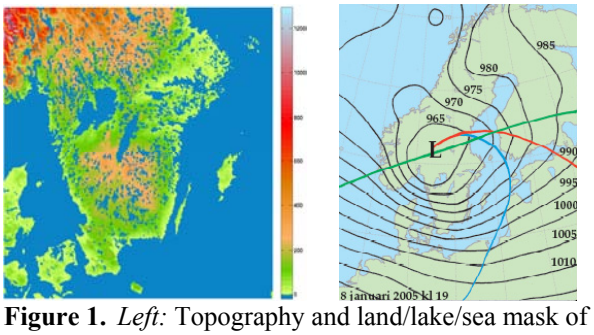

Figure 1. *Left:* Topography and land/lake/sea mask of the domain used in the *AROME* simulation. *Right:* MSLP of the Gudrun windstorm at 20050108 18UTC.

The simulated surface pressure was evaluated using available SYNOP and automatic stations (Figure 2) before transforming to mean sea-level pressure (MSLP). The simulated pressure is close to the observed pressure despite no data assimilation was used (Figure 2). The minor discrepancies are not important because the focus is not on an exact representation of this specific windstorm event, but rather to get a spatially complete coverage of a realistic windstorm event to sample from.

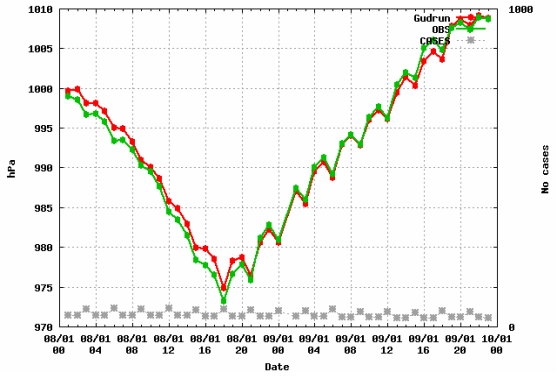

Figure 2. Temporal evolution of the average surface pressure at 61 stations (red) and the corresponding simulated values (green).

Geostrophic winds were then calculated from 10 000 randomly placed triplets of gridcells (Figure 3). The gridcells were selected so that the triangles were approximately equilateral within 20% at 500 km, as well as at 250 km thus mimicking different station network densities.

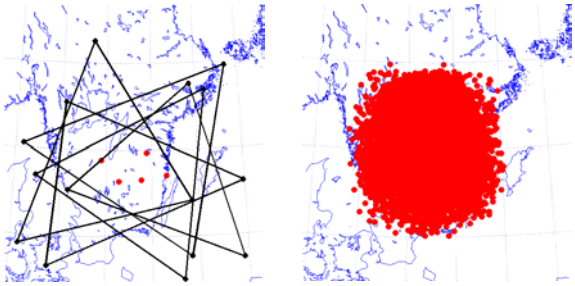

Figure 3. *Left:* Five randomly located pressure triangles having gridcell spacing of ~500 km and their centres. *Right:* The spatial coverage produced by 10 000 randomly located triangles.

The Eulerian storminess indices were taken from Bärring and Fortuniak (2009):

i. the annual number of pressure observation below 980 hPa (N_{p980}),

ii. annual number of absolute pressure tendencies exceeding 25 hPa/24 h ($N_{\Delta p/\Delta t}$),

iii. intra-annual 99-percentile of the absolute pressure differences in 8 h ($P99_{\Delta p/\Delta t}$).

Because we analyse only one windstorm event, the indices as such cannot be calculated. But the underlying measure of storm intensity is for *i*) the occurrence of pressure below the threshold 980 hPa, and for ii) and iii) the occurrence of $|\Delta p|/\Delta t$ above combinations of thresholds and timesteps.

3. Results

We calculate basic statistics of geostrophic windspeed (cf. Figure 4 for an example) and analyse how different observation intervals influence the statistics.

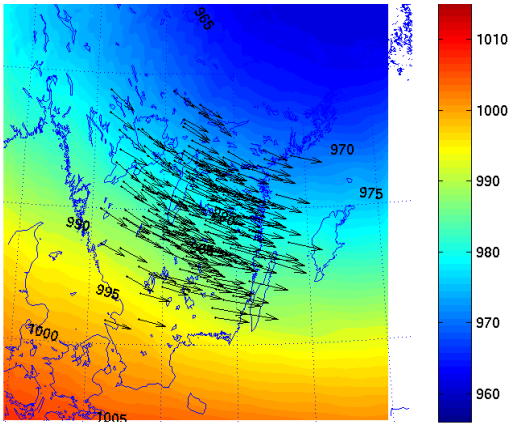

Figure 4. MSLP and geostrophic wind vectors (n=200) at 2005-01-09 00UTC (near peak storm intensity), min=32.8 m s^{-1}, mean=41.9 m s^{-1} and max=54.3 m s^{-1}.

Figure 5 (left) shows that with high-frequency air pressure measurements the index N_{p980} would identify a windstorm for roughly 60% of the region. The region of guaranteed detection – i.e. the region where the longest uninterrupted time period below the threshold is longer than the sampling interval - successively contracts towards N, and finally towards NE when the sampling frequency decreases (Figure 5 right).

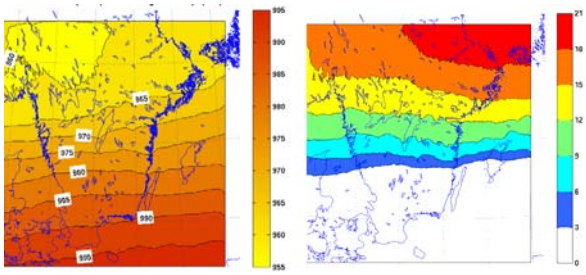

Figure 5. *Left:* Minimum MSLP for all timesteps. *Right:* Longest period (3h intervals) the MSLP stays below 980 hPa. This indicates the region of guaranteed detection of the windstorm using the N_{p980} index given different observation frequencies.

From Figure 5 (right) it is clear that the calculated geostrophic wind will be sensitive to the position of the individual stations (gridcells) making up the triangles. This is clearly evident in Figure 6 where widely different continuous periods of geostrophic winds above 25 m s^{-1} are mixed. The only geographic stratification is that the longest periods are confined to a smaller region slightly more to the east. While geostrophic windspeeds exceeding 25 m s^{-1} are infrequent in southern Scandinavia (about 2% of the time), the Gudrun event was one of the most intense windstorms observed in Sweden. The rather long periods

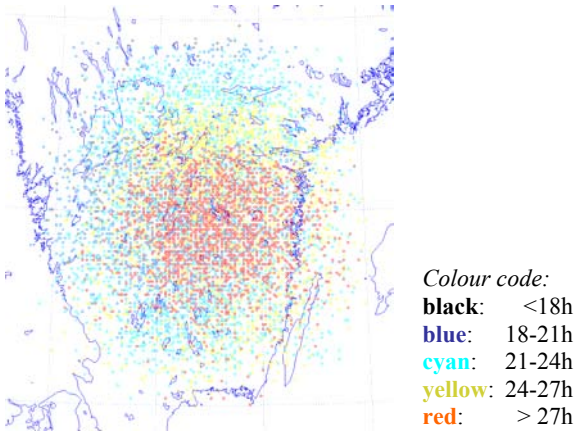

Figure 6. Maximum continuous period where the geostrophic wind exceeds 25 m s^{-1} derived from the 10 000 triangles (500 km).

shown in Figure 6 is thus not surprising but show that with most common sampling frequencies the Gudrun windstorm would have been detected by a geostrophic wind index using 25 m s^{-1} as threshold for windstorms.

4. Concluding remark

We have in this initial study shown that a high-resolution gridded dataset can be useful for assessing sampling characteristics of several storminess indices. This analysis of a high-resolution simulation of one extreme windstorm will be complemented with a similar analysis a gridded data set covering a longer time period.

References

Andrae, U.: SMHI ALADIN implementation. *HIRLAM Newsletter No. 51*, 36-43. October 2006.

Alexandersson H., Schmith T. and Tuomenvirta H.: Long-term variations of the storm climate over NW Europe. *Global Atmos. Ocean System*, 6, 97-120. 1998.

Alexandersson H., et al.: Trends of storms in NW Europe derived from an updated pressure data set. *Clim Res.* 14, 71-73. 2000.

Bärring L. and von Storch H.: Scandinavian storminess since about 1800. *Geophys. Res. Lett.*, 31, L20202, 1-4. 2004.

Bärring L. and Fortuniak, K.: Multi-indices analysis of southern Scandinavian storminess 1780-2005 and links to interdecadal variations in the NW Europe-North Sea region. *Int. J. Climatol.* 29, 373-384. 2009

Carretero J.C. et al.: Changing waves and storms in the northeast Atlantic? *Bull. Amer. Met. Soc.*, 79, 741 760. 1998.

Matulla C. et al.: European storminess: late nineteenth century to present. *Clim. Dyn.*, 31, 125-130. 2008.

Schmidt H. and von Storch H.: German Bight storms analyzed. *Nature*, 365, 791-791. 1993.

Trenberth K.E. et al.: Observations: surface and atmospheric climate change. In: *Climate Change 2007: The Physical Science Basis*. Cambridge Univ. Press. pp. 236-336. 2007.

Ulbrich, U. et al.: Changing northern hemisphere storm tracks in an ensemble of IPCC climate change simulations. *J. Clim.*, 21, 1669-1679, 2008

Weisse, R. et al.: Regional meteo-marine reanalyses and climate change projections: Results for Northern Europe and potentials for coastal and offshore applications, *Bull. Amer. Meteor. Soc*. in press. 2009.

MesoClim – A mesoscale alpine climatology using VERA-re-analyses

Benedikt Bica, Stefan Sperka and Reinhold Steinacker

Department of Meteorology and Geophysics, University of Vienna, Austria. Benedikt.Bica@univie.ac.at

1. Introduction

Many efforts are being made in the quantitative capture of regional-scale climate changes and the assessment of socio-economic consequences of future climatic conditions.
The present study is intended to provide insight into the mesoscale climatic conditions and their recent change in the Alpine region. The work is being done within the MesoClim project, carried out at the Department of Meteorology and Geophysics at the University of Vienna and funded by the Austrian Science Fund, FWF.

2. Data

Observation data were retrieved from ECMWF's MARS and ERA40 archives and were complemented by additional station data from the national weather services of Austria, Germany and Switzerland in order to obtain a very dense observation network (Fig. 1).

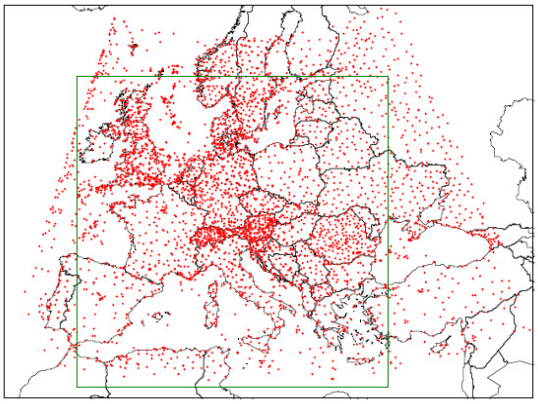

Figure 1. MesoClim-stations and analysis domain. Analysis domain size: 3000 km x 3000 km.

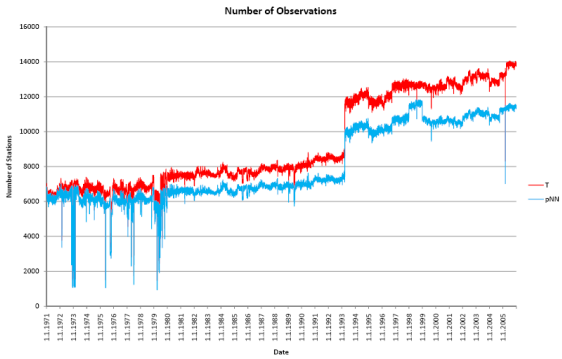

Figure 2. Number of available temperature and pressure observations 1971-2005 used in MesoClim.

The observations used within MesoClim range back to the early 1970s and thus encompass a time period of 35 years (1971-2005, Fig. 2). The data is checked with a multilevel quality control tool and further processed with the VERA analysis method.

3. VERA

VERA (Vienna Enhanced Resolution Analysis) is a high resolution analysis and downscaling tool with embedded quality control, which is particularly intended for use over complex topography. The basic philosophy of VERA is to use physical a priori knowledge (the so-called fingerprints) of typical meteorological patterns that occur over complex terrain. If the fingerprint patterns are a priori known, their signals can be detected in data-rich regions and they can subsequently be impressed to the field in data-sparse regions, i.e. data is transferred from data-rich to data-sparse regions.
Hence, VERA enables the user to efficiently downscale meteorological information without making use of any further model input, i.e. it is data self-consistent. VERA is related to the thin-plate spline method, but calculation is done by using finite differences.

4. Data processing and main achievements

VERA is used to provide a spatially (2 to 16 km) and temporally highly resolved climatology of the Alpine region. The analyses are calculated in 3-hourly intervals for the entire MesoClim dataset and for the following parameters:

- mean sea level pressure
- potential temperature
- equivalent potential temperature
- wind
- precipitation

Reanalyses are currently carried out, with first evaluations being already on hand. The main achievements of MesoClim are expected to comprise amongst others

- high resolution reanalyses of air mass characteristics in terms of equivalent potential temperature for a climate normal period
- investigation of the mesoscale flow patterns over the Alps for a climate normal period
- climatological evaluation of 3-hourly isallobaric fields over the Alps.

5. Acknowledgements

The financial support by the Austrian Science Fund FWF under grant No. P18296 is gratefully acknowledged.

References

Bica, B., T. Knabl, R. Steinacker, M. Ratheiser, M. Dorninger, C. Lotteraner, S. Schneider, B. Chimani, W. Gepp, and S. Tschannett: Thermally and Dynamically Induced Pressure Features over Complex Terrain from High Resolution Analyses, *J. Appl. Meteor.*, 46, pp. 50-65, 2007

Bica, B., R. Steinacker, C. Lotteraner, and M. Suklitsch: A new concept for high resolution temperature analysis over complex terrain. *Theor. Appl. Climatol.*, 90, pp. 173-183, 2007

Steinacker, R., Ch. Häberli and W. Pöttschacher: A Transparent Method for the Analysis and Quality Evaluation of Irregularly Distributed and Noisy Observational Data, *Mon. Wea. Rev.*, 128, No.7, pp. 2303-2316, 2000

Steinacker, R., M. Ratheiser, B. Bica, B. Chimani, M. Dorninger, W. Gepp, C. Lotteraner, S. Schneider, and S. Tschannett: A Mesoscale Data Analysis and Downscaling Method over Complex Topography, *Mon. Wea. Rev.*, 134, pp. 2758-2771, 2006

Observed and modeled extremes indices in the CECILIA project

Ole B Christensen[1], Fredrik Boberg[1], Martin Hirschi[2], Sonia Seneviratne[2] and Petr Stepanek[3]

[1]Danish Meteorological Institute, Copenhagen, Denmark. obc@dmi.dk
[2]Institute for Atmospheric and Climate Science, ETH Zürich, Switzerland
[3]Czech Hydrological and Meteorological Institute, Prague, Czech Republic

1. Introduction

The EU FP6 research project CECILIA deals with Central and Eastern European climate change. Regional climate models are being run in very high resolution, around 10 km, for Central European areas. Various impacts models are also being employed, using this high-resolution climate model output in order to study future changes of e.g. agriculture, forestry and pollution.

One important aspect of the project is the analysis of changes in various extremes indices based on daily values of temperature and precipitation. For validation purposes an unprecedented collection of observational data has been collected from the involved national meteorological and hydrological services of the region.

In this study, relevant extremes indices will be presented both based on observations and on climate simulations. Both validation and climate change will be discussed.

2. Extremes Indices

In the CECILIA project a list of more than 100 extremes indices has been constructed through discussions between national meteorological services in Central Europe and regional climate modelers, and based on existing indices collections from STARDEX, ETCCDI and ECA&D.

The entire set of indices has been calculated for the ENSEMBLES and PRUDENCE data sets of regional model output, as well as for the ECA&D collection of station observations (Klein Tank et al. 2002) and the ENSEMBLES gridded observations (Haylock et al. 2008). Furthermore, the involved meteorological services have provided many indices at a density of observation stations, which has not been seen for the Central European area before.

Finally, output from the high-resolution regional climate simulations of the CECILIA project will be calculated and included as far as possible.

We will present and compare results here.

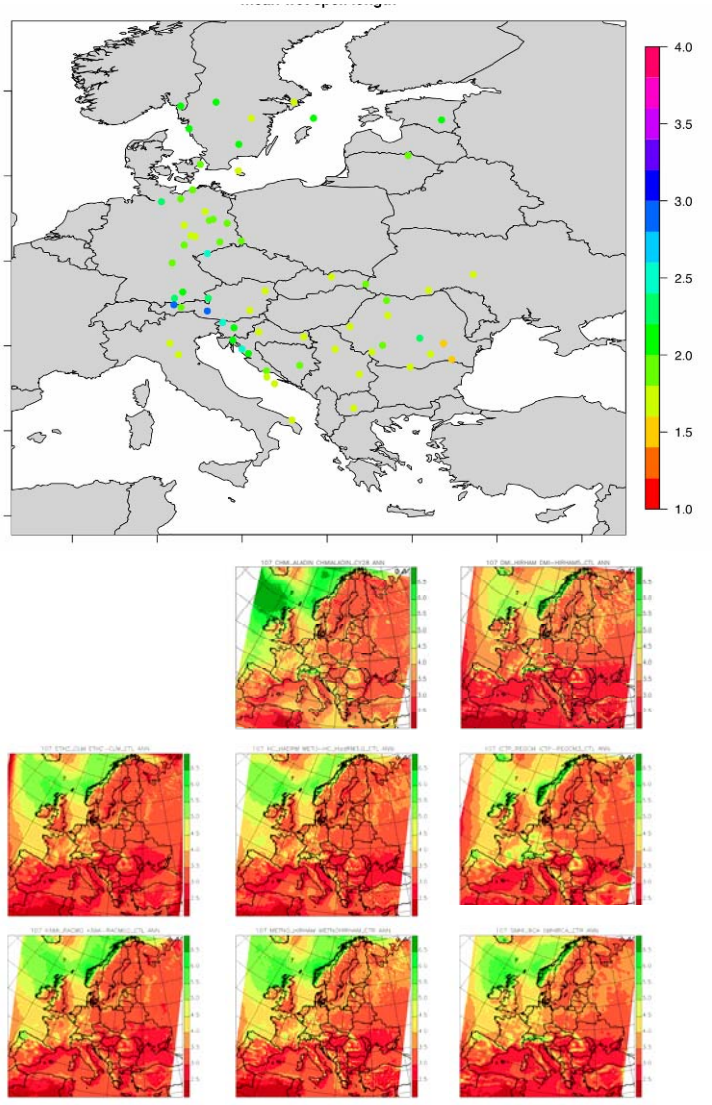

Figure 1. 99th percentile of daily precipitation for a) ECA&D and b) a set of ENSEMBLES simulations.

References

Haylock, M. R., N. Hofstra, A. M. G. Klein Tank, E. J. Klok, P. D. Jones, and M. New. A European daily high-resolution gridded dataset of surface temperature and precipitation for 1950–2006. J. Geophys. Res., 113(D20119):doi:10.1029/2008JD010201, 2008

Klein Tank, A. M. G., et al. Daily dataset of 20th-century surface air temperature and precipitation series for the European Climate Assessment. *Int. J. Climatol.*, 22, 1441–1453, 2002

Dynamical downscaling of surface wind circulations over complex terrain

Pedro A. Jiménez[1,2], J. Fidel González-Rouco[1], Juan P. Montávez[3], E. García-Bustamante[1,2] and J. Navarro[2]

(1) Dto. Astrofísica y CC Atmósfera, Universidad Complutense de Madrid, pedro.jimenez@fis.ucm.es
(2) Dto. Energías renovables, CIEMAT and (3) Dto. de física, Universidad de Murcia

Estimating and/or forecasting the surface wind flows over a region is important for quite different applications such as the transport and dispersion of pollutants over an area, the extinction of forest fires, or the decision making involved with risk meteorological situations associated with strong winds. Recently, there is an increasing demand of wind estimations and forecasts by the wind energy sector as a consequence of its large development experimented during the last years. Accurate wind estimations at the regional scale can be used to identify potential locations adequate for its wind energy exploitation. In turn, the forecast is useful in routine activities on the already existing wind farms. For instance, it can be used to identify adequate periods to perform maintenance operations on the wind turbines, or to estimate the wind power production of the wind farms.

The surface wind behavior over a region largely depends on the large scale atmospheric circulations over the area, and its particular topography which strongly modify the large scale circulations through channeling, forced ascents, blocking, etc. Topography is also capable to generate thermally driven circulations associated with a differential surface heating. An example of these kind of circulations are the up- and down valley winds or the mountain-plain system circulations (Whiteman 2000). Increasing terrain complexity produces a rich variability on the surface wind field converting its estimation into a challenging issue.

Regional climate models (RCMs) are a standard tool used to provide estimations/forecasts of the surface wind field. These models allow to achieve a high spatial resolution without compromising in excess the computational resources required to accomplish the estimation. RCMs can provide a realistic representation of the terrain features over a region, and therefore they are potentially appropriate tools to estimate the surface circulations over complex terrain areas. The model outputs should be compared to observations in order to confirm the capability of the simulation to reproduce the surface circulations.

The evaluation of model based estimations meets some uncertainties when comparison with local information is involved. Usually, *in situ* observations are compared against the nearest simulated grid points. However, two main reasons are worth to stress as responsible for the uncertainty introduced in this particular type of comparison. First, the simulated variables represent averaged quantities over atmospheric volumes whose comparison against *in situ* observations can be problematic at those locations affected by local features. Secondly, the discretization introduced by the simulation smooths the complexity of the orography, which can cause that the simulated volume including the actual location of the stations is not the most representative one; being surrounding volumes more adequate. Reid and Turner 2001 compared the volume averaged wind from a coarse simulation (40 km) against averaged observations within the grid cells. Averaging the observations mitigates the influence of local effects on the time series (noise) and thus, enhances the regional signal providing more appropriated time series for comparison. This was reflected in stronger relationships than the traditional comparison between observations and nearest grid points.

The present study uses the Reid and Turner 2001 concept of regional evaluation to analyze the capability of a numerical simulation performed with the Weather Research and Forecast model (WRF, Skamarock et al. 2005) to reproduce the surface circulations over a complex terrain region. The evaluation is performed on a daily basis in order to mitigate the influence of thermally induced circulations and thus focus on dynamically induced circulations associated with the interactions between the orography and the atmospheric dynamics. The capability of the simulation to reproduce both the wind variability and the climatological flows is evaluated. Special emphasis is paid during the evaluation to understand the influence that the topography and large scale representation exert over the surface wind estimations.

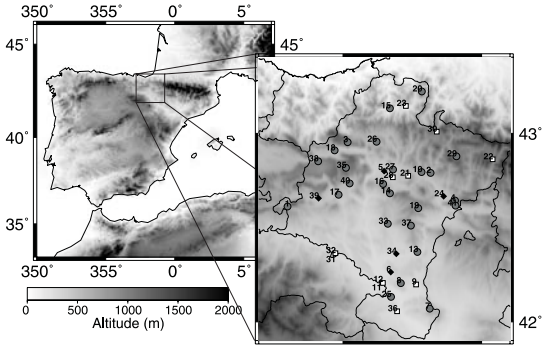

Figure 1. Location of the CFN within the Iberian Peninsula. The right panel shows the location of the observational sites (circles).

The Comunidad Foral de Navarra (CFN) a complex terrain region located in the Northeast of the Iberian Peninsula is selected for the study (Fig. 1). The CFN is characterized by strong wind conditions that have favored the large development of the wind energy over the area. In addition, it has a reasonable dense network of surface observations with wind observations available since 1992. The CFN constitutes given the existence of observations and a relatively complex terrain an interesting area for evaluating the numerical simulation performance for future wind energy applications.

The complete observational period from 1992 to 2005 is simulated at a high horizontal resolution of 2 km over the CFN. This simulation provides both, a high spatial resolution to adequately represent the topography over the region, and a long simulated period to robustly analyze the large scale influence on the surface wind estimations. To our knowledge, there are no previous simulations that

analyzed the surface wind behavior over such an extended temporal period (over thirteen years) at such a high horizontal resolution (2 km).

The wind variability over the area is analyzed in a first step using the information from the observational network (Jiménez et al. 2008a). The analysis consists in the identification of areas of coherent wind behavior. This classification is accomplished with a twofold objective. In first place, it contributes to understand the surface wind variability over the CFN and secondly, it provides an appropriate framework to evaluate the simulation performance. The regionalization is accomplished by classifying together those observational sites with similar temporal wind variability. A total of four regions in concordance with the topographic features of the terrain are identified. The meridional wind variability is rather similar at the four subregions being the zonal wind variability which causes the differences between the subregions.

Evaluating the model performance at the regional scale provides certain advantages than the traditional evaluation at the sites (Jiménez et al 2008b). The averaging of the time series to obtain the regional ones mitigates the influence of local effects in the observational time series and representativeness errors in the simulated ones, enhancing the regional signal and thus providing more appropriated time series for comparison. The analysis reveals the capability of the WRF simulation to reproduce areas of coherent wind behavior.

A further understanding of the wind circulations over the CFN is obtained by analyzing the climatological surface flows over the area. This is accomplished by classifying the observed wind fields with similar structure into groups of typical surface circulation or wind patterns (WPs, Jiménez et al. 2009). The resulting classification is also used to evaluate the WRF simulation performance in reproducing the climatological flows over the area. A total of six WPs are identified. The WPs tend to show a northwest or southeast orientation of the flow. This result shows the strong influence that orography produces over the surface circulations, since the valleys over the region are mainly oriented in the NW-SE direction (Fig. 1). The WPs are more frequent in some seasons than others showing a certain annual evolution. In order to understand the large scale mechanisms that originate the regional circulations, the sea level pressure (SLP) fields over the area are classified into pressure patterns (PPs) and related to the WPs already identified. The relationships found between the PPs and the WPs reveal the strong influence exerted by the ageostrophic balance over the CFN surface circulations, and the wind intensification produced by the pressure gradient along the valleys.

The WRF simulation reproduces reasonable well the spatial structure of the flow of the WPs. However, the simulation underestimates the wind on the mountain stations (the windiest sites) and tend to overestimate the wind at the valley subregions (the less windy areas), causing an underestimation of the spatial variability of the wind speed field. This behavior is partially related with the smoother orography used in the simulation. However, there are some WPs under which the wind speed is underestimated over the valley subregions being this behavior contrary to the general tendency of underestimating the wind speed over the valleys. The knowledge of the synoptic forcings, the PPs, that generate the regional wind variability, the WPs, allows to look for possible explanations in the large scale. The analysis reveals limitations of the numerical simulation to reproduce certain large scale fields. In particular, the misrepresentation underestimates the pressure gradient along the valleys of the CFN which in turn produces the wind speed underestimation. Therefore, both the topography representation and the large scale reproducibility introduce biases on the surface wind simulation. This suggests that the potential improvement expected by increasing the horizontal resolution may be at least partially hampered if the large scale can not be appropriately represented.

In summary, the WRF simulation shows a reasonable good accuracy to reproduce the wind variability over the area, with certain biases in reproducing the climatological flow. This finding encourages to extend the simulation in order to analyze the wind variability over the CFN before 1992 when wind observations are very limited. A certain correction seems to be necessary to suppress the systematic errors introduced by the downscaling in order to extend our understanding of the climatological flows over the area. One possible correction could relay on the use of the SLP classification to correct the biases introduced in the wind estimations by each PP. The extended simulation can be used for instance to analyze the sustainability of the wind farms already installed in the region. This is an important issue at the view of the increasing humankind demand for electricity.

References

Jiménez, P.A., J. F. González-Rouco, J. P. Montávez, J. Navarro, E. García-Bustamante and F. Valero, Surface wind regionalization in complex terrain, *J. applied Meteor. & Climatol.*, Vol., 47., pp. 308-325, 2008a.

Jiménez, P.A., J. F. González-Rouco, J. P. Montávez, E. García-Bustamante and J. Navarro, Climatology of wind patterns in the northeast of the Iberian Peninsula, *Int. J. Climatol.*, Doi 10.1002/joc.1705, 2009 (in press.)

Jiménez, P.A., J. F. González-Rouco, E. García-Bustamante, J. Navarro, J. P. Montávez, J. Vilà-Gerau de Arellano, J. Dudhia and A. Muñoz-Roldan, Surface wind regionalization over complex terrain: an evaluation of a high resolution WRF simulation, *J. applied Meteor. & Climatol., (Submitted)* 2008b.

Reid, S. and R. Turner, Correlation of real and model wind speeds in different terrains, , *Wea. Forecasting*, Vol., 16., pp. 620-627, 2001.

Skamarock, W. C., J. B., Klemp, J. Dudhia, D. O. Gill, D. M. Barker, W. Wang, and J. G. Powers, A description of the advanced research WRF Version 2. Thechical Report TN-468+STR, NCAR, 2005.

Whiteman, C. D., Mountain meteorology: fundamentals and applications. Oxford University Press, 355 pp., 2000.

JP10: 59-year 10 km dynamical downscaling of re-analysis over Japan

Hideki Kanamaru, Kei Yoshimura, Wataru Ohfuchi, Kozo Ninomiya and Masao Kanamitsu

Climate Change and Bioenergy Unit, Viale delle Terme di Caracalla 00153 Rome, Italy. Hideki.Kanamaru@fao.org

1. Introduction

To date, multi-decadal dynamical downscaling simulations driven by the Reanalysis data have been completed over many regions (e.g., Vidale *et al.*, 2003), but only a few are in *very high* resolution, which is required for application studies such as agricultural study or energy and water resources management. As one such very high resolution long-term simulation, Kanamitsu and Kanamaru (2007; KK07 hereafter) conducted a 10 km resolution run over California for a half-century. KK07 revealed that these simulations had better skill than the regional Reanalysis product, NARR, whose spatial resolution (32 km) is coarser than the dynamical downscaling simulations (10 km), because the current data assimilation system is incapable of effectively utilizing high-density near-surface observations, and places more weight on the initial guess produced by the regional high-resolution numerical model.

In this study, we conduct a similar long-term high resolution dynamical downscaling as CaRD10 over Japan. The product is hereafter called JP10. The major objective is to demonstrate that the dynamical downscaling is capable of reproducing small scale detail which agrees better with station observations than the coarse resolution analysis, without injecting small scale observation. To do so, the accuracy of JP10 will be compared with independent high density in-situ observation data, and how JP10 reproduces some historical extreme events will be also investigated.

2. Model and Observation

The Regional Spectral Model (RSM; Juang and Kanamitsu 1994) originates from the one used at the National Centers for Environmental Prediction (NCEP), but the code was updated with greater flexibility and much higher efficiency (Kanamitsu et al. 2005) at the Scripps Institution of Oceanography. The RSM utilizes a spectral method (with sine and cosine series) in two dimensions. A unique aspect of the model is that the spectral decomposition is applied to the difference between the full field and the time-evolving background global analysis field. The model configuration and the downscaling method in this study are basically the same as that of CaRD10 (10 km California Reanalysis Downscaling; Kanamitsu and Kanamaru, 2007) but for a domain covering Japan Islands (22.123°–49.163°N and 119.960°–151.577°E; shown in Figure 1a with topography) for 1948 to 2006, and with narrower lateral boundary nudging zones that extends only 2.5% of the total width in each of four lateral boundaries instead of 11.5% in CaRD10 to increase the useable domain.

As same as CaRD10, a spectral nudging scheme, i.e., scale selective bias correction (SSBC, Kanamaru and Kanamitsu 2007), is applied to the Reanalysis large scale thermodynamic fields for a 10 km horizontal resolution downscaling simulation, to reduce the growth of large-scale error spanning the regional domain. The scheme consists of three components: 1) dampening the large-scale (more than 1000 km scale) part of the wind perturbation toward zero, with dampening coefficient of 0.9, 2) removing the area average perturbation of temperature and moisture at every model level, and 3) adjusting the area mean perturbation logarithm of surface pressure to the corresponding difference of logarithm of surface pressure due to the area mean difference in the global and regional topography.

For verification of the JP10 dataset, this study uses hourly precipitation, surface temperature, and surface wind direction and speed from the AMeDAS re-statistic dataset (JMBSC, 2007), which is a surface meteorological observation dataset of 29 years (1976-2004) from over 1,300 Japanese automated meteorological data-acquisition system (AMeDAS) sites. These observation sites are distributed across Japan at intervals of about 20 km on average. The locations of all the observatories are shown in Figure 1b. These about 1300 sites are divided into 9 groups in accordance to the geographical divisions in Japan Meteorology Agency (JMA).

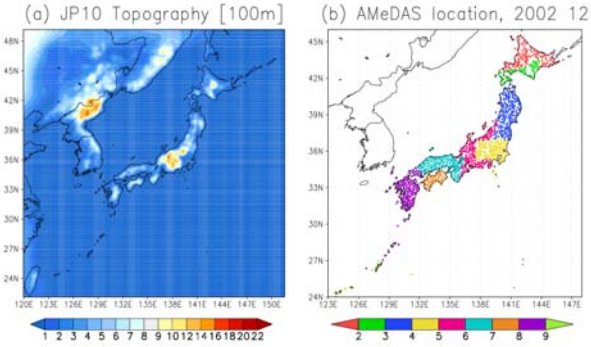

Figure 1. (a) Domain and topography and (b) AMeDAS observatories location. Nine regions are classified as N-Hokkaido (red), S-Hokkaido (green), Tohoku (blue), Kanto (yellow), Chubu (pink), Kinki (sky blue), Shikoku (orange), Kyushu (purple), and Okinawa (light green).

3. Results

Climatology

Figure 2 shows monthly climatology variations averaged over each of the nine AMeDAS regions. It is notable that there is significant systematic over estimation of precipitation all over Japan whereas air temperature is almost perfectly agreed. By intensive investigations, we found that this is due to the over correction of humidity field by this version of SSBC.

Daily variations

As shown in Figure 2, downscaled daily variations of surface meteorology at one of the AMeDAS observatories in Okinawa Island are well reproduced, particularly for wind and air temperature. Precipitation includes errors in amount and timing. In Figure 3, daily air temperature in a month at each observatory is compared with those of JP10, and the distributions of their correlation coefficients are shown for four months (Feb., May, Aug., and Nov.) in 1976. This figure indicates that high frequency variations of the air temperature associated with the synoptic scale weather changes are accurately captured in the downscaled product (in average, more than 0.8 of correlation coefficient), whereas the original coarse scale Reanalysis could not reproduce them in this degree of accuracy. Note that the accuracy is relatively low in

summer particularly in the Pacific side, indicating that not only synoptic scale behavior but also finer scale feature may take an important role by, such as, localized disturbances. The wind fields are similarly reproduced as air temperature (figure not shown).

In contrast, precipitation is not reproduced as well as temperature and wind by the JP10, with averaged correlation coefficient of 0.3~0.7. Figure 4 shows the same but for precipitation, with significantly larger number of the observatories. Interestingly, the seasonality of the scores is more apparent in precipitation, i.e., summer and Pacific side precipitation is more difficult, due to sub-grid scale convective activity and also low quantitative reproducibility of typhoon and Baiu systems by the model and analysis.

Hazardous snow events

In Figure 5, monthly mean snow water equivalent (SWE) amount is averaged over all Honshu Island. According to the hazard record in Japan reported by JMA, there were deadly severe events in the winters of 1960-61, 62-63, 73-74, 76-77, 80-81, 83-86, and 2005-06. These hazardous events are captured in this preliminary analysis of JP10 to some extent. Note that there is no official record before 1960.

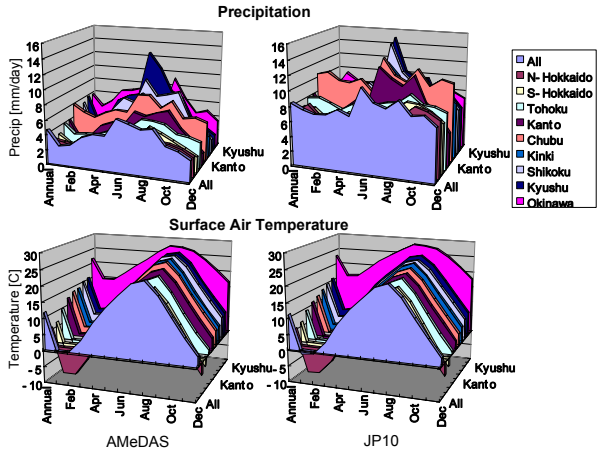

Figure 2. Monthly climatology of precipitation and surface air temperature averaged over the nine AMeDAS regions.

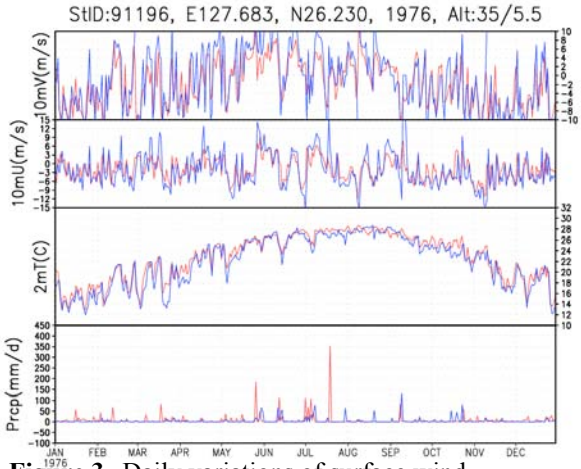

Figure 3. Daily variations of surface wind components, air temperature, and precipitation of AMeDAS observation (blue) and JP10 (red) in Okinawa Island.

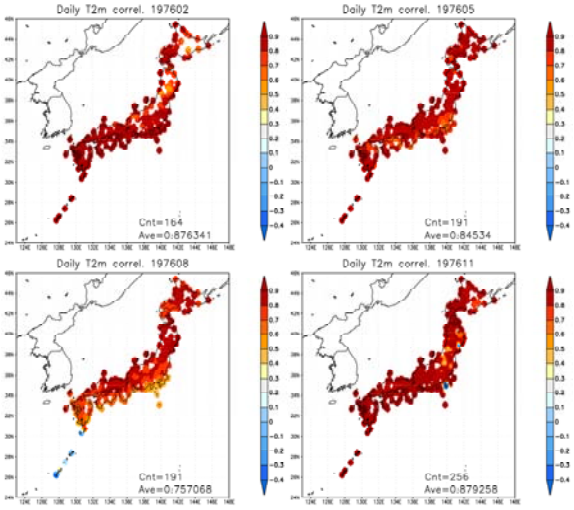

Figure 4. Distributions of correlation coefficients of monthly-long daily precipitation in four seasons. Number of the observation sites and arithmetic average of the coefficients of all sites are also shown.

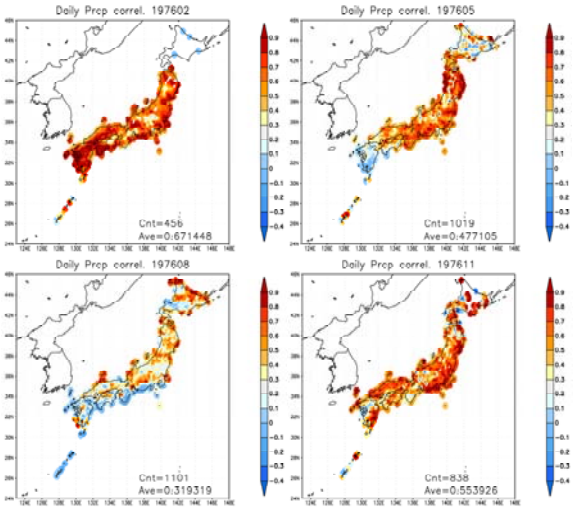

Figure 5. Same as Figure 3, but for precipitation.

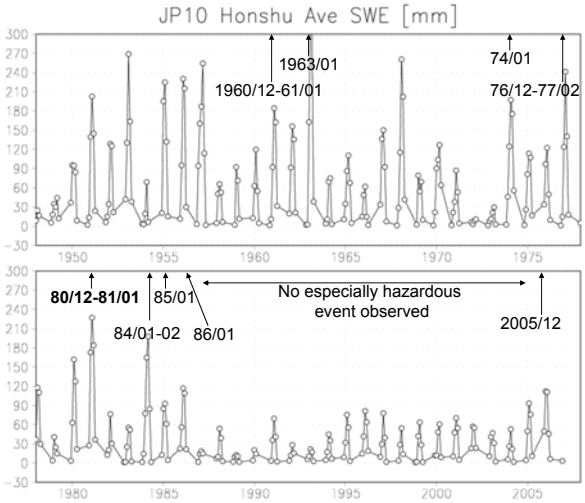

Figure 6. JP10 monthly mean SWE averaged over all Honshu Island and historical hazardous snow events.

Satellite-based datasets for validation of regional climate models: The CM-SAF product suite and new possibilities for processing with 'climate data operators'

F. Kaspar (1), J. Schulz (1), P. Fuchs (1), R. Hollmann (1), M. Schröder (1), R. Müller (1), K.-G. Karlsson (2), R. Roebeling (3), A. Riihelä (4), B. de Paepe (5), R. Stöckli (6) and U. Schulzweida (7)

(1) Satellite Application Facility on Climate Monitoring (CM-SAF), Deutscher Wetterdienst, Offenbach, Germany (frank.kaspar@dwd.de), (2) CM-SAF, Swedish Meteorological and Hydrological Institute, (3) CM-SAF, Royal Netherlands Meteorological Institute, (4) CM-SAF, Finnish Meteorological Institute, (5) CM-SAF, Royal Meteorological Institute of Belgium, (6) CM-SAF, MeteoSwiss, (7) Max-Planck-Institute for Meteorology, Hamburg, Germany

1. Introduction: EUMETSAT's Satellite Application Facility on Climate Monitoring (CM-SAF)

Increasing the confidence in model-based climate projections requires evaluation of climate simulations with high-quality observational datasets. Satellite data provide information on the climate system that are not available or difficult to measure from the Earth's surface like top of atmosphere radiation, cloud properties or humidity in the upper atmosphere. In particular over ocean and sparsely populated areas space-based observations are largely the only data source. Especially for evaluating the generality of climate models across varying locations, satellite-derived datasets have the strong advantage of consistent measurements and processing methodologies across regions. Existing satellite time series, especially from operational meteorological satellites, now reach a length that makes them useful for climate analysis.

Following this idea, EUMETSAT's Satellite Application Facility on Climate Monitoring (CM-SAF) is dedicated to the high-quality long-term monitoring of the climate system's state and variability. CM-SAF supports the analysis and diagnosis of climate parameters in order to detect and understand changes in the climate system. One goal is to support the climate modelling communities by the provision of satellite-derived geophysical parameter data sets.

CM-SAF provides data sets of several cloud parameters, surface albedo, radiation fluxes at top of the atmosphere and at the surface, atmospheric temperature and water vapour profiles as well as vertically integrated water vapour (total, layered integrated). They are derived from geostationary (SEVIRI and GERB instruments) and polar-orbiting (AVHRR, ATOVS and SSM/I instruments) meteorological satellites (*Schulz et al*., 2008).

Products from the SEVIRI instrument on-board the geostationary Meteosat Second Generation satellites cover the full visible Earth disk, that extends from South America to the Middle East, with Africa fully included and Europe in the North. Products derived from the AVHRR-sensor on-board the polar-orbiting satellites cover Europe, the East Atlantic and the Inner Arctic. For these sensors, cloud and radiation products are generated at original pixel resolution of a few kilometres. These intermediate products are then aggregated to daily and monthly averages in equal-area projections. SSM/I (over ocean only) and ATOVS water vapour products offer global coverage. The SSM/I total column water vapour series based on intercalibrated radiances already covers almost 20 years with a quality sufficient to perform studies of inter-annual variability and possibly trends.

2. The CM-SAF product suite

The following products are currently available and can be ordered free-of-charge at www.cmsaf.eu:

Cloud parameters: Cloud fractional cover (CFC), cloud type (CTY), cloud top pressure, height and temperature (CTP/CTH/CTT), cloud phase (CPH), cloud optical thickness (COT), cloud water path (CWP).
These products are available at a spatial resolution of $(15\text{km})^2$. For the *CM-SAF Baseline Area* (30°N to 80°N, 60°W to 60°E, i.e. Europe and the North Atlantic) they are derived from the AVHRR sensor and are available since 01.01.2004. For the *Meteosat Disc Area* (see Figure 1) they are derived from the SEVIRI sensor and are available since 01.09.2005.

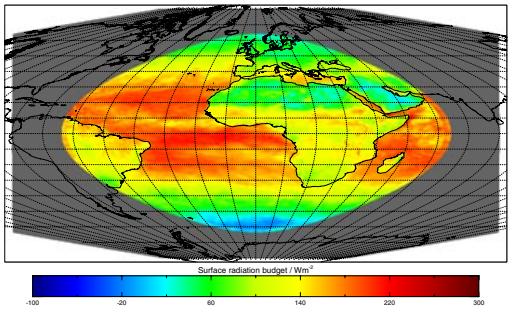

Figure 1. Monthly mean surface radiation budget for September 2007 [W/m^2] derived from Meteosat-9 / SEVIRI observations (geostationary satellite)

Humidity products: Total (HTW) and layered (HLW) precipitable water. Mean temperature and relative humidity for 5 layers as well as specific humidity and temperature at the six layer boundaries (HSH).
Spatial resolution is $(90\text{km})^2$. The products are derived from the ATOVS sensor, have global coverage and are available from 01.01.2004 onwards.

Surface radiation: Incoming short-wave radiation (SIS) surface albedo (SAL), net shortwave radiation (SNS) net longwave radiation (SNL), downward long-wave radiation (SDL), outgoing long-wave radiation (SOL), surface radiation budget (SRB)
Spatial resolution is $(15\text{km})^2$. For the *CM-SAF Baseline Area* they are derived from AVHRR and are available

since 01.01.2004. For the *Meteosat Disc Area* they are derived from SEVIRI and are available since 01.09.2005.

Top-of-atmosphere radiation: Incoming solar radiative flux (TIS), reflected solar radiative flux (TRS), emitted thermal radiative flux (TET). Spatial resolution is $(45km)^2$. The products are derived from GERB and CERES for the *CM-SAF Baseline area* and *Meteosat disc Area*. They are available from 01.02.2004 onwards.

The above mentioned products are produced as first-guess products in near-real time on a day-to-day basis. Intermediate products on higher spatial and temporal resolution are available on request. CM-SAF currently prepares reprocessing of long-times series which will be based on carefully intercalibrated radiances. These time-series will cover periods of up to 20 years and will become available in 2010 and 2011.

3. New products for the Inner Arctic

With January 2009, CM-SAF's product suite has been extended to the Inner Arctic (see Figure 2). Several cloud parameters (cloud fraction; cloud type; cloud top height/temperature/pressure) as well as surface albedo are derived from the Advanced Very High Resolution Radiometers (AVHRR) on-board polar-orbiting satellites (NOAA-17, NOAA-18 and MetOP2).

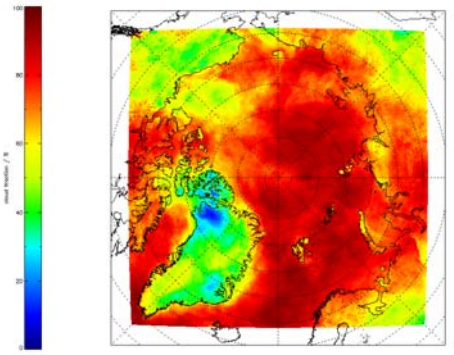

Figure 2. Monthly mean cloud fraction in the Inner Arctic [%] for August 2007.

The processing exploits AVHRR data at full spatial resolution (~1.1 km at nadir) for all available overpaths of the polar-orbiters (~ 43 per day for the three satellites) and is based on a multi-spectral threshold technique applied to each pixel of the satellite scenes.
Selected months in 2007 have already been generated for product validation. First comparisons have shown that the monthly mean cloud cover products over the Arctic region in the polar summer of 2007 are capable of reproducing similar results as those based on the more sophisticated and spectrally superior MODIS instrument. Validation against ground-based measurements (synoptic observations) also shows that the product is within the required accuracy. In agreement with other studies, the data indicate that for some part of the Arctic, low cloud amounts occurred in summer 2007 which could be a contributing factor to the unprecedented rapid melting of sea ice during the polar summer of 2007. The new CM-SAF products for the Arctic offer additional opportunities for such analyses and regular monitoring of such processes. The data could be valuable for validation of process studies within the International Polar Year (*Kaspar et al*., 2009)

4. Processing of CM-SAF datasets with the 'climate data operator' package

In the past a drawback for model-data-comparisons and similar validation studies have been the different data formats of both communities.

CM-SAF's climate monitoring products are provided as HDF5 (Hierarchical Data Format, release 5). Reasons for selecting HDF5 were its high compression efficiency and the features to include several data models and self-describing datasets. In order to allow easy access to CM-SAF datasets for the climate modeling community, the possibility to import CM-SAF data has recently been integrated into the ‚climate data operators' (CDO) which is a well-established conversion tool in the climate modelling community http://www.mpimet.mpg.de/~cdo). This package was originally developed for processing and analysis of data produced by a variety of climate and numerical weather prediciton models (e.g. for file operations, simple statistics, arithmetics, interpolation or the calculation of climate indices).

Besides the pure conversion of CM-SAF-HDF5-files to NetCDF and GRIB, this offers additional possibilities for preprocessing the data for validation studies, especially interpolation to other grid types and selection of regions. The implementation considers special features, e.g. methods for interpolation of non-continuous datasets as e.g. cloud types. Daily and monthly mean products of CM-SAF are provided in equal-area projections that are described in the metadata entries of the HDF5-files. CDO employs this information for spatial operations on these final products. Processing of CM-SAF intermediate products on original pixel-resolution for polar-orbiting satellites as well as geostationary satellites is also facilitated when pixel-related geolocation is available. This allows access to datasets with high spatial resolution of a few kilometres.

References

Kaspar, F., R. Hollmann, M. Lockhoff, K.-G. Karlsson, A. Dybbroe, P. Fuchs, N. Selbach, D. Stein, J. Schulz: Operational generation of AVHRR-based cloud products for Europe and the Arctic at EUMETSAT's Satellite Application Facility on Climate Monitoring (CM-SAF), *submitted to Adv. Sci. Res*, 2009.

Schulz, J., W. Thomas, R. Müller, H.-D. Behr, D. Caprion, H. Deneke, S. Dewitte, B. Dürr, P. Fuchs, A. Gratzki, R. Hollmann, K.-G. Karlsson, T. Manninen, M. Reuter, A. Riihelä, R. Roebeling, N. Selbach, A. Tetzlaff, E. Wolters, A. Zelenka, M. Werscheck: Operational climate monitoring from space: the EUMETSAT satellite application facility on climate monitoring (CM-SAF), *Atmos. Chem. Phys. Discuss*., 8, 8517-8563, 2008, accepted for publication in *Atmos. Chem. Phys.*

Reflection of shifts in upper-air wind regime in surface meteorological parameters in Estonia during recent decades

Sirje Keevallik[1] and Tarmo Soomere[2]

[1] Marine Systems Institute at TUT, Tallinn, Estonia. sirje.keevallik@gmail.com
[2] Institute of Cybernetics at TUT, Tallinn, Estonia. soomere@cs.ioc.ee

1. Regime shifts in the free atmosphere

Most of the analysis of the gradual change of the climate of the Baltic Sea region has been concentrated on extracting linear trends and/or periodic variability in local meteorological parameters (*BACC* 2008). Recent studies have shown that a new type of systematic behaviour of the climate system – switch-like events with largely varying periods between abrupt changes (shifts) in certain decisive parameters, perhaps most widely discussed in paleoclimatology, are able to essentially disturb otherwise more or less gradual or cyclic evolution of the Earth systems (*Scheffer et al*. 2001).

There is very little information on such switch-like behaviour of the climate system in the Baltic Sea region. In our earlier paper (*Keevallik and Soomere* 2008) we demonstrated evidence about shift-like changes of the winter-to-spring switch-time of the upper air flow regime at 850 and 500 hPa levels over the north-eastern Baltic Sea, inferred from a data set recorded at Tallinn Aerological station during 1955–2007.

The annual course of the upper air flow over this region has two typical regimes: a relatively intense north-westerly flow during the autumn and winter season (September–February) and a less intense south-westerly flow during the spring and summer season (April–August). The flow transition is quite abrupt at the beginning of the summer season, but fairly smooth at its end.

The key outcome of the analysis of the nature of the flow with the use of the switch-detection technology of *Rodionov* (2004) was that the long-term variation of the transition time hosts neither simple linear trend nor periodic behaviour. Instead, it exhibits certain clearly defined multiple regime shifts. The largest changes have occurred in March. In the middle of the 1960s the average air flow in March turned from NW to W at the 500 hPa level. The original regime was restored in the mid-1990s (Fig. 1). Analogous changes (the turn of the air flow from WNW to WSW and back) occurred also in the air flow at the 850 hPa level.

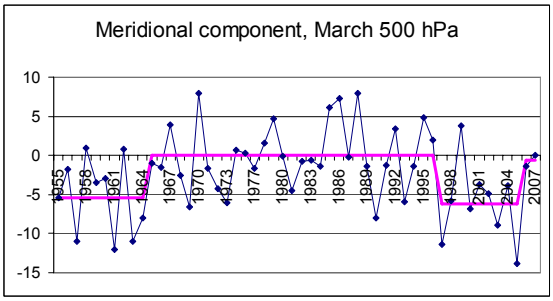

Figure 1. Regime shifts in the meridional wind component on the 500 hPa level in March (*Keevallik and Soomere* 2008).

As the local meteorological parameters not necessarily exactly mirror the nature of or changes in the upper air flow, detection of such shifts from surface data is a highly nontrivial problem. The best candidate for the analysis is the marine wind that reflects many properties of the flow in upper layers. Also, records made on the coasts of a large lake may contain a certain signal from such shifts.

In this paper, we present the first evidence of switch-like behaviour of certain local meteorological parameters on Estonian coasts. Shown is that (i) major shifts have taken place in the average direction of the surface air flow in the northern Baltic Proper and (ii) clearly detectable shifts exist in records of temperature, precipitation and cloud cover over the western coast of Lake Peipsi.

2. Average air flow at the surface

The analysis of wind data at Vilsandi meteorological station (58°23'N, 21°29'E) was carried out for the years of 1966–2003. Meteorological data at Vilsandi have been recorded since 1897, but due to major changes in measurement regime, using of earlier wind data are not recommended (*Keevallik and Soomere 2008*). The observation site on this small island in the western Estonian archipelago is located about 120 m from the coastline on a small limestone plateau, about 5 m above the mean water level. The site is completely open to dominant marine wind directions from SW to NNW and has been shown to adequately reflect marine wind properties (*Soomere and Keevallik* 2001)

The average wind speed for 1966–2003 was 6.30 m/s. At the same time, the average zonal component of the wind vector was only 1.23 m/s and meridional component 0.71 m/s. Therefore, the average air flow was only 1.41 m/s. The large difference between the mean wind speed and the average air flow shows that wind direction at this site is extremely variable (Fig. 2), a feature which is not unexpected in the Baltic Sea meteorological system.

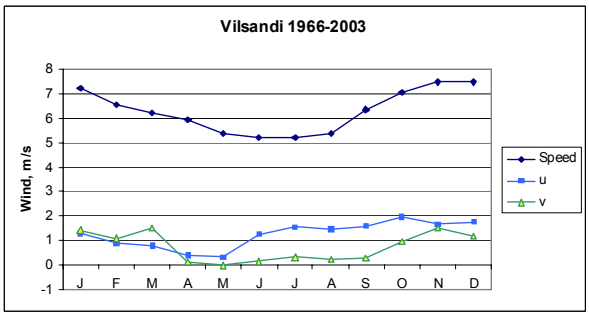

Figure 2. Average wind speed and air flow components at Vilsandi. Here *u* is the zonal component and *v* is the meridional component.

Trend analysis reveals significant changes in the average meridional and zonal components of the air flow in January and February (Fig. 3). While the average flow was predominantly directed to the West in the 1960s and the 1970s, it has turned to the East since about 1980. On the other hand, no trend can be noticed in the wind speed.

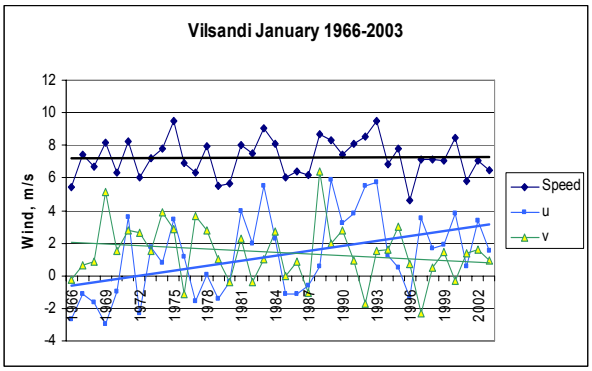

Figure 3. Trends in wind speed and air flow components in January. Here *u* is the zonal component and *v* is the meridional component.

The changes in the average air flow become even more clearly evident when one plots the vectors representing the monthly average direction of the air flow at the beginning and at the end of the time interval in question (Fig. 4).

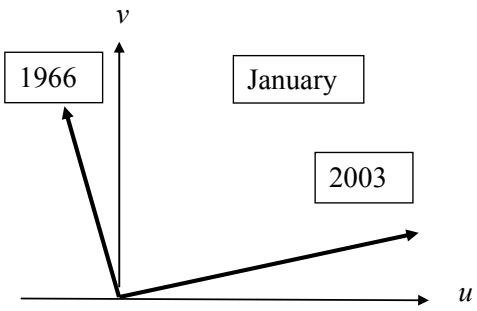

Figure 4. Changes in the average air flow vector at Vilsandi in January.

Figure 4 demonstrates that the average air flow has somewhat strengthened during 1966–2003. A much more fascinating change is that the average direction of the flow has turned remarkably, clockwise by 90 degrees. A similar turning was detected also in the winds on the 500 hPa level by *Keevallik and Soomere* (2008).

A similar analysis for other months reveals the features that somewhat deviate from the conclusions made for the changes in the upper-air flow. For example, identifiable changes exist neither in the wind speed nor in the wind components in June in the upper air flow for the same time interval. Surface data, however, show clearly that the average air flow has turned counter-clockwise and strengthened (Fig. 5).

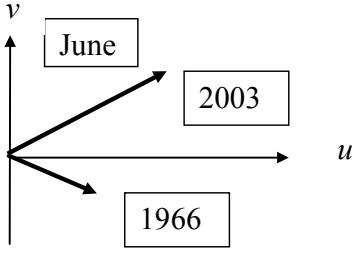

Figure 5. Changes in the average air flow vector at Vilsandi in June.

3. Regime shifts over Lake Peipsi

A significant rising trend in temperature, accompanied by increase in the amount of precipitation and low clouds was established for Tiirikoja meteorological station (58°12'N, 26°57'E) during 1955–1995 (*Keevallik* 2003). This site well described the meteorological situation over the northwestern part of Lake Peipsi. Figure 6 demonstrates that rather a major regime shift has occurred in this region in 1988–89.

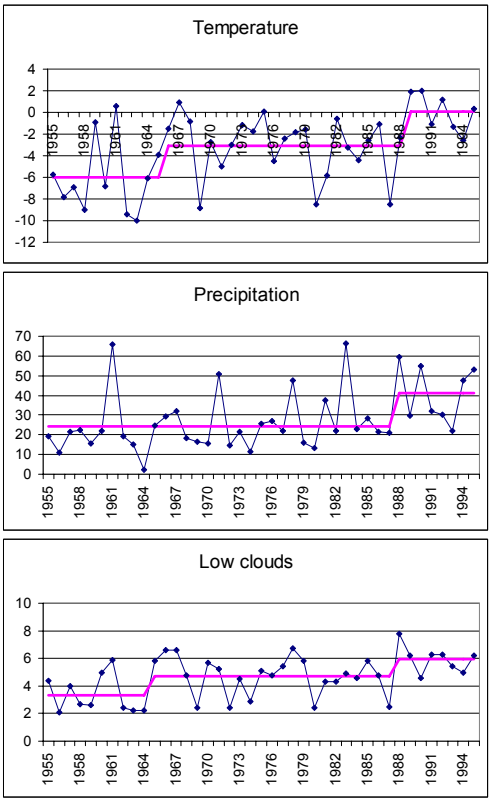

Figure 6. Regime shifts in meteorological parameters at Tiirikoja in March

The presence of (multiple) shifts of different meteorological parameters suggests that the climate system (either its gradual changes or its natural variability) over Estonia comprises considerable nontrivial, switch-like variability with time scales of about 20–30 years.

References

Keevallik S. Changes in spring weather conditions and atmospheric circulation in Estonia (1955–95), *Int. J. Climatology,* **23**, 263–270, 2003.

Keevallik S., Soomere T. Shifts in early wind regime in North-East Europe (1955–2007),*Climate of the Past*, 4, 147–152, 2008.

Rodionov S.N. A sequential algorithm for testing climate regime shifts, *Geophys. Res. Lett.*, **31**, L09204, 2004.

Scheffer M., Carpenter S., Foley J.A., Folke C., Walker B. Catastrophic shifts in ecosystems, Nature **413** (6856), 591–596, 2001.

Soomere T., Keevallik, S. Anisotropy of moderate and strong winds in the Baltic Proper, *Proc. Estonian Acad. Sci. Eng.*, **7**, 35–49, 2001.

Regional features of recent climate change in Europe: Aggregated index approach

Valeriy N. Khokhlov and Lyudmila G. Latysh

Hydrometeorological Institute, OSEU, Lvovskaya str. 15, Odessa 65016, Ukraine, e-mail: vkhokhlov@ukr.net

1. Introduction

Considering for the climate in the widest sense, i.e. as a state of system consisting of five main components: atmosphere, hydrosphere, cryosphere, earth surface, and biosphere, many parameters, more or less significant from a variability view, must be taken into account separately and/or together to describe its changes.

The trend of global temperature is, due to its obviousness, one of the most frequently used parameters. During the last one hundred years, the global temperature increased by ~0.74°C, and this warming is most probably determined by the anthropogenic impact (*IPCC*, 2007). Also, the warming was associated with the sea level rise and the decrease of snow cover in Northern Hemisphere. From the other hand, some regions (e.g. South Atlantic, Alaska etc.) were getting colder. Furthermore, overall rise of temperature against the increasing annual precipitation were observed over Eurasia with the exception of East Asia where the precipitation were reduced. In other words, the changes of these climate parameters are in whole not connected to each other, which is explained by a complexity of processes progressing in the global climatic system. It is thus necessary not only to investigate regional climate changes, but to produce also some approach permitting a quantitative assessment for the complex concept of "climate change". It's for that *Giorgi* (2006) and *Baettig et al.* (2007) introduced the notion of "Climate Change Index" (CCI), which summarizes as far as possible the quantitative indicators of climate such as statistics for the variability of temperature and precipitation.

This communication purposes to describe spatial distribution of the CCI proposed by *Baettig et al.* (2007) to reveal regional features of recent climate change in Europe.

2. Data and Methodology

Baettig et al. (2007) presented an aggregated CCI summarizing various climatic information into single value, a possible measure for projected climate change. This CCI is composed of different temperature and precipitation indicators. This communication adopts the original approach of *Baettig et al.* (2007) to reveal regional features of climate change using the monthly surface temperature and monthly precipitation form 1949 to 2006. We use the period 1949-1977 as reference and 1978-2006 as control. The length of both periods is almost "conventional" in the climate sense (30 years). Moreover, it is well known that the decrease of temperature in the Europe was observed from end of 1940-th up to end of 1970-th whereupon the decrease of temperature began. Therefore, such a choice of periods looks as reasonable.

The main data source is the NCEP/NACR Reanalysis data in the domain bounded with 30N and 80 N, 20W and 60E; grid steps along latitude and longitude are 1.875º and ~1.9º respectively. To detail regional features of climate change, the information from meteorological sites (at the average, 4-5 sites per grid cell over land) are used.

Following *Baettig et al.* (2007), we calculate the indicators of four groups (see Table 1). All indicators are calculated according to the same principle, i.e. to identify the "1 in 20 years" most extreme event of the reference period and to calculate the occurrence of such an event within the control period. This method is based on the assumption that climate change and climate impacts manifest themselves through an increased occurrence of extreme events over a longer time period. To calculate the indicators, a cumulative density function was fitted to the data of the reference period and into those of the scenario period. The quantile corresponding to the 95th (and 5th) percentile was determined using the reference period distribution function; then the probability of this quantile was calculated under the control period. Indicator values are between 0 and 19 and express additional extreme events within 20 years.

Table 1. Indicator groups and individual indicators that are aggregated to the CCI

Indicator Group *Individual Indicator*
Change in annual temperature
1. Additional hottest years
2. Additional coldest years
Change in annual precipitation
3. Additional driest years
4. Additional wettest years
Change in extreme temperature events
5. Additional extremely warm JJA
6. Additional extremely cold JJA
7. Additional extremely warm DJF
8. Additional extremely cold DJF
Change in extreme precipitation events
9. Additional extremely dry JJA
10. Additional extremely wet JJA
11. Additional extremely dry DJF
12. Additional extremely wet DJF

Note that in contrast to the original formulation of *Baettig et al.* (2007) we use twelve indicators (additional coldest years, additional extremely cold JJA, and additional extremely cold DJF).

For the aggregation, each indicator group was assigned a total weight of one. Within the groups, weights were equally distributed among the indicators. Then, the CCI was calculated as the weighted mean of the indicators. It can thus assume values between 0 and 19 (see *Baettig et al.* (2007) for details).

3. Results and Discussion

Against the overall increase of anomalous hottest and coldest years, there are some regions, e.g. the Arctics, Northern Europe, Western Mediterranean, with very large increase. It is noteworthy that this quantity is well correlated with the results based on the linear trends. Moreover, the regions most sensitive to the temperature anomalies are located close to Arctic and Atlantic Oceans and Mediterranean, although unambiguous conclusion on the low continentality of climate change can not be made.

As expected, the climate changes associated with anomalies of precipitation are defined by large

heterogeneity. For example, large anomalies of precipitation are observed in Central Europe, Balkans, and Northeast Turkey. From the other hand, both the temperature and precipitation in North Atlantic and the Arctic are distributed almost identical.

Before analyzing spatial distribution of CCI, let us divide its values into the three conditional ranks: low (CCI = 0 ÷ 2), moderate (CCI = 2 ÷ 4), and large (CCI > 4) climate change. Then, the distribution of aggregated CCI (see Fig. 1) shows that the most striking changes are observed northward of 70N, in Central Europe, North Sea, Pyrenees, western and central parts of Mediterranean. From the other hand, Russia and most part of Ukraine are defined by the low climate change.

It must be noted that the large climate change in regions are more frequent caused by the anomalies in the precipitation with the exception of the Arctics, where both the temperature and precipitation anomalies have an one-way influence on the CCI. Moreover, the large heterogeneity distinctive for the CCI indicates that a global process, to be referred to as a climate change, reveals in different regions in different ways, and some regularity can not be definitely detected using climatic concepts such as maritime climate, continentality etc.

References

Baettig M.B., Wild M., Imboden D.M., A climate change index: Where climate change may be most prominent in the 21st century, *Geophysical Research Letters*, Vol. 34, No. 1, L01705, 2007

IPCC, Climate Change 2007: The Physical Science Basis. Summary for Policymakers, Geneva, 2007

Giorgi F., Climate change hot-spots, *Geophysical Research Letters*, Vol. 33, No. 8 L08707, 2006

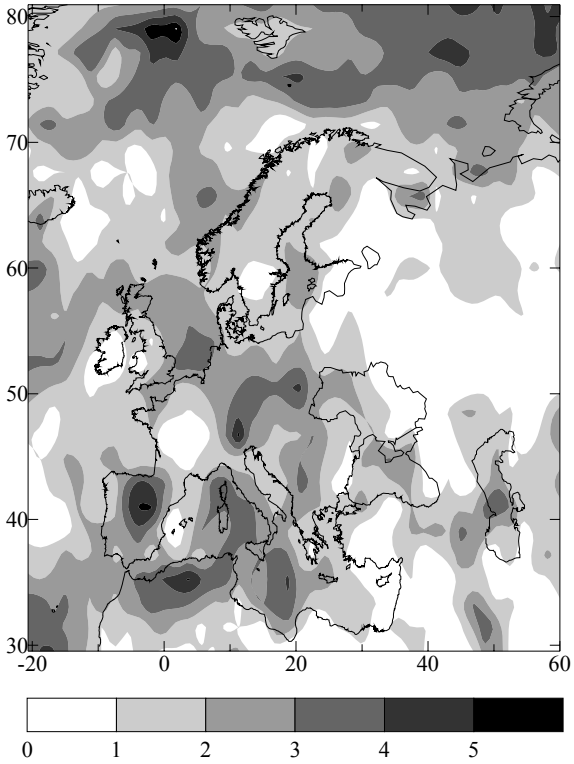

Figure 1. The aggregated CCI (additional number in 20 years) for the control period 1978–2006 with respect to reference period 1949–1977

Hindcasting Europe's climate – A user perspective

Thomas Klein

European Environment Agency, Copenhagen, Denmark. thomas.klein@eea.europa.eu

1. Needs

There is a general need for a consistent historical European coverage of climate data to support water, ecosystems and climate change-related integrated assessments, supporting EU policies, including the 6th Environment Action Plan, and complementing the GMES initiative with high quality and high resolution information on the physical state and past trends of the climate.

From an EEA perspective, the availability of sound and detailed European climate monitoring information is essential. In 2008, the EEA in partnership with the Joint Research Centre and World Health Organisation Europe produced the report "Impacts of Europe's changing climate" based on more than 40 indicators covering physical, biological and health impacts (EEA, 2008). The report shows widespread and increasing changes associated with climate change outside the most conservative estimates from the IPCC 2007 report.

However, the report also identifies data gaps such as the lack of consistent European data at the spatio-temporal resolution required for regional and local assessments. More detailed and quantitative, tailor-made information are especially needed for regional climate impact assessments and the development of cost-effective adaptation strategies.

2. The EURRA concept

The needs and data gaps outlined above are consistent with earlier findings which led to discussions between EEA and ECMWF and a workshop (ECMWF, 2005) with representatives of EEA, ECMWF and European National Meteorological and Hydrological Services about the concept of a high-resolution Europe-wide reanalysis, nested into climate quality global reanalyses. Such a European Regional Reanalysis (EURRA) could provide multi-decadal information on variables describing the state of the atmosphere, coastal ocean, snow cover and land surfaces (including vegetation and soil moisture).

European regional-scale high-resolution reanalysis requires basically three major components:

- A global-scale reanalysis system providing boundary fields for the regional system;
- A regional reanalysis system, together with additional downscaling techniques for the provision of very high-resolution information for specific surface and near-surface variables;
- Observational databases for space-based and terrestrial information to be assimilated.

Designing and building reusable European capacity consisting of the above components is essential to allow for gradual improvements of data quality and resolution in an iterative process. Updates of data sets can be performed when justified by sufficient improvements of system components, computational power and/or by the availability of better/more observational data in the input databases.

3. Outlook

In early 2009, the EEA held an expert meeting on climate information services based on atmospheric reanalyses, considering also the wider perspective of a GMES climate change service (EEA, 2009). The meeting was attended by the European Commission (DG ENV, DG JRC, DG RTD), ECMWF, EUMETNET, ESA, EUMETSAT, EEA, GEO and GCOS representatives as well as several country representatives. Confirming the need for consistent long-term data series with high quality and high resolution information on both basic essential climate variables as well as climate change indicators of impact and vulnerability, the meeting also identified the EURRA idea as a feasible way to address the requirements. In particular, EURRA is expected to serve many specific demands at European and local level, regarding indicators e.g. EEA/JRC/WHO report, the Commission's green paper and white paper on climate change, impacts assessments and adaptation measures, assessment of ecosystem services, hydrological applications etc.

At this stage, EURRA is still a concept, developed in response to evolving user needs which will need to be refined in an ongoing process. Moving from concept to project will require taking into account a number of project demands, such as the need for integration of large amounts of physical and socio-economic data, integrating space and in-situ, data discovery and recovery and high computer processing capacity. In addition to the technical requirements, EURRA will need a huge organizational effort, involvement of many potential actors, funding for capacity building and operation (e.g. through existing European funding mechanisms), access to observational data and a coherent dialogue and cooperation between data providers and users.

The next steps of the EURRA initiative will include a further consolidation of user requirements, identification of funding options, and, in particular, the communication and promotion of the EURRA concept in forthcoming workshops. It will also be crucial to learn from existing reanalysis experiences, including both global (e.g., ERA-40/ERA-Interim, NCEP/NCAR, JRA, ACRE) and regional (e.g., North American Regional Reanalysis, the Arctic System Reanalysis or the BALTEX Regional Reanalysis) reanalysis initiatives.

References

ECMWF, 2005: http://www.ecmwf.int/newsevents/meetings/workshops/2005/EURRA/index.html.

EEA, 2008: Impacts of Europe's changing climate – 2008 indicator-based assessment. European Environment Agency, Copenhagen.

EEA, 2009: http://eea.eionet.europa.eu/Public/irc/eionet-circle/gmes/library?l=/eurra.

Analysis of surface air temperatures over Ireland from re-analysis data and observational data

Priscilla A. Mooney[1], Frank J. Mulligan[2] and Rowan Fealy[1]

[1] Irish Climate Analysis and Research Units, National University of Ireland Maynooth, Kildare, Ireland.
priscilla.a.mooney@nuim.ie
[2] Department of Experimental Physics, National University of Ireland Maynooth, Kildare, Ireland.

1. Abstract

Since the observational data used in both ERA-40 and NCEP/NCAR Reanalysis data are largely identical, it is frequently assumed that either dataset is equally valid in the assessment of climate models. However, comparisons of these two dataset shows that subtle differences do exist and it is important to compare them to observational data in the region of interest to determine which reanalysis dataset should be used.

In this study, surface air temperatures at 2 m altitude predicted by ERA-40 and NCEP/NCAR reanalysis (NNRP-1) have been compared with observations at eleven synoptic stations in Ireland over the period 1958-2000. Both reanalysis datasets show good agreement with the observed data and with each other. Slopes of the least-squares line to scatter plots of reanalysis data to observational data show small differences between the two reanalyses, with NNRP-1 slopes and ERA-40 slopes ranging between (0.75-0.97) ±0.01 and (0.79-1.0) ±0.01, respectively. Summary statistics and the monthly mean temperatures over the 1979-2000 period showed that both reanalyses predicted significantly warmer winters than the observations which caused the slopes of the best fit lines to be consistently less than unity.

2. Introduction

Over the past decade reanalysis data has found widespread application in many areas of research ranging from studies of climatic trends (Ciccarelli et al, 2008) and climate modeling (Fealy and Sweeney, 2007) to estimation of renewable energy resources (Henfridsson et al, 2007). It is advantageous to use reanalysis data in certain research areas where observational data is sparse or when knowledge of the state of the atmosphere on a uniform grid is required.

Some of the most well known reanalysis data sets are NCEP/NCAR (NNRP-1), NCEP/DOE (NNRP-2), ERA-15, ERA-40 and ERA interim. NNRP-1 and ERA-40 are two of the most widely used reanalysis archives. Although they use similar observational data, previous studies have shown subtle differences between them (Escoffier and Provost, 1998; Li et al., 2004; Gleiser et al., 2005; Ruti et al., 2008).

Simmons et al., 2004 compared surface air temperature anomalies from CRUTEM2v with ERA-40 and NNRP-1. They found that ERA-40 showed better agreement with CRUTEM2v than NNRP-1 over the time periods 1958-2001 and 1979-2001. In addition they reported closer agreement between ERA-40 and CRUTEM2v over the period 1979-2001 compared with the period 1958-1979. This was attributed to the greater observational coverage after 1979.

3. Surface Temperature Datasets

NNRP-1 reanalysis data was produced by the National Centers for Environmental Predication (NCEP) in collaboration with the National Center for Atmospheric Research (NCAR). The assimilation system used in the NCEP/NCAR reanalysis is described in detail in Kalnay et al., 1996. The NNRP-1 data used in this study was obtained from the NOAA/OAR/ESRL PSD, Boulder, Colorado, USA web site at http://www.cdc.noaa.gov/.

ERA-40 data was produced by the European Center for Medium range Weather Forecasting (Uppala et al, 2005) in collaboration with several other institutions with an interest in climate analysis and weather forecasting. The ERA-40 data used in this study was obtained from the ECMWF data server (http://data.ecmwf.int/data/).

The observed station data used in this study for the period 1958-2000 was obtained from Met Éireann, the Irish national meteorological service, for 11 synoptic weather stations. The synoptic stations, which are geographically dispersed around Ireland (figure 1), represent mixture of both coastal and inland locations. This study did not perform any homogeneity analysis of the data. However, the data is from the synoptic network which is manned by experienced meteorological officers and the data is considered to be of high quality.

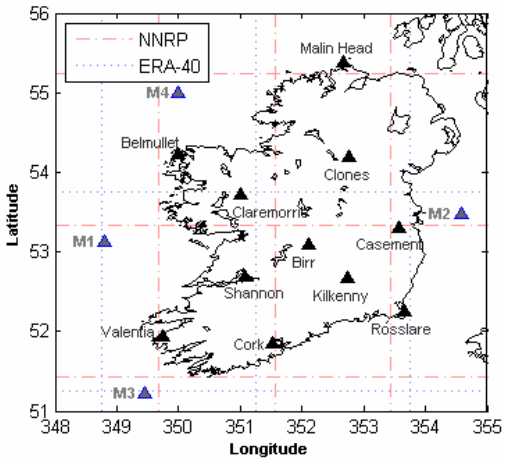

Figure 1. Map of Ireland showing the location of the eleven meteorological stations and the marine buoys M1 and M4. The map is overlaid with grids for NNRP (red --- line) and ERA-40 (blue… lines).

4. Collocation Method

Spatially, the parameter values in the reanalysis data sets represent the value of that parameter in a 'grid box' centred on the geographic coordinates given in the dataset. This presents a difficulty when comparing the station data with the reanalysis data, since the station data represents a single site within a grid box. Additional complications are introduced by the fact that the grid sizes in ERA-40 and NNRP-1 are different, the grid centres in the two reanalysis data sets are not coincident and the location of a station in the grid box can vary from the centre of the grid box to its edge. This is illustrated in figure 1 where the grids used by ERA-40 and NNRP-1 are plotted together with the location of the stations and marine buoys.

The approach used in this study obtains a weighted average of the reanalysis values of the 4 grid boxes whose centres lie closest to the station and assigns this value to the reanalysis for comparison with the station value. The average of the four grid boxes is obtained from the inverse distance weighted average (Stahl et al., 2006).

5. Analysis and Results

The study reported here compares the air temperature at 2 m in the NNRP-1 and ERA-40 data sets with observational data over Ireland for the period 1958-2000. This variable is examined at the 2 m height because there is a substantial quantity of observational data available for comparison at this vertical height. Previous comparisons of reanalysis datasets with observational data have tended to divide the data into two periods – pre- and post-1979 – on the basis that the reanalysis datasets after 1979 have significantly more observational data. This approach is also adopted here.

We examine the slopes of the best fit lines to scatter plots of reanalysis data with observational data at eleven synoptic weather stations. The best fit lines are the lines fitted to the data using the least squares method. This method shows that the reanalysis are consistent with the observations and with each other.

The analysis also includes a study of the mean temperature of each month over the period 1979-2000. Summary statistics (mean, mean absolute deviation, kurtosis and skewness) for the winter and summer season are also examined over the same period. These statistics show that both NNRP-1 and ERA-40 predicted significantly warmer winters than the observations.

References

Ciccarelli N, von Hardenberg J, Provenzale A, Ronchi C, Vargiu A, Pelosini R. Climate variability in north-western Italy during the second half of the 20th century. *Global and Planetary Change*, **63**:185-195. 2008.

Escoffier C, Provost C. Surface forcing over the South West Atlantic according to NCEP and ECMWF re-analyses over the period 1979-1990. *Phys. Chem. Earth* **23**(5-6): 537-542. 1998

Fealy R, Sweeney J. Statistical downscaling of precipitation for a selection of sites in Ireland employing a generalised linear modelling approach. *Int. J. Climatol*., **27**:2083-2094. 2007

Gleiser H, Thejll P, Stendel M, Kaas E, Machenhauer B. Solar signals in Tropospheric re-analysis data: comparing NCEP/NCAR and ERA-40. *J. Atmos. Solar Terr. Phys.*, **67**:785-791. 2005

Henfridsson U, Neimane V, Strand K, Kapper R, Bernhoff H, Danielsson O, Leijon M, Sundberg J, Thorburn K, Ericsson E, Bergman K. Wave potential in the Baltic Sea and the Danish part of the North Sea, with reflections on the Skagerrak. *Rewewable Energy*, **32**:2069-2084. 2007

Kalnay E, Kanamitsu M, Kistler R, Collins W, Deaven D, Gandin L, Iredell M, Saha S, White G, Woolen J, Zhu Y, Chelliah M, Ebisuzaki W, Higgins W, Janowiak J, Mo K, Ropelewski C, Wang J, Leetmaa A, Reynolds R, Jenne R, Joseph D. The NCEP/NCAR 40-year re-analysis project. *Bulletin of the American Meteorological Society,* **77** : 437-471. 1996

Li H, Robock A, Liu S, Mo X, Viterbo P. Evaluation of reanalysis soil moisture simulations using updated Chinese soil moisture observations. 2004. *ERA-40 Project Report Series* **20**. 2004

Ruti PM, Marullo S, D'Ortenzio F, Tremont M. Comparison of analyzed and measured wind speeds in the perspective of oceanic simulations over the Mediterranean basin: Analyses, Quickscat and buoy data. *J. Marine Systems* **70**:33-48. 2008

Stahl K, Moore RD, Foyer JA, Asplin MG, McKendry IG. Comparison of approaches for spatial interpolation of daily air temperature in a large region with complex topography and highly variable station density. *Agric. Forest Meteorol,* **139**:224-236. 2006

Uppala SM, Kållberg PW, Simmmons AJ, Andrea U, da Costa Bechtold V, Fiorino M, Gibson JK, Haseler J, Hernandez A, Kelly GA, Li X, Onogi K, Saarinen S, Sokka N, Allan RP, Andersson E, Arpe K, Balmaseda MA, Beljaars ACM, Van de Berg L, Bidlot J, Bormann N, Caires S, Chevallier F, Dethof A, Dragosavac M, Fisher M, Fuentes M, Hagemann S, Hólm E, Hoskin BJ, Isaken L, Janssen PAEM, Jenne R, McNally AP, Mahfouf J-F, Morcrette J-J, Rayner NA, Saunders RW, Simon P, Sterl A, Trenberth KE, Untch A, Vasiljevic D, Viterbo P, Woollen J. The ERA-40 re-analysis. *Q.J.R. Meteorol. Soc,* **131**:2961-3012. 2005

Environmental database and the Geographic Information System for socio-economic planning

Francis Omidiora Olakunle[1] and Ahmed Balogun[2]

[1] Earth Observation & Remote Sensing Division, Katholieke Universiteit Leuven , Belgium
[2] School of Process, Environmental and Material Engineering Energy and Resources Research Institute

The Geographic Information System (GIS) has helped in taking integrated land – resource inventory with other geo-coded statistics. These environmental databases are used in predicting disasters such as flood, erosion and drought. Also it is used to estimate the wind speed frequency distribution at OSU, Nigeria. A GIS is designed to accept large volume of spatial data derived from a variety of sources including remote sensing sensors and to effectively store, retrieve, manipulate, analyze and display these data according to user – defined specifications. Planning organization needs a vast amount of accurate and timely information on physical resources and related socio-economic factors to help guide their management and planning decisions.

Applications also include

1. Environmental impact of forestry plantation
2. Biomass production (Herbal eons and forestry plants) for energetic and industrial uses .
3. Near Earth object risk assessment and reduction

The AMMA field campaign and its potential for model validation

Jan Polcher and the AMMA Partners

IPSL/CNRS, 4 Place Jussieu, 75252 Paris Cedex

The AMMA project, fund ed by a large number of agencies (France, UK, US and Africa) and has been the beneficiary of a major financial contribution from the European Community's Sixth Framework Programme, has carried out a large scale field campaign in West Africa. During the period 2005 to 2007 instruments were deployed on a variety of platforms in order to monitor the evolution of the ocean, land surfaces and the physical as well as the chemical properties of the atmosphere. During the year 2006 the field campaign was intensified with the extra deployment of research aircraft, balloons and vertical sounders in order to sample more precisely the atmospheric processes. All this data is now collected in a central database which is now accessible to the larger scientific research community.

This presentation will discuss the the observation strategy which was chosen by AMMA and give an overview of the data collected. We will discuss the observations available for validating fine scale processes in models as diverse as convection, the planetary boundary layer, hydrology or the land and ocean interactions with the atmosphere. The data which allows to verify at a larger spatial and temporal scale the seasonal cycle of the monsoon in regional climate models will also be presented. The project has for its own research created some composite data sets which provide a regional analysis of the land surfaces, atmosphere and oceans and which can also be useful. These datasets, although less detailed provide gridded data which is easier to use for model validation.

Climate change and water pollution interactions in the Republic of Belarus

Veranika Selitskaya and Alena Kamarouskaya

Republican Center for Radiation Control and Environtmental Monitoring, Minsk, Belarus; pustynia1@ya.ru

This article deals with interactions of climatic and hydrochemical changes. The climate changes are reported to have been occurred since 1989. But the warmest years were 1989, 1990, 1999, 2000, when the meaning of temperature added 1,5ºC to its normal value. The hydrochemical situation in the Republic of Belarus also underwent changes during this period of observations. Especially it concerned biogenic matter and biochemical oxygen demand. For instance, the average annual concentrations of phosphorus compound in the waters of the Zapadnaya Dvina increased almost at all points of observation in 1990.

The article will include graphic material, tabular material with average annual concentrations of biogenic matter and analysis of climate change and water pollution interactions.

Current-climate downscaling of winds and precipitation for the Eastern Mediterranean

Scott Swerdlin[1], Thomas Warner[1], Andrea Hahmann[2], Dorita Rostkier-Edelstein[3] and Yubao Liu[1]

[1]National Center for Atmospheric Research, Boulder, Colorado,USA; swerdlin@ucar.edu
[2]Risø National Laboratory for Sustainable Energy, Technical University of Denmark
[3]Israel Institute of Biological Research, Ness-Ziona, Israel

1. Introduction

The use of a four-dimensional data-assimilation (FDDA) system for generating mesoscale climatographies is demonstrated. This dynamical downscaling method utilizes the Penn State University – National Center for Atmospheric Research Mesoscale Model Version 5 (MM5), wherein Newtonian-relaxation terms in the prognostic equations continually nudge the model solution toward surface and upper-air observations. When applied for mesoscale climatography development, the system is called Climate-FDDA (CFDDA). In this example application of CFDDA, it is used to downscale weather in the Eastern Mediterranean region for January and July. This region was chosen because of its interesting weather and climate (e.g., geographic contrasts, inter-annual and inter-seasonal variability).

We verify the performance of the downscaling method by using independent gridded observations of monthly rainfall, QuikSCAT ocean-surface winds, TRMM and gauge rainfall, and hourly boundary-layer winds from near-coastal tall-tower sites. The verification focuses on the ability of the mesoscale model to represent the frequency distributions of atmospheric states, rather than the simple zero-order statistics. Earlier results for this study are published in Hahmann et al. (2007).

2. The model configuration

The model uses 36 computational levels, with approximately 12 levels within the lowest 1 km and with the model top at 50 HPa. Figure 1 displays the geographic location of the model grids, and the surface elevation on each domain. The model has a horizontal grid increment of 45 km on the outer grid (D1), which covers most of the Mediterranean Sea and extends eastwards to cover the Black and Caspian Seas. The first nested grid (D2), which has a grid increment of 15 km, covers the Eastern Mediterranean and Middle East regions. A third nested domain (D3), with a grid increment of 5 km, is located along the easternmost portion of the Mediterranean coast. The three domains contain 81 × 111, 124 × 178, and 102 × 102 grid points, respectively.

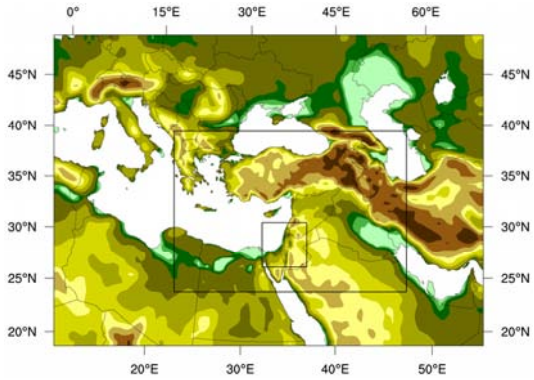

Figure 1. The model grids used for the downscaling simulations. See the text for details.

3. Example results

The downscaling method represents very well the statistics of precipitation over this region. Not only are monthly averages and their geographic distribution well simulated, but also the frequency distributions of daily rainfall are accurately diagnosed for various regions of the Levant. The inter-annual variability of the January rainfall is also well represented for the regions of heavy precipitation in the Levant and southern Turkey. The verification with QuikSCAT-estimated wind speeds over the ocean shows some systematic errors. The CFDDA-simulated winds tend to be slower than those defined by QuikSCAT, especially in winter. These errors are easily corrected by simple regression equations. In contrast, over land, the C-FDDA-derived wind climatography overestimates the boundary-layer wind speeds, especially in winter. However, most of the errors can be explained by poorly resolved orography and coastal configuration in the mesoscale model. Figure 2 shows the QuickSCAT-observed and model downscaled winds during July for the period 2000-2007.

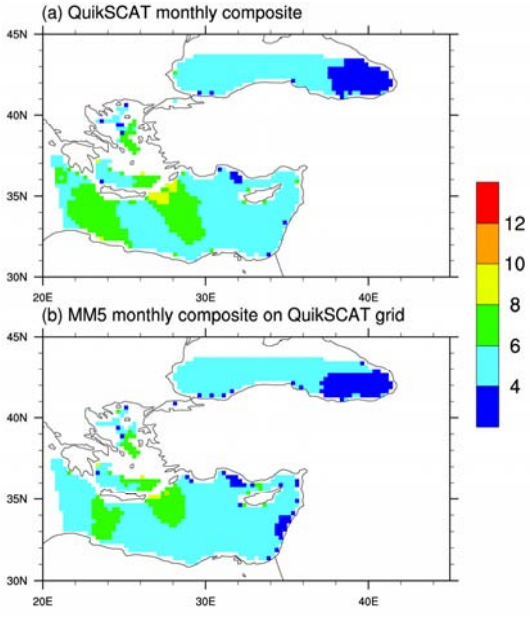

Figure 2. July (2000–2007) composite of 10-meter winds from (a) QuikSCAT and (b) the CFDDA simulations (MM5 D2). The colorbar shows wind speeds in meters per second.

During summer, winds over the Mediterranean Sea are dominated by steady local wind systems, and the CFFDA system is able to capture the wind distribution observed by QuikSCAT. The areas of observed wind funneling through the straits to the east and west of Crete (Zecchetto and DeBiasio 2007) are clearly seen in the CFDDA analysis. Mean absolute differences between QuikSCAT and the model are mostly below 1 m/s over more than 90% of the ocean grid points in Domain 2.

References

Hahmann, A. N., D. Rostkier-Edelstein, T. T. Warner, Y. Liu, F. Vandenberghe, S. P. Swerdlin, 2007: Climate downscaling for the eastern Mediterranean. *Advances in Geosciences* (EGU), **12**, 159-164.

Zecchetto, S., and F. de Biasio, 2007: Sea surface winds over the Mediterranean Basin from satellite data (2000-04): Meso- and local-scale features on annual and seasonal time scales. *J. Appl. Meteor. Climatol.,* **46**, 814–827.

Current-climate downscaling at the National Center for Atmospheric Research (NCAR)

Thomas Warner, Scott Swerdlin, Yubao Liu and Daran Rife

National Center for Atmospheric Research, Boulder, Colorado, USA; warner@ucar.edu

1. Introduction

Mesoscale analyses of current climates can be used for many purposes, including optimal siting of wind-energy farms and airports, calculating the most probable direction of the transport of hazardous material at some future date and time, and scheduling the time and season for events that require specific meteorological conditions. To construct such climatologies for the many areas of the world where there are few routine four-dimensional (4D) observations of the atmosphere, NCAR has developed a Climate Four-Dimensional Data Assimilation (CFDDA) system. The CFDDA system uses the Penn State University – National Center for Atmospheric Research Mesoscale Model Version 5 (MM5), and the Weather Research and Forecasting (WRF) model, wherein Newtonian-relaxation terms in the prognostic equations continually nudge the model solution toward surface, radiosonde, aircraft, and satellite-based observations. This is one of the few current-climate downscaling systems that relaxes the model solution to observations rather than to gridded analyses of observations.

The CFDDA system is able to generate a 4D description of the diurnal and seasonal evolution of regional atmospheric processes, with a focus on the boundary layer. Unlike point measurements, the gridded fields define coherent multi-dimensional realizations of complete physical systems. Not only does the CFDDA system define mean values of variables as a function of season and time of day, extremes are also estimated, and example days are produced. See Hahmann et al. (2007) for an early application of CFDDA.

2. Example applications of CFDDA

The specific application of CFDDA determines the configuration of the model. For limited-area applications, lateral-boundary conditions are defined from the NCEP-NCAR or NCEP-DOE reanalyses. For situations where high-resolution analyses are required globally, a global version of WRF or MM5 is used.

As an example of a limited-area application of CFDDA, Fig. 1 shows a map of the probability that 30-m above-ground-level (AGL) winds will exceed 10 m s^{-1} in the month of February in southern Europe, where such an analysis would be valuable for wind-energy prospecting. These statistics are based on a 20-year downscaling from the NCEP-NCAR Reanalysis Project (NNRP) global data set.

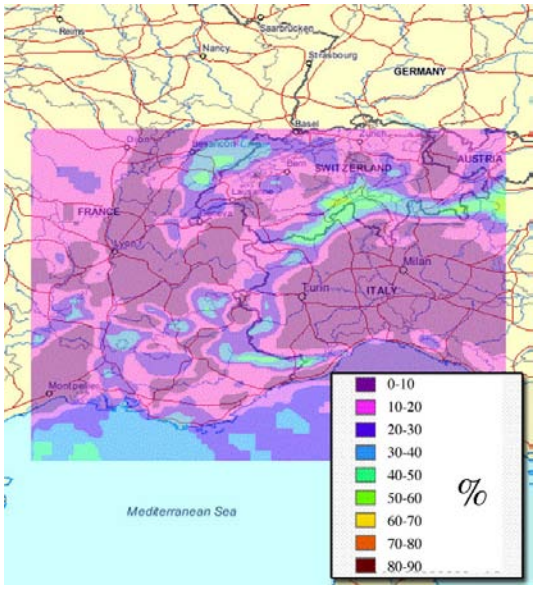

Figure 1. CFDDA-generated map of the probability that the 30-m AGL winds will exceed 10 m s^{-1} in the month of February, for southern Europe (based on a 20 year data-assimilation period).

In a global application of CFDDA, a 21-year reanalysis has been produced, with hourly output, using a 40-km grid increment. A composite-mesh technique was used with MM5, wherein twin polar stereographic grids, one centered over each pole, are integrated separately, then joined to form a seamless global analysis. The solutions are constrained by both the driving NCEP-DOE Reanalysis (an improved version of the NNRP) and the assimilated surface and radiosonde observations. The large-scale climates of CFDDA and the NCEP-DOE Reanalysis remain synchronized, while the mesoscale model and observations simultaneously define the small-scale features. Figure 2 shows example output from the model, and illustrates the ability of CFDDA to represent complex atmospheric structures across a spectrum of scales, as well as climate extremes. The infrared satellite image is shown with the CFDDA analysis for 0230 UTC 5 January 2001, when tropical cyclone Ando was active over the Indian Ocean. The CFDDA-analyzed cyclone has a remarkable resemblance to that observed. Also reasonably represented is the diurnal pattern of moist convection over Africa, as well as the wave patterns in the higher latitudes. In terms of cyclone Ando, CFDDA produced a storm whose structure remained highly similar to that observed throughout its life cycle, and the simulated storm

followed nearly the correct path. And this took place within the data void of the Indian Ocean.

References

Hahmann, A. N., D. Rostkier-Edelstein, T. T. Warner, Y. Liu, F. Vandenberghe, S. P. Swerdlin, 2007: Climate downscaling for the eastern Mediterranean. *Advances in Geosciences* (EGU), **12**, 159-164.

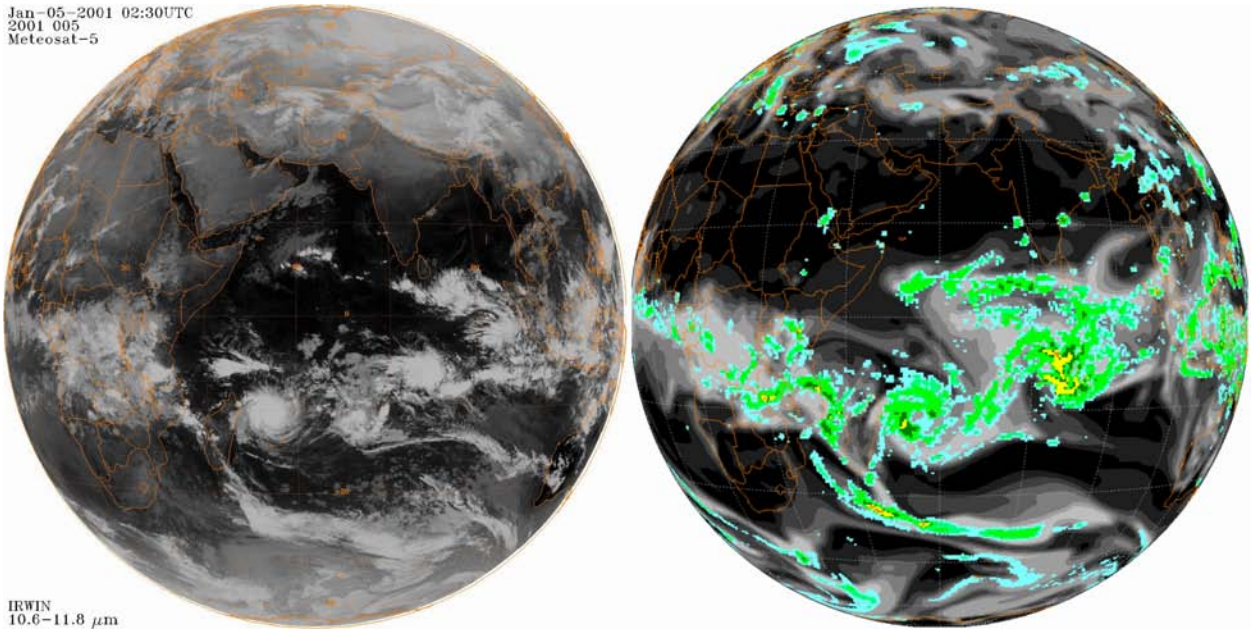

Figure 2. Comparison of infrared satellite imagery (left) and the CFDDA solution (right) for 0230 UTC 5 January 2001, when tropical cyclone Ando was active over the Indian Ocean. Surface precipitation accumulation (colors) for CFDDA is plotted with the 500 hPa humidity field (gray shades). Warmer colors indicate higher precipitation intensity.

Verification of simulated near surface wind speeds by a multi model ensemble with focus on coastal regions

Ivonne Anders[1,2], Hans von Storch[1] and Burkhardt Rockel[1]

1) GKSS Research Center, Max-Planck-Str. 1, 21502 Geesthacht, Germany, 2) Central Institute for Meteorology and Geodynamics, Hohe Warte 38, 1190 Vienna, Austria; Ivonne.Anders@zamg.ac.at

1. Introduction

The knowledge of the wind climate at specific locations is of vital importance for risk assessment, engineering, and wind power assessment. Results from regional climate models (RCM) are getting more and more important to enlarge the investigation from local to regional scale.

With help of GCM- and RCM-simulations *Leckebusch and Ulbrich (1994)* investigate the relationship between cyclones and extreme windstorm events over Europe. It is clearly visible that with the higher temporal and spatial resolution, especially in coastal areas the RCM lead to an improvement in simulating the extreme wind speeds compared to the GCM. For open ocean areas *Winterfeld (2008)* shows no adding value for RCM modeling compared to reanalysis forcing in the wind speed frequency distributions, whereas in coastal regions RCM results - especially for higher wind speed percentiles - are closer to the observations than the forcing data. *Rockel and Woth (2007)* focused on near-surface wind speed over Europe and identified that most of the RCMs have not been able to simulate wind velocities above 8 Bft.

In this study we investigate the simulated near surface wind speed by a multi model ensemble carried out in the EU funded project ENSEMBLES. The special focus is on the coastal regions of the Netherlands and Germany. The Southern North Sea and the German Bight are Luvcoasts, that means the winds blow onshore or parallel to the coast. The main wind direction in this area is West to Southwest.

Figure 1. Locations of all measurements available for the time period 1971-1983

2. Observation Data and their Homogeneity

The German Weather Service (DWD) provided measurements for 31 stations across the German coastal area. The data contains the mean speed and the mean direction of the wind in 10m height as a mean over the preceding hour. Beside these values the daily maximum of the wind speed is available. Until the end of the year 1974 the wind direction measured in degree was transformed into the 32-scale wind classes. From 1.1.1975 the number of these classes has been changed to 36.

The wind measurements network of the Netherlands Meteorological Institute (KNMI) contains more than 50 stations across the Netherlands. For these stations hourly values are available for the mean speed and the mean direction of the wind over the last 10 minute period in the preceding hour, the hourly mean of the wind speed and the maximum wind speed in the preceding hour.

Wind measurements are very strongly influenced by changes in e.g. surface roughness and by shadowing effects from trees and buildings, but also changes in the instrument, the measuring height or the location are reasons for the inhomogeneity of the data.

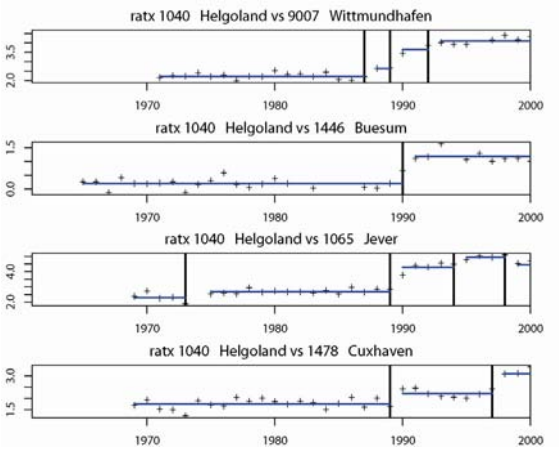

Figure 2. Example for breaks detected in difference in wind speed series (in m/s) from Helgoland vs. Wittmundhafen, Buesum, Jever and Cuxhaven.

A homogenization of wind measurement is critical due the measurements are influenced by local wind effects. Stations history is often incomplete and changes in the stations surrounding (growing trees, new buildings in the neighbourhood) are rarely documented.

In this investigation we used an algorithm for detecting breaks in the time series (*Caussinus and Mestre, 2004)*) based on monthly mean wind speed in the time period from 1961 to 2000. Figure 2 shows the breaks in difference series from Helgoland compared to the closest stations around. The change in the location of the measuring site at the island in 1989 is clearly visible. Together with the provided stations histories we defined two time windows where as many as possible of the measurements are less disturbed. For the Netherlands we choose observation data of 10 stations for the time periods 1971-1983 and 5 stations from 1971 to 2000, for the German coast it is 13 and 10 stations respectively (cf. Figure 1).

3. The Multi Model Ensemble

Within the ENSEMBLES project 14 participating European institutions and one Canadian Research Institute run their RCMs for the same European domain (including the Mediterranean and Island) with the same grid size of 0.44° (~50km) and in a second simulation 0.22° (~25km). For these simulations the ERA40 reanalysis (*Uppala et al. 2005*) were used as forcing data. The simulations cover at least the time period from 1961 to 2000. As far as provided from RCMs daily means of the simulated 10-m wind speed are analysed in this study.

4. Verification of the Simulated Wind Speed

For each station the covering gridcell of each model as well as the driving ERA40 reanalysis data was used for bias, root mean squared error (RMSE), and quantiles assessment.

The bias is small and most of the year at all stations positive with values between -0.5 and 2.5 m/s. At few stations directly located at the coastline for almost all models the bias is negative over the whole year with values down to -2.5 m/s.

All models perform standard deviation quite well and are well correlated with station data. Correlation values are between 0.7 and 0.8. Results from one model using the spectral nudging technique is higher correlated (0.85 to 0.9) with the station data.

The RMSE, combining correlation and bias, gives values between 0.5 and 2 m/s for sites away the coast and higher values up to 3 m/s for the stations at the coastline. For the RMSE there is no distinct additional gain for the simulated wind speeds from grid boxes with the 25km resolution compared to the 50km.

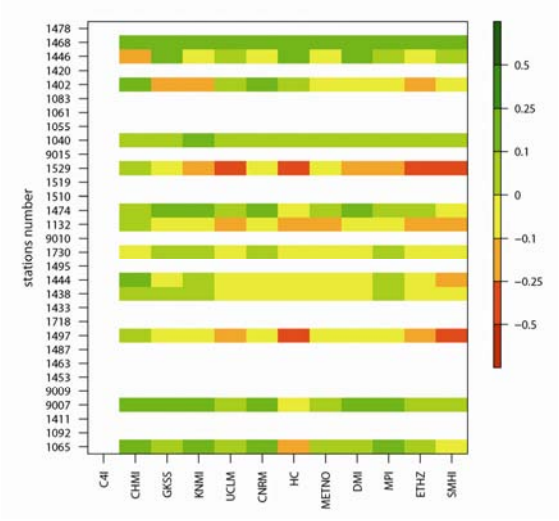

Figure 3. Differences in Perkins Score for the RCMs (50km) and ERA40 reanalysis from 1971 to 1983. (Negative values indicate an added value for the ERA40 reanalysis, positive values for the RCMs.; white: no data available for observation and/or model output.)

The results in the quantiles of the models and the observation are varying for most of the locations with no clear behavior. At stations more than 50km off the coast where in general smaller wind speeds are observed, the RCM´s quantiles fir very well with the observed ones. For the Helgoland (No. 1040) island ERA40 reanalysis data underestimate the wind speed over all quantiles. We can see a clear added value from all RCMs in the quantiles assessment compared to the ERA40 forcing data. All models define the corresponding gridbox as water.

With the help of Skill Scores it is possible to quantify models performance in simulating the surface wind speed compared to the ERA40 reanalysis forcing. We applied the Brier Skill Score (BSS) and a score described by *Perkins et al. (2007)* in a modified way. While the BSS is a relation of the RMSE from the RCMs compared to the RMSE from ERA40 forcing, the Perkins Score is a very simple measure to estimate the relative similarity between simulated and observed Probability Density Functions (PDF). For the available observations in the time period from 1971 to 1983 Figure 3 shows the Perkins Score from each RCMs in relation to the Score for the ERA40 reanalysis as the difference between both scores. The value -1 is full agreement in the PDFs from ERA40 and the observations and no similarity between the PDF from RCM and that one from the observations. The value 1 is the opposite and indicates the gain due to considering the RCM. For many stations we identified a a strong similarity between the PDFs derived from simulated surface wind speed from RCMs and ERA40 reanalysis compared to the observed PDFs. At few sites an added value for the RCMs was detected.

5. Conclusion

Here, we test the performance of 14 RCMs concerning the simulated surface wind speed in coastal regions, especially the North Sea area. We applied several measures and skill scores to analyse the RCMs performance compared to the driving field and to evaluate accuracy gain by including higher spatial resolution of the grid cell Results for bias, RMSE, standard deviation but also for Brier Skill Score and Perkins adapted skill score don't show strong seasonal dependence. The differences can be addressed to the calm summer periods and the stormy autumn and winter month where large scale events are more important than local effects.

At few stations e.g. Helgoland RCMs show an added value concerning the quantiles assessment of daily mean surface wind speed compared to the driving field.

References

Caussinus, H. and Mestre, O., Detection and correction of artificial shifts in climate series, *Appl. Statist.*, Vol. 53, Part 3, pp. 405-425, 2004

Leckebusch, G.C. and Ulbrich, U., On the relationship between cyclones and extreme windstorm events over Europe under climate change, *Global and Planetary Change*, No. 4, pp. 181-193, 1994

Perkins S.E. et.al, Evaluation of the AR4 Climate Models' Simulated Daily Maximum Temperature, Minimum Temperature, and Precipitation over Australia Using Probability Density Functions, *J. Clim.*, Vol. 20, pp. 4356–4376, 2007

Rockel, B. and Woth, K., Extremes of near-surface wind speed over Europe and their future changes as estimated from an ensemble of RCM simulations, *Climate Change*, pp. 267-280, 2007

Uppala, S.M., et al. The ERA-40 re-analysis. *Quart. J. R. Meteorol. Soc.*, No. 131, pp. 2961-3012, 2005

Winterfeldt, J., Comparison of measured and simulated wind speed data in the North Atlantic, GKSS Report, No. 2, 2008

The North American Regional Climate Change Assessment Program (NARCCAP): Status and results

Raymond W. Arritt for the NARCCAP Team

Department of Agronomy, Iowa State University, Ames, Iowa 50011 USA (rwarritt@bruce.agron.iastate.edu)

1. Overview

The North American Regional Climate Change Assessment Program (NARCCAP) is an international program that is generating projections of climate change for the U.S., Canada, and northern Mexico at decision-relevant regional scales. NARCCAP uses multiple limited-area regional climate models (RCMs) with a nominal grid spacing of 50 km nested within results from multiple atmosphere-ocean general circulation models (AOGCMs). The use of multiple regional and global models allows us to investigate the uncertainty in model responses to future emissions (here, the A2 SRES scenario).

Six regional climate models are used in NARCCAP:

- Regional Spectral Model, being run by project participants at the Scripps Institution of Oceanography / University of California at San Diego
- Canadian Regional Climate Model, by participants at the consortium Ouranos
- RegCM3, by participants at the University of California at Santa Cruz
- MM5, by participants at Iowa State University
- WRF (Weather Research and Forecasting Model), by participants at Pacific Northwest National Laboratories
- HadRM3, by participants at the UK Meteorological Office Hadley Centre

The four global climate models providing initial and boundary conditions for the regional models are:

- HadCM3, from the UK Meteorological Office Hadley Centre
- CGCM3, from the Canadian Centre for Climate Modelling and Analysis
- CCSM3.0, from the National Center for Atmospheric Research
- CM2.1 from the NOAA Geophysical Fluid Dynamics Laboratory

The project also includes global time-slice experiments at the same discretization used for the regional models (50 km) by the GFDL atmospheric model (AM2.1) and the NCAR atmospheric model (CAM3).

2. NARCCAP Phases and Progress

Phase I of the experiment uses the regional models nested within the NCEP/DOE reanalysis for the period 1979-2004 in order to establish uncertainty attributable to the RCMs themselves. Phase II of the project then nests the RCMs within results from the current and future runs of the AOGCMs to explore the cascade of uncertainty from the global to the regional models.

In NARCCAP Phase II each RCM-AOGCM pair performs two simulations: one for the period 1971-2000, and another for 2041-2070. The difference between these two can then be used to infer regional climate change. Performance of the coupled RCM-AOGCM simulation for 1971-2000 can be compared to the reanalysis-driven results from Phase I in order to deduce errors and uncertainty arising from the use of the AOGCM to represent current climate.

Phase I has been completed and the results to be shown include pronounced variations in skill across the model domain as well as findings that spectral nudging is beneficial in some regions but not in others. Phase II is nearing completion and some preliminary results will be shown.

3. Users and Data

NARCCAP seeks to accommodate the needs of three classes of users of the model results:

- Users who intend to perform analyses of the NARCCAP output, such as process-oriented studies or climate change analyses for specific regions.
- Users who will apply NARCCAP results to climate change impacts studies.
- Users who will perform further downscaling of NARCAP results, whether using dynamical downscaling (e.g., using the NARCCAP results as initial and boundary conditions for a fine-resolution numerical model) or statistical downscaling.

NARCCAP data are formatted into a netCDF-based standard largely following that used for the AOGCM data archive developed for the IPCC Fourth Assessment Report. Data and metadata are checked for adherence to project standards and then are made available through the Earth System Grid (http://www.earthsystemgrid.org/). The uniform data format greatly simplifies the ability of end-users to compare results from different NARCCAP simulations.

4. Further Information

For further information please consult the project web site at http://www.narccap.ucar.edu

MRED: Multi-RCM Ensemble Downscaling of global seasonal forecasts

Raymond W. Arritt for the MRED Team

Department of Agronomy, Iowa State University, Ames, Iowa 50011 USA (rwarritt@bruce.agron.iastate.edu)

1. Motivation

The Multi-Regional Climate Model Ensemble Downscaling (MRED) project was recently initiated to address the question, *Do regional climate models provide additional useful information for seasonal forecasts?* Regional climate models (RCMs) have long been used to downscale global climate simulations. In contrast the ability of RCMs to downscale seasonal climate forecasts has received little attention. MRED will systematically test the RCM downscaling methodology by using a suite of RCMs to downscale seasonal forecasts produced by the National Centers for Environmental Prediction (NCEP) Climate Forecast System (CFS) and the NASA GEOS5 system. The initial focus will be on wintertime forecasts in order to evaluate topographic forcing, snowmelt, and the potential usefulness of higher resolution, especially for near-surface fields influenced by highly irregular orography.

Each RCM will cover the conterminous United States at approximately 32 km node spacing, comparable to the grid spacing of the North American Regional Reanalysis which will be used to evaluate the models (Figure 1). The forecast ensemble for each RCM will be comprised of 15 members over a period of 22+ years (from 1982 to 2003+) for the forecast period 1 December – 30 April. The RCMs will be continually updated at their lateral boundaries using 6-hourly output from CFS or GEOS5. Each RCM will provide hydrometeorological output in a standard netCDF-based format for a common analysis grid. MRED will compare individual RCM and global forecasts as well as ensemble precipitation and temperature forecasts which are currently being used to drive macroscale land surface models (LSMs). The project also will evaluate wind, humidity, radiation, and turbulent heat fluxes, which are important for more advanced coupled macro-scale hydrologic models. Metrics of ensemble spread will also be evaluated. Extensive analysis will be performed to link improvements in downscaled forecast skill to regional forcings and physical mechanisms. Our overarching goal is to determine what additional skill can be provided by a community ensemble of high resolution regional models, which we believe will eventually define a strategy for more skillful and useful regional seasonal climate forecasts.

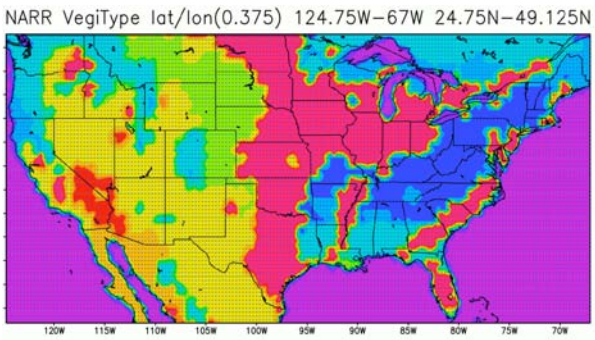

Figure 1. MRED analysis domain and vegetation

2. Participating Models

The regional climate models participating in MRED are:

- MM5, being executed at Iowa State University.
- WRF-NMM, at Iowa State University and NOAA Global Systems Division. This is the version of WRF used for U.S. operational short-range weather forecasting by NCEP.
- WRF-ARW, the Advanced Research version of WRF, at Pacific Northwest National Laboratories.
- CWRF, a version of the WRF model that has been specially adapted for climate simulation, at the Illinois State Water Survey.
- Eta/SSiB, at the University of California Los Angeles.
- RAMS (Regional Atmospheric Modeling System) at Colorado State University and the University of Colorado.
- RSM (Regional Spectral Model), at the Scripps Institution of Oceanography / University of California at Santa Barbara.

The initial global seasonal forecast model to be downscaled is the T62L64 version of the NOAA CFS. A seasonal forecast model based on the NASA Goddard Space Flight Center GEOS5 GCM, currently in development, also will be downscaled when results become available.

3. Further Information

For further information consult the project web site at http://rcmlab.agron.iastate.edu/mred/

An atmosphere-ocean regional climate model for the Mediterranean area: Present climate and XXI scenario simulations

V. Artale, S. Calmanti, A. Carillo, A. Dell'Aquila, M. Herrmann, G. Pisacane, PM Ruti * and G. Sannino, MV Struglia

ACS/CLIM-MOD, ENEA, Roma, Italy; paolo.ruti@enea.it

F. Giorgi, X. Bi, J.S. Pal and S. Rauscher

Abdus Salam ICTP,Trieste, Italy

In the framework of CIRCE EU Project, an atmosphere-ocean regional climate model (AORCM) for the Mediterranean basin, called the PROTHEUS system, is presented. The PROTHEUS system is composed of the regional climate model RegCM3 as atmospheric component and a regional configuration of the MITgcm model as oceanic component.

The model is applied to an area encompassing the Mediterranean Sea and the adjacent basin (Fig. 1), where the fine scale feedbacks associated with air-sea interactions can substantially influence the spatial and temporal structure of regional climate. We compare a 40-year simulation with the PROTHEUS system driven by ERA40 reanalysis fields at the lateral boundaries with a corresponding simulation performed with the stand-alone configuration of the atmospheric model RegCM3. We show that the coupled system produces realistic features of atmospheric circulations, land surface climate, ocean sea surface temperature (SST), ocean surface circulations and air-sea fluxes.

The main improvement associated with the use of the coupled system is found by considering the high spatio-temporal variability of surface fields. First, the coupled model is able to capture the fine scale spatio-temporal evolution of observed SST. Second, large changes in air-sea fluxes are associated to the changes in SST and yield a better simulation of fine temporal scale climate variability. Given the successful development of the coupled model system here described we envisage a number of possible applications of the PROTHEUS system.

In this perspective, we have also performed a 1951-2050 scenario simulation driven by ECHAM5-MPIOM fields at the lateral boundaries. Preliminary results from this run are here shown.

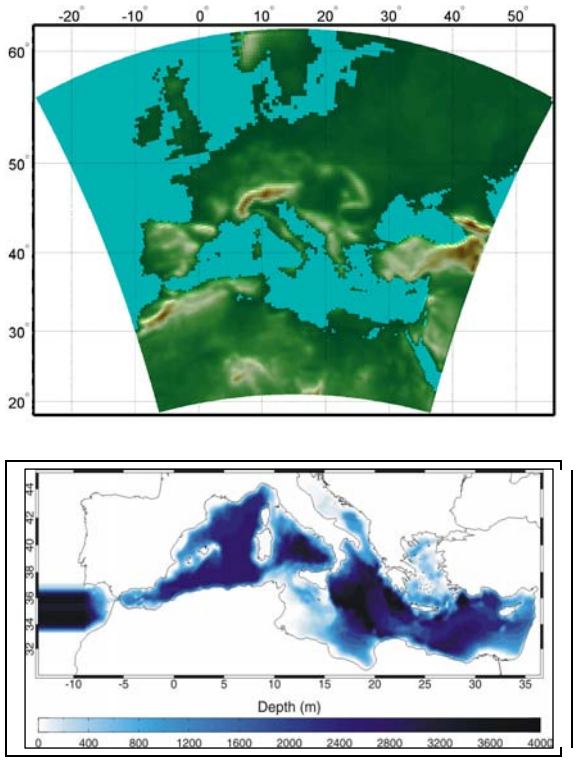

Figure 1. Domain for: a) RegCM and b) MITgcm with corresponding topography. Units are m.

Regional climate modeling in Morocco within the project IMPETUS Westafrica

K. Born, H. Paeth, K. Piecha, and A. H. Fink

Institute for Geophysics and Meteorology, University Cologne, Kerpener Str. 13, 50937 Cologne, Germany.

1. Introduction

In IMPETUS Westafrica (http://www.impetus.uni-koeln.de), consequences of possible future climate change impacts on local economic and social conditions in two river catchments were investigated: the Drâa in Morocco and the Ouémé in Benin. Climate changes were assessed using a model hierarchy from global down to local scales. Different techniques of dynamical, statistical and statistical-dynamical downscaling had to be applied in order to fulfill demands of hydrological and socio-economic models.

2. The Hierachy of Climate Models

In Morocco, climate ranges from High Mountain climates to steppe and deserts. Due to this strong spatial heterogeneity, different techniques had to be applied in order to assess future climate change patterns. An overview of the downscaling techniques is shown in Figure 1.

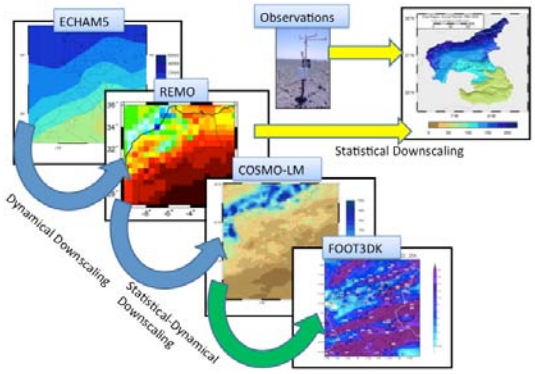

Figure 1. IMPETUS hierarchy of climate models and according downscaling techniques.

Climate model applications started on the global scale using results from the consortium runs of ECHAM5 performed by the Max-Planck Institute for Meteorology in Hamburg, accompanied by ECHAM5 climate simulations using a vegetation model adapted to the peculiarities of West African climate, which were performed at the University of Cologne. The first downscaling step was a dynamical downscaling from ECHAM5 to synoptic scales using the regional climate model REMO with 0.5° Lon/Lat resolution. The ECHAM5 simulations covered the 20th century climate and the future climate using greenhouse gas emissions defined by the SRRES A1B and B1 scenarios up to 2100, the REMO simulations covered the period 1960-2050. Details about the REMO climate simulations may be found in *Paeth et al.* (2005) and *Paeth et al.* (2009).

For Morocco, climate simulations for the 21st century reveal a continuation of the drying trend, which can already be seen for the 20th century observations. A classification of the Koeppen climate zones is presented in Fig. 2. The climate model data show a considerable dry bias compared to CRU TS2.1. An analysis of wet and dry periods for Morocco suggest that this is due to an increase of the number and strength of dry periods, whereas the nature of wet periods seems to be unchanged (*Born et al.*, 2008). Besides changes in rainfall variability, the most important change is the rise of the snowline due to the greenhouse gas induced warming.

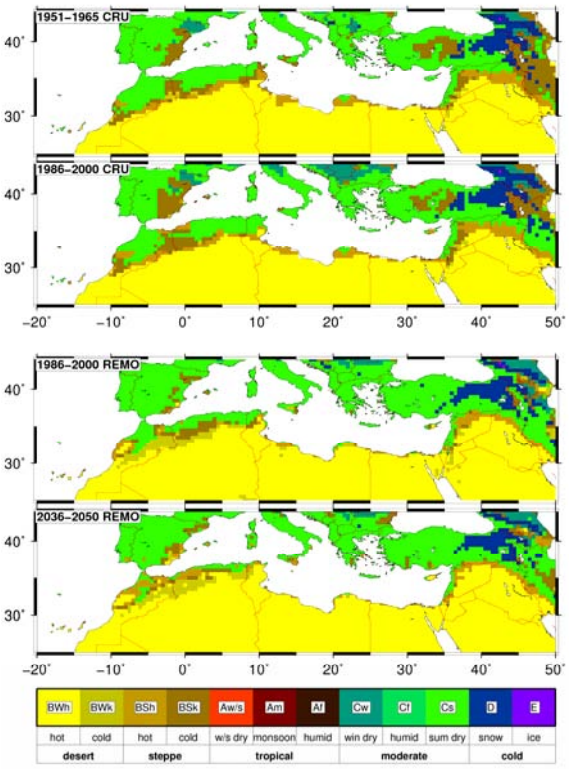

Figure 2. Koeppen climate classification for CRU TS2.1 data and for REMO regional climate simulations.

For smaller scale regional climate scenarios, statistical-dynamical and statistical techniques were applied in order to circumvent the large computational effort. In this step, first the COSMO-LM – embedded in REMO model output and into analysis data – has been applied for single years under present day and future climate conditions. The grid spacing was 0.25°, 0.1° and 0.0625° on a rotated grid, corresponding to about 27 km, 11 km and 7 km, respectively. From these simulations, shorter episodes have been simulated with 3km and 1km resolution using FOOT3DK, which was nested into the COSMO-LM. The episodes were chosen to be representative for typical, climate relevant weather situations and could be "recombined" using weights depending on frequencies of occurrence in order to estimate patterns of small-scale climatic scale.

Alternatively, the dynamic and statistical-dynamical approaches have been supplemented by a statistical regionalization method. This had to be applied because (1) climate model data and observations have – especially with the focus on hydrological modeling – dramatically

different rainfall characteristic; and (2) the statistical-dynamical approach had to be complemented in order to allow for a construction of continuous time series.

3. Statistical-Dynamical Downscaling

The usual, one-way dynamical approach of downscaling by nesting the smaller scale climate model into a larger scale model output is straightforward and not commented here. The statistical-dynamical technique uses in a first step the dynamical (one-way) approach, but only for certain episodes, which represent weather type classes. These episodes have to be chosen to be relevant for the focus of the question. For a general estimation of climate conditions, results of a weather classification on dynamic flow directions and circulations after *Jones et al.* (1993) into so-called circulation weather types (CWT) have been used. The adaptation of the classification technique to Morocco and the discussion of results can be found in *Knippertz et al.* (2003). The advantage of this technique is that smaller scale dynamic features of orography and land cover are considered, but the results strongly depend on the quality of the weather type classification. The estimated rainfall for present day and differences to future climate conditions for this approach are presented in Fig. 3.

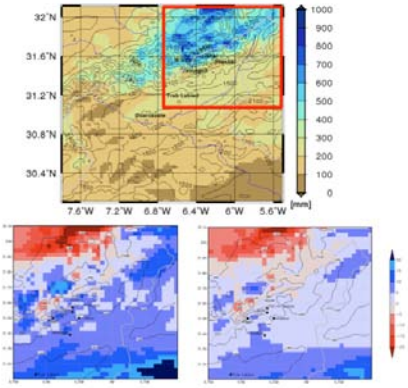

Figure 3. Rainfall from statistical-dynamical downscaling with FOOT3DK. Top: annual rainfall 2002. Bottom: difference (2036-2050) minus (1986-2000); SRES scanario A1B (left) and B1 (right).

4. Statistical Downscaling

The statistical downscaling used directly the model output of the transient REMO simulations. Statistical characteristics of model rainfall can be very different from observations, because the model rainfall has to be understood as an aggregate over a model grid box. Therefore, the model tends to smaller rainfall rates and to more frequent rainfall events. These changed characteristics have a large impact on results of hydrological models.

In order to generate rainfall data with statistical characteristics of observations, the annual cycle of rainfall probability was extracted from observations, which cover at least all different climatic zones of the region of interest. The rainfall probability and, thus, the numbers of rainy days were taken from observations; whereas the monthly rainfall sums were preserved. In addition, a multiple regression with topographic characteristics (surface elevation, exposition, geographical position) generates predictors for small-scale, topographically induced heterogeneities. This method results in less frequent events with higher rainfall rates. The advantage of the corrected statistics is achieved by a abandoning the ability to estimate the future changes of daily rainfall probability.

Another constraint was that the amount of data had to be reduced in order to fit into a desktop computer application, which support decision makers. The reduction was achieved by definition of climatic similar zones. Time series of climate parameters were given for these zones (see an example in Fig. 4).

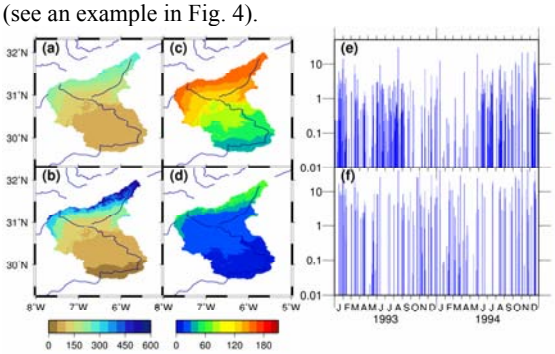

Figure 4: Results of statistical downscaling for the catchment of Qued Drâa. Top row: REMO rainfall 1960-2000 using multiple regression coefficients obtained from climate model data and topography: (a) mean annual rainfall sums, (c) average number of rainy days per year, (e) exemplary time series of daily rainfall for the high mountain zone. Bottom row: (b), (d) and (f) shows the same for rainfall interpolated using regression coefficients from climate station observations.

5. Conclusions

The demand of reliable and applicable climate data in IMPETUS lead to the development of different regionalization techniques. Depending on the focus of the question, special downscaling methods had to be used. Even with sufficient computational resources, dynamical downscaling showed considerable discrepancy and had to be corrected by post-processing, which again resulted in the expansion of the regionalization method by inclusion of statistical techniques.

References

Born, K., A. Fink, H. Paeth, 2008: Dry and Wet Periods in the Northwestern Maghreb for Present Day and Future Climate Conditions. *Meteorol. Z.* **17**, 533-551.

Jones, P. D., M. Hulme, K. R. Briffa, 1993: A comparison of Lamb weather types with an objective classification scheme. *Int. J. Climatol.* **13**, 655-663.

Knippertz, P.; Christoph, M.; Speth, P., 2003: Long-term precipitation variability in Morocco and the link to the large-scale circulation in recent and future climates. *Meteorology and Atmospheric Physics*, **83**, 67–88.

Mitchell, T. D., P. D. Jones, 2005: An improved method of constructing a database of monthly climate observations and associated high resolution grids. *Int. J. Climatol.* **25**, 693-712.

Paeth, H., K. Born, R. Podzun, D. Jacob, 2005, Regional dynamic downscaling over West Africa: Model evaluation and comparison of wet and dry years. *Meteorol. Z.* **14**, 349-367

Paeth, H., K. Born, R. Girmes, R. Podzun, and D. Jacob, 2009: Regional Climate Change in Tropical and Northern Africa due to Greenhouse Forcing and Land Use Changes. *J. Climate*, **22**, 114–132

Will future summer time temperatures go berserk?

Jens H. Christensen, Fredrik Boberg, Philippe Lucas-Picher, and Ole B. Christensen

Danish Meteorological Institute, Lyngbyvej 100, DK-2100 Copenhagen Ø, Denmark; jhc@dmi.dk

1. Temperature bias in perfect boundary experiments

In a recent analysis of monthly mean model temperature bias over Europe of the complete ensemble of regional climate models (RCMs) participating in the EU FP6 project ENSEMBLES, it was demonstrated that models tend to have a common behavior when temperatures are getting very high *Christensen et al.* (2008). Monthly mean temperature bias in most RCMs tends to increase (in a positive direction) as the simulated temperature increase, *e.g.* typically, summers are simulated warmer than they are in reality.

Figure 1a depicts the essentials of the work presented in *Christensen et al.* (2008). The figure shows monthly mean model bias with respect to modeled monthly mean temperature for a region covering most of the Mediterranean region (see *Christensen & Christensen* (2007) for details) covering the period 1961-2000. Here we have chosen to show bias wrt. model temperature, whereas *Christensen et al.* showed bias wrt. observed temperature. Obviously these are equivalent, but the former is chosen for reasons that will become obvious. The figure indicates the bias for the individual months as simulated by three models, REMO, RACMO and RCA when nested in ERA40, shown by dots (more models will be included when the paper is presented). The full lines represent the best fitted second order polynomial fit, while the dashed lines represent the extension of this functional relation into a warmer regime not yet realized by the simulations.

2. Climate change simulations

Currently, the ENSEMBLES RCMs are providing their results from climate change experiments taking boundary conditions from a suite of GCMs. These are being archived and are publicly available. Only three models were fully completed and fully available in time for this manuscript. However, the three models all provide information until the end of the 21st century.

Figure 1b illustrates how the monthly mean temperatures for different 30 year periods change with respect to the simulated mean temperature in the particular cases of 1961-1990, 2011-2040, and 2071-2100. Figure 1c shows how the bias as estimated by the best fit curve deduced in Figure 1a can be used to adjust the simulated values as it is clear that the warmer the month in concern is, the larger also the bias is. Thus all temperatures are shifted to a somewhat lower level depending on the actual temperature (see *Christensen et al.* 2008 for details).

Figure 1d shows the adjusted (non-linearly) bias corrected monthly mean climate change temperatures. It is seen that for two of the models the bias correction almost entirely eliminates the seasonal warming signal. The third model did not show this behavior. This is explained by the almost temperature independent behavior of the bias, while the two other models apparently exhibit quite a strong temperature dependent bias.

3. Conclusion and discussion

There appears to be a non-linear bias behavior in the ability of some RCMs to simulate the annual cycle of monthly mean temperatures. This behavior indicates the possibility that when these models are used to simulate climate change due to an increase in greenhouse gas concentrations, they are likely to overestimate the warming, particularly in the warmest months. Here we have illustrated that for two models participating in ENSEMBLES, a correction for this bias leads to a more uniform temperature increase throughout the year. The last model, which apparently does not exhibit a large temperature dependent bias still shows a marked warming

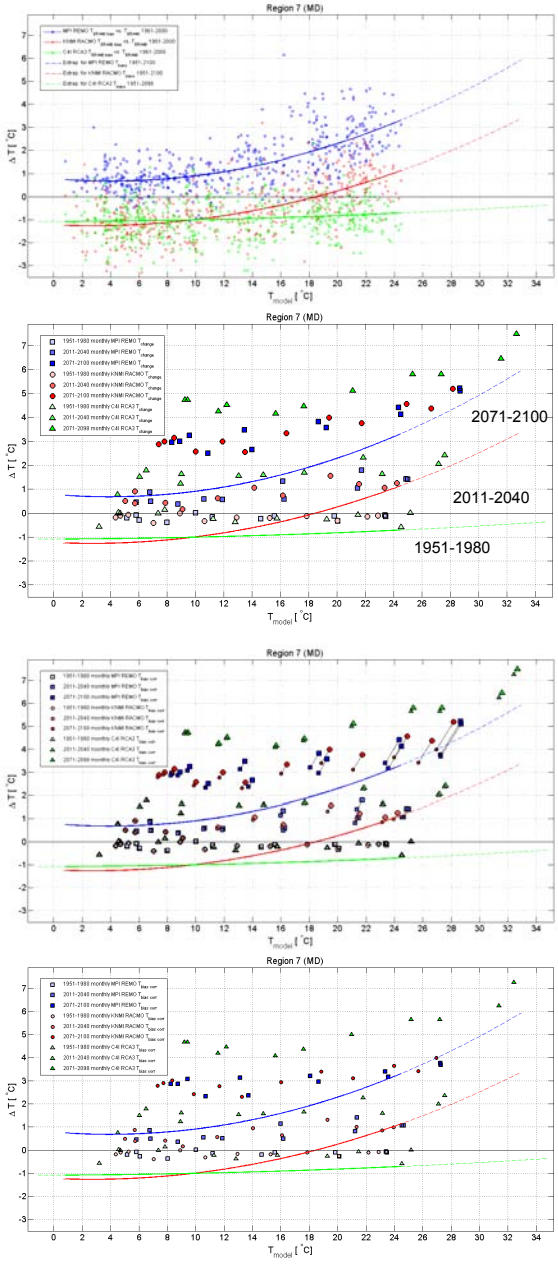

Figure 1. Monthly mean temperature bias (top) and warming for three ENSEMBLES RCMs. For details see text

with increasing temperature. More model results will be available as the paper will be presented.
This model, on the other hand shows a marked warming with increasing temperature. However in the future, the model experiences such temperature levels throughout the year that nearly 40% of all months are warmer than anything experienced under current conditions. If the bias behavior of the two other models represents a general model behavior (as indeed supported by *Christensen et al.* 2008), this latter model may just happen to have its bias curvature at a higher temperature than experienced under present conditions. Note for example that the excess warming does not appear to be present before the last 30 year period. If so, one could speculate on wehter this model would also need to be corrected downwards in a similar way as the others, particularly at the warmest months.

Acknowledgements

We are indebted to our partners in the ENSEMBLES project, who have provided their ERA40 driven and GCM driven climate simulation to the ENSEMBLES RCM archive hosted by the DMI

References

Christensen, J. H., F. Boberg, O. B. Christensen, and P. Lucas-Picher, On the need for bias correction of regional climate change projections of temperature and precipitation, Geophys. Res. Lett., 35, L20709, doi:10.1029/2008GL035694, 2008

Christensen, J.H. and O.B. Christensen, A summary of the PRUDENCE model projections of changes in European climate by the end of this century, Climatic Change, 81 Supl. 1, 7-30, doi:10.1007/s10584-006-9210-7, 2007

An atmosphere-ocean coupled model for the Mediterranean climate simulation

Alberto Elizalde, Daniela Jacob and Uwe Mikolajewicz

Max Planck Institute for Meteorology, Bundesstraße 53, 20146 Hamburg, Germany. alberto.elizalde@zmaw.de

1. Introduction

Preliminary results of a coupled model are presented. A regional coupled model was developed using a composition of three models: REMO for the atmospheric component, MPIOM for the oceanic component and HDModel for the hydrological part. The goal of this development is to study the Mediterranean climate and the impact of the climate change over this region with a special interest on the water cycle. A coupled model simulation permits, through the comprehension of the atmosphere-ocean interaction, a better understanding of the processes' mechanisms involved on each component of such cycle, *Somot et al*. (2008); *Aldrian et al*. (2005), like: cloud formation, precipitation, evaporation, runoff, processes interaction, feedbacks, etc.

2. Coupling Strategy

At present, global models and reanalysis datasets have not resolution enough to solve the relative small scale local processes, derived from the complex orography, coastal line and straits (*Fig*. 1), *Lorenz and Jacob* (2005); *Sotillo et al*. (2005). A high resolution on the configuration of the coupled model is needed for this task. The spatial resolution established for our experiment is as follow: REMO spatial resolution is 25 km and 31 vertical levels, a limited version of the Max-Planck-Institute Ocean Model (MPI-OM) has a ~11 km resolution with 41 vertical levels and the Hydrological Discharge model (HD model) has a 50 km spatial resolution. The coupling is carried out using the OASIS coupler. REMO calculates fluxes of heat, momentum and freshwater, runoff and drainage, the last two diagnostics are used to calculate river discharge by the HD model. MPIOM provides the SST to REMO (*Fig*. 2). The domain for the atmospheric component was chosen in such way that it catches all the influential regional atmospheric processes that affect the hydrological cycle (not shown), with the Nile catchment as an exception.

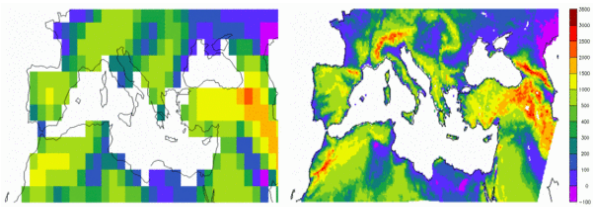

Figure 1. Orography (in meters) of ECHAM5 global model (~200 km horizontal resolution, left) and REMO regional model (~25 km, right).

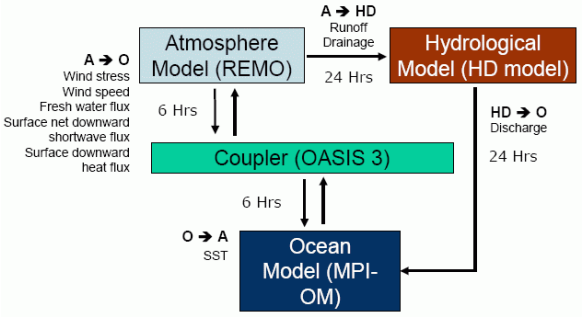

Figure 2. Coupled model configuration. Exchange variables and coupling.

This work is within the EU-funded CIRCE project. Climate simulations over the Mediterranean region are carried out using the coupled model and non-coupled models. The configuration of the coupling is discussed and preliminary results are compared. Both simulations, from the coupled and non-coupled models, are run with boundary conditions from ERA40 reanalysis dataset. The results are compared to observations for the simulated period. The performance of the model and its applicability on Mediterranean region is discussed.

References

Aldrian E., D. V. Sein, D. Jacob, L. D. Gates, and R. Podzun, Modeling Indonesian rainfall with a coupled regional model. *Climate Dyn.*, Vol. 25, pp. 1–17, 2005.

Lorenz, P., and D. Jacob, Influence of regional scale information on the global circulation: A two-way nesting climate simulation, *Geophys. Res. Lett.*, Vol. 32, L18706, doi:10.1029/2005GL023351, 2005.

Somot S., Sevault F., Deque M. and Crepon M., 21st century climate change scenario for the Mediterranean using a coupled atmosphere-ocean regional climate model, *Global and Planetary Change*, Vol. 63, No. 2-3, pp. 112-126, 2008.

Sotillo, M. G., Ratsimandresey, A.W., Carretero, J. C., Bentamy, A., Valero, F., and Gonz´alez-Rouco, J. F.: A high-resolution 44-year atmospheric hindcast for the Mediterranean Basin: Contribution to the regional improvement of global reanalysis, *Clim. Dyn.,* Vol. 25, pp. 219–236, 2005.

Inter-comparison of Asian monsoon simulated by RCMs in Phase II of RMIP for Asia

Jinming Feng, Congbin Fu, Shuyu Wang, Jianping Tang, D. Lee, Y. Sato, H. Kato, J. Mcgregor et al.

Institute of Atmospheric Physics, Chinese Academy of Sciences, Beijing, China. fengjm@tea.ac.cn

1. Abstract

In phase II of the Regional Climate Model Inter-comparison Project (RMIP) for Asia, the regional climate has been simulated for July 1988 through December 1998 by five regional climate models and one global variable resolution model. Comparison of the 10-year simulated precipitation with the observations was carried out. The results show that most models have the capacity to reproduce the basic spatial pattern of precipitation for Asia, and the main rainbelt can be reproduced by most models, but there are distinctions in the location and the intensity. Most models overestimate the precipitation over most continental regions. Interannual variability of the precipitation can also be basically simulated, while differences exist between various models and the observations. The biases in the stream field are important reasons behind the simulation errors of the Regional Climate Models (RCMs). The cumulus scheme and land surface process have large influences on the precipitation simulation. Generally, the Grell cumulus scheme produces more precipitation than the Kuo-Anthes scheme.

2. Design of experiments

In order to understand the performance of RCMs on simulating Asian, especially East Asian climate, the Regional Climate Model Inter-comparison Project (RMIP) for Asia was launched by START Regional Center for Temperate East Asia in 2000 (Fu et al., 2005). There are six participant models in phase II of RMIP, of which five are RCMs and one is a global variable-resolution model. They include: RIEMS (Fu et al., 2000), NJU MM5, MRI JSM_BAIM, RegCM2b, SNU RCM, CSIRO CCAM. The experiment domain is the same as phase I, which contains a large part of the Asian continent, western Pacific, Bay of Bengal and the South China Sea (Fig. 1). The horizontal resolution of the models is 60 km, with a 151×111 grid in the east-west and north-south directions. The simulation period is from July 1988 to December 1998. The driving fields come from NCEP-II reanalysis data, with a 15-grid buffer zone. The NCAR terrain data are used in the model integration with a horizontal resolution of 0.5°×0.5°, in addition to satellite land surface data supplied by NASA. The same driving field, topography, land surface vegetation, simulation domain and horizontal resolution ensure the comparability of the simulation results.

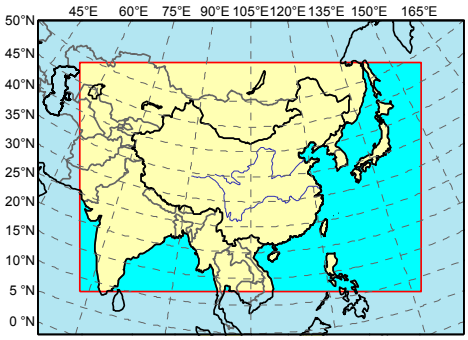

Fig.1. Simulation domain for RMIP

3. Some results

The driving fields come from the NCEP-II reanalysis data, but these reanalysis data have some biases. The spatial distribution of the NCEP-II bias has some similarities with the results of most models over the continental region, such as the positive bias over most areas of Mongolia and the southwest of China, and the negative bias over the north of India, etc. Because of the few observation stations in Northwest China and the Tibetan Plateau, the observed data used to validate the models almost come from the CRU precipitation data, so a larger bias may exist. Hence, maybe the biases of the large-scale forcing fields and the deficiency of the validation data are one of the possible reasons for the biases of the simulation.

In summer, the southeastern and southwestern monsoons prevail in the East Asian continent. The strong summer monsoon transports the abundant vapor northwardly from the Bay of Bengal and West Pacific, thereby generating a large amount of precipitation in South China, Changjiang-Huaihe and later in North China. For the summer monsoon current located to the south of 30ºN, it is underestimated by MRI compared to the NCEP-II data. So the precipitation simulated by MRI is much smaller in summer, while it is greater in the other models. The summer monsoon current simulated by RIEMS is much stronger and the region of strong monsoon current is extended further northward. This is the main reason that RIEMS simulates much more precipitation in the summer. The summer monsoon current simulated by SNU is close to NCEP-II, and the bias of the simulated precipitation is smaller relatively. Hence, the biases of the monsoon current are important reasons for the simulation errors of RCMs.

4. Some conclusions

Most models overestimate the precipitation in most continental regions. The seasonal variation of precipitation can be simulated, but there are large differences in the regional precipitation among the models.

The biases of the stream fields are important reasons behind the simulation errors of RCMs. Also, the deviation of the large-scale driving fields may be one reason for the simulation biases. The cumulus parameterization scheme and land surface process have a large influence on the precipitation simulation.

Most models can basically simulate the trend of the interannual variation of precipitation, but there are large differences in the magnitude of precipitation among the models.

References

Fu, C. B., and coauthors, Regional Climate Model Intercomparison Project for Asia. Bull. Amer. Meteor. Soc., 86, 257-266., 2005.

Fu Congbin, Wei Heilin, and Qian Yun, Documentation on a Regional Integrated Environment Model System (RIEMS version 1). TEACOM Science Report No.1, START Regional Committee for Temperate East Asia, Beijing, China, 1-26, 2000.

From droughts to floods: A statistical assessment from RCM

Garcia, S.G. and Giraldo, J.D.

Departamento de Ingeniera Térmica y de Fluidos, UPCT, Paseo Alfonso XIII, 52. Cartagena (30203) MurciaUPCT, Spain

Hazards related with heavy rain, results in floods and crop damage that have significant impacts on environment and human activities (society and economy) in West Africa. On the other hand, changes on spatial distribution of precipitation and frequency of droughts will have implications for the planning and management of water resources. Extracting useful predictions of these events from RCMs, according to stakeholders and resource planners needs in West Africa, should represent a significant challenge for the research community. The present work analysis the spatiotemporal precipitation patterns in Senegal river basin, from RCM. A multi-parametric approach is used by means of the analysis of the variability and trends of frequency and magnitude of different types of extreme rain events (moderate, heavy and very heavy events based on thresholds of daily rain), and length of dry spells (with thresholds of daily rain < 1mm and <10 mm). Nonparametric and parametric tests, are applied for analysis of trends and dynamics of rainfall.

Key words: climate change, impacts assessment, natural hazards, West Africa, AMMA

On the validation of RCMs in terms of reproducing the annual cycle

Tomas Halenka, Petr Skalak and Michal Belda

Department of Meteorology and Environment Protection, Charles University; tomas.halenka@mff.cuni.cz

1. Climate models and annual cycle

There are many aspects of the validation of climate models. In addition to standard statistical characteristics a more in-depth analysis of annual cycle performance can provide more information on ability of the models to reproduce properly the physical processes which strongly affect the behavior of climate parameters during the year. Global Circulation Models (GCMs) can reproduce climate features on large scales, but their accuracy decreases when proceeding from continental to regional and local scales because of the lack of resolution and thus on the regional scale they are very often rather poor in reproducing the annual cycle. The more detail analysis of 15 RCMs used in EC FP6 IP ENSEMBLES in ERA 40 driven experiment on 25 km resolution for the period of 1961-2000 in different PRUDENCE regions presents the comparison of the models and their validation in terms of annual cycle reproduction. While for the temperature the performance of the models is mostly very good and quite consistent, there are some models with rather significant problems in some regions in reproducing annual cycle of precipitation.

2. ENSEMBLES RCMs assessment in terms of annual cycle

The quality of reproducing the annual course in the model simulations is believed to be good indication of quality of different atmospheric processes description which affects the overall model performance. However, to compare the annual course patterns with those based on observational data is not simple and unambiguous task, for the purpose of the use in the weighting methods in ENSEMBLES project some objective method is required. The problem of the annual course analysis is that we cannot use just one simple characteristic as bias, basically at least three patters are of importance, i.e. in addition to the bias it is the amplitude and shift in period, either as a whole or partly in some seasons. *Taylor (2001)* presented so called Taylor diagram, which is used for presenting the data in terms of RMS error, standard deviation and correlation and show just the analysis of models simulations with emphasis on annual cycle. Actually, although these characteristics are not completely independent, we can see the analogue between the bias and RMS error, as well as in between amplitude and standard deviation, correlation being good representation of the shifts in the annual course. For purpose of the weighting we propose to use the score index

$$S = \frac{4(1+R)}{\left(\sigma + 1/\sigma\right)^2 (1+R_0)}$$

where R_0 is the maximum correlation attainable. For simplicity we used maximum value R_0=1. Parameter R is the correlation coefficient with respect to the observation dataset used for comparison, σ is standard deviation of the model results σ_m normalized by standard deviation of the observational dataset used for validation σ. We have made calculations both for first degree formulation as above and fourth degree one discussed in *Taylor (2001)*, which reads

$$S = \frac{4(1+R)^4}{\left(\sigma + 1/\sigma\right)^2 (1+R_0)^4}.$$

Additionally, we have tested the second degree formulation as well, basically the higher degree penalizes the lower correlation, for computations in this analysis seems to be usefull to use the 4th order formulation for temperature to resolve the differences between otherwise very high scores, for precipitation the scores are not so high anyway and the first degree is enough to resolve the performance of the individual models. All the calculations were performed for individual PRUDENCE regions, quite significant differences appears between the models for some regions. To compare these score annual cycles for temperature and precipitation are presented in Fig. 1 and 2, respectively, using ENSEMBLES gridded data (E-obs, *Haylock et al., 2008*). Original CRU databases are shown for comparison as well, although for precipitation there are some differences between the climatologies the resulting scores are not so significantly affected.

It should be mentioned that this method is validating the general performance of the models anyway, for temperature, where the variance of the complete monthly data is usually nearly of order higher than interannual variance (year by year) of data for individual months, this performance well correspond with the performance of annual cycle. The results for precipitation are not so clear, the variance of all the time series is basically the similar as the interannual variability of individual monthly data so that the overall performance and quality of annual cycle cannot be well resolved by this method. Proper choice of R_0 for precipitation could be of great importance for further application of the method.

Annual courses of temperature as well as precipitation will be presented for individual models and regions. Taylor's diagrams will show the models validation against E-Obs.

Acknowledgements

This work is supported in framework of EC FP6 IP ENSEMBLES. Some contributions to the tasks are supported from local sources as well under Research Plan of MSMT, No. MSM 0021620860. We acknowledge the E-Obs dataset from the EU-FP6 project ENSEMBLES (http://www.ensembles-eu.org) and the data providers in the ECA&D project (http://eca.knmi.nl).

References

Haylock, M.R., N. Hofstra, A.M.G. Klein Tank, E.J. Klok, P.D. Jones, M. New, A European daily high-resolution gridded dataset of surface temperature and precipitation. *J. Geophys. Res (Atmospheres)*, 113, D20119, doi:10.1029/2008JD10201, 2008.

Taylor, Karl E., Summarizing multiple aspects of model performance in single diagram, *J. Geophys. Res.*, 106, D7, 7183--7192, 2001.

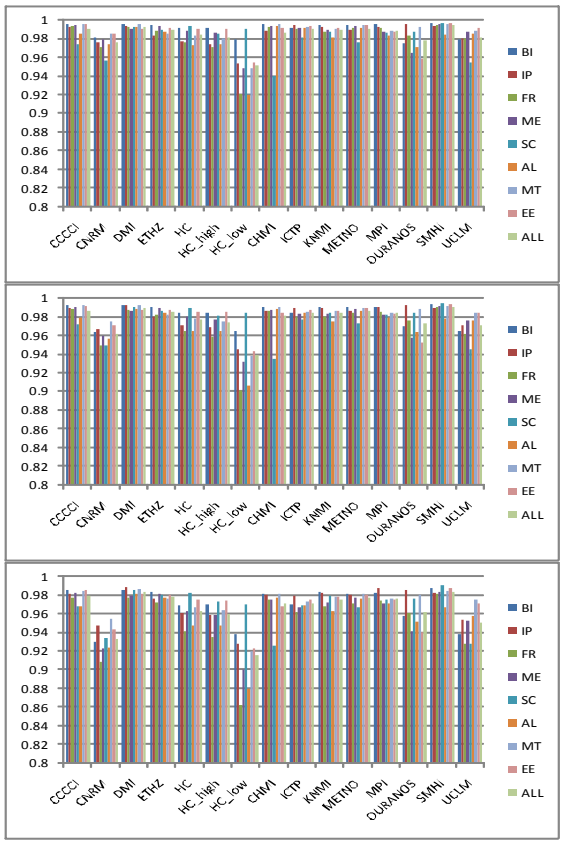

Figure 1. Taylor's scores for the first, second and fourth order, temperature.

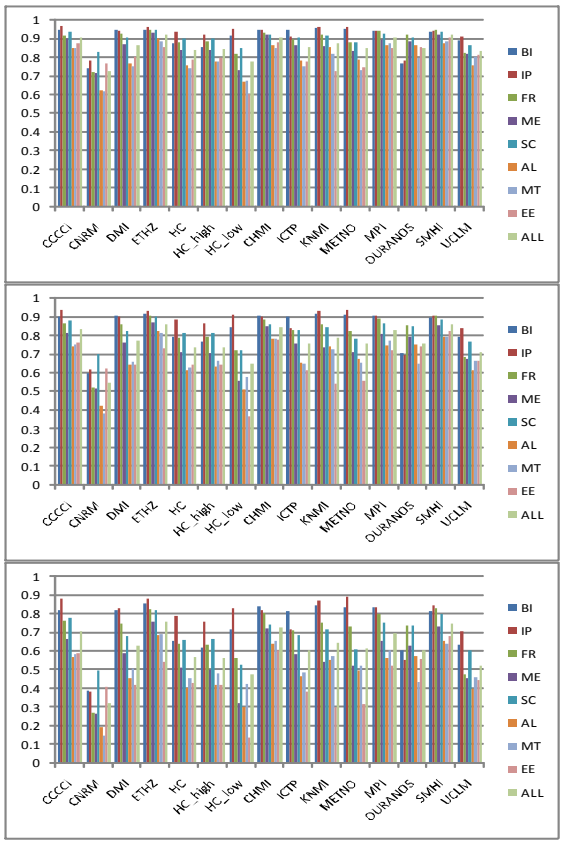

Figure 2. Taylor's scores for the first, second and fourth order, precipitation

AMMA-Model Intercomparison Project

F Hourdin., J Polcher, F Guichard, F Favot, JP Lafore, JL Redelsperger, Ruti PM*., A Dell'Aquila, T Losada., AK Traoer

paolo.ruti@enea.it

AMMA-MIP is a Model Intercomparison Project developed in the frame of the African Monsoon Multi disciplinary Analysis project (AMMA). It is a light exercise of intercomparison and evaluation of both global and regional atmospheric models, focused on the study of the seasonal and intraseasonal variations of the climate and rainfall over Sahel. Taking advantage of the relative zonal symmetry of the West African climate, one major target of the exercise is the documentation of a meridional cross section made of zonally averaged (10W-10E) outputs.

The African Monsoon is characterized by a well defined meridional structure of albedo and vegetation (Fig. 1 A), with weaker longitudinal variations. This structure is tightly connected to that of the mean rainfall (Fig. 1 B), with maximum rainfall occuring in the Sudanian region (8N-12N) during northern summer, and a sharp transition over Sahel (12N-20N), a particularly sensitive region which has undergone a strong drought in the late 70s and 80s. The meridional structure of the mean rainfall is itself related to the mean meridional circulation with a near surface monsoon flow which brings to the African continent water evaporated over the Guinea gulf. This monsoon flow converges with a southward dry air flow coming from Sahara at the "intertropical discontinuity", in the region of the Saharian heat low where dry convection occurs. The return branch of this Hadley circulation at around 600 hPa is associated through angular momentum budget and thermal wind balance with the African Easterly Jet which, in turn, carries additional water from the Indian ocean. At around 10N, one finds the Inter Tropical Convergence Zone where most of the convective rainfall occurs, with a mean upward motion which reaches 200 hPa where the Tropopause Easterly Jet takes place.

We present here the main diagnostics tailored for the West African monsoon dynamics and we discuss first results and further extension.

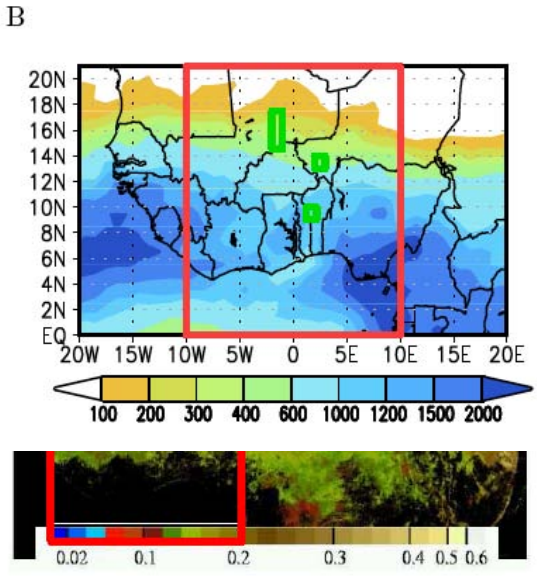

Figure 1:Picture of West Africa albedo (A) (source EUMETSAT/GEM,http://wwwgem.jrc.it/stars/ albedo.htm) and GPCP cumulated rainfall (B) for year 2000 (mm). The red rectangle corresponds to the zone retained for the AMMA-CROSS section and the green rectangles to the meso-scale AMMA sites.

Projection of the changes in the future extremes over Japan using a cloud-resolving model (JMA-NHM): Change in heavy precipitation

Sachie Kanada, M. Nakano, M. Nakamura, S. Hayashi, T. Kato, H. Sasaki, T. Uchiyama, K. Aranami, Y. Honda, K. Kurihara, A. Kitoh

Advanced Earth Science & Technology Organization (AESTO)/ Meteorological Research Institute (MRI), 1-1 Nagamine, Tsukuba, Ibaraki, 305-0052, JAPAN;: skanada@mri-jma.go.jp

1. Introduction

Warming of the climate system is now evident and changes in the present climate due to global warming, including changes in precipitation and aspects of extremes, are of the highest priority to be researched (IPCC, 2007). Several numerical simulations have been conducted; however, most of them have been performed by general circulation models using a horizontal grid larger than several tens of kilometers. Wakazuki et al. (2008) studied precipitation-based extreme indices from the results of both relatively fine-mesh experiments with a 20-km horizontal grid hydrostatic atmospheric general circulation model (AGCM-20km: TL959L60) and a non-hydrostatic model with a horizontal resolution of 5km, and they concluded that the intense precipitation tends to be underestimated even by the AGCM-20km. It is a well-known fact that the horizontal distribution of precipitation depends on the topography and that intense precipitation tends to concentrate in limited areas. Therefore, finer-mesh experiments with a horizontal resolution of several km should be appropriate.

2. Model descriptions

In order to study changes in the regional climate due to global warming, especially those of the extremes, in the vicinity of Japan during the summer rainy season, experiments by a semi-cloud resolving non-hydrostatic model (JMA-NHM; Saito et al. 2001, 2006) with a horizontal resolution of 5km (NHM-5km) have been conducted from June to October by nesting within the results of the 10-year time-integrated experiments using the improved AGCM-20km for the present (1990-1999), near-future (2026-2035) and future climates (2086-2095). Detailed descriptions of the NHM-5km are presented by Nakano et al. at this RCM2009-WS. The results of the present and future climates will be shown. A domain for the NHM-5km experiments is shown in Fig. 1.

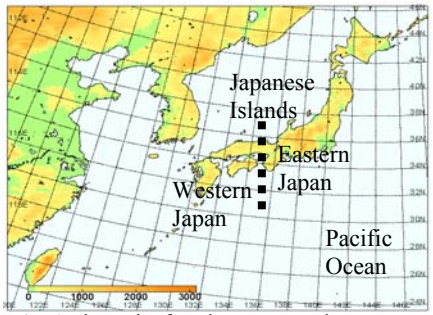

Figure 1. A domain for the NHM-5km.

The results of the preliminary experiments with the NHM-5km have been already published by Kanada et al. (2008).

3. Results of the NHM-5km experiments

Our results on the precipitation show that intense precipitations exceeding 150 - 300 mm day^{-1} will increase in the vicinity of Japan in the future climate. The 90th percentiles of regional largest values among maximum daily precipitations (R-MDPs) grow 156 to 207 mm/day between the present and future climates. The STARDEX indices of precipitation extremes (e.g., prec90p, 646SDII, Fig. 2) show that the intense precipitation on the Pacific side of Japan will increase.

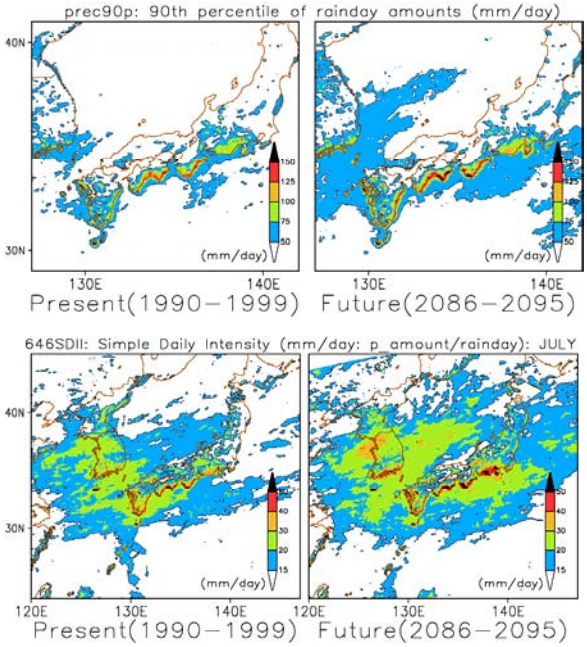

Figure 2. 90th percentile of rainday amount (upper row) and simple daily intensity (lower row) in the present (left) and future (right) climates.

In general, the number of rain day (> 1.0 mm day^{-1}) will decrease in the future climate, while the number of heavy rain day (> 100.0 mm day^{-1}) will increase in western Japan in August and September and on the Pacific side of eastern Japan in July and August (Fig. 3). Heavy precipitations (defined by daily precipitations larger than 90th percentiles at each model grids) frequently appear in July in western Japan in both the present and future climates, because the Baiu front extends from the west to the east along the Japanese Islands. Moreover, heavy precipitations in western and eastern Japan in the future climate will continue to appear at a high frequency rate even in August due to the stagnation of the Baiu front in the vicinity of Japan (not shown).

4. Results of the NHM-2km experiments

Further detailed experiments have been conducted by a cloud-resolving model with a horizontal resolution of 2km (NHM-2km) as well, since it is well-known that the finer-mesh models are strongly required for the precipitation extremes, and horizontal distributions of precipitation much depends on the complex topography in the vicinity of Japan. The finer topography and no cumulus

parameterization are used in the NHM-2km experiments. The results of verification experiments with perfect boundary conditions produced from objective analysis data show a quite good agreement with the observational data in both the quality and quantity on precipitation (not shown). Tentative comparisons between the results of the NHM-5km and NHM-2km experiments reveal that the NHM-2km can re-produce more detailed and realistic horizontal distributions of rainfall in many cases (Fig. 4).

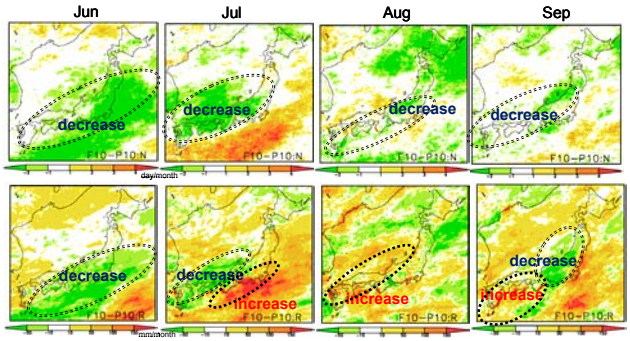

Figure 3. Changes in precipitation frequencies (upper row) and monthly precipitation amounts (lower row) from June to September from in the present to future climates.

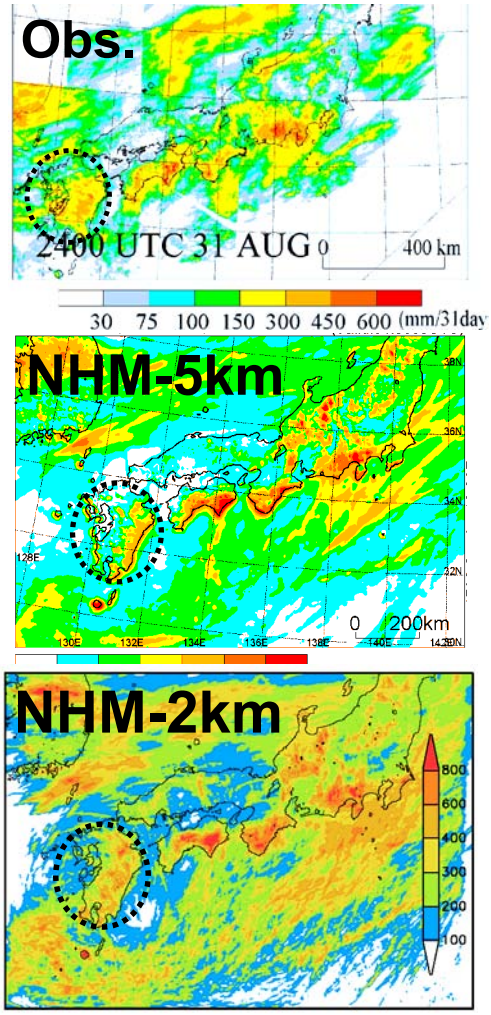

Figure 4. Monthly precipitation amounts in August 2003 by the observation, NHM-5km and NHM-2km.

5. Summary and Future Plan

In the future climate, the frequency of rain day (> 1.0 mm day^{-1}) will decrease overall Japan, while the number of heavy rain day (> 100.0 mm day^{-1}) will increase in western Japan in August and September and on the Pacific side of eastern Japan in July and August.

Further experiments without any cumulus parameterizations are conducted by the NHM-2km. Early results prove a satisfactory performance of the NHM-2km in precipitations.

The NHM-2km experiments is going to be conducted from June to October for 10-25 years for the present (1990-1999), near-future (2026-2035) and future climates (2086-2095), respectively. Further analysis, especially on the precipitation extremes will be planed by using the results of the experiments.

The NHM-5km adopts the Kain-Fritsch scheme for a cumulus parameterization. A topography-dependent tendency in horizontal distribution of the precipitation by this scheme is pointed out by Narita, M. (2008) and Kanada, et al. (2008). Therefore, the improved Kain-Fritsch scheme also has been under development.

Acknowledgements

This study is supported by the Ministry of Education, Culture, Sports, Science and Technology under the framework of the "KAKUSHIN" program. Numerical simulations are performed in the Earth Simulator. The authors are grateful to "KAKUSHIN-3" modeling group for carrying out the project.

References

IPCC, Climate Change 2007: Synthesis Report. Contribution of Working Groups I, II and III to the Fourth Assessment Report of the Intergovernmental Panel on Climate Change [Core Writing Team, Pachauri, R.K. and Reisinger, A. (eds.)]. *IPCC*, Geneva, Switzerland, 104 pp, 2007.

Kanada, S., M. Nakano, S. Hayashi, T. Kato, M. Nakamura, K. Kurihara and A. Kitoh, Reproducibility of Maximum Daily Precipitation Amount over Japan by a High-resolution Non-hydrostatic Model. *SOLA*, Vol. 4, pp.105-108, 2008.

Narita, M., Improvement and adjustment of Kain-Fritsh sheme. *Separate volume of annual report of NPD*, 54, 103-111, 2008. (in Japanese)

Saito, K., T. Kato, H. Eito and C. Muroi, Documentation of the meteorological research institute / numerical prediction division unified nonhydrostatic model. *Tech. Rep. of MRI.,* 42, pp133, 2001.

Saito, K., T. Fujita, Y. Yamada, J. Ishida, Y. Kumagai, K. Aranami, S. Ohmori, R. Nagasawa, S. Kumagai, C. Muroi, T. Kato, H. Eito and Y. Yamazaki, The operational JMA nonhydrostatic mesoscale model. *Mon. Wea. Rev.*, 134, 1266-1298, 2006.

Wakazuki, Y., M. Nakamura, S. Kanada and C. Muroi, Climatological Reproducibility Evaluation and Future Climate Projection of Extreme Precipitation Events in the Baiu Season Using a High-Resolution Non-Hydrostatic RCM in Comparison with an AGCM. *J. Meteor. Soc. Japan,* Vol. 86, pp. 951-967, 2008.

Predicting water resources in West Africa for 2050

Karambiri H.[(1)], Garcia S.[(2)], Adamou H.[(3)], Decroix L.[(4)], Mariko A.[(5)], Sambou S.[(6)] and Vissin E.[(7)]

[(1)]2iE, Burkina Faso; [(2)]UPC, Spain; [(3)]UAM, Niger; [(4)]IRD, France; [(5)]UB, Mali; [(6)]UCAD, Senegal; [(7)]UAC, Benin

Water resources play a key role in the socio-economic development, human activities, environmental and ecosystems preservation. In West Africa, these vital resources are very vulnerable to global changes and human pressures. The current and future availability and dynamic of water resources need to be better assessed and analyzed to ensure a sustainable and integrated management and planning. In the AMMA-EU project, the WP3.3 aims to assess the impacts of climate and land use change on the water resources in West Africa for a number of river basins on different scales, different agro-climatic areas and different uses (Senegal, Volta and Oueme). The assessment of water resources for future horizons (2050) is done through hydrological modelling coupled or forced with climate models outputs. Up today, global climate predictions using GCMs were intensively and widely used. Even if these coarse simulations allow bringing broad tendencies on water resources availability and distribution, they do not bring relevant answers on the availability and variability of water resources locally. The recent advances in climate sciences and their capacity to provide fine scaled results using regional/sub-regional models (RCM) or downscaling techniques should be discussed with the climate community, in order to provide detailed assessments of climate change impacts on water resources corresponding to the needs of stakeholders, decision-makers and communities in West Africa.

Key words: Climate change, Impacts assessment, water resources, West Africa, AMMA.

Evaluation of European snow cover as simulated by an ensemble of regional climate models

Sven Kotlarski, Daniel Lüthi and Christoph Schär

Institute for Atmospheric and Climate Science, ETH Zurich, sven.kotlarski@env.ethz.ch

1. Introduction

In many regions land surface characteristics are strongly influenced by the presence of seasonal snow cover. A correct description of snow characteristics is therefore of major importance for the simulation of surface-atmosphere energy fluxes in regional climate models (RCMs). At the same time snow modelling poses special challenges due to the non-linear processes involved and their pronounced spatial variability. If the future evolution of regional snow cover is of interest, the ability of RCMs to reproduce present-day conditions should be investigated beforehand.

The present contribution evaluates the performance of a set of state-of-the-art RCMs with respect to snow cover extent and snow depth in Europe. A special focus is laid on the European Alps, an area with a pronounced topography and a high economic significance of snow cover.

2. Data and Methods

The investigated RCM experiments were carried out within the ENSEMBLES project for the period 1960-2000 at a horizontal resolution of approx. 25 km. In all cases the lateral boundary forcing was provided by the ERA40 re-analysis. The simulated snow characteristics (snow cover extent, snow depth, number of snow days) in Europe are compared to different observational datasets. For this purpose both ground based and remote-sensed datasets are used.

3. Results

The detailed comparison of simulated and observed snow cover characteristics reveals an overall good performance of the RCMs. The basic characteristics of seasonal snow cover on a European scale are well reproduced. Still, pronounced differences exist between individual RCMs, for instance with respect to winter snow extent (Figure 1).

Furthermore, important biases appear for individual models in some regions. For instance, the timing of spring snowmelt is often shifted by several weeks in the models. One example of these biases is shown in Figures 2 and 3 which depict the mean annual cycle (1981-2000) of the number of snow days for distinct elevation intervals in Germany. With respect to the observational dataset most models show a pronounced delay of the spring snowmelt and an overestimation of the total number of snow days in wintertime.

In some cases model deficiencies can be traced back to the treatment of snow in the land surface scheme of the respective RCM. Furthermore, biases in atmospheric parameters (temperature and precipitation) can partly be linked to shortcomings in the representation of surface snow cover.

4. Conclusions

The detailed validation of the simulated snow characteristics in an ensemble of state-of-the-art RCMs reveals an overall good model performance for the period 1961-2000. However, important biases in basic parameters in individual regions (e.g., the timing of spring snowmelt) question the direct use of the simulated snow parameters in impact studies (e.g., hydrological modeling).

Regarding regional climate change scenarios for the 21st century confidence has been gained that state-of-the-art RCMs are able to capture basic climate change effects on snow extent and snow depth. These experiments will be analyzed in a second step.

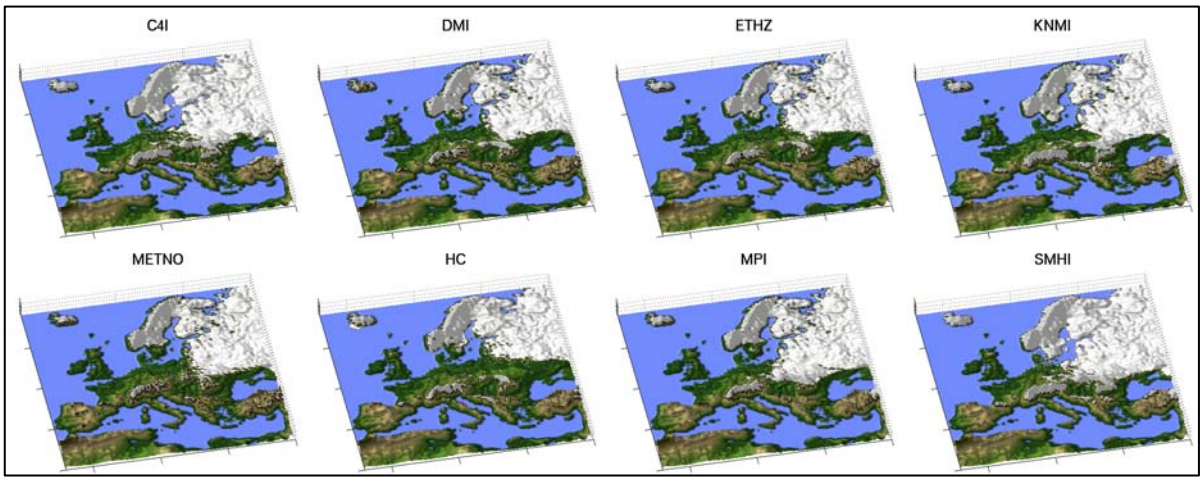

Figure 1. Mean extent of winter (DJF) snow cover in 8 ENSEMBLES RCMs (1961-2000). White: Areas with a mean winter snow depth of more then 3 cm w.e.

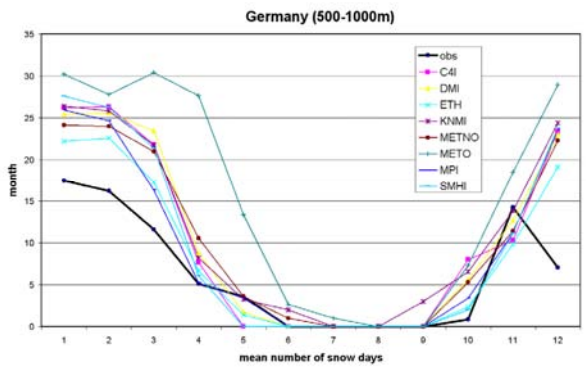

Figure 3. Mean annual cycle (1981-2000) of the number of snow days in Germany (elevation interval 500-1000m) as derived from observations (black line) and as simulated by 8 ENSEMBLES RCMs (colored lines).

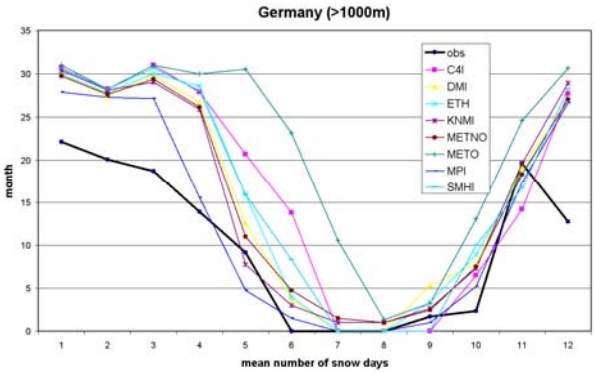

Figure 2. Mean annual cycle (1981-2000) of the number of snow days in Germany (elevation >1000m) as derived from observations (black line) and as simulated by 8 ENSEMBLES RCMs (colored lines).

Projections of eastern Mediterranean climate change simulated in a transient RCM experiment with RegCM3

Simon Krichak, Pinhas Alpert and Pavel Kunin

Department of Geophysics and Planetary Sciences, Tel Aviv University, Tel Aviv, Israel

1. Introduction

The climate conditions of the eastern Mediterranean (EM hereafter) are characterized by changeable rainy weather with moderate temperatures during the cool seasons and dry and hot weather during summers. The climate conditions fit the "Mediterranean" type of the *Koppen and Geiger's* (1936) classification and are strongly determined by the region's location in the zone dominated by polar front activity in winter and that of subtropical high-pressure system during summer. The EM region's climate is influenced by the effects of annual variations in the area of the Asian monsoon (*Bedi et al*., 1976; *Rodwell and Hoskins*, 1996). During the cool season the EM climate is also affected by specific synoptic processes associated with interaction of the upper-troposphere jet stream with the regional terrain over northern Africa (*Krichak et al*., 1997). Winters in the EM are characterized by passing disturbances known as Cyprus cyclones and between them intrusions of high pressure systems and polar air masses (*Alpert et al.* 1990, *Saaroni et al.* 1996, *Levin and Saaroni*, 1999). In the summer the EM is under the influence of a quasi-stationary system, a Persian Gulf trough, an extension of the Asian monsoon, and in the southern parts, and extension of the Azores anticyclone. The system is characterized by westerly winds and a diurnal breeze mechanism and is limited to an average height of about 1000 m. Above it is dominated by the subtropical anticyclone causing subsidence and almost absolute absence of rainfall (*Bitan and Saaroni,* 1992) These conditions are permanent during mid-June to mid-September. During intermediate seasons there are several different synoptic mechanisms acting. Among those are Sharav cyclones and Red Sea Trough systems. The thermal low pressure systems known as the north-African (Sharav) cyclone, move fast along the north-African shore area, especially during spring. They cause very high temperatures and low humidity when the EM is ahead of and below the warm sector of cyclone (*Alpert and Ziv,* 1989, Levin and Saaroni 1999). The Red Sea trough (RST) is common in both spring (less typical) and autumn (Tsvieli and Zangvil 2005; Ziv et al. 2005). The RST is an extension of the African monsoon trough. Intensity of the associated with the trough weather processes is significantly determined by the position of the inter-tropical convective zone (ICTZ). During October and April the ITCZ is located approximately at 15ºN-20ºN (along the 0ºE). The RST is a low-level trough extending from the Red Sea northward. The air-low in the EM depends on the location of the trough's axis (*Dayan,* 1986). The EM weather conditions associated with the RST systems are usually dry. Intense EM precipitation events are typical however in the cases of development of Active Red Sea Troughs, with lower level RST accompanied by extending southward upper-level trough (*Kahana et al*. 2002).eral biases in results of simulation of the EM climate have been noted (*Evans et al*., 2004; *Krichak et al.* 2007). Among those a negative bias in representation of the regional precipitation was also noted. (*Evans et al*., 2004; *Giorgi et al*., 2004; *Krichak et al.*, 2007).

The analysis was focused on optimization of the climate simulation results over the region centered over the Israeli part of the EM region and realization of a transient regional climate change simulation experiment.

2. Justification of model configuration

Synoptic processes over a large geographic area from the Atlantic to the east-Europe and Middle East participate in formation of the EM climate. Intense EM rainy periods are usually associated with powerful synoptic developments and cold-air intrusions taking place over a large zone. Ten climate simulation experiments driven from the lateral boundaries by the NCAR/NCEP Reanalysis data are realized to understand the role of model domain configuration in the RCM over the region. Sensitivity of the model results over the area to the positioning of the lateral boundaries of the domain is evaluated. An optimal configuration of the domain is finally selected.

3. Transient climate change RCM experiment

Climate change trends over the EM region are simulated in a regional climate simulation experiment with the ICTP RegCM3 model (Pal et al. 2007) driven from the lateral boundaries by results of ECHAM5/MPI-OM1 (Roeckner et al. 2003) transient climate simulation from 1960 to 2060 (SRES A1B emission scenario after 2001). The trends projected for the southern part of the eastern Mediterranean region include a 20-30% precipitation drop during winter (the period with major rains take place) and its rise during autumn (20-25%) and spring (5%); also projected is a 1.5-2.0°C mean seasonal 2m air temperature rise during winter and spring, somewhat lower one (1.0–1.5°C) in summer and a non-significant (0.3°C) temperature rise during autumn from 1961-1990 to 2021-2050. The climate change signal is not uniform over the region however. Notable mean seasonal precipitation rises from the current climate conditions are projected over the southern part of the region during winter and summer, whereas a drop in summer rains is projected for the north-eastern part of the EM. During winter and summer seasons the warming process seems to be mainly controlled by the Middle East effects – leading to maximum air temperature changes over eastern part of the region. During spring however the zone with the maximum warming is found over the northern part of the EM. During autumn the major zone with the maximum warming up is found over the Mediterranean Sea area. The transient RCM simulation experiment projects significant decadal oscillations of the EM climate parameters during the coming decades however which may be indicating a time-lagged contribution of climate change processes over remote areas. The roles of several possible external effects are evaluated.

Acknowledgments

The research was supported by German-Israeli research grant (GLOWA - Jordan River) from the Israeli Ministry of Science and Technology; and the German Bundesministerium fuer Bildung und Forschung (BMBF) and by integrated project granted by the European Commission's Sixth Framework Programme, Priority 1.1.6.3 Global Change and Ecosystems (CIRCE), Contract no.:036961.

References

Alpert P, SO Krichak, H. Shafir, D. Haim, I. Osetinsky Climatic trends to extremes employing regional modeling and statistical interpretation over the E. Mediterranean, *Global and Planetary Change*, Vol. 63, pp. 163-170, 2008

Alpert P, B. Ziv, The Sharav cyclone - observations and some theoretical considerations. *J. Geophys. Res*., Vol., 94 pp. 18495–18514, 1989

Bedi HS, RK Datta, SO. Krichak Numerical forecast of summer monsoon flow patterns. *Soviet Meteorology and Hydrology* 5, pp. 39-45, 1976

Bitan A, Saaroni H., The horizontal and vertical extension of the Persian Gulf pressure trough. *Int. J. Climatology*, Vol. 12, pp. 733–747, 1992

Dayan U., Climatology of back-trajectories from Israel based on synoptic analysis. *J. Climate Appl. Meteor.,* Vol. 25, pp. 591–595, 1986

Evans JP, Smith RB, Oglesby RJ Middle East climate simulation and dominant precipitation processes, *Int. J. Climatol.* Vol. 24, pp. 1671-1694, 2004

GoldreichY.,Regional variation of phase in the seasonal march of rainfall in Israel. *Isr. J. Earth Sci.,* Vol. 25, pp. 133–137, 1976

IPCC Climate change - the physical science basis. Contribution of working group I to the Fourth Assessment Report of the Intergovernmental Panel on Climate Change [Solomon, S., D. Qin, M. Manning, Z. Chen, M. Marquis, K.B. Averyt, M. Tignor and H.L. Miller (eds.)]. Cambridge University Press, Cambridge, United Kingdom and New York, NY, USA, 996 pp, 2007

Kahana, R., Ziv, B., Enzel, Y., Dayan, U. Synoptic climatology of major floods in the Negev desert, Israel, *Int. J. Climatol*. Vol. 22, pp. 867-882, 2002

Köppen W, Geiger R Das geographische system der klimate. In: Handbuch der klimatologie (eds Köppen W & Geiger R), Bd 1, Teil C. Verlag Gebrüder Bornträger, Berlin, 44 p., 1936

Krichak SO, M. Tsidulko and P. Alpert Monthly synoptic patterns with wet/dry conditions in the eastern Mediterranean, *Teor. Appl. Climatol*. Vol. 65, 215-229, 2000

Krichak SO, Alpert P, Bassat K, Kunin P The surface climatology of the eastern Mediterranean region obtained in a three-member ensemble climate change simulation experiment, *Adv. Geosci*., 12, 67–80, 2007

Krichak SO Regional Climate Model simulation of present-day regional climate over European part of Russia with RegCM3, *Russian Meteorology and Hydrology*, Vol. 1, pp. 31-41, 2008

Levin N., H. Saaroni Fire Weather in Israel—Synoptic *Climatological Analysis GeoJournal* Vol. 47, pp. 523–538, 1999.

Pal JS, Giorgi F, Bi X, Elguindi N, et al. The ICTP RegCM3 and RegCNET: regional climate modeling for the developing world. *Bull. Amer. Meteorol. Soc.* Vol. 88, 9, pp. 1395-1409, 2007

Rodwell MJ, Hoskins B Monsoons and the dynamic of deserts. *Quart J. of the Royal Meteorol Soc*, Vol. 122 pp. 1385–1404, 1996

Roeckner E, and co-authors., The atmospheric general circulation model ECHAM5, Part I, Max-Plank Inst for Meteorology, Report no. 349, 127 p., 2003

Saaroni H., Bitan A., Alpert P. and Ziv Continental polar outbreaks into the eastern Mediterranean. *Int. J. of Climatology*, Vol. 16, pp. 1175–1191

Saaroni H. ,Ziv B., Bitan A. and P. Alpert, Easterly windstorms over Israel. *Theoretical and Applied Climatology,* 59:61–77, 1998

Tsvieli Y, A. and Zangvil, Synoptic climatological analysis of wet and dry Red Sea troughs over Israel. *Int. J. Climatol*. Vol. 25, pp. 1997-2015, 2005

Ziv, B, U. Dayan and D. Sharon, A mid-winter, tropical extreme flood-producing storm in southern Israel: Synoptic scale analysis, *Meteorol. Atmos. Phys* Vol. 88**,** 1-2, pp. 53-63, 2005

Atmospheric river induced heavy precipitation and flooding in the NARCCAP simulations

L. Ruby Leung and Yun Qian

Pacific Northwest National Laboratory, Richland, WA, USA; Ruby.Leung@pnl.gov

1. Introduction

The western U.S. receives precipitation predominantly during the cold season when storms approach from the Pacific Ocean. Several studies in recent years have clarified the role of atmospheric rivers (AR) in producing heavy precipitation and floods in the mountainous regions of the West. Atmospheric rivers are narrow bands of enhanced water vapor associated with the warm sector of extratropical cyclones over the Pacific and Atlantic oceans (Zhu and Newell 1998; Ralph et al. 2004]. Because of the strong winds and neutral stability, atmospheric rivers often lead to heavy precipitation due to large orographic enhancement during landfall on the U.S. west coast. This study aims to investigate how global warming may affect the frequency and water vapor fluxes of atmospheric rivers and the potential impacts on heavy precipitation and flooding in the western U.S.

2. Numerical Simulations

As part of the North American Regional Climate Change Assessment Program (NARCCAP), the Weather Research and Forecasting (WRF) model (Skamarock et al. 2005) has been used to simulate the regional climate of North America. In this study, we first analyzed the simulation driven by the NCEP/DOE global reanalysis for 1980-1999. We used the standard NARCCAP domain that covers North America and the adjacent oceans at 50 km grid resolution. A simple nudging scheme was used to blend the lateral boundary conditions from the global reanalysis with the WRF simulation in a 10-grid point wide buffer zone, with nudging coefficients following a linear-exponential function. Several AR events in this simulation have been compared to elucidate atmospheric and hydrologic ingredients that lead to heavy precipitation and flooding in the western U.S.

A second set of simulations, in which WRF was driven by the current (1970-2000) and future (2040-2070) climate simulated by the Community Climate System Model (CCSM), are being analyzed to investigate the potential impacts of climate change on AR characteristics and the resulting heavy precipitation and flooding in the mountainous regions.

3. Comparison of Two AR Events

Atmospheric rivers have large impacts on heavy precipitation and flooding along the west coasts where the complex terrains effectively extract the low-level moisture from the ARs. To examine the hydrologic impacts of AR, we selected two specific AR events, the 1986 President Day (PD) event and the 1997 New Year Day (ND) event, to contrast the precipitation and flooding conditions. Our analysis highlights the role of both atmospheric and land surface conditions in flooding associated with AR. Atmospheric stability plays a role in determining the spatial distribution of precipitation of the 1986 PD and 1997 ND events, as atmospheric stability can modify the orographic precipitation signature through changes in low level flow over terrain. This study suggests that the Froude number, defined by atmospheric stability and low level wind speed, can be a useful parameter for predicting or diagnosing orographic precipitation pattern. This may also be true for heavy precipitation such as those associated with AR, as even small deviations from moist neutral stability can lead to important differences in both precipitation amounts and spatial distributions.

For precipitation to generate floods, our results underscore the important role of antecedent soil moisture, as well as precipitation phase (or snow level), which depends on temperature, and possibly melting of existing snowpack due to rain-on-snow. The 1997 ND event was found to produce much larger flooding than the 1986 PD event because the former was characterized by high antecedent soil moisture, warmer temperature, which produces a higher ratio of rainfall to snowfall, and larger existing snowpack, which may increase runoff through rain on snow. For a climate simulation to realistically characterize extreme precipitation and flood in the western U.S., the model must be able to simulate AR and its atmospheric structures, as well as the land surface conditions. The latter requires realistic simulation of both temporal and spatial variability of precipitation.

4. Potential Changes of AR in the Future Climate

Analysis is being performed to compare the AR characteristics simulated by CCSM for the current and future conditions. Preliminary results suggest a small increase in AR frequency, particularly AR that makes landfall in the Pacific Northwest, in the future (2040-2070) compared to the current (1970-2000) conditions. In addition, the ARs in the future are associated with more water vapor content, which is consistent with the warmer temperature that can hold more moisture. An increase in AR frequency and water vapor flux suggests that heavy precipitation and flooding may increase in the future climate. Analysis is being performed using the WRF downscaled climate change scenarios to examine how AR, the associated precipitation, and land surface conditions may be affected by climate change to alter extreme precipitation and flooding in the western U.S.

References

Ralph, F.M., P.J. Neiman, and G.A. Wick (2004), Satellite and CALJET aircraft observations of atmospheric rivers over the eastern North-Pacific Ocean during the winter of 1997/98, *Mon. Wea. Rev.*, *132*, 1721-1745.

Skamarock, W.C., J.B. Klemp, J. Dudhia, D.O. Gill, D.M. Barker, W. Wang, and J.G. Powers (2005), *A Description of the Advanced Research WRF Version 2*. NCAR Technical Note NCAR/TN-468+STR, 88pp.

Zhu, Y., and R.E. Newell (1998), A proposed algorithm for moisture fluxes from atmospheric rivers, *Mon. Wea. Rev.*, *126*, 725-735.

Intra-seasonal evolution of the West African monsoon: Results from multiple RCM simulations

Neil MacKellar, Philippe Lucas-Picher, Jens Christensen and Ole Christensen

Danish Climate Centre, Danish Meteorological Institute, Copenhagen, Denmark, ncm@dmi.dk

1. Introduction

The West African monsoon (WAM) is characterized by three distinct phases (*Le Barbé et al.,* 2002, *Gallée et al.,* 2004). The primary phase occurs between March and June, when rainfall begins along the Guinea Coast and extends progressively northward. The second phase occurs over the Sahelian region between July and September and is not characterized by a smooth transition from the primary phase, but rather an abrupt northward shift in the rainband. The third phase, however, is a gradual southward movement of the rainfall core between September and November. The timing of these three phases are critical to the population of the region, given a heavy reliance on rain-fed agriculture. When applying a dynamical model over this domain for the purpose of seasonal forecasting or projecting long-term climate changes, due consideration should therefore be given to the model's skill in replicating the intra-seasonal phases of the WAM.

2. Aim

The purpose of this study is to perform a quantitative evaluation of the skill of multiple regional climate models (RCMs) in simulating the intra-seasonal evolution of WAM rainfall. Emphasis is placed on the models' ability to replicate the timing of rainfall onset and cessation for the three phases of the monsoon cycle.

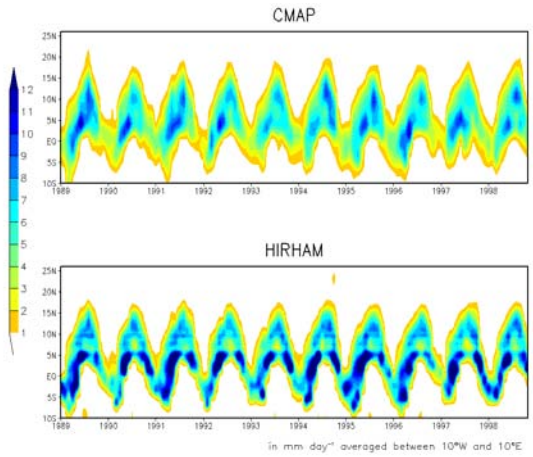

Figure 1: Hovmöller plot showing temporal evolution of rainfall over West Africa represented by (top) the CMAP analysis and (bottom) the HIRHAM RCM.

3. Data and method

The RCM simulations to be used for this analysis are the results of coordinated experiments currently being undertaken by multiple institutions as part of the ENSEMBLES project. Within ENSEMBLES, 10 institutions are conducting RCM simulations in collaboration with the African Monsoon Multidisciplinary Analyses (AMMA) project. All simulations share a common domain covering the West African region at a 50 km horizontal resolution. Boundary conditions for a set of validation runs covering the period 1989-2007 are provided by the ERA-Interim reanalysis. Further experiments using boundary conditions from selected general circulation model simulations are also being conducted for the period 1990-2050 to provide climate change scenarios. The output of these simulations will provide an unprecedented resource for inter-model comparison over West Africa. The present study will contribute to such a comparison by deriving appropriate measures of monsoon onset and cessation and using these to identify relative strengths and weaknesses of the RCMs.

4. Preliminary results

An initial evaluation of the HIRHAM RCM shows promising results. The spatial distribution of mean summer rainfall over West Africa is well replicated. The positions and magnitudes of local maxima, as well as dominant spatial gradients are simulated with remarkable accuracy. Temporal progression of the monsoon is also very well simulated (Figure 1). Meridional positioning of the rainband core appears realistic, but rainfall magnitude is possibly too high. An important feature of the HIRHAM simulation is that the second phase of the WAM cycle is correctly simulated as separate from the primary phase. More detailed analysis is ongoing and a quantitative inter-model comparison will reveal valuable information about the performance of the RCMs.

References

Gallée, H., Moufouma-Okia, W., Bechtold, P., Brasseur, O., Dupays, I., Marbaix, P., Messager, C., Ramel, R., Lebel, T., A high-resolution simulation of a West African rainy season using a regional climate model, *Journal of Geophysical Research*, Vol. 109, D05108, 2004.

Le Barbé, L., Lebel, T., Tapsoba, D, Rainfall variability in West Africa during the years 1950-90, *Journal of Climate*, Vol. 15, pp. 187-202, 2002.

CLARIS project: Towards climate downscaling in South America using RCA3

Claudio G. Menéndez (1, 2), Anna Sörensson (1), Patrick Samuelsson (3), Ulrika Willén (3), Ulf Hansson (3), Manuel de Castro (4), Jean-Philippe Boulanger (5)

1. Centro de Investigaciones del Mar y la Atmósfera, CONICET-UBA, Buenos Aires, Argentina, menendez@cima.fcen.uba.ar
2. Departamento de Ciencias de la Atmósfera y los Océanos, FCEN, Universidad de Buenos Aires, Argentina
3. Rossby Centre, SMHI, Norrköping, Sweden
4. Facultad de Ciencias del Medio Ambiente, Universidad de Castilla-La Mancha, Toledo, Spain
5. Laboratoire d'Océanographie et du Climat, UMR CNRS/IRD/UPMC, Paris, France

1. Introduction

This paper documents coordinated work carried out with the Rossby Centre regional atmospheric climate model (RCA3, Kjellström et al., 2005) within the work package on downscaling in the sub-tropical and mid-latitude South America of the European Union project 'A Europe-South America Network for Climate Change Assessment and Impact Studies' (CLARIS, http://www.claris-eu.org).

The goal of this 3-year interdisciplinary project was to build an integrated European-South American network dedicated to promote common research strategies to observe and predict climate changes and their consequent socio-economic impacts taking into account the climate and societal peculiarities of South America. CLARIS was built on experience obtained through other European Projects such as e.g. PRUDENCE, MICE and ENSEMBLES and was, in a more modest way, a counterpart of these projects in South America. Details on the project and its main results are summarized in Boulanger et al. (2009).

The work package on downscaling has promoted the co-ordinated participation of European and South American research teams in the use and development of regional dynamical models and statistical downscaling techniques. In particular, a collaboration between Rossby Centre (Sweden) and the Centro de Investigaciones del Mar y la Atmósfera (Argentina) was established with the purpose of pursuing climate research in South America using RCA3.

Concerning dynamical downscaling activities within CLARIS, two multi-RCM ensemble downscaling were carried-out: (i) Case studies of months with observed extreme precipitation in south-eastern South America (hereafter EXP1), and (ii) Multiyear simulations of the recent present climate (EXP2). Models were run at horizontal spatial scales of ~50 km and were driven by reanalysis data ERA-40. In addition, regional climate change scenarios were generated during the last part of the project (e.g. Nuñez et al., 2008; Sörensson et al., 2009a).

For details on models participating in CLARIS downscaling activities the reader is referred to Boulanger et al. (2009) and Menéndez et al. (2009). More detailed information on RCA3 setup for South America can be found in Sörensson et al. (2009b).

The first part of this study (section 2) briefly evaluates the ability of models forced by analyzed boundary conditions (i.e. quasi-observed) to simulate case studies of intense precipitation in the monthly time-scale near the Rio de la Plata (EXP1) and a 10 year period (EXP2). The analysis is focused on the comparison between RCA3, CLARIS ensembles and observations. Simulations were evaluated against high-resolution data compiled by the Climatic Research Unit (CRU) (New et al., 2000).

In the second part (section 3) a regional climate change scenario developed for the CLARIS project is presented. RCA3 is nested into a coupled global model to study the effects of twenty-first-century climate change over South America. Three 20-year time-slice simulations were performed for the periods 1980-1999 (using reanalysis and global model driving fields) and 2080-2099. We assess the response of temperature and precipitation both in terms of seasonal means and changes in distributions for daily and monthly-to-annual time-scales.

2. Ensemble RCM experiments within CLARIS

The CLARIS ensemble for EXP1 consists of simulations performed with five RCMs (MM5, PROMES, RCA3, REMO and WRF) and one stretched-grid global model (LMDZ). The domain of analysis is restricted to southern South America where CLARIS is exploring models' behaviour and sources of uncertainty in more detail. For a description of the main results of the ensemble of model simulations over South Eastern South America (southern Brazil, Uruguay, north-eastern Argentina), including a comparison with station data and with results from a statistical downscaling method, we refer the reader to Menéndez et al. (2009).

The CLARIS ensemble for EXP2 consists of regional simulations performed with four models (LMDZ, PROMES, RCA3 and REMO) for the period 1991-2000. Models' domains are somewhat different from model to model but include most of South America (the domain of analysis covers from 50S to the equator and 85W to 35W). The CLARIS ensemble is able to reproduce the basic large-scale characteristics of the observed precipitation, such as the migration of rainfall associated with the South American monsoon system and the precipitation maximum associated with the South Atlantic Convergence Zone. The relatively good performance of the multi-model ensemble average compared to any one individual model, already found in previous studies with global models and with RCMs for other regions, is true in this regional study over South America as well. Nevertheless, this results from the cancellation of offsetting errors in the individual models.

Models have difficulties in capturing accurate mean precipitation amounts over the Amazon and La Plata basins (the two main hydrological basins of the region).

RCA3 exhibits a reasonably good agreement with observations, but underestimates the annual mean rainfall of south-eastern South America (wintertime is too dry in this model) and overestimates precipitation in parts of western and southern Amazonia and along the Andes. These biases are often also found in other global and

regional models (Christensen et al., 2007). However, it should be mentioned that as South America is a data-sparse region, the actual model skill is masked by existing uncertainties in the observational-based datasets used to evaluate models.
A collaborative research for studying the regional climate with more detail as simulated by this CLARIS ensemble is in progress.

3. Regional climate change experiment

In this section we examine a regional climate change scenario carried out with RCA3. The model has a continental-scale domain and is forced, for present climate (1980-1999, 20C3M scenario, simulation hereafter called RCA20) and future climate (2080-2099, IPCC SRES A1B scenario, hereafter RCA21), with lateral boundary conditions and SSTs updated every six hours from a coupled global model, ECHAM5/MPI-OM (Jungclaus et al., 2006). An additional 20-year experiment, where RCA3 is forced by ERA40 reanalysis data (Uppala et al., 2005, hereafter RCAERA), aids in the identification of the sources of the biases for the present climate.
RCA3 does inherit certain large-scaleerrors from the driving coupled model, in particular concerning the position of the convergence zones in the Atlantic Ocean. As a consequence, RCA20 presents spurious large rainfall and too cold surface temperature over northeastern Brazil. In other regions such as Southern Amazonia, the positive large precipitation bias in RCAERA is attenuated in the global model driven simulation. But in general, the geographical pattern of precipitation is more correct in the reanalysis driven simulation, except for the austral spring season (SON) when both simulations show a reasonable pattern, and RCA20 actually is closer to the observed precipitation intensity.
The seasonal mean surface air temperature response to the A1B scenario was found to be largest in the Amazon region, especially during SON. The seasonal mean precipitation response is largest during the monsoon seasons (SON and DJF). However, when assessing the response, it should be kept in mind that the present day biases are larger in magnitude than the model's response to large-scale changes in circulation and SSTs for future climate. In SON the precipitation response is negative, suggesting a longer dry season and a delayed onset of the monsoon circulation in austral spring while in the mature monsoon phase (DJF) the response is positive in large areas of Western and Northern Amazonia.
Changes in daily temperature are consistent with less cold temperature extremes and more warm temperature extremes throughout the continent. The distribution of precipitation on different intensity classes shows a tendency toward an increase in the number of dry days and a decrease in the number of precipitation events in many regions during the monsoon onset (SON). During the mature monsoon (DJF) the amount of dry days decreases and the strong and heavy precipitation events increases over most of the continent. The Southern Amazonia and Southern Andes regions show an increase of dry days for all seasons.

References

Boulanger J.P., G. Brasseur, A. F. Carril, M. Castro, N. Degallier, C. Ereño, J. Marengo, H. Le Treut, C. Menéndez, M. Nuñez, O. Penalba, A. Rolla, M. Rusticucci, R. Terra, The European CLARIS Project: A Europe-South America Network for Climate Change Assessment and Impact Studies. *Climatic Change*, in press, 2009

Christensen, J.H. et al., Regional Climate Projections. In: Climate Change 2007: The Physical Science Basis. Contribution of Working Group I to the Fourth Assessment Report of the Intergovernmental Panel on Climate Change [Solomon, S., D. Qin, M. Manning, Z. Chen, M. Marquis, K.B. Averyt, M. Tignor and H.L. Miller (eds.)]. Cambridge University Press, Cambridge, United Kingdom and New York, NY, USA, 2007

Jungclaus J. H., N. Keenlyside, M. Botzet, H. Haak, J.-J. Luo, M. Latif, J. Marotzke, U. Mikolajewicz, and E. Roeckner, Ocean Circulation and Tropical Variability in the Coupled Model ECHAM5/MPI-OM. *J. Clim*., 19, 3952–3972, 2006

Kjellström E., L. Bärring, S. Gollvik, U. Hansson, C. Jones, P. Samuelsson, M. Rummukainen, A. Ullerstig, U. Willén, K. Wyser, A 140-year simulation of European climate with the new version of the Rossby Centre regional atmospheric climate model (RCA3). *Reports Meteorology and Climatology* No. 108, SMHI, SE-60176 Norrköping, Sweden, 54pp, 2005

Menéndez C.G., M. de Castro, J.P. Boulanger, A. D'Onofrio, E. Sanchez, A. A. Sörensson, J. Blazquez, A. Elizalde, U. Hansson, H. Le Treut, Z. X. Li , M. N. Núñez, S. Pfeiffer, N. Pessacg, M. Rojas, P. Samuelsson, S. A. Solman, C. Teichmann, Downscaling extreme month-long anomalies in southern South America. *Climatic Change*, in press, 2009

New M, Hulme M, Jones P Representing twentieth-century space time climate variability. Part II: Development of 1901-1996 monthly grids of terrestrial surface climate. *J. Clim* 13, 2217-2238, 2000

Nuñez M.N., S.A. Solman, M.F. Cabré, Regional climate change experiments over southern South America. II: Climate change scenarios in the late twenty-first century. *Clim. Dyn*., DOI 10.1007/s00382-008-0449-8, 2008

Sörensson A.A., R. Ruscica, C.G. Menéndez, P. Alexander, U. Hansson, P. Samuelsson, U. Willen, South America's present and future climate as simulated by Rossby Centre Regional Atmospheric Model. Extended abstracts of the *9th International Conference on Southern Hemisphere Meteorology and Oceanography*. American Meteorological Society. Melbourne, Australia, 9 to 13 February 2009 (a)

Sörensson A.A., C.G. Menéndez, P. Samuelsson, U. Willén, U. Hansson, Soil-precipitation feedbacks during the South American Monsoon as simulated by a regional climate model. *Climatic Change*, in press, 2009 (b)

Uppala, S. M., et al., The ERA-40 re-analysis. *Quart. J. R. Meteorol. Soc.,* 131, 2961-3012, 2005

Influence of soil moisture initialization on regional climate model simulations of the West African monsoon

Wilfran Moufouma-Okia and Dave Rowell

Met Office Hadley Centre, Exeter, UK

The Met Office Hadley Centre regional climate model HadRM3P is used to investigate the relative impact of initial soil moisture and lateral boundary conditions on simulations of the West African Monsoon. Soil moisture data that are in balance with our particular model are generated using a 10-year (1997-2007) simulation of HadRM3P nested within the NCEP-R2 reanalyses. Three sets of experiments are then performed for six April-October seasons (2000 and 2003-2007) to assess the sensitivity to different sources of initial soil moisture data and lateral boundary data. The results show that the main impact of the initial soil moisture anomalies on precipitation is to generate random intraseasonal, interannual and spatial variations. In comparison, the influence of the lateral boundary conditions dominates both in terms of magnitude and spatial coherency.

1. Objectives

The objective of the present study is to improve our understanding of the influence of initial SM and lateral boundary conditions (LBCs) on Regional Climate Model (RCM) simulations of the West African Monsoon (WAM) climate in the framework of the West African Monsoon Modeling and Evaluation initiative (WAMME, Xue et al, 2008). For this, we performed four sets of experiment using the Hadley Centre RCM to assess the relative sensitivity of the wet season evolution over West Africa to SM initialization and LBC specification. In addition to the advantage of a higher resolution than the GCMs, the RCM can isolate the regional scale impact of initial SM conditions.

2. Model and experimental design

The RCM used here is the HadRM3P which is a high resolution limited area hydrostatic grid-point model, locatable over any part of the globe, and based on the atmospheric component of the HadCM3 coupled atmosphere-ocean GCM (Pope et al., 2000) with some modifications to the model physics. There are 19 vertical levels and the latitude-longitude grid is rotated so that the equator lies inside the region of interest, in order to obtain a quasi-uniform grid box area throughout the region of interest. The horizontal resolution is 0.44ºx0.44º, which roughly corresponds to 50km at the equator of the rotated grid, and the model timestep is 5 minutes.

HadRM3P was first integrated continuously for 10 years (1997-2007) with the quasi-observed LBCs from the National Centers for Environmental Prediction and Department of Energy (DOE) Atmospheric Model Intercomparison Project Reanalysis II (NCEP-R2, Kanamitsu et al., 2002). The aim of this long-term integration, denoted NCEP_RM3PL, is to produce initial SM conditions that are fully consistent with the RCM formulation, and therefore capable of providing more appropriate estimates of initial SM moisture conditions for use in our model.

Three further sets of 7-month long sensitivity simulations, on which our analysis is based, were conducted using HadRM3P for the following six years, which have different climatic characteristics across most areas of the Sahel and portions of the Guinea coast region: the WAMME years (2000, 2003, 2004, and 2005; Xue et al. 2009), 2006 and 2007. Each individual simulation runs from April 1 to November 31, with the month of April considered as a spin-up period, so that only data from May to October (MJJASO) are used for the analysis.

The first set of sensitivity simulations, referred to as NCEP_RM3P, is the control experiment and consists of HadRM3P seasonal integrations forced by the 6-hourly LBCs from NCEP-R2 dataset and initial SM conditions from the continuous 10-yr NCEP_RM3PL simulation.

The second set of simulations, referred to as NCEP_ERA, is identical to the control, except that it uses initial SM conditions from the 40-year ECMWF Reanalysis project (ERA-40, Simmons and Gibson, 2000). This model configuration is similar to the standard WAMME experimental design (Druyan et al., 2009); except that here ERA-40 initial SM conditions are used instead of NCEP-R2 initial SM conditions. The main purpose of the NCEP_ERA experiment is to investigate the impact of early spring anomalous SM conditions on the subsequent monsoon precipitation over West Africa.

The third set of simulations, referred to as C20C_RM3P, is identical to the control, except that it uses LBCs from the Hadley Centre global atmospheric GCM (HadAM3, Pope et al., 2000; Good et al., 2007), which itself was forced by observed SSTs (see below) and integrated from 1949 to 2007. The objective of this RCM experiment is to investigate the impact of using a different LBC specification.

3. Results

The analysis of the response to early spring initial SM anomalies reveals many distinct features. Over the Soudan-Sahel and East-Soudan-Sahel, the initial SM anomalies persist for several months after the start of the simulation, although with gradually decaying magnitude. This then affects evapotranspiration, but in the experiments discussed here, is not of sufficient magnitude to have a systematic impact on precipitation. Rather, it appears that these initial SM perturbations generate only random internal variations that have considerable intraseasonal, interannual and spatial variability. Over the Guinea coast region, evapotranspiration is not limited by SM availability, and again the only impact of the initial SM anomalies on precipitation is to generate chaotic variability on a range of time and space scales. In comparison, the impact of of LBCs on the RCM simulations is substantially larger, though perhaps not surprisingly also shows some systematic impact of the slightly different climatology of the driving data.

References

Druyan L, Feng J, Cook KH, Xue Y, Fulakeza M, Hagos SM, Konare A, Moufouma-Okia W, Rowell DP , Vizy EK (2009) The WAMME regional model intercomparison study. Submitted to Climate. Dynamics.

Good P, Lowe JA Collins M, Moufouma-Okia W (2008) An objective tropical Atlantic sea surface temperature gradient index for studies of south Amazon dry-season climate variability and change. Phil. Trans. R. Soc. B 363, 1761-1766, DOI: 10.1098/rstb20070024.

Pope VD, Gallani ML, Rowntree PR, Stratton RA (2000) The impact of new physical parametrizations in the Hadley Centre climate model: HadAM3. Climate Dynamics 16: 123-146 doi 10.1007/s003820050009.

Simmons AJ, Gibson JK (2000) The ERA-40 project plan. ERA-40 Project Report Series 1, Shinfield Park, Reading, United Kingdom, 63pp.

Xue Y, Lau K-M, Cook K, Rowell DP, Boone A, Feng J, Konare A, Bruecher T, De Sales F, Dirmeyer P, Druyan L, Fink A, Fulakeza M, Guo Z, Hagos S, Kim K-M, Kitoh A, Kumar V, Lonergan P, Pasqui M, Poccard-Leclercq I, Mahowald N, Moufouma-Okia W, Pegion P, Sanda I, Schemm J^3, Schubert S, Sealy A, Thiaw W, Vintzileos A, Vizy E, Williams S, Wu M-L (2008) The West African Monsoon Modeling and Evaluation project (WAMME) and its First Model Intercomparison Experiment. Submitted to Bull Am Meteorol Soc.

Projection of the Changes in the Future Extremes over Japan Using a Cloud-Resolving Model (JMA-NHM) : Model Verification and First Results

Masuo Nakano, S. Kanada, M. Nakamura, S. Hayashi, T. kato, H. Sasaki, T. Uchiyama, K. Aranami, Y. Honda, K. Kurihara and A. Kitoh

Advanced Earth Science & Technology Organization (AESTO) / Meteorological Research Institute (MRI), 1-1 Nagamine, Tsukuba, Ibaraki, 305-0052, JAPAN; mnakano@mri-jma.go.jp

1. Introduction

Some extreme weather phenomena occur every year around Japan in the warm season (from June to October). For example, mesoscale convective systems around the Baiu frontal zone often bring heavy rainfall over the Japan islands. Typhoons also cause wind and flood damage. We also experience drought or extremely high temperature in the summer season. The changes in these extreme weather phenomena in the future climate are great concerns. Due to complex topography in the Japan islands, a super-high resolution model is desired to represent extreme phenomena.
The Ministry of Education, Culture, Sports, Science and Technology (MEXT) has launched a 5-year (FY2007-2011) program, called as KAKUSHIN program, to contribute to IPCC AR5. Under the framework of KAKUSHIN program, our team is conducting global climate projection using a 20 km-mesh AGCM (AGCM-20km) and regional climate projection in the vicinity of Japan using a 5 or 2 km-mesh non-hydrostatic model (JMA-NHM). This paper focused on the verification and first results of 5 km-mesh JMA-NHM (NHM-5km).

2. Model

The model utilized in this study is JMA-NHM (*Saito et al.* 2006, 2007), which is developed at Meteorological Research Institute (MRI) and Japan Meteorological Agency (JMA). The horizontal resolution of JMA-NHM is set to be 5 km (NHM-5km). The model domain is shown in Figure 1. In NHM-5km, terrain-following vertical coordinate z* is employed. The vertical grid in NHM-5km contains 50 levels with variable grid intervals of 40 m (near surface) to 886 m (model top). The model top is located at a 21.8 km height.
The Kain-Fritsch cumulus parameterization scheme and improved Mellor-Yamada level 3 turbulence scheme proposed by *Nakanishi and Niino* (2004) are utilized in NHM-5km. The spectral boundary coupling (SBC) method, developed at MRI by *Kida et al.* (1991) and implemented in the JMA-NHM by *Yasunaga et al.* (2005), is employed in NHM-5km simulations to reduce phase errors between the outer model and NHM-5km.

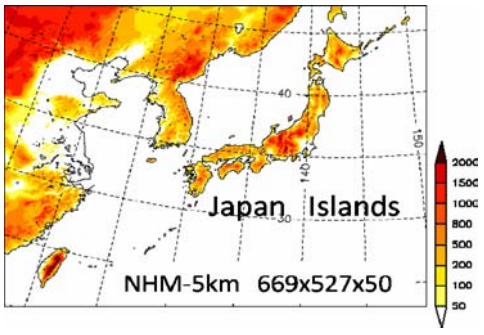

Figure 1. NHM-5km domain and topography

3. Experimental Design

Since our targets are extreme phenomena from June to Octorber, NHM-5km is initialized at 00UTC 17 May every experiment year, and the time integrations are performed until 00UTC 1 November.
First, in order to validate the accuracy of NHM-5km simulations, perfect boundary experiments are conducted using initial and boundary conditions produced from the JMA operational regional analysis data (RANAL), which have a horizontal resolution of 20 km. The experiments are performed for 5 warm seasons from 2002 to 2006.
Second, NHM-5km is nested within the simulations of AGCM-20km (TL959L60; *Mizuta et al.,* 2006) experiments in the present (1990-1999) and future (2086-2095) climates. In the AGCM-20km experiment for present climate, observed SST and sea ice distribution are utilized as bottom boundary conditions. On the other hand, for future climate experiments, averaged SST/sea ice increment and trend predicted by CMIP3 models are added to detrended observed SST and sea ice distribution. More detail can be found in *Mizuta et al.* (2008). The SRES-A1B emission scenario is used in this study.

4. Perfect boundary experiments

The results of perfect boundary experiments are verified using observed precipitation and temperature data by Automated Meteorological Data Acquisition System (AMeDAS) of the JMA. The AMeDAS has about 1300 rain gauges over Japan (horizontal resolution of approximately 17 km) and about 850 stations for temperature, wind and sun shine duration observation over the Japan islands (horizontal resolution of approximately 21 km).
The NHM-5km results show a good agreement with observed monthly rainfall amount (e.g., Fig. 2). Appearance frequency of simulated daily precipitation amount exceeding 100 mm is slightly overestimated. Simulated monthly mean temperature has warm bias of 1 K. The simulated number of maximum consecutive dry days by NHM-5km also agrees with the observed one.
Fifty nine typhoons come into NHM-5km domain during 2002-2006. Track of typhoons and their accompanying precipitation distribution and amount observed in Japan are also simulated well.

5. Present Climate and Future projection experiments

The NHM-5km results are compared with 1990s observed rainfall and temperature data. Less monthly precipitation amount in June (-22%) and more precipitation amount in July (+20%) are simulated by NHM-5km. These gaps are mainly brought from the poor reproducibility of the Baiu front in the AGCM-20km. Less precipitation amount is also simulated in September (-33%). This gap is mainly brought from the underestimation of number of typhoon

approach to Japan; approximately half of typhoons approach to Japan in AGCM-20km results.
Although the reproducibility of Baiu and typhoons is poor in AGCM-20km, we can discuss changes in the climatological property of rainfall and temperature in the future climate. In future climate experiments, appearance frequency of daily precipitation amount exceeding 100 mm, simulated by NHM-5km, increases more than 20%. The number of maximum consecutive dry days increases in most regions of Japan (Fig. 3). Several extremely hot days (maximum temperature is greater than 35 degrees centigrade) become to appear in some plain regions in future September.

6. Future plan

From 2009, new series of experiments are planed using improved AGCM-20km and NHM-5km. In new AGCM-20km, new cumulus convection scheme will be implemented to improve the reproducibility of the Baiu front and typhoons in Asia. In new NHM-5km, simple biosphere model (SiB) will be implemented to improve the accuracy of temperature projection. In addition, Kain-Fritsch scheme will be improved to reduce artificial precipitation pattern. The integrations in 25 warm seasons will be performed for present (1979-2003), near-future (2015-2039) and future (2075-2099) climates

.

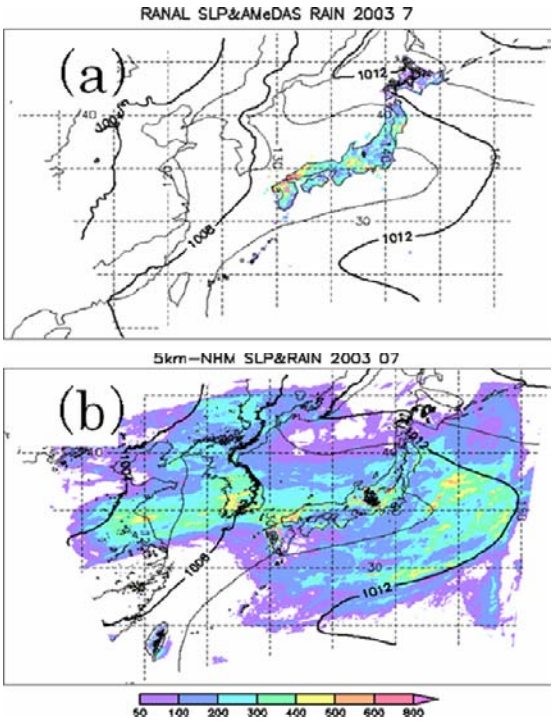

Figure 2. (a) Observed and (b) simulated monthly mean sea level pressure and precipitation in July 2003.

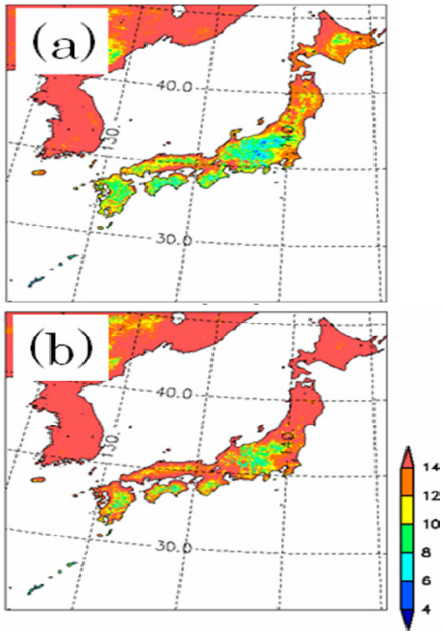

Figure 3. Maximum consecutive dry days in JJA in the (a) present and (b) future climates.

Acknowledgements

This work was conducted under the framework of the KAKUSHIN Program of the Ministry of Education, Culture, Sports, Science, and Technology (MEXT). The calculations were performed on the Earth Simulator.

References

Kida, H., T. Koide, H. Sasaki and M. Chiba, A New Approach fo Coupling a Limited Area Model to a GCM for Regional Climate Simulations, *J. Meteor. Soc. Japan*, Vol. 69, No. 6, pp. 723-728, 1991

Mizuta, R., Y. Adachi, S. Yukimoto and S. Kusunoki, Estimation of the Future Distribution of Sea Surface Temperature and Sea Ice Using the CMIP3 Multi-model Ensamble Mean, *Tech. Rep. MRI*, Vol. 56, pp. 1-28, 2008

Nakanishi, M., and H. Niino, An Improved Mellor–Yamada Level-3 Model with Condensation Physics: Its Design and Verification, *Boundary-Layer Meteor.*, Vol. 112, No. 1, pp. 1-31, 2004

Saito, K., T. Fujita, Y. Yamada, J. Ishida, Y. Kumagai, K. Aranami, S. Ohmori, R. Nagasawa, S. Kumagai, C. Muroi, T. Kato, H. Eito and Y. Yamazaki, The Operational JMA Nonhydrostatic Model, *Mon. Wea. Rev.*, Vol. 134, No. 4, pp. 1266-1298, 2006

Saito, K., J. Ishida, K. Aranami, T. Hara, T. Segawa, M. Narita and Y. Honda, Nonhydrostatic Atmospheric Models and Operational Development at JMA, *J. Meteor. Soc. Japan*, Vol. 85B, pp. 271-304, 2007

Yasunaga, K., H. Sasaki, Y. Wakazuki, T. Kato, C. Muroi, A. Hashimoto, S. Kanada, K. Kurihara, M. Yoshizaki and Y. Sato, Performance of Long-Term Integrations of the Japan Meteorological Agency Nonhydrostatic Model Using the Spectral Boundary Coupling Method, *Wea. Forecasting*, Vol. 20, No. 6, pp. 1061-1072, 2005

Regional climate model studies in CEOP: The Inter-Continental Transferability Study (ICTS)

Burkhardt Rockel, Beate Geyer, William J. Gutowski Jr., C.G. Jones, Z. Kodhavala, I. Meinke, D. Paquin and A. Zadra

GKSS Research Centre Geesthacht, Germany; Burkhardt.Rockel@gkss.de

1. Introduction

Regional Climate Models (RCMs) are often developed on the basis of existing weather forecast models. These are applied to a specific domain (e.g. Europe, America) and validated for present weather situations. However, is the model also flexible enough to be able to calculate a projected future climate correctly? A few things can already be ascertained about the model's flexibility. One way to test a model's flexibility is to carry out long-term simulations for different regions of the world, taking into account as many climate zones as possible. Takle et al. [2007] provide a survey of past and present activities in this field. They include an overview of transferability studies with several other RCMs. It has to be mentioned that in these studies for specific regions (e.g. for West Africa: Vizy and Cook [2002], Paeth et al. [2005], Druyan et al. [2007]) generally a testing and adaptation process precedes the actual simuations.

In the Inter-Continental Transferability Study (ICTS; Rockel et al. [2005]), which is part of the Coordinated Energy and Water Cycle Observation Pro ject (CEOP; Koike [2004]) within the Global Energy and Water Cycle Experiment (GEWEX; http://www.gewex.org) the model setup as the same for all regions.

The two major objectives of ICTS are:

Study the transferability of regional climate models to areas of different continental scale experiments (i.e. to different climate regimes)

Apply CEOP (satellite, reference sites, global analysis and model data) and other available observational data sets to validate the energy and water cycle in regional models

Eight institutions show there interest in taking part in the ICTS exercise Four managed to perform simulations over all regions with their RCMs and delivered data. These are the RSM, CRCM, GEMLAM, CLM

Model domains and setup

Seven computation areas were defined (Fig. 1). Each of the domains corresponds to a certain Regional Hydrology Project (RHP) in GEWEX. Several aspects were considered in defining the domains. For instance the model boundaries should not cut through mountain ridges and typical features for a region should be included in the model domain. Furthermore the domain should be large enough to minimize the influence of the driving model. In addition several test simulations are performed to find the optimal domain. In order to minimize these tests the choice of the domain size is based on the experiences of other groups who already performed simulations on these domains.

Areas cover the Mackenzie GEWEX Study (MAGS), the GEWEX Americas Prediction Project (GAPP), the Large-Scale Biosphere-Atmosphere Experiment in Amazonia (LBA) and the La Plata region, the BALTEX catchment, the AMMA (African Monsoon Multidisciplinary Analysis) region, the GEWEX Asian Monsoon Experiment (GAME) region, and the MDB (Murray-Darling-Basin Water Budget Pro ject) .

A requirement in ICTS was to use the same model settings for each domain. Participants in ICTS interpolated the results of their simulations onto a common geographical grid and common domains. The rectangles in Fig. 1 show the outline of these domains.

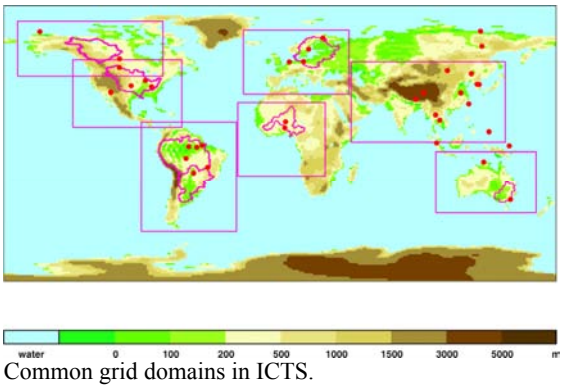

Common grid domains in ICTS.

Initial and boundary data was taken from the NCEP (National Centers for Environmental Prediction) reanalysis II data set (Kanamitsu et al. [2002]). This data is available or 00, 06, 12, and 18 UTC each day on a Gaussian grid with a horizontal resolution in the meridional of 1.875◦ .

The simulation period is July 1999 to December 2004, with the first six months considered as spin-up period.

Results of the simulations are stored in the CEOP model data archive at the WDCC (World Data Centre for Climate) in Hamburg and are freely available to the science community. Two kind of data sets were produced: daily values of gridded data on a common 0.5 degree grid and 3hourly values as MOLTS (Model Output Location Time Series) for the reference sites within CEOP (denoted by the red dots in Fig.1).

2. Data for Intercomparison

Global gridded data sets

Global analysis data sets from GCMs of eight weather centres around the world are part of the CEOP model data set and are available for the two years time period 2003/2004 through the WDCC. These data sets are used in ICTS for comparison with the regional climate models.

In addition several freely available observational gridded data sets were taken into account (e.g. GPCC4, Matsuura-Willmot, TRMM)

CEOP Reference Site data

In a coordinated activity numerous meteorological stations around the world served as reference sites within CEOP. Time series in 1hourly resolution or less of several meteorological parameters are stored in the CEOP reference data archive. Participants in ICTS uses these valuable data set e.g. for studies of the diurnal cycle and frequency distributions of quantities.

3. Results

I. Meinke, J. Roads, and M. Kanamitsu (2007) compared gridded observations of the Global Precipitation Climatology Project (GPCP) and the Global Precipitation Climatology Center (GPCC), as well as CEOP reference site precipitation observations with the RSM simulated precipitation for the first half of the CEOP Enhanced Observation Period (EOP) III (October 2002 to March 2003). After estimating the uncertainty ranges of both the model and the observations, model deficiencies were obtained for almost all model domains in terms of the amount of simulated precipitation. Although the RSM is able to accurately simulate the seasonal evolution and spatial distribution of precipitation, the RSM has an almost uniform positive bias (i.e., RSM values are greater than observed values) over almost all the domains. Most of the positive bias is associated with convection in the Intertropical Convergence Zone (ITCZ) or monsoonal convection in Southeast Asia. Predicted stratiform precipitation is also excessive over areas of elevated topography. As the control simulations used a Relaxed Arakawa-Schubert scheme (RAS), sensitivity tests with three additional convection schemes were then carried out to assess whether the simulations could be improved. The additional convection schemes were: 1) the Simplified Arakawa-Schubert scheme (SAS); 2) the Kain-Fritsch scheme (KF); and 3) the National Centers for Atmospheric Research (NCAR) Community Climate Model (CCM) scheme. The precipitation simulation was significantly improved for almost all domains when using either the KF scheme or the SAS scheme. The best simulations of ITCZ convective precipitation and Southeast Asian monsoon convective precipitation were achieved using the SAS convection scheme.

B. Rockel and B. Geyer (2008) perfomed similar comparison as I. Meinke et al. but with the regional climate model CLM. As expected, the quality of the simulations for temperate and continental climates is similar to those over Europe. Tropical climates, however, display systematic differences with a land-sea contrast. Here, precipitation is overestimated over warm oceans and underestimated over land. Another similarity in all regions is the positive bias in precipitation occurring over high and narrow mountain ranges which stand perpendicular to the main wind direction. In these cases, the CLM produces higher precipitation values than those given in the Global Precipitation Climatology Project (GPCP) data set. A comparison to three other regional climate models indicates that the findings are not CLM-specific. It also stresses the major role of the convection scheme in tropical regions. The study confirms the assumption that in order to gain optimal results, one standard model setup is not appropriate for all climate zones.

Dominique Paquin (Ouranos) has looked at a mini-ensemble of ICTS runs for the large Asia/Himalaya domain. In addition to the requested simulations over 7 domains, supplementary simulations with the CRCM over the GAME domain (Asia) were generated with the aim of estimating the internal variability of the model. This estimation is needed to assess how much of the inter-model variance observed in this domain can be explained simply by model internal variability (sensitivity to initial conditions), rather than model configuration differences.

Two different configurations were used: a) the standard configuration of the model that includes spectral nudging of the horizontal wind in the higher levels of the atmosphere, and b) a configuration without spectral nudging. Each configuration was run twice with different initial dates (twin simulations).

The internal variability responses of the two configurations are evaluated for temperature and precipitation over observation points. Time series and diurnal cycle are studied. Results show that at some locations internal variability for simulations without spectral nudging can be as large as are the differences between different model configurations or other models.

Z. Kodhavala (University of Quebec) and others compared MOLTS data of ICTS regional model results with CEOP reference sites observations with respect to frequency distributions and diurnal cycle.

B. Gutowski (Iowa State University) and others performed studies on the diurnal cycle.

References

Christensen , , J. H., T. R. Carter, M. Rummukainen, and G. Amanatidis, Evaluating the performance and utility of climate models: the PRUDENCE pro ject, Climatic Change, 81, 1–6, doi:10.1007/s10584-006-9211-6, 2007

Druyan , L., M. Fulakeza, and P. Lonergan, Spatial variability of regional model simulated June-September mean precipitation over West Africa, Geophys. Res. Lett., 34, L18709, doi:doi: 10.1029/2007GL031270, 2007

Kanamitsu , M., A. Kumar, H. M. H. Juang, J. K. Schemm, W. Q. Wang, F. L. Yang, S. Y. Hong, P. T. Peng, W. Chen, S. Moorthi, and M. Ji, NCEP dynamical seasonal forecast system 2000, Bulletin of the American Meteorological Society, 83 (7), 1019–1037, 2002.

Koike, T., The coordinated enhanced observing period – an initial step for integrated global water cycle observation, WMO Bulletin, 53, 9, 2004

Meinke, I., J. Roads, and M. Kanamitsu, Evaluation of the RSM Simulated Precipitation During CEOP, Vol. 85A, pp.145-166, 2007.

Paeth , H., K. Born, R. Podzun, and D. Jacob, Regional dynamical downscaling over West Africa: Model evaluation and comparison of wet and dry years, Meteorol. Z., 14, 349–367 2005

Rockel , B., I. Meinke, J. Roads, W. J. Gutowski, Jr., R. W. Arrit, E. S. Takle, and C. Jones, The Inter-CSE Transferability Study, CEOP Newsletter, 8, 4–5, 2005

Rockel, B. and B. Geyer, 2008: The performance of the regional climate model CLM in di□erent climate regions, based on the example of precipitation, Meteorol. Z., Volume 12, Number 4, 487-49

Takle, , E. S., K. Roads, B. Rockel, W. J. Gutowski, Jr., R. W. Arrit, I. Meinke, C. G. Jones, and A. Zadra, Transferability intercomparison: An opportunity for new insight on the global water cycle and energy budget, Bul l. Amer. Soc, 88, 375–384, 2005

Vizy E. K., and K. H. Cook (2002), Development and application of a mesoscale climate model for the tropics: Influence of sea surface temperature anomalies on the West African monsoon, J. Geophys. Res., 107(D3), 4023, doi:doi: 10.1029/2001JD000686., 2002

ENSEMBLES regional climate model simulations for Western Africa (the "AMMA" region)

Markku Rummukainen[1], Filippo Giorgi[2] and the ENSEMBLES RT3 participants

[1]SMHI, SE-601 76 Norrköping, Sweden. Markku.Rummukainen@smhi.se
[2]ICTP, Strada Costiera 11, IT- 34014 Trieste, Italy

1. Introduction

This presentation introduces and discusses common aspects and lessons learnt in a co-ordinated regional climate modeling experiment for Western Africa, performed within the EU Integrated Project ENSEMBLES, see e.g. *Hewitt and Griggs* (2004), and collaborating with the AMMA project (*Redelsperger et al.* 2006).

2. Regional climate and Africa

While the threat of climate change to Europe is real, the threat to other regions of the world is far greater both from a climate change perspective and due to vulnerability. This is especially true for Africa, as is emphasized in *Boko et al* (2007). At the same time, there is a deep lack of climate data on regional and local scales both on the recent past and on possible future conditions (cf. *Christensen et al.* 2007). Whereas information on the recent past conditions is important in characterizations of climate variability including extremes, as well as in development and evaluation of seasonal forecasting and impact models, future projections in turn are needed for weather and water related risk assessments and adaptation efforts. Estimates of regional/local climate change are therefore an important question for Africa.

3. ENSEMBLES regional climate modelling

One research theme of the EU Integrated Project ENSEMBLES is on regional climate models (RCM). In particular, there is co-ordinated experimentation with a number of European and one Canadian RCM. These simulations are made in two patches. One is for a recent past period (not least for assessing RCM performance), using global reanalysis (ERA40, *Uppala et al.* (2006)) data as boundary conditions, in runs performed for Europe, followed with climate change projections, with ENSEMBLES global model projections providing the boundary conditions, run mostly with the SRES A1B emissions. Similar set-up is now made for Western Africa.

The ENSEMBLES regional climate model study covers the so-called AMMA region. Again, there are two simulation streams. The first one covers 1989-2007, relying on ERA-Interim reanalysis data for boundary conditions (see www.ecmwf.int). As for Europe, a second stream consists of climate change projections, for the 1990-2050 period and run at 50 km resolution, relying on few GCMs for boundary conditions and again the A1B emission scenario (*Nakićenović et al.* 2000).

The RCM runs for western Africa are performed by 11 regional climate modeling groups, with almost as many RCMs (HIRHAM (in two versions), RCA3 (by two groups9, RACMO2, RegCM, HadRM, REMO, PROMES, ALADIN CY28T3, CCLM). Whenever possible, the models are run with the same (minimum) domain with perfectly overlapping grids (so as to provide for easier comparisons). As some the RCMs have different co-ordinate systems, some of the models have slightly different grids compared to the body of the contributing models.

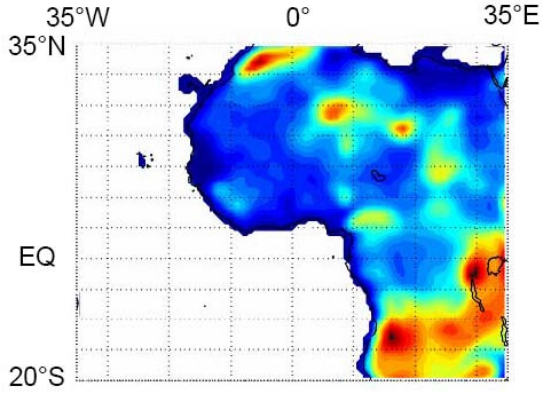

Figure 1. ENSEMBLES general Western Africa minimum RCM domain.

4. ENSEMBLES – AMMA collaboration

The RCM simulations have been set up and are evaluated in dialogue with the EU/AMMA project. Herein focus is on one hand on relevant climate aspects for significant impact applications, and on the other hand, the capture of important climate phenomena in the region. Indeed, whereas ENSEMBLES benefits from the experience of applying the RCMs in another region, thus putting them to test under a different climate regime (cf. *Rockel et al.* 2005), EU/AMMA gains a database covering the past two decades and extending to the middle 21st Century. Compared to earlier, rather sporadic regional climate model simulations for the region, this constitutes a major resource for impact research.

5. Models and data

The RCM runs have been underway in 2008-2009. Various evaluation data are collected. Especially the databases collected by AMMA are valuable for this purpose. The first analyses concerned temperature, precipitation and surface energy fluxes. Some of the comparisons were made for specific regions, such as river catchments. Continued evaluation efforts are to extend to look at the course and character of such meteorological phenomena as the timing of the monsoon season, diurnal cycles and variability on different scales.

In many respects, the RCMs exhibit skill in reproducing the regional climate, but also deficiencies can be found. These provide information for model development efforts and also for identifying data needs.

6. Next steps

The ENSEMBLES RCM efforts will include joint analyses and RCM intercomparisons for both the simulations over the recent climate period (see above) and the future scenario period. The model data will be available for other researchers' efforts, thus facilitating

new and more comprehensive climate, climate change and climate impacts for the region.
The simulations will also serve as a learning platform for future co-ordinated RCM experiments for other world regions, and not least those that so far are less extensively studied.

7. Acknowledgement

We acknowledge the ENSEMBLES project, funded by the European Commission's 6th Framework Programme through contract GOCE-CT-2003-505539.
The AMMA participants and project are acknowledged for provision of various observed and modeled data.

References

Boko, M., I. Niang, A. Nyong, C. Vogel, A. Githeko, M. Medany, B. Osman-Elasha, R. Tabo and P. Yanda, 2007: Africa. *Climate Change 2007: Impacts, Adaptation and Vulnerability.* Contribution of Working Group II to the Fourth Assessment Report of the Intergovernmental Panel on Climate Change, M.L. Parry, O.F. Canziani, J.P. Palutikof, P.J. van der Linden and C.E. Hanson, Eds., Cambridge University Press, Cambridge UK, 433-467.

Christensen, J.H., B. Hewitson, A. Busuioc, A. Chen, X. Gao, I. Held, R. Jones, R.K. Kolli, W.-T. Kwon, R. Laprise, V. Magaña Rueda, L. Mearns, C.G. Menéndez, J. Räisänen, A. Rinke, A. Sarr and P. Whetton, 2007: Regional Climate Projections. In: *Climate Change 2007: The Physical Science Basis.* Contribution of Working Group I to the Fourth Assessment Report of the Intergovernmental Panel on Climate Change [Solomon, S., D. Qin, M. Manning, Z. Chen, M. Marquis, K.B. Averyt, M. Tignor and H.L. Miller (eds.)]. Cambridge University Press, Cambridge, United Kingdom and New York, NY, USA.

Hewitt, C. and Griggs, D. Ensembles-Based Predictions of Climate Changes and Their Impacts (ENSEMBLES) *Eos,* Vol. 85, No. 52, 566, 2004.

Nakićenović, N. et al. *Emission scenarios. A Special Report of Working Group III of the Intergovernmental Panel on Climate Change.* Cambridge University Press, 599 pp, 2000.

Redelsperger, J.L., Thorncroft, C., Diedhiou, A., Lebel, T., Parker, D.J. and Polcher, J. African Monsoon Multidisciplinary Analysis (AMMA): An International Research Project and Field Campaign. *BAMS,* Vol 87, Issue 12, pp. 1739–1746, 2006.

Rockel, B., Meinke, I., Roads, J., Gutowski, W. J. Jr. Arritt, R., Takle, W E. S. and Jones, C. The Inter-CSE Transferability Study. *CEOP Newsletter* No.8, 2005.

Uppala S. M. et al. The ERA-40 Re-analysis. *Q. J. Roy. Meteorol. Soc.,* Vol 131, 2961—3012, 2006.

Assessing the performance of seasonal snow in the NARCCAP RCMs – An analyses for the Upper Colorado River Basin

Nadine Salzmann (1,2,3) and Linda Mearns (3)

(1) University of Zurich, Department of Geography, Switzerland, nadine.salzmann@geo.uzh.ch
(2) University of Fribourg, Department of Geosciences, Switzerland
(3) National Center for Atmospheric Research, Institute for the Study of Society and Environment (NCAR/ISSE), Boulder, CO, USA

1. Introduction

Seasonal snow is a major component of the hydrological cycle and thus of the climate system *Cohen and Rind* (1991). The dynamics of the snow cover depends on the atmospheric circulation, which in turn is thermodynamically influenced by the snow pack.

In mountain regions, the dynamics of the seasonal snow cover is a key factor for hydrological run off and consequent availability of water for human consumption, irrigation and power generation e.g. *Barnett et al.* (2005). Due to the proximity to the melting point, snow is particular sensitive to changes in the atmospheric conditions with significant effects on the timing and magnitude of hydrological run off.

Among the most promising tools for assessing future changes in the hydrological run off in mountain regions is Regional Climate Models (RCMs). They are able to simulate and provide climate input variables on a regional scale and for heterogeneous landscapes such as mountain topography *Leung and Qian* (2003). However, so far only a few studies analyzed the performance of mountain snow in RCMs. There are many reasons for that, including foremost the general difficulties associated with process-modeling in complex topography and the lack of ample snow observations in most mountain regions worldwide for validation purposes.

Despite these limitations, here, we aim at assessing the performance of the seasonal snow in the RCM simulations calculated for the international RCM program NARCCAP (North American Climate Change Program, *www.narccap.ucar.edu*) *Mearns et al.* (2005).

2. Study site and data

The following analyses are conducted for the region of the Upper Colorado River Basin (UCRB) in the U.S. Rocky Mountains. Here, the seasonal snow pack of the highest peaks contributes about 70 % of the Colorado River's total annual run off *Christensen et al.* (2004). Within the perimeter of the UCRB, 45 SNOTEL observation stations exist, most of them measuring Snow Water Equivalent (SWE), 2m Temperature (2mT) and precipitation (Precip), since 1981 and before. In addition to these point measurements, a second source of 'observation' is used in this study; the gridded NARR data (North American Regional Re-analyses), with a horizontal resolution of 32 km. SNOTEL and NARR are compared in the following with results from NARCCAP simulations. Only NCEP-driven NARCCAP runs are used in a first step. The comparison includes the following RCMs, listed with the respective Landsurface Scheme (LSS) used in each RCM. It is in the LSS, where the processes concerning the snow dynamics are defined.

ECPC (Experimental Climate Prediction Center) from Scripps Institution of Oceanography, La Jolla, CA, USA.
LSS: NOAH

MRCC (Modèle Régional Canadien du Climat) from Ouranos Consortium, Montreal (Quebec), Canada.
LSS: CLASS

RegCM3 (REGional Climate Model) from UC Santa Cruz, ITCP, USA.
LSS: BATS

WRF (Weather Research and Forecasting Model) from Pacific Northwest National Lab, Washington, USA.
LSS: NOAH

MM5 (Mesoscale Meteorologic Model) from Iowa State University, Iowa, USA.
LSS: NOAH

All RCMs are run with a grid spacing of 50 km and cover the UCRB by 10 grid boxes.

3. Analyses and some results

'SWE' and the two related variables '2mT' and 'Precip' were compared and analyzed in various spatial and temporal terms.

It was found that NARCCAP RCMs generally simulate higher air temperatures than NARR and particularly than SNOTEL. However, the departures are relatively constant within different elevation levels, indicating that theoretically a lapse rate correction could be applied for adjusting the NARCCAP results towards the SNOTEL measurements. Though, based on the relatively small elevation difference between the SNOTEL and NARCCAP topography, the lapse-rate factor only explains a minor part of the deviation.

Regarding precipitation the NARCCAP models are in general too dry compared to SNOTEL.
A large-scale factor that influences the climate and particularly precipitation on the Colorado Plateau is the ENSO. Major El Niño events as e.g. in 1982-83, 1992-93 and 1994-95 produce during winter exceptionally wet weather in the region. It is thus of interest, if these events are reflected in the datasets. However, no clear evidence is found in any of the datasets used here, pointing towards ENSO events.

Finally, SWE, shows significant departures between the different RCMs, and also compared to SNOTEL and NARR. While the annual cycle is captured relatively well, the amount of snow as well as the duration and the time of maximum vertical snow depth are significantly underestimated by the NARCCAP RCMs and NARR

compared to SNOTEL. The departures can partly be attributed to the too high temperatures simulated by NARCCAP RCMs compared to SNOTEL. Another reason for the partially great deviations is that SNOTEL probably in general overestimates snow cover depth. The SNOTEL stations were placed based on the goal to collect information primarily for run off forecasting purposes, and not to measure and monitor snow as a climate variable. Therefore, SNOTEL sites are mostly located in troughs, shadowed areas and generally, where the seasonal snow pack lasts a relatively long time.

In order to gain some insights into possible reasons and sources leading to the biases found, some analyses regarding the LSS were undertaken. The LSS dictates and forces the processes related to snow in a RCM. Here, there was no obvious larger similarity found between RCMs using the same LSS. In particular also NARR, which uses the same LSS (NOAH), as the RCMs WRF, MM5 and ECPC, did not show specific similarities with the respective RCMs. Therefore, it seems that the LSS's function is marginal for the final output regarding snow and that the biases found can not directly be attributed to the LSS used by the RCM.

4. Conclusion and Perspectives

It can be concluded so far that the annual snow cycle is, in general, represented relatively well by the NARCCAP simulations but underestimates the amount of snow. Quantifying this underestimation in absolute values is, however, difficult. This is because the SNOTEL measurements most probably overestimate the effective snow depth due to the primary goal of the SNOTEL network as mentioned above. Furthermore, a comparison between point measurements and gridded data is always somewhat questionable. Additionally, a detailed attribution of the biases to e.g. the LSS or the elevation differences between models and reality is finally not possible. Because of the many uncertainties associated with such analyses, it is advised and proposed to refer to such analyses as 'an assessment or evaluation of the performance of the models' rather than as 'a validation of models'.

Nevertheless such analyses are fundamental for the impacts community. It is essential that impacts modeler know about the range of uncertainty associated with RCM outputs and that they account accordingly for it in their studies.

References

Barnett, T.P., Adam, J.C., Lettenmaier, D.P., Potential impacts of a warming climate on water availability in snow-dominated regions, *Nature* 438, 303-309, 2005

Cohen, J., & Rind, D., The effect of snow cover on the climate, J. Climate, 689-706, 1991

Christensen, N.S., Wood, A.W., Voisin, N., Lettenmaier, D.P., Palmer, N., The effect of climate change on the hydrology and water resources of the Colorado River Basin. *Climate Change* 62, 337-363, 2004

Leung, L., R. & Qian, Y., The sensitivity of precipitation and snowpack simulations to model resolution via nesting in regions of complex terrain, *J. Hydrometerology* 4, 1025-1043, 2003

Mearns, L.O. et al., 2005: NARCCAP, North American Regional Climate Change Assessment Program, A multiple AOGCM and RCM climate scenario project over North America. Preprints of the American Meteorological Society 16th Conference on Climate Variations and Change. 9-13 January, 2005. Paper
16 J6.10, pp. 235-238 Washington, D.C.

Applying the Rossby Centre Regional Climate Model (RCA3.5) over the ENSEMBLES-AMMA region: Sensitivity studies and future scenarios

Patrick Samuelsson, Ulrika Willén, Erik Kjellström and Colin Jones

Rossby Centre, SMHI, SE-601 76 Norrköping, Sweden; patrick.samuelsson@smhi.se

1. Introduction

Western Africa is a region subject to decadal variability in rainfall including devastating droughts in the Sahel region during the last decades of the 20th century. Changes in Sahel precipitation may be related to the response of the African monsoon to oceanic forcing amplified by land-atmosphere interaction (*Trenberth et al.* 2007). Although AGCMs are able to simulate basic patterns of rainfall trends during the second half of the 20th century there are uncertainties related to their ability of simulating for instance interannual variability in rainfall and the exact position of the African Easterly Jet (*Christensen et al.* 2007). AOGCMs have even larger problems including biases in sea surface temperatures (SST), displacements in the intertropical convergence zone and distortions in the monsoonal climate. Possibly RCMs can be used to improve the understanding of the processes regulating the climate in this region. So far only few RCM simulations exist for this area although efforts are currently undertaken in the AMMA (*Redelsperger et al.* 2006), WAMME (*Cook and Vizy* 2006) and ENSEMBLES (*Hewitt and Griggs* 2005) projects. In this paper we present results from one RCM for this area.

2. RCA 3.5

We have used an updated version of the Rossby Centre regional climate model RCA3 (*Kjellström et al.* 2005, *Samuelsson et al.* 2006). RCA3 is developed at Rossby Centre, SMHI, and has been extensively used in a number of climate scenario studies. RCA3 is one of the RCMs in the European projects PRUDENCE (*Jacob et al.* 2007) and ENSEMBLES (*Sanchez-Gomez et al*. 2008). RCA3 includes parameterizations for radiation (*Savijärvi* 1990; *Sass et al.* 1994), turbulence (*Cuxart et al.* 2000), large-scale clouds and microphysics (*Rasch and Kristjánsson* 1998), convection (*Kain and Fritsch* 1993; *Jones and Sanchez* 2002), and land surface (*Samuelsson et al.* 2006). In the updated version RCA3.5 we have replaced the original lake model PROBE (*Ljungemyr et al*. 1996) by FLake (*Mironov* 2008) and replaced the land-surface physiographic information by ECOCLIMAP (*Masson et al.* 2003). The convection parameterisation is based on *Bechtold et al*. (2001) which is a development from the one by *Kain and Fritsch* (1993) now separating shallow and deep convection.

3. RCA3.5 over ENSEMBLES-AMMA

The RCA3.5 ENSEMBLES-AMMA domain is shown in Figure 1. The domain is set up on a regular grid resolved by 168x142 grid points covering -39 – 35°E and -23 – 39°N which corresponds to 0.4° or 50km horizontal resolution. In the vertical we have used 24 and 40 levels, respectively.

For hind-cast simulations we have used ERA INTERIM as forcing for lateral boundary conditions and for sea-surface temperature. The analyzed period cover 1990-1997 with one year spin-up time before that.

For the scenario simulation we take lateral boundary conditions and sea surface temperatures from the HadCM3 model (*Collins et al.* 2006) operating under the SRES A1B emission scenario (*Nakićenović et al.* 2000). The scenario simulation covers the period 1961-2100.

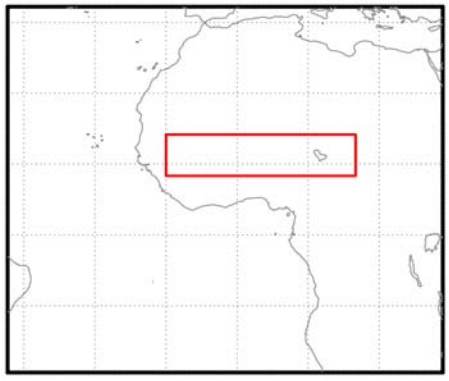

Figure 1. The RCA3.5 ENSEMBLES-AMMA domain including the Sahel region as used for area-averaging.

4. Sensitivity tests

In Figure 2 it is shown how the simulated annual cycle of precipitation depends on the number of vertical levels used. The results represent averaged values over the Sahel region as shown in Figure 1.

The improvement of the model to capture the large amount of precipitation during the rain period due to increased number of vertical levels is obvious. However, over this area, the too early on set of the rainy season gets even more pronounced.

We will present results based on some more tests including the sensitivity of the simulated African Easterly Jet and precipitation patterns on albedo and SST.

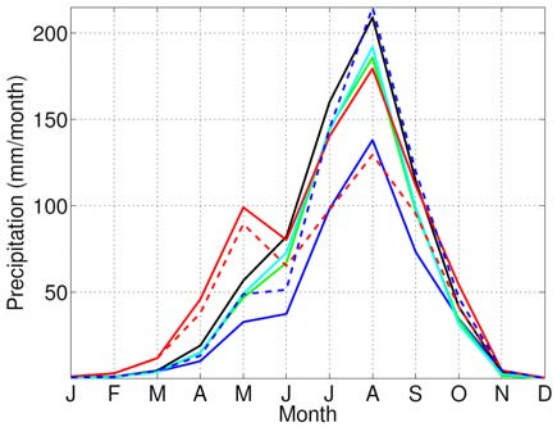

Figure 2. Annual cycle of precipitation over the step region. The lines represent: RCA3.5 40 levels (solid red), RCA3.5 24 levels (dashed red), ERA INTERIM (dashed blue), ERA40 (solid blue), CRU (green), GPCP (black) and Willmott (cyan).

5. Future climate

We will compare the simulated climate in the 20th century to observational climatologies. Focus is on evaluating the ability of the combination HadCM3-RCA3 to simulate aspects of the atmospheric circulation in the area and the associated rainfall patterns and their seasonal migration. In a next step it will be illustrated how these aspects change in a changing climate and to what degree the regional climate model alters the signal given by the global model.

6. Acknowledgements

This work is part of the ENSEMBLES project funded by the EC through contract GOCE-CT-2003-505539. The Hadley Centre is acknowledged for providing boundary data. The model simulations with RCA3 were performed on the climate computing resource Tornado funded with a grant from the Knut and Alice Wallenberg foundation.

References

Bechtold P., Bazile E., Guichard F., Mascart P. and Richard E. 2001: A mass-flux convection scheme for regional and global models. Quarterly Journal Royal Meteorological Society. 127. 869-886.

Christensen, J.H. et al., 2007: Regional Climate Projections. In: Climate Change 2007: The Physical Science Basis. Contribution of Working Group I to the Fourth Assessment Report of the Intergovernmental Panel on Climate Change [Solomon, S., D. Qin, M. Manning, Z. Chen, M. Marquis, K.B. Averyt, M. Tignor and H.L. Miller (eds.)]. Cambridge University Press, Cambridge, United Kingdom and New York, NY, USA.

Collins et al, 2006, Clim. Dyn., DOI 10.1007/s00382-006-0121-0

Cook K.-H. and E.K. Vizy, 2006: Coupled Model Simulations of the West African Monsoon System: 20th century Simulations and 21st Century Predictions. J. Climate, 19, 3681-3703.

Cuxart, J., Bougeault, Ph. and Redelsperger, J-L., 2000. A turbulences scheme allowing for mesoscale and large eddy simulations. Q. J. R. Meteorol. Soc., 126, 1-30.

Hewitt, C.D and Griggs, D.J., 2004: Ensembles-based predictions of climate changes and their impacts. Eos, 85, 566.

Jacob, D. et al., 2007. An inter-comparison of regional climate models for Europe: Design of the experiments and model performance. Climatic Change. 81, 31-52. doi:10007/s10584-006-9213-4.

Jones C.G. and Sanchez, E., 2002. The representation of shallow cumulus convection and associated cloud fields in the Rossby Centre Atmospheric Model. HIRLAM Newsletter 41, Available on request from SMHI, S-60176 Norrköping, Sweden.

Kain, J.S. and J.M. Fritsch, 1993. Convective parameterizations for Mesoscale Models: The Kain-Fritsch scheme. In: The representation of cumulus convection in numerical models, Eds: K.A. Emanuel and D.J. Raymond. AMS Monograph, 46, 246 pp.

Kjellström, E., Bärring, L., Gollvik, S., Hansson, U., Jones, C., Samuelsson, P., Rummukainen, M., Ullerstig, A., Willén U. and Wyser, K., 2005. A 140-year simulation of European climate with the new version of the Rossby Centre regional atmospheric climate model (RCA3). Reports Meteorology and Climatology 108, SMHI, SE-60176 Norrköping, Sweden, 54 pp.

Ljungemyr P., Gustafsson N. and Omstedt A., 1996. Parameterization of lake thermodynamics in a high resolution weather forecasting model. Tellus, 48A, 608–621.

Masson, V., J.L. Champeaux, F. Chauvin, C. Mériguet and R. Lacaze, 2003, A global database of land surface parameters at 1km resolution for use in meteorological and climate models. J. Climate, 16, pp 1261-1282.

Mironov D.V. 2008. Parameterization of lakes in numerical weather prediction. Description of a lake model. COSMO Technical Report, No. 11, Deutscher Wetterdienst, Offenbach am Main, Germany, 41 pp.

Nakićenović, N., Alcamo, J., Davis, G., de Vries, B., Fenhann, J., Gaffin, S., Gregory, K., Grübler, A., et al., 2000. Emission scenarios. A Special Report of Working Group III of the Intergovernmental Panel on Climate Change. Cambridge University Press, 599 pp.

Rasch, P.J. and Kristjansson, J.E., 1998. A comparison of the CCM3 model climate using diagnosed and predicted condensate parameterisations, J. Climate, 11, 1587-1614.

Redelsperger, J.L., Thorncroft, C., Diedhiou, A., Lebel, T., Parker, D.J. and J. Polcher (2006): African Monsoon Multidisciplinary Analysis (AMMA): An International Research Project and Field Campaign. Published in BAMS, Volume 87, Issue 12 (December 2006) , pp. 1739–1746.

Samuelsson, P., Gollvik, S. and Ullerstig, A. 2006. The land-surface scheme of the Rossby Centre regional atmospheric climate model (RCA3). SMHI Meteorologi No 122 . 25 pp.

Sanchez-Gomez E., Somot S. and Déqué M., 2008: Ability of an ensemble of regional climate models to reproduce weather regimes over Europe-Atlantic during the period 1961-2000, Clim. Dyn., 10.1007/s00382-008-0502-7.

Sass B.H., Rontu L., Savijärvi H., Räisänen P., 1994. HIRLAM-2 Radiation scheme: Documentation and tests. Hirlam technical report No 16., SMHI. SE-601 76 Norrköping, Sweden, 43 pp.

Savijärvi H., 1990. A fast radiation scheme for mesoscale model and short-range forecast models. J. Appl. Met., 29, 437-447.

Trenberth, K.E., P.D. Jones, P. Ambenje, R. Bojariu, D. Easterling, A. Klein Tank, D. Parker, F. Rahimzadeh, J.A. Renwick, M. Rusticucci, B. Soden and P. Zhai, 2007: Observations: Surface and Atmospheric Climate Change. In: Climate Change 2007: The Physical Science Basis. Contribution of Working Group I to the Fourth Assessment Report of the Intergovernmental Panel on Climate Change [Solomon, S., D. Qin, M. Manning, Z. Chen, M. Marquis, K.B. Averyt, M. Tignor and H.L. Miller (eds.)]. Cambridge University Press, Cambridge, United Kingdom and New York, NY, USA.

Interactions between European shelves and the Atlantic simulated with a coupled regional atmosphere-ocean-biogeochemistry model

Dmitry V. Sein, Joachim Segschneider, Uwe Mikolajewicz and Ernst Maier-Reimer

Max Planck Institute for Meteorology, Bundesstrasse 53, 20146 Hamburg, Germany; dimitry.sein@zmaw.de

1. Introduction

In the framework of NORDATLANTIK project the numerical investigations of interactions of the water masses on the European shelves with the Atlantic were carried out. A regionally coupled model consists of the regional atmosphere model REMO, the global ocean model MPI-OM and the marine biogeochemical model HAMOCC, which simulates biogeochemical tracers in the oceanic water column and in the sediment (*Mikolajewicz et al.* 2005, *Maier-Reimer et al. 2005*). The coupled domain includes Europe, the North-East Atlantic and parts of the Arctic Ocean (Fig.1).

The lateral atmospheric and the upper oceanic boundary conditions outside the coupled domain were prescribed using ERA40 reanalysis data. No momentum and heat flux corrections was applied.

2. Model simulations

For better understanding of the influence of tidal dynamics on long term ocean variability the model was run both with (run A) and without (run B) tidal forcing, derived from the full ephemeridic luni-solar tidal potential .

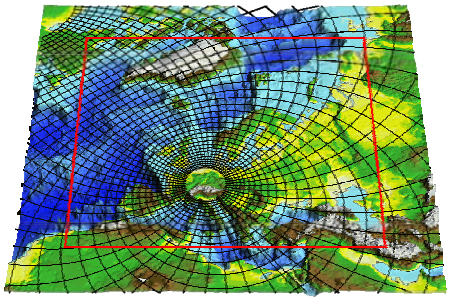

Figure 1. Coupled REMO/MPI-OM configuration. The red rectangle indicates the domain of coupling. Only every fourth line of the formally global ocean grid is shown (black line)

The "dynamical" effect of tides on the mean North Atlantic circulation leads to a small reduction of the mean current in the open ocean and an amplification along the North European shelf edge.

Tidally induced mixing leads to a reduction of North Atlantic SST. However, warming (up to 3K) occurs near the amphidromic points of the M2 and S2 tidal constituents near Iceland and in the middle of the North Atlantic (Fig.2).

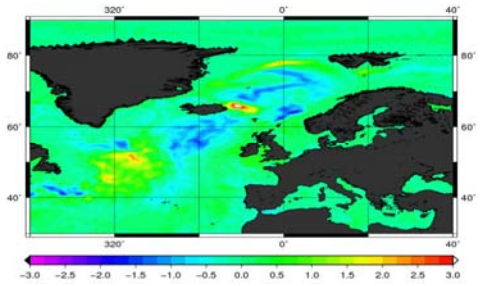

Figure 2. Tidal influence on SST. The difference in mean SST (C) between run A and B

3. Biogeochemistry

The biogeochemical model HAMOCC5 has been spun-up with anthropogenic CO2 concentrations starting in 1860 and using atmospheric forcing from the ERA40 reanalysis. For years before 1958, the forcing was repeated in several cycles beginning in 1860, so as to prevent a model drift for 1958 when the reanalyzed data become available. Therefore, physical conditions before 1958 deviate from the true state, whereas after 1958 they correspond to the true state within the usual limitations (model errors, forcing errors etc.).

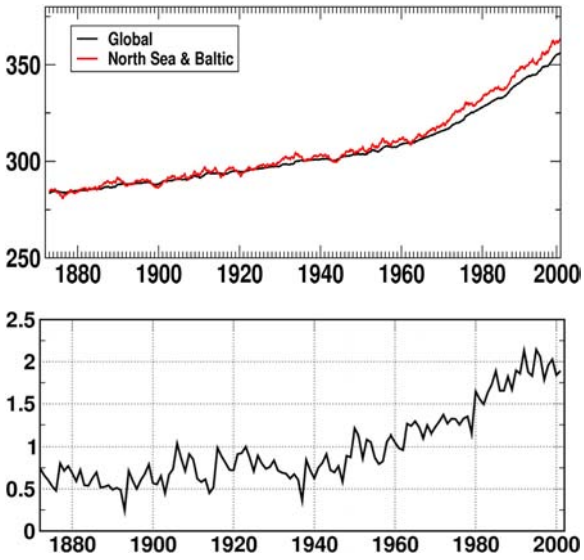

Figure 3. Time series of oceanic pCO2 (top) as global mean (black line) and for the North Sea and Baltic (red line) and oceanic uptake of CO_2 in GtC/a (bottom)

The simulated increase in oceanic pCO2 is shown in Fig. 3 as global average (black curve) and averaged over the

North and the Baltic Sea (red curve). Note the stronger than global average increase for the North Sea and the Baltic area, implying that these marginal seas may serve as a precursor for the global ocean with regard to CO2 increase.

Further features of the biogeochemical model are artificial tracers, marking tropical, polar, and northwest European shelf water masses. Tropical and polar tracers decay with a half-time constant of 30 years, the northwest European shelf tracer with a half-time constant of 3 years. These tracers were computed into equilibrium over a period of 200 years. Afterwards, the ERA forcing was used for the years 1958 to 2001. The distribution for the year 2001 is shown in Fig. 4. The figures show the northward spreading of tropical water masses with the Gulf Stream and along the Norwegian coast (upper panel), the southward spreading of the polar water masses in the north-western Atlantic (centre panel) as well as the spreading of water masses from the northwest European shelf into the deep water formation regions between Greenland and Svalbard (bottom panel)

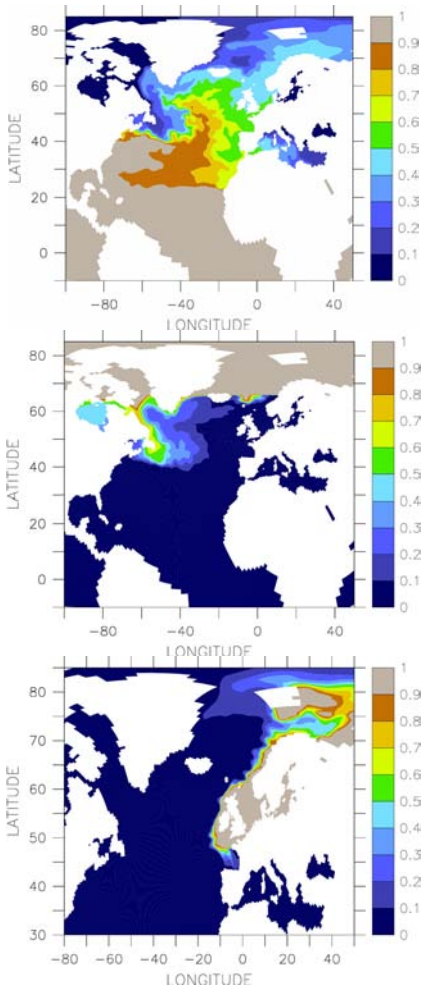

Figure 4. Concentrations of the artificial tracers in the 2001 from the model integration with ERA forcing. From top to bottom: tropical, polar, and north west European shelf water mass tracers.

One application of the artificial tracer is to determine changes in the water masses e.g. in the North Sea where recently an increase in subtropical species has been observed in the fauna. It is not clear yet, whether this is due to a local increase in temperature due to e.g. global warming or a change in inflowing water masses. The artificial tracers show a relative increase of the contribution of tropical water masses in the North Sea for the last 20 years, indicating that changing circulation patterns may be the cause.

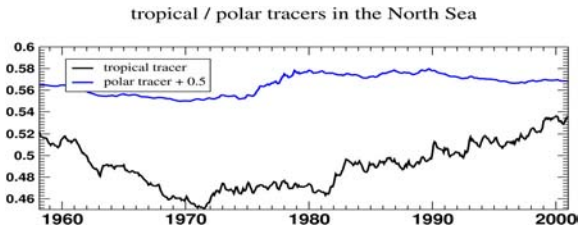

Figure 5. Time series of the concentration of artificial tracers averaged over the North Sea for a tropical (black) and a polar (blue) tracer.

4. Summary and future work

A coupled AOGCM including ocean biogeochemistry was successfully validated for the period 1958-2001. As a next step further simulations of the anthropogenic climate change are planned.

5. Acknowledgements

This work was supported by the BMBF through the NORDATLANTIK project. We thank ECMWF for supplying the reanalysis data used for model forcing and validation.

References

Maier-Reimer, E., I. Kriest, J. Segschneider and P. Wetzel: The HAMburg Ocean Carbon Cycle Model HAMOCC5.1, Technical Description, *Berichte zur Erdsystemforschung* 14/2005, 2005

Mikolajewicz.,U., D.V.Sein, D.Jacob, T.Kahl, R.Podzun, T.Semmler: Simulating Arctic sea ice variability with a coupled regional atmosphere-ocean-sea ice model, *Meteorologische Zeitschrift,* 14, No. 6, pp. 793-800, 2005

ALADIN-Climate/CZ simulation of the 21st century climate in the Czech Republic for the A1B emission scenario

Petr Skalak, Petr Stepanek and Ales Farda

Czech Hydrometeorological Institute, Na Sabatce 17, Praha 4 – Komorany, 143 06, Czech Republic, skalak@chmi.cz

1. Introduction

In the frame of the EC FP6 project CECILIA, two simulations of the future climate conditions in the Central Europe were performed by the regional climate model ALADIN-Climate/CZ under high resolution of 10 km. The simulations according to the IPCC A1B emission scenario cover 30-years time intervals in the middle (2021-2050) and end of the 21st century (2071-2100). The regional model was driven by the general circulation model (GCM) ARPEGE-Climate over the Central Europe domain shown on *Fig. 1*.
The analysis of the expected climate change is focused only on the Czech Republic that represents a part of the integration domain. There are 789 model's grid points over the Czech Republic.

2. Methodology

Before the analysis of the future climate, the model data were corrected according to validation results carried out for the period 1961-1990. For this task a new gridded dataset of station observation was created from all available data records stored in the climatological database of the Czech Hydrometeorological Institute. All input station observations were quality controlled and homogenized in daily scale and then recalculated to the ALADIN-Climate/CZ's grid of 10 km horizontal resolution while taking into account the model's elevation and distance from an individual grid point.
Gridded dataset of station observations was then compared with the past climate (1961-1990) GCM driven ALADIN-Climate/CZ simulation in each grid point. According to relationship between these two datasets, outputs of A1B scenario integrations of the future climate were corrected applying an approach of *Déqué* (2007) that is based on a variable correction using individual percentiles. After the correction, the model outputs are fully compatible with the station (measured) data.
The gridding and all data processing including the presented analysis were done by ProClimDB database software for processing of climatological datasets (*Stepanek*, 2009).

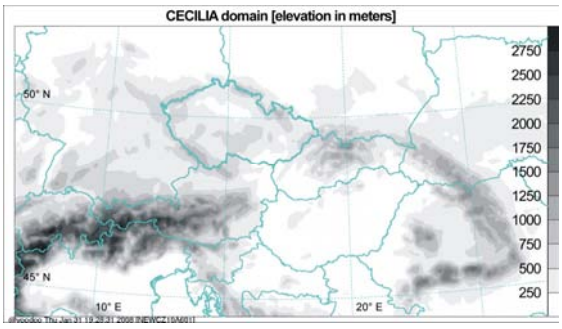

Figure 1. Orography over the Central European model's integration domain. The Czech Republic is upper left of the domain center.

3. Results

The analysis of the 21st century climate in the Czech Republic was focused on four basic meteorological elements: daily mean, maximum and minimum 2-meter temperature and precipitation. Spatial distribution of the projected changes and the temporal evolution over the periods 1961-2050 (1961-2100) for individual seasons was studied (*Fig 2*). A special emphasis was put on the investigation of the selected extreme characteristics for 2-meter temperature (minimum and maximum) and precipitation. The obtained information on the future climate was compared to both, ALADIN-Climate/CZ historic run (1961-1990) and station observations.

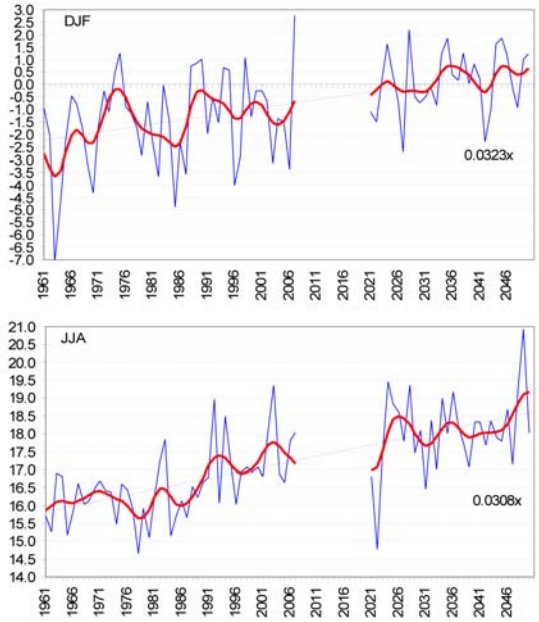

Figure 2. Fluctuations of averaged seasonal winter (top) and summer (bottom) air temperature for the Czech Republic calculated from gridded dataset of station observations (1961-2007) and corrected A1B scenario model runs (2021-2050). Smoothed by Gaussian low-pass filter for 10 years.

References

Déqué, M., Frequency of precipitation and temperature extremes over France in an anthropogenic scenario: Model results and statistical correction according to observed values, *Global Planet. Change*, 57, pp. 16-26, 2007

Stepanek, P., ProClimDB, *http://www.climahom.eu*, 2009

Overview of the research project of Multi-model ensembles and down-scaling methods for assessment of climate change impact, supported by MoE Japan

Izuru Takayabu

Meteorological Research Institute, 1-1 Nagamine Tsukuba Ibaraki 305-0052 JAPAN; takayabu@mri-jma.go.jp

1. Introduction

With a strong determination to fill in the gap between the result of climate prediction by the whole atmospheric model and the study of impact statement, we started the project S-5-3 supported by Ministry of the Environment, Japan. Now we are in the third year of it. Unfortunately we haven't made yet a specific formation of the big system that we had in mind when we applied it for permission in figure 1. However, each part of it has been making its clear formation, thanks to the effort made by each participating institution. The accomplishment report for the last two years is outlined as follows.

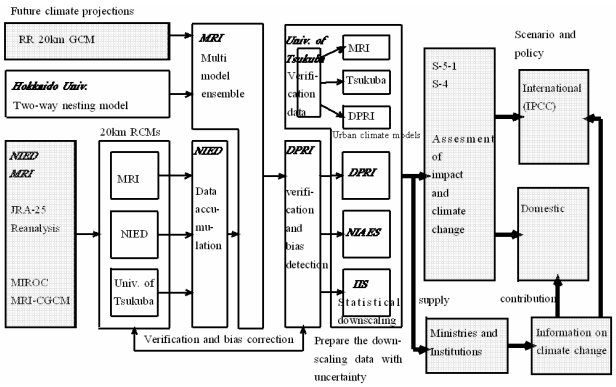

Fig.1: Summary of the project

2. To Reduce the model uncertainty

To reduce the uncertainty of the RCMs result, we integrate many 20km RCMs parallel over the field of Japan Islands (Fig. 2). Three institutions and universities (Natiolnal Institute for Earth science and Disaster prevention (NIED), University of Tsukuba and Meteorological Research Institute (MRI)) integrated their 20km resolutions regional climate models for three years (2002 – 2004), by using JRA-25 (reanalysis data) as the boundary forcing data. They are NIED-RAMS (Dairaku et al., 2009), TERC-RAMS (University of Tsukuba), MRI-NHM (Sasaki et al., 2007) and MRI RCM (Murazaki et al., 2008). With the cooperation of Tanaka (2008, personal communication), we have made advances in our studies of bias specification and model tuning, as shown in figure 3. Using the calculational result from them, Tanaka (2008, personal communication) has started to study a bias correction method of precipitation and surface air temperature, as shown in figure 4.

We also apply pseudo global warming method (PGWM) and do the integration of the WRF model. Hara et al. (2008) succeeded to simulate the snow depth pattern around Japan Islands caused by the Asian winter monsoon. Kawase et al. (2009) succeeded to simulate the Meiyu-Baiu forntal rainbands appearing at the Asian summer monsoon season with the lateral boundary forcing by the ensemble results of CMIP3 AO-GCMs.

We also have a two way nesting system. Inatsu and Kimoto (2009) have succeeded to drive their two way nesting model around the Japan Islands, and simulate the effect of its method of nesting on the northern hemisphere storm track activity.

By comparing these valuable methods of driving RCM, we try to reduce the model uncertainty.

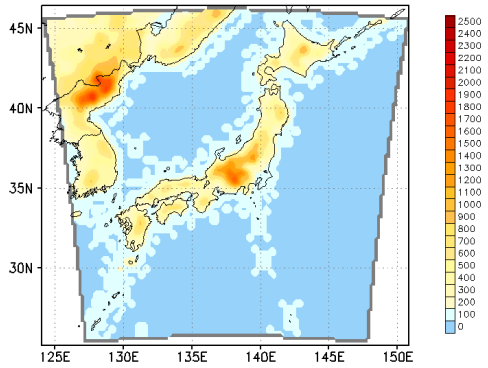

Fig.2: The requested area of calculation in this project.

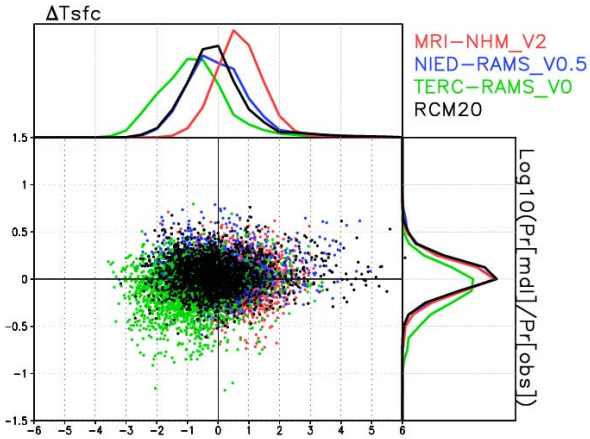

Fig.3: Monthly mean surface temperature bias vs. monthly accumulated precipitation bias. Red: NHM of MRI, blue: RAMS of NIED, green: RAMS of Tsukuba University, black: RCM of MRI. All but RCM of MRI are non-hydrostatic model. These dots are drawn every month for each prefecture in Japan. The observation data comes from the AWS network of Japan Meteorological Agency (AMeDAS). PDFs are drawn on the top and right hand side of the figure.

3. To bridge the results to the impact research

In the area of the dynamic downscaling which is no less important than the statistical downscaling, the study about the city area was developed by using urban canopy schemes (University of Tsukuba , MRI and DPRI). At MRI (Aoyagi et al., 2009), the regional climate model was put together with an urban canopy scheme and an

experiment of recreating the present climate was done. In addition to this, at University of Tsukuba (Kusaka et al., 2008), a pseudo global warming experiment was done by using the result of the MIROC-HI model as the boundary and they succeeded in showing the future increase in the temperature in the Tokyo metropolitan district as shown in figure 5.

(a)

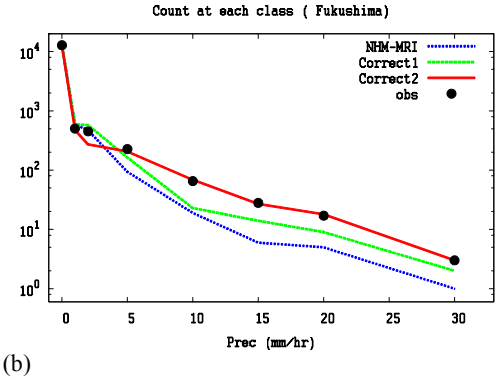

(b)

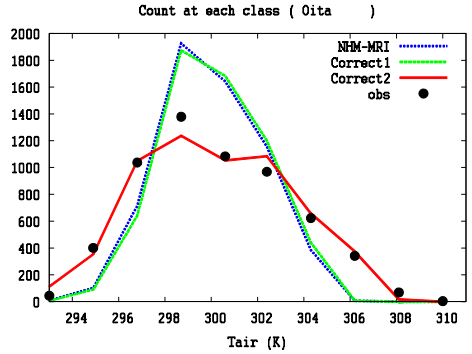

Fig. 4: Frequency histogram of the daily total precipitation (a) and dayly mean temperature (b). Black dots: AWS observation, blue line: MRI-NHM original value, green line: Corrected the total value, red: corrected also the frequency. The value of one prefecture in Japan is displayed (Tanaka, 2009, personal communication).

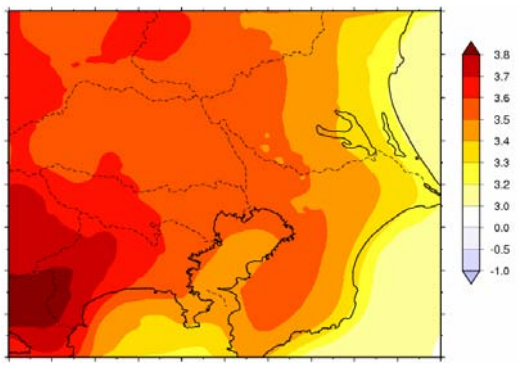

Fig. 5: The temperature increase of August to 2070, by using TERC-RAMS model nested into the MIROC AO-GCM by using PGWM. The map is around the metropolitan area of Japan (Kusaka et al., 2008)

We also apply statistical downscaling method to get the finer structure up to 1km grid, in the rural area. We try to get the projection data accurate enough to drive the impact model of both hydrology and agriculture.

4. The response to the present results

This is the report mainly about the comments made in the meeting for the advisory report base on remarks by those who represent various institutions. The prediction information with specific names of different places gave a strong impact to media representatives. As far as the regional climate model is concerned, assessment was conducted in each prefecture respectively and the method of evaluating warming of the climate in each prefecture was presented, to which many people took a strong interest. And when using the urban model, we were able to produce an almost pinpointing prediction result, which gave a very strong impression on many people. We think that this resulted from the method in which we presented it, but it seemed to give a good impression.

Acknowledgements

This work was supported by the Global Environment Research Fund (S-5-3) of the Ministry of the Environment, Japan. We are deeply grateful to all the members participating to this project.

References

Aoyagi, T. and N. Seino, A sensitivity study on anthropogenic heat release and building / street aspect ratio using a mesoscale model in Tokyo Metropolitan area, Japan. 89th American Meteorological Society Annual Meeting, P1.4. 2009.

Dairaku, K., S. Iizuka, W. Sasaki, R. A. Pielke Sr, and A. Beltran, Assessment of dynamical downscaling in river basins in Japan using the Regional Atmospheric Modeling System (RAMS). RCM2009, 2009.

Hara, M., T. Yoshikane, H. Kawase, and F. Kimura, Estimation of the impact of global warming on snow depth in Japan by the pseudo-global-warming method. Hydrological Research Letters, 2, 61-64. 2008.

Inatsu, M., and M. Kimoto, A scale interaction study on East Asian cyclogenesis using a general circulation model with an interactively nested regional model. *Mon. Wea. Rev.*, 2009 (revised).

Kawase, H., T. Yoshikane, M, Hara, F. Kimura, T. Yasunari, B. Ailikun, H. Ueda, and T. Inoue, Assessment of future changes in the Baiu rainband using the pseudo-global warming downscaling method, J. Geophisical Letters, 2009 (submitted).

Kusaka, H., S. Adachi, F. Kimura, M. Hara, and T. Hanyu, Urban climate prediction using the regional climate models (in Japanese), Annual meeting of the Association of Japanese Geographers, 2008.

Murazaki K., Kazuo Kurihara, Hidetaka Sasaki, Izuru Takayabu, Takao Uchiyama. A Regional climate simulation over Japan nested with JRA-25.Third WCRP International Conference on Reanalysis, P2-22, 2008

Sasaki H., K. Kurihara, I. Takayabu and T. Uchiyama, Preliminary experiments of reproducing the present climate using the non-hydrostatic regional climate model, *SOLA*, Vol.4, pp. 025-028, 2008

Takayabu I., and N. Ishizaki. An impact of weather events on the reproducibility of local climate with MRI/JMA non-hydrostatic regional climate model, AGU fall meeting GC53A-0689, 2008.

Simulation of Asian monsoon climate by RMIP Models

Shuyu Wang, Jinming Feng, Zhe Xiong and Congbing Fu

Institute of Atmospheric Physics, CAS, Beijing 100029, China, wsy@tea.ac.cn

1. Introduction

Regional climate model has shown its great abilities to add regional details in climate and climate change signals, which are forced by mesco-scale forcings such as topography, inland water body, the coastline, land use/land cover changes, ect. However, more systematic evaluation of RCM to adequately assess its performance and uncertainty in reproducing the regional climate information is required. To fully assess the regional climate model's advantages and disadvantages in simulating the Asian monsoonal climate, and to provide better confidence in projecting regional climate change, the Regional Climate Model Intercomparison Project (RMIP) for East Asia has been established to study the performance of an ensemble of regional climate models (RCMs) when simulating Asian climate. Started in 2000, RMIP is under the joint support of Asia-Pacific Network for Global Change Research (APN), the Global Change System for Analysis, Research and Training (START), the Chinese Academy of Sciences (CAS), and other national projects. RMIP seeks to improve further the RCM simulations of East Asian climate by evaluating their strengths and weaknesses in a common framework (Fu et al., 2000).

RMIP are carried out to improve RCMs simulation of East Asian climate by evaluating their strengths and weaknesses in a common framework. The specific objectives of RMIP are: (1) to assess the current status of East Asian regional climate simulation; (2) to provide a scientific basis for further RCM improvement; (3) to provide scenarios of East Asian regional climate change in the 21st century based on an ensemble of RCMs that are nested with GCMs.

A two-phase simulation program has been conducted to meet these objectives.

Phase-one, the 18-month simulation (March 1997- August 1998) covers a full annual cycle and contains two climatic extremes, i.e., the East Asian drought in summer 1997 and the floods in the Yangtze and Songhua River Valleys of China, as well as in Korea and Japan during summer 1998. The tasks of phase-one are to examine the models' capabilities to reproduce the seasonal cycle of East Asian Monsoon Climate, and to capture the basic character of two extreme climatic events. Totally nine models, including eight RCMs and one conformal-cubic Atmospheric Model, from five countries have taken part into the RMIP's phase one simulation. 1998 is the weak summer monsoon year, and the results phase one are used to examine the models' performances on simulating this abnormal monsoon year.

Phase-two is 10-year continuous simulation (January 1989 - December 1998) was conducted to assess the models' abilities to reproduce the statistical behavior of the average Asian model climate.

2. RMIP models' simulation of weak monsoon year of 1998

The main components of East Asian Summer Monsoon System includes the Australian cold anticyclone, the cross equatorial flow, the Indian South West Monsoon flow, ITCZ over South China Sea and the tropical western Pacific, the western Pacific subtropical High and tropical easterly flow and the Meiyu Front zones.

As a weak East Asian Monsoon year of 1998, the weak monsoon circulation produces too much precipitation over Yangtze River valley, which caused severe flooding. Most models captured the extreme heavy rainfall in 1998, though the models simulated intensities are different from that of observation (Fig.1). The results also show that models tend to overestimate the precipitation at the higher latitude.

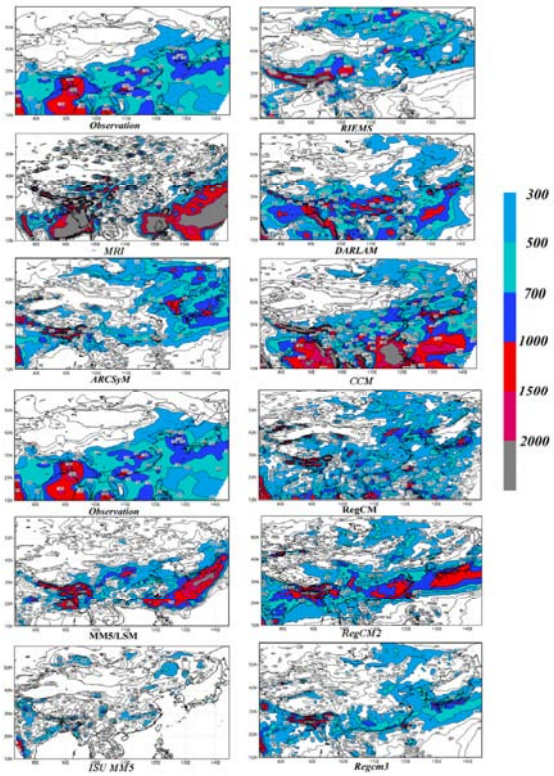

Figure 1. the total summer precipitation (mm) by RMIP Models.

3. Mean Monsoon Climate by RMIP models

The East Asian summer monsoon begins following the onset of the South and East Asia monsoons. Fig.2 shows the spatial distribution of 10-year mean summer total precipitation from RMIP Phase-Two results. All models reproduce the main monsoon rainfall center over Yangtze Valley of China, but either overestimate or underestimate the rainfall amount compared with observations.

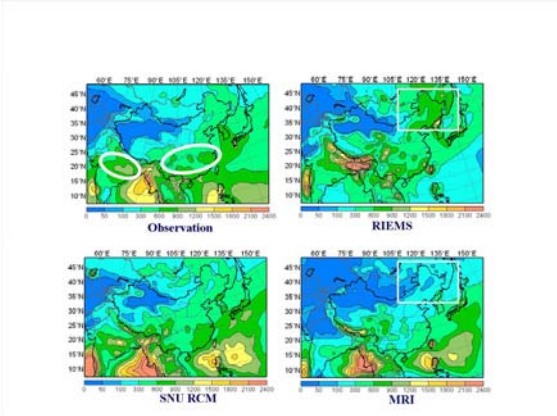

Figure 2. the 10-year averaged summer monsoon precipitation (mm)

4. Interannual Variability of East Asian Monsoon Climate by RMIP models

The model can simulate the interannual variability of monsoon precipitation, as shown in Fig. 3. The high variability regions such as North India, south-east China are reasonably captured by most RMIP models. The differences between model results and observations are not significant.

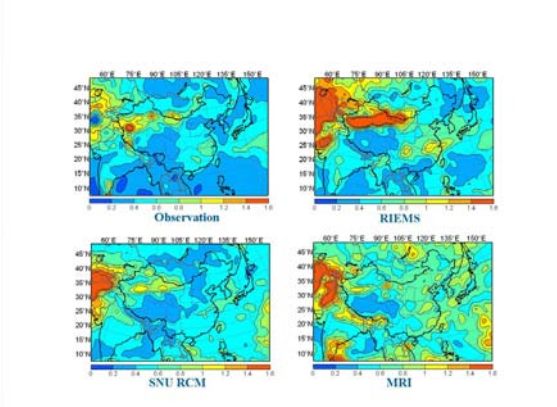

Figure 3. Interannual variability of East Asian Summer Monsoon Prec. (generated by July total precipitation)

5. Conclusions

Most RMIP model can simulate the averaged East Asian Monsoon precipitation as well as its variability. However, models' abilities on producing the main rainfall centers and intensities can be further improved by better simulation of monsoon circulation and better understand the impacts of the model physical processes on East Asian monsoon system.

Use of regional climate models in regional attribution studies

Christopher J. Anderson[1], William J. Gutowski[1], Jr., Martin P. Hoerling[2] and Xiaowei Quan[2]

[1]3010 Agronomy Hall, Iowa State University, Ames, 50011-1010, cjames@iastate.edu
[2]Earth Systems Research Laboratory, Physical Sciences Division, 325 Broadway, Boulder, CO, 80305-3328

1. Introduction

Attribution is the scientific process whether an identified change is consistent with an expected response to a combination of external forcing mechanisms and inconsistent with alternative, plausible explanations for which important elements are excluded from the combination of forcing mechanisms. Currently, the IPCC (*IPCC*, 2007) concludes:

"Difficulties remain in attributing temperature changes on smaller than continental scales and over time scales of less than 50 years. Attribution at these scales, with limited exceptions, has not yet been established. Averaging over smaller regions reduces the natural variability less than does averaging over large regions, making it more difficult to distinguish between changes expected from different external forcings, or between external forcing and variability."

An alternative to reducing dimensionality by averaging is to apply attribution techniques to a particular physical process rather than over a summation of all processes. Two examples are provided herein.

2. Attribution of Seasonal Extremes of Water Vapor Flux Convergence

An increasing trend over the past century in frequency and intensity of precipitation >4" has been found to be statistically significant in the upper Midwest United States (*CCSP*, 2008). Precipitation has large spatial variability, especially high-rate precipitation, making attribution studies susceptible to poor signal-to-noise ratio. Furthermore, it is difficult to simulate these extreme precipitation rates whether using global or regional climate models. However, the representation of the linkages between atmospheric processes and extreme precipitation in the Midwest United States by regional climate models is superior to that of analysis used to drive them (Anderson et al. 2003), and provides the possibility of focusing attribution studies on the processes that lead to extreme precipitation rather than extreme precipitation itself.

The attribution problem is one in which a one-way downscaling technique is appropriate for the following two reasons. First, the convective processes and feedback into the large-scale circulation is believed to be largely constrained to the region of heavy rainfall and regions nearby. Second, the convective processes require the ability to simulate correctly the coupling of mesoscale circulations.

The attribution approach begins with downscaling two global climate model simulations of the 20th century: one with increasing greenhouse gas concentrations and one with constant pre-industrial values. What is important to analyze is the components of the water vapor flux convergence, which is comprised of the product of water vapor and velocity convergence added to the advection of water vapor. Because the atmospheric processes have a larger scale and slower time evolution than storms that produce precipitation >4", it is less likely to be subject to the same signal-to-noise ratio problem. Furthermore, the components of the moisture flux convergence may be related to different expected responses to climate change. In particular, the velocity convergence will be related to the position of the storm track and its volatility; whereas, the water vapor advection will be related to the moisture content of the air due to evaporation from the Gulf of Mexico sea surface and evapotranspiration in nearby land regions. Thus, the interpretation of how climate change affects conditions conducive to >4" precipitation may be much cleaner than the interpretation for >4" precipitation itself.

3. Attribution of a climate extreme

One-way downscaling with regional climate models may also be used for attribution of an individual extreme event. In this case, the forcing mechanisms of interest evolve on a seasonal or sub-seasonal scale rather than over multiple decades. Attribution of the 2008 Midwest flood is one example.

The attribution methodology first seeks to determine whether the precipitation that led to the 2008 Midwest flood is consistent with the precipitation that is expected given the slowly-varying global sea surface temperatures or some particular pattern within the global sea surface temperatures. The main tool used in this analysis would be a global climate model with specified sea surface temperature as a lower boundary condition (an external forcing mechanism).

Another slowly varying factor to consider is the surface wetness. The feedback of soil moisture into precipitation is a process that is much easier to isolate than heavy precipitation rates themselves. In this attribution problem, an estimate of the soil moisture is provided as a boundary condition and atmospheric analyses rather than global climate model simulations are used as lateral boundary conditions to a regional model. Thus, there are two external forcing mechanisms: the large-scale circulation and the soil moisture pattern. An ensemble is used to assess the precipitation variability and is generated by initializing on different dates but retaining the estimated soil moisture pattern as a boundary condition. It is necessary to define an alternative pattern to examine whether other soil moisture patterns produce a similar response. Candidates for alternative patterns might include a soil moisture anomaly of opposite phase or a climatological soil moisture pattern.

4. Summary

The role of regional climate models in attribution studies is likely to expand as interest shifts to examination of regional climate change. A different perspective on attribution is described here. Rather than averaging fields to reduce variability, it is proposed that regional attribution studies focus on coherent regional mechanisms that are better simulated in regional models than global models.

References

Anderson, C. J., and PIRCS coauthors, Hydrological processes in regional climate model simulations of the central United States Flood of June-July 1993, *J. Hydrometeor.*, Vol. 4, No. 3, pp. 584—598, 2003.

CCSP, Weather and climate extremes in a changing climate. A report by the U. S. Climate Change Science Program and the Subcommittee on Global Change Research, [Thomas R. Karl, Gerald A. Meehl, Christopher D. Miller, Susan J. Hassol, Anne M. Waple, and William L. Murray (eds.)], Department of Commerce, NOAA's National Climatic Data Center, Washington, D. C., USA, pp. 164, 2008.

IPCC, Climate Change 2007: The physical science basis. Contribution of working group I to the fourth assessment report of the intergovernmental panel on climate change [Solomon, S., D. Qin, et al. (eds.)]. Cambridge University Press, Cambridge, United Kingdom and New York, NY, pp. 996, 2007

Wave estimations using winds from RCA, the Rossby regional climate model

Barry Broman[1] and Ekaterini.E. Kriezi[2]

[1]Swedish Meteorological and Hydrological Institute, Rossby Centre, Norrköping, Sweden; Barry.Broman@smhi.se
[2]Swedish Meteorological and Hydrological Institute, Göteborg, Sweden; Ekaterini.Kriezi@smhi.se

1. Introduction

Waves have now been used in the projections of the climate. The model SWAN running with winds from the Rossby Regional Climate Atmospheric model, (RCA). The first results of this were presented at the International Symposium US/EU-Baltic 2008 in Tallinn.

2. Future Wave Climate

Hind casts of waves were made with winds from RCA. When the results were compared to measurements they were to low. The reason is that the winds in RCA are too week due to among other thing averaging over the grid cell. In order to get better results a method were used to "correct" the winds by using both winds and gusts. This was a great improvement but more work is needed. In maps and graphs the comparisons will be given. Below in figure 1 you se an example of the climate effect on winds after taking the difference between a reference period and a future projection.

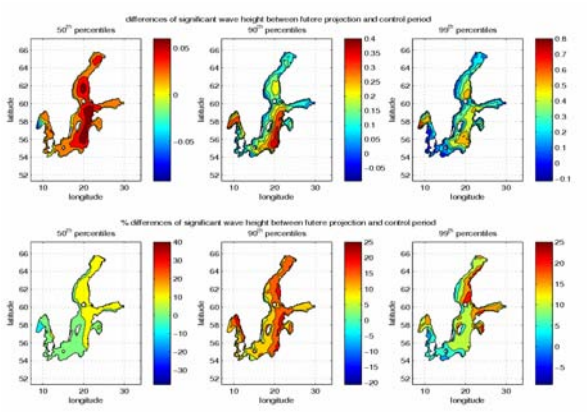

Figure 1. example of results with the SWAN model (significant wave heights): differences in percentiles between control period and future projection

3. Future plans

The plan is to use results from a coming coupled run between RCA, the atmospheric model and RCO the oceanographic model. These will give both winds and ice which is needed in order to make estimation of eventually changing wave climate in the Baltic

References

Booij, N., Ris, R.C., Holthuijsen, L.H., 1999. A third-generation wave model for coastal regions, 1. Model description and validation. J. Geophys. Res. 104 (C4), 7649–7666.

Broman B, 2007. Estimation of the wave climate for the Baltic Sea. Poster, Baltic Science Conference, Rostock 2007.

Broman, B., Hammarklint T., Soomere T., Valdmann A., 2006, Trends and extremes of wave fields in the north-eastern part of the Baltic Proper" ,OCEANOLOGICA,48,2006 pp 165-184.

Davis F. and Newstein H. 1968. The variation of Gust Factors with Mean wind Speed and with Height. Journal of Applied Meteorology, Jume 1968, volume 7, 372-378

Gill G.C. 1969. Comments on "The variation of Gust Factors with

Mean wind Speed and with Height". Journal of Applied Meteorology, Notes and correspondence, february 1969, 167

Grabemann I. and Weisse R. 2007 Climate changes Impact on Extreme Wave conditions in the Noth Sea: An Esemble Study. Ocean Dynamics, Submitted

Häggmark L., Ivarsson K-I., Gollvik S. and Olofsson P-O, 2000.

Mesan, an operational mesocale analysis system. Tellus,52 A,2-20

Kjellström E., Bärring L., Gollvik S., Hansson U., Jones C, Samuelsson P, Rummukainen M., Ullerstig A., Willén U. and Wyser K., 2005. A 140-year simulation European climate with new version of the Rossby Centre regional atmospheric climate model (RCA3), SMHI, Reports Meteorology and climatology 108

Jönsson A., Broman B., and Rahm L., 2003. Variations in the Baltic Sea wave fields. Ocean Engineering, Volume 30, Issue 1, January 2003, 107-126

Nerheim S. 2008. Growing demands for downscaling of climate

information – examples from predictions of future sea levels. US/EUBaltic2008

International Symposium, Tallinn Estonia, 27-29 May 2008

Ris, R. C. 1997: Spectral modelling of wind waves in coastal areas. PhD Thesis, Delft University of Technology, Delft, Netherlands.

Räisänsen J, Hansson U, Ullerstig A., Döscher R., Graham L.P., Jones C., Meier M., Samuelsson R., Willén U., 2003. GCM driven simulations of recent and future climate with the Rossby Centre coupled Atmospheric – Baltic Sea regional climate model RCAO. SMHI, Reports Meteorology and climatology 101

Van der Westhuysen, A.J., M. Zijlema and J.A. Battjes, 2007.

Nonlinear saturation-based whitecapping dissipation in SWAN for deep and shallow water. Coastal Engineering, 54, 151-170.

Ekrietsi E. and Broman B. Past and future wave climate in the Baltic Sea produced by SWAN model with forcing from the regional climate model RCA of the Rossby Centre. US/EU-Baltic 2008, Tallinn may 27 -29 2008.

Development of a Regional Arctic Climate System Model (RACM)

John J. Cassano, Wieslaw Maslowski, William Gutowski and Dennis Lettenmaier

John J. Cassano, University of Colorado, Cooperative Institute for Research in Environmental Sciences, Boulder, Co. USA
john.cassano@colorado.edu

1. Introduction

Observations and global climate system model projections indicate significant changes in the state of the Arctic climate (IPCC, 2007). These changes are impacting many aspects of the climate system (atmosphere, ocean, sea ice, land) and changes in one component of the climate system are intimately linked to changes in other components of the climate system. In order to understand the forcing for observed change in the Arctic and to increase confidence in future projections of Arctic climate change it is necessary to consider coupled changes in the Arctic climate system.

Global climate system models include many, but not all, components of the Arctic climate system, yet errors remain in their simulation of the current and past state of the Arctic. These errors arise from many sources including errors propagating into the Arctic from lower latitudes, inadequate representation of polar climate processes, and coarse model resolution. One way to address these shortcomings is through the use of an Arctic regional climate system model. An Arctic regional climate system model allows increased horizontal and vertical resolution and improved model physics that are optimized for polar regions, as well as the use of "perfect" lateral boundary conditions for retrospective simulations.

This extend abstract, and associated presentation at the 2nd Lund Regional-Scale Climate Modeling workshop, discusses plans for and the status of a collaborative project to develop a state-of-the-art Regional Arctic Climate system Model (RACM) including high-resolution atmosphere, land, ocean, sea ice and land hydrology components. The ultimate goal of this project is to perform multi-decadal numerical experiments with RACM using high performance computers to minimize uncertainties and fundamentally improve current predictions of climate change in the northern polar regions.

The project involves PIs from four institutions: Naval Postgraduate School (lead institution, PD/PI - Wieslaw Maslowski), University of Colorado in Boulder (co-PI - John J. Cassano), Iowa State University (co-PI - William J. Gutowski) and the University of Washington (co-PI - Dennis P. Lettenmaier) funded by the United States Department of Energy. In addition, collaborators from the University of Alaska – Fairbanks Arctic Regions Supercomputing Center and International Arctic Research Center (Andrew Roberts, Juanxiong He, and Greg Newby) are actively involved in this effort, while several other international experts in Arctic climate modeling are contributing to this project.

2. Regional Arctic Climate System Model

The regional Arctic climate system model (RACM) that is currently under development couples atmosphere, ocean, sea ice, and land component models. The atmospheric model used in RACM is a version of the National Center for Atmospheric Research (NCAR) Weather Research and Forecasting (WRF) model that has been optimized for the polar regions. The ocean and sea ice models are basically the same as those used in the NCAR Community Climate System Model (CCSM3), although used on a regional domain: the Los Alamos National Laboratory POP ocean model and CICE sea ice model. Land surface processes and hydrology will be represented by the Variable Infiltration Capacity (VIC) model. These four climate system component models are being coupled using the NCAR CCSM coupler CPL7.

The simulation domain of RACM covers the entire pan-Arctic region and includes all sea ice covered regions in the Northern Hemisphere as well as all terrestrial drainage basins that drain to the Arctic Ocean. The simulation domain is shown in Figure 1, with the red line indicating the extent of the atmosphere and land model domains and the blue line indicating the extent of the ocean and sea ice model domains. The ocean and sea ice model will use a horizontal grid spacing of less than 10 km, while the atmosphere and land component models will use a horizontal grid spacing of 50 km or less.

3. Benefits and Outcomes

A major product of this effort, and a principal community benefit, will be the development of a high-resolution pan-Arctic climate system model that combines all major climate elements in an internally consistent framework for focused studies. The coupling framework will allow straightforward implementation of additional climate-system components, thereby extending its capacity to cover a range of natural and human impacts.

A primary focus of the project is to improve our understanding of processes leading to reductions in Arctic sea ice cover. One outcome from this effort will be improved prediction of ice-free Arctic Ocean for use in policy planning.

This project will facilitate synthesis and integration of historical and new observations with model results. It will involve undergraduate, graduate, and postdoctoral students, who will receive practical training in coupled climate system modeling and/or analysis of model output.

References

IPCC, Climate Change 2007: The Physical Science Basis. Contribution of Working Group I to the Fourth Assessment Report of the Intergovernmental Panel on Climate Change [Solomon, S., D. Qin, M. Manning, Z. Chen, M. Marquis, K.B. Averyt, M. Tignor and H.L. Miller (eds.)]. Cambridge University Press, Cambridge, United Kingdom and New York, NY, USA, 996 pp, 2007

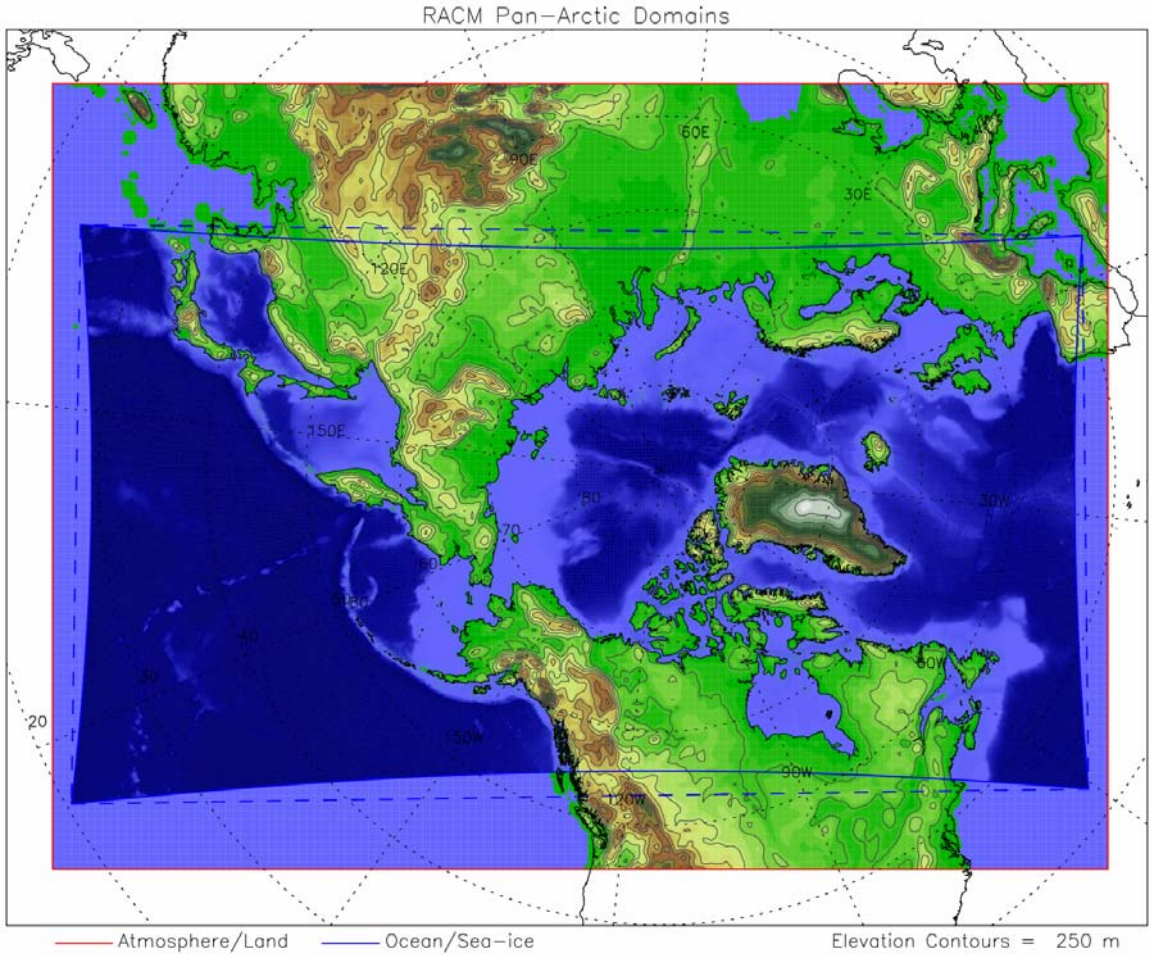

Figure 1. Model domain for the regional Arctic climate system model. The extent of the atmosphere and land model domains is shown by the red line and the extent of the ocean and sea ice model domains is shown by the solid blue line. Land topography and ocean bathymetry are given by color shading.

Regional climate simulation with mosaic GCMs

Michel Déqué

Météo-France/CNRM, CNRS/GAME, 42 avenue Coriolis, 31057 Toulouse Cédex 1, France; deque@meteo.fr

1. Introduction

The next IPCC exercise will include contributions of regional models on areas of the globe that have not be covered in the past by international multimodel projects like NARCCAP or ENSEMBLES. The target resolution will be 50 km. Ideally, the best exercise would be to run a global model at 50 km resolution driven by sea surface temperatures (SST) from lower resolution coupled model. If local biases in SST are too detrimental to some regional climates, they can be corrected. But such an exercise is unaffordable for many modelling groups, and very heavy (e.g. ARPEGE model needs one year with a full 8-processor node on a NEC-SX8 computer) for other groups. A more flexible approach is proposed here.

2. Scope of the study

The ARPEGE model has the capability of variable resolution with maximum resolution around a pole of interest. If the whole globe is considered, then several poles must be used, and then several versions of the model must be run. Given well known geometrical properties of the sphere, a good number of poles is 20, because the icosahedron (20 vertices) is the largest possible regular polyhedron (see Figure 1).
Two AMIP 10-year experiments are used for the analysis. They use each versions of ARPEGE at different poles. The spectral truncation is TL179 and the stretching factor is two. If we build a composite grid with the maximum resolution everywhere, the mean resolution is 57 km with a maximum of 54 km and a minimum of 65 km. If we consider an individual model, the minimum resolution (at the antipodes) is 200 km. In the first experiment, the models are run independently. It is possible to build composites of climate parameters like seasonal mean or standard deviation. But it is not possible to reconstruct daily fields, because each run has its own history, and using the same SST is not enough to constrain the atmosphere daily fields. Thus a second experiment is proposed. A preliminary AMIP simulation has been run by the same model with homogeneous TL159 120 km horizontal resolution. This is the "pacemaker" simulation. Then the variable resolution models are run with driving conditions from this run. For each model, the relaxation coefficient is zero where the resolution is the maximum of the 20 grids, and maximum (6-hour e-folding time) where the resolution is less than that of the driving model (i.e. 120 km).

3. Content of the presentation

In the presentation, we will use eight such GCMs surrounding Europe and Africa. The reference is a 10-year run with a version of ARPEGE at homogeneous TL319 60 km resolution (perfect model exercise). We will analyze the effects of the "seams" in the composite fields and examine whether imposing a relaxation is detrimental to or improving the simulation in the area of high resolution.

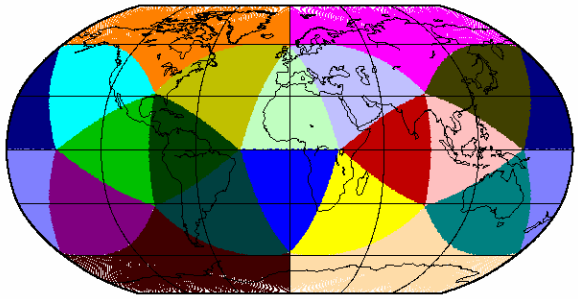

Figure 1: The 20 equal-area on which a stretched GCM may focus.

A coupled regional climate model as a tool for understanding and improving feedback processes in Arctic climate simulations

Wolfgang Dorn, Klaus Dethloff and Annette Rinke

Alfred Wegener Institute for Polar and Marine Research, Telegrafenberg A43, 14473 Potsdam, Germany;
Wolfgang.Dorn@awi.de

1. Motivation

A realistic representation of sea ice in coupled climate models is an essential precondition for reliable simulations of the Arctic climate. Intercomparison studies of coupled models have shown that there are still large deviations in the simulation of Arctic sea ice among the models (e.g., *Holland and Bitz*, 2003). The representation of the processes at the interface between atmosphere and sea ice is often oversimplified due to poor knowledge of the underlying physics of feedback processes between the climate subsystems. While such feedbacks are completely absent in stand-alone models for the subsystems, their accurate simulation plays a key role in the performance of coupled regional and global models.

2. The coupled regional climate model HIRHAM-NAOSIM

The coupled model is a composite of the regional atmospheric climate model HIRHAM (*Christensen et al.*, 1996; *Dethloff et al.*, 1996) and the high-resolution version of the North Atlantic/Arctic Ocean sea-ice model NAOSIM (*Karcher et al.*, 2003; *Kauker et al.*, 2003). Both model components were well adapted for Arctic climate simulations and successfully applied for a wide range of Arctic climate studies.

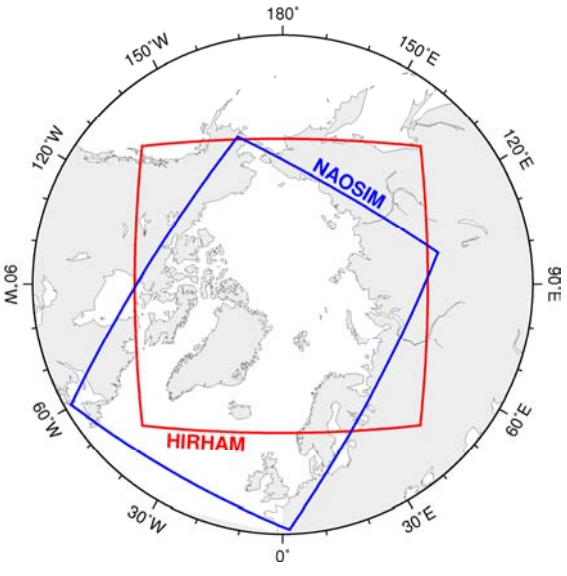

Figure 1. Geographical locations of the coupled model's atmosphere domain (HIRHAM) and its ocean-ice domain (NAOSIM). The domain of coupling is given by the overlap area and covers the whole Arctic Ocean, including all marginal seas, the Nordic Seas, and parts of the northern North Atlantic.

The coupled model system, first introduced by *Rinke et al.* (2003), was described in detail by *Dorn et al.* (2007). The integration domains of the two model components are shown in Figure 1. The horizontal resolutions currently used in the coupled model system are 0.5° (~50 km) in HIRHAM and 0.25° (~25 km) in NAOSIM. In the vertical, the atmosphere is subdivided into 19 unevenly spaced levels in hybrid sigma-pressure coordinates and the ocean into 30 unevenly spaced z-coordinate levels. In the near future, a sophisticated land surface model (LSM) with 6 soil layers will be incorporated into the coupled model system too.

3. Improvement in the model representation of feedback processes

Feedback processes, in which sea ice is involved, like the ice-albedo feedback, play an important role in the Arctic climate system and may be regarded as crucial factors in the polar amplification of climate change. In order to improve the simulation of the ice-albedo feedback, more sophisticated schemes for the ice growth/melting, the snow and ice albedo as well as the snow cover fraction on ice have been implemented into HIRHAM-NAOSIM and tested in a series of sensitivity experiments (see *Dorn et al.*, 2008b).

It is found that the simulation of Arctic summer sea ice responds very sensitively to the parameterization of the snow and ice albedo but also to a sub-grid-scale separation of the heat fluxes within the ice growth scheme. The parameterization of the snow cover fraction on ice plays an important role in the onset of summertime ice melt. This has crucial impact on summer ice decay when more sophisticated schemes for ice growth and ice albedo are used. It is shown that in case of using a harmonized combination of more sophisticated parameterizations the simulation of the summer minimum in ice extent can be considerably improved due to a better timing of the snow and ice ablating periods.

4. Linkage between atmospheric and sea-ice variability

The patterns of maximum amplitude of interannual variability of the Arctic summer sea-ice cover have been analyzed in HIRHAM-NAOSIM simulations for the 1980s and 1990s and compared with SSM/I satellite-derived sea-ice concentrations. It is found that natural variability of the summer sea-ice cover is almost exclusively restricted to its peripheral zone. Furthermore, summers with low sea-ice extent are associated with anomalously high atmospheric pressure over the western Arctic Ocean.

The presence of a high pressure area over the Arctic Ocean is usually related to lower cloud cover and more anticyclonic and divergent ice motion accompanied by a more pronounced transpolar drift and stronger sea-ice export through the Fram Strait (see Figure 2). These conditions represent favorable factors for low sea-ice extent at the end of the summer. *Dorn et al.* (2008a) noted that large-scale variations in the atmospheric circulation are likely to represent the main driver for sea-ice variability, also with respect to the strong decline of the Arctic summer sea-ice cover in recent years.

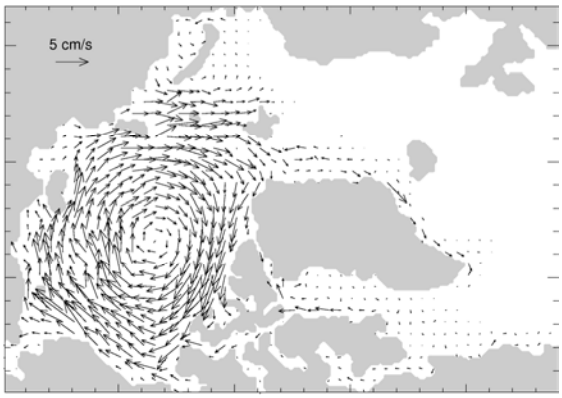

Figure 2. Difference between "low-ice" and "high-ice" years of simulated mean sea-ice drift velocity during summer (June to September). For clarity reasons, only every fifth difference vector is displayed.

In order to achieve a realistic regional distribution of sea-ice in late summer, it requires that the coupled model reproduces the observed atmospheric circulation during the preceding summer months. Unrealistic sea-ice cover, in turn, may favor model deviations in the atmospheric circulation, but these deviations can clearly differ in their strength, probably in consequence of regional feedback processes. It is a future task to identify the key regions in the Arctic where a more realistic simulation of such feedback processes is important.

References

Christensen, J. H., Christensen, O. B., Lopez, P., van Meijgaard, E., Botzet, M., The HIRHAM4 regional atmospheric climate model, DMI Sci. Rep. 96-4, Dan. Meteorol. Inst., Copenhagen, Denmark, 51 pp., 1996.

Dethloff, K., Rinke, A., Lehmann, R., Christensen, J. H., Botzet, M., Machenhauer, B., Regional climate model of the Arctic atmosphere, *J. Geophys. Res.*, 101, 23401-23422, 1996.

Dorn, W., Dethloff, K., Rinke, A., Frickenhaus, S., Gerdes, R., Karcher, M., Kauker, F., Sensitivities and uncertainties in a coupled regional atmosphere-ocean-ice model with respect to the simulation of Arctic sea ice, *J. Geophys. Res.*, 112, D10118, doi:10.1029/2006JD007814, 2007.

Dorn, W., Dethloff, K., Rinke, A., Kurgansky, M., The recent decline of the Arctic summer sea-ice cover in the context of internal climate variability, *Open Atmos. Sci. J.*, 2, 91-100, doi:10.2174/1874282300802010091, 2008a.

Dorn, W., Dethloff, K., Rinke, A., Improved simulation of feedbacks between atmosphere and sea ice over the Arctic Ocean in a coupled regional climate model, *Ocean Model.*, submitted, 2008b.

Holland, M. M., Bitz, C. M., Polar amplification of climate change in coupled models, *Clim. Dyn*., 21, 221-232, doi:10.1007/s00382-003-0332-6, 2003.

Karcher, M. J., Gerdes, R., Kauker, F., Köberle, C., Arctic warming: Evolution and spreading of the 1990s warm event in the Nordic seas and the Arctic Ocean, *J. Geophys. Res.*, 108, 3034, doi:10.1029/2001JC001265, 2003.

Kauker, F., Gerdes, R., Karcher, M., Köberle, C., Lieser, J. L., Variability of Arctic and North Atlantic sea ice: A combined analysis of model results and observations from 1978 to 2001, *J. Geophys. Res.*, 108, 3182, doi:10.1029/2002JC001573, 2003.

Rinke, A., Gerdes, R., Dethloff, K., Kandlbinder, T., Karcher, M., Kauker, F., Frickenhaus, S., Köberle, C., Hiller, W., A case study of the anomalous Arctic sea ice conditions during 1990: Insights from coupled and uncoupled regional climate model simulations, *J. Geophys. Res.*, 108, 4275, doi:10.1029/2002JD003146, 2003.

Arctic regional coupled downscaling of recent and possible future climates

R. Döscher*, T. Königk*, K. Wyser,* H. E. M. Meier** and P. Pemberton***

*SMHI/Rossby Centre, **SMHI and Univ. Stockholm, ***SMHI, ralf.doescher@smhi.se

1. A regional coupled ocean-sea ice-atmosphere model of the Arctic

SMHI/Rossby Centre has developed a regional coupled ocean-sea ice-atmosphere model of the Arctic (The Rossby Centre Atmosphere Ocean model RCAO). After validation of recent climate representation, first regional climate scenario experiments have been carried out based on two global scenario simulations (ECHAM5/MPI-OM and BCM) and the emission scenario A1B.

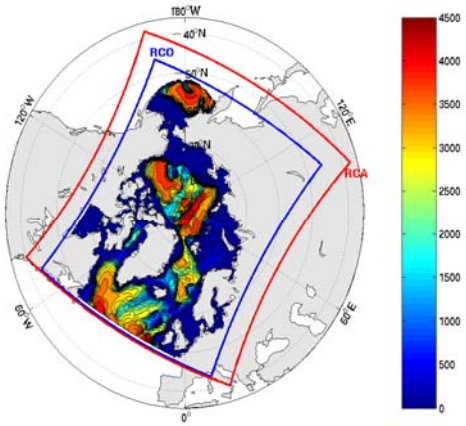

The RCAO Arctic model domain for the ocean (RCO, blue) and the atmosphere (RCA, red), together with the ocean topography.

2. Validation and Predictability

Within the EU-DAMOCLES project, validation of recent climate has been carried out under the conditions of the ECMWF reanalysis (ERA-40) and control periods of the global scenario simulations. Central validation parameters are the Arctic sea ice parameters and its relation with large scale atmospheric circulation. Significant correlations between the winter North Atlantic Oscillation index and the summer Arctic sea ice thickness and summer sea ice extent are found in agreement with observations. The ice thickness trend is found to be related to large scale atmospheric forcing. In an ensemble experiment, Arctic predictability has been assessed in order to quantify uncertainty due to non-linear interannual variability generated internally within the Arctic coupled system. Results indicate that the variability generated by the external forcing is more important in most regions than the internally generated variability. However, both are in the same order of magnitude. Local areas such as the Northern Greenland coast together with Fram Straits and parts of the Greenland Sea show a strong importance of internally generated variability, which is associated with wind direction variability due to interaction with atmospheric dynamics on the Greenland ice sheet. High predictability of sea ice extent is supported by north-easterly winds from the Arctic ocean to Scandinavia.

3. Regional Arctic scenario downscaling

The regional scenario downscaling exercise has been set up as a set of scenario experiments covering the role of different processes and forcing on possible future climates. Initially, the regional scenarios have been run under different treatments of sea surface salinity and lateral boundary conditions. First results indicate that occurrence of rapid change events in the Arctic are very much dependent on the hemisphere-scale atmospheric circulation. The local response in the regional scenarios tends to be stronger than in the global scenarios.

A regionally coupled atmosphere-ocean and sea ice model of the Arctic

Ksenia Glushak, Dmitry Sein and Uwe Mikolajewicz

Max-Planck Institute for Meteorology, Bundesstrasse 53, 20146 Hamburg. Germany; ksenia.glushak@zmaw.de

1. Introduction

To correctly understand the latest changes with decline Arctic sea ice, as well as the changes on decadal and interannual scale, it is necessary to consider the dynamics of atmosphere, ocean and sea ice. The atmosphere, as well as the ocean shows significant decadal and interannual changes in this remote region. Unfortunately, global coupled climate models do not have sufficient resolution to represent key processes in this area. A regional climate model in this case may show a better result, due to increased horizontal resolution and the more flexible model setup.

2. Model description

To simulate the climate of the last decades the regional atmospheric model REMO coupled to the global ocean model MPIOM was used. REMO was used in different versions. It has 27 vertical levels and horizontal resolutions of 1º or 0.5º. The ocean model was configured in such a way that one pole of the bipolar grid was located over western Canada and the over one over southern Russia. This setup results in horizontal resolution of 10 to 15 km over the Arctic basin (see e.g. Fig. 1). The individual models were coupled using the Oasis coupler.

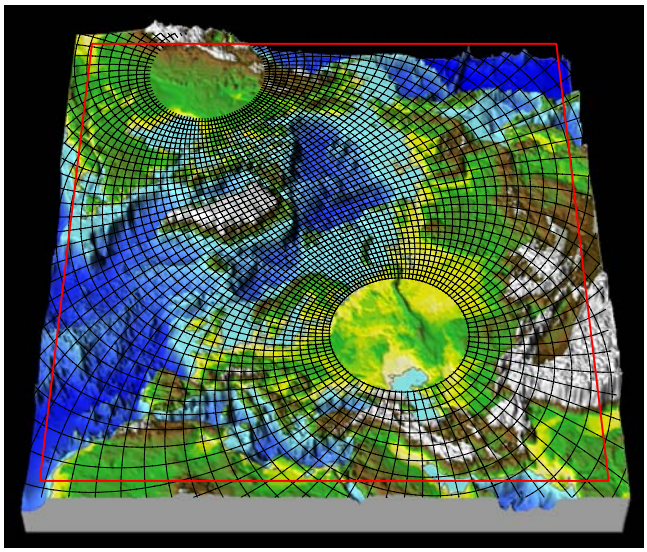

Figure 1. Grid setup. Red border is the REMO area.

Beside the difference in the horizontal resolutions, different forcing was used to drive the REMO model. NCEP-NCAR and ERA40 re-analysis covered almost the same time slices, except that NCEP-NCAR is started ten years early than ERA40 in 1948, and continue after August 2002. Our knowledge about the climate of the Arctic region suffers from lack of the observations within the central Arctic basin, especially before the "satellite era", which started in 1979. The difference between the two reanalysis is bigger in this time period, and it is important to drive the model with both reanalysis to understand how sensitive the model to the choice of the driving forcing.

To validate the model different reanalysis were used as well as observations data. Unfortunately, back in time over the central basin the observation data had a big gaps, and some of the fields like total cloud cover are very hard to evaluate on the decadal scale.

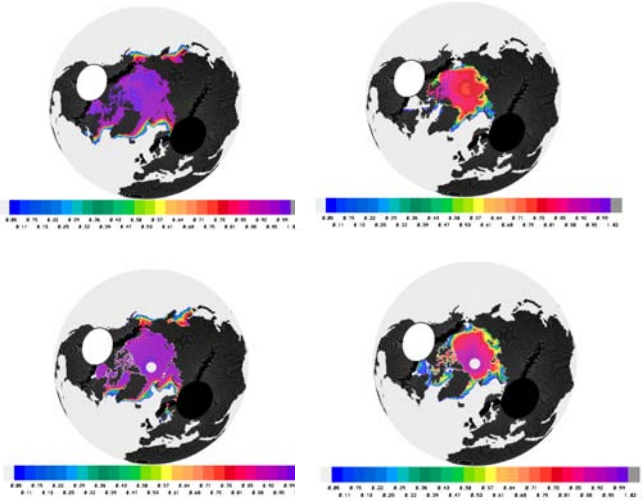

Figure 2. Sea ice concentration from the model simulations (top) and from satellite data (NSIDC, bottom). Mean February (left) and July (right) values calculated over 1980-1990.

Currently we are testing the model in the coarser resolution version. Preliminary results indicate a good reproduction of the observed climatology (see e.g. Fig. 2). After availability of the new next generation super computer HLRE II at DKRZ (Deutsches Klimarechenzentrum), which is scheduled for the next weeks, we will perform a set of simulations with different model setups. The results will be presented on the poster.

As next step we will couple the land hydrology. The set up of the atmospheric model has been chosen to include the catchment of all rivers ending in the Arctic Ocean. With this model we will study the water cycle of the Arctic, and its variations.

Convection-resolving regional climate modeling and extreme event statistics for recent and future summer climate

Christoph Knote[1], Günther Heinemann[2] and Burkhardt Rockel[3]

[1)] christoph.knote@empa.ch, Empa Materials Science and Technology, Überlandstr. 129, 8600 Dübendorf, Switzerland
[2)] Environmental meteorology, University of Trier, Behringstr. 21, 54286 Trier, Germany
[3)] GKSS research centre, Max-Planck-Str. 1, 21502 Geesthacht, Germany

1. Introduction

Global and regional climate models are currently employed on horizontal resolutions up to 5 km. State-of-the-art numerical weather prediction (NWP) models though have arrived at the kilometer-scale. At this resolution explicit calculation of convection becomes feasible and effects of small-scale topographic features (e.g. valleys) can be accounted for. It is assumed that consequently extremes like wind gusts, thunderstorms or heavy rain will be modelled more realistic.

Extreme events exert the most imminent effect on people's lifes, which reasons a detailed treatment of possible changes within future climate scenarios. Changes in extreme events do not necessarily origin in changes of the mean. An increase in variability is another possible source of change, as has recently been shown for the summer heat wave over Europe in 2003 by *Schär et. al (2004)*. Extreme value development is therefore not equivalent to mean development and requires special analysis.

The combination of convection resolving regional climate simulations with a state-of-the-art extreme value analysis is believed to result in more accurate and more detailed information about the changes in extremes in a future climate.

2. Modeling

The COSMO-CLM version 4.2 has been employed in simulations at 1.3 km resolution over the region of Rhineland-Palatine in Germany. The simulations are nested in simulations at 5 km which are based on the COSMO-CLM consortial runs as reported in *Hollweg et al. (2008)*. Two time slices of 10 years (1960-69 and 2015-24) show changes in extremes for the IPCC A1B scenario. Due to computational demand only the summer months June, July and August of each year have been modelled.

3. Extreme value analysis

A "peaks over threshold" (POT) extreme value analysis gives information about changes in extremes of near-surface wind speed, screen level temperature and precipitation. This method is commonly used for the analysis of extreme values of meteorological data, e. g. in *Brabson and Palutikof (2000)*. The modelled extreme values are fitted to a GPD function to achieve comparable return value statistics for the selected variables. Return values are widely used in urban planning, disaster management and insurance. This methodology is applied to regional means as well as to single grid points to derive information about mean changes as well as the regional differences.

4. Accuracy assessment

To assess the accuracy of the statistical procedure a non-parametric method called "moving-block bootstrapping" after *Wilks (1997)* is used. Therein the simulation data itself forms the basis of a synthetic sample from which statistical error properties of the POT procedure can be inferred, without an a priori assumption about its distribution.

5. Results

It can be shown that the simulations result in added variability when compared to simulations on a coarser grid. Comparison of the two time slices results in positive changes of daily extremes of temperature variables, including an increasing variability between daily minima, mean and maxima values. Wind speed and gust extremes show no significant changes. These results are in accordance with findings in the PRUDENCE project (*Kjellström et al. (2007)*, *Beniston et al. (2007)*). Bootstrapping shows that the extreme value analysis itself is stable.

References

Beniston, M., Stephenson, D. B., Christensen, O. B., Ferro, C. A. T., Frei, C., Goyette, S., Halsnaes, K., Holt, T., Jylhä, K., Koffi, B., Palutikof, J., Schöll, R., Semmler, T., and Woth, K., Future extreme events in european climate: an exploration of regional climate model projections, *Climatic Change*, 81, pp. 71–95, 2007

Brabson, B. B. and Palutikof, J. P., Tests of the Generalized Pareto Distribution for predicting extreme wind speeds, *Journal of Applied Meteorology*, 39, pp. 1627–1640, 2000

Hollweg, H.-D., Boehm, U., Fast, I., Hennemuth, B., Keuler, K., Keup-Thiel, E., Lautenschlager, M., Legutke, S., Radtke, K., Rockel, B., Schubert, M., Will, A., Woldt, M., and Wunram, C., Ensemble simulations over europe with the regional climate model CLM forced with IPCC AR4 global scenarios, *Technical report, Max-Planck-Institut fuer Meteorologie*, Hamburg, 2008

Kjellström, E., Bärring, L., Jacob, D., Jones, R., Lenderink, G., and Schär, C., Modelling daily temperature extremes: recent climate and future changes over Europe, *Climatic Change*, 81, pp. 249–265, 2007

Schär, C., Vidale, P. L., Lüthi, D., Frei, C., Häberli, C., Liniger, M. A., and Appenzeller, C., The role of increasing temperature variability in european summer heatwaves, *Nature*, 427, pp. 332–336, 2004

Wilks, D. S., Resampling hypothesis test for autocorrelated fields, *Journal of Climate*, 10, 1, pp. 65–82, 1997

Numerical modeling of trace species cycles in regional climate model systems

Bärbel Langmann

Institute of Geophysics, University of Hamburg, Bundesstr. 55, Germany, baerbel.langmann@zmaw.de

1. Introduction

In recent years, numerous atmospheric regional and global climate models have been extended by modules for transport and transformation of trace species (Zhang, 2008) to improve the numerical simulation of atmospheric trace species cycles, their impact on climate and vice versa. This is an important step from the chemical and climate point of view, as the on-line methodology offers several advantages compared to the off-line methodology, where chemical and meteorological processes are determined in separate models. Examples for such regional scale models are GATOR-GCMM (Jacobson, 2001), REMOTE (Langmann, 2000) and WRF (Grell et al., 2005).

A further extension towards regional Earth system models is to couple ocean and atmosphere biogeochemical models on the regional scale, with the potential to offer new insights into exchange processes of climate relevant trace species between the ocean and the atmosphere. Aerosols in the marine atmosphere influence solar irradiation over the world's ocean directly by backscattering incoming solar radiation and indirectly, by forming cloud condensation nuclei thereby affecting the cloud albedo. In recent years, the role of natural organic aerosol (OC) in the marine environment has received increasing attention. Measurements indicate that the increase of the marine biological activity is accompanied by a considerable increase of the contribution of OC to the submicron marine aerosol (e.g. O'Dowd et al., 2004) exceeding the mass fraction of nss sulfate by a factor of more than two. Here the recent developments of and future plans with the regional scale climate-chemistry/aerosol model REMOTE are presented together with selected applications.

2. Model description

The regional scale three-dimensional on-line atmosphere-chemistry/aerosol model REMOTE (Regional Model with Tracer Extension, www.mpimet.mpg.de/en/wissenschaft/modelle/remote.html) (Langmann, 2000; Langmann et al., 2008) is one of the few regional climate models that determines the physical, photochemical and aerosol state of the atmosphere at every time step thus offering the possibility to consider trace species effects on climate as well (e.g. Langmann, 2007). The dynamical part of the model is based on the former regional weather forecast system of the German Weather Service (Majewski, 1991) which is using a hydrostatic assumption for the vertical pressure gradient. In addition to the German Weather Service physical parameterisations, those of the global climate model ECHAM-4 (Roeckner et al., 1996) have been implemented in REMOTE and are used for most applications since 2000.

There are different trace species modules available: a photochemical module, stable water isotopes have been studied (e.g. Sturm et al., 2005), carbon dioxide (e.g. Karstens et al., 2006) and recently an aerosol microphysical module has been implemented in addition to the photochemical one (Langmann et al., 2008). A study on the second indirect aerosol effect is described in Langmann (2007). The model is flexible to be applied all over the world: many applications focus on Europe, some studies on Indonesia, South America, Nicaragua and India. Meanwhile the model is applied in Indonesia, China, Germany, UK and Ireland, where it is further developed to study a variety of scientific questions.

3. Selected applications

Recently, O'Dowd et al. (2008) published a novel approach to develop a combined organic-inorganic sub-micron sea-spray source function for inclusion in large-scale models. It requires wind speed and surface ocean chlorophyll-a concentration as input parameters. The combined organic-inorganic source function was implemented in REMOTE and sea-spray fields are predicted with particular focus on the North East Atlantic. The model predictions for primary organic carbon (POC) using the new source functions (Fig. 1, 2) compare well with observations of total sea-spray mass and organic carbon fraction in sea-spray aerosol.

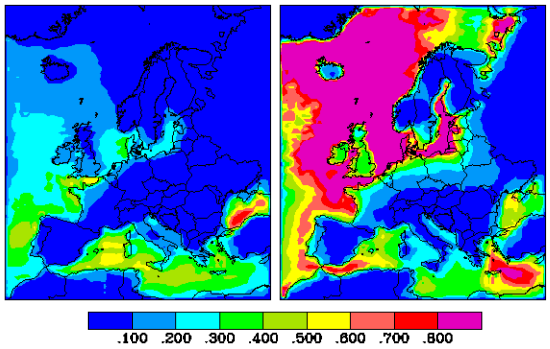

Figure 1. REMOTE model results for marine POC [ug/m^3] in surface air during January (left figure) and June 2003 (right figure).

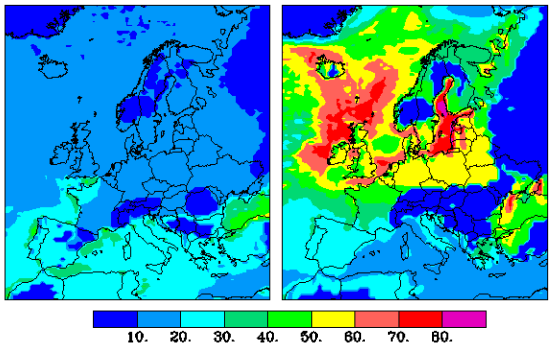

Figure 2. REMOTE model results for the fraction of marine POC in accumulation mode sea-spray [%] in surface air during January (left figure) and June 2003 (right figure).

4. Outlook

Currently a coupled ocean-atmosphere biogeochemical model system is set-up with REMOTE as atmospheric component. REMOTE will provide information about the input of nutrients into the ocean in addition to the usually transferred information of heat fluxes and precipitation. Experiences to couple REMOTE with ocean models are available (e.g. Aldrian, 2003). The ocean model will provide sea surface temperature, chlorophyll-a content and maybe whitecap coverage for the determination of ocean-atmosphere trace species fluxes. In a first step it is planned to apply the coupled ocean-atmosphere model system over the NE Pacific ocean to study phytoplankton growth due to volcanic ash nutrients and its impact on climate via modifications of atmospheric CO_2 and marine cloud formation.

References

Aldrian, E., Simulation of Indonesian Rainfall with a Hierarchy of Climate Models, University Hamburg, Dissertation, 2003.

Grell, G. A., S. E. Peckham, R. Schmitz, S. A. McKeen, G. Frost, W. C. Skamarock, B. Eder, Fully coupled ‚online' chemistry within the WRF model, Atm. Environ. 39, 6957-6975, 2005.

Jacobson, M. Z., A global-through urban-scale air pollution and weather forecast model 1. Model design and treatment of subgrid soil, vegetation, roots, rooftops, water, sea, ice, and snow, J. Geophys. Res. 106, 5385-5401, 2001.

Karstens, U., M. Gloor, M. Heimann and C. Roedenbeck, Insights from simulations with high-resolution transport and process models on sampling of the atmosphere for constraining mid-latitude land carbon sinks, J. Geophys. Res. 111, D12301, 2006

Langmann, B., Numerical modeling of regional scale transport and photochemistry directly together with meteorological processes, Atmos. Environ. 34, 3585-3598, 2000.

Langmann, B., A model study of the smoke-haze influence on clouds and warm precipitation formation in Indonesia 1997/1998, Atmos. Environ. 41, 6838-6852, 2007.

Langmann, B., S. Varghese, E. Marmer, E. Vignati, J. Wilson, P. Stier, C. O'Dowd, Aerosol distribution over Europe: a model evaluation study with detailed aerosol microphysics, Atmos. Chem. Phys. 8, 1591-1607, 2008.

Majewski, D., The Europa Modell of the Deutscher Wetterdienst. Seminar Proceedings ECMWF Vol. 2, 147-191, 1991.

Roeckner, E., K. Arpe, L. Bengtsson, M. Christoph, M. Claussen, L. Duemenil, M. Esch, M. Giorgetta, M. Schlese, U. Schulzweida, The atmospheric general circulation model ECHAM-4: Model description and simulation of present-day climate. MPI Report No. 218. Hamburg, Germany, 1996.

O'Dowd, C., M. C. Facchini, F. Cavalli, D. Ceburnis, M. Mircea, M. Decesari, S. Fuzzi, Y. J. Yoon, J.-P. Putaud, Biologically driven organic contribution to marine aerosol. Nature 431, 676–680, 2004.

O'Dowd, C., B. Langmann, S. Varghese, C. Scannell, D. Ceburnis and M. C. Facchini, A combined organic-inorganic sea-spray source function, Geophys. Res. Lett. 35, L01801, doi:10.1029/2007GL030331, 2008.

Sturm, K., G. Hoffmann, B. Langmann and W. Stichler, Simulation of delta 18O in precipitation by the regional circulation model REMOiso, Hydrological Processes 19, 3425-3444, doi:10.1002/hyp.5978, 2005.

Zhang, Y., Online-coupled meteorology and chemistry models, history, current status, and outlook, Atmos. Chem. Phys. 8, 2895-2932, 2008.

The impact of atmospheric thermodynamics on local climate change predictability: A plea for very high resolution climate modeling

G. Lenderink and E. van Meijgaard

KNMI, Wilhelminalaan 10, 3730 AE, De Bilt, The Netherlands; lenderin@knmi.nl

1. Introduction

It is well accepted that regional/local climate change is less predictable than the global mean climate. This is largely based on the concept that uncertainty "propagates" from the global scale to the continental scale, to the regional and eventually to the local scale, in each step broadening the distribution of possible outcomes. This often leads to the conclusion that the future local climate is highly uncertain or even unpredictable. In two examples we show that, while the notion of propagation of uncertainty may have a general value, thermodynamic processes acting on a local scale may cause a higher level of predictability than expected.

2. Extreme precipitation

Global mean precipitation amounts are generally predicted to increase by 1-3 % per degree global warming (*Held and Soden,* 2006) On a regional level, however, uncertainties increase, mainly due to uncertainty in the atmospheric circulation response. For example, for the Netherlands it is uncertain whether mean precipitation will increase or decrease in summer (*Van Ulden and Van Oldenborgh* 2006). However, it is more certain how precipitation extremes will evolve, and increases in summertime daily extremes are consistently obtained in regional climate simulations (*Lenderink et al.* 2007). The result that increases in extremes are more predictable than the changes in the means may appear contra intuitive. However, there is a simple and robust thermo-dynamic explanation: the fact that the maximum precipitable water in the atmosphere increases with temperature at a rate predicted by the Clausius-Clapeyron relation (7 % per degree) and, roughly speaking, that this higher water holding capacity causes higher extremes when essentially all available water is raining out.

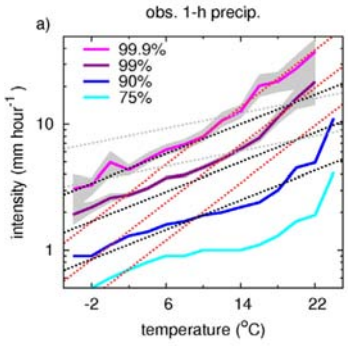

Figure 1. Scaling relation of hourly precipitation as a function of daily mean temperature derived from observations in De Bilt (The Netherlands). The black (red) stippled lines denote increases of 7 (14) % per degree. Shown are extreme precipitation intensities (70 to 99.9th percentiles) of wet hours only.

Increases in daily precipitation extremes with temperature can also be found in station observations, for example for De Bilt (The Netherlands). By binning the daily precipitation sum on the daily mean temperature, we obtained an increase in the extremes with temperature. However, the scaling behavior of precipitation extremes on temperature is not very well defined: for lower temperature it is roughly 7 % per degree, whereas for higher temperatures the temperature dependency is generally lower (*Lenderink and Van Meijgaard* 2008).

For shorter time scales a stronger and better defined relation between temperature and precipitation extremes is found. For days with mean temperatures above 10 ^{o}C, the observed hourly intensities of De Bilt show an exponential increase of 14 % per degree temperature rise for the extreme events (Figure 1) (*Lenderink and Van Meijgaard* 2008). Results of stations in Belgium and Switzerland show very similar dependencies.

Model results at 25 km resolution (present state of the art in regional climate modeling) only partly reproduce these dependencies. This could be due to model errors related to convection, but the results suggest that the scale difference between station scale of the observations and grid box averages of the model play an important role as well.

3. Coastal precipitation

The precipitation distribution within the Netherlands is strongly influenced by the temperature of the North Sea. In spring, the coastal area (< 30 km from the coastline) is relatively dry compared to the inland area due the low temperatures of the North Sea which lead to a suppression of shower activity. In autumn the situation is reversed and showers arise and strengthen above the warm water (Figure 2).

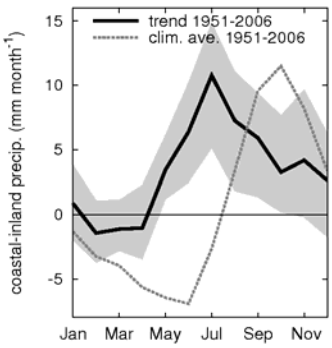

Figure 2. Precipitation difference between the coastal zone and the inland zone as a function of month. Shown is the climatology over the period 1951-2006 (dashed line) and the trend over this period (change in mm month^{-1} per 55 year) (thick solid line, with the grey band indicating the 10-90% uncertainty range).

Since the North Sea is a shallow coastal sea, temperatures are expected to respond relatively fast to climate changes, and this could potentially change the precipitation

distribution within the Netherlands. Indeed, over the last 55 years already a trend in the difference between the coastal zone and inland area is observed. The coastal area has become wetter compared to the inland area (Figure 2). Also, the period with the largest difference between coastal zone and inland area has shifted from the autumn season to late summer.

From daily observations the dependency of precipitation intensity on the sea surface temperature can be derived (*Lenderink et al.* 2009). Also high resolution model simulations can be used to derive these dependencies on a case basis. Both show that under specific circulation conditions (mostly cold cyclonic conditions) the dependency can be large. In the coastal area up to 10-15 % more precipitation could fall per degree temperature rise of the North Sea.

4. Relation to Clausius-Clapeyron

Increases of precipitation with temperature are generally found to be equal or lower than the Clausius-Clapeyron relation. However, we show that for the shorter time scales (hourly) and the local scale (coastal zone, station) dependencies can be much larger. These stronger dependencies are likely due to positive feedbacks in the intensity of updrafts in the convective clouds (*Lenderink and Van Meijgaard,* 2008) and locally strong dependencies of sea surface evaporation on temperature (*Lenderink et al.* 2009).

5. A plea for high resolution modeling

The resolution in present-day state of the art regional climate simulations is order 25 km (ENSEMBLES, *Hewitt and Griggs* 2004). In addition, regional modeling systems do not generally contain an ocean component, but obtain sea surface temperatures from global model simulation directly. In particular, for coastal seas temperature responses to changing atmospheric conditions could therefore be strongly underestimated. Thus, our present models only partly resolve the processes that may lead to strong extremes on the local (here and now) level. Considering the societal relevance of these extremes we therefore make a strong plea for high resolution (< 10 km resolution) coupled regional modeling systems.

References

Held, I. M. & Soden, B. J., Robust responses of the hydrological cycle to global warming. *J. Clim.* **19**, 5686–5699, 2006.

Hewitt, C. & Griggs, D. Ensembles-based predictions of climate changes and their impacts (ENSEMBLES). *Eos* **85**, 566, 2004.

Lenderink, G., van Ulden, A., van den Hurk, B. & Keller, F. A study on combining global and regional climate model results for generating climate scenarios of temperature and precipitation for the Netherlands. *Clim. Dyn.* **29**, 157–176, 2007.

Lenderink G. & Van Meijgaard E. Increase in hourly precipitation extremes beyond expectations from temperature changes, *Nature Geoscience,* **1**, 8, 511-514, 2008.

Lenderink, G., E. van Meijgaard & Selten F., Intense coastal rainfall in the Netherlands in response to high sea surface temperatures: analysis of the event of August 2006 from the perspective of a changing climate. *Clim. Dyn.*, **32**, 19-33, 2009.

Van Ulden, A. P. & van Oldenborgh, G., Large-scale atmospheric circulation biases in global climate model simulations and their importance for climate change in central Europe. *Atmos. Chem. Phys.* **6**, 863–881, 2006.

Chances of the global-regional two-way nesting approach

Philip Lorenz and Daniela Jacob

Max Planck Institute for Meteorology, Hamburg, Germany; philip.lorenz@zmaw.de

1. Introduction

Large scale atmospheric processes influence smaller ones, which in turn affect the evolution of the regional climate: this paradigm is the basis for one-way nested simulations with regional climate models (RCMs) driven by data from general circulation models (GCMs).

However, small scale processes are at least influencing large scale processes too and could have in key regions significant impacts on the evolution of the general circulation: this paradigm was the main motivation for the development of a two-way nested GCM-RCM climate model system, in which feedback from the RCM to the GCM takes place in a selected region (see figure 1). This feedback is accounting for processes which are not resolved by the relative coarse resolution of the GCM, but which are resolved by the finer resolution of the RCM.

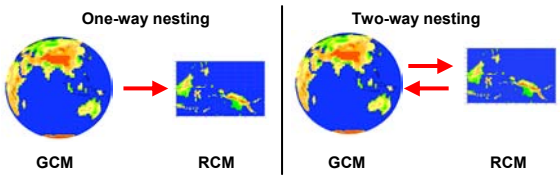

Figure 1. Illustration of one-way nesting versus two-way nesting.

Another motivation for performing two-way in contrast to one-way nested RCM simulations is a higher compatibility between the RCM's internal dynamics and the lateral boundary conditions. The GCM adapts to the large scale state of the RCM by the two-way nesting technique feedback, and is providing therefore more consistent boundary data.

For investigating the former mentioned questions, a two-way nested global – regional climate model system has been developed and applied in several simulations. A description of the model system and introductions to different analysis will be given within the following sections.

2. The two-way nested model system

The developed two-way nested model system consists of Max Planck Institute (MPI-M) climate models, the GCM ECHAM4 and the RCM REMO. Both the spectral GCM ECHAM4 and the grid-point RCM REMO use the same set of physical parameterisations. The feedback from the RCM to the GCM on all prognostic variables takes place at every time of the GCM (24 min. in T42 resolution). More details about the two-way nested model system are given in *Lorenz and Jacob* (2005).

10-year integrations using observed sea surface temperature data (AMIP; 1980-1989) have been carried out with the two-way nested model system for different two-way nested regions. In all simulations the GCM was applied in a spectral T42 horizontal resolution (~250 km in grid-point space), and the RCM in a 0.5° (~55 km) horizontal resolution.

3. Influence on the general circulation

For the analysis of the effects of the two-way nesting approach on the general circulation, a stand-alone ECHAM4 run has been performed and compared against two-way nested GCM-RCM runs. At least for the two-way nested region covering the tropical Maritime Continent a positive influence on the general circulation was analyzed and published in *Lorenz and Jacob* (2005).

4. One-way versus two-way nested RCM simulations

Additional one-way nested RCM simulations have been carried out for some of the domains used for the two-way nested GCM-RCM simulations. The comparison of one-way versus two-way RCM results reveal a significant reduction of typical RCM boundary artefacts (like unrealistic precipitation close to the lateral boundaries) in the two-way nested simulations, and furthermore an influence on the interior of the regional model domains.

5. Influence of the lateral boundary data update frequency in one-way nested simulations

Most state of the art RCM's use 6-hourly output from GCMs or (re-)analysis as lateral boundary data. Within the framework of the two-way nested model system it is possible to perform one-way nested RCM simulations using GCM output down to a time interval of 24 minutes, which is the internal time step of ECHAM4 in T42 resolution. For the domain covering the Maritime Continent only very small differences were found between RCM runs with the usual 6 hourly update frequency and runs with an increased update frequency of 24 minutes.

6. Conclusions

An overview of the major results of the investigations within the two-way nested model system framework will be presented; and prospects and limits of the two-way nesting approach will be discussed.

References

Lorenz, P. and Jacob, D., Influence of regional scale information on the global circulation: a two-way nesting climate simulation, *Geophysical Research Letters*, Vol.32, L18706, doi:10.1029/2005GL023351, 2005

Very high-resolution regional climate simulations over Greenland with the HIRHAM model

Philippe Lucas-Picher, Jens H. Christensen, Martin Stendel and Gudfinna Aðalgeirsdóttir

Danish Meteorological Institute, Lyngbyvej 100, DK-2100 Copenhagen Ø, Denmark; plp@dmi.dk

1. Introduction

Recent progress in available computer power allows regional climate models to run at an increasingly higher horizontal resolution, down to the order of a few kilometers. At this resolution, climate simulations over Greenland become more realistic, in part due to the enhanced description of the rugged topography of the ice cap that affects the atmospheric circulation. Climate simulations at such resolution are very interesting for permafrost models, which require detail values of temperature and precipitation on the margin of the Greenland glacier. Moreover, the description of climate variable at high resolution is also very useful for glacier model to compute the surface mass balance of the glacier. Thus, a RCM simulation at 5 km simulation is presented. At the same time, it is also interesting to assess the added value of high-resolution simulations over Greenland, by comparing regional climate simulations with different resolutions.

2. Methodology

Three regional climate model simulations are performed with the HIRHAM model using three different resolutions (5, 25 and 75 km) for a similar domain covering the entire Greenland. The simulations cover the period 1989-2005 with 31 vertical levels and use the ERA-Interim as lateral boundary conditions. The analysis focuses on the validation of these simulations by using observation records from ground stations and on the emerging climate details that accompany increasing resolution.

3. Preliminary results

This work is in progress. When writing the abstract, the simulations are ongoing in the supercomputer. A preliminary simulation was executed to get a first idea of the performance of the HIRHAM model at 5 km resolution. The simulation covers the same period (1989-2005) and resolution (5 km) with 19 levels for a domain covering south of Greenland. The domain contains 386 x 386 grid cells. At first sight, the simulation makes sense when comparing with observation data as CRU (not shown). However, a deeper analysis with observation records from ground stations is required to validate the simulation because spatial observation database is only available at coarse resolution and is produced from ground stations, which are sparsely distributed over Greenland. Figure 1 shows a zoom of the topography and of the 1989-2005 precipitation climatology in summer (JJA) in the south of the domain. We can see in Fig. 1b the details of the precipitation pattern, which is in agreement with the topography in Fig. 1a. Such details for the precipitation pattern are promising to feed permafrost and glacier models.

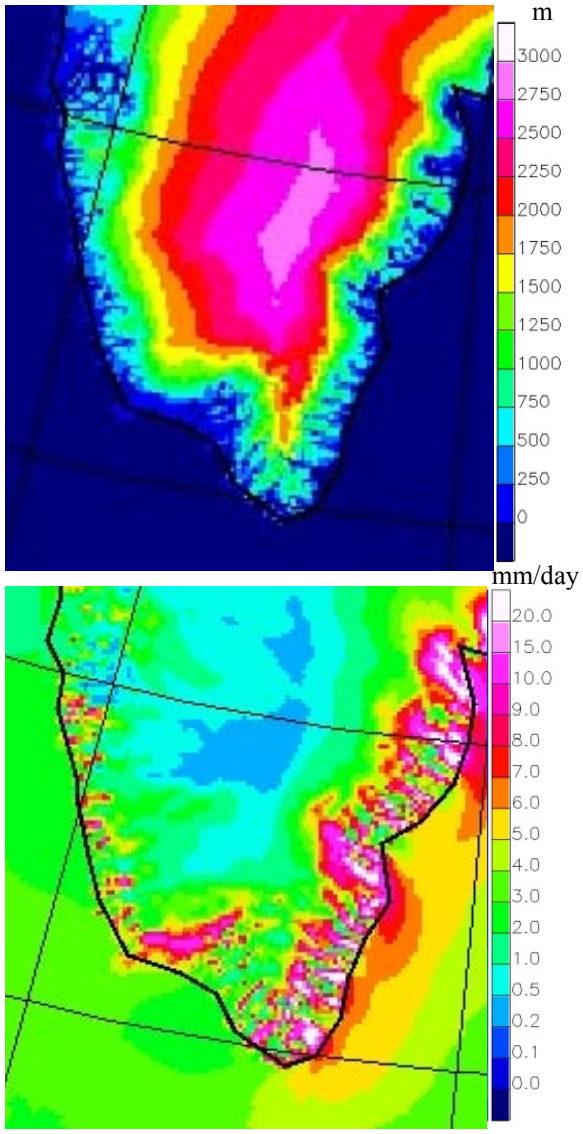

Figure 1. Zoom of the south of the domain for a) the topography in meters and for b) the 1989-2005 precipitation climatology in summer (June-July-August) in mm/day.

4. Coming next…

A deeper validation of the simulations will be done using available observation records from ground stations. We will particularly pay attention to the quality of the precipitation, which is one of the controlling fields for a good simulation of the surface mass balance of the glacier and permafrost conditions surrounding the ice sheet.

Time invariant input parameter processing for applications in the COSMO-CLM Model

Gerhard Smiatek[1], Goran Georgievski[2] and Hermann Asensio[3]

[1]Institute for Meteorology and Climate Research, Atmospheric Environmental Research (IMK-IFU), Forschungszentrum Karlsruhe GmbH (gerhard.smiatek@imk.fzk.de
[2]BTU Cottbus, Chair of Environmental Meteorology (goran.georgievski@tu-cottbus.de)
[3]Deutscher Wetterdienst, (hermann.asensio@dwd.de)

1. Introduction

Topography, soil characteristics, land use and land cover as well as associated vegetation parameters are key information in Soil-vegetation-Atmosphere-Transfer (SVAT) schemes widely applied in atmospheric models in parameterization of surface exchange processes. With exception of seasonal changes in the leaf area index (LAI), vegetation fraction or roughness length, the geodata input is usually kept constant in a simulation and can therefore be considered as a time-invariant parameter..

2. Data Processing

The quality of the data input can have a significant influence on the simulation results. Block (2007) has shown changes of annual mean values in the order of 0.25 K for the 2m-temperature related to the source of the leaf area index data, vegetation cover, soil data, and derived parameters. Box and Rinke (2003) identified systematic model biases of GTOPO30 elevation data set over Greenland. In 50 km grid cells employed by the HIRHAM regional climate model the errors ranged up to −840 meters.

Errors result not only from the quality of the globally available data sets on topography, soil characteristics and land use but also from way how these data are processed. Investigations with various compilers and compiler options revealed differences up to 20 meters in the average elevation in some model grid cells covering complex terrain. Slightly reduced precision in the domain coordinates might yield even higher differences (see Figure 1).

The paper presents in broad term the time invariant data preprocessor PEP (Smiatek et. al., 2008) used in the COSMO-CLM (COnsortium for Small-scale MOdeling in CLimate Mode). The preprocessor is used to transform various global geospatial data into geometrical resolution and into rotated coordinates system specified by the model user. Especially newly available data, such as the Harmonized World Soil Database at 30 arc-second resolution, or Global Database of Land Surface Parameters (ECOCLIMAP) (Masson et al., 2003) will be presented.

Furthermore, issues resulting from the data processing and data aggregation and interpolation into the rotated coordinates system will be discussed.

In the third part the paper concentrates upon the question how the errors resulting from the time invariant data preprocessing propagate in a long term COSMO-CLM simulation driven with ECHAM 5 boundary forcings.

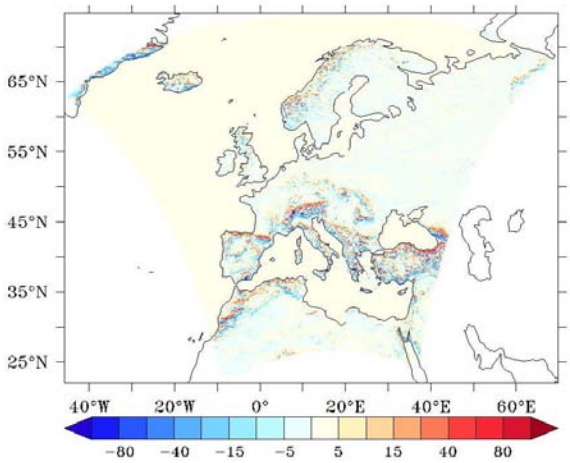

Figure 1 Differences in elevation in meters in a COSMO-CLM domain resulting from reduced precision in calculation of the domain coordinates

References

Block, A. Uncertainties of surface and soil parameters and their impacts on regional climate simulations (in german), Ph.D. thesis, BTU Cottbus, Fakultät für Umweltwissenschaften, 2007

Box J.E., and A.Rinke, Evaluation of Greenland ice sheet surface climate in the {HIRHAM} regional climate model using automatic weather station data., J. Climate, Vol. 16,1 302–--1319, 2003

Masson V., J.-L. Champeaux, F. Chauvin, C. Meriguet, and R. Lacaze, A global database of land surface parameters at 1-km resolution in meteorological and climate models, Journal of Climate, Vol. 16, 1261-1282, 2003

Smiatek, G., Rockel, B. and U. Schättler, Time invariant data preprocessor for the climate version of the COSMO model (COSMO-CLM), Meteorologische Zeitschrift, Vol 17., No. 4, pp. 395-405, 2008

Impact of convective parameterization on high ressolution precipitation climatology using WRF for Indian summer monsoon

Sourav Taraphdar, P. Mukhopadhyay, B. N. Goswami and K. Krishnakumar

Indian Institute of Tropical Meteorology, Pune – 411008, India. sourav@tropmet.res.in

1. Introduction

The Indian monsoon rainfall shows significant variability in spatial and temporal scale. The temporal variability causes intraseasonal, interannual and multi-decadal scale oscillations and spatial variability causes the heterogeneous precipitation distribution from north to south and east to west. These variabilities are caused by two types of forcing namely slowly varying large scale surface boundary conditions e. g. sea surface temperature (SST), snow cover etc. and the regional forcing from topography e. g. Himalayas and Western Ghats etc. Thus resolving the regional heterogeneity is one of the key to improve the precipitation distribution over the region (Giorgi and Mearns 1991). It is also reported that higher resolution AGCM helps in improving the monsoon simulation, however very high resolution AGCM requires large computational resources. Thus the computationally less expensive strategy of running regional models embedded in AGCM gain popularity in simulating regional climate at higher resolution since mid 90s.

To evaluate the sensitivity of convective parameterization schemes on monsoon simulation, several attempts were made. Ratnam and Kumar (2005) simulated two contrasting years of monsoon 1987 and 1988 by a mesoscale model (MM5) at 45 km resolution with variety of cumulus parameterization schemes. They found Betts-Miller-Janjic (BMJ) and Kain-Fritsch (KF) has certain merits compared to Grell. At this resolution, large scale monsoonal features can be captured but to resolve the physiographical heterogeneity due to topography, ocean etc. of the region, higher resolution regional climate models (RCM) are required (Im et al. 2006). Thus, it remains to be seen whether the mean monsoon rainfall bias improves with a high resolution (Less than 20 km) mesoscale model. Therefore, the first objective of the present paper is to produce robust daily monsoon climatology over Indian region at high resolution by various cumulus parameterization schemes and its validation with available observed rainfall data. Along with this attempt will also be made to identify the models ability to correctly capture the underlying spatio-temporal variability of precipitation. The detail investigation of this kind only can help to decipher the weakness in the formulation of moist convection which can be improved further. To gain sufficient insight for further development that would reduce the uncertainties in the simulations, the third goal of the paper is to investigate and identify the possible sources of deviations in simulation arising from different convective closures.

2. Model, data used and experimental design

The non-hydrostatic, fully compressible with a terrain following sigma mass co-ordinate mesoscale model WRF-ARW version 2.2 developed by National Center for Atmospheric Research (NCAR) has been used for the present study. The model is used with two nested domains with horizontal resolutions of 45 and 15 km and 31 sigma levels with model top at 10 hPa. The model mother domain covers the large scale Indian monsoon region where the nested domain focuses mainly on the Indian land masses. The physical parameterizations schemes used in the model is with Lin microphysics, Monin-Obukhov similarity scheme for surface layer, Yonsei university scheme for PBL, RRTM scheme for long wave and Dudhia scheme for short wave in all the numerical experiments. The experiments are differing only by three convective parameterization schemes namely KF (Kain and Fritsch 1993), BMJ (Betts-Miller (1986); Janjic 1994) and Grell-Devenyi (GD; Grell and Devenyi 2002).

In this study, the mother domain simulations are driven by the National Center for Environmental Prediction (NCEP)/ NCAR reanalysis data at a resolution of 2.5°. The 6-hourly SST was obtained by linearly interpolating the daily SSTs of RTG and used as the slowly varying lower boundary condition for the model. The model simulation spans from 1 May to 31 October for the year 2001 to 2007. The daily precipitation simulated by the model is compared with the daily gridded rainfall data of India Meteorological Department (IMD) at 1°x1° resolutions for the land areas and for the land-ocean area the GPCP and TRMM rainfall are used.

3. Results and Discussion

a. The monsoon circulation pattern

It is important to examine whether the driving field in the mother domain are adequate for the nested domain particularly in connection with synoptic scale climatic features of Indian summer monsoon. So the JJAS mean wind (2001-2007) at 850 hPa for each of the three schemes and from NCEP/NCAR (NNRP) reanalysis are showed in Fig. 1. The large scale southwesterly flow over Arabian Sea and Bay of Bengal (BOB) and a cyclonic vorticity in the north of BOB are reasonably captured by all the three cumulus schemes (Figs. 1b-d) as compared to the NNRP (Fig. 1a).

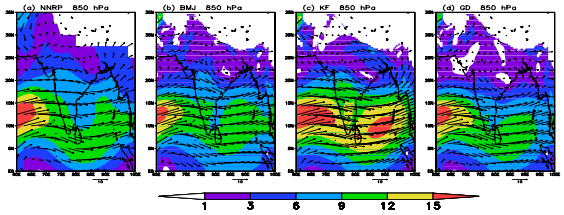

Figure 1. JJAS averaged mean 850 hPa wind (m s^{-1}) from (a) NNRP, (b) BMJ, (c) KF and (d) GD for the year 2001-2007.

However the wind field by KF (Fig. 1c) over the Arabian Sea and BOB appears to be stronger than the observation (Fig. 1a). The BMJ is found to have (Fig. 1b) simulated the most realistic wind field in both the oceanic basin where as the GD (Fig. 1d) has produced a weaker wind field over BOB although the Arabian Sea branch is reasonably reproduced. The upper air (200 hpa) easterly and the Tibetan anticyclone are captured by all the three experiments with BMJ, KF and GD (Figures not shown) but with varied intensity. The center of the anticyclone is

found to be shifted eastwards in all the three experiments as compared to the NNRP. In general it can be said that compared to KF and GD, BMJ is in good agreement with the observation in both the level.

b. Distribution of mean monsoonal precipitation and underlying variability

In comparing three convective parameterization schemes from IMD, KF is found to have high moist bias over central Indian region along with the west coast (Fig. 2b) in the seasonal mean. GD (Fig. 2c) on the other hand shows the opposite, where as BMJ (Fig. 2a) is found to produce most reasonable seasonal distribution of rainfall out of the three convective schemes.

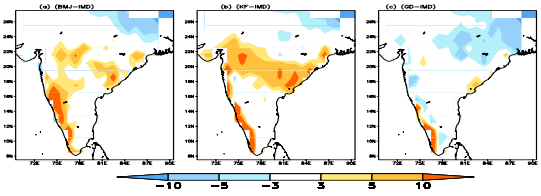

Figure 2. Spatial distribution of model simulated JJAS averaged precipitation difference of (a) BMJ, (b) KF, and (c) GD from IMD observation.

To investigate the spatio-temporal variability of precipitation superimposed in the seasonal mean, daily mean rainfall PDFs are computed for different range of rain-rates. The PDF plot indicates that BMJ and KF underestimates the observation for lighter rain-rates (<10 mm/day) and overestimates for rain-rate categories more than 10 mm/day. GD on the other hand shows a mixed distribution with initially the PDF being higher than observation for lighter rain-rate and lower in the moderate (between 10-40 mm/day) category followed by an overestimation in the heavy (> 40 mm/day) category. The time evolutions of PDF for the above three rain rate categories are computed. In the lighter category GD shows a systematic overestimation throughout the season whereas BMJ and KF have problem (overestimation) during the first 30 days of integrations. In the moderate rain-rate category GD has systematically underestimated the observed PDF throughout the season. BMJ and KF have underestimated the observed PDF for the first 30 days and are in good agreement in the rest of the season for the same category. In the heavy category KF has significantly overestimated the observed PDF throughout the season. Further by analyzing the percentage contributions of each rain-rate to the total seasonal rain for each of the three schemes, it is found that GD has substantially large contribution to the total rain by the light rain-rate bins and significantly lesser contribution from moderate rain-rates. BMJ appears to produce the closest possible contribution amongst the three for all the rain-rate categories. The higher percentage contribution by KF from the rain-rate bins of 25 mm/day or more along with significant overestimation of observed PDF in the high rain-rate category can be attributed to the positive biases in seasonal mean precipitation by KF. To gain further insight about the role of each scheme in adding dry or moist bias in the evolution of seasonal rain and its spatial patterns, the time evolution and also the spatial pattern of percentage of rainy grid cells are computed. This brings out that the underestimation of precipitation in GD mainly came from the moderate rain-rate and overestimation of KF is because of heavy rain-rate.
After identifying details of biases for each convection schemes arising from different rain-rate category and its manifestation on spatio-temporal variability of precipitation, a critical evolution of apparent heat source (Q_1) and moisture sink (Q_2) is carried out over mother domain to determine the physical reason behind the deficiency in reproducing seasonal mean precipitation. The seasonal evolution of Q_1 and Q_2 clearly tells about the competition between the evaporation and condensation throughout the season. It is found that KF could not reproduce the domination of evaporation over condensation at the time of withdrawal which means KF continues to produce rain even at the end of the season. Whereas GD shows a very weak seasonal cycle with the natural cycle of evaporation and condensation is totally missing. On the other hand BMJ could realistically depict the domination of evaporation compared to condensation till the mid June prominently. The enhancement of condensation over evaporation after the monsoon onset and followed by a maxima in the July-August and reduction of condensation at the time of withdrawal is only reasonably captured by BMJ.

4. Conclusion

The erroneous spatio-temporal evolution of apparent heat source and moisture sink is the main reason behind the seasonal bias of precipitation by different convective closures. KF appears to produce stronger instability and intense updraft and end up with a large moist bias. GD on the other hand produces weaker instability and weaker updraft to produce relatively dry bias. BMJ is found to be better than KF and GD but it also shows certain biases compared to observation. The improvement in formulation that can give a more accurate profile of Q_1 and Q_2 and remove the deficiency of producing the right PDF at correct proportion could result in the improvement of the precipitation bias significantly in weather and climate mode of application of regional model.

References

Betts, A. K., and M. J. Miller, A new convective adjustment scheme. Part II: Single column tests using GATE wave, BOMEX, and arctic air-mass data sets. *Quart. J. Roy. Meteor. Soc.,* 112**,** 693–709, 1986.

Giorgi, F., L. O. Mearns, Approaches to the simulation of regional climate change: A review, *Rev. Geophys.,* 29, 191–216, 1991.

Grell, G. A., and D. Devenyi, A generalized approach to parameterizing convection combining ensemble and data assimilation techniques. *Geophys. Res. Lett.,* 29**,** 1693, 2002.

Im, E-S., E-H. Park, W-T. Kwon, and F. Giorgi, Present climate simulations over Korea with a regional climate model using a one way double nested system, *Theor. Appl. Climatol*, 86, 187–200, 2006.

Janjic, Z. I., The step-mountain eta coordinate model: Further developments of the convection, viscous sublayer, and turbulence closure schemes, *Mon. Wea. Rev.,* 122**,** 927–945, 1994.

Kain, J. S., and J. M. Fritsch, Convective parameterization for mesoscale models: The Kain–Fritcsh scheme. The Representation of Cumulus Convection in Numerical Models*, Meteor. Monogr., 24*, 165–170, 1993.

Ratnam, J. V., and K. KrishnaKumar, Sensitivity of the simulated monsoons of 1987 and 1988 to convective parameterization schemes in MM5, *J. Climate*, 18, 2724–2743, 2005.

Development of a regional ocean-atmosphere coupled model and its performance in simulating the western North Pacific summer monsoon

Liwei Zou, Tianjun Zhou and Rucong Yu

LASG, Institute of Atmospheric Physics, Chinese Academy of Science, Beijing 100029, China.
zoulw@mail.iap.ac.cn

1. Abstract

A regional ocean-atmosphere coupled model is developed with the aim to improve Asian monsoon simulations. It consists of the Regional Climate model (CREM) developed at the State Key Laboratory of Numerical Modeling for Atmospherics Sciences and Geophysical Fluid Dynamics / Institute of Atmospheric Physics (LASG/IAP) and the revised Princeton Ocean Model (POM2000) developed by Princeton University. The exchanges of coupling fields, including sea surface temperature (SST), heat flux and wind stress, are synchronized by Ocean Atmosphere Sea Ice Soil 3.0 (OASIS3.0) coupler developed at CERFACS (Toulouse, France).

The performance of the coupled model in simulating the Western North Pacific Summer Monsoon (WNPSM) during the warm season (May-August) in 1998 is compared with a stand-alone CREM simulation. The results show that the rainfall and heat fluxes, especially the latent flux over Western North Pacific (WNP), are significantly improved in the coupled model. The coupled simulation improves the spatial pattern of the rainfall and increases the intensity of the rainfall over the WNP. Furthermore, the intra-seasonal oscillation is better reproduced in coupled simulation. However, the model overestimates the rainfall over the western northern flank of the western Pacific subtropical high and SST over the whole domain.

2. Model configuration and experiment design

The configuration of the coupled model is illustrated in Fig.1.The atmospheric component of the coupled model is CREM which is developed at LASG/IAP based on a numerical forecast model. The CREM is a hydro-static, primitive-equation, grid point model and has uneven 32 vertical levels in an eta (η) coordinate, with the model top at 10 hPa. The Arakawa E-grid is employed in CREM and the spatial resolution is 37 km in current version. The Biosphere-Atmosphere Transfer Scheme version 1e (BATS1e) is used to compute the exchanges between the land and atmosphere, and the modified Betts-Miller cumulus parameterization scheme is applied to calculate the convective rainfall (Shi et al., 2009)

The ocean component is the Princeton Ocean Model 2000 (POM2000). It is a three-dimensional, primitive equation model using a sigma vertical coordinate and a free ocean surface with embedded turbulence. The version used in this study was improved by Qian (2000). The model employs a horizontal resolution of 0.5°×0.5°, and there are 16 levels in the vertical direction. A simple radiation method is adopted as the open boundary condition.

The OASIS3.0 coupler is used to bridge the atmospheric model (CREM) and ocean model (POM2000). The heat flux and wind stress which are necessary to drive POM2000 are derived from CREM, while the SST provided by POM2000 is used as the lower boundary of CREM.

The model domain covers the region of -5°S-40°N, 100°E-160°E. The couple model is integrated from May 1 to Aug 31 in 1998 (Coupled Run). In order to facilitate comparison, a stand-alone CREM simulation (Control Run) forced by weekly OISST is also performed in the same period. The daily GPCP rainfall data (resolution: 1°×1°) are used as observational evidence for model assessment.

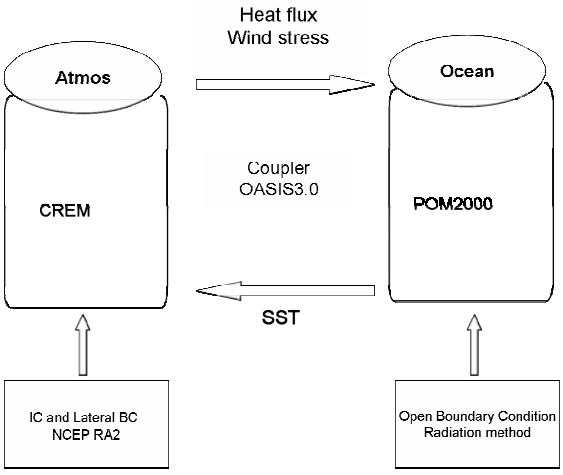

Figure 1. Schematic description of the coupled model; initial condition and lateral boundary condition of the CREM are obtained from NCEP RA2. A simple radiation method is adopted to deal with the open boundary problem of the regional ocean model (POM2000). The CREM and POM2000 are coupled sequentially with an interval of 3hr.

3. Some results

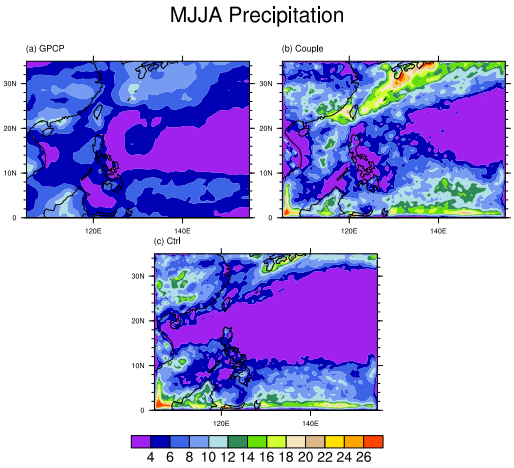

Figure 2. The spatial distribution of the rainfall (units: mm/day) over WNP area averaged during the simulation period from (a) GPCP (b) Coupled Run (c) Control Run

The averaged rainfall for the whole simulated period from GPCP, Coupled Run and Control Run are compared in Fig.2. The major rain band is located over the equatorial region and the western north flank of the subtropical high in the GPCP data. The coupled run well simulates these typical characteristics. The spatial correlation coefficient between the coupled run and GPCP is 0.59(0.31) over ocean (land), while that of the control run is 0.41(0.17). These indicate that the coupled run improves the simulation of the spatial pattern of rainfall over both land and ocean. However, both the control run and coupled run produce a narrow rain belt near the south boundary of the model. In addition, the coupled run overestimates the rainfall over the western northern flank of the western Pacific subtropical high.

The evolution of rainfall averaged over the central area of WNP (10°N-25°N, 130°E-150°E) is shown in Fig.3. The control run underestimates the intensity of rainfall, while the coupled run significantly increases the intensity. The correlation coefficient between the GPCP and control run (coupled run) is 0.43(0.61), both are statistically significant at the 5% level.

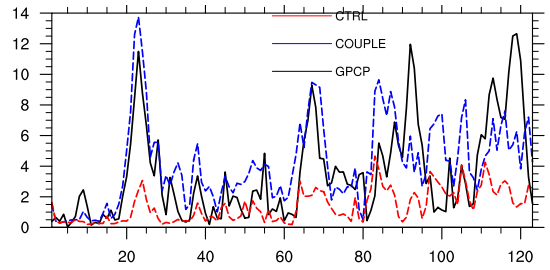

Figure 3. The evolution of rainfall averaged within (10°N-25°N, 130°E-150°E). Black line: GPCP; Red line: Control Run; Blue line: Coupled Run. The tick mark of the abscissa denotes days from May 1 to August 31 in 1998. The unit of the ordinate is mm/day.

Figure 4 shows the time- longitude cross section of the rainfall averaged between 5°N -25°N. An intra-seasonal oscillation is evident in the GPCP data. This feature is reasonably reproduced in the coupled run, but poorly in the uncoupled control run, suggesting the importance of air-sea coupling.

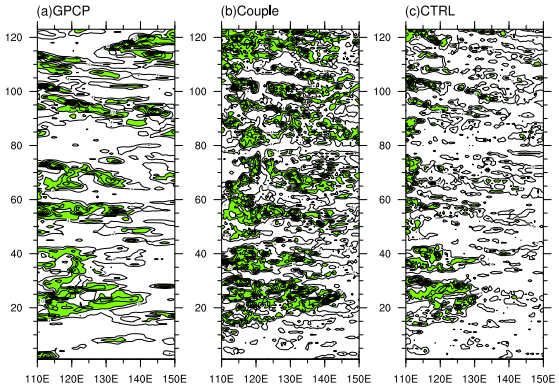

Figure 4. The time- longitude cross section of the rainfall averaged between 5°N -25°N. The tick mark of the ordinate denotes the day. The rainfall intensity larger than 6mm/day are shaded.

The mean latent heat flux, sensible heat flux, shortwave radiation and longwave radiation averaged within 10°N-25°N, 130°E-150°E are given in Table 1.The latent heat, sensible heat and longwave radiation are increased evidently in the coupled run, especially for the latent heat which is significantly underestimated in control run. The improvement of the simulation of the surface heat fluxes in the coupled run reveals the crucial role of the air-sea coupling over this region.

	Latent heat	Sensible heat	Shortwave radiation	Longwave radiation
OAFLX	112.12	5.77	260.84	43.98
Coupled	123.80	2.79	249.82	32.26
CTRL	56.17	-1.13	266.47	29.13

Table 1. The mean latent heat, sensible heat, shortwave radiation and longwave radiation (units: w/m^2) averaged within 10°N-25°N, 130°E-150°E.

4. Concluding remarks

A regional ocean-atmosphere coupled model is developed. Case studies of the WNPSM in 1998 indicate the improvement of coupled model due to the inclusion of air-sea coupling. The mechanisms behind this improvement deserve further study. Future works will also examine more cases with the model.

Reference

Shi HB, Yu RC, Li J, Zhou TJ. Development of a regional climate model and evaluation on its simulation of summer climate over eastern China, *Journal of the Meteorological Society of Japan*, 2009. (in press)

Qian YF. Simulation of the annual cycle of the South China Sea temperature by POM, *Chinese Journal of Atmospheric Sciences*, 24, 373-380, 2000. (In Chinese).

Regional climate change impact studies in the upper Danube and upper Brahmaputra river basin using CLM projections

B.Ahrens and A.Dobler

Institute for Atmosphere and Environment, Goethe-University, Frankfurt/M., Germany (Bodo.Ahrens@iau.uni-frankfurt.de)

1. Introduction

This contribution focuses on regional impact studies based on climate change projections from the regional climate model CLM (the climate version of the COSMO-model, see www.clm-community.eu) in two alpine regions. To this end, CLM simulations have been carried out in two domains, one containing the upper Danube river basin (UDRB, see Fig. 1) in the European Alps, the other containing the upper Brahmaputra river basin (UBRB, see Fig. 2) in the Himalayas. The model configurations are detailed in *Dobler and Ahrens* (2008). Inside the two major river basins (RBs), five sub-basins of interest are considered: Lech RB, Salzach RB, Assam, Lhasa RB, and Wang-Chu RB.

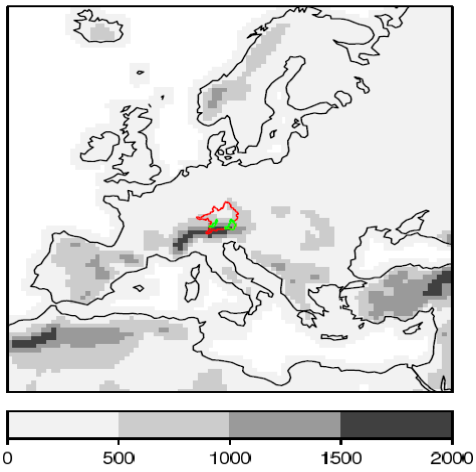

Figure 1: Orography (m) used for the regional climate simulations with the CLM. The colored areas denote the Upper Danube (red), the Lech (left), and the Salzach (right) river basins.

2. Methods

Coarse-scale projections from the ECHAM5/MPI-OM AR4 projections (*Roeckner et al.* 2003) have been dynamically downscaled from about 2° grid resolution to 0.44° for the years 1960-2100 using the CLM. The simulations cover the four SRES scenarios A1B, A2, B1, and the commitment scenario.

Besides annual and seasonal temperature and precipitation amounts, daily precipitation indices are calculated for four seasons on a yearly basis. For the European regions the four seasons used are: spring (MAM), summer (JJA), autumn (SON) and winter (DJF). For the South Asian regions these are: summer (MAM), monsoon (JJAS), post-monsoon (ON) and winter (DJF). An overview on the applied precipitation indices is provided in Table 1. The linear trends of these indices are tested for significance at 5% significance level using the Mann-Kendall trend test.

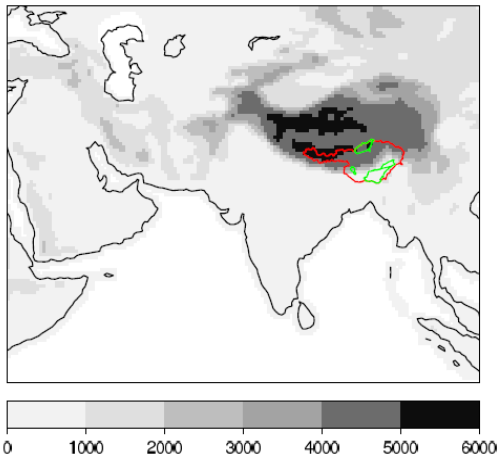

Figure 2: As for Fig. 1, but for the South Asian computational domain with the Assam region (bottom right) and the Upper Brahmaputra (red), the Lhasa (top) and the Wang-Chu (bottom left) river basins.

To remove constant model biases, a normalization via division by the mean value of the reference period 1971-2000 has been carried out. This bias has to be corrected for application of the downscaled projections in inmpact research. This assumes that the bias is constant – an assumption that is debated.

Acronym	Description	Unit
PFRE	Fraction of wet days	1
PINT	Mean precipitation amount on wet days	mm/d
PQ90	90% quantile of wet days precipitation	mm/d
PX5D	Max. 5-day precipitation	mm
PCDD	Longest period of consecutive dry days	d

Table 1: List of daily precipitation statistics.

3. Results and conclusions

An overview on the projected precipitation statistics for the A1B scenario and the years 1960-2080 is given in *Ahrens and Dobler* (2008). While the focus therein is on one single scenario, we here present the results from all four scenario runs. With this we are able to examine the impact uncertainties coming from the different scenarios

and to find possible connections between future emissions and trends in the indices.

Consider for example the statistics "longest period of consecutive dry days", PCDD, as an indicator for possible trends in dry spells. Table 2 shows the different projected changes from the four scenario runs in the UDRB, the UBRB and their sub-areas for the 3rd season (summer in Europe and monsoonal in South-Asia) of the years 1960 to 2080.

The table shows that the two scenarios with the highest emissions (A1B and A2) show a larger positive trend in consecutive dry days. Note that in these two scenarios the emission up to the year 2070 is higher in A1B than in A2. The B1 and commitment scenario (with emissions fixed at the year 2000 level) trends are smaller and in most river basins not significant. This indicates a direct connection between future emissions and trends in summer dry spells. Besides these trends only the positive PCDD trend in winter for the Brahmaputra river basins are significant. It is interesting to note that the PCDD trends are quite consistent in the projections by ECHAM5 and by CLM.

The other indicators show a more heterogeneous picture. For example, precipitation intensities increase in spring and autumn in the European basin, but in the monsoon season in the South Asian basin. A positive trend in maximum precipitation in five days, PX5D, is significant only in spring in Europe. These trends are also less consistent between the ECHAM5 and the CLM projections. The similarities and differences in ECHAM5 and CLM trends have to be carefully investigated to understand and assess the potential added value of downscaling for the presented indicators.

Summer (JJA)	A2	A1B	B1	COM
UDRB	**26**	**31**	08	18
Lech RB	**22**	**29**	8	7
Salzach RB	**21**	**30**	1	7
Monsoon (JJAS)				
UBRB	**16**	**21**	**12**	12
Assam	**20**	**26**	9	8
Wang-Chu RB	13	**16**	5	0
Lhasa RB	**36**	**52**	**25**	**23**

Table 2: Seasonal changes of PCDD (% / 100 years) in different areas during the time period 1960-2080. For normalization, the yearly values have been divided by the mean of the reference period 1971-2000. Bold values are statistically significant (at the 0.05 level).

References

Ahrens, B., A. Dobler (2008): Climate change projections in the upper Danube (European Alps) and the upper Brahmaputra (Himalayas)**,** *17th Conference on Applied Climatology (Extended Abstract),* pp. 6.

Dobler, A., B. Ahrens (2008): Precipitation by a regional climate model and bias correction in Europe and South-Asia. Meteorol. Zeitschrift, 17(4), 499-509.

Roeckner, E., et al. (2003): *The Atmospheric General Circulation Model ECHAM5. Part I: Model Description*. MPI Report 349, Max Planck Institute for Meteorology, Hamburg, Germany, 127 pp.

River runoff projection of future climate in Latvia

Elga Apsīte, Anda Bakute and Līga Kurpniece

University of Latvia, Faculty of Geography and Earth Sciences, Raina blvd. 19, Riga LV-1586, Latvia, E-mail: elga.apsite@lu.lv

1. Introduction

Traditionally, climate change studies include identification of natural climate variability, attempt to detect a climate signals in historical data and elaboration of possible scenarios for the future (Hisdal et al., 2006). Therefore, different projects and national programs are developed in many countries. In 2006, the Research Program *Climate change impact on water environment in Latvia* (2006-2009) was started (http://kalme.daba.lv). Generic goal of the Programme is to assess short, medium, and long-term impact of climate change on the environment and ecosystems of the inner waters of Latvia and the Baltic Sea, and to create a scientific basis for adaptation of environmental and sectorial policies of Latvia to climate change. This study is a part of the mentioned programme aimed to carry out a simulation of hydrological processes in different river basins and to forecast climate change impact on runoff and nutrient loading in the future.

In Latvia, during the last twenty years, several versions of mathematical models of hydrological processes have been developed: METUL (Krams and Ziverts, 1993), METQ96 (Ziverts and Jauja, 1996), METQ98 (Ziverts and Jauja, 1999), METQ2005 and METQ2006, and the latest version of the METQ2007BDOPT with semi-automatic calibration performance (Apsite et al., 2008). The model is successfully applied to small and relatively large catchments, the brook Vienziemīte (A=5.92 km^2) and the River Daugava (A=81,000 km^2 at the Pļaviņas HPP) respectively. Furthermore, the METQ model has been used for different hydrological tasks, e.g. to evaluate the model performance before and after drainage construction and to estimate the eventual maximum flood (Ziverts and Jauja, 1999), to study eutrophication and hydrotechnical problems of lakes, including climate change effects (Bilaletdin et al., 2004; Ziverts and Apsite, 2005).

This paper addresses: (1) the results of the METQ model, the latest version of the METQ2007BDOPT, calibration and validation for five different river basins in Latvia, and (2) the analysis of meteorological and hydrological data series in projection of future climate, based on a control period (1961-1990) and scenarios (2071-2100).

2. Data and methods

The hydrological model METQ, applied for each of the five river basins with a daily time step in this study, is used to simulate hydrological behaviour of the river runoff particularly for past and future changed climate conditions. The METQ is conceptual rainfall-runoff model of catchment's hydrology, originally developed using Latvian catchments. The latest version of the METQ2007BDOPT has 23 parameters and most of them can be kept constant for different river catchments. The model consists of different routines, including the runoff and hydraulic (if there is a lake in the river basin which considerably influences the hydrological regime of the river). The total runoff consists of three runoff components: Q_1 - surface runoff, Q_2 - subsurface runoff (runoff from the groundwater upper zone) and Q_3 - base flow (runoff from the groundwater lower zone). For more detailed description of this model find Ziverts and Jauja, 1999; Apsite et al., 2008. In general, the structure and simulation of hydrological processes by the METQ model are similar to the HBV (Bergström, 1976; Bergström, 1992) model developed in Sweden.

In this study, the conceptual METQ2007BDOPT model was calibrated and validated for the following differently sized river basins at the gauging stations: the Salaca (A=3220 km^2), the Bērze (A=904 km^2), the Iecava (A=566 km^2), the Imula (A=232 km^2) and the Vienziemīte (A=5.92 km^2). The calibration period was selected from 1961 to 1990 (30-years as the control climate) with an aim to simulate the scenario climate from 2071 to 2100 in the future, and validation period – next ten years from 1991 to 2000.

In the terms of data, the study was based on meteorological and hydrological observed data series from the *Latvian Environment, Geology and Meteorology Agency* and SIA *Meliorprojekts* national data bases. As input data for the METQ2007BDOPT model calibration and validation, daily measurements of air temperature (^{o}C), precipitation (mm) and vapour pressure deficit (hPa) at eleven meteorological stations and daily river discharge (m^3 s^{-1}) and water level (m) of the lake and water reservoir of five hydrological gauging stations, were applied. A statistical criterion R^2 (Nash and Sutcliffe, 1970), a correlation coefficient r, mean values and graphical representation were used in the analysis of the model calibration results.

Meteorological data series (daily air temperature, precipitation and vapour pressure deficit) provided by the National Research Program *Climate change impact on water environment in Latvia* were used for the simulation and the study of the river runoff under changed climate conditions. These data series were developed by the *Faculty of Physics and Mathematics* (FPM) of *University of Latvia*. FPM analyzed 21 regional climate models (RCM) from the EU project PRUDENCE and selected HCCTL model from SMHI (driving from GCM HadAM3H) as the best applicable for Latvian conditions. Description of the used methodology can be found in Bethers et al. (2008). Therefore, in this study the calculated data series of HCCTL present the control period from 1961 to 1990, and HCA2 and HCB2 scenarios from 2071 to 2100.

3. Results and discussions

In this study, the conceptual METQ2007BDOPT model was calibrated and validated to five different size river basins in Latvia. The results of the model calibration for these river basins showed a good coincidence between the observed and simulated daily discharges from 1961 to 1990: the Nach-Sutcliffe efficiency R^2 varies from 0.86 to 0.50 and correlation coefficient r – from 0.91 to 0.71. The best coincidence was obtained for the brook Vienziemīte R^2 – 0.86 and r – 0.91. On one hand, it could be explained by the fact that catchment area is small (only 5.92 km^2) and used meteorological data fit very well to this drainage area, to describe the simulation of hydrological processes. On other hand, we obtained rather good calibration results also for a large river basin such as the River Salaca at Lagaste: R^2 – 0.80 and r – 0.88. The lowest statistical

criterions were found for the rivers Imula and Iecava. The validation of model was done for the next 10-years period - from 1991 to 2000, except for the river gauging stations Imula-Pilskalni and Iecava-Dupši which was closed in 1995. We obtained lower statistical criterions comparing with calibration period for studied gauging stations in this study: the statistical efficiency R^2 varies from 0.77 to 0.44 and correlation coefficient r – from 0.87 to 0.70. One of the main reasons of difference between the simulated and observed runoff values is the quality of precipitation and vapour pressure deficit input data, and location of the available meteorological stations characterising the spatial and temporal distribution of precipitation in the studied drainage area. Another explanation of the above mentioned calibration differences could be a broad palufied flood plain, a high percentage of wetlands in the sub-basins of the river Salaca and a lack of the channel measurements at the outlet of the lake Burtnieks. These reasons determine a specific hydrological regime and additional riverbed measurements for the better simulation of the hydrological processes within the studied catchments.

After learning the results of many researches in Europe and the Baltic region (Hisdal el al. 2006; Danker et al, 2007; Bolle et al, 2008; etc.), we can conclude that in this study we have identified similar tendencies of meteorological and hydrological trends in projections of future climate changes. Analysis of the climate change conditions metrological data in the studied river basins show an average increase in the annual atmospheric temperature by 3.8-4.1 ^{o}C for the HCA2 scenario and by 2.5-2.7 for the HCB2 scenario in the period of 2071 to 2100 comparing to the control period of 1961-1990. The most considerable temperature increase is forecasted for the winter and autumn seasons: 4.1-4.9 ^{o}C HCA2 and 3.0 ^{o}C HCBA2 respectively. Atmospheric precipitation, at the same time, will increase by 11-12% according to the HCA2 scenario and by 8-9% according to the HCB2 scenario. The highest atmospheric precipitation increase is registered in winter, but the major decrease – in the summer and autumn seasons. Climate scenario data, particularly the HCA2 scenario, allows forecasting the eventual decrease of total annual river runoff by 15-20% in the future. The highest increase in the river runoff is registered in winter due to the increase of the mean atmospheric temperature and precipitation, while the decreased river runoff is forecasted for the second half of the year, particularly in autumn. The mentioned changes in the river runoff regimes can be explained by the higher atmospheric temperatures and particularly increased total evaporation as well as decreased amount of precipitation.

References

Apsīte E., Zīverts A., Bakute A. Application of conceptual rainfall-runoff model METQ for simulation of daily runoff and water level: the case of the Lake Burtnieks watershed. *Proc. of Latv. Acad. Sci.,* B 1/2:62, pp. 47-54, 2008

Bergström S. Development and application of a conceptual runoff model for Scandianvian catchments, SMHI, report No.RHO7, Norrköping, 1976

Bergström S. The HBV Model - Its Structure and Applications. *SMHI Reports Hydrology,* 4 (April), 33 pp., 1992.

Bethers U., Seņņikovs J., Timuhins A. Employment of regional climate models as data source for hydrological modeling. Eds.: Sveinsson O., Gardarsson S., Gunnlaugsdottir S. The XXV Nordic Hydrological Conference „Nordic Water 2008", 11-13 August, Reykjavik, Iceland, pp. 373-383, 2008

Bilaletdin Ä., Frisk T., Kaipainen H., Paananen A., Perttula H., Klavins M., Apsite E., Ziverts A. Water Protection Project of Lake Burtnieks. *The Finnish Environment* 670, Pirkanmaa Regional Environment Centre, Tampere, 92 pp., 2004

Bolle H.J., Menenti M., Rasool I. (eds.) Assessment of Climate Change for the Baltic Sea Basin. Regional Climate Studies. Springer-Verlag Berlin Heidelberg, 474 pp., 200

Dankers R., Feyen L., Christensen O.B., Roo A. Future changes in flood and drought hazards in Europe. Ed. by M. Heinonen, 3rd Internationa Conference on Climate and Water, Helsinki, Finland, 4.-7.09.2007. Publisher Finnish Environment Institute, pp. 115-120, 2007

Hisdal H., Roald L.A. and Beldring S. Past and future changes in flood and drought in the Nordic countries. Ed. by S. Demuth, Climate Variability and Change - Hydrological Impacts, IAHS Publ. no. 308, pp. 502-507, 2006

Krams M., Ziverts A. Experiments of Conceptual Mathematical Groundwater Dynamics and Runoff Modelling in Latvia. *Nordic Hydrology* 24, pp. 243-262, 1993

Nash J.E., Sutcliffe J.V. River Flow Forecasting Through Conceptual Models. Part I-A discussion of principles. *Journal of Hydrology* 10, pp. 282-290, 1970

Zīverts A., Jauja I. Konceptuālais matemātiskais modelis METQ96 ikdienas caurplūdumu aprēķināšanai izmantojot meteoroloģiskos novērojumus (Conceptual Mathematical Model METQ96 for the Calculation of daily Discharge using Meteorological Observations). *LLU Raksti* 6, pp. 126-133, (in Latvian – summary in English), 1996

Ziverts A., Jauja I. Mathematical model of hydrological processes METQ98 and its applications. *Nordic Hydrology,* 30, pp. 109-128, 1999

Ziverts, A., Apsite, E. 2005. Simulation of Daily Runoff and Water Level for the Lake Burtnieks. *19th European Conference on Modelling and Simulation ECMS 2005*, Simulation in Wider Europe, 1-4 June, Riga, 633-637.

Acknowledgements

This study was supported by the National Research Program *Climate change impact on water environment in Latvia* and data were provided by *Latvian Environment, Geology and Meteorology Agency* and SIA *Meliorprojekts*.

Application of regional-scale climate modelling to account for climate change in hydrological design for dam safety in Sweden

Sten Bergström, Johan Andréasson and L. Phil Graham

Swedish Meteorological and Hydrological Institute, SE 601 76 Norrköping Sweden, sten.bergstrom@smhi.se

1. Background

Accounting for the impact of climate change on dam safety is not a trivial task in the Nordic climate where, a mix of snowmelt and extreme rainfall determines the most extreme hydrological conditions. Nevertheless, this is required in the new edition of the Swedish guidelines for the determination of design floods for dams (*Svenska Kraftnät, Svensk energi and SveMin,* 2007). Therefore a study has been initiated to assess the impact of climate change on the national guidelines for design floods. The basic question is how to best use regional-scale climate scenarios to account for climate change in hydrological design studies.

2. Methods

The work relies on climate scenarios from the Rossby Centre and the European Ensembles project, the HBV hydrological model and the simulation scheme for design of dams as prescribed in the Swedish guidelines for dam design. Development of the interface between the climate model output and the hydrological simulations is a major effort. It is treated by two methods, *delta change*, where the climate change signal is superimposed upon an observed climate record, and *scaling* were the output from the climate models is used directly after bias-correction (*Yang et al*., 2008).

A number of drainage basins and dams relevant to the power industry have been selected for the studies of dams according to Design Flood Category I (Fig.1).This category represents dams with the greatest consequences in case of a failure.

Figure 1. Basins where climate impact studies for dams according to Design Flood Category I of the Swedish guidelines are carried out.

For dams where the consequences in case of failure are less serious, Design Flood Category II, the 100 year flood is prescribed as criteria for design. The development of 100-year floods in a changing climate is therefore studied in a larger sample of 65 basins in Sweden. The location of these basins is shown in Fig. 2.

Design floods are calculated both according to present day climate conditions and with available climate scenarios. Focus for the design studies in a changing climate is on the first half of the century, but simulations will also be made up to the year 2100.

Figure 2. Location of the 65 test basins used for analysis of the development of the 100-year flood in a climate change perspective.

3. Preliminary results.

A lot of effort has been spent on the scaling interface. It is a complex process to go from a climate model to an off-line hydrological simulation without loosing statistical information. At present the regional climate scenarios from the Ensembles project are being processed and analysed as they appear. Fig. 3 shows an example of the development of 100-year floods according to a number of climate scenarios for River Byskeälven in northern Sweden. It is based on a running frequency analysis with a window width of 30 years.

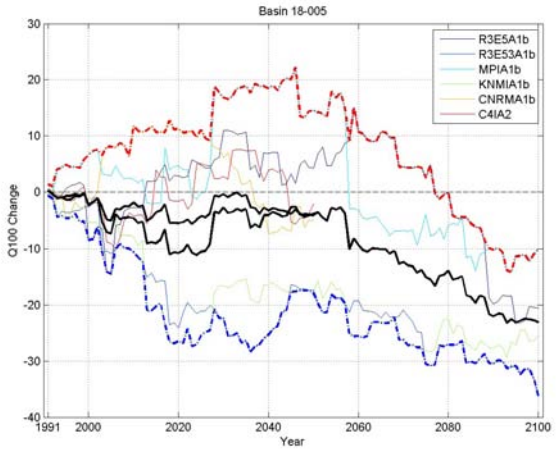

Figure 3. Example of the development of 100-year floods according to a number of climate scenarios for River Byskeälven in northern Sweden. The scale is percent change in relation to the reference period 1961-1990.

4. Future work

Design floods will be carried out for the whole Ensembles-matrix of climate scenarios and all the selected test basins during 2009. The work is carefully monitored by a special committee with representatives from the dam safety authority, the power industry, the mining industry and SMHI. The task of this committee is to recommend how climate change shall be accounted for in future design studies. This will have strong impact on future design of dams but also on the physical planning along the shorelines in Sweden, as the same flood criteria are used for flood risk mapping.

In parallel the results will be discussed with colleagues from Norway, Finland, Iceland, Latvia and Lithuania within the Climate and Energy Systems project.

5. Acknowledgements

The national research is financed by the Swedish dam safety authority (Svenska Kraftnät) and the power industry via Elforsk. The Nordic co-operation, within the CES-project, is financed by Nordic Energy Research. The scientific contribution from the Ensembles project, the staff of the Research department of SMHI and our colleagues within the CES-project is also gratefully acknowledged.

References

Yang, W., Andréasson, J., Graham, L.P, Olsson, J., Rosberg, J. och Wetterhall, F. A scaling method for applying RCM simulations to climate change impact studies in hydrology. *Proceedings from the Nordic Hydrological Conference - Reykjavik, Iceland, 11-13 August 2008, Vol.1, pp.256-265, 2008.*

Svensk Energi, Svenska Kraftnät och SveMin. Riktlinjer för bestämning av dimensionerande flöden för damm-anläggningar – Nyutgåva 2007 (Guidelines for the determination of design floods for Swedish dams – New edition). 2007.

Local air mass dependence of extreme temperature minima in the Gstettneralm Sinkhole with regard to global climate change

Benedikt Bica and Reinhold Steinacker

Department of Meteorology and Geophysics, University of Vienna, Austria; Benedikt.Bica@univie.ac.at
UZA II, Althanstraße 14, 1090 Vienna, Austria

1. Introduction

The 150-m-deep Gstettneralm sinkhole (1270 m asl) in the eastern Austrian Alps is known for having recorded the lowest temperatures in Central Europe (-52.6°C in February 1932). In 14 consecutive winters between 1928 and 1942, the nocturnal temperature minima dropped at least eight times below -50°C.

This historic data set is completed by measurements that were collected in the course of a large field experiment taking place in 2001/02 and by automatic temperature registrations that have been carried out on a more limited scale over the last eight years (Fig. 1).

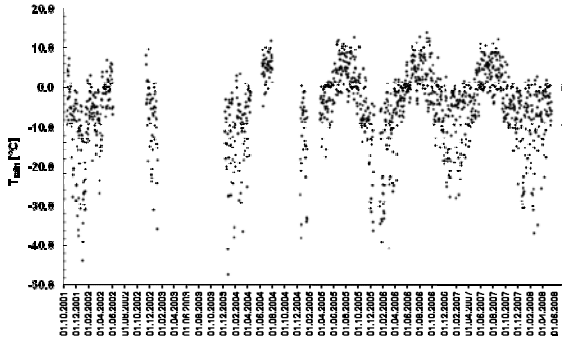

Figure 1. Nocturnal temperature minima at the bottom of Gstettneralm sinkhole between 2001/10/18 and 2008/05/12.

On the other hand, the Sonnblick observatory (Salzburg, Austria, 3106 m MSL) provides one of the longest time series in the Alpine region, with climate observations ranging back as far as 1886. From Sonnblick observatory, in addition to current data, a comprehensive set of observations of the free atmosphere is available for the thirties of the last century.

2. Evaluation of correlations

Both historic and current nocturnal temperature minima in the sinkhole have been related to the respective prevailing air mass properties in terms of equivalent potential temperature θ_e, which can easily be determined from Sonnblick observations. Correlation coefficients up to 0.9 between these two locations prove that there is a significant interrelation between Sonnblick air mass energy content and Gstettneralm temperature minima (Fig. 2).

3. Problem

Between 2001 and today, nocturnal temperature minima have never dropped below -50° although the ambient conditions in the sinkhole, which is located in a very remote area, should not have changed as compared to former times. Direct anthropogenic influence can be completely excluded at this place. Moreover, it was found that even under the same air mass properties in terms of θ_e, today's minima appear to be higher as compared to the 1930s.

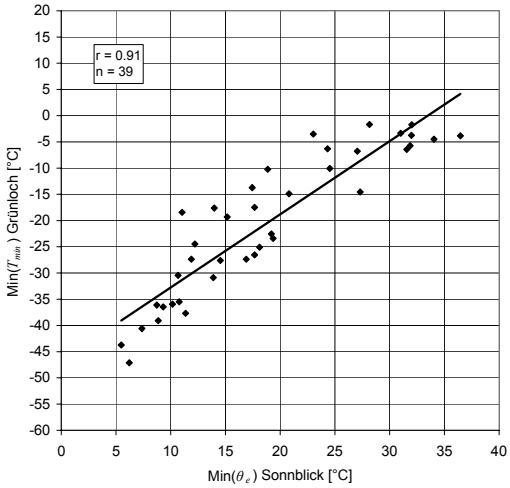

Figure 2. Scatterplot of correlations between Min(θ_e) Sonnblick and Min(T_{min}) Gstettneralm based on 40 day - intervals. Current data: 2001/10/18 - 2008/04/01.

This raises the question if the observed reduction in the amount of nocturnal cooling might be due to other reasons such as changes in the radiation budget of the sinkhole.

4. Conclusions

It is well known that the amount of radiative nocturnal cooling in a sinkhole strongly depends on the amount of atmospheric back radiation: increased back radiation is a distinct reason for an increased level of nocturnal temperature minima in a sinkhole. On the other hand, the interrelation of increased atmospheric greenhouse gas concentration and changed radiative budget is beyond dispute. We hypothesize that evaluation of historic and current data from the Gstettneralm sinkhole help to quantify the anthropogenic influence on climate change in an innovative way.

References

Easterling, D.R., B. Horton, P.D. Jones, T.C. Peterson, T.R. Karl, D.E. Parker, M.J. Salinger, V. Razuvayev, N. Plummer, P. Jamason, C.K. Folland: Maximum and Minimum Temperature Trends for the Globe. *Science*, 277, pp. 364 – 367, 1997

Sauberer, F., I. Dirmhirn: Über die Entstehung der extremen Temperaturminima in der Doline Gstettner-Alm (On the occurrence of extreme temperature minima in the Gstettner-Alm Doline). *Arch. Meteor. Geophys. Bioclimatol.*, 5B, pp. 307–326, 1954

Steinacker, R., C.D. Whiteman, M. Dorninger, B. Pospichal, S. Eisenbach, A.M. Holzer, P. Weihs, E. Mursch-Radlgruber, K. Baumann: A Sinkhole Experiment in the Eastern Alps, *BAMS,* 88, pp. 701-716, 2007

IPCC: Climate Change 2007: The Physical Science Basis. Contribution of Working Group I to the Fourth Assessment Report of the Intergovernmental Panel on Climate Change [Solomon, S., D. Qin, M. Manning, Z. Chen, M. Marquis, K.B. Averyt, M. Tignor and H.L. Miller (eds.)]. *Cambridge University Press*, Cambridge, United Kingdom and New York, NY, USA, 996 pp., 2007

Impact of vegetation on the simulation of seasonal monsoon rainfall over the Indian region using a regional model

Surya K. Dutta, Someshwar Das, S.C. Kar, V.S. Prasad and Prasanta Mali

National Centre for Medium Range Weather Forecasting, A50, Institutional Area, Phase-II, Sector-62, Noida – 201307, Uttar Pradesh, India; surya@ncmrwf.gov.in, dutta_surya@yahoo.co.in

1. Introduction: Different vegetation types with varied spatial coverage have a marked influence on precipitation patterns, whose effects have also been observed on the forecast models; Kar (1990). Change in the type of vegetation fraction can induce major changes in the local effects such as local evaporation, surface radiation, etc. that in turn induces changes in the model simulated outputs. Present study deals with the effects of vegetation in climate modeling over Indian region using mesoscale model MM5. An attempt has been made to examine the influence of vegetation on the Indian Monsoon Rainfall as simulated by the model. Main objective of the study is to compare the model performance based on ISRO (Indian Space Research Organization) generated vegetation data (derived from SPOT satellite) with that of USGS (United States Geological Survey) data. Consequently, identify the superior quality vegetation data over the Indian region for use in forecast models.

2. Experiment: The present study has been conducted for five monsoon seasons (1998-2002), giving emphasis over the two contrasting southwest monsoon seasons of 1998 (normal) and 2002 (deficient). Non-hydrostatic version of the MM5 modeling system developed at Penn State University/ National Centre for Atmospheric Research (PSU/NCAR) has been used for this study. The model preprocessor was modified to read the NCMRWF's (National Centre for Medium Range Weather Forecasting) global model T80L18 (Triangular Truncation at wave number 80 with 18 vertical layers) output in order to prepare the initial and boundary conditions for the MM5 model, which are updated every 12 hourly.

MM5 model has been simulated in two nested domains of resolution 90 km. and 30 km., respectively. In the present context, we have discussed the results mainly for the inner domain-2 (30 km. resolution). For detailed rainfall study, seven small regions within the Indian Domain (4.2^0 N – 38.7^0 N, 67.0^0 E – 104.8^0 E) are considered, which are important for rainfall prediction, and have wide variability of rainfall within it. The model was integrated based on the initial conditions at 00GMT of 16^{th} May. Starting from this date the simulation was carried forward for all the four months of Southwest Monsoon Season over the specified region, till 00GMT of 10^{th} October. MM5 simulations for the five years have been made independently, by using USGS (United States Geological Survey) and ISRO (Indian Space Research Organization) generated vegetation data. TRMM (Tropical Rainfall Measuring Mission) data has been used here as a ground truth for the verification of rainfall simulations by the mesoscale model. Daily mean data of NCEP-Reanalysis II has been used here for verification of the wind fields and surface parameters simulated by the model; Kanamitsu, et al. (2002). They serve as the observational component for the validation of model outputs, in particular, the winds and surface parameters.

3. Results and Discussion: Study of MM5 simulations with USGS and ISRO vegetation data show that ISRO vegetation has some positive impact on MM5 simulations. It has performed better over northeastern region and along the western coast. Considering all the five years (1998-2002), performance of MM5-USGS (MM5 simulations using USGS data) has an edge over MM5-ISRO (MM5 simulations using ISRO data) in terms of All India JJAS Rainfall RMSE and Bias. Also, JJAS total rainfall over North India and Deccan Coast is better simulated using the USGS vegetation. But, MM5-USGS has greater tendency of over estimation of rainfall. Higher standard deviation of MM5-USGS shows that it induces a dispersive effect on the rainfall simulation. In all the five years of study, it is seen that July and JJAS RMSE for All India Rainfall is mostly lower for MM5-ISRO. Also, July and JJAS bias for the same is mostly closer to unity for MM5-ISRO.

The wind fields at 850 and 200hPa are also better simulated by MM5 using ISRO vegetation. The synoptic features like Somali Jet and Tibetan anticyclone are simulated closer to the verification analysis by MM5-ISRO.

From this study the obvious impact of vegetation on regional climate simulation is revealed. By changing the type of vegetation fraction used for the regional climate simulation by a meso-scale model, significant change in rainfall and wind field is observed. Surface parameters like temperature at 2 meter above the ground, latent heat flux, sensible heat flux and relative humidity at 2 meter above the ground are the most important parameters that are intimately linked with the type of vegetation cover. However, the results do not show much change in the parameters in the simulations based on USGS and ISRO generated vegetation (Das, et al., 2007). 2m-air temperature is better simulated by MM5-ISRO over the northeastern India, showing greater spatial variability over the region. Over northwest India, MM5-USGS simulated sensible heat flux is closer to the verification analysis.

Through this investigation the impact of ISRO vegetation is clearly visible, but persistence and nature of the impact is yet to be studied in detail. Though mostly USGS vegetation is scoring over ISRO vegetation, but still it is difficult to justify the superior vegetation fraction among the two. The results are not the same always for all the seven demarcated regions within the Indian sub-continent. Individually over the smaller regions USGS does not always score over ISRO. For probing the probable reasons of inconsistency of ISRO vegetation throughout the Indian region, intensive study in detail is

required over the smaller regions separately. The difference in vegetation fraction for different regions among USGS and ISRO along with the variation in the type of vegetation and their respective coverage over month and years has to be studied. Error incorporated in the SPOT satellite data itself may be one of the reasons. Error might also get incorporated during the process of retrieval.

References:

Das, Someshwar, Surya K. Dutta, S.C. Kar, U.C. Mohanty and P.C. Joshi. 2007. Impact of Vegetation and Downscaling on Simulation of the Indian Summer Monsoon using a Regional Climate Model. NCMRWF-IIT Delhi Joint Research Report, 226 pp.

Kanamitsu, M., W. Ebisuzaki, J. Woollen, S-K Yang, J.J. Hnilo, M. Fiorino, and G. L. Potter. 2002. NCEP-DOE AMIP-II Reanalysis (R-2). Bul. of the Atmos. Met. Soc. 1631-1643.

Kar, S.C. 1990. Influence of vegetation cover in the ECMWF global spectral model. Proc. of Indo-US seminar on Physical Processes in Atmospheric Models held at IITM, Pune, 1990" Ed.by D.R. Sikka and S.S. Singh, 525-536

Climate change impacts on the water quality: A case study of the Rosetta Branch in the Nile Delta, Egypt

Alaa El-Sadek[1]

[1]Researcher, Drainage Research Institute, National Water Research Center, Delta Barrage, P.O.Box 13621/5, Cairo, Egypt. alaa_elsadek@yahoo.com

A physico-chemical water quality model has been developed for the Rosetta Branch in the Nile Delta, making use of the MIKE11 river modelling software of DHI Water & Environment (DHI, 2002). The physico-chemical water quality (WQ) module of MIKE11 was linked with a detailed full hydrodynamic (HD) model developed for the same Rosetta Branch, and also implemented in the MIKE11 modelling system. The WQ model aims to describe and predict concentrations of dissolved oxygen (DO), biochemical oxygen demand (BOD) and nitrogen in the form of ammonia (NH_4-N) and nitrate (NO_3-N), taking into consideration advection, dispersion and the most important biological, chemical and physical processes. All significant pollution sources along the Rosetta Branch were considered. The objective of this research is to study the effect of the climate change in terms of temperature on the water quality statues in Rosetta branch in the Nile Delta of Egypt. The results of this research indicated that, climate change is likely to increase the stress on rivers already under pressure from salinity, over-allocation and declining water quality. Higher water temperatures and reduced stream flows will tend to adversely affect water quality - water temperature, oxygenation, nutrient and pollution loads, salinity and other water chemistry - affecting habitat values for aquatic and riparian species and affecting human uses.
Changes in water quality could have implications for all types of uses. For example, higher temperatures and changes in water supply and quality could affect recreational use of rivers or productivity of freshwater fisheries. Finally, the research concluded that, with respect to water quality, most climate change impacts can be attributed to changes in either discharge or in water temperature. To a minor degree climate change may also affect the levels of direct atmospheric input of nutrients and other elements to the surface waters. The discharge controls dilution and residence times. When temperature increases, oxygen diffusion to water decreases and biological activity is enhanced. The development of water quality will depend essentially on the future evolution of human activities. The effectiveness of wastewater treatment, agricultural practices, water withdrawals and many other factors will play an important role.

Direct radiative forcing of various aerosol species over East Asia with a coupled Regional Climate/Chemistry model

Zhiwei Han

Key Laboratory of Regional Climate-Environment for East Asia (RCE-TEA),Institute of Atmospheric Physics (IAP), Chinese Academy of Sciences (CAS), Beijing 100029, China. hzw@mail.iap.ac.cn

The Regional Integrated Environmental Model System (RIEMS) was developed at RCE-TEA, IAP/CAS and has been utilized to predict regional climate in East Asia (Fu et al., 2005). RIEMS was further developed recently by incorporating tropospheric chemistry and aerosol processes to explore potential impacts of anthropogenic agents (O_3, aerosols etc) on regional climate over East Asia where intense human activity and continuous economic growth occur. Gas phase chemical mechanism is represented by CB-IV mechanism, ISSOROPIA has been used to calculate physical state and composition of inorganic aerosols. Black carbon, organic carbon (both primary and secondary), soil dust and sea salt aerosols are also included in RIEMS based on previous works on aerosols (Han et al., 2004; Han et al., 2008).

The time period of this study is March, 2006, with the study domain covering most of the East Asia (85-145ºE, 15-55ºN). The reanalysis data, four times a day with 1º×1º resolution are derived from National Centers for Environmental Prediction (NCEP) to provide initial and boundary conditions for RIEMS. The Lambert projection was used, with horizontal resolution of 60 km, and 16 levels from the surface to 100 mb. Emission inventories of SO_2, NO_x, CO, NMVOC, BC and OC are from Streets et al. (2003) and interpolated to RIEMS projection.

Figure 1a-1d shows the model predicted monthly mean surface direct radiative forcing (DRF) by sulfate, BC, OC, soil dust and sea salt aerosols, respectively. Strong cooling by sulfate at the surface (< -10 W m^{-2}) occurred over large areas of east China, with a maximum of < -20 W m^{-2} around Chongqing city in Sichuan Province. DRF by sulfate at the top of the atmosphere (TOA) is negative (not shown) and almost the same as the DRF at the surface. BC and OC aerosols exert cooling effects at the surface, with maximum values being -10 W m^{-2} and -2 W m^{-2} over the regions similar to that of sulfate. Soil dust aerosol cause negative forcing at the surface, showing cooling effect predicted mainly over the northwestern China and parts of the eastern China, as a result of dust deflation in arid regions and subsequent southeastward transport. The sign of DRF at TOA by soil dust is geographically dependent, either negative or positive. The maximum surface cooling by soil dust can be larger than -10 W m^{-2}, implying the potentially important climatic impact of Asian soil dust in springtime. The total surface forcing by all the five aerosols (Figure 1e) predicted with an assumption of external mixture is negative in the study domain, with strong cooling of ~ -30 W m^{-2} occurring over the middle reaches of the Yangtze River. Korean peninsula exhibits moderate cooling of -6 ~ -3 W m^{-2}, and the predicted DRF over Japan is generally in a range of -6 ~ 0 W m^{-2}.

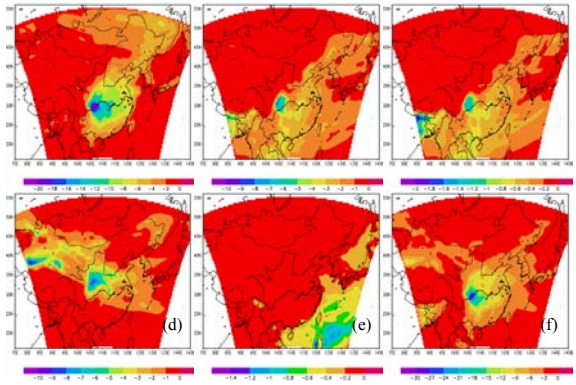

Figure 1 The predicted monthly mean surface DRF by (a) sulfate, (b) BC, (c) OC, (d) soil dust, (e) sea salt (f) external mixture of the aerosols

References

Fu Congbin et al., Regional Climate Model Intercomparison Project for Asia, Bulletin of American Meteorological Society, 86(2),257-266. 2005.

Han, Zhiwei et al., Model study on particle size segregation and deposition during Asian dust events in March 2002, Journal of Geophysical Research, 109,D19205, doi: 10.1029 /2004jd004920. 2004

Han Zhiwei et al.,. Regional modeling of organic aerosols over China in summertime. Journal of Geophysical Research, 113, D11202, doi:10.1029/2007JD009436. 2008.

Streets, D.G. et al., An inventory of gaseous and primary emissions in Asia in the year 2000. Journal of Geophysical Research 108 (D21), 8809, doi:10.1029/2002JD003093. 2003.

Influence of soil moisture-near surface temperature feedback on present and future climate simulations over the Iberian Peninsula

S. Jerez (1), J.P. Montavez (1), P. Jimenez-Guerrero (1), J.J. Gomez-Navarro (1) and J.F. Gonzalez-Rouco (2)

(1) Universidad de Murcia, Spain (sonia.jerez@gmail.com), (2) Universidad Complutense de Madrid, Spain

1. Introduction

Regional Climate Models are widely extended tools to evaluate the global warming impact at regional scales. Some of these models have a wide spectrum of physical options in order to parametrize the implemented processes, such as land-atmosphere interactions. This work assesses the implications of the election of the land-surface model within a climate version of the MM5 mesoscale model (Grell et al., 1994) in the present and future modeling of the climate of the Iberian Peninsula (IP). Often such interactions are modeled by a simple soil model, 'Simple Five-Layers Soil Model' (Dudhia, 1996), whose main weakness comes conditioned by the fact that the content of soil moisture is prescribed to fixed seasonal values. Previous works (Fernandez et al., 2007) pointed that this leads to an underestimation of summer temperatures, among other limitations. A more complex soil parametrization, 'Noah Land-Surface Model' (Chen et al., 2001), can be coupled to the atmospheric part of MM5. Noah dynamically models the evolution of the soil moisture, allowing the development of some feedback processes between the soil and the atmosphere that otherwise would remain inhibited.

Hence, the aim of this work is to characterize the influence of such processes to accurately reproduce the current climatology of the Iberian Peninsula, and the projected warming that can be attributed to them. Other authors have already highlighted about the contribution of land-atmosphere coupling to some climate change phenomena over Europe, such as the occurrence of heat waves (Fischer at al., 2007) and the projected higher temperature temporal variability (Seneviratne et al., 2006). These results also motivate this work.

2. Experiments

The spatial configuration of the domains employed in the simulations consists of two two-way nested domains, arising a resolution of 30 km over the IP. Vertically, 24 sigma levels with the top at 100 mb are considered. The common physics options are: *RRTM* radiation scheme, *Simple Ice* for microphysics processes, *Grell* for cumulus formation and *MRF* PBL parametrization.

Two sets of simulations have been performed:

- Hindcast simulations: using ERA40 data as initial and boundary conditions to simulate the period 1958-2002. The simulation denoted as HS uses the simple soil model, and the named HN uses Noah.
- Climate change simulations: 1961-1990 and 2070-2099 periods have been simulated using outputs from the ECHO-G global model under SRES A2 scenario for the future period. CS and CN denote the projections performed with the simple soil model and with Noah respectively.

3. Methodology

This work focuses on two aspects of the monthly mean temperature simulation: multiyear mean values (anual cycle) and variability of the anomalies series (substracted the annual cycle) defined as the standar deviation. For the latter summer series (contaning May to September months) and winter ones (with November to March months) have been considered separately. During those periods the soil moisture contain in the simple simulations remains constant. To asses the skill of the hindcasts a real data base (refered to as OBS) of monthly mean temperature series from 55 points is used covering the whole IP.

4. Results

4.1. Hindcast simulations

- Mean values:

The most important weakness of HS is the underestimation of summer months temperature, speacially inland and toward the south of the IP, rising values of more than 5 degrees (Fig. 1). With HN, since north-south heterogeneities are better captured and more realistics surface heat fluxes are reproduced, such error is notably reduced (more than 3 degrees in some places, Fig. 2) and the obtained spatial patterns are in better agreement with those observed. In winter months, while HS overestimates the temperature in general, HN underestimates it. But in both cases the error is under 2 degrees and does not present a defined spatial estructure.

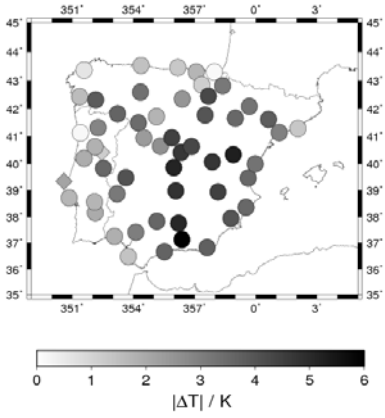

Figure 1: HS minus OBS in multiyear monthly mean August temperature. Circles represents negative values and diamonds positive.

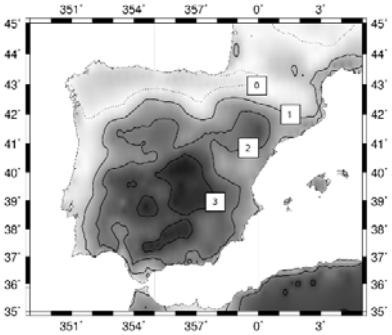

Figure 2: HN minus HS in multiyear monthly mean August temperature. Interval contour is one degree.

- Variability:

Temporal correlation between simulated and instrumental series of anomalies for monthly mean temperature is poorer in summer than in winter, but it is never under 0.8. In this sense, HN is not better than HS. Nevertheless HN reproduces more realistic patterns of summer series variability. This magnitude is systematically underestimated, but with HN it increases 30% with respect to HS in some areas of the eastern IP (Fig. 3). Differences between HS and HN in this variability study are clearly related to the soil moisture evolution simulated by Noah.

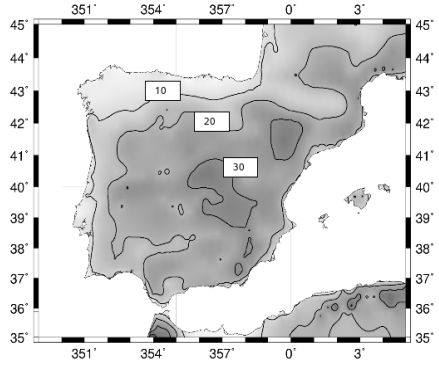

Figure 3: Increase in the standar deviation of the summer series (of monthly mean anomalies temperatures) introduced by HN with respect to HS (in %). Interval contour is 10.

4.1. Climate change simulations

- Mean values:

Patterns of impact due to the utilization of Noah Land-Surface Model obtained from hindcast experiments are reproduced from climate change simulations, finding an intensification of the impact in the future. Albeit such patterns do not fit with the warming ones, whose spatial structure is the same in both CS and CN, there are significant differences between them in future projections:

CN projects a temperature increase for summer months over 7 degrees in northwestern areas, 2 degrees higher than the projected by CS. Furthermore, CN projects a larger increase for the maximum monthly mean temperatures than for the minimum ones, while such aspect is not reproduced in CS.

- Variability:

Present impact patterns differ from the obtained with the hindcast simulations. Major signal appears moved towards the north-west in summer, where CN projects an increase of the variability for summer series of about 20% greater than CS.

5. Conclusions

When soil moisture content is dynamically modeled, spatial heterogeneities between areas that do not suffer from hydric stress during summer and the ones subjected to drought periods are better captured. The former are not notably affected by the use of the more complex soil model, neither other seasons.

In HN simulation, superficial sensible heat fluxes dominate in the center and south of the IP during summer, at the expense of the latent ones. Such land-atmosphere positive feedback leads to an increase of the simulated temperatures, and therefore to a better estimation (when comparing to observations).

Besides, experiments confirm that the dynamical modelling of soil moisture is related to the higer variability of the temperature anomalies summer series, a systematically underestimated magnitude. Nevertheless, this higher variability does not entail a better temporal correlation between simulated and instrumental series. Hence, the sense of the evolution of those series should respond to advective causes.

By one hand, these results advice to use realistic soil moisture parametrizations for future climate projections (in fact, the impact patterns due to its dynamic modelling appear intensified in the future). In that case, more intense warming patterns and also a larger signal of variability increse are found, although their spatial structure is the same in both CS and CN experiments. Regarding to the warming patterns of maximum and minimum monthly mean temperatures, CN projects an increasing amplitude (differences between them), which is disguised in CS.

On the other hand, the weak skill of regional models to accurately simulate the precipitation (which is managed by the soil model), together with the shown results, open a new uncertainty source for realistic temperature projections.

References

Chen, F. and J. Dudhia, Coupling an advanced land surface-hidrology model with the Penn State-Ncar MM5 modeling system. Part I: Model implementation and sensitivity, *Mon. Wea. Rev.,* 129, 569–585, 2001

Chen, F. and J. Dudhia, Coupling an advanced land surface-hidrology model with the Penn State-Ncar MM5 modeling system. Part II: Preliminary model validation, *Mon. Wea. Rev.,* 129, 587–604, 2001

Dudhia, J., A multi-layer soil-temperature model for MM5, *Sixth PSU/NCAR Mesoscale Model Users Workshop*, pages 49–50, Boulder, CO, 1996

Fernández, J., J. P. Montávez, J. Sáenz, J. F. González-Rouco, and E. Zorita, Sensitivity of MM5 mesoscale model to physical parameterizations for regional climate studies: Annual cycle, *J. Geophys. Res.*, 112, D04101, 2007

Fischer, E.M., S.I. Seneviratne, D. Lüthi and C. Sächr, Contribution of land-atmosphere coupling to recent european summer heat waves, *Geophysical Research Letters*, 34, L06707, 2007

Grell, G.A., J. Dudhia and D.R. Stauffer, A description of the fifth-generation Penn State/NCAR Mesoscale Model (MM5), *Technical Report*, NCAR/TN-398+STR, 1994

Seneviratne, S.I., D. Lüthi, M. Litschi and C. Sächr, Land-atmosphere coupling and climate change in Europe, *Nature*, 443, 05095, 2006

Forest damage in a changing climate

Anna Maria Jönsson[1] and Lars Bärring[2]

1) Department of Physical Geography and Ecosystems Analysis, Geobiosphere Science Centre, Lund University, Sölvegatan 12, SE- 223 62 Lund, Sweden E-mail: Anna_Maria.Jonsson@nateko.lu.se
2) Rossby Centre, Swedish Meteorological and Hydrological Institute, SE-601 76, Norrköping; Sweden

1. Extreme weather events

Annual mean temperature and precipitation influence the large-scale distribution of terrestrial biomes. Extreme weather events such as drought, flooding, storm and frost events can have large impacts on plant species composition at finer scales through the differential effects on competition among species. Rapid climate change is likely to change both temperature and precipitation regimes in Northern Europe, including the frequency and severity of extreme events (IPCC 2007), and these changes may have direct consequences for competitive relationships in most ecosystems. In Swedish forest ecosystems the positive effects of increased warmth and growing season length have the potential to increase wood production; however adaptation of current forest management regimes is likely to be required to reduce the risk of damage and to preserve biodiversity (SOU 2007).

2. Assessments of biological response

Biological responses to changes in climate can be explored by developing impact models based on data from experimental studies and monitoring sites. The impact assessments are dependent on the representativity and quality of climate model data. An interpretation of results from impact studies must consider uncertainties associated with climate modeling. Developmental processes related to accumulation of temperature sums, non-linear relationships between ambient temperature and biological response magnitude, as well as responses induced after crossing of sharp temperature thresholds increase the risk for amplification of otherwise modest bias in climate data. The more complex models, the higher the risk for systematic errors caused by carry-over effects.

3. Spruce bark beetle

Extreme weather events are driving factors in forest disturbance dynamics. Insects and pathogens may utilize trees killed or weakened by disturbances as breeding material, and some herbivorous insect species has the potential to aggravate the damage caused by disturbance. Norway spruce (*Picea abies*) is one of the dominating tree species in the boreal forest of Northern Europe, and the spruce bark beetle, *Ips typographus* is one of the most destructive pests of mature Norway spruce. The damaging potential of *I. typographus* is expected to be affected by climate change as swarming activity and developmental rate is influenced by temperature (Jönsson et al. 2007). Impact modelling indicated that global warming can result in increased frequency and length of late summer swarming events. In south Scandinavia, *I. typographus* may shift from primarily univoltinism to bivoltinism (Jönsson et al. 2009a). An increased frequency of three generations per year may occur in central Europe (Jönsson et al 2009b).

4. Spring backlashes

Earlier timing of spring events has been observed in response to the raise in temperature during the last decades[1]. An earlier onset of spring phenology have raised concern about an increased risk for frost damage, as this may occur already in the beginning of the year when the seasonal temperature progression is slow and the risk of temperature backlashes with sudden frost episodes is high (Jönsson et al. 2004).

5. Integrated assessments

Integrated impact assessments, capturing both aspects related to forest growth potential and tree vitality, *i.e.* risk for damage and susceptibility to pests and pathogens are required. Tree species and provenances, forest management and soil properties (such as nutrient status and water holding capacity) set the stage for how a forest stand will respond to changes in climate. This may include substantial increase in productivity, acute damage triggered by extreme weather such as severe spring frost or drought and opportunistic pests and pathogens attacking trees that are weakened by damage, contributing to decline in tree vitality or even mortality.

References

IPCC, Climate Change 2007: Impacts, Adaptation and Vulnerability. Contribution of Working Group II to the Fourth Assessment Report of the Intergovernmental Panel on Climate Change, M.L. Parry, et al. Eds., Cambridge University Press, Cambridge, UK, 976pp. 2007

SOU (Sweden facing climate change - threats and opportunities SOU 2007:60, Swedish Government Official Report 21 December 2007, Ministry of the Environment, Stockholm: Fritze, pp. 679. 2007

Jönsson, A.M., Linderson, M.-L., Stjernquist, I., Schlyter, P. and Bärring, L. Climate change and the effect of temperature backlashes causing frost damage in *Picea abies*. *Global and Planetary Change* 44:195-207. 2004.

Jönsson, A.M., Harding, S., Bärring, L., & Ravn, H.P. Impact of climate change on the population dynamics of Ips typographus in southern Sweden. *Agricultural and Forest Meteorology, 146*, 70-81, 2007.

Jönsson, A.M., Appelberg, G., Harding, S., & Bärring, L. Spatio-temporal impact of climate change on the activity and voltinism of the spruce bark beetle, Ips typographus In, *Global Change Biology* (pp. 486-499) 2009a.

Jönsson, A.M., Harding, S., Krokene, P., Lange, H., Lindelöw, Å., Økland, B., & Schroeder, L.M. Modelling the potential impact of global warming on Ips typographus voltinism and reproductive diapause. *submitted* 2009b

Climate change and air pollution interactions in the Republic of Belarus

Alena Kamarouskaya and Aliksandr Behanski

Republican Center for Radiation Control and Environtmental Monitoring, Minsk, Belarus; clim@by.mecom.ru

The indexes of air monitoring are used for the quantification of regional impacts of environmental pollution in the context of global climate change. It gives the opportunity to compare past and recent climate variability and change with the impacts of air pollution.

Since 1989 it has been the longest period of temperature rising. The only time, when the average annual temperature was a little lower than normal meaning was in 1996, other years this parameter was much higher. During the warmest years – 1989, 1990, 1999, 2000 – the meaning of temperature added 1,5ºC to its normal value.

The period of active temperature rising (at the end of XX century) had no effect on the annual amount and precipitation distribution. The amount of precipitation fall wasn't equal in different observation periods during the year. These features in addition to temperature rising lead to droughty conditions.

Due to air monitoring data this period was notified as the most complicated because of smog processing. This process took place in Belarus in 1992 and 2002 (August and September) and was accompanied with rising of total solid particles' (TSP) concentrations, concentrations of nitrogen oxide (NOx), carbon oxide (CO) and benzapiren BaP. The influence of smog situation was the greatest on the background territories: concentrations of TSP exceeded WHO standards. At the same time rising of alkalinity precipitation was noticed.

Future challenges for regional coupled climate and environmental modeling in the Baltic Sea Region

H.E. Markus Meier[1], Thorsten Blenckner[2], Boris Chubarenko[3], Anna Gårdmark[4], Bo G. Gustafsson[2], Jonathan Havenhand[5], Brian MacKenzie[6], Björn-Ola Linnér[7], Thomas Neumann[8], Urmas Raudsepp[9], Tuija Ruoho-Airola[10], Jan-Marcin Weslawski[11], and Eduardo Zorita[12]

[1]Swedish Meteorological and Hydrological Institute, Norrköping, Sweden, markus.meier@smhi.se, [2]Baltic Nest Institute, Stockholm, Sweden, [3]Atlantic Branch of P.P. Shirshov Institute of Oceanology, Russian Academy of Sciences, Kaliningrad, Russia, [4]Swedish Board of Fisheries, Öregrund, Sweden, [5]Dept. Marine Ecology - Tjärnö, Göteborg University, Strömstad, Sweden, [6]DTU-Aqua, Technical University of Denmark, Charlottenlund, Denmark, [7]Center for Climate Science and Policy Research, Linköping University, Linköping, Sweden, [8]Baltic Sea Research Institute Warnemünde, Rostock, Germany, [9]Marine Systems Institute at Tallinn University of Technology, Tallinn, Estonia, [10]Finnish Meteorological Institute, Helsinki, Finland, [11]GKSS-Research Centre Geesthacht GmbH, Geesthacht, Germany, [12]Institute of Oceanology Polish Academy of Sciences, Sopot, Poland

1. Background

Within the recently performed BALTEX Assessment of Climate Change for the Baltic Sea Basin (BACC, www.baltex-research.eu/BACC) it was concluded that "identified trends in temperature and related variables (during the past 100 years) are consistent with regional climate change scenarios prepared with climate models". Regional climate model (RCM) results suggest that global warming may cause increased water temperatures of the Baltic Sea, reduced sea ice cover, increased winter mean wind speeds causing increased vertical mixing, and increased river runoff causing reduced salinity.

The projected hydrographic changes could therefore have significant impacts on the Baltic Sea ecosystem, i.e. its biodiversity, species distributions, growth and reproduction of organisms including zooplankton, benthos and fish. These could include the complete loss of entire species, and major restructuring of the food web and trophic flows. In addition, acidification of the coastal oceans is an emerging and potentially critical threat to Baltic Sea ecosystems. In the last 150 years, fossil fuel burning has caused the pH of the global oceans to fall by 0.1 units, and by the year 2100 oceanic pH is predicted to be $\leq$ 0.4 units lower than at present. Decadal records of pH in the Baltic Sea and Skagerrak show acidification proceeding at rates 2 – 5 times faster than in the open ocean. The effects of these changes and their interaction with other climate variables, in mediating both gradual changes and abrupt shifts in Baltic Sea ecosystems are currently unknown but likely to be considerable.

Thus, it will be a challenge for future research to develop dynamical downscaling methods adding necessary regional details (e.g. more accurate land-sea masks) and providing consistent scenarios with coupled models such that the impact on the Baltic ecosystem could be studied. In this presentation a recently started project will be introduced: ECOSUPPORT (An advanced modelling tool for scenarios of the Baltic Sea Ecosystem to support decision making) is an inter-disciplinary cooperation between 11 partner institutes from 7 Baltic Sea countries. First results will be shown and challenges for regional-scale climate modelling will be discussed in a wider perspective.

2. Methods

Within ECOSUPPORT we will apply a hierarchy of existing state-of-the-art sub-models of the Earth system (Fig.1). The main emphasis is the coupling of these sub-models and ensemble simulations. This is the key, novel, contribution that ECOSUPPORT will make toward obtaining an integrated predictive understanding of marine ecosystems.

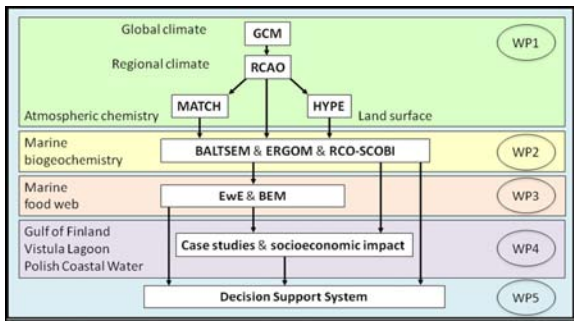

Fig.1: Model hierarchy in ECOSUPPORT. The schematic is highly simplified neglecting complex interactions (e.g. fish predation pressure on zooplankton, changing society/policy will affect climate and nutrient load scenarios).

Regional climate modeling

For dynamical downscaling a high-resolution coupled atmosphere-ice-ocean-land surface model (the Rossby Centre Atmosphere Ocean model, **RCAO**) with lateral boundary data from GCMs will be applied to calculate future climate of the Baltic Sea region [1]. The regional scenario simulations will differ depending on the applied GCM at the lateral boundaries and depending on the utilized greenhouse gas and aerosol emission scenario.

To calculate future river flow and riverborne nutrient loadings a new hydrological model developed at SMHI (**HYPE**, HYdrological Predictions for the Environment) is used. It simulates a range of hydrological variables including phosphorus and nitrogen in soils, rivers and lakes. The model is a further development of the earlier HBV model [2].

The transient changes in atmospheric near-surface concentrations of trace species, that were simulated with an advanced photochemical transport model (**MATCH**, Multiple-scale Atmospheric Chemistry and Transport modelling system [3,4]), will be analyzed to estimate changing airborne nutrient deposition over the Baltic Sea.

Marine biogeochemical modeling

Three state-of-the-art coupled physical-biogeochemical models will be used to calculate changing concentrations

of nitrate, ammonium, phosphate, diatoms, flagellates, cyanobacteria, zooplankton, detritus, and oxygen: **BALTSEM** [5,6], **ERGOM** [7], and **RCO-SCOBI** [8]. The models are structurally different in that ERGOM and RCO-SCOBI are 3D circulation models comprising sub-basin scale processes while BALTSEM resolves the Baltic Sea spatially in 13 sub-basins. The biogeochemical sub-models are of similar type but the process descriptions differ. For the case studies in the Gulf of Finland and Vistula Lagoon two regional models forced with lateral boundary data from the basin-wide models are used during selected time slices.

Food web modeling

The food web of the Baltic Sea will be simulated by applying the ecological software **EwE** (www.ecopath.org). An existing food web model for the Baltic Sea has already been used, and contains 15 functional groups from primary producers to seals and fishery [9]. The model was parameterized with a focus on fish (sprat, herring and cod). EwE is an excellent tool to: a) address ecological questions; b) evaluate ecosystem effects of fishing; c) explore management policy options; d) evaluate impact and placement of marine protected areas; and e) evaluate effects of environmental changes.

At present, **process-based** and **statistical models for Baltic Sea fish species** can link climatic forcing and lower trophic level processes to fish dynamics. These models will be integrated within ECOSUPPORT by linking them to outputs from physical-biogeochemical models. Dynamics of cod, herring and sprat have been shown to be driven partly by fluctuations in climate, eutrophication and lower trophic level processes, including those which directly affect reproductive success [10], feeding and survival of larvae, and feeding and growth of adults [11].

We will generate **Bioclimatic Envelope Models** (**BEMs**) for key species in the Baltic Sea system (and in the models used here) to assess the susceptibility of these taxa to range-extension and possible local extinction arising from climate change. BEMs will be constructed using statistical modelling (CART, [12]) trained with historical distribution data for key taxa, and corresponding oceanographic environmental data [13].

Socioeconomic impact assessment

For the **focus study sites**, Gulf of Finland, Vistula Lagoon and the Polish coastal waters, we will conduct assessments of the impact of climate change on the regional and local development. The **economic assessment of the ecosystem goods and services** delivered from key ecosystems/habitats within the Baltic Sea (*Fucus* beds, mussel beds, seagrass, shallow soft bottom habitats) and processes (benthic-pelagic coupling, filtration) follows the methods of [14]. In order to develop management strategies for sustainable use and conservation in the marine environment, reliable and meaningful, but integrated ecological information is needed. Biological valuation maps that compile and summarize all available biological and ecological information can be used as baseline maps for future spatial planning at sea. Rather than a general strategy for protecting areas that have some ecological significance, biological valuation is a tool for calling attention to areas which have particularly high ecological or biological significance and to facilitate provision of a greater-than-usual degree of risk aversion in management of activities in such areas.

The regional results from the focus study sites will be scaled up to the Baltic Sea scale. This will support the **charting of socioeconomic implications** from different climate scenarios (e.g. [15,16]). Especially, the costs of nutrient load reductions of defined ecological targets of Baltic Sea water quality in present and future climates will be calculated with the **Nest economic model** [17]. The metric difference between the results will provide us with a first estimate of costs related to changing climate.

3. First results

First results from scenario simulations of biogeochemical cycles are now available calculated with the coupled physical-biogeochemical model RCO-SCOBI. The ocean model is forced with atmospheric and hydrological fields from the regional climate model RCAO driven with lateral boundary from ECHAM4/OPYC3 (or HadAM3H, not shown). As an example Figure 2 shows annual mean phytoplankton concentrations in present and future climates assuming four socioeconomic scenarios with corresponding nutrient loadings from land. The results suggest that climate change may have a significant impact on the ecosystem and needs therefore to be considered in the Baltic Sea management.

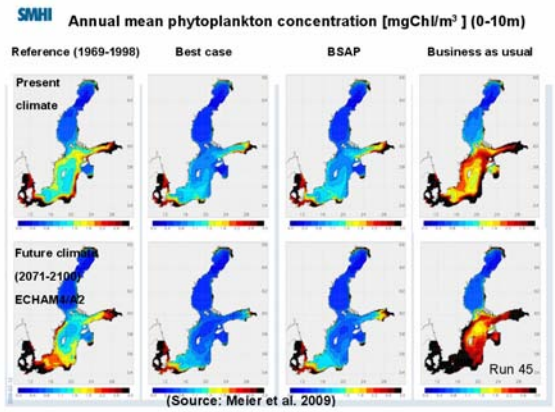

Fig. 2: Annual mean phytoplankton concentration [mgChl/m^3] (0-10m). Present climate (upper panels), future climate according to ECHAM4/A2 for 2071-2100 (lower panels), reference conditions of nutrient supply during 1969-1998 (first column), nutrient load scenarios following the most optimistic (best) case (second column), the Baltic Sea Action Plan (third column), and the most pessimistic case assuming business as usual (fourth column). The nutrient load scenarios have been developed by the Baltic Nest Institute.

References

[1] Räisänen et al. 2004, Clim. Dyn., **[2]** Lindström et al. 1997, J. Hydrol., **[3]** Robertson et al. 1999, J. Appl. Meteor., **[4]** Engardt & Foltescu 2007, SMHI Meteorologi No. 125, **[5]** Gustafsson et al. 2008, Göteborg University, Report No.C82, **[6]** Savchuk & Wulff 1999, Hydrobiologia, **[7]** Neumann et al. 2002, Global Biogeochemical Cycles, **[8]** Eilola et al. 2009, J. Mar. Sys.**,** **[9]** Österblom et al. 2007, Ecosystems, **[10]** MacKenzie & Köster 2004, Ecology, **[11]** Casini et al. 2006, Oikos, **[12]** Breiman et al. 1984, Wadsworth, Belmont, **[13]** Lima et al. 2007, Global Change Biology, **[14]** Weslawski et al. 2006, Oceanologia, **[15]** Kaivo-Oja et al. 2004, Boreal Env. Res., **[16]** Holman et al. 2005, Climatic Change, **[17]** Gren and Wulff 2004, Regional Envi-ron. Change

Linking climate factors and adaptation strategies in the rural Sahel-Sudan zone of West Africa

Ole Mertz-1, Cheikh Mbow-2, Jonas Ø. Nielsen-1, Abdou Maiga-3, Alioune Ka-4, rissa Diallo-5, Pierre Cissé-5, Drissa Coulibaly-5, Bruno Barbier-6, Dapola DA-7, Tanga Pierre Zoungrana-7, Ibrahim Bouzou Moussa-8, Waziri Mato Maman-8, Boureima Amadou-8, Addo Mahaman-8, Alio Mahaman-8, Amadou Oumarou-8, Daniel Dabi-9, Vincent Ihemegbulem-9, Awa Diouf-2, Malick Zoromé-6, Ibrahim Ouattara-7, Mamadou Kabré-7, Anette Reenberg-1, Kjeld Rsamussen-1, Inge Sandholt-1

1-DGGUC, Denmark, 2-UCAD, Dakar, Senegal, 3-University of Montreal, Canada, 4-CSE, Senegal, 5-Université de Bamako, Mali, 6-2ie, Ouagadougou, Burkina Faso, 7-Université de Ouagadougou, Burkina Faso, 8-UAM, Niamey, Niger, 9-University of Jos, Nigeria

Although there is an increasing realization of the interplay between different driving forces for rural development and environmental change in developing countries, understanding the relative impact of climate factors on land use change and local livelihoods is still not straight forward. However, without a better knowledge of these relationships it becomes difficult to devise specific and well targeted adaptation strategies to climate change and variability – at best, adaptation becomes a collection of 'no regret' actions, which in any case would have benefited development; in worst case scenarios, adaptation could become counter-productive if based on the wrong assumptions. In this paper we aim to estimate the relative weight of climate factors in the decision making process of rural household in the Sahel-Sudan zone of West Africa during the past 20 years and compare these with strategies described in National Adaptation Programmes of Action (NAPA. We interviewed 1354 households in 16 sites in Senegal, Mali, Burkina Faso, Niger and Nigeria distributed across a rainfall gradient divided into three zones: 400-500 mm, 500-700 mm, and 700-900 mm. Group interviews were also carried out with 3-5 groups in each site.

Household income sources have increasingly become diversified. A majority states that income from remittances, irrigated vegetable farming, and various businesses has increased while a decrease in rainfed agriculture mentioned by 63% of respondents is perceived to be due to decreased rainfall. Many different reasons are given for a decrease in livestock income. Poor rainfall is by far the main cause mentioned of decreases in millet and maize production, though soil fertility decline is equally important in the humid zone. Causes for decreases in livestock holdings were much more diverse with sale for family needs, diseases, theft and inadequate pastures being more important than rainfall. When asked directly about impacts of climate change, the climate impact on rainfed agriculture was reiterated as were the more complex and less important impacts on livestock. Adaptation measures taken in response to decreasing agricultural production were very diverse – soil fertilization and alternative income sources were frequent, but the most often cited was various types of 'prayer', indicating that many farmers do not see a technical solution. Adaptation of livestock production was more concrete, including veterinary control, fodder complements and increased transhumance. The group interviews largely corroborated the household survey.

The adaptation projects proposed in the NAPAs are generally not reflected in the adaptation options chosen by people in villages studied as very few households mentioned improved irrigation, new crop species and agro-meteorological information as solutions. This may be due to ignorance or lack of access to such possibilities. The study concludes that the while the rainfed agricultural sector is perceived to be under significant stress, the livestock sector seems to be a more promising pathway for developing agriculture in the Sahel.

Keywords: Adaptation to climate change, Land use change, Society-environment-climate interactions, Agriculture, Livestock, Household economy, Livelihoods

Projected changes in daily temperature variability over Europe in an ensemble of RCM simulations

Grigory Nikulin, Erik Kjellström and Lars Bärring

Rossby Centre, Swedish Meteorological and Hydrological Institute, Sweden (grigory.nikulin@smhi.se)

1. Introduction

Future climate scenarios show not only possible changes in the mean state but also changes in variability. In addition to shifts in the mean, enhanced or reduced variability also influences weather extremes which may become more or less frequent. Together with a pronounced warming over Europe an increase in summer temperature variability (interannual and intraseasonal) have been found from an ensemble of regional climate model (RCM) simulations driven by one global climate model (GCM) *Vidale et al.* (2007) and *Fischer and Schär* (2009). Boundary conditions only from one GCM substantially define the behaviour of the entire ensemble of RCM simulations. In order to supplement the above results we use an ensemble of integrations with one RCM driven by different GCMs, focusing on the question "How does a possible future climate with increased greenhouse gas concentration influence daily temperature variability over Europe in summer and winter?"

2. Data and method

For downscaling of GCM scenarios over Europe we use the Rossby Center Regional Climate Model (RCA3) *Kjellström et al.* (2005) with a horizontal resolution of 0.44° (approximately 50 km). The regional simulations are driven by boundary conditions from five different GCMs: ECHAM5 (MPI, Germany), CCSM3 (NCAR, USA), HadCM3 (Hadley Center, UK), CNRM (CNRM, France), BCM (NERSC, Norway) *Meehl et al.* 2007. All simulations have employed the A1B scenario and two periods are chosen to represent the recent (1961-1990, CTL) and future (2071-2100, SCN) climates. As a measure of daily temperature variability we use the variance (or standard deviation) of daily temperature at the 2 meter level and separate the total variability into four components, namely: seasonal-cycle, interannual, intraseasonal and trend-induced variability, accordingly to the methodology by *Fischer and Schär* (2009). The simulated variability for the CTL period is evaluated against the gridded ENSEMBLES observational dataset (ENSOBS) *Haylock et al.* (2008).

3. Summer

In summer and for the CTL period (Fig. 1 top) the ensemble mean total temperature variability has a band of large values stretching from the Iberian Peninsula throughout central to eastern Europe. Comparison to ENSOBS (not shown) reveals that the ensemble mean variability is well captured over central and eastern Europe while underestimated in Scandinavia and the Alps (20-30%) and overestimated in the in the Pyrenees (up to 50%). In the SCN period (Fig. 1 bottom) the simulated summer total temperature variability is significantly enhanced over a substantial part of the domain, approximately south of 50°N, with the maximum increase up to 20-30% over southern and eastern Europe. Detailed analysis of all four components of the total variability shows that on average two main contributors to the total variability increase are the seasonal-cycle (50%) and intraseasonal (30%) variability while the interannual component explains about 10 % of the total change.

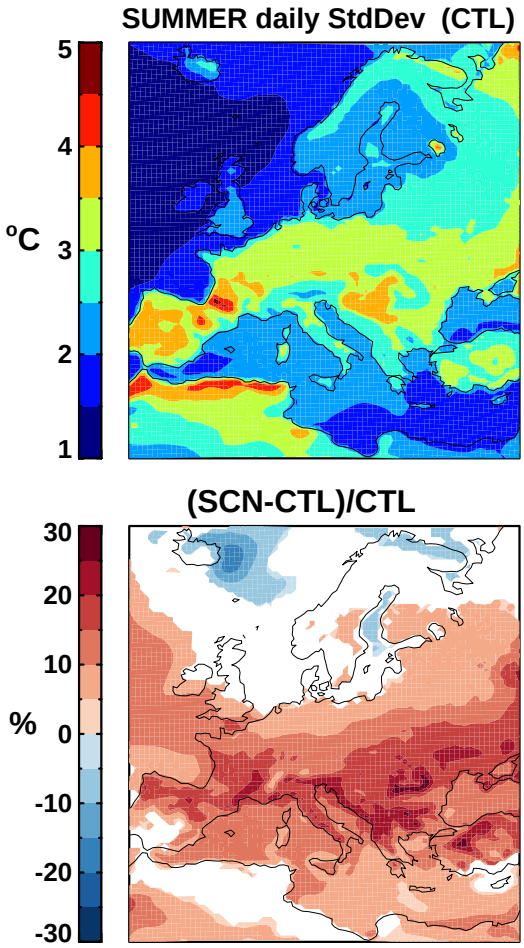

Figure 1. (top) The simulated summer total daily standard deviation of the 2m temperature for 1961-1990 and (bottom) the relative change in the standard deviation in 2071-2100 wrt 1961-1990. Only differences significant at 5% level are shown.

4. Winter

The simulated winter total temperature variability (CTL) shows a gradual increase from south to north with local maxima over Iceland, northern Scandinavia and the Barents Sea (Fig. 2 top). The winter variability is generally underestimated in continental Europe (10-20%) and overestimated in the Alps (50%), south part of the Iberian Peninsula (40%) and northern Scandinavia (10-20%) The overestimation in northern Scandinavia is mainly due to the BCM and CNRM driven simulations which heavily (up to 100%) overestimate the total variability in this region that may reflect a problem with the modeled sea ice in the Barents Sea in those driving

GCMs. In the end of the 21st century (Fig. 2 bottom), the projected winter total temperature variability is significantly reduced over northern Europe and the Alps with the largest decrease (30-40%) over Scandinavia. The change in the intraseasonal variability strongly dominates explaining about 80% of the total decrease while the interannual component explains about 15%.

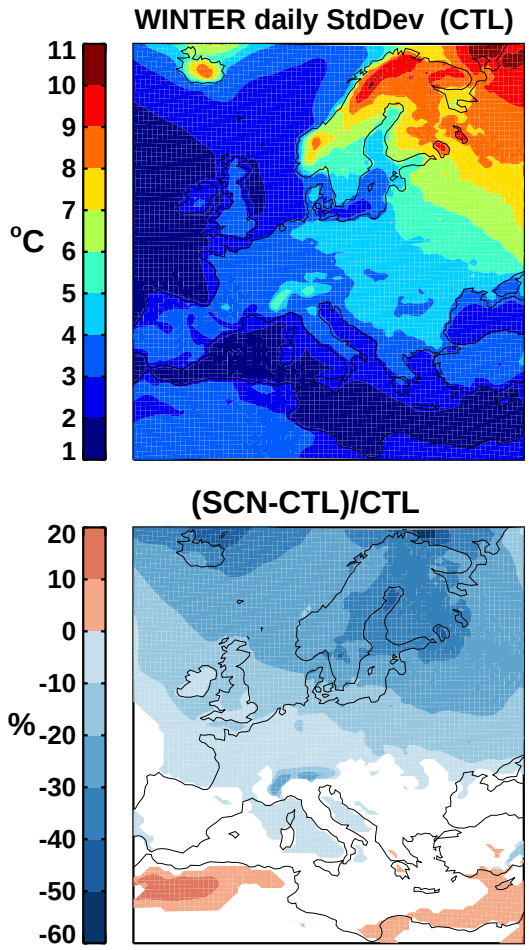

Figure 2. As Fig.1 but for winter.

5. Summary

The future projection (2071-2100) of European climate based on the ensemble of RCA3 simulations driven by 5 different GCMs have shown an increase (up to 30%) of daily temperature variability over central and southern Europe in summer and a decrease (up to 40%) over northern Europe and the Alps in winter. The simulated changes in temperature variability (not shown) is found in the both cold and warm tails of daily temperature distribution that, in addition to the mean warming, leads to higher occurrence of hot days in summer and lower occurrence of cold days in winter. The ensemble mean enhancement of summer temperature variability over central and southern Europe is in good agreement with the results of *Vidale et al.* (2007) and *Fischer and Schär* (2009) based on the ensemble of different RCMs driven by one GCM. Also here, the change in the mean temperature has the same sign and spatial patterns although with different magnitudes among the members of the ensemble. On the other hand change in the temperature variability has only in general the same sign while spatial patterns and magnitudes of the change strongly depend on choice of driving GCM. It means that when we look at regional climate changes in higher-order quantities rather than in usual means uncertainties related to driving GCMs become more important.

Acknowledgements

This work is part of the Mistra-SWECIA programme, funded by Mistra (the Foundation for Strategic Environmental Research), and of the ENSEMBLES project funded by the EC through contract GOCE-CT-2003-505539. The GCM groups are acknowledged for providing models and boundary data. The model simulations with RCA3 were performed on the climate computing resource Tornado funded with a grant from the Knut and Alice Wallenberg foundation. We acknowledge the E-Obs dataset from the EU-FP6 project ENSEMBLES (http://www.ensembles-eu.org) and the data providers in the ECA&D project (http://eca.knmi.nl).

References

Fischer, E.M. and Schär C., Future changes in daily summer temperature variability: driving processes and role for temperature extremes, *Clym. Dyn.*, 32., doi:10.1007/s00382-008-0473-8, 2009

Haylock, M.R., Hofstra, N., Klein Tank, A.M.G., Klok, E.J., Jones, P.D. and New, M., A European daily high-resolution gridded data set of surface temperature and precipitation for 1950-2006, *J. Geophys. Res.*, 113, D20119, doi:10.1029/2008JD010201, 2008

Kjellström, E., Bärring, L., Gollvik, S., Hansson, U., Jones, C., Samuelsson, P., Rummukainen, M., Ullerstig, A., Willén U. and Wyser, K., A 140-year simulation of European climate with the new version of the Rossby Centre regional atmospheric climate model (RCA3), *Reports Meteorology and Climatology*, 108, SMHI, pp. 54, 2005

Meehl, G.A. and coathors , Global Climate Projections. In: Climate Change 2007: The Physical Science Basis. Contribution of Working Group I to the Fourth Assessment Report of the Intergovernmental Panel on Climate Change. *Cambridge University Press*, 2007.

Vidale, P., Lüthi, D., Wegmann, R. and Schär C., European summer climate variability in a heterogeneous multi-model ensemble, *Clim. Change*, 81, Supp. 1, pp. 209-232, 2007.

Climate change impact assessment in central and eastern Europe: The CLAVIER project

Susanne Pfeifer [(1)], Daniela Jacob [(1)], Gabor Balint [(2)], Dan Balteanu [(3)], Andreas Gobiet [(4)], Andras Horanyi [(5)], Laurent Li [(6)], Franz Prettenthaler [(8)], Tamas Palvolgyi [(7)] and Gabriella Szepszo[(5)]

[(1)]Max Planck Institute for Meteorology Hamburg, Germany (susanne.pfeifer@zmaw.de)
[(2)] Environmental Protection and Water Management Research Institute (VITUKI), Budapest, Hungary
[(3)] Institute of Geography, Romanian Academy, Bucharest, Romania
[(4)] Wegener Center for Climate and Global Change, University of Graz, Austria
[(5)] Hungarian Meteorological Service (HMS), Budapest, Hungary
[(6)] Institut Pierre Simon Laplace, Centre National de la Recherche Scientifique, Paris, France
[(7)] Env-in-Cent Ltd. (EiC), Budapest, Hungary
[(8)]Institute of Technology and Regional Policy, JOANNEUM RESEARCH Forschungsgesellschaft mbH, Graz, Austria

1. The CLAVIER project

The CLAVIER project (Climate Change and Variability: Impact on Central and Eastern Europe) is supported by the European Commission's 6th Framework Programme as a 3 year Specific Targeted Research Project from 2006 to 2009 under the Thematic Sub-Priority "Global Change and Ecosystems". The CLAVIER consortium consists of 13 partners from 6 countries, most of them coming from the CLAVIER target countries Hungary, Romania and Bulgaria. Based on a set of climate change simulations from different regional climate models, linkages between climate change and its impact on weather patterns, air pollution, extreme events, and on water resources are investigated. Furthermore, an evaluation of the economic impact on agriculture, tourism, energy supply and the public sector is conducted.
Figure 1 shows the case study regions for economic impact assessment which have been defined based on the expert knowledge of the local CLAVIER partners.

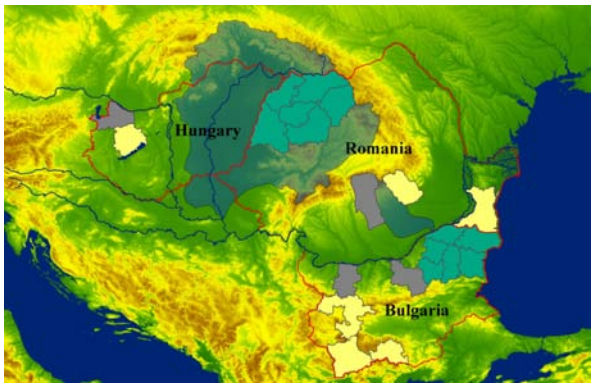

figure 1: CLAVIER study regions for impact assessment. Green: hydrology, yellow: tourism, grey: energy, cyan: agriculture.

2. The CLAVIER model ensemble

The CLAVIER model ensemble consists of three regional climate models, namely REMO from the Max Planck Institute for Meteorology (MPI-M) in Hamburg, used in Version 5.7 by MPI-M and REMO5.0 used by the Hungarian Meteorological Service in Budapest, and the LMDZ model developed at CNRS in Paris. From all models, A1B scenario simulations driven by the global climate model ECHAM5 are available for the period of 1950 to 2050 with a horizontal resolution of about 25 to 30 km. For LMDZ, additional simulations driven by the IPSL global model are available for the A1B scenario.

3. Interface climate simulations – impact studies

One main challenge of conducting climate change impact assessment is the multidisciplinary knowledge which is needed. CLAVIER joins disciplines such as climate modelers, hydrologists, geographers, engineers and economists. To facilitate the communication and the data flow, an interfacing work package has been established which bridges the gap between the model simulation data and the needed input data for the impact studies. Among others, this work package is carrying out a bias correction procedure to account for the known biases of the regional climate models.

4. Physical Impact Assessment

The impact of climate change on different sectors has been studied. Among others, analyzes have been and will be carried out on: the water levels of the Lake Balaton, the hydrological regime of the Tisza river basin, possible changes in weather extremes, landslide and mud flow risks in the Sub-Carpathian regions, the risk of road damages in Hungary, and possible changes in typical weather regimes for Central and Eastern Europe and their implications to air pollution levels.

5. Economic Impact Assessment

The economic impact assessment concentrates on the four economic sectors with the highest expected impacts, agriculture, tourism, energy supply and the public sector. Based on the climate change information and on economic data for the respective sector (e.g. temperatures, precipitation from the climate simulations, sectoral economic data e.g. on tourism revenues, overnight stays, number and types of hotels, tourism infrastructure, restaurants, shops, beaches etc. for the tourism studies), the sensitivity and the exposure to a changing climate is assessed in 10 case study regions on the NUTS II and NUTS III level and finally translated into expected changes in regional macroeconomic indicators, such as the sectoral Climate Change impact on Gross Regional Product (GRP) allowing also for first estimates on the impact on Gross Domestic Product (GDP) on the national level respectively.

This workshop contribution will give an overview on the results of the CLAVIER project.

References

http://www.clavier-eu.org

Climate change impacts on extreme wind speeds

S.C. Pryor[1,2], R.J. Barthelmie[1,2], N.E. Claussen[2], N.M. Nielsen[2], E. Kjellström[3] and M. Drews[4]

[1] Indiana University, Bloomington, IN 47405 USA spryor@indiana.edu
[2] Risø DTU National Laboratory for Sustainable Energy, Roskilde, Denmark
[3] Rossby Centre, SMHI, Norrköping, Sweden
[4] Danish Meteorological Institute, Copenhagen, Denmark

1. Introduction and objectives

Our objective is to quantify potential changes in extreme wind speeds across northern Europe under a variety of climate change scenarios. For wind energy applications we conform to the Wind Turbine design criteria, which define the suitable class of wind turbines based on the 50-year return period wind speed (U_{50yr}). We determine extreme winds based on the Gumbel distribution so:

$$U_T = \frac{-1}{\alpha}\ln\left[\ln\left(\frac{T}{T-1}\right)\right] + \beta \quad (1)$$

U_T wind speed for a given return period (T), and α and β are the distribution parameters.

2. Methods

Two downscaling tools are applied to AOGCM output to generate higher resolution realizations of surface winds from which we calculate the extreme wind speeds:

1. Dynamically downscaled time series of grid-cell averaged wind speeds are used from two applications of Regional Climate Models (RCMs): (a) Simulations conducted using the Rossby Centre RCAO lateral boundary conditions from two General Circulation Models (ECHAM4/OPYC3 and HadAM3H) and two emission scenarios (SRES A2 and B2) (Pryor et al. 2005). (b) Simulations conducted using the HIRHAM RCM and lateral boundary conditions from ECHAM5/MPI-OM for the A1B SRES. Simulated time series of annual maximum wind speeds are used to compute U_{50yr} using the method of moments to determine α and β:

$$\alpha = \frac{\ln 2}{2b_1 - \overline{U^{\max}}} \quad (2)$$

$$\beta = \overline{U^{\max}} - \frac{\gamma}{\alpha} \quad (3)$$

$$b_1 = \frac{1}{n}\sum_{i=1}^{n}\frac{i-1}{n-1}U_i^{\max} \quad (4)$$

The uncertainty on U_T is given by:

$$\sigma(U_T) = \frac{\pi}{\alpha}\sqrt{\frac{1+1.14k_T+1.10k_T^2}{6n}} \quad (5)$$

Where n is the sample size, the frequency factor (k_T) is:

$$k_T = -\frac{\sqrt{6}}{\pi}\left(\ln\left[\ln\left(\frac{T}{T-1}\right)\right] - \gamma\right) \quad (6)$$

Where γ = Euler's constant (0.577216)

Assuming a Gaussian distribution of U_T, then 95% of all realizations will lie with $\pm 1.96\sigma$ of the mean, and thus σ can be used to provide 95% confidence intervals on the estimates of extreme winds with any return period.

2. Empirical downscaling is used to develop site specific estimates of extreme wind speeds using output from eight AOGCMs; BCCR-BCM2.0, CGCM3.1, CNRM-CM3, ECHAM5/MPI-OM, GFDL-CM2.0, GISS-ModelE20/Russell, IPSL-CM4, and MRI-CGCM2.3.2. AOGCM output for two historical periods (1982-2000 and 1961-1990) are taken from climate simulations of the twentieth century. AOGCM output for 2046-2065 and 2081-2100 are from simulations conducted using the A2 SRES. Wind speed observations (1982-2000) at 10-m for 43 stations used to condition the transfer functions are as in Pryor et al. (2006). This empirical downscaling technique develops a probability distribution of wind speeds during a specific time window rather than a time series of wind speeds. Thus the downscaled parameters are the scale (A) and shape (k) of the Weibull distribution:

$$P(U) = 1 - \exp\left[-\left(\frac{U}{A}\right)^k\right] \quad (7)$$

This approach is advantageous in the current context because it avoids a focus on mean conditions, underestimation of variance, and difficulties associated with reproducing the time structure of wind speeds.

Downscaled Weibull A and k for each time period, AOGCM and station are used to compute U_{50yr} using eq. (1) and:

$$\alpha = \frac{k}{A}\left((\ln(n))^{1-\frac{1}{k}}\right) \quad (8)$$

$$\beta = A(\ln(n))^{1/k} \quad (9)$$

Where n is the number of independent observations

For the 8 AOGCMs presented and the 43 stations, the range of downscaled U_{50yr} for 1961-1990 lie within ±4% of the mean U_{50yr} and 95% lie within ±2%, so the downscaling results for extreme winds from the Weibull A and k parameters are relatively consistent for the historical period. Estimates from the future time periods are defined as being different from the historical period (1961-1990) if they lie beyond the 95% confidence intervals derived based on propagation of the uncertainty in A and k.

3. Dynamically downscaled extreme wind speeds

RCAO simulations for the end of the C21st conducted using boundary conditions from HadAM3 imply little change in U_{50yr} (Table 1). Estimated U_{50yr} for the future period (and both SRES) generally lie within the 95% confidence intervals derived for the control period simulations (O(4-15%) of the U_{50yr} in 1961-1990). This is also the case for simulations conducted using lateral boundary conditions from ECHAM4/OPYC3, although in those simulations U_{50yr} for the future period under either SRES show increases particularly in the southwest of the study domain (Figure 1). The choice of SRES appears to have little influence on the $d(U_{50yr})$ in either set of runs.

Table 1. Fraction of grid cells (in %) that exhibit a significant increase, decrease or no change for the 4 future simulations (2071-2100) relative to 1961-1990.

	Declines	No change	Increases
ECHAM4: A2	0.1	73.2	26.7
ECHAM4: B2	0.1	72.9	27.0
HadAM3: A2	6.0	90.1	3.9
HadAM3: B2	1.8	95.8	2.4

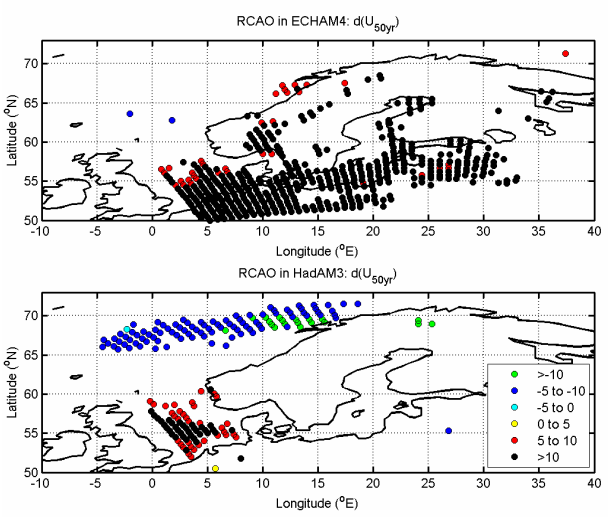

Figure 1. Magnitude (in %) of statistically significant differences in U_{50yr} computed by grid cell for 2071-2100 v 1961-1990 for simulations nested within (above) ECHAM4/OPYC3 and (below) HadAM3 for the A2 SRES.

4. Empirically downscaled extreme wind speeds

U_{50yr} for each observational station were computed from the downscaled Weibull A and k parameters for the 8 AOGCMs for three time periods; 1961-1990, 2046-2065 and 2081-2100. The ensemble mean U_{50yr} for 1961-1990 and the ensemble average change between 1961-1990 v 2081-2100 are shown in Figure 2 and Table 2. In the ensemble average there are a large number of stations that exhibit no change in U_{50yr} (26 of 43 stations for 2046-2065, and 14 of 43 for 2081-2100 exhibit change of less than 1% relative to 1961-1990), this is also true for the majority of individually downscaled AOGCMs. However, of the stations that exhibit a $|d(U_{50yr})|$ >1% between 1961-1990 and the future period, the majority exhibit increases. Seventeen of 43 stations (i.e. 40%) exhibit an ensemble average increase in U_{50yr} of 1-5% in 2046-2065 relative to 1961-1990. Twenty-seven of 43 stations (i.e. 63%) exhibit an ensemble average increase in U_{50yr} of 1-10% in 2081-2100 relative to 1961-1990. This bias towards increased extreme wind speeds is also exhibited in results from the majority of individually downscaled AOGCMs. However, for the majority of stations considered, results from at least one downscaled AOGCM exhibit declining U_{50yr}. A further key caveat that should be noted is that application of the Weibull method to compute U_{50yr} is subject to some uncertainty related to the accuracy of the Weibull fit. The 95% confidence intervals computed for the 1961-1990 period are -12% to +10%. Downscaling of only two AOGCMs exhibit any single station for which the difference in U_{50yr} in the historical period (1961-1990) and future time periods (2046-2065 or 2081-2100) exceeds the 95% confidence intervals computed for 1961-1990.

Table 2. Ensemble average $d(U_{50yr})$ from the empirically downscaled Weibull A and k expressed in terms of the number of stations from which U_{50yr} estimates show a change of the specified magnitude (in %) between the future period and 1961-1990 (if positive the future period exhibits a higher U_{50yr} than the historical period).

% change	2046-65 v 1961-90	2081-2100 v 1961-90
-10 to -5	0	0
-5 to 0	6	7
0 to 5	37	33
5 to 10	0	3

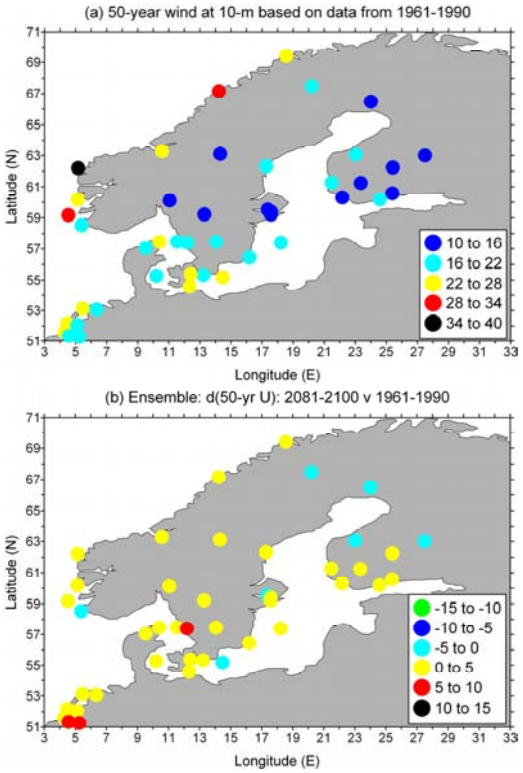

Figure 2. (a) U_{50yr} at 10-m empirically downscaled for 1961-1990 (ms^{-1}), (b) the ensemble average change (%) in U_{50yr} computed from the 8 AOGCMs for 2081-2100 relative to 1961-1990 (if positive the future period exhibits a higher U_{50yr} than 1961-1990).

5. Concluding remarks

U_{50yr} computed using both dynamically and empirically downscaled wind speeds exhibit some weak evidence for an increase in extreme wind speeds at sites in northern Europe during the middle and end of the C21st relative to 1961-1990. The spatial distribution of simulated changes in U_{50yr} between the RCAO and the empirical downscaling are to some degree consistent – showing maximal changes in the southwest of the study domain, though the relative changes are of larger magnitude from the RCAO in simulations conducted with lateral boundaries from ECHAM4/OPYC3. The increase in U_{50yr} from the ECHAM4/OPYC3 nested runs exceeds 10% for many grid cells, but the majority of grid cells show no change beyond the 95% confidence intervals for 1961-1990. This tendency towards 'no statistically significant change' is even more marked in HadAM3 nested RCAO simulations. Uncertainty calculations presented herein illustrate the challenge of estimating climate change impacts on geophysical extremes, but also provide critical context for interpreting the results of such analyses.

Acknowledgements

Financial support was supplied by the National Science Foundation (grants # 0618364 & 0647868), Nordic Energy Research and the energy sector in the Nordic countries.

References

Pryor SC, Barthelmie RJ, Kjellström E (2005). Climate Dynamics 25:815-835

Pryor SC, Schoof JT, Barthelmie RJ (2006). Geophysical Research Letters 33:doi:10.1029/2006GL026000

Winter storms with high loss potential in a changing climate from a regional point of view

Monika Rauthe, Michael Kunz and Susanna Mohr

Institute for Meteorology and Climate Research, University Karlsruhe/Forschungszentrum Karlsruhe,
monika.rauthe@imk.uka.de

1. Introduction

According to the recent publications of the IPCC, global climate changes are unequivocal (IPCC, 2007). Many more changes in the global climate systems are very likely in the following decades and centuries. Concerning winter storms in global climate models, an enhancement especially of severe cyclones over Europe is found (see review by Ulbrich et al., 2009 and references therein). But changes of strength and/or occurrence of extreme natural hazards on the regional scale are more or less unknown. Due to the low resolution of current global climate models, regional effects can be hardly estimated – especially for parameters like wind speed and precipitation, which are strongly amplified by local scale conditions (e.g. orographic effects). Because of the high loss potential of winter storms the knowledge about changes of the storm climate on the regional scales is very important (see Figure 1).

In the RESTER (Strategien zur Reduzierung des Sturmschadensrisikos für Wälder) project the impacts of extreme storm events on the forests are analysed. The investigations are conducted in the framework of the cooperative research project "Herausforderung Klimawandel" funded by the federal state of Baden-Württemberg. Various institutions from different research fields investigate the effects and impacts of climate change on the regional scale. Within the RESTER project our institute characterises the changes in winter storm climate in Germany with a special focus on the region of Baden-Württemberg in the southwest of Germany.

Figure 1. Losses after the winter storm 'Lothar' in the Black Forest near Oberkirch in Baden-Württemberg (Photo: Georg Müller).

2. Data and Methods

This study is based on different data sets from regional climate models. In addition to the output of REMO also that of CLM is used. These regional climate models are both forced by the global circulation model ECHAM5. The ECHAM5 and REMO model runs were all conducted at the Max-Planck-Institute for Meteorology in Hamburg. In contrast to ECHAM5 with its horizontal resolution of about 210 km, REMO and CLM have a resolution of about 10 and 18 km, respectively. The REMO simulations were commissioned by the German Federal Environment Agency. The CLM simulations are part of the so-called "Konsortialläufe". For the projection period the calculations are based on the IPCC SRES emission scenarios A1B, A2 and B1 (IPCC, 2007). Details of the regional climate simulations are summarized in Table 1.

Extreme value statistics are applied to quantify the storm climate. The analyses are based on the time series of wind gusts at each grid point. The maximum gusts of the 100 strongest events are fitted with a statistical distribution. The generalized Pareto distribution (GPD) allows for the best description of the data (Hosking and Wallis, 1987; Palutikof et al., 1999). From the fitted probability distribution, the strength of storms of a specific return period is estimated. This analysis is applied to every single grid point for both the control period (1971–2000) and the projection period (2021–2050).

	REMO	CLM-KL run 1	CLM-KL run 2
Forcing	ECHAM5 run 1	ECHAM5 run 1	ECHAM5 run 2
Emission scenario	A1B, A2, B1	A1B	A1B
Resolution	0.088° ≈ 10 km	0.167° ≈ 18 km	0.167° ≈ 18 km

Table 1. Details of the regional climate simulations.

3. Results

To estimate the reliability of the regional climate data, they are evaluated for the control period against point measurements and results of the so-called storm hazard map from CEDIM (Center of Disaster Management and Risk Reduction Technology) published by Heneka et al. (2006) and Hofherr and Kunz (2009). Despite the systematic underestimation of the wind speeds in the gusts the spatial patterns due to the underlying orography are well reproduced by the regional models. These results are also confirmed by observations at several SYNOP stations. Additionally, a dependency on the elevation above sea level is clearly visible. Stations at higher elevations show larger differences between observations and model data than those at lower elevations. But the effect exists only if the elevation differences are large enough. Altogether, the regional climate models are able to resolve the local amplifications of wind speeds e.g. due to orography and land use. This is a big advantage over the coarse resolution of the global models. The underestimation of the absolute gust wind speeds in the

simulations is not relevant in the following discussion, because only relative climate change signals are quantified.
The future changes of the storm climate is analysed for the guest speeds with a 10 year return period. They vary in the different parts of Germany. The results of REMO with A1B scenario shows that the storm activity in Northern Germany will increase in the future by about 10%. Also in Central Germany gusts with a 10 year return period will become more frequent, but their amplitude is smaller. However, south of 50° N there is no clear trend, i.e. no changes of storm climate has to be expected in Southern Germany according to these analyses.
The results for the other simulations of REMO and CLM are generally in agreement with the results of the REMO model run with A1B scenario, but there are a few local differences. It has to be noted though that the changes of the storm climate in regional models are greatly depended on the changes found in the global model used.
To get a better survey of all results an ensemble of the five runs is created on a common grid determined by the model with the lowest resolution. The ensemble composite shows which changes of the storm climate are most likely. In Northern Germany the increase of gust is supported by a high probability. In Central and Southern Germany the trends are indifferent and in some parts a decrease of the storm activity seems to be possible. Finally, it has to be emphasized that such a differentiation between the regions of Germany is only possible by means of regional climate models.

4. Outlook

Apart from the data presented here, CLM simulations with a resolution of about 7 km are available in our institute. These data will be integrated in the ensemble results.
In addition to the strength of the storms their horizontal extent is also an important factor for the loss potential. A so-called storm index, which takes both the strength and horizontal extension of storms into account, is calculated following Della-Marta et al. (2008). In future these results will be linked with the financial and other losses caused by the storms.

References

Della-Marta, P., H. Mathis, C. Frei, M. A. Liniger, J. Kleinn and C. Appenzeller, The return period of wind storms over Europe, *Int. J. of Climatology*, published online, doi:10.1002/joc.1794, 2008.

Heneka, P., T. Hofherr, B. Ruck and Ch. Kottmeier: Winter storm risk of residential structures – model development and application to the German state of Baden-Württemberg, *Nat. Hazards Earth Syst. Sci.*, 6(5), 721–733, 2006.

Hofherr, T. and M. Kunz, Assessment and mapping of extreme wind speeds related to winter storms in Germany, *Int. J. of Climatology*, submitted, 2009.

Hosking, J. R. M. and J. F. Wallis, Parameter and quantile estimation for the generalized paretro distribution, *Technometrics*, 29(3), 339–349, 1987.

IPCC: Climate Change 2007, The Physical Science Basis, Contribution of Working Group I to the Fourth Assessment. Report of the Intergovernmental Panel on Climate Change [S. Solomon, D. Qin, M. Manning, Z. Chen, M. Marquis, K. B. Averyt, M. Tignor and H. L. Miller (eds.)]. Cambridge University Press, Cambridge, United Kingdom and New York, NY, USA, 996 p, 2007.

Palutikof, J. P., B. B. Brabson, D. H. Lister and S. T. Adcock, A review of methods to calculate extreme wind speeds, *Meteor. Appl.*, 6, 119–132, 1999.

Ulbrich, U., G. C. Leckebusch and J. G. Pinto, Extra-tropical cyclones in the present and future climate: a review, *Theoret. and Appl. Climatology*, published online, doi: 10.1007/s00704-008-0083-8, 2009.

The impact of land use change at ShanGanNing Border areas on climate with RegCM3 Study

Xueli Shi(1), Yiming Liu(1), and Jianping Liu(2)

(1) National Climate Ceneter, China Meteorological Administration, No.46 Zhongguancun Nandajie, Haidian District, Beijing 100081, P.R. China; shixl@cma.gov.cn
(2) Ningxia Meteorological Bureau, Ningxia, P.R. China

1. Abstract

The land use and land cover change can impact regional/local climate through land-atmosphere interactions. In this paper, the land use change impacts of the "conversion of cropland to forest" at the ShanGanNing Border Areas (SGNBA) in Western China were investigated by using the regional climate model (RegCM3) simulation experiments. Two sets of simulations are conducted with the same large-scale forcing data from NCEP/NCAR reanalysis II dataset. The control simulation use the original model land cover dataset used in standard RegCM3 simulations, which are noted as CTL. In another set, the yearly updated remote dataset in the "key SBA area" are used for the simulation, which are noted as MOD. Besides the assessment of the CTL performance, differences between the MOD and CTL will also be presented to understand the climate effects of the land use change.

2. Introduction

The impacts of land use and land cover change on climate have been and still will be the study interests all around the world, such as Correia et al. (2008) in Amazonia and Douglas et al. (2006)) at the Indian Monsoon belt. Pielke et al. (2007) presented an overview on their regional impacts on rainfall. In East Asia and China, Fu et al. (2001) studied the impacts of recovering natural vegetation on summer climate and environmental conditions in East Asia. Zhang and Gao (2009) investigated the atmospheric dynamical response to land-use change with general circulation model and regional climate model.

But not too many models studies are focused on the SGNBA because of the limitation of available dataset and complicated features of climate, land-surface and sensitive ecosystem. The returning natural forest in SGNBA has started from 1999 in China aimed at improving the conditions there. But how much are the change and their impacts? In our work, the land cover mapping obtained from remote sensing was used to quantify land cover change during March – October from 1999 to 2007 in the SGNBA. The dataset are introduced into the RegCM3 (Pal et al., 2007) to study their impacts on climate.

The model has a 20km horizental resolution, with the model domain including part of the high land in the west (Figure 1). The key area (SGNBA) is located at center of model domain, which is also the region where the land cover dataset is replaced. The CTL simulation has proven the model performance in reproducing the basic climate features. Differences between MOD and CTL shown the significant effects of land cover change at the key area, which will be presented during the meeting.

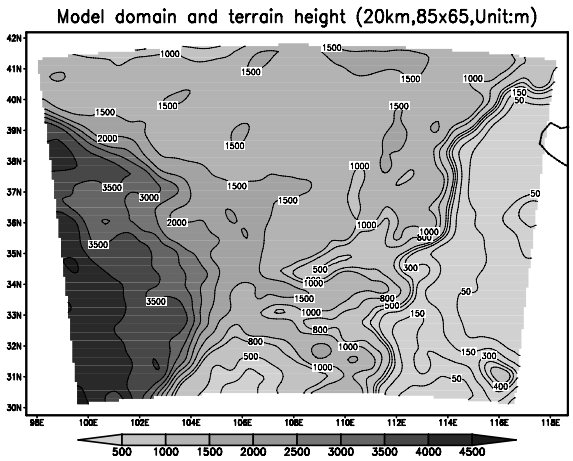

Figure 1. The model domain and terrain height. (Unit: m)

References

Correia F.W.S., Alvala R.C.S., and Manzi A.O., 2008: Modeling the impacts of land cover change in Amazonia: a regional climate model (RCM) simulation study. *Theor. Appl. Climatol.*, 93, pp. 225-244.

Douglas E., Niyogi D. and Frolking S., et al., Changes in moisture and irrigation in the Indian Monsoon, belt, *Geophys. Res. Lett.*, 33: L14403, doi:10.1029/2006GL026550.

Fu C.B., Yuan H.L., A virtual numerical experiment to understand the impacts of recovering natural vegetation in East Asia, *China Sci. Bull.*, 50, pp. 620-628, 2007

Pal J.S., et al., Regional climate modeling for the developing world: the ICTP RegCM3 and RegCNET, *Bull. Atmos. Meteor. Soc.*, 88, pp. 1395-1409, 2007.

Pielke R.A., Adegoke J., and Beltran-przekurat A., et al., An overview of regional land-use and land-cover impacts on rainfall, *Tellus*, 29B, 3, pp. 587-601, 2007.

Zhang H.Q., and Gao X.J., On the atmospheric synamical responses to land-use change in East Asian monsoon region, *Clim. Dyn*, doi:10.1007/s00382-008-0472-9, 2009.

Numerical investigations into the impact of urbanization on tropical mesoscale events

Himesh S[1], Goswami P[1] and Goud BS[2]

1. CSIR Centre for Mathematical Modeling and Computer Simulation, NAL Belur Campus, Wind Tunnel Road, Bangalore-560037, India; himesh@cmmacs.ernet.in

2. UVCE, Department of Civil Engineering, Bangalore University, Bangalore-560056, India

1. Summary

Worldwide there is growing trend in urbanization, leading to development of mega cities, with south-east Asia in the lead. These mega cities, through variety of effects like Urban Heat Island (UHI) affect local weather; of primary concern is the change in intensity and duration of extreme weather events. It is, however, necessary to study these effects through models that comprehensively describe local atmospheric dynamics in a large-scale environment. In this work we examine the impact of urbanization on evolution of three heavy rainfall events occurred over Indian monsoonal region in different seasons at three different cities (Mumbai, Bangalore and Chennai) with very high population density and located in different climatic regions. Numerical experiments for each of the events were carried out using a 3-nest configuration (MM5V3 model) with 2-km resolution of innermost domain. Simulations were carried out for two scenarios; partially urban and fully (hypothetical) urban. The results show that increased urbanization affected both intensity and spatial distribution of rain. Partial urbanization was found to be associated with more total rain, larger spatial extant of distribution and less intense, while the converse is true for fully urban scenario.

2. Introduction

In recent times there has been increase in intensity and frequency of heavy rainfall events over Indian Monsoon region resulting in loss of lives and property in many Indian cities. Increased urbanization, due to altered thermodynamic and mechanical properties of land surface has known to modulate local weather and trigger high impact weather events like heavy rainfall. **Franklin et al. (2004)** studied the impact of urbanization on water budget in Nairobi City using limited area model (GESIMA). He observed that urban heat island effect and increased surface roughness length due to urbanization induce thermal instability, increases mechanical turbulence, and also produce enhanced rainfall around downwind of the urban area. **Gero et al. (2006)**, through numerical simulations had shown that highly urbanized cities like Sydney trigger severe convective storms. This study assumes significance in the context of disaster management and mitigation associated with high impact weather events in India.

3. Model and Data

The fifth generation NCAR /Penn State mesoscale model MM5V3 used in this study (Dudhia et al. 2004) is a mesoscale model with options for parameterization of various processes like cumulus convection, Planetary Boundary Layer (PBL) and radiative forcing. It can support multiple nests with varying horizontal resolution and has non-hydrostatic dynamics. The details of model configuration are given in **Table 1**. Global Tropospheric Analysis 1^ox1^o degree data (NCEP/NCAR) was used to generate initial and lateral boundary conditions including SST fields (monthly climatology). Terrestrial data includes terrain elevation (2-minute), Land-use (USGS-24 Category 2 minute), vegetation fraction (10 minute).

Table 1 Model configuration and data

Model Version	NCAR MM5V3
Number of Nests	3-Nest, 2-way
Moisture Scheme	Graupel (reisner2)
Microphysical Scheme	Simple Ice
Radiation Scheme	Dudhia
Vertical Levels	23
Land Surface Model	NOAH LSM
PBL	MRF
Boundary Condition	Relaxation
Non-Hydrostatic	Yes

Domain D1 and D2 consists of 250x250 grid points in X and Y direction with grid size of 18 and 6-km respectively. Domain D3 consists of 100x100 grid points with 2-km grid size.

4. Description of Events

We have considered three heavy rainfall events; Mumbai (03UTC, 26th July to 03UTC 27th July 2005), Bangalore (15UTC, 22nd Oct to 15UTC 23rd Oct 2005) and Chennai (06UTC, 26th Oct to 06UTC 27th Oct 2005) over three different locations covering different climatic regions and seasons. The Mumbai event was a very high intensity event that occurred over the west coast of India during the summer monsoon season. The other two events occurred during the winter (north-east monsoon) season; of these, one was over the east coast of India (Chennai 13.5N, 80.17E), while the other was over a continental location (Bangalore 12.59N, 77.35E). The extreme rainfall event that flooded the metropolis of Mumbai on the west coast of India (72.52E and 18.52N) was an intense and highly localized meso-scale convective system, with a spatial scale of only about 30 Kms.

5. Design of Experiments

Numerical experiments involve a set of six simulations with control and test simulation for each of the event. Control simulation essentially represents old land use scenario(less urbanized) and test simulations represent modified land surface (current) due increased urbanization. Only the innermost domain (D3) was modified in all the test runs to reflect current condition of increased urbanization by modifying land surface properties (surface roughness length, albedo, thermal inertia and moisture availability) with typical urban (50 cm, 18 %, 0.03 cal.cm^{-2}K^{-1} S$^{-1/2}$ and 10%) values. In all the experiments, model was integrated for 3 days starting from 2005-07-25:00 Hour (Mumbai), 2005-10-22:00 (Bangalore) and 2005-10-25:00 (Chennai) respectively.

6. Analysis of Results (Rain)

The Figure 2., below show spatial distribution of 24-hour accumulated (event window) rain in domain D2 ; difference between control and test (control-test) simulations and observed rain (10-km satellite data).

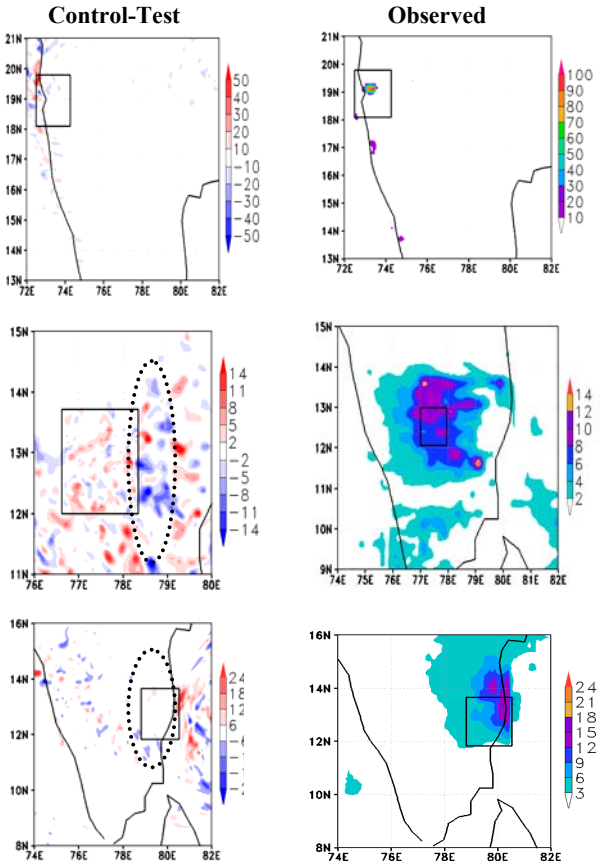

Figure 1. Spatial distribution of 24-hour accumulated simulated (left) and observed (right) rain. High intensity spots concentrated around the periphery of urban zone (D3 indicated by boxes) may be seen (around dotted ellipse).

Distribution of 24-hour accumulated rain in domain D2 and for different events was found to be spatially more extensive for control simulation compared to test simulation but rain was seen to be more intensified in test runs with intense spots located around the periphery of the urban zone. The difference between control and test runs confirms this as shown by dotted ellipse regions in Figure.1. It may also be noted that simulated events (control and test) can be reasonably compared with observation with intensity captured fairly accurately by the model in all the three events. Test simulations with modified land surface conditions (hypothetical, more urbanized) offer less of moisture which most probably resulted in the reduced spatial extent of rainfall distribution compared to control runs (less or partially urbanized). Based on this study following observations can be made; rainfall over urban areas tend to be less in spatial extent, discontinuous in distribution with more number of isolated intense cells clustering around the periphery of the urban zone. This is particularly true for land locked cities like the one (Bangalore event) discussed here. Another important observation is that test cases (modified land surface with more urbanization) have simulated the event better than control cases in terms of intensity, distribution and location. Time evolution profiles of maximum rain (Figure not shown here) for different events have shown that compared to control runs, test runs (more urbanize) maintained high intensity through out event life cycle.

7. Analysis of Results (Surface Energy Fluxes)

Surface energy fluxes (w/m^2) play critical role in the evolution and dynamics of mesoscale convective systems like heavy rainfall events. Land surface properties (thermodynamic and mechanical) largely affect surface energy partitioning. Availability of moisture would be more in partially urbanized areas (control) and LHF should be relatively more in such areas compared to urbanized areas (test). Converse is true for SHF. Higher latent heat flux (6-hour, pre-event, time integrated) was found to be more in control cases for all the three events (Mumbai, Bangalore and Chennai), rainfall distribution was also found to be spatially more extensive in control runs. Higher sensible heat flux associated with urban areas on the other hand contributes to the early formation of clouds (due to the availability of more heating at surface) and intensification of the event. In general it is in agreement with our earlier discussion on the time evolution of maximum accumulated rain

8. Conclusions

Impact of urbanization on intensity and distribution of rain was investigated using mesoscale model (MM5V3). Results presented above are based on the investigation of three events occurred in different seasons and different geographical locations. All the three events discussed here have shown that urban areas tend to modify the intensity and spatial distribution of rain. In general it was found that total rain (accumulated domain averaged rain) was more in semi-urban or partially urbanized areas (control) than urbanized areas (test).It was also found that intensification was more in urban areas with more rain accumulated around the boundary of urban zone or around urban-semi-urban interface zone. Such intensification would eventually contribute to flooding. Urbanization seems to have influenced heavy rainfall events differently over different locations, nevertheless all the events significantly affected by urbanization. In the case of Chennai event, location and intensity of event was found to be more accurate in urban experiment (test) than control experiment though it was slightly overestimated.

References

Dudhia, J., PSU/NCAR Mesoscale Modeling System Tutorial Class Notes and User's Guide; MM5 Modeling System Version 3, 2004

Franklin, J.O. and Joseph, R.M., On the influence of urbanization on water budget in Nairobi city: A numerical study. *GeoJournal.* No. 61, pp. 121-129, 2004

Gero, A.F., Pitman, A.J., Narsima, G.T., Jacobson, C. and Pielke, R.A., The impact of land cover change on storms in the Sydney Basin, Australia. *Global and Planetary Change*, 54, pp. 57-78, 2006.

Observation and simulation with RegCM3 for the 2005-2006 rainy season over the southeast of Brazil

Maria Elisa Siqueira Silva and Diogo Ladvocat Negrão Couto

Department of Geography, University of São Paulo, Brazil, mariaelisa.siqueirasilva@gmail.com

1. Introduction

Vegetation at central-southeast of Brazil and Amazonian region has great potential to provide changes, both due to the increase of dioxide carbon concentration in atmosphere and by the rapid use of land (Ferniside, 2005), replacing natural vegetation by crops or deforested areas. Salazar et al. (2007) verified the relationship between climate and geographical distribution of vegetation over South America, dealing with biogeographic modeling. They defined spatial distributions of vegetation based on 15 climatic models for two emissions sceneries (A2 and B1) from IPCC (Moss et al., 2008), considering the dioxide carbon increase in the atmosphere for many future decades (2020-2029; 2050-2059; 2090-2099). All models indicated different levels of aridization, mainly over central areas of South America. Besides the development of studies focused on climatic simulations, there are initiatives in order to going on with biosphere-atmosphere observation over different types of coverage, as is the case of the project *Biosphere-Atmosphere Interaction Phase II: Cerrados and Changing the Landuse* (Rocha, 2004), from which is possible to obtain surface energy fluxes data, since 2002, over sugar cane and Eucalyptus crops and, Cerrado (savannah-like vegetation).

Considering locally observed data (those observed in the context of the cited project) and simulation results, the objective in this study is to estimate, through the use of RegCM3, the rainy impact over the central-southeast of Brazil due to modification of vegetation type accordingly to Salazar et al. (2007), for the period comprised between 2020 and 2029. In this period, the reduction observed in tropical forest is about 3%. The dryness of vegetation is taken in account, as provided by Salazar et al. (2007), as consequence of the increase of CO_2 concentration in the atmosphere.

2. Data and Model

The simulations were generated with the regional model RegCM3 for the major part of South America considering a domain centered in 22S and 55W, and covering an area of 160x120 grid points with resolution of 50 km. RegCM3 is originated from MM4, as documented by Giorgi et al. (1993). Soil-plant-atmosphere interaction processes are described by BATS, providing calculation of momentum, heat and water vapor turbulent changes between surface and atmosphere and solving prognostic equations for each grid point. In this study, deep cumulus convection is parameterized after Grell (1993). Reanalysis I (Kalnay et al., 1996) is used as initial and boundary conditions.

To prevent dryness of atmosphere due to low evapotranspiration, some adjustments were made in the model for tropical forest vegetation type. The rate of root between the two upper soil layers was modified to 0.40, instead of 0.80, providing more water to be extracted by roots from deeper soil layers. The depths of soil and root layer were also increased to 4.5 and 3 m, respectively.

The model was run from July to December of 2005. Results show the last three month of simulation by the model (Oct-Dec) (period defined by the beginning of local rainy season) while the first three months (Jul-Sep) were cut off to prevent considering spin up problem.

Two different experiments were run: CTR, control experiment and SAVAN, considering the aridization proposed by Salazar et al. (2007). Observed data are compared to those simulated for verification.

3. Results

As shown in Figure 1, it is possible to see the good representation of averaged rain (Oct-Dec, 2005) by RegCM3 when compared to CMAP data (not shown). South Atlantic Convergence Zone (SACZ) is very well positioned.

The comparison between simulated and local observed data, for the north of São Paulo State (as mentioned earlier) shows diurnal evolution of minimum and maximum air temperature near surface, sensible and latent heat fluxes (Figure 2). Local observed temperature shows greater diurnal temperature amplitude in comparison to that simulated by the model (Figure 2a). Diurnal variability appears to be very well simulated in comparison to observation. Although latent and sensible heat fluxes appear to be well simulated, in terms of absolute values, latent heat flux is overestimated for the whole period (Figure b,c). The increase of latent flux during the simulated period is accompanied by increase in precipitation (figure not shown).

The simulation results considering vegetation change over the southeast of Brazil, replacing evergreen shrub and crop areas by deciduous shrub, show the diminishing of precipitation over São Paulo state (Figure 3). Blue line contours in Figure 3 show negative impact (experiment minus control run).

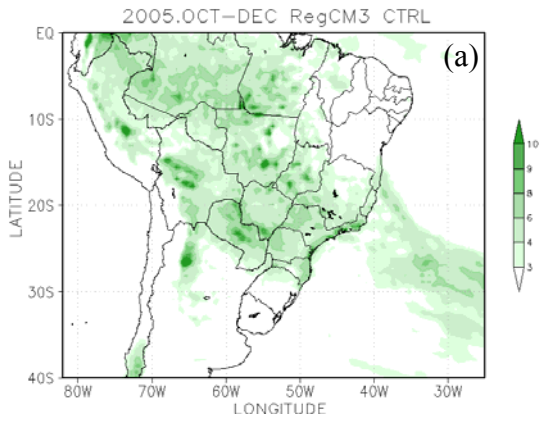

Figure 1. (a) Precipitation simulated (RegCM3) for South America, 2005 OCT-DEC.

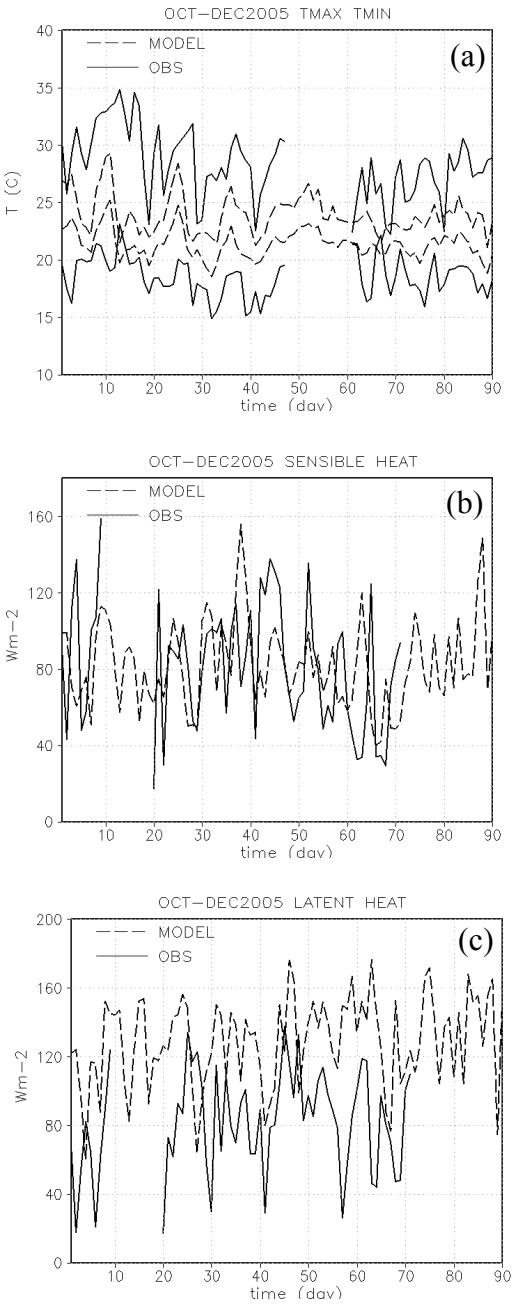

Figure 2. Precipitation and anomaly for 2005 OCT-DEC, the beginning of rainy season, based on CMAP data.

4. Discussion and Conclusions

The use of RegCM3 for South America shows very good simulations. Simulation considering Emmanuel parameterization provides wetter rainy season (figures not shown) than those run with Grell schemes.

This aspect can be particularly important when we try to simulate different periods (wetter and drier), as is the case of 2005 and 2006 years that show significantly distinct photossintetically albedo radiation for the considered region.

Another important aspect of simulation results considering Grell parameterization is the SACZ positioning during the rainy season. Also in this case compared to that simulated by the model with Emmanuel parameterization.

In general, the values of minimum and maximum air temperature, latent and sensible heat fluxes are well simulated when compared to those observed.

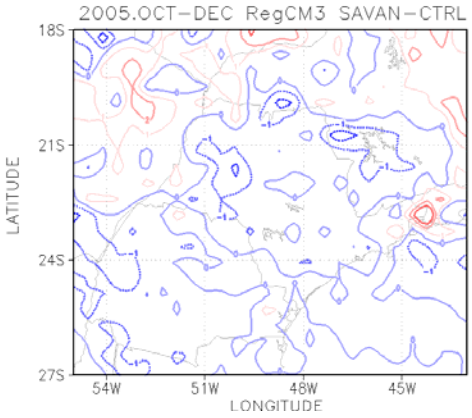

Figure 3. Impact of vegetation change for São Paulo state, SAVAN minus CTR experiment precipitation, during Oct-Dec, 2005. Blue (red) contour shows negative (positive) values.

Acknowledgments. We gratefully acknowledge the financial support provided by FAPESP, Process No 2007/07834-3.

References

Dickinson, RE, A Henderson-Sellers, PJ Kennedy, MF, Wilson, 1986. Biosphere-Atmosphere Transfer Scheme (BATS) for the NCAR Community Climate Model. *NCAR Technical Note*, NCAR/TN-275+STR, 69p.

Fearnside, PM, 2005. Global implications of Amazon frontier settlement: Carbon, Kyoto and the role of Amazonian deforestation. pp. 36-64. In: A. Hall (ed.) *Global Impact, Local Action: New Environmental Policy in Latin America*. University of London, School of Advanced Studies, Institute for the Study of the Americas, London, U.K. 321 pp.

Giorgi, F., M.R. Marinucci, G.T. Bates, 1993: Development of a second-generation regional climate model (RegCM2). Part II: Convective processes and assimilation of lateral boundary conditions. *Mon. Wea. Rev.*, 121, 2814-2832.

Grell, G.A., 1993: Prognostic evaluation of assumptions used by cumulus parameterizations. *Mon. Wea. Rev.*, 121, 764-787.

Kalnay, E. and Coauthors, 1996: The NCEP/NCAR Reanalysis 40-year Project. *Bull. Amer. Meteor. Soc.*, 77, 437-471.

Moss, R. and Coauthors, 2008. Towards New Scenarios for Analysis of Emissions, Climate Change, Impacts, and Response Strategies. *Intergovernmental Panel on Climate Change,* Geneva, 132 pp.

Rocha, H.R., 2004. Projeto Temático Interação Biosfera-Atmosfera Fase 2: Cerrados e Mudanças de Uso da Terra, financiado pela Fapesp.

Salazar, L F; Nobre, C A; Oyama, M D, 2007. Climate change consequences on the biome distribution in tropical South America. Geoph. Res. Letters, v. 34, p. 1-6.

Sellers, P.J.; D.A. Randall; C.J. Collatz; J.A. Berry; C.B. Field; D.A. Dalzich; C. Zhang; G.D. Collelo, 1996. A revised land surface parameterization (SiB2) for atmospheric GCMs, Part I: Model formulation. J. Climate, 9, 676-705.

Simulating cold palaeo climate conditions in Europe with a regional climate model

Gustav Strandberg, Jenny Brandefelt, Erik Kjellström and Benjamin Smith

Gustav Strandberg, SMHI, SE-601 76 Norrköping, Sweden, gustav.strandberg@smhi.se
Jenny Brandefelt, Dept. of Mech. KTH, SE-100 44 Stockholm, Sweden
Erik Kjellström, , SMHI, SE-601 76 Norrköping, Sweden
Ben Smith, Dept. of Physical Geography and Ecosystems Analysis, Lund University, SE-223 62 Lund, Sweden

1. Introduction

A fully coupled atmosphere-ocean general circulation model (AOGCM) is used to simulate Last Glacial Maximum (LGM, ~21ka BP) and conditions representative of a stadial during Marine Isotope Stage 3 (MIS 3, ~44ka BP). Both periods are much colder than today. Selected periods of these runs are dynamically downscaled with a regional climate model (RCM) operating on 50 km horizontal resolution over Europe. The high resolution of the RCM simulation is important for a better representation of the boundary conditions (e.g. the topography associated with the ice sheets covering Scandinavia during these periods). Simulating past climates can be a way to evaluate the models, firstly to see if it is able to reproduce a climate very different from today at all, and also by comparing model results with climate reconstructions of the periods.

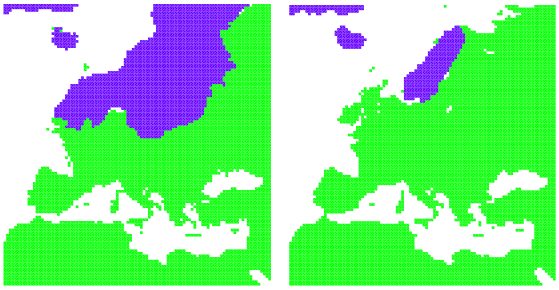

Figure 1. Land (green) and ice extent (blue) in RCA3 in Europe in LGM (left) and MIS 3 (right). Grid boxes with a land fraction lower than 20% are not filled.

2. Method

The AOGCM (CCSM3) was run for more than 1000 model years to get a climate in equilibrium for each period. Time slices of 50 years were selected for downscaling with the RCM (RCA3). The results from the RCM were used in a vegetation model (LPJ-GUESS) to get vegetation that is in accordance with the simulated climate. The new vegetation is then used in a second RCA3 run. LGM is characterised by a large ice sheet. MIS 3 is also a cold period, but with a smaller ice sheet (Fig. 1). The CO_2 levels are set to 185 (200) ppm for LGM (MIS 3). Because of the large ice sheets the sea surface in both periods is much lower than today, exposing new land areas. See Kjellström et al. (2009) for further details on the simulations.

3. Results

LGM is much colder than the recent past (RP, 1961-1990). RCA3 simulates temperatures of the coldest month at least 25˚C colder than RP conditions in Scandinavia and around 5˚C colder around the Mediterranean Sea (Fig. 2). In summer Scandinavia is around 15˚C colder than the RP and the area around the Mediterranean Sea about 5-10˚C colder (Fig. 3). Europe north of Paris has an annual average temperature below 0˚C. Precipitation is lower compared with RP conditions in northern Europe, partly because of changed topography, and partly because of reduced evaporation from the Atlantic, which to a large degree is ice covered in the winter (not shown). However, precipitation in LGM compared with RP is larger on the edge of the ice sheet northwest of Fennoscandia and the British Isles as a result of the orographic forcing. In southern Europe, the Iberian Peninsula and the southern Alps and Italy gets more precipitation than in the RP climate due to changed atmospheric circulation in winter (southward shift of the North Atlantic storm track).

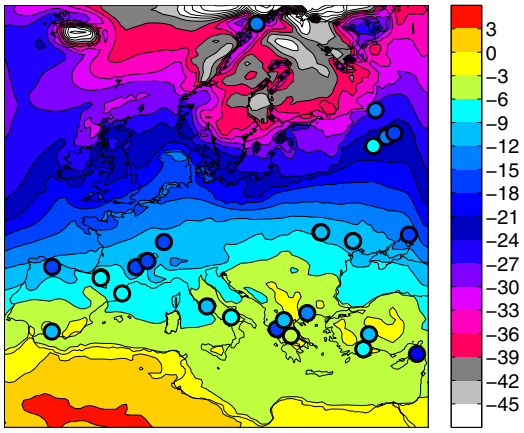

Figure 2. Mean temperature of the coldest month in LGM as compared to recent past climate. Corresponding temperatures as given by proxy based reconstructions are denoted in the filled circles. Units are ˚C.

The simulation is colder than SST proxies over the North Atlantic, possibly indicating a too cold climate in the region and also potentially in northern Europe. Compared to proxy-based data from southern Europe the regional climate model show a good agreement for all seasons except summer when it is colder by some 2-5˚C than the reconstructions show (Fig. 2). A comparison to proxy data of precipitation in southern Europe for LGM conditions shows that the geographical distribution of simulated changes in precipitation is similar to the proxy data.

The simulation of MIS 3 is the first long run with a fully coupled AOGCM. CCSM3 simulates a cold, but not as cold as LGM, climate compared to RP conditions. This is manifested in the downscaling experiment with RCA3 as exemplified by the 0°C isotherm for annual mean temperature that goes south of Ireland, through England and the southern parts of Denmark, just south of Sweden and then eastwards (not shown). All Europe but the Mediterranean area has average winter temperatures below zero (Fig. 4). In summer only the ice covered areas are

that cold (Fig. 5). Winter temperatures are on a scale from around 5°C colder than RP in southern Europe to around 15°C colder in southern Scandinavia and more than 30°C colder in the ice covered areas. In summer southern and western Europe are 3-6°C colder and eastern Europe 0-3°C colder than in the RP. Ice covered areas are around 15°C colder than RP conditions. Around the Mediterranean Sea, precipitation amounts are about the same as in the recent past although with more precipitation in the southwest (not shown). Most of central Europe gets 10-20 mm/month less precipitation than today. The largest difference is over the Norwegian Sea where the sea ice prevents evaporation and thereby convection and precipitation.

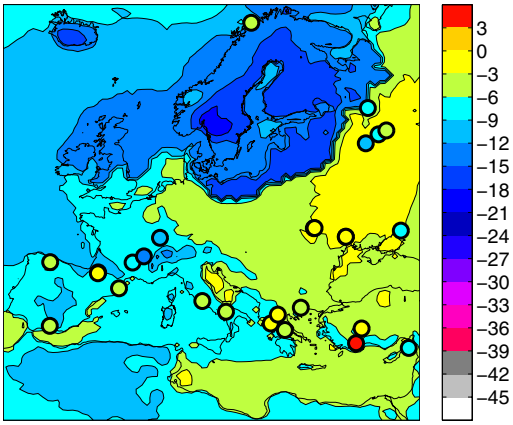

Figure 3. Mean temperature of the warmest month in LGM as compared to recent past climate. Corresponding temperatures as given by proxy based reconstructions are denoted in the filled circles. Units are ˚C.

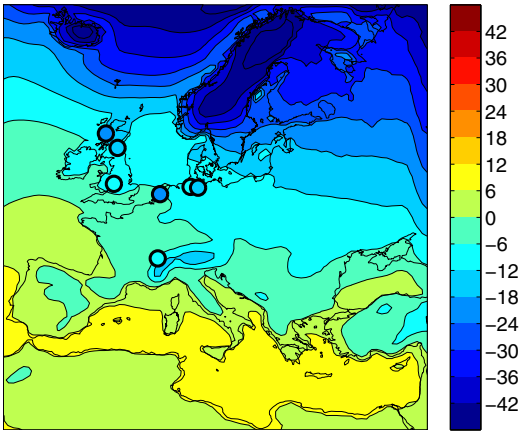

Figure 4. Mean temperature of the coldest month in MIS 3. Corresponding temperatures as given by proxy based reconstructions are denoted in the filled circles. Units are ˚C.

Proxy data are sparse which limits any profound evaluation of the model results. The single point of SST proxies at high latitudes in the Atlantic is in better agreement with the simulation than the corresponding agreement in LGM, however the comparison of terrestrial proxies with the regional climate model results shows that RCA3 is colder than recorded at the three available sites in the British Isles for the warmest month of the year (Fig. 5). This may indicate that summertime SSTs in parts of the North Atlantic are indeed too low. For all the other locations in western Europe the agreement between simulation and proxy data is reasonable and within the uncertainty ranges assigned to the proxies.

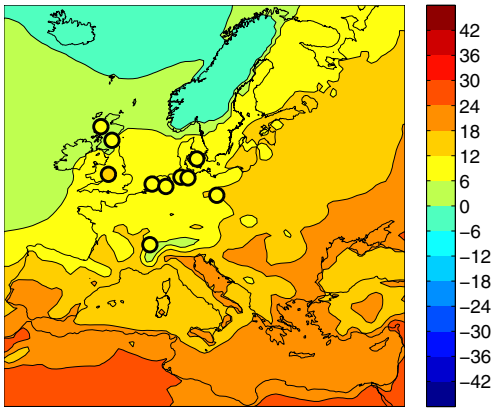

Figure 5. Mean temperature of the warmest month in MIS 3. Corresponding temperatures as given by proxy based reconstructions are denoted in the filled circles. Units are ˚C.

4. Concluding remarks

RCA3 is able to reproduce climates very different from today. The results are in broad agreement with available proxy data and other climate model simulations. The resulting climate is in a qualitative agreement with the imposed extent of ice sheets and types of vegetation for the respective climate case. In particular we show that the results for the cold MIS 3 case are consistent with ice free conditions in south-central Fennoscandia. The results of the iterative simulations with the regional climate model and the dynamic vegetation model show that this is indeed a viable approach as the resulting vegetation is close to the vegetation in the LGM as estimated by other models and to the vegetation in MIS 3 as deduced from palaeo data.

5. Acknowledgements

This project was initiated by Svensk Kärnbränslehantering AB (SKB). Joel Guiot, Masa Kageyama, Antje Voelker and Barbara Wohlfarth kindly provided proxy data. This research uses data provided by the Community Climate System Model project supported by the Directorate for Geosciences of the National Science Foundation and the Office of Biological and Environmental Research of the U.S. Department of Energy. All model simulations with the global and regional climate models were performed on the climate computing resource Tornado operated by the National Supercomputer Centre at Linköping University. Tornado is funded with a grant from the Knut and Alice Wallenberg foundation.

References

Kjellström, E., Brandefelt, J., Näslund, J-O., Smith, B., Strandberg G., Wohlfart, B., Climate conditions in Sweden in a 100,000-year time perspective, Svensk Kärnbränslehantering AB, *report TR-09-04*, pp. 128, 2009

Coupling climate and crop models

B. Sultan[a], A. Alhassane, P. Oettli, S. Traoré, C. Baron, B. Muller[b], and M. Dingkuhn[b]

a) IPSL/CNRS, 4 Place Jussieu, 75252 Paris Cedex
b) CIRAD, Montpellier, France

Global circulation models (GCM) are increasingly capable of making relevant predictions of seasonal and long-term climate variability, thus improving prospects of predicting impact on crop yields. This is particularly important for semi-arid West Africa where climate variability and drought threaten food security. Translating GCM outputs into attainable crop yields is difficult because GCM grid boxes are of larger scale than the processes governing yield, involving partitioning of rain among runoff, evaporation, transpiration, drainage and storage at plot scale. This study will analyze the bias introduced to crop simulation when climatic data is aggregated spatially or in time, resulting in loss of relevant variation. It will also show some downscaling perspectives and results from the AMMA program focused on the use of IPCC AR5 simulations to estimate future yields in West Africa.

Streamflow in the upper Mississippi river basin as simulated by SWAT driven by 20C results of NARCCAP regional climate models

E. S. Takle, M. Jha, E. Lu, R. W. Arritt, W. J. Gutowski, Jr., and the NARCCAP Team

Iowa State University, Ames, IA 50011 USA, gstakle@iatate.edu

1. Introduction

Major hydrological quantities in the Upper Mississippi River Basin (UMRB) in the last two decades of the 20C are evaluated with the Soil and Water Assessment Tool (SWAT) in comparison with observed streamflow. Inputs to SWAT are provided by the daily meteorological quantities from observed at weather stations in the basin and from daily meteorological conditions simulated by a subset of regional climate models reporting to the archive of the North American Regional Climate Change Assessment Program (NARCCAP, 2009) driven by reanalysis boundary conditions. Results show that regional models correctly simulate the seasonal cycle of precipitation, temperature, and streamflow within the basin. Regional models also capture interannual extremes represented by the flood of 1993 and the dry conditions of 2000.

2. Soil and Water Assessment Tool

The SWAT (Arnold and Fohrer, 2005) is a physically based, continuous time, long-term, watershed scale hydrology and water quality model. SWAT version 2005 was used for this analysis. Meteorological input to SWAT includes daily values of maximum and minimum temperature, total precipitation, mean wind speed, total solar radiation, and mean relative humidity. The hydrologic cycle as simulated by SWAT at the HRU level is based on the balance of precipitation, surface runoff, percolation, evapotranspiration, and soil water storage. SWAT takes total daily precipitation from models or observations and classifies it as rain or snow using the average daily temperature. When climate model output is provided, SWAT uses only total liquid precipitation and does its own partitioning to rain or snow. Snow cover is allowed to be non-uniform cover due to shading, drifting, topography and land cover and is allowed to decline non-linearly based on an areal depletion curve. Snowmelt, a critical factor in partitioning between runoff and baseflow, is controlled by the air and snow pack temperature, the melting rate, and the areal coverage of snow. On days when the maximum temperature exceeds 0ºC, snow melts according to a linear relationship of the difference between the average snow pack maximum temperature and the base or threshold temperature for snowmelt. The melt factor varies seasonally, and melted snow is treated the same as rainfall for estimating runoff and percolation. Further details can also be found in the SWAT User's manual (Neitsch et al., 2002).

3. Regional Climate Models

A preliminary analysis is presented of three regional climate models reporting to the NARCCAP archive: MM5I run at Iowa State University, RCM3 run by the University of California – Santa Cruz, and the WRFP model run at the Pacific Northwest National Laboratory. The 20C simulations of NARCCAP consist of simulations over North America for 1980-2004 driven by NCEP reanalysis data at lateral boundaries.

4. Preliminary Results

Mean monthly precipitation and streamflow (Fig 1) for these three models demonstrate skill in simulating seasonal distributions and also interannual variability.

a)

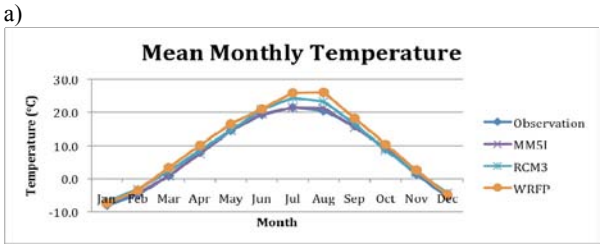

b)

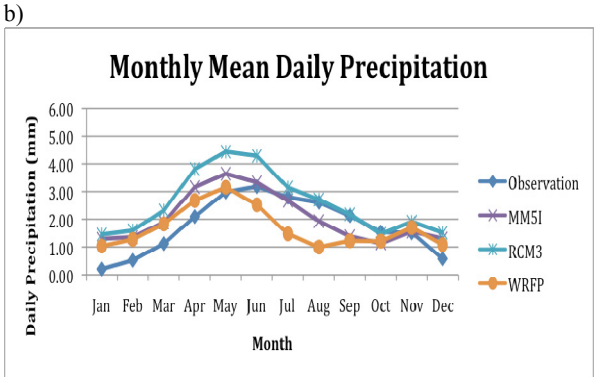

c)

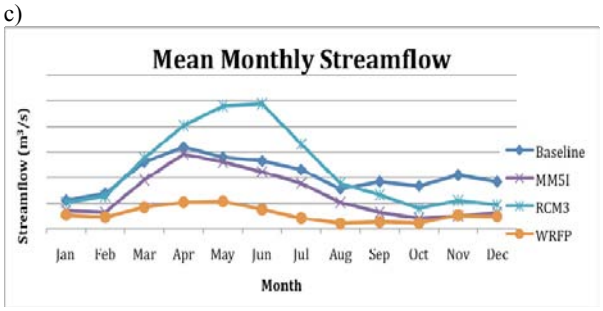

d)

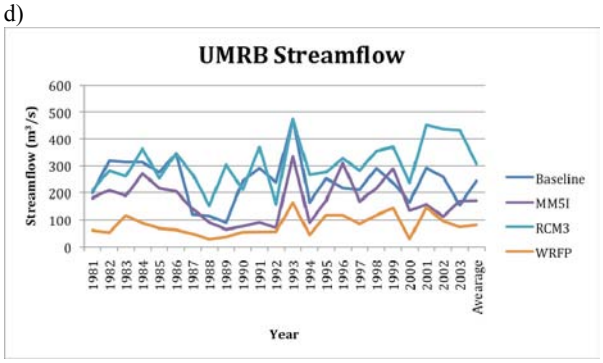

Figure 1. RCM/SWAT simulations of a) temperature, b) precipitation, c) monthly streamflow, and d) interannual streamflow.

The models generally show a warm bias in summer for this region but lower bias in winter. By contrast, precipitation amounts simulated for winter are higher than observations, and the annual maximum generally occurs about one month earlier than is observed. The spring-to-summer decrease in precipitation is more abrupt in the models than in observations.

The delayed peak in seasonal precipitation in the models leads to a delayed seasonal peak in streamflow as well, as shown in Fig. 1c. The range of results for streamflow is larger than the range in either temperature or precipitation. For instance if a model is both too warm and too dry it has two factors leading to a low simulations of streamflow.

All regional models capture two major features of the interannual variability that occurred during the period of 1980-2004. The major flood of 1993 was the dominant hydrological feature of this region over the period simulated. Individual models have systematic biases over the entire simulated record, but all capture the flood of 1993, albeit with reduced or amplified (depending on bias) difference from the long term mean. All models also capture the weaker extreme dry period of 2000, although with less distinctiveness than the flood year. Small interannual variations are simulated differently by individual models, with some showing much less variability, particularly in the first half of the record.

5. Future Results

SWAT simulations with results of additional NARCCAP models are in progress and will be reported at the workshop.

6. Acknowledgement

We acknowledge the North American Regional Climate Change Assessment Program (NARCCAP) including the climate modeling groups and the NCAR/LLNL archiving teams (http://www.narccap.ucar.edu/about/participants.html) for providing the data used in this publication. NARCCAP is funded by the US National Science Foundation, US Department of Energy, the National Oceanic and Atmospheric Administration (NOAA) and the U. S. Environmental Protection Agency Office of Research and Development. Partial support for this work was provided by USDA National Research Initiative Grant #20063561516724.

References

NARCCAP, 2009: North American Regional Climate Change Assessment Program. [Available online at http://www.narccap.ucar.edu]

Neitsch, S.L., J.G. Arnold, J.R. Kiniry, R. Srinivasan, and J.R. Williams (2002), Soil and Water Assessment Tool: User Manual, Version 2000, *Texas Water Resour. Inst. TR-192*, GSWRL 02-02, BRC 02-06. 455 pp.

Dynamical downscaling of urban climate using CReSiBUC with inclusion of detailed land surface parameters

Kenji Tanaka[1], Kazuyoshi Souma[2], Takahiro Fujii[1] and Makoto Yamauchi[1]

[1]WRRC, DPRI, Kyoto University, Gokasho Uji, 611-0011, Japan, E-mail: tanaka@wrcs.dpri.kyoto-u.ac.jp
[2]IPRC, SOEST, University of Hawaii, 1680 East West Road, POST Bldg., 4th Floor, Honolulu, HI 96822 U.S.A.

1. Introduction

Recently, a sense of impending crisis for the global warming came to be realized, and the social needs for the concrete description of future climate has been increasing. Regional climate model (RCM) might be indispensable on predicting detailed characteristics of climate change. Although RCMs have accomplished remarkable development in recent years, the requirement from user side on the resolution and the accuracy has been increasing more and more. Thus, there is still a gap between precision realized by models and that required from users.

The research project of S-5-3 "Multi-model ensemble and downscaling for global warming impact assessment study" is an ongoing project under the global environment research fund of Japanese Ministry of Environment. The final goal of S-5-3 is to provide the detailed and reliable future climate scenario around Japan for climate change impact assessment community. Since most of populations are concentrated in the city area, concrete description of future urban climate is an important issue. In this study, dynamical downscaling is performed by the non-hydrostatic meteorological model CReSiBUC (Moteki et al., 2005) to include the effect of urban area as realistically as possible.

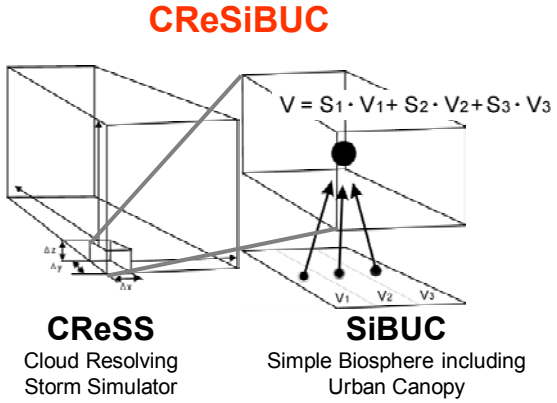

Figure 1. Coupled model of CReSS and SiBUC.

2. CReSiBUC

Figure 1 shows a schematic image of a coupling of the non-hydrostatic meteorological model CReSS (Cloud Resolving Storm Simulator) and the precise land surface model SiBUC (Simple Biosphere model including Urban Canopy). The CReSS is a non-hydrostatic meteorological model developed in Hydrospheric Atmospheric Research Center, Nagoya University (Tsuboki and Sakakibara, 2002). The CReSS has a high calculation efficiency that satisfies a condition to use the "Earth Simulator," which is one of the fastest super computers in the world. The SiBUC is a land surface processes model developed in Water Resources Research Center, Disaster Prevention Research Institute, Kyoto University (Tanaka, 2004). The SiBUC calculates surface fluxes and related hydrological quantities considering detailed processes. In the normal CReSS, the land surface processes are calculated with empirical constant values of albedo, evaporation efficiency, and roughness for simplifying calculations. To the contrary, the SiBUC calculates budgets of radiation, heat, water, and momentum while changing parameters for the surface condition. For example, for an urban area in the SiBUC, irregularity associated with buildings is considered on the basis of the urban canyon concept. As shown in Figure 2, roof height distribution in one model grid cell can be directly incorporated as geometrical information of urban area. Additionally, the SiBUC adopts a "mosaic" approach. In case that a horizontal grid of the CReSS is including a number of various land use categories, values on each category are calculated and a value averaged for these is returned to the CReSS. This mosaic scheme is an effective facility especially for the domain where multiple artificial landuse categories of urban, paddy, etc. are mixed as like Japan.

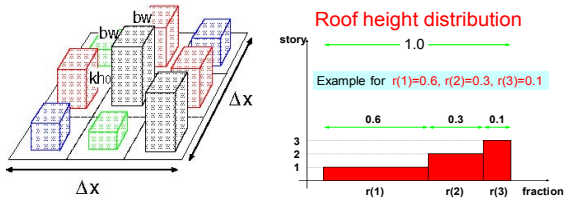

Figure 2. Roof height distribution in urban canopy.

3. Land Surface Parameters

Various kind of land surface information must be prepared to enable the realistic setting of land surface condition. As for landuse and soil type, 100m resolution datasets are provided from National and Regional Planning Bureau in MLIT (http://nlftp.mlit.go.jp/ksj/). SPOT VEGETATION Products (http://free.vgt.vito.be) are utilized for time-varying vegetation parameters in 1km resolution.

Tokyo Metropolitan Governmental Office has established the precise GIS database of urban geometrical information. Figure 3 is an example of building floor number dataset for Shinjuku area (about 5km x 5km area). As seen from this figure, this is a vector data of individual buildings. This information is converted into roof height distribution in each model grid. Owing to this kind of precise information, spatial distribution and its typical diurnal cycle of anthropogenic heat can be estimated following the method of Senoo et al.(2004). Figure 4 shows the spatial distribution of anthropogenic heat around Tokyo at 12JST.

4. Initial and Boundary Conditions

In this S-5-3 project, dynamical downscaling of urban climate is executed only for the summer season (July and August). Then, initial condition of land surface state variables (especially soil wetness) is a big issue when accounting for the effect of the inter-annual variability (wet summer & dry summer). Although there are numerous surface weather observation sites in Japan, few observe the state of the land surface. We have developed a

land data assimilation system (LDAS) to initialize the spatial distribution of the land surface state for short-term weather prediction (Souma et al., 2008). In this study, the offline simulation of this LDAS was performed using the model grid of CReSiBUC to get the initial land surface states (soil wetness, temperature, etc.). As shown in Figure 5, different values of initial soil wetness are adopted for each year in this downscaling experiment.

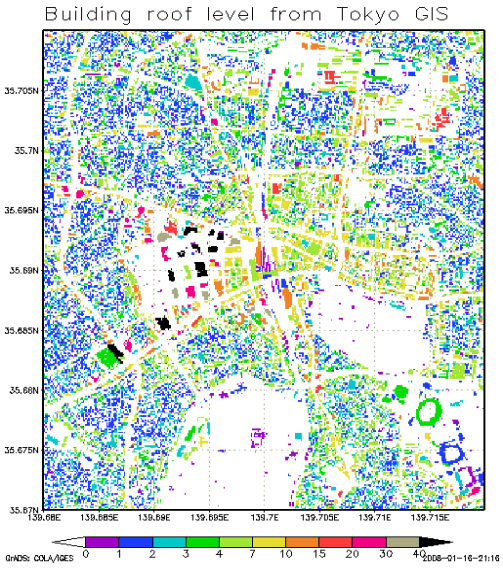

Figure 3. Example of GIS information of building floor number in Tokyo Metropolitan area.

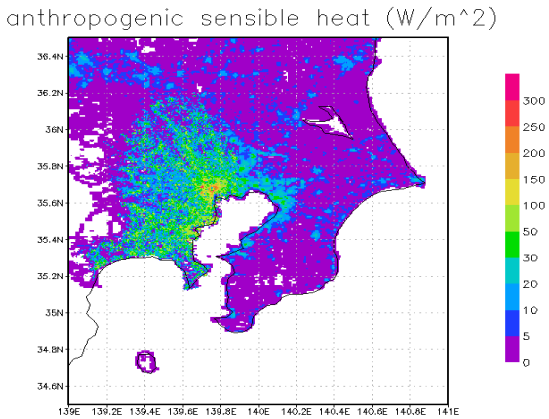

Figure 4. Spatial distribution of anthropogenic heat around Tokyo at 12JST (local time).

Since Japan is surrounded by sea and most of the big cities are located near sea shore, land-sea breeze plays an important role for the urban climate. Land-sea breeze is driven by the contrast of land and sea surface temperature. Sea surface temperature (SST) can be predicted by the water body model in SiBUC. As for initial SST, Pathfinder ver5 monthly 4km resolution product is provided from NASA (http://podaac-www.jpl.nasa.gov). In this way, different values of initial SST are also adopted for each year in this downscaling experiment.

As for the initial and lateral boundary conditions for atmospheric variables, meso-scale analysis product (MANAL) is provided from JMA with 6 hour interval and 10km resolution. Considering the computational load, horizontal grid number is selected as 103 x 103 with 2km resolution. The model domain should include most part of densely populated area and enough sea area for land-sea breeze. As a result, model domain was selected as Figure 5 (center: N35.4, E140.4, projection: Lambert).

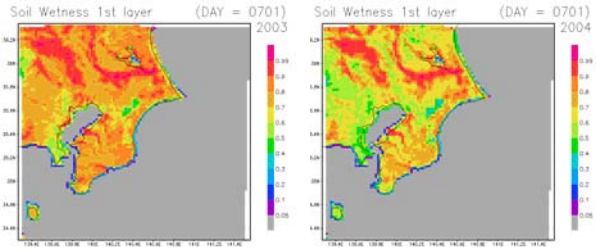

Figure 5. Spatial distribution of initial soil wetness for July 1st (left:2003, right: 2004).

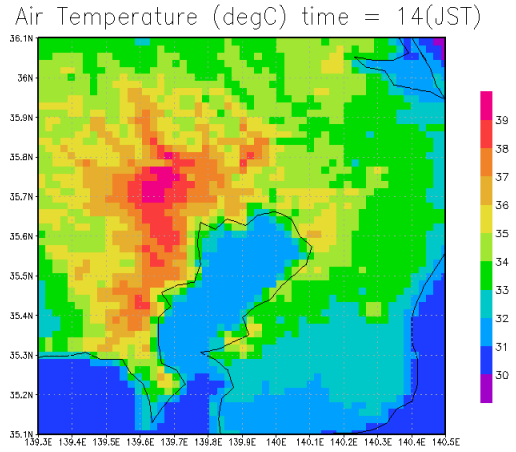

Figure 6. Surface air temperature on hottest day (2003 Aug 14th, 14JST).

5. Results

Figure 6 shows the spatial distribution of surface air temperature at 14JST on 20th July 2004, the hottest day during the simulation period. The air temperature at Nerima reaches to 39 degrees Celsius, that is coincides with observation.

References

Moteki,Q., Y.Ito, K.Yorozu, K.Souma, A.Sakakibara, K.Tsuboki, T.Kato, K.Tanaka, and S.Ikebuchi, Estimation for Effects of Existence of Urban on Development of Cumulonimbus Clouds Using Atmosphere-Land Coupled Model of CReSiBUC, *Annuals of Disas. Prev. Res. Inst., Kyoto Univ.*, No.48 C, pp.197-208, 2005.

Senoo,H., M. Kanda, T. Kinouchi, A. Hagishima, Estimation of anthrpogenic heat and vapor emission and the impact of regional urban climate, Annual Journal of Hydraulic Engineering, JSCE, Vol.48, pp.169-174, 2004(in Japanese).

Souma, K., K. Tanaka, E. Nakakita, S. Ikebuchi, and K. Takara, Effect of the LDAS Derived Realistic Distribution of Soil Moisture on a Summertime Heat Thunderstorm Prediction in Japan, Proc. of 4th Intl. Conf. on Water Resources and Environment Research, pp.2339-2349, 2008.

Tanaka, K., Development of the new land surface scheme SiBUC commonly applicable to basin water management and numerical weather prediction model, *doctoral dissertation, Kyoto Univ.*, 284pp., 2004.

Tsuboki, K. and A. Sakakibara, Large-scale parallel computing of Cloud Resolving Storm Simulator, *High Performance Computing, Springer*, pp.243-259, 2002.

Impact of megacities on the regional air quality: A South American case study

Claas Teichmann and Daniela Jacob

Max-Planck-Institute for Meteorology, Hamburg, claas.teichmann@zmaw.de

1. Introduction

Natural as well as anthropogenic emissions determine the aerosol and chemical composition of the atmosphere. This has a major impact on cloud formation, on the hydrological cycle and on air quality. In many South American regions the effects of megacities - such as São Paulo, Buenos Aires, etc. - are crucial and have an impact on a regional scale. In other regions the emissions are dominated by natural sources as well as by land-use change and biomass burning. The goal of the study is to estimate the impacts of different emission sources on the regional air quality.

In South America the Andes have a significant influence on the atmospheric circulation and on the transport of chemical species, because of the pronounced orographic features. An adequate representation of the Andes within a climate model is only possible with the relatively high horizontal resolution of a regional climate model. The high resolution is also needed to resolve the megacities with their highly concentrated emissions and the corresponding chemical reactions.

2. The regional model REMO including online chemistry and tracer transport

In this study the newest operational version of the regional climate model REMO (*Jacob et al.*, 2001, 2007) is used including on-line chemistry and tracer transport. The chemistry module is based on the second generation Regional Acid Deposition Model (RADM2) (*Stockwell et al.*, 1990).

The model calculates the meteorological processes directly together with photochemistry and tracer transport. The advantage over off-line chemistry-transport models – which are driven by the, e.g., hourly output from a meteorological model – is the direct coupling of meteorological and chemical fields, which both are available for each model timestep.

In the current model setup, the atmospheric mechanisms influence the chemical mechanism and the tracer transport, while there is no feedback from chemistry and tracer concentrations onto the atmospheric properties and processes (see Fig 1).

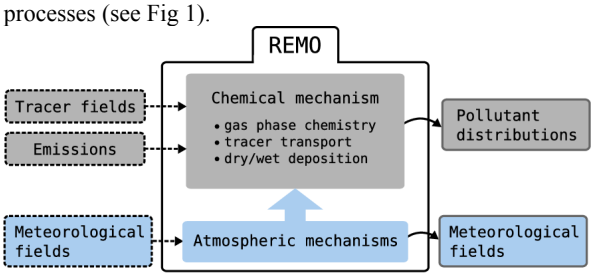

Fig 1. REMO with chemistry and tracer transport

The advantage of this setup is that different case studies, e.g., with modified emission inventories, are subject to exactly the same meteorological conditions. Differences in resulting trace gas concentrations can be attributed to the chemical mechanism and to the modifications made, e.g., to the emission inventory.

3. Boundary data

Boundary and initial data for the chemical species concentrations is provided by global model output from the Model for Ozone and Related Chemical Tracers (MOZART) (*Kinnison et al.*, 2007). Anthropogenic emission data and fire emission data is taken from the REanalysis of the TROpospheric chemical composition over the past 40 years (RETRO) emission database (e.g., *Schultz et al.*, 2008).

Meteorological boundary conditions are provided by ERA-40 re-analysis data (*Uppala et al.*,2005).

4. Model simulations

In order to assess the impact of the different emission sources, several model runs are performed in a case study for the year 2000. They include the full chemistry and tracer transport and are embedded in a hindcast which comprises the whole ERA-40 period for meteorology only.

A so called *reference run* includes the full emission inventory, natural as well as anthropogenic emissions. In two sensitivity runs the emissions from different sources are modified.

Emissions from eight megacities (cities with more than five million inhabitants) are reduced by 90% in the first sensitivity run (denoted as *reduced megacity emissions run*). In the second sensitivity run, denoted as *no-fires run*, fire emissions are removed from the emission inventory. In a comparison, the impact of the different emission sources on the regional air quality is obtained.

5. Results

As an example, results from two sensitivity runs are shown for the simulated April 2000. As April is not part of the main fire season, the impact of the fire-emissions is relatively low, compared to the maximum fire impact of the year.

In Figure 2 the maximum weighted difference between the sensitivity runs and the reference run of near surface CO concentrations (lowest model layer) is shown for the reduced megacity emissions run. Figure 3 shows the maximum weighted difference of CO concentrations for the no-fires run. This gives an impression of the extent of air pollution episodes originating from megacities compared to fire emissions and shows which regions are affected.

As South American megacities are located mainly in coastal regions, pollution can be transported long distances over the ocean. This is shown for Buenos Aires where the CO pollution plume reaches far over the southern Atlantic with a relative impact (i.e., the increase from the reduced megacity emissions to the reference case) of more than 10%.

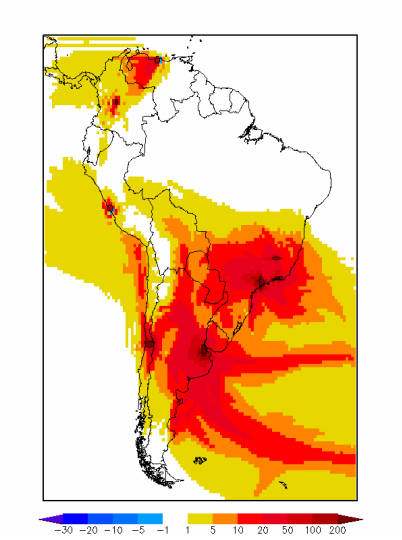

Fig 2. Normalized difference of CO concentrations in the lowest model level between the reference run and the reduced megacity emissions run. Red colors indicate an impact of more than 10%.

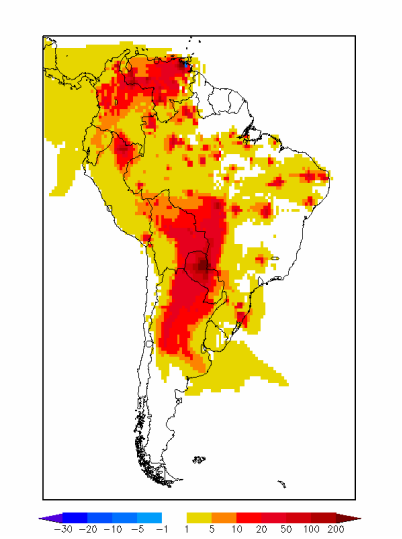

Fig 3. Normalized difference of CO concentrations in the lowest model level between the reference run and the no-fires run. Red colors indicate an impact of more than 10%.

We see that coastal regions are more affected by megacities than by the fires in the southern part of South America. The impact of Santiago de Chile, e.g., can reach up to the coast of Peru, although it is simulated to be less than 10% at maximum at the coast of southern Peru.
The impact of fire emissions in the Amazon region does hardly reach the coastal areas while large parts of northern Argentina, Paraguay and parts of Brazil and Bolivia are affected by more then 20% by fire emissions.

6. Conclusions

Our results suggest that during a one month time period air pollution episodes caused by megacities can affect areas on a continental scale. They affect especially the relatively high populated coastal regions of South America.

In April 2000, the fire emissions are relatively low, but produce an impact area of comparable size to the impact area of megacitiy emissions, which is mostly located away form coastal regions.
During the fire-season, the fire impact area is much larger, while the impact of the megacity emissions on air quality is of the same magnitude (not shown).
Further research will lead to a deeper understanding and quantification of the impact of the different emission sources on regional air quality.

References

Jacob, D., Bärring, L., Christensen, O. B., Christensen, J. H., de Castro, M., Déqué, M., Giorgi, F., Hagemann, S., Hirschi, M., Jones, R., Kjellström, E., Lenderink, G., Rockel, B., Sánchez, E., Schär, C., Seneviratne, S. I., Somot, S., van Ulden, A. & van den Hurk, B., 'An inter-comparison of regional climate models for Europe: model performance in present-day climate', *Climatic Change* , 81, pp. 31-52, 2007

Jacob, D., Van den Hurk, B. J. J. M., Andrae, U., Elgered, G., Fortelius, C., Graham, L. P., Jackson, S. D., Karstens, U., Kopken, C., Lindau, R., Podzun, R., Rockel, B., Rubel, F., Sass, B. H., Smith, R. N. B. & Yang, X., 'A comprehensive model inter-comparison study investigating the water budget during the BALTEX-PIDCAP period', *Meteorology and Atmospheric Physics,* 77, 1-4, 19-43, 2001

Kinnison, D. E., Brasseur, G. P., Walters, S., Garcia, R. R., Marsh, D. R., Sassi, F., Harvey, V. L., Randall, C. E., Emmons, L., Lamarque, J. F., Hess, P., Orlando, J. J., Tie, X. X., Randel, W., Pan, L. L., Gettelman, A., Granier, C., Diehl, T., Niemeier, U. & Simmons, A. J., 'Sensitivity of chemical tracers to meteorological parameters in the MOZART-3 chemical transport model', *Journal Of Geophysical Research-Atmospheres* 112, D20, D20302, 2007

Schultz, M. G., Heil, A., Hoelzemann, J. J., Spessa, A., Thonicke, K., Goldammer, J. G., Held, A. C., Pereira, J. M. C. & van het Bolscher, M., 'Global wildland fire emissions from 1960 to 2000', *Global Biogeochem. Cycles,* 22, GB2002, 2008

Stockwell, W. R., Middleton, P., Chang, J. S. & Tang, X. Y., 'The 2nd Generation Regional Acid Deposition Model Chemical Mechanism For Regional Air-Quality Modeling', *Journal Of Geophysical Research-Atmospheres,* 95, D10, 16343-16367, 1990

Uppala, S. M., Kallberg, P. W., Simmons, A. J., Andrae, U., Bechtold, V. D., Fiorino, M., Gibson, J. K., Haseler, J., Hernandez, A., Kelly, G. A., Li, X., Onogi, K., Saarinen, S., Sokka, N., Allan, R. P., Andersson, E., Arpe, K., Balmaseda, M. A., Beljaars, A. C. M., Van De Berg, L., Bidlot, J., Bormann, N., Caires, S., Chevallier, F., Dethof, A., Dragosavac, M., Fisher, M., Fuentes, M., Hagemann, S., Holm, E., Hoskins, B. J., Isaksen, L., Janssen, P. A. E. M., Jenne, R., McNally, A. P., Mahfouf, J. F., Morcrette, J. J., Rayner, N. A., Saunders, R. W., Simon, P., Sterl, A., Trenberth, K. E., Untch, A., Vasiljevic, D., Viterbo, P. & Woollen, J., 'The ERA-40 re-analysis', *Quarterly Journal Of The Royal Meteorological Society,* 131, 612, pp. 2961-3012, 2005

Validation of RCM simulations using a conceptual runoff model

Claudia Teutschbein, Jan Seibert

Department of Physical Geography and Quaternary Geology, Stockholm University, 106 91 Stockholm, Sweden, claudia.teutschbein@natgeo.su.se

1. Introduction

Hydrological modeling for climate change impact assessment implies simulations using temperature and precipitation series generated by climate models, e.g. regional climate models (RCMs). The ability to correctly reproduce current conditions provides confidence in the simulation of future scenarios. While simulated temperature and precipitation series can be compared directly to observations, we were in this study also interested in the combined effect on runoff simulations. In this study we, therefore, investigated how well current conditions were reproduced for both temperature, precipitation and runoff for 5 Swedish catchments.

A comparison of RCM control-run data with observations was performed for precipitation and temperature. Moreover, the runoff simulated with these time series has been compared with measured values. Reanalysis data was also included in the investigation for comparison.

2. Methods

The analysis has been performed for 5 Swedish catchments with areas of 150 to 300 km^2. These catchments, namely Ostträsket (OST), Tännån (TAN), Fyrisån (FYR), Emån (EMA) and Rönne Å (RON), represent different typical climatic conditions and land-use types in Sweden (Fig. 1).

RCM precipitation and temperature data from 16 different RCMs – all driven by ERA40 reanalysis data - were obtained from the ENSEMBLES EU project.

After comparing the results of each RCM with observed data in terms of accuracy and frequency of extreme events (Fig. 2), spatial and temporal differences were analyzed as well.

For comparison, reanalysis data (ERA-MESAN, ERA-INTERIM) were also included.

In a second step, the best performing RCMs were picked for further hydrological investigations. The runoff in the study catchments was simulated with the conceptual runoff model HBV, forced by the RCM data as well as reanalysis time series. This approach is advantageous because hydrological effects of inaccuracies of simulated precipitation and temperature from the RCMs can be assessed. Furthermore, the catchment runoff integrates over a larger area which corresponds better to the RCM grid data than meteorological point measurements.

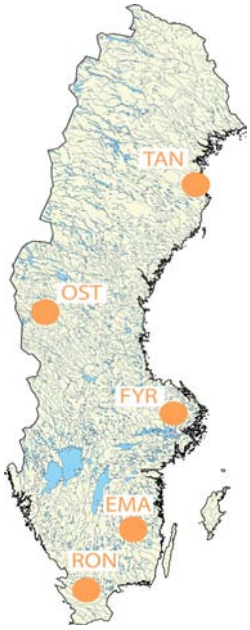

Figure 1. Catchment areas in Sweden.

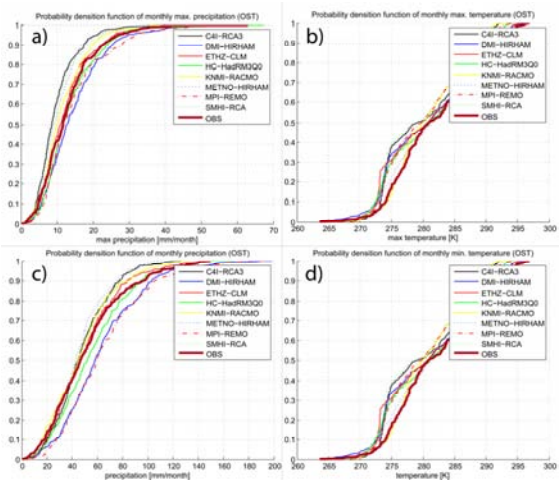

Figure 2. Ability of several RCMs to simulate monthly climate parameters for Ostträsket. (a) max precipitation, (b) max temperature, (c) sum precipitation, (d) min temperature.

Impacts of vegetation on global water and energy budget as represented by the Community Atmosphere Model (CAM3)

Zhongfeng XU and Congbin FU

RCE-TEA, Institute of Atmospheric Physics, Chinese Academy of Sciences, Beijing, 100029, China, xuzhf@tea.ac.cn

1. Introduction

Vegetation exerts very important influences on the climate system through modifying momentum, energy, and water flux between land and air. Over the last decades many studies have been focused on the climatic impacts of vegetation over various regions such as the tropical forest (e.g., Dickinson and Henderson-Sellers, 1988), temperate forests and grasslands (e.g., Bounoua et al 2002; Fu, 2003), boreal forests (e.g., Bonan et al, 1992), and dry lands (e.g., Charney 1975; Xue, 1997). The previous studies showed that the effect of vegetation is different from place to place and from season to season. In a general sense how much the Earth's climate depends on vegetation? This study is aiming to estimate the contributions of vegetation to global and regional hydrological cycle and land surface energy budget by using a community atmosphere model.

2. Model and experimental design

The model used is the NCAR community atmosphere model (CAM3) with the resolution T85 and 26 layers in the vertical. Two numerical experiments were performed. The first one, ctrl run, was integrated by using the standard vegetation type map supplied with the CLM distribution. In the second one, noveg run, the standard vegetation type map was replaced by bare ground. The soil color, percentages of lake and glacier in each gridcell were not changed. Each simulation is integrated 15 years with prescribed monthly varying SST forcing periodically. The first three years of the simulation were discarded for spin up.

3. Influence on global water and energy budget

The annual mean water and energy budget are shown in Figure 1 in which the bold fonts indicate the difference between the ctrl run and noveg run at the confidence level of 95%. In the ctrl run, land surface evapotranspiration and precipitation increase by 10.6% and 1.5%, respectively, indicating an enhanced water exchange between land and atmosphere when the vegetation is included. Meanwhile the runoff reduces by 13.2% due to the enhanced evapotranspiration. The atmospheric precipitable water content increases by 1.5% over land. In addition, the evaporation significantly reduces by 1.1% over the oceans (Fig. 1a).

The land-surface energy balance is also widely influenced by vegetation (Fig. 1b). In the ctrl run, the reflected solar radiation decreases by 6.7%, while the incident solar radiation decreases only 0.6%, indicating a reduced land surface albedo. As a result, there is a 1.3% increase in the solar radiation absorbed by the continents (Fig. 1b). The decrease of incident solar radiation suggests the increase of cloud albedo associated with the increasing precipitation over the continents (Fig. 1a). The net longwave radiation at land surface decreases by 3.6%, although the incident and reflected longwave radiations both show a slight decrease (0.1% and 0.8%, respectively). The increasing land-surface evapotranspiration leads to a considerable increase in the latent heat flux (7.9%). However, no significant change can be found in the sensible heat flux between the ctrl run and noveg run. This is likely related to the following two effects of vegetation: (1) the inclusion of vegetation leads to an increase in net solar radiation due to the reduced land-surface albedo and a decrease in net longwave radiation at land surface, which tends to increase the land surface temperature. (2) On the other hand, the presence of vegetation leads to a considerable increase in evapotranspiration which tends to decrease the land surface temperature. In this case, the annual mean global land-surface temperature doesn't show significant difference between the ctrl run and the noveg run because two effects are largely offset with each other. Thus the influence of vegetation on annual and global mean sensible heat flux appears to be insensitive. However, the relative contributions of two effects of vegetation to surface temperature vary with time and space, therefore substantial difference of sensible heat flux can still be found in some latitudes.

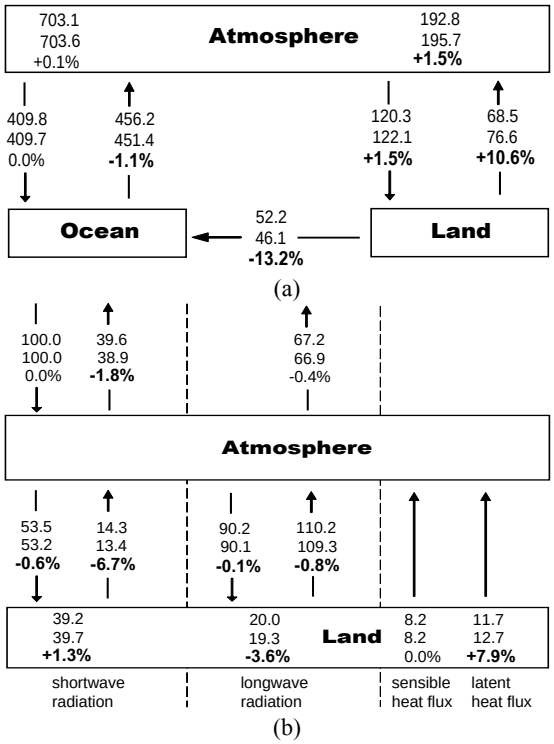

Figure 1. Annual means of (a) global water cycle and (b) the surface energy balance over land for the noveg (upper), ctrl (middle) run, and ctrl minus noveg in percent (lower). Annual mean water fluxs in 10^{15} kg yr^{-1}, precipitable water in 10^{15} kg, and heat/radiative fluxes in percent incoming radiation (100% = 341.3 W m^{-2}). Bold fonts indicate the difference between the ctrl run and the noveg run at significance level of 0.05.

4. Hydrological cycle and energy budget in different latitudes

To examine the effects of vegetation on land surface energy and water budget in different latitudes, Figure 2 shows the zonal mean differences of some key variables between the ctrl run and noveg run as a function of

latitude in July. In the ctrl run, the zonal mean sensible heat flux shows a significant decrease over EQ-25°N and significant increase over 10°-20°S, 30°-35°N, and 55°-65°N relative to that in the noveg run (Fig. 2a), which are highly consistent with the difference of absorbed solar radiation between the ctrl run and noveg run (Fig. 2b). The inclusion of vegetation modifies the energy budget at land surface which in turn impacts the sensible heat and land surface temperature. The vegetation-induced energy modification is not the only factor influencing sensible heat flux and land surface temperature although it likely plays a dominant role in most latitudes. For example, the negative difference of surface temperature at the latitude of 10°S-EQ mainly results from the substantial increase of evapotranspiration even where the absorbed solar radiation appears to be significantly increased when the vegetation is introduced (Fig. 2b-d). As a matter of fact, the evapotranspiration increases almost everywhere after introducing the vegetation effects, especially over the latitudes of 10°S-5°N and 40°-60°N where the maximum differences of vegetation density are found between the ctrl run and noveg run (Fig. 2d). The influence of vegetation on precipitation also appears to be significant in some latitudes such as EQ-20°N and around 50°N (Fig. 2e). The enhanced land evapotranspiration leads to a dramatic increase of vertically integrated atmospheric precipitable water over the latitude around 50°N (Figure not shown), which brings air closer to saturation and therefore closer to precipitation. Sensitive experiments with changing soil moisture confirm this effect (Rowntree and Bolton, 1983). In the tropical continents of EQ-20°N, however, the precipitation is significantly decreased although the evaporation is enhanced (Fig. 2d, e). As a result, the runoff is dramatically decreased in the boreal tropical continents (Fig. 2f). Clearly, vegetation plays different role in different latitudes in influencing precipitation. In boreal tropics, the land covers only about 24% of the total area of boreal tropical zone (EQ-20°N); the atmospheric moisture content is mainly dominated by the evaporation over the tropical oceans. Therefore, the evapotranspiration plays a minor role in the formation of precipitation in the tropical land relative to that in the mid-latitudinal land of 45°-55°N where the land covers about 57% of the total area. However, the land surface heating is likely more important to the formation of precipitation in the moist tropic than in the relatively dry mid-latitudes. In summer, the warm land surface could induce a shallow circulation between the tropical land and ocean. Then, maritime air with high moisture content comes to converge into the low pressure system formed over the land, and cumulus convection and precipitation is formed (Webster 1987). It is seen in Figure 2a that the monthly-mean sensible heat flux significantly decreases by about 3 W m^{-2} in the tropical zone (EQ-20°N) when the vegetation is introduced. The decreased sensible heat flux tends to lower the probability of the formation of tropical convection.

5. Conclusions

We examine the possible contributions of vegetation to global energy and water cycle by using the CAM3. The main conclusions are briefly summarized as follows: The annual and global mean evapotranspiration, precipitation, and vertically integrated precipitable water increase, respectively, by 10.6%, 1.5%, and 1.5% over continent, however the runoff reduces by 13.2% when the vegetation effects are incorporated. The latent heat flux increases by 7.9% in association with the increasing evapotranspiration. The annual mean net solar radiation absorbed by land significantly increases by 1.3% due to the reduced land surface albedo.

Vegetation plays different roles in different latitudes. In the tropical zone, the inclusion of vegetation reduces the heating of land surface, which stabilize the troposphere and therefore leads to less convective precipitation. In the middle latitudes of around 50°N, the effect of vegetation help to enhances the summer evapotranspiration and precipitable water over land, which brings air closer to saturation and therefore closer to precipitation.

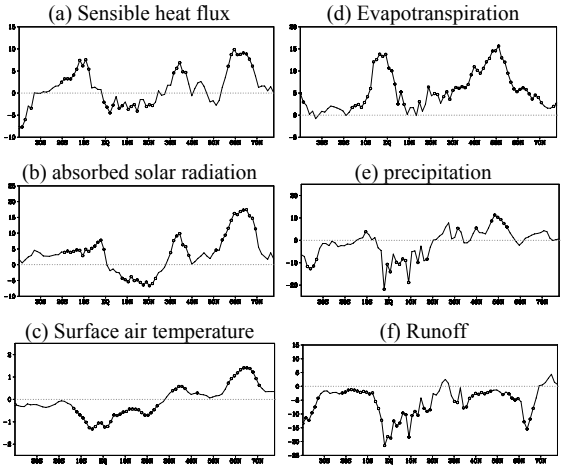

Figure 2. The zonal mean differences of (a) land surface sensible heat flux, (b) absorbed solar radiation, (c) surface air temperature, (d) Evapotranspiration, (e) precipitation, and (f) runoff between the ctrl run and noveg run in July. Unit: (a, c) in W m^{-2}, (b) in °C, (d, e, f) in mm $month^{-1}$. The open circles indicate the latitudes where the difference is significant at the 95% confidence level.

Acknowledgements

We are supported by the Foundation of Jiangsu Key Laboratory of Meteorological Disaster KLME0704.

References

Bonan GB, Pollard D, Thompson SL, Effects of boreal forest vegetation on global climate. *Nature* 359,716-718, 1992

Bounoua L, DeFries R, Collatz GJ, Sellers P, Khan H, Effects of land cover conversion on surface climate. *Climatic Change* 52, 29-64, 2002

Charney JG, Dynamics of deserts and droughts. *Q. J. R. Meteorol. Soc.* 101, 193-202, 1975

Dickinson RE, Henderson-Sellers A, Modelling tropical deforestation: a study of GCM landsurface parameterizations. *Q. J. R. Meteorol. Soc.* 114, 439-462, 1988

Fu CB, Potential impacts of human-induced land cover change on East Asia monsoon. *Global and Planetary Change* 37, 219–229, 2003

Rowntree PR, Bolton JA, Simulation of the atmospheric response to soil moisture anomalies over Europe. *Q. J. R. Meteorol. Soc.* 109, 501-526, 1983

Webster PJ, The elementary monsoon. Monsoons, Fein JS, Stephens PL, eds., John Wiley, New York, NY, 3–32, 1987

Xue Y, Biosphere feedback on regional climate in tropical North Africa. *Q. J. R. Meteorol. Soc.* 123, 1483-1515, 1997

International BALTEX Secretariat Publication Series

ISSN 1681-6471

No. 1: Minutes of First Meeting of the BALTEX Science Steering Group held at GKSS Research Centre in Geesthacht, Germany, 16-17 May, 1994. August 1994.

No. 2: Baltic Sea Experiment BALTEX – Initial Implementation Plan, 84 pages. March 1995.

No. 3: First Study Conference on BALTEX, Visby, Sweden, August 28 – September 1, 1995. Conference Proceedings. Editor: A. Omstedt, SMHI Norrköping, Sweden, 190 pages. August 1995.

No. 4: Minutes of Second Meeting of the BALTEX Science Steering Group held at Finnish Institute of Marine Research in Helsinki, Finland, 25-27 January, 1995. October 1995.

No. 5: Minutes of Third Meeting of the BALTEX Science Steering Group held at Strand Hotel in Visby, Sweden, September 2, 1995. March 1996.

No. 6: BALTEX Radar Research – A Plan for Future Action, 46 pages. October 1996.

No. 7: Minutes of Fourth Meeting of the BALTEX Science Steering Group held at Institute of Oceanology PAS in Sopot, Poland, 3-5 June, 1996. February 1997.

No. 8: *Hydrological, Oceanic and Atmospheric Experience from BALTEX.* Extended Abstracts of the XXII EGS Assembly, Vienna, Austria, 21-25 April, 1997. Editors: M. Alestalo and H.-J. Isemer, 172 pages. August 1997.

No. 9: The Main BALTEX Experiment 1999-2001 – *BRIDGE*. Strategic Plan, 78 pages. October 1997.

No. 10: Minutes of Fifth Meeting of the BALTEX Science Steering Group held at Latvian Hydro-meteorological Agency in Riga, Latvia, 14-16 April, 1997. January 1998.

No. 11: Second Study Conference on BALTEX, Juliusruh, Island of Rügen, Germany, 25-29 May 1998. Conference Proceedings. Editors: E. Raschke and H.-J. Isemer, 251 pages. May 1998.

No. 12: Minutes of 7th Meeting of the BALTEX Science Steering Group held at Hotel Aquamaris in Juliusruh, Island of Rügen, Germany, 26 May 1998. November 1998.

No. 13: Minutes of 6th Meeting of the BALTEX Science Steering Group held at Danish Meteorological Institute in Copenhagen, Denmark, 2-4 March 1998. January 1999.

No. 14: BALTEX – BASIS Data Report 1998. Editor: Jouko Launiainen, 96 pages. March 1999.

No. 15: Minutes of 8th Meeting of the Science Steering Group held at Stockholm University in Stockholm, Sweden, 8-10 December 1998. May 1999

No. 16: Minutes of 9th Meeting of the BALTEX Science Steering Group held at Finnish Meteorological Institute in Helsinki, Finland, 19-20 May 1999. July 1999.

No. 17: Parameterization of surface fluxes, atmospheric planetary boundary layer and ocean mixed layer turbulence for BRIDGE – What can we learn from field experiments? Editor: Nils Gustafsson. April 2000.

No. 18: Minutes of 10th Meeting of the BALTEX Science Steering Group held in Warsaw, Poland, 7-9 February 2000. April 2000.

No. 19: BALTEX-BASIS: Final Report, Editors: Jouko Launiainen and Timo Vihma. May 2001.

No. 20: Third Study Conference on BALTEX, Mariehamn, Island of Åland, Finland, 2-6 July 2001, Conference Proceedings. Editor: Jens Meywerk, 264 pages. July 2001.

No. 21: Minutes of 11th Meeting of the BALTEX Science Steering Group held at Max-Planck-Institute for Meteorology in Hamburg, Germany, 13-14 November 2000. July 2001.

No. 22: Minutes of 12th Meeting of the BALTEX Science Steering Group held at Royal Netherlands Meteorological Institute (KNMI), De Bilt, The Netherlands, 12-14 November 2001. April 2002.

No. 23: Minutes of 13th Meeting of the BALTEX Science Steering Group held at Estonian Business School (EBS), Centre for Baltic Studies, Tallinn, Estonia, 17-19 June 2002. September 2002.

No. 24: The eight BALTIMOS Field Experiments 1998-2001. Field Reports and Examples of Measurements. Editors: Burghard Brümmer, Gerd Müller, David Schröder, Amélie Kirchgäßner, Jouko Launiainen, Timo Vihma. 138 pages. April 2003,.

No. 25: Minutes of 14th Meeting of the BALTEX Science Steering Group held at Lund University, Department of Physical Geography and Ecosystems Analysis, Lund, Sweden, 18 - 20 November 2002. May 2003.

No. 26: CLIWA-NET: BALTEX BRIDGE Cloud Liquid Water Network. Final Report. Editors: Susanne Crewell, Clemens Simmer, Arnout Feijt, Erik van Meijgaard, 53 pages. July 2003.

No. 27: Minutes of 15th Meeting of the BALTEX Science Steering Group held at Risø National Laboratory, Wind Energy Department, Roskilde, Denmark, 8 - 10 September 2003. January 2004.

No. 28: Science Plan for BALTEX Phase II 2003 – 2012. February 2004, 43 pages.

No. 29: Fourth Study Conference on BALTEX, Gudhjem, Bornholm, Denmark, 24 - 28 May 2004, Conference Proceedings. Editor: Hans-Jörg Isemer,

189 pages. May 2004.

No. 30: Minutes of 16th Meeting of the BALTEX Science Steering Group held at Gudhjem Bibliotek, Gudhjem, Bornholm, Denmark, 23 May 2004. October 2004.

No. 31: BALTEX Phase I 1993-2002 – State of the Art Report. Editors: Daniela Jacob and Anders Omstedt, 181 pages, October 2005.

No. 32: Minutes of 17th Meeting of the BALTEX Science Steering Group held at Poznan, Poland, 24 – 26 November 2004. November 2005.

No. 33: Minutes of 18th Meeting of the BALTEX Science Steering Group held at Meteorological Observatory Lindenberg – Richard Aßmann Observatory, Germany, 18 – 20 October 2005. February 2006.

No. 34: BALTEX Phase II 2003 – 2012 Science Framework and Implementation Strategy, 95 pages. April 2006.

No. 35: BALTEX Assessment of Climate Change for the Baltic Sea Basin. Summary. Editors: The BACC lead author group, 26 pages. June 2006.

No. 36: Minutes of 19th Meeting of the BALTEX Science Steering Group held at Ågrenska Villan of Göteborg University Sweden, 23 – 24 May 2006. October 2006.

No. 37: Minutes of 20th Meeting of the BALTEX Science Steering Group held at St. Petersburg, Russia, 6 – 7 December 2006. March 2007.

No. 38: Fifth Study Conference on BALTEX, Kuressaare, Saaremaa, Estonia, 4 - 8 June 2007. Conference Proceedings. Editor: Hans-Jörg Isemer, 209 pages. May 2007.

No. 39: Minutes of 21th Meeting of the BALTEX Science Steering Group held at Kuressaare, Saaremaa, Estonia, 3 June 2007. September 2007.

No. 40: Minutes of 22nd Meeting of the BALTEX Science Steering Group held at SMHI, Norrköping, Sweden, 23-25 January 2008. May 2008.

No. 41: 2nd International Lund RCM Workshop: 21st Challenges in Regional-scale Climate Modelling. Lund University, 4-8 May 2009. Workshop Proceedings. Editors: Burkhardt Rockel, Lars Bärring and Marcus Reckermann. 292 pages, April 2009.

Copies are available upon request from the International BALTEX Secretariat.